

Histogenesis of Merkel cell carcinoma

(Titel der Dissertation)

Dissertation zur Erlangung des
naturwissenschaftlichen Doktorgrades
der Julius-Maximilians-Universität Würzburg

vorgelegt von

Thibault Kervarrec

(Vor- und Familienname)

Mont Saint Aignan, France

(Geburtsort)

Würzburg, 22/11/2019

(Erscheinungsjahr der Dissertation)



Eingereicht am: 30/09/2019

Mitglieder der Promotionskommission:

Vorsitzender: Prof. Philippe Roingeard, University of Tours, France
Gutachter: Prof. Mahtab Samimi, University of Tours, France
Gutachter: Dr. Vladimir Soukhorukov, University of Würzburg, Germany
Gutachter: Prof. Jürgen Becker, University of Duisburg-Essen, Germany
Gutachter: Dr. Houben, University of Würzburg, Germany
Gutachter: Prof. Nicolas Ortonne, UPEC University, France
Gutachter: Prof. Axel zur Hausen, University of Maastricht, Netherlands

Tag des Promotionskolloquiums: 22/11/2019

Doktorurkunde ausgehändigt am:

To the Tumor Biology Forschung Laboratory,

ABBREVIATIONS

AJCC: American Joint Committee on Cancer
ALTO: Alternate frame of the Large T Open reading frame
ATOH1: Atonal homolog 1
CD: Cluster of Differentiation
CLL: Chronic lymphocytic leukaemia
eNEC: Extracutaneous neuroendocrine carcinoma
EpCAM: Epithelial cell adhesion molecule (CD326)
DTS: digital transcriptome subtraction
HaPv: Hamster Polyomavirus
HHV8: Human herpesvirus 8
INSM1: Insulinoma-associated protein 1
KRT: Keratin
LSD: LT stabilization domain
LT: Large T
PML: progressive multifocal encephalopathy
MC: Merkel cell
MCC: Merkel cell carcinoma
MCPyV: Merkel cell polyomavirus
MuPyV: Murine Polyomavirus
NCCR: Non coding control region
NHEK: Normal human epidermal primary keratinocytes
NLS: Nuclear localization signal
PAX5: Paired box-5
PML: Progressive multifocal encephalopathy
PP2A: Protein phosphatase 2 A
PP4C: Protein phosphatase 4 C
RaPv: Raccoon Polyomavirus
RB1: Retinoblastoma protein 1
SATB2: Special AT-rich sequence binding protein 2
SHH: Sonic Hedgehog
sT: Small T
SOX: SRY-box
SV40: Simian virus 40
TAg: « Tumor » antigens
TB: trichoblastoma
TdT: Terminal deoxynucleotidyl transferase
TTF-1: Thyroid transcription factor-1
WHO: World Health organization

ACKNOWLEDGMENTS

I would like to express my sincere gratitude to Dr. Roland Houben and Dr. David Schrama for the continuous support of my PhD study and related research, for their patience, motivation, and immense knowledge. I learned a lot from them and hope we will continue the Würzburg-Tours collaboration for a long time.

I want to express my sincere gratitude to Prof. Mahtab Samimi and Prof. Antoine Touzé for their help and contributions to this work. They support me since many years and I am grateful for that. My wish is to continue to work with them in the MCC research field. I also would like to thank Prof. Touzé's wife for her support and good spirit.

I would like to thank Dr. Soukhorukov, for accepting to be my supervisor and to come in France for my PhD defense.

I would like to thank Prof. Becker, Prof. Ortonne, Prof. Roingeard and Prof. Zür Hausen, for accepting to be member of my thesis committee. It is an honor to get the opportunity to present my work in front of such experts of the field.

I want to express my gratitude to the members of the Pathology department of Tours, notably Prof. Guyétant, Prof. de Pinieux, Dr. de Muret and Dr. Machel. They support me since more than ten years and largely contributed to my education in Pathology as well as to the success of this work.

My sincere thanks also go to all members of the TBFL and BIP teams notably, Dr Hesbacher, Dr. Arnold, Dr. Leblond, Dr. Berthon, Mrs. Sarma, Mrs. Sarosi, Mrs. Neuss, Mrs. Vogtmann, Mrs. Faber, Mrs Esnault and Mrs. Schweinitzer. I am grateful for their help and support. I also would like to thank Prof. Goebeler for his support.

I would like to thank all peoples which contribute to the present work especially the dermatologists and pathologists, who help to the cohort constitution. I would like specially to thank Dr. Julia Zaragoza for her help and support. My sincere thanks also go to Prof. Bernard Cribier and Dr. Marie-Laure Jullié, who identified and provided the MCC-trichoblastoma combined tumors.

I want to express my gratitude to my colleagues especially Dr. Elodie Standley, Dr. Matthias Tallegas, Dr. Damien Sizaret. I am convinced that we will be a fantastic pathology team in the future.

I would like to thank your close collaborators especially Dr Anne Tallet, Dr Christine Collin from the molecular biology platform, and all of the McSaf team, notably Prof. Marie-claude Viaud-Massuard, Dr. Camille Martin and Dr. Ludovic Juen.

Finally, I would like to express my sincere gratitude to my wonderful wife, to my parents and my sister without whom nothing would have been possible.

TABLE OF CONTENT

INTRODUCTION.....	5
I. Merkel cell carcinoma.....	5
1. Historical perspectives and current definition	5
2. Epidemiology.....	7
3. Clinical features	7
4. Histology.....	8
a. Tumor classification.....	8
b. Morphology	11
c. Immunohistochemical profile.....	13
5. Staging, treatment and survival	14
II. MCC Etiologic factors	16
1. Merkel cell polyomavirus	16
a. Merkel cell polyomavirus identification	16
b. Polyomavirus overview	17
c. Polyomaviruses structure	20
d. MCPyV life-cycle.....	23
e. MCPyV: an oncogenic agent.....	25
2. MCPyV-negative tumors	33
III. Histogenesis of MCC.....	35
1. The Merkel cell: the historical candidate.....	35
2. Putative mechanism of a “non-MC” origin for MCC.....	40
3. A non-MC epithelial origin	43
4. A fibroblastic origin.....	49
5. A pre/pro or pre-B-cell origin	50
CONTEXT AND OBJECTIVES	54
RESULTS	59
I. Article 1. Diagnostic accuracy of a panel of immunohistochemical and molecular markers to distinguish Merkel cell carcinoma from other neuroendocrine carcinomas.....	60
II. Article 2. Morphologic and immunophenotypical features distinguishing Merkel cell polyomavirus-positive and negative Merkel cell carcinoma.	73
III. Article 3. Differentiating Merkel cell carcinoma of lymph nodes without a detectable primary skin tumor from other metastatic neuroendocrine carcinomas: The ELECTHIP criteria.	85
IV. Article 4. Merkel cell carcinoma of lymph nodes without skin primary tumor are metastatic neoplasia associated with an efficient immune response.....	97

V. Article 5. Detection of the Merkel cell polyomavirus in the neuroendocrine component of combined Merkel cell carcinoma.....	122
VI. Article 6. Polyomavirus-positive Merkel cell carcinoma derived from a TB suggests an epithelial origin of this Merkel cell carcinoma.....	135
VII. Article 7. Merkel cell Polyomavirus T antigens promote Merkel cell differentiation in epithelial progenitors of the skin	179
DISCUSSION	223
I. Conclusions on the origin of MCC based on the phenotypic characterization of the tumors.....	223
1. Do morphological differences reflect the nature of the oncogenic factors driving MCC development?.....	224
2. Do immunohistochemical differences reflect the nature of the oncogenic factors driving MCC development?.....	225
3. Do prognostic differences reflect the nature of the oncogenic factors driving MCC development?.....	226
II. Conclusions on the origin of MCC based on the characterization of combined tumors	227
1. Are Squamous cell carcinoma/MCC combined tumors indicative of the cell of origin of MCPyV-negative MCC?	227
2. Are Trichoblastoma/MCC combined tumors indicative of the cell of origin of MCPyV-positive MCC?.....	232
III. Are the MCPyV T Antigens capable of promoting Merkel cell like differentiation?	238
IV. How could the MCPyV T Antigens promote Merkel cell like differentiation?	240
SUPPLEMENTS: OTHER PUBLICATIONS OF THE CANDIDATE DURING THE PhD	244
REFERENCES.....	245
ABSTRACT	263

INTRODUCTION

I. Merkel cell carcinoma

1. Historical perspectives and current definition

In 1878, Friedrich Sigmund Merkel, a German anatomist and histopathologist, identified a new cell type located on the basal layer of the epidermis (Figure 1) (Halata et al. 2003). These so-called Merkel cells (MCs) are more frequently observed in acral skin and are often located in contact with the terminal part of dermal nerve fibers. Electronic microscopy studies later confirmed the close contact between these MCs and small nerve endings (Halata et al. 2003), suggesting a mechanoreceptor function. In addition, ultrastructural detection of neurosecretory granules in MCs cytoplasm linked these cells to the disseminated endocrine system (Halata et al. 2003).

In 1972, Toker reported five observations of "trabecular carcinomas" of the skin (Figure 1) (Toker 1972). This new tumor entity was characterized by nests of tumor cells, located in the deeper parts of the skin (dermis or subcutis), without connection to the overlying epidermis. Although, based on morphology, Toker initially postulated an adnexal origin of this tumor, the ultrastructural study performed in 1978 by the same group revealed the presence of neurosecretory granules (Figure 1) (Tang and Toker 1978). Consequently, the authors hypothesized that trabecular carcinoma of the skin derives from MCs and accordingly the name of this entity was changed into "Merkel cell carcinoma" (MCC).

Currently, MCC is defined in the updated World Health Organization (WHO) classification of the skin tumors (WHO 2018) as "the eponymous name for primary neuroendocrine carcinoma of the skin". Interestingly, although, the MCC chapter is now included in the epidermal tumors part, the authors stated that "the cell of origin of MCC is unknown, the assumption that MCC derives from normal MC is now in doubt and alternative histogenetic contenders include cutaneous stem cells, pro/pre-B cells and either cancer stem cells or lineage specific cancer stem cells capable of neometaplasia".

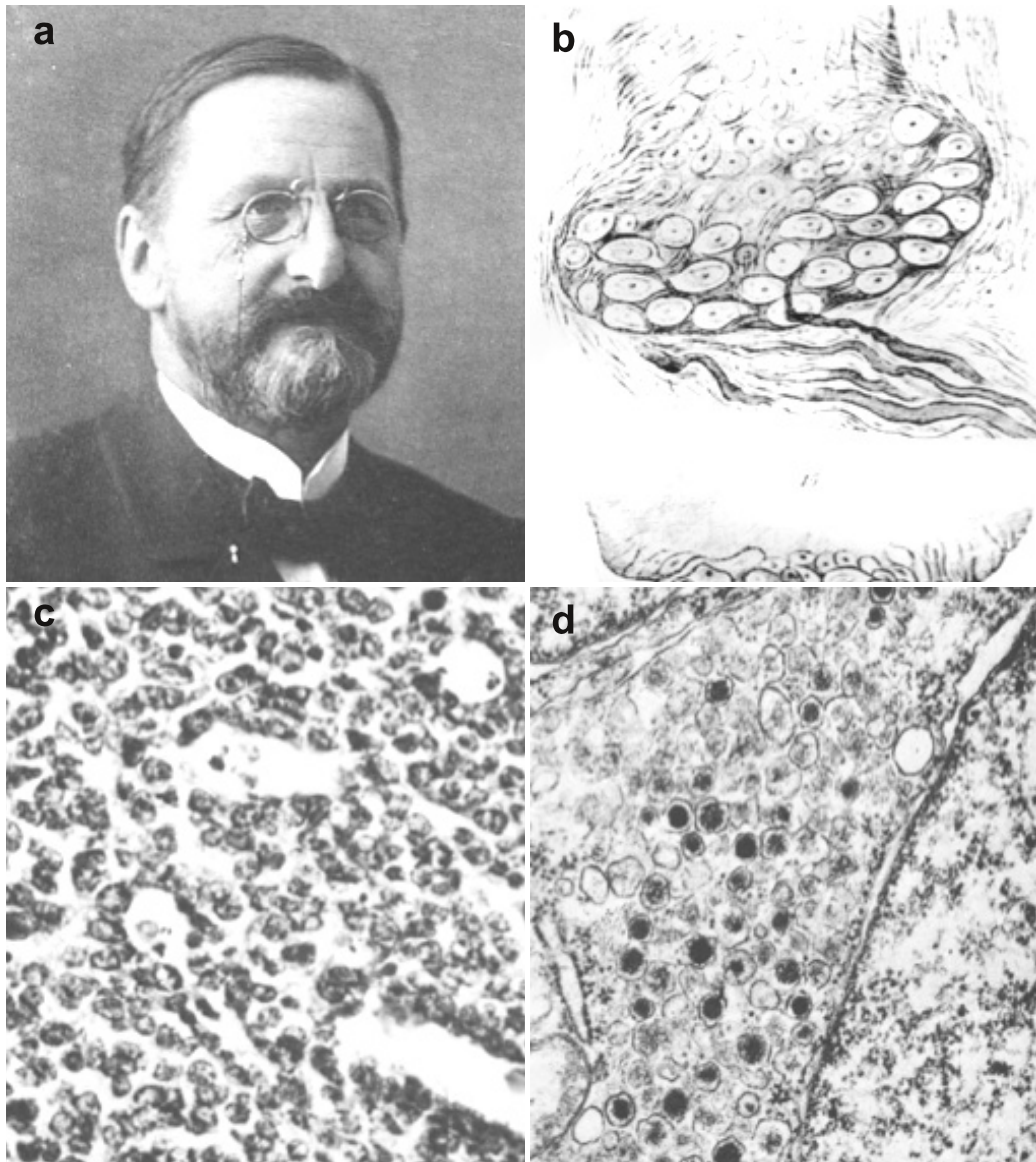


Figure 1. Historical description of Merkel cells and Merkel cell Carcinoma. a: portrait of Friedrich Sigmund Merkel; b: initial draft of MCs by Friedrich Sigmund Merkel (adapted from Halata. 2003); c-d: microscopic and ultrastructural features of « trabecular carcinoma of the skin (adapted from Tang and Toker. 1978): microscopic examination of trabecular carcinoma of the skin (c) revealed a diffuse proliferation of tumor cells with high nucleocytoplasmic ratio. Ultrastructural investigation revealed in tumor cells the presence of dense core granule, a hallmark of MCs in the skin.

2. Epidemiology

Due to the rarity of MCC and the lack of a large international registry, the MCC incidence rate is difficult to evaluate (Schadendorf et al. 2017). Around 1600 new cases are diagnosed each year in the United States (Paulson et al. 2018) and estimated incidence rates of 0.70 and 0.17-0.30 cases/100 000 persons/years have been reported in the United States (Fitzgerald et al. 2015) and in European populations (Eisemann et al. 2014; Kieny et al. 2019), respectively. Although rare, most of the recent publications revealed a dramatic increase in MCC incidence over the two last decades (Schadendorf et al. 2017).

MCC arises mostly in elderly, with a median age at diagnosis of 75 years and less than 5% of the patients are diagnosed before 50 years of age (Albores-Saavedra et al. 2010). Of note, exceptional pediatric cases have been reported (Köksal et al. 2009). In addition, MCC predominantly occurs in white peoples; about 95% of the cases (Albores-Saavedra et al. 2010), and a slight male predominance has been observed (Schadendorf et al. 2017). Immunosuppression including hematologic malignancies, organ transplants, autoimmune diseases and HIV infection appears to be associated with an increased risk of MCC (Asgari et al. 2014; Cook et al. 2019). Indeed, a ten-fold increased incidence is observed in HIV patients (Engels et al. 2002) and patients with chronic lymphoid leukemia further have a 30-fold risk of developing MCC (Cook et al. 2019; Heath et al. 2008). Of note, poor outcome has been reported in such immunocompromised patients (Cook et al. 2019; Paulson et al. 2013). An additional risk factor is sun exposure, a conclusion supported by predominance of MCC in sun exposed areas (about 80% of the cases (Heath et al. 2008)) and by the higher MCC incidence rate observed in high UV-index countries such as Australia (reported incidence rate: 1.6 cases/100 000 persons/years (Youlden et al. 2014)).

3. Clinical features

MCC mostly appears as a fast growing, painless solitary nodule, almost always without epidermal alterations (Figure 2). Clinical features of MCC have been summarized in the AEIOU criteria (Heath et al. 2008): Asymptomatic, Expanding rapidly (< 3 months), Immunosuppression, Older than 50 years, UV exposed site. However, although 89% of MCC cases fulfill at least three of these criteria, the clinical presentation is actually quite unspecific and based only on physical examination, MCC cases are frequently misdiagnosed as benign skin tumor or cyst (Heath et al. 2008). While MCC arise preferentially in sun exposed area

especially head and neck (Heath et al. 2008; Schadendorf et al. 2017), these tumors can also be observed in any skin location. Moreover, MCC arising on mucosae (Islam et al. 2018; Lewis et al. 2010) or appearing as lymph node metastasis without skin primary tumors (de Biase et al. 2012; Pan et al. 2014) have been reported. At diagnosis, median tumor size is around 2 cm but can vary from 0.1 to more than 7 cm (Iyer et al. 2014). Use of dermoscopy has been proposed (Dalle et al. 2012; Harting et al. 2012; Jalilian et al. 2013) and might contribute to the diagnosis of cutaneous tumors which in any case has anyway to be confirmed by microscopic examination. Paraneoplastic syndromes seem to be exceptionally associated with MCC and only few published cases reported Myasthenia/Lambert-Eaton syndrome as well as hyponatremia (Iyer et al. 2016; Nguyen et al. 2019).



Figure 2. Clinical features of MCC tumors. An MCC tumor arising in the face in a 87-years old woman is depicted. MCC tumors frequently develop in sun exposed area and appear as fast-growing nodule lacking specific clinical features (adapted from Samimi. 2015).

4. Histology

a. Tumor classification

Tumor classification system is based on the phenotypic similarities between tumor cells and the healthy tissues and according to Boyd : "Rare cancers, have historically been divided into two groups: cancers defined by their unusual histogenesis (cell of origin or differentiation state)—including chordomas or adult granulosa cell tumours—and histologically defined

subtypes of common cancers” (Boyd et al. 2016). In this context, although the initial assumption that MCC derives from MCs would fit with the first category, the current WHO definition defining MCC as a primary neuroendocrine carcinoma of the skin clearly belongs to the second category.

Indeed “neuro”-“endocrine” differentiation, defining a subgroup of human cancers, is a complex concept referring to the phenotypic similarities of tumor cells with the physiological disseminated neuroendocrine system. Although endocrine organs have been identified for a long time, the concept of neuroendocrinology arose at the beginning of the 20th century based on the observation of the pancreas and digestive tissues. In 1902, Bayliss and Starling identified in the digestive tract a first human hormone they called “secretin” suggesting that this organ harbors endocrine secretion properties (Vinik 2000). Subsequently, based on the tinctorial affinities of endocrine cells for silver and chromium, a new population of so-called enterochromaffin cells or Kulchitsky cells or “Helle Zellen” (clear cells) were described as disseminated elements in digestive tissues and pancreas (Champaneria et al. 2006; Modlin et al. 2006). In 1938, based on i) morphologic and histochemical characterizations of these “clear cells”, ii) their comparison with hypothalamus and adrenal glands, iii) the proof of a chemical transmission by nerves, Feyrter and Masson proposed that these “clear cells” derived from the nervous system. Subsequently, they introduced the concept of a diffuse integrated neuroendocrine network contributing to the regulation of intestinal tissue network (Champaneria et al. 2006; Feyrter 1938). In line with this hypothesis, Pearse later demonstrated that a group of previously unrelated cells with a widespread distribution over the human body (including clear cell of the pancreas, and enterochromaffin cells of the intestine) had the same ability to produce amino hormone. The author reported them as the APUD system (amine precursor uptake and decarboxylation) (Pearse 1969) including the MCs (Hartschuh and Grube 1979; Winkelmann 1977). Histochemical and ultrastructural studies then provided proof that these APUD cells producing small polypeptide hormone. APUD cells are characterized by a common phenotype with respect to expression of proteins necessary for hormone production (Pearse 1969; Pearse 1968). Ultrastructural analysis notably revealed presence of dense core granules containing secretion products (Scalettar et al. 2012), a structure closely related to what was observed in the neurons synapses. Based on these similarities between neurons and APUD cells, Pearse proposed a common embryologic

neurectodermal origin and additionally suggested a neural crest origin of the APUD cells (Pearse 1968). This hypothesis was initially supported by the results obtained in a chimeric quail-chicken models investigating the thyroid C cells which were also regarded as neural crest derived. However, there is currently clear evidences that such C cells are deriving from the endodermis and acquire secondary a neuroendocrine differentiation (Johansson et al. 2015). Therefore, the current view is that neurons and neuroendocrine cells acquire a common phenotype, despite of different embryologic origin (Modlin et al. 2006).

Tumors harboring neuroendocrine differentiation virtually arise from all parts of the body. Initial description in the digestive tract in 1907 referred such as “Karzinoïd” tumors due to their relatively low aggressiveness potential compared to other carcinoma arising from the same site (Oronsky et al. 2017). The term neuroendocrine neoplasia describes nowadays a very heterogeneous tumor group also including aggressive tumors entities (Oronsky et al. 2017). Indeed based on behavior, neuroendocrine tumors (NET) also previously referred as carcinoïds, have a more indolent course and are frequently observed in the digestive tract whereas neuroendocrine carcinomas are an aggressive tumor entity (Oronsky et al. 2017). The latter subgroup is further divided in small cell and large cell types based on morphological variations which are expected to reflect different genetic background (Rekhtman et al. 2016). While Large cell carcinoma tumor cells harbor abundant cytoplasm and prominent nucleoli, small cell carcinoma cases are characterized by high nucleocytoplasmic ratio and granular chromatin. In this setting, small cell neuroendocrine carcinoma are characterized by *TP53* and *RB1* alterations regardless to the primary site (Zheng et al. 2015). Interestingly, following the same argumentation as used by Pearse to propose a neural crest origin of APUD cells, an APUD and neural crest origin of small cell lung neuroendocrine carcinomas has been proposed (Tischler 1978; Yesner 1980). However, an epithelial origin of these cancers has now been provided (Yazawa 2015; Yoshimoto et al. 2018), suggesting that the neuroendocrine phenotype might arise during the oncogenesis and may reflect of specific oncogenetics alterations (Meder et al. 2016).

b. Morphology

According to the WHO definition (WHO 2018), microscopic examination of MCC reveals a proliferation of tumor cells harboring high-grade neuroendocrine carcinoma features (Figure 3). Tumor cells almost always massively infiltrate the dermis and/or subcutaneous tissues without any connection with the overlying epidermis. Connections with appendages might be observed (Walsh 2001). Tumor cells have intermediate size, although few cases of large cell neuroendocrine carcinoma of the skin cases have been reported (Nagase et al. 2016; Walsh 2001). Classical MCC tumor cells features include high nucleocytoplasmic ratio, scant cytoplasm, round nucleus with frequent nuclear molding and fine, granular so called “salt and pepper” chromatin. Mitotic figures and large areas of necrosis are frequent and reflect tumor aggressiveness. Trabecular, diffuse or solid architectures have been described without significant impact on prognosis (Pilotti et al. 1988) and it should be noted that such architectural patterns are frequently intermixed in tumor specimens. Interestingly, a trabecular pattern has been reported as specific of MCC among neuroendocrine carcinoma (Bandino et al. 2018). Unusual features are presence of ulceration (Nagase et al. 2019), intraepidermal involvement (Jour et al. 2017), association with epidermal tumors or presence of a divergent differentiation (Carter et al. 2018; Martin et al. 2013; Walsh 2001). Depending on MCC etiology, several variations in tumor morphology, which will be discussed later, have been reported (Iwasaki et al. 2013b; Kuwamoto et al. 2011a). Here, it is important to note that the current WHO MCC definition does not include etiology and accordingly, no recommendations regarding etiologic factor determination are currently available.

Since MCC belongs to the spectrum of small, round and blue cells proliferations, the main differential diagnosis included hematological malignancies (acute leukaemia and chronic lymphocytic leukaemia), sarcomas (primary neuroectodermal tumors, rhabdomyosarcoma, synoviosarcoma) and small cell variants of melanoma. MCC diagnosis has also to be considered in the context of basal cell carcinoma (Stanoszek et al. 2017). In current pathological practice, metastasis of another neuroendocrine carcinoma remains the most challenging differential diagnosis of MCC, underlining the need for a thorough immunohistochemical analysis.

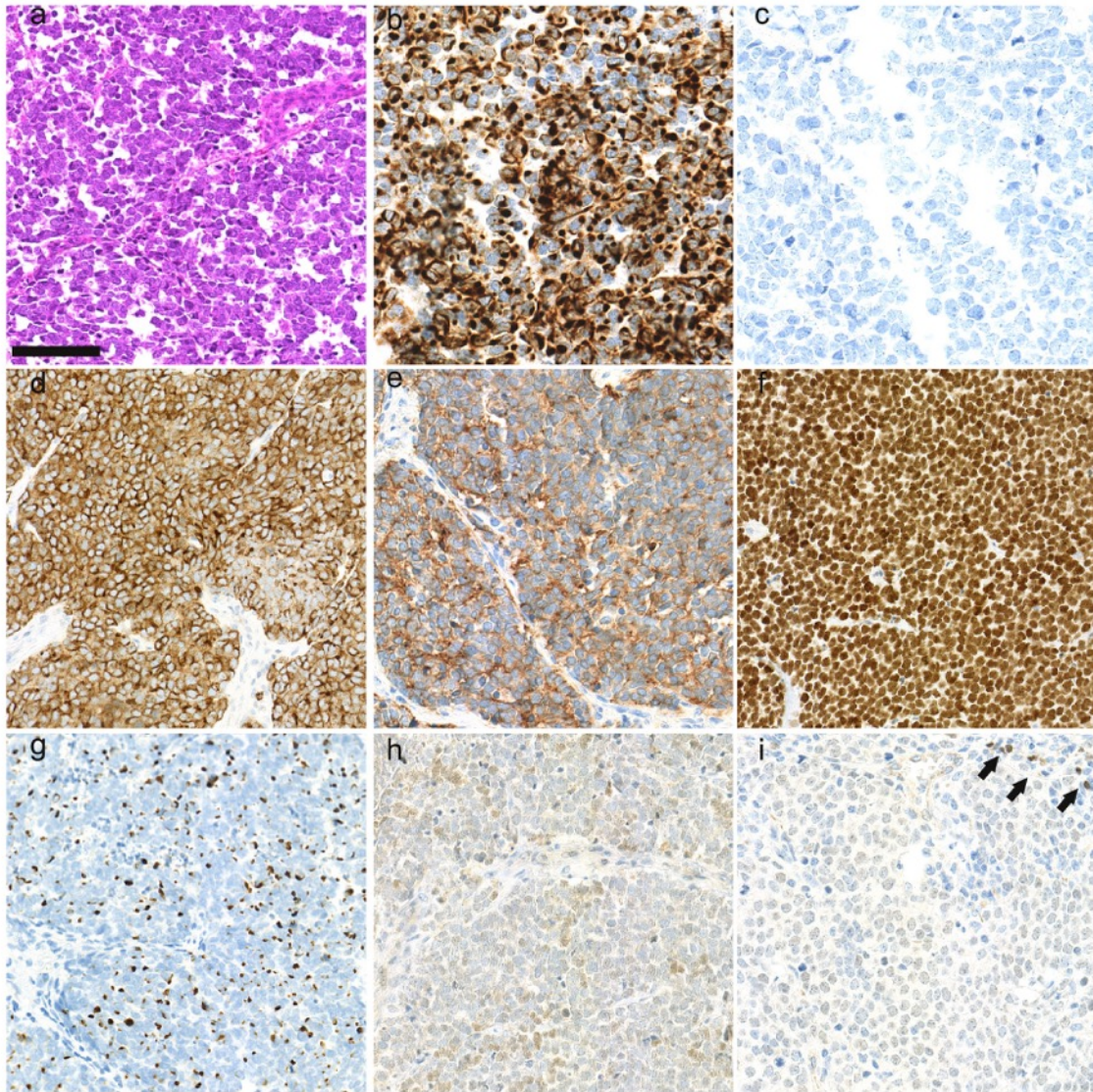


Figure 3. Morphological and immunohistochemical features of Merkel cell carcinoma. a: Microscopic observation of an MCC tissue section (hematein-phloxin-saffron staining) reveals a diffuse proliferation of tumor cells harboring scant cytoplasm, round nucleus and dusty chromatin. Immunohistochemical analysis (b-h) demonstrates: b: cytokeratin 20 expression with paranuclear dot-like pattern; c: thyroid transcription factor-1 negativity; d: chromogranin A cytoplasmic positivity; e: membranous CD56 expression; f: special AT-rich sequence-binding protein 2 (SATB2) nuclear expression; g: neurofilament expression with a dot-like pattern; h: terminal deoxynucleotidyl transferase weak/moderate expression; i: low paired box 5 weak expression in tumor cells in comparison to intratumoral lymphocytes (arrows). Adapted from Kervarrec et al 2018.

c. Immunohistochemical profile

Immunohistochemical investigations confirm the dual epithelial and neuroendocrine differentiation of MCC tumor cells (Figure 3) in accordance with the WHO classification definition (WHO 2018). Indeed, MCC tumors express epithelial markers notably pancytokeratins such AE1/AE3 and KL1 and display frequent positivity for EPCAM (García-Caballero et al. 2003; WHO 2018) whereas a panel of markers is used to confirm neuroendocrine differentiation including chromogranin A, synaptophysin, CD56 (Fernández-Figueras et al. 2007) and more recently INSM1 (Leblebici et al. 2019b; Lilo et al. 2018).

Since MCC belongs to the spectrum of the neuroendocrine carcinomas, several markers are available to distinguish MCC from extracutaneous neuroendocrine carcinomas (eNECs). Although, extension work-up by imaging contributes to distinguish cutaneous primary MCC from metastatic eNEC, MCC cases without skin primary remain a diagnosis challenge and immunohistochemistry is a crucial tool in such setting (Kotteas and Pavlidis 2015; Pan et al. 2014). Indeed, most MCC cases harbor cytokeratin 20 (KRT20) (Chan et al. 1997; Cheuk et al. 2001) with paranuclear dot-like pattern as well as Neurofilament (Schmidt et al. 1998; Stanoszek et al. 2019) and the recently described marker SATB2 (Bellizzi 2019; Fukuhara et al. 2016) whereas these markers are almost lacking in eNEC. A subset of MCC (5-10%) can express TTF-1 and/or KRT7 which are more frequently observed in eNEC cases (Calder et al. 2007; Pasternak et al. 2018; Reddi and Puri 2013). As for MCs (Halata et al. 2003; Moll et al. 2005), an expression of cytokeratin 8, 18 and 19 is also common in MCC but might also be observed in eNEC (Badzio et al. 2019). Although, more predominant in MCC, dot-like pattern expression of the cytokeratins is an hallmark of extracutaneous small cell neuroendocrine carcinomas (Badzio et al. 2019).

Of note, neuroendocrine differentiation might be observed in other epithelial skin tumors: i) exceptional cases of low-grade neuroendocrine tumors of the skin have been reported (Goto et al. 2017), ii) various degree of neuroendocrine marker expression is observed in endocrine mucin-producing sweat gland carcinoma (WHO 2018), iii) frequent expression of such markers are also detected in basal cell carcinoma (Houcine et al. 2017). However, no expression of KRT20, SATB2 or neurofilament is observed in these entities.

Moreover, MCC frequently expresses CD99 (55 to 100% of cases) and consequently should not be misdiagnosed as Ewing sarcoma (Domínguez-Malagón et al. 2016; Rajagopalan et al. 2013). Similarly, MCC frequently harbors a B cell phenotype with positivity of lymphoid markers (PAX5: 100%, TdT: 73%, immunoglobulin light and heavy chains: about 50% of cases) which should not lead to the diagnosis of leukemia (Zur Hausen et al. 2013).

5. Staging, treatment and survival

Disease extension is evaluated according the 8th edition of the AJCC stage as detailed below. At the time of diagnosis, MCC patients present with localized tumor, lymph node involvement or distant metastases in 66, 26 and 8 % of the cases (Harms et al. 2016) with a five-year overall survival estimated at 51, 35, and 14 %, respectively (Harms et al. 2016). Patients with nodal metastasis without detectable skin primary tumor, have been shown to experiment improved prognosis compared to those with a skin primary (estimated overall survival of 42 vs. 27 %) (Harms et al. 2016). Treatment of localized stages consists in complete excision surgery with 1-2 cm margins combined with sentinel lymph node procedure (Becker et al. 2019). Adjuvant radiotherapy of the primary tumor bed and the lymph node area should be considered on an individual basis (Becker et al. 2019; Tseng et al. 2017). Until recently, advanced metastatic MCC cases (unresectable stage III or stage IV disease) received platinum salts based chemotherapy without evidence of benefit on survival (Becker et al. 2017; Nghiem et al. 2017). Although, response rates up to 50% were observed in first line setting with such chemotherapy, patients experimented short term recurrences (median response duration: 3 months) and important toxicities (Nghiem et al. 2017; Samimi 2019). The unmet need for innovating therapies in advanced stages led to several single-arm trials investigating immune checkpoint inhibitors (CPI), either blocking PD-1 (pembrolizumab and nivolumab) or PD-L1 (avelumab). Such immunotherapies allow responses in 50% of metastatic, chemo-naïve MCC patients (first-line setting) and 30% of chemoresistant MCC patients (second-line setting). Importantly, these responses are durable overtime (75% at one year) (D'Angelo et al. 2018; Kaufman et al. 2018a; Kaufman et al. 2018b; Kaufman et al. 2016; Nghiem et al. 2019; Nghiem et al. 2016). Although not assessed in randomized studies in comparison with chemotherapy, rates and durability of responses with CPIs were meaningful enough to allow authorities and experts to consider such strategies as a standard of care in metastatic MCC. Avelumab is approved since 2017 in USA and Europe for treating patients with advanced MCC and

pembrolizumab was approved by the US FDA in December 2018 in the same setting. The 2018 US NCCN and 2019 S2K German guidelines currently recommend Check-point inhibitors in a first line setting for all patients with advanced MCC (Becker et al. 2019b; Bichakjian et al. 2018).

Table: Staging of Merkel cell carcinoma according to the 8th edition of the AJCC stage (Harms et al. 2016)

Site	Stage	Criteria
Primary tumor (pT)	pTX	primary tumor cannot be assessed
	pT0	no evidence of primary tumor
	pTis	in situ primary tumor
	pT1	maximum clinical tumor diameter ≤ 2 cm
	pT2	maximum clinical tumor diameter > 2 cm but ≤ 5 cm
	pT3	maximum clinical tumor diameter > 5 cm
	pT4	primary tumor invades fascia, muscle, cartilage or bone
Regional lymph nodes (pN)	pNX	cannot be assessed
	pN0:	no regional metastasis detected
	pN1a	microscopic lymph node metastasis clinically occult
	pN1b	microscopic confirmation of clinically detected regional lymph node metastasis
	pN2	in transit metastasis without lymph node metastasis
pN3	in transit metastasis with lymph node metastases	
Distant metastasis (pM)	pM0	no evidence of distant metastasis by clinical or radiological examination
	pM1a	microscopic confirmation of metastases to skin, distant subcutaneous tissue or distant lymph nodes
	pM1b	microscopic confirmation of metastases to lung
	pM1c:	microscopic confirmation of metastases to all other distant sites

AJCC pathological prognostic stage groups (pTNM)

Stage group 0:	Tis	N0	M0
Stage group I:	T1	N0	M0
Stage group IIA:	T2 - T3	N0	M0
Stage group IIB:	T4	N0	M0
Stage group IIIA:	T1 - T4	N1a(sn) or N1a	M0
	T0	N1b	M0
Stage group IIIB:	T1 - T4	N1b - N3	M0
Stage group IV:	T0 - 4	N0 - N3	M1

II. MCC Etiologic factors

1. Merkel cell polyomavirus

a. Merkel cell polyomavirus identification

Genetic alterations driving MCC oncogenesis remained, for a long time, unknown (Houben et al. 2009; Kanitakis 2008). Indeed although alterations in the PDGF-R gene have been described, it was unclear at that time if these changes would represent only single nucleotide variants or real mutations (Swick et al. 2008). In addition, while high expression levels of KIT have been observed in tumors, no activating mutations of *KIT* were detected in the investigated MCC samples (Su et al. 2002; Swick et al. 2013; Swick et al. 2007). Similarly, lack of MAP kinase pathway activation had been described in MCC tumor cells (Houben et al. 2006). MCC karyotype investigation revealed frequent loss of chromosome 10 long arm, which harbor the tumor suppressor gene *PTEN*. However, the authors were not sure about a crucial involvement of *PTEN* inactivation in MCC development (Van Gele et al. 2001).

Based on increased MCC incidence in the immunocompromised individuals, an infectious etiology of MCC was further suggested (Kanitakis 2008). However, no involvement of Human papillomaviruses or EBV in MCC development were evidenced (Kanitakis et al. 2006; Shaw et al. 2006).

The discovery of Merkel cell polyoma virus integrated in the genome of MCC tumor cells in 2008, then received a lot of attention because it was not only the starting point for understanding MCC carcinogenesis but also the first identification of a polyomavirus-induced cancer in humans (Feng et al. 2008). The research group, that had already identified the contribution of the Human Herpes virus 8 (HHV8) to Kaposi disease, developed a new method called digital transcriptome subtraction (DTS), in order to identify foreign non-human transcripts in MCC. Comparing MCC tumor cDNA with human sequences databases, they identified non-human transcripts harboring high homology levels with known polyomavirus sequences. The sequence of this new polyomavirus, therefore called Merkel cell polyomavirus (MCPyV), was further detected in 80% of the tested MCC cases (n=8/10) and was in addition shown to be integrated into the tumor cell genome.

b. Polyomavirus overview

From an historical view, discovery of the polyomaviruses widely contributed to our understanding of tumor biology (Gross 1953; Morgan 2014). Indeed, in 1953, Gross et al. demonstrated for the first time that injection of a viral agent, the murine Polyomavirus (MuPyV), promoted tumor development in salivary glands and in other solid tissues in mice (Gross 1953; Morgan 2014). Accordingly, Stewart and Eddy proposed to call this new virus « poly » « oma » due to their ability to induce multi-organs tumors *in vivo* (Stewart et al. 1958). Further researches on MuPyV especially allowed the identification of the Phosphoinositide 3-kinase (PI3K) pathway (Kaplan et al. 1987; Shuda et al. 2011). A further important step was the isolation of the simian virus SV40 from a monkey kidney cell lines (Atkin et al. 2009; Sweet and Hilleman 1960). Its ability to transform human cell lines and to induce cancer in hamsters, led to the identification of the *TP53* gene (Tan et al. 1986), again underlining the crucial impact of polyomavirus research on our cancer understanding on the molecular basis of cancer. Of note, SV40 involvement in human cancer development is still a controversial issue, since approximately 100 millions people received a SV40 contaminated poliovirus vaccine between 1955 and 1963 in the USA (Poulin and DeCaprio 2006). Although, clear oncogenic abilities of the virus were demonstrated *in vitro*, evidences of association with cancer or of any oncogenic properties have not been provided in human (Poulin and DeCaprio 2006).

In 1971, the two first human Polyomaviruses, BK and JC were respectively identified in urine and brain of patients with kidney transplant and progressive multifocal encephalopathy (PML) respectively (Gardner et al. 1971; Padgett et al. 1971). Additional investigations revealed widespread latent infections of the healthy population by these viruses (Kardas et al. 2015) and that their reactivation upon immunosuppression can result in either BK-induced nephropathy or JC related-PML. Although debated for a long time, recent advances suggest that BK virus might be oncogenic in kidney-transplant patients by contributing to the oncogenesis of urothelial carcinoma (Müller et al. 2018; Papadimitriou et al. 2016; Sirohi et al. 2018).

While polyomaviruses and papillomaviruses were initially considered to belong to the same family (referred as Papoviridae), the international Committee on Taxonomy of Virus recognized them as two distinct families in 1999 (International Committee on Taxonomy of

Viruses et al. 2000). The Polyomavirus family was then divided in 4 genera with alpha-polyomaviruses including MCPyV whereas BK and JC belong to the beta-polyomaviruses (Moens et al. 2017). HPyV 6 and 7 are members of delta-polyomaviruses whereas gamma-polyomaviruses are observed in birds (Moens et al. 2017).

Up to now, about 100 different polyomaviruses have been identified in several species including mammals, reptiles, birds, fishes and invertebrates (Buck et al. 2016). Although some of them induce severe, acute, sometimes lethal diseases like for bird polyomaviruses, pathogenicity of the others is widely unknown. Of note, oncogenic abilities in the natural host were only demonstrated in four of them (MuPyV, MCPyV, Hamster Polyomavirus (HaPv) and Raccoon Polyomavirus (RaPv) (Dela Cruz et al. 2013).

In humans, 13 polyomaviruses have been identified (genomic sizes: 4776-5387 pb) and while a 14th one called Lyon IARC HPyV has been reported, its natural host(s), humans or cats, still needs to be clarified (Fahsbender et al. 2019; Gheit et al. 2017). Most of the human polyomaviruses have been detected in pathologic conditions as shown below, however the causal pathogenic properties remain to be demonstrated for most of them. *Trichodysplasia spinulosa* associated Polyomavirus (TSPyV) is involved in the eponym disease characterized by follicular papules of the face associated with skin thickening and alopecia occurring in immunocompromised young people (van der Meijden et al. 2010; Rouanet et al. 2016; Sheu et al. 2019). HPyV6 and 7 were identified by rolling circle amplification from healthy skin swabs and both viruses seem to be involved in pruritic and dyskeratotic dermatoses with characteristic “peacock plumage” histology observed in immunocompromised people especially bone marrow transplant patients (Ho et al. 2015; Nguyen et al. 2017; Schowalter et al. 2010). Further involvement of HPyV6 in epithelial proliferations arising in patients treated with BRAF inhibitors and in keratoacanthoma were reported (Beckervordersandforth et al. 2016; Schrama et al. 2014; Sheu et al. 2019).

To conclude, infection during childhood followed by latent infectious state in a majority of healthy individuals, and reactivation upon host immunosuppression with potential acquisition of pathogenic properties appear as common features of human polyomaviruses.

Table : Identified Human Polyomaviruses and potential related diseases, adapted from (Moens et al. 2017b)

Virus	Genome (bp)	Associated-Disease
HPyV1 (BKPyV)	5153	BK-associated nephropathy (Hirsch 2005)
		haemorrhagic cystitis (Erard et al. 2004)
		ureteral stenosis (Coleman et al. 1978)
		progressive multifocal leukoencephalopathy (Reploeg et al. 2001)
		meningitis and encephalitis (Chittick et al. 2013)
		Retinitis (Reploeg et al. 2001)
		Pneumonitis (Akazawa et al. 2012)
		prostate cancer (Delbue et al. 2014)
		HIV-associated salivary gland disease (Jeffers and Webster-Cyriaque 2011)
		renal carcinoma (Kenan et al. 2017)
HPyV2 (JCPyV)	5130	progressive multifocal leukoencephalopathy (Calabrese et al. 2015)
		multiple sclerosis (Brew et al. 2010)
		colon cancer (Niv et al. 2005)
HPyV3 (KIPyV)	5040	respiratory disease (Dehority et al. 2017)
HPyV4 (WUPyV)	5229	respiratory disease (Toptan et al. 2016)
HPyV5 (MCPyV)	5387	Merkel cell carcinoma (Feng et al. 2008a)
HPyV6	4926	Keratoacanthoma (Beckervordersandforth et al. 2016)
		Kimura disease (Rascovan et al. 2016)
		pruritic and dyskeratotic dermatosis (Nguyen et al. 2017)
HPyV7	4952	Thymoma (Rennspiess et al. 2015)
		pruritic and dyskeratotic dermatosis (Ho et al. 2015; Nguyen et al. 2017)
HPyV8 (TSPyV)	5232	<i>Trichodysplasia spinulosa</i> (van der Meijden et al. 2010)
HPyV9	5026	Unknown
HPyV10 (MWPyV)	4927	Unknown
HPyV11 (STLPyV)	4776	Unknown
HPyV12	5033	Unknown
HPyV13 (NJPyV)	5108	Vasculitis (Mishra et al. 2014)

c. Polyomaviruses structure

Polyomaviruses are naked viruses with a double stranded DNA genome consisting in about 5000 bp (MCPyV= 5387bp) (Figure 4). Such viruses harbor a conserved genomic organization with an early region encoding the “Tumor” T Antigens (TAg), expressed during the early steps of the viral cycle, and a late region containing the structural capsid proteins sequences, expressed after the replication. A bidirectional non coding control region (NCCR) including the replication origin (ori), promoters and enhancer elements is located between early and late regions. From the early region one single pre-mRNA is transcribed giving rise to 2 to 5 proteins by alternative splicing as well as occasional use of an alternative reading frame (e.g. ALTO). Universally a small (sT) and a Large T (LT) are encoded by all polyomaviruses, while further proteins like Middle T of MuPyV or 57kT and ALTO of MCPyV are specific to certain members of the family (Figure 5). Structures of sT and LT are highly conserved among polyomaviruses (Pipas 1992) since such proteins are crucial for viral life cycle and are involved in viral replication, regulation of the early and late genes transcription and viral assembly (Kwun et al. 2009). As described for other polyomaviruses, MCPyV sT binds to PP2A whereas wild type Large T sequesters pRB and p53 thus hijacking the cell cycle. Moreover, LT harbors an origin binding domain and a core Helicase/ATPase which are both necessary for viral replication (Houben et al. 2015; Shuda et al. 2011; Wendzicki et al. 2015). Functional domains and oncogenic properties of the oncoproteins will be described in detail below.

Polyomavirus virion size is about 40-50 nm and the capsid consists in 72 capsomeres harboring icosahedral T=7 symmetry (Figure 6). Each capsomere includes 5 major capsid proteins (VP1=40-50 kDa) with C-term residues interacting with the neighboring pentamer and N-term part connected to the viral genome (Ben-nun-Shaul et al. 2009). A single copy of the VP2 protein (=39 kDa) is present at the center of the capsomere (Schowalter and Buck 2013). VP3 is expected not to be expressed in MCPyV (Schowalter and Buck 2013).

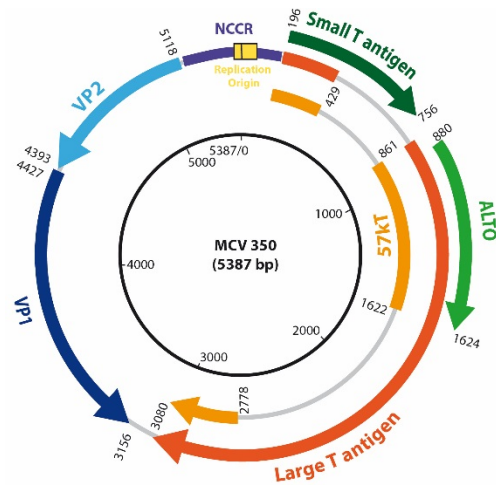


Figure 4. Merkel cell polyomavirus genomic organization. Polyomaviruses harbor double stranded DNA genome consisting of about 5000 bp (MCPyV= 5387bp). The early region encodes the T Antigens comprising small (sT), medium (57kT/ALTO) and Large T (LT) which are obtained by alternative splicings, while the late region contains the capsid protein sequences. A bidirectional non coding control region (NCCR) including the replication origin (ori), promoter and enhancer elements is located between early and late regions (Figure kindly provided by Dr Schrama and Dr Houben).

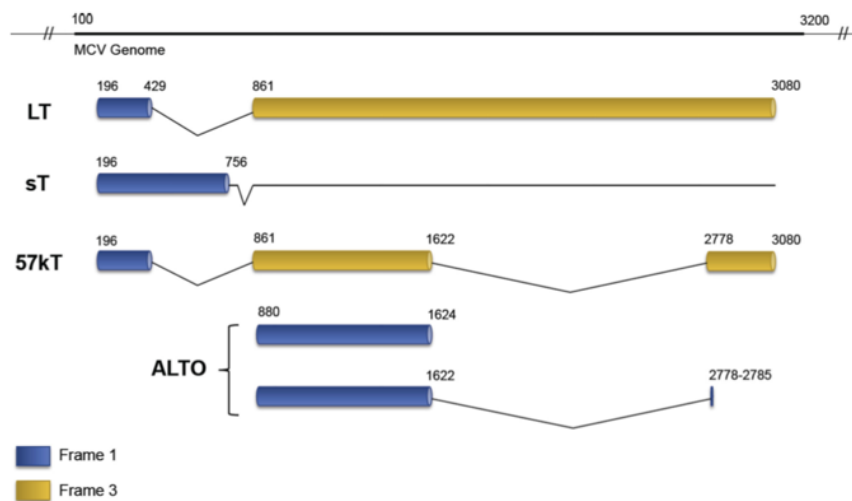


Figure 5. MCPyV T antigens structures. T Antigens are produced by alternative splicing. The N-terminal part of the first exon encodes the initial 78 aminoacids shared by sT and LT. ALTO is expected to be the product of an alternative open reading frame however it is unclear whether ALTO is expressed in MCC tumors (adapted from Wendzicki 2015).

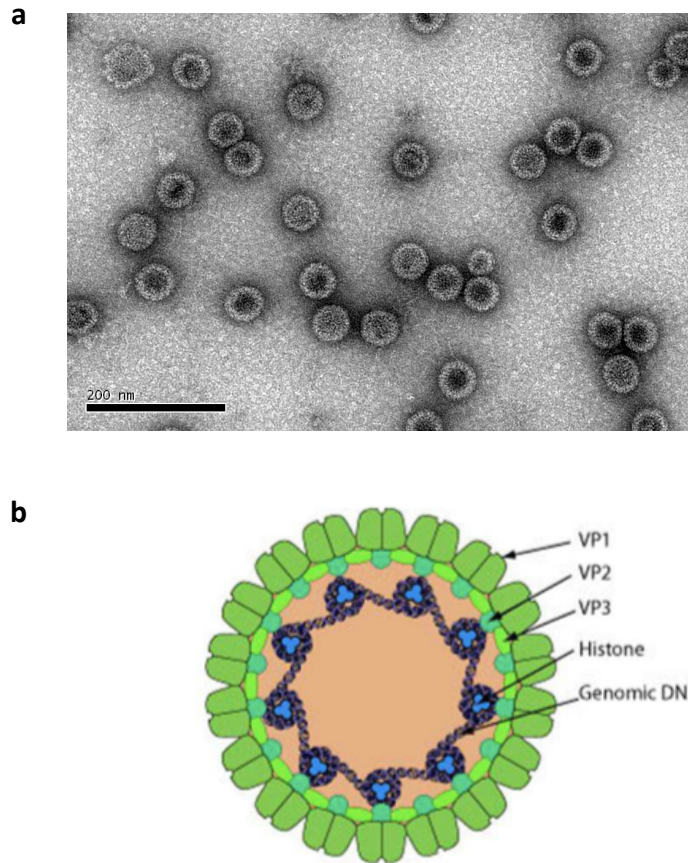


Figure 6. Polyomavirus viral particle structure. a. Ultrastructural features of MCPyV pseudo-particles (kindly provided by Pr. Antoine Touzé); b. Graphic representation of the SV40 infectious particle. Association of major (VP1) and minor (VP2-VP3) capsid proteins leads to the viral particle assembly containing DNA genome associated cellular histones (adapted from Swiss Institute of Bioinformatic, <http://expasy.org>).

d. MCPyV life-cycle

As for other human polyomaviruses, asymptomatic primary MCPyV infection arises in childhood with a seroprevalence reaching more than 75% in healthy adults. (Martel-Jantin et al. 2013; Nicol et al. 2013; Pastrana et al. 2009; Tolstov et al. 2011; Tolstov et al. 2009; Touzé et al. 2010). Respiratory and/or cutaneous transmission routes have been proposed (Cason et al. 2018; Foulongne et al. 2010; Iaria et al. 2015; Shikova et al. 2017). Indeed, frequent detection of MCPyV genome in skin swabs of healthy donors (Schowalter et al. 2010; Wieland et al. 2009) and further detection in the environment (Foulongne et al. 2010) indicate the skin as a main infection site, although MCPyV has been detected in a wide range of other tissues (Goh et al. 2009; Kantola et al. 2009; Mancuso et al. 2017; Mertz et al. 2010). In the skin, dermal fibroblasts have been proposed as MCPyV natural cellular host (Liu et al. 2016), a conclusion suggested by their ability to support the complete viral cycle *in vitro*, while the ability of MCPyV to enter in a wide range type of cell types was also shown (Liu et al. 2016).

MCPyV viral entry process involves initial interactions of the VP1 with glycosaminoglycans such as heparan sulfates and/or chondroitin sulfates. Sialic acid (Neu5Ac) seems to be secondarily required for MCPyV attachment to the target cell (Neu et al. 2012; Schowalter et al. 2011). Minor capsid protein, VP2, might play a role in post-attachment steps (Schowalter and Buck 2013). MCPyV entry is dependent on caveolar/lipid raft-mediated endocytosis (Becker et al. 2019). Following the decapsidation step in the endosomal compartment, the binding of the host cell RNA polymerase II to the NCCR results in the transcription of a single precursor mRNA which will generate several early antigens by alternative splicing. LT is expected to be the first viral protein expressed followed by 57kT, and sT (Feng et al. 2011). The alternative protein named "Alternate frame of the LT Open reading frame" (ALTO) as result of an overprinting open reading frame might also be expressed (Carter et al. 2013). As for other polyomaviruses, transfer of the oncoproteins to nucleus due to the nuclear localization signal (NLS) sequence of the LT is followed by recognition by LT of the origin replication sequence consisting of repeated G(A/G)GGC pentamers (Harrison et al. 2011; Kwun et al. 2009). Subsequent steps are likely to be similar to what was described for SV40 with LT assembly into double hexameric structures, recruitment of DNA binding proteins and topoisomerase I (Fanning and Zhao 2009) and finally initiation of the replication. Contribution

of sT to the MCPyV replication as a coeffector, in a LT stabilization-independent manner, has been proposed (Feng et al. 2011) and binding of iron /sulfur clusters to sT cysteins are required for this function (Tsang et al. 2016). LT phosphorylation status (Diaz et al. 2014), and cellular components such as bromodomain containing 4 protein (BRD4) (Wang et al. 2012) and DNA damage repair system (Tsang et al. 2014) are involved in the regulation of MCPyV replication. Replication initiation is associated with the downregulation of early genes expression and transcription of the two capsids proteins VP1 and VP2. VP3 capsid protein might be generated from an alternative start codon in VP2 sequence but was not yet detected in experimental models (Schowalter and Buck 2013). VP1 protein also harbors a Nuclear localization signal (NLS) sequence allowing its targeting to the nucleus. Whereas NLS were identified on VP2/3 proteins in others PyV, such sequences were not predicted for MCPyV, suggesting that the transfer to the nucleus is passive and due to interaction with VP1. In the nucleus, viral particle self assembles around the viral genome associated with cellular histones (Schowalter and Buck 2013). Cell lysis is then expected in order to release virions during productive infection which therefore results in cell death rather than transformation.

After primary infection, MCPyV is expected to persist in a latent phase in most of healthy individuals (Krump et al. 2018) as attested by high MCPyV seroprevalence (Martel-Jantin et al. 2014; Martel-Jantin et al. 2013; Nicol et al. 2013; Tolstov et al. 2011). By contrast to the productive cycle, such latency is characterized lack of infectious particles production and replication of the viral genome in such setting might therefore be mainly dependent of cell host division. Ubiquitination and subsequent degradation of phosphorylated LT by the cellular E3 ubiquitin ligases Fbw7, β TrCP, and Skp2 Skp-F-box-cullin (SCF) (Kwun et al. 2017) as well as miR expression (Seo et al. 2009) have been identified as crucial regulators in the latent phase. Alternatively, combination of low viral load production and establishment of viral immune escape mechanisms might allow MCPyV persistence (Krump et al. 2018).

As described for other polyomaviruses (Krump et al. 2018), MCPyV reactivation upon immunosuppression appears as a required step for MCPyV pathogenicity, i.e. resulting in genomic integration and subsequent cell transformation (Wiedinger et al. 2014). Although, molecular determinants of this step are poorly understood, sT expression induction by UV

radiation (Mogha et al. 2010) might explain why MCPyV-positive MCC arise mostly in sun exposed area while no UV signature is detected in tumor cells (Sunshine et al. 2018).

e. MCPyV: an oncogenic agent

i. MCPyV in MCC tumors

Two hallmarks distinguish MCC-associated MCPyV genome from wild-type viral genome detected in healthy tissue or in the environment. First, MCPyV genome is always found to be integrated in the genome of the MCC tumor cells (Feng et al. 2008) and second, mutations or deletions in the LT antigen coding sequence resulting in the expression of a truncated LT are always present (Shuda et al. 2008). Although the molecular determinants and mechanisms leading to these two key features are largely unknown, genomic integration of the MCPyV might result from the genome fragmentation occurring during the viral replication step (Harms et al. 2018; Kwun et al. 2009). No preferential site of integration or hotspot have been detected neither in the human nor the viral genome, and consequently disruption of cellular genes (either inactivation of tumor suppressor or activation of oncogenes) is unlikely to represent a main oncogenic mechanism in MCC (Sastre-Garau et al. 2009).

Evidence of a clonal integration pattern in MCPyV-positive tumor cells as well as presence of the conserved integration points in primary tumor and related metastases strongly suggest that viral integration occurs prior to clonal expansion (Houben et al. 2015; Laude et al. 2010; Shuda et al. 2008). In MCC tumors, clonal integration is always associated with mutation or deletion of the viral sequences, which are likely to occur prior or during viral integration, a notion supported by cases with concatemer integration (Schrama et al. 2019). Of note, since both MCPyV genome mutation and integration are required for MCC development, the low probability of both events happening in combination might explain the low incidence of MCC (Harms et al. 2018).

Although T antigen mutations are different for each MCC tumor case, they always result in the expression of a truncated LT harboring an intact pRb1 binding site but lacking the C-terminal part including p53 binding site, ori, ATPase/helicase domain (Hesbacher et al. 2016; Shuda et al. 2008). Accordingly, no viral replication (Kwun et al. 2009) and no expression of the late proteins are observed in MCC tumor cells (Shuda et al. 2008; Touzé et al. 2011).

Interestingly, ectopic expression of wild type LT *in vitro* results in p53 pathway and DNA damage repair activation, leading to cell death (Li et al. 2013). Moreover, growth inhibitory activities of the C-terminal part of the LT, which is lacking in MCC tumors, have been demonstrated (Cheng et al. 2013). Therefore, the constant detection of a mutated LT in MCC tumor cells is likely to be due to selection pressure. In addition to the impairment of viral replication and capsid proteins expression, truncation of the LT additionally results in overexpression of both sT and truncated LT (Borchert et al. 2014; Kwun et al. 2009; Rodig et al. 2012; Shuda et al. 2008). Accordingly, the clear expression of these two viral proteins in MCPyV-positive tumors (Houben et al. 2015; Shuda et al. 2011) suggest these two factors as potential actors of MCPyV-positive MCC oncogenesis.

ii. Oncogenic properties of the TAG

Several observations suggest a causative role of TAGs in MCC development: the detection of MCPyV integration in 80% of MCC cases together with constant mutation of the LT sequence; evidence of TAGs overexpression in MCC tumors; similarities between MCPyV and others oncogenic polyomaviruses (such as MPyV and SV40). In addition, two independent experimental demonstrations of TAGs oncogenic properties were provided. First, knock-down of the T-antigens in MCC tumor cells results in cell cycle arrest and death *in vitro* and in xenograft mice model (Houben et al. 2012; Houben et al. 2010). Second, ectopic overexpression of both TAGs in the epidermis of transgenic mice induces epithelial transformation (Spurgeon et al. 2015).

Oncogenic functions of sT were further supported by its ability to induce cell transformation in fibroblasts *in vitro* (Shuda et al. 2011). Ectopic expression of sT alone leads to the development of anaplastic tumors in transgenic mice (Shuda et al. 2015) while combined expression of sT with Atonal homolog-1, the main transcription factor driving MC differentiation, induces formation of MCC-like tumor aggregates in mice epidermis (Verhaegen et al. 2017a). Although controversial (Shuda et al. 2014), sT expression does not seem to be required for tumor growth in MCC cell lines, as shown by sT knock-down experiments, or ectopic reintroduction of sT expression after TAGs knock-down (Angermeyer et al. 2013). By contrast, LT expression is crucial in this setting and ectopic re-expression of LT in TAGs knock-down cells resulted in complete rescue of tumor cells growth. Therefore, the

TAgS are now recognized as the two main oncogenic triggers of MCPyV-positive MCC. Whereas sT harbors transforming abilities, LT expression is required for tumor growth maintenance (Angermeyer et al. 2013; Harms et al. 2018a; Shuda et al. 2015).

iii. TAg structures and related oncogenic functions

Both sT and LT structures are provided in Figure 7. While the 78 N-terminus amino-acids are common to the two proteins, the remaining C-terminal parts are obtained by alternative splicing.

The common part the TAgS is composed of a J domain and the Psycho motif including a YGT sequence. Similarly to the DnaJ chaperone protein from *E. coli* (Kelley and Georgopoulos 1997), the MCPyV DnaJ sequence including the conserved region CR1 (LXXLL) and the Hsc70 binding sequence (HPDKGG), binds to the ATPase domain of the heat shock protein 70 (Hsc70), subsequently inducing activation of this protein (Adam et al. 2014; Wendzicki et al. 2015). Interestingly, the DnaJ domain was demonstrated to be necessary for both virus replication and MCPyV-positive MCC tumor growth *in vitro* (Houben et al. 2015; Kwun et al. 2009) as confirmed by the reduction of tumor growth upon pharmacological HSP70 inhibition in a MCC mouse model (Adam et al. 2014). Conservation of the DnaJ sequence was further identified as necessary for pRB sequestration by LT (Houben et al. 2015). The YGT sequence and Psycho motif are dispensable for MCC tumor cell proliferation (Houben et al. 2015) but are thought to modulate folding of DnaJ and pRB binding sites respectively (Johnson 2010; Kim et al. 2001).

In addition to the common part, sT harbors a LT stabilization domain (LSD) (Shuda et al. 2011), as well as PP4C (Abdul-Sada et al. 2017) and PP2A (Shuda et al. 2011) binding sites (Wendzicki et al. 2015). While other polyomaviruses such as SV40 affect cell cycle via sT-PP2A interaction therefore impacting on the *AKT-mTor* pathway (Gjoerup and Chang 2010), this function is dispensable for MCPyV sT transforming abilities (Shuda et al. 2011; Verhaegen et al. 2017) accompanied by only a restricted ability of MCPyV sT to inhibit PP2A B subunit assembly (Kwun et al. 2015). Transforming potential of sT is indeed related to the LSD domain which prevents degradation of other oncogenic proteins including LT (Kwun et al. 2013). Although Kwun et al.

reported this stabilization as a consequence of Fbw7 E3-ubiquitin ligase inhibition, this interaction could not be confirmed by others (Dye et al. 2019). The LSD also promotes cap-dependent translation via the eukaryotic translation initiation factor 4E-binding protein 1 (4E-BP1) (Shuda et al. 2011).

Moreover, sT binding to L-MYC allows the recruitment of the EP400 histone acetyltransferase and chromatin remodeling complex, and L-MYC and EP400 have been shown as essential to maintain tumor cell viability (Cheng et al. 2017). Together, the sT-L-MYC-EP400 complex transactivates specific target genes such as MDM2 and casein kinase 1, a serine-threonine kinase targeting MDM4. Subsequent overexpression or activation of MDM2 and MDM4 lead to the ubiquitination of p53 and inhibition of p53 functions (Park et al. 2019).

sT additionally alters metabolism pathways by increasing aerobic glycolysis and, in line with these findings, inhibition of the monocarboxylate lactate transporter MCT1 leads to the loss of the transforming abilities of sT (Berrios et al. 2016). Furthermore, interaction of sT with PP4C is expected to inhibit the NF- κ B pathway and cause cytoskeleton disruption therefore improving mobility and invasiveness of tumor cells (Abdul-Sada et al. 2017; Griffiths et al. 2013; Knight et al. 2015).

In addition to the common part harboring the Hsc70 binding site, the LT sequence includes a Merkel unique region (MUR) 1, the Vamp6 binding domain and the Rb binding site followed by the MUR2, the nuclear location signal, the origin of replication binding site and ATPase/helicase domain (Wendzicki et al. 2015). MUR1 and MUR2 regions are specific for MCPyV and were not observed in the polyomaviruses discovered prior to MCPyV identification (Gjoerup and Chang 2010; Johnson 2010). Although, they are not essential for tumor cell growth *in vitro*, both might slightly contribute to tumor growth promotion by LT (Houben et al. 2015). In addition, MUR1 contributes to maintaining high LT expression in MCC cell lines (Houben et al. 2015). The Vamp6 binding domain is included in the MUR1 region and induces relocation and sequestration of this lysosomal protein into the nucleus (Liu et al. 2011). Mutation of the Vamp6 binding domain leads to increased genome replication *in vitro* (Feng et al. 2011).

Truncated LT promotes tumor growth by sequestering pRB via the LxCxE motif (Houben et al. 2012). Indeed among the pocket proteins, the MCPyV LT exhibits a specific affinity for pRB

(Giacinti and Giordano 2006; Hesbacher et al. 2016) and subsequent sequestration of such protein induces the release of E2F family transcription factors thereby promoting G1/S transition and tumor growth (Chen et al. 2009; Hesbacher et al. 2016). Indeed, several lines of evidence clearly demonstrate the crucial role of pRB sequestration in MCC tumor promotion. First TAGs knock-down can be totally rescued by *RB1* knock-down (Hesbacher et al. 2016). Second, MCC cell lines with deletion of *RB1* gene are insensitive to TAGs knock-down (Hesbacher et al. 2016). Finally, ectopic expression of a LT construct with mutated pRB binding site fails to rescue MCC cell lines after TAGs knock-down (Houben et al. 2015). Of note, phosphorylation of serine 220 was demonstrated as crucial for LT-pRB interaction and accordingly mutation of this serine into alanine results in tumor cell growth arrest (Schrama et al. 2016).

The MUR2 region including the NLS (RK RK) in position 277– 280 is located after the pRB binding site in the LT sequence. Nakamura et al. firstly reported high conservation of the NLS motif (Nakamura et al. 2010), however this sequence is actually lacking in several tumors and cell lines and a mixed nuclear and cytoplasmic location of LT is observed in such cases (Houben et al. 2015). Indeed, premature stop codon leading to the LT truncation frequently occurs in MUR2 region resulting in loss of the p53 and ATPase/helicase domains. Besides loss of viral replication and lack of the late region transcription (Shuda et al. 2008), several other changes are induced by the truncation resulting in enhanced LT oncogenicity compared to the wild type form. Indeed, truncated LT is expressed at higher levels and harbor higher affinity for pRB than full length LT (Borchert et al. 2014). Furthermore, truncated LT yields similar or higher potential than the full length protein to transform the cells when associated with sT (Borchert et al. 2014), and accordingly is more efficient than full length LT in promoting fibroblast growth in culture (Cheng et al. 2013). In contrast to other polyomaviruses which are able to sequester p53 (Gjoerup and Chang 2010), no direct binding of wild type MCPyV LT to p53 was observed although an inhibitory effect of wild type LT expression on p53 targeted genes was confirmed (Borchert et al. 2014). By contrast, truncated LT lacking the p53 binding site had no inhibitory effect (Houben et al. 2013) or even induce p53 activation (Borchert et al. 2014). This findings might be detrimental for tumor development, although they are counterbalanced by p53 inhibitory properties of sT (Park et al. 2019).

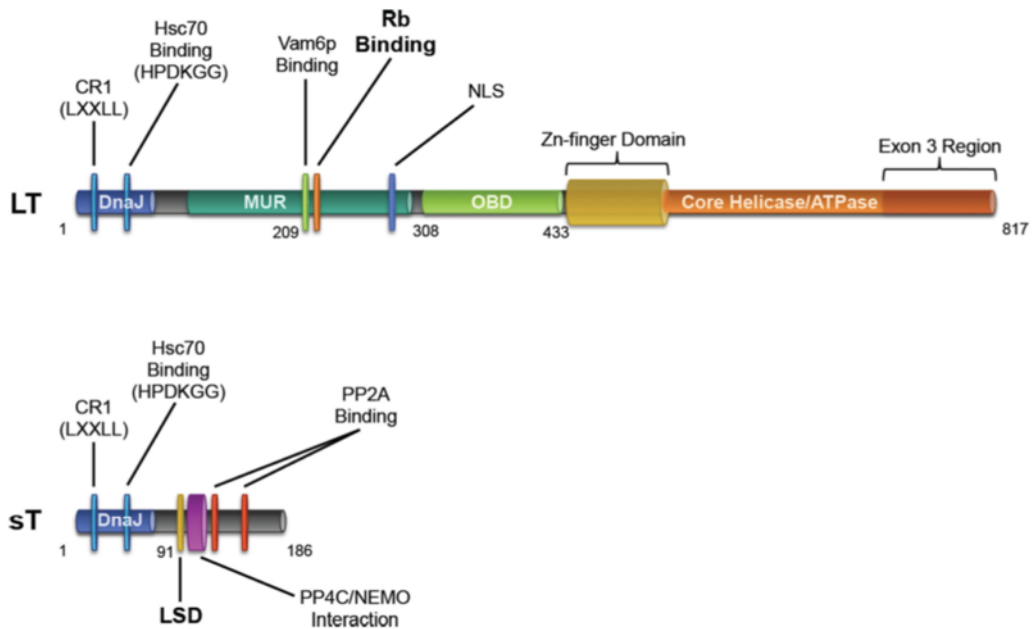


Figure 7. Functional domains of Merkel cell polyomavirus small T and Large T. The first N terminal 78 amino acids are common to the two T antigens and contain the Heat shock protein binding site. The sT protein also harbors a Large T stabilisation domain (LSD) as well as PP2A and PP4C binding sites. Wild Type large T protein contains Vam6p, RB1 binding sites associated with a helicase and ATPase domain required for viral replication. MUR (Merkel unique regions) 1 and 2 are not observed in most other polyomaviruses (adapted from Wendzicki 2015).

iv. MCPyV detection in medical practice

Regarding the specific association between MCPyV and MCC, the detection of MCPyV may be a useful diagnostic tool in difficult to diagnose MCCs cases (unusual phenotype, absence of primary skin tumour, metastasis revealing the disease). However, low loads of the episomal virus are present in the skin of healthy subjects (Foulongne et al. 2010) and can also be detected in non-MCC tumors (Bellott et al. 2017; Hillen et al. 2017; Kassem et al. 2010; Mertz et al. 2013; Ota et al. 2012; Scola et al. 2012). In this context, diagnosis procedures based on MCPyV detection should discriminate MCC-associated MCPyV from the episomal virus. For this purpose, two commercial antibodies allowing the recognition of T antigen expression are now available (CM2B4 and 2T2 clones). The use of semi-quantitative score according the Allred's method has been proposed for the interpretation of the CM2B4 staining (Figure 8) (Moshiri et al. 2017) and a positivity rate of 60% is reported in MCC tumors using this protocol. Of note, some immune cells, especially lymphocytes, can be positive using this technique. In addition, various molecular methods have been proposed to demonstrate virus integration (PCR, real-time PCR, Detection of integrated polyomavirus sequences-PCR (DIPS), next generation sequencing, Fluorescence in situ Hybridation (FISH) (Duncavage et al. 2011; Eid et al. 2017; Haugg et al. 2014; Iwasaki et al. 2013c; Sastre-Garau et al. 2009)) while most of these methods are not available in current practice. The detection of LT mutation by exon 2 sequencing and the detection of the MCPyV genome by FISH which might differentiate between integrated and episomal forms, could additionally be considered (Figure 8) (Haugg et al. 2014). Quantitative methods controlling the detection threshold can alternatively be used (Eid et al. 2017). Indeed, only low viral loads are observed in case of episomal virus, therefore the use of a sufficiently high detection limit makes it possible to rule out false positives.

Behind such diagnostic considerations, detection of the serological response against MCPyV components in MCC patients have been shown as relevant markers for prognostic and follow-up. Indeed high titers of antibodies against VP1 in serum of MCC patients at the diagnosis time are associated with better outcome (Touzé et al. 2011) whereas an increase in LT antibody titers during the follow up predicts recurrence (Paulson et al. 2010; Samimi et al. 2016).

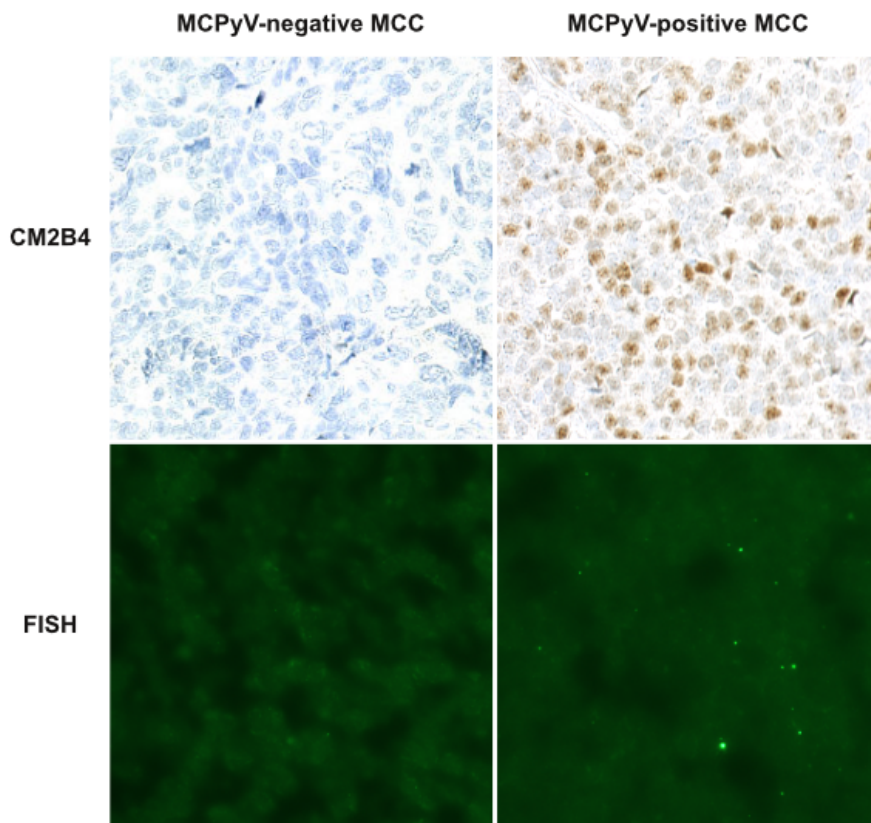


Figure 8. MCPyV detection in MCC tumor samples. In tumor samples, nuclear large T expression can be detected by immunohistochemistry (clone CM2B4), while MCPyV genome is evidenced by FISH (illustrations of the FISH were kindly provided by Mr. Klufah/Pr. Zur Hausen) (of note, the samples investigated by immunohistochemistry and FISH were independents).

2. MCPyV-negative tumors

In addition to MCPyV-induced tumors, about 20% of the MCC cases are not related to viral integration. DNA damages caused by UV radiations are regarded as the main oncogenic factor of such MCPyV-negative tumors, as suggested by several findings: i) high mutation burden similar to those observed in melanoma (around 1100 somatic single nucleotide variants per-exome) (Carter et al. 2018; Goh et al. 2016; Starrett et al. 2017; Sunshine et al. 2018; Yarchoan et al. 2019), ii) predominant UV signature with C to T transition (Carter et al. 2018; Goh et al. 2016; Starrett et al. 2017), iii) association of MCPyV-negative MCC with other UV-induced neoplasia such as Bowen's disease (Walsh 2001). Frequent damaging mutations of *TP53* and *RB1* (Carter et al. 2013; Goh et al. 2016; Starrett et al. 2017), alterations of PIK3C, HRAS, and NOTCH pathways (Harms et al. 2015) as well as mutations in genes involved in chromatin modification (*ASXL1*, *MLL2*, and *MLL3*) and in DNA-damage repair (*ATM*, *MSH2*, and *BRCA1*) (Goh et al. 2016a) are observed in this subset. Furthermore, arsenic exposure has been proposed as an alternative etiologic factor of MCPyV-negative MCC (Ho et al. 2005; Lien et al. 1999).

Interestingly, alteration of the same oncogenic pathways (especially inactivation of pRB and p53) either by TAg or somatic mutations, may account for the common neuroendocrine phenotype observed in virus-positive and negative MCCs (González-Vela et al. 2017; Kaplan-Lefko et al. 2003; Starrett et al. 2017; Syder et al. 2004). Nevertheless, variations in phenotype and behavior have been reported between the two subsets. Although controversial, MCPyV-negative cases seems to be associated with worst outcome (Moshiri et al. 2017; Schrama et al. 2011). Under microscopic examination, distinct cytological features of tumor cells have been reported (Iwasaki et al. 2013; Kuwamoto et al. 2011). Indeed, MCPyV-positive tumor cells typically harbor scant cytoplasm and round nuclei, with clear chromatin, whereas more irregular nuclei and more abundant clear cytoplasm are observed in MCPyV-negative cases (Iwasaki et al. 2013; Kuwamoto et al. 2011). Additionally, presence of a divergent component is suggestive of MCPyV-negative tumors (Carter et al. 2018; Foschini and Eusebi 2000; Martin et al. 2013). Ulceration, hyperkeratosis or an intraepidermal component are also associated with MCPyV-negative cases (Kervarrec et al. 2019; Nagase et al. 2019). Moreover, MCPyV-negative cases display a so-called “aberrant” immunohistochemical profile

(Pasternak et al. 2018a) with frequent KRT20-negativity (Miner et al. 2015). Such variations in phenotype and behavior are likely to reflect significant differences in genetic background between MCPyV-positive and -negative MCC cases.

Table: Distinct features of MCPyV-positive and –negative MCC cases

Compared to the MCPyV-positive MCC cells, MCPyV-negative MCC tumor cells have been described to harbor more irregular nuclei, more abundant cytoplasm and display more frequently so-called divergent differentiation. Moreover, MCPyV-negative cases are characterized by a specific immunohistochemical profile with frequent lack of expression of KRT20 and neurofilaments, and more frequent positivity for TTF1 and KRT7. Finally, a very high mutational burden with UV signature are observed only in MCPyV-negative cases.

Features	MCPyV(+) Merkel cell carcinoma	MCPyV(-) Merkel cell carcinoma
Morphology Nucleus Cytoplasm Divergent differentiation	Round (Iwasaki et al. 2013; Kuwamoto et al. 2011) Few (Iwasaki et al. 2013; Kuwamoto et al. 2011) No (Busam et al. 2009; Martin et al. 2013)	irregular/spindle (Iwasaki et al. 2013; Kuwamoto et al. 2011) more abundant (Iwasaki et al. 2013; Kuwamoto et al. 2011) yes (Busam et al. 2009; Martin et al. 2013)
Immunohistochemical markers KRT20 KRT7 TTF1 Neurofilament	+ (Harms et al. 2016; Pasternak et al. 2018) - (Pasternak et al. 2018) - (Czapiewski et al. 2016; Pasternak et al. 2018) + (Pasternak et al. 2018; Pulitzer et al. 2015; Stanoszek et al. 2018)	+/- (Harms et al. 2016; Pasternak et al. 2018) +/- (Pasternak et al. 2018) +/- (Czapiewski et al. 2016; Pasternak et al. 2018) +/- (Pasternak et al. 2018; Pulitzer et al. 2015; Stanoszek et al. 2018)
Oncogenic triggers	MCPyV TAg (Feng et al. 2008; Houben et al. 2012b; Shuda et al. 2015; Shuda et al. 2011)	UV induced genetic alterations (Goh et al. 2016; Harms et al. 2015; Wong et al. 2015)
Mutation load	Low (Goh et al. 2016; Harms et al. 2015; Wong et al. 2015)	High (Goh et al. 2016; Harms et al. 2015; Wong et al. 2015)

(+): frequent positivity of the marker; (-): frequent negativity of the marker, (+/-) increased or decrease expression frequency of this marker compared to the MCPyV(+) subset.

III. Histogenesis of MCC

Despite identification of both viral and UV-induced oncogenetic triggers in MCC, the nature of the cell where MCC oncogenesis occurs remains unknown (Harms et al. 2018). Actually, several hypotheses have been presented. The aim of this section is to provide a comprehensive overview of current knowledge of the histogenesis of MCC.

1. The Merkel cell: the historical candidate

According to Boyd *et al.*, rare cancer types identified before the molecular biology era were “either tumours presumed to originate from or resemble a cell type that infrequently gave rise to cancer, or histologically defined subsets within a more common type of cancer” (Boyd et al. 2016). MCC, a perfect illustration of the first group, was classified according to its similarities with skin physiological Merkel cells. MCs are highly specialized epithelial cells located in the basal layer of the epidermis and in the external part of the hair follicle (Figure 9). They have been shown to act as mechanoreceptors by transforming tactile stimuli into Ca^{2+} -action potentials (Ikeda et al. 2014) and serotonin release (Chang et al. 2016) and transmit these signals on to afferent nerve endings. The protein allowing transformation of mechanic into electric signals is the ion channel Piezo2 (Ikeda et al. 2014), which is also highly expressed by MCC cells [(Harms et al. 2013), unpublished data]. Expression of this MC-characteristic molecule is only one of many features shared by MCs and MCC cells. Indeed in addition to the numerous neuroendocrine granules containing dense cores, observed in MCC tumor cells by Tang and Toker (Tang and Toker 1978), further immunohistochemical analysis revealed a shared expression of many markers in MCs and MCC (Godlewski et al. 2013), whereas only a few markers distinguish them from each other, as detailed in the Table below. Indeed, both MCs and MCC express KRT 20 ((Cheuk et al. 2001; Van Keymeulen et al. 2009), neuroendocrine markers chromogranin A and synaptophysin (Koljonen et al. 2005a; Moll et al. 1995) and neuropeptides (Godlewski et al. 2013; Halata et al. 2003). By contrast, the expression of vasoactive intestinal peptide and metenkephalin (Nguyen and McCullough 2002) are specific to MCs, whereas CD117 and CD171 are detected only in MCC cells (Deichmann et al. 2003; Su et al. 2002).

Despite the remarkable phenotypic similarity of phenotypic features, several points argue against MCC deriving directly from MCs. First, in other organs such as the lung, strong data suggest that neuroendocrine carcinoma rather derives from epithelial progenitors than neuroendocrine cells (Yazawa 2015; Yoshimoto et al. 2018). Second, MCs are mainly post-mitotic cells (Van Keymeulen et al. 2009) and thus have low sensitivity to oncogenic stimuli. Accordingly, ectopic expression of sT antigen in MCs failed to induce cell proliferation or transformation in a transgenic mouse model (Shuda et al. 2015). Of note, hyperplasia of MCs as well as mitotic activity in keratin 20-positive cells has been reported in pathologic conditions (Kanitakis et al. 1998; Narisawa et al. 2018). However, whether these observations are due to proliferation of already differentiated MCs or to a MC differentiation process is still unclear. Third, MCs are most frequently present in the palms and soles in humans (Fradette et al. 1995; Vela-Romera et al. 2018), whereas MCC occurs mainly in sun-exposed areas [head and neck, limbs (Kervarrec et al. 2017; Miller and Rabkin 1999)]. Moreover, no infection of MCs by MCPyV has been reported (Tilling and Moll 2012a). Finally, in an *in vitro* model, MCPyV pseudovirions could barely infect KRT20-positive cells obtained from the fetal scalp (0.8%) (Liu et al. 2016). Overall, these data argue against an efficient MCPyV infection triggering MCC oncogenesis in an already differentiated MC.

Table: Markers expressed by physiological Merkel cells and Merkel cell carcinoma

Markers	Merkel cells	Merkel cell carcinoma
Epithelial markers		
Cytokeratin 20	+(Perdigoto et al. 2016; Van Keymeulen et al. 2009)	+(Kervarrec et al. 2018; WHO 2018)
Cytokeratin 8	+(Perdigoto et al. 2016; Van Keymeulen et al. 2009)	+(Baudoin et al. 1993)
Cytokeratin 18	+(Perdigoto et al. 2016; Van Keymeulen et al. 2009)	+(Kontochristopoulos et al. 2000; Li et al. 2015)
β1 integrin	+(Tilling et al. 2014)	lacking data
LRIG1	+(Tilling et al. 2014)	lacking data
CSPG4	+(Tilling et al. 2014)	lacking data
Neuroendocrine markers		
Chromogranin A	+(García-Mesa et al. 2017; Moll et al. 1995)	+(Koljonen et al. 2005)
Synaptophysin	+(García-Mesa et al. 2017; Moll et al. 1995)	+(Koljonen et al. 2005)
CD56	+(Boulais et al. 2009; Mouchet et al. 2014)	+(Fernández-Figueras et al. 2007)
ISL1	+(Perdigoto et al. 2014) lacking data	+(Agaimy et al. 2013)
INSM1	+(Hoefler et al. 1984; Nguyen and McCullough 2002)	+(Lilo et al. 2018)
Vasoactive intestinal peptide	+(Hoefler et al. 1984; Nguyen and McCullough 2002)	-(Hoefler et al. 1984; Nguyen and McCullough 2002)
Metenkephalin	+(Hoefler et al. 1984; Nguyen and McCullough 2002)	-(Hoefler et al. 1984; Nguyen and McCullough 2002)
MAO A and B	+(Vitalis et al. 2003)	lacking data
Neurogenic/ mechanoreceptor markers		
Neuropeptides	+(Godlewski et al. 2013)	+(Halata et al. 2003)
Neurofilament	-(Moll et al. 1995)	+(Kervarrec et al. 2018; Stanoszek et al. 2018)
CD171	-(Deichmann et al. 2003)	+(Deichmann et al. 2003)
SATB2	+(Fukuhara et al. 2016)	+(Fukuhara et al. 2016; Kervarrec et al. 2018)
PIEZO2	+(García-Mesa et al. 2017)	+(unpublished data)
PGP9.5	+(Sebastian et al. 2017)	+(Inoue et al. 1997)
SOX2	+(Perdigoto et al. 2014)	+(Azmahani et al. 2016; Lasithiotaki et al. 2017)
WNT1	+(Szeder et al. 2003)	lacking data
TUBB3	+(Sebastian et al. 2017)	+(Jirásek et al. 2009)
p75NTR	+(Sieber-Blum et al. 2004)	lacking data
TrkC	+(Sieber-Blum et al. 2004)	lacking data
NT-3	+(Sieber-Blum et al. 2004)	lacking data
Advillin	+(Hunter et al. 2018)	lacking data
B cell markers		

CD117 (c-KIT) PAX5	-(Grichnik et al. 1996) lacking data	+(Su et al. 2002) +((Johansson et al. 2018; Kervarrec et al. 2018; Zur Hausen et al. 2013)
TdT	lacking data	+(Johansson et al. 2018; Kervarrec et al. 2018; Zur Hausen et al. 2013)
Immunoglobulins	lacking data	+(Murakami et al. 2014; Sauer et al. 2017)

(+): positivity of the marker; (-): negativity of the marker, CSPG4: chondroitin sulfate proteoglycan 4, INSM1: insulinoma associated 1, ISL1: Islet-1, LRIG1: leucine rich repeats and immunoglobulin like domains 1, MAO: monoamine oxidase, NT-3: neurotrophin 3, p75NTR: neurotrophin receptor p75, PAX5: paired box 5, PGP9.5: ubiquitin C-terminal hydrolase L1, SATB2: special AT-rich sequence binding site 2, SOX2: SRY-box2, TdT: terminal deoxynucleotidyltransferase, TRKC: neurotrophic tyrosine kinase receptor type 3, TUBB3: tubulin beta 3 class III, WNT1: Wnt family member 1.

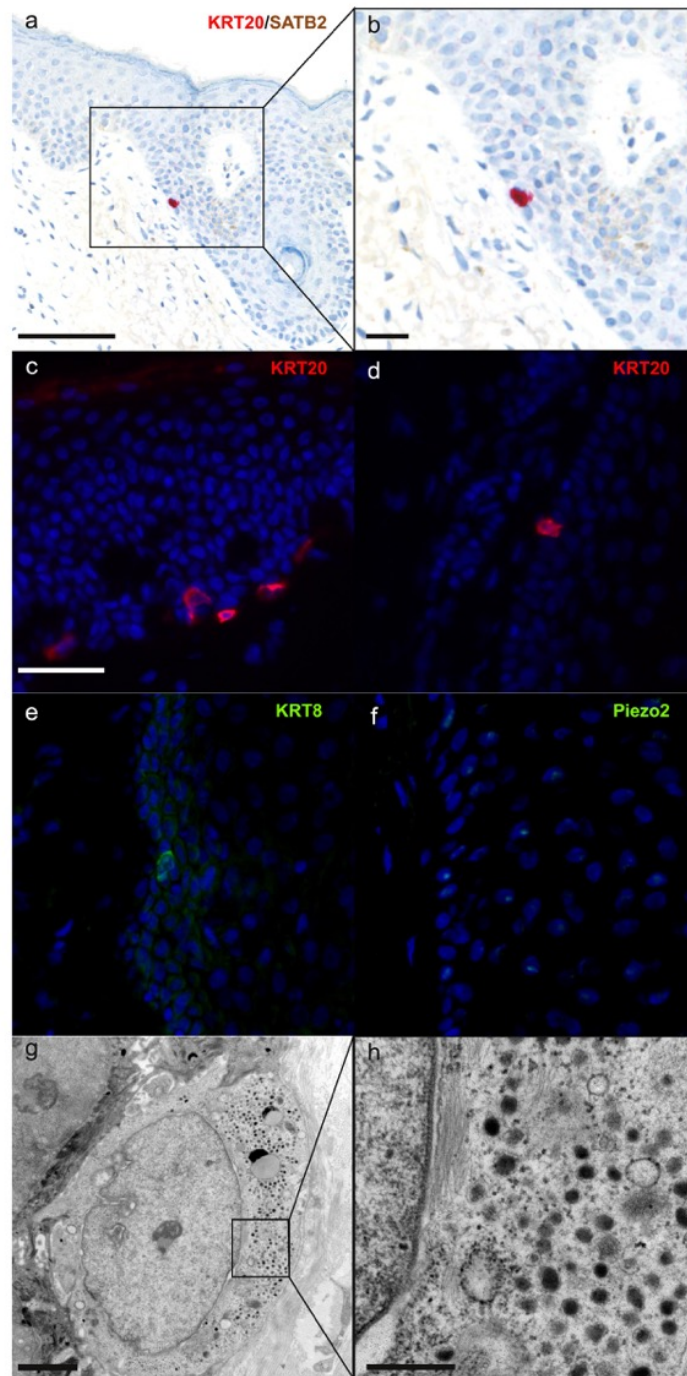


Figure 9. Immunohistochemical and ultrastructural features of physiological Merkel cells: immunohistochemical staining of normal skin (a,b) revealing one Merkel cell located in the infundibulum of a hair follicle and coexpression of cytokeratin 20 (cytoplasmic expression in red) and SATB2 (nuclear expression in brown) (bar = 100 and 50 μm for A,B). Immunofluorescence staining of healthy skin revealing some Merkel cells expressing cytokeratin 20 (c,d), cytokeratin 8 (e) and Piezo2 (f) in the epidermis (c) and in hair follicles (d–f) (bar = 40 μm for c–f). Electron microscopy of a Merkel cell (g,h) revealing numerous dense-core granules (bars = 2 and 0.5 μm for g,h respectively). A cropped region is shown in the inset (h). Adapted from Kervarrec et al. 2019

2. Putative mechanism of a “non-MC” origin for MCC

The tumour classification system is based on tumour differentiation and should not be considered a direct indicator of tumour histogenesis (Fletcher 2006). Indeed, several phenotypic changes occurring during the oncogenic process contribute to the final differentiation profile of tumour cells, which consequently differs from the primary cell in which the first oncogenic event took place (Fletcher 2006). Accordingly, acquisition of an MC-like phenotype including neuroendocrine differentiation (Chteinberg et al. 2018) during MCC oncogenesis could explain the similarities between MCs and MCC (Harms et al. 2018b). In MCC, both UV and virus-induced oncogenic triggers are thought to impact shared molecular pathways, accounting for the common phenotype between MCPyV-positive and -negative tumours (González-Vela et al. 2017). In this respect, disruption of pRB function occurs by somatic mutations and repression of protein expression in virus-negative tumours (Harms et al. 2015a), whereas sequestration by MCPyV LT antigen inactivates pRB in virus-positive MCC cells (Houben et al. 2012a). Interestingly, disruption of this pathway has been identified as a main driver of the acquisition of a neuroendocrine phenotype in tumours of other organs (Meder et al. 2016; Shamir et al. 2018; Syder et al. 2004).

In the skin, MC differentiation occurs in specific epithelial precursors upon expression of one main transcription factor, atonal homolog 1 (ATOH1) (Van Keymeulen et al. 2009). Under physiologic conditions, ATOH1 expression in the skin is restricted to MCs (Van Keymeulen et al. 2009). Because ATOH1 is also observed in MCC, its expression could explain the shared phenotype between MCs and MCC (Gambichler et al. 2016). Moreover, genetic ablation of *Rb1* and the related Rb-family gene *p130* in the intestinal epithelium in a mouse model leads to increased expression of *Atoh1* (Haigis et al. 2006), which suggests that *Atoh1* induction could occur during an oncogenic process associated with *Rb1* inactivation.

Considering these findings, a non-MC could also be candidate for the ancestry of MCC. As such, an epithelial non-MC, as well as fibroblastic, neuronal and B-cell origin have been proposed (Figure 10).

Table: Pros and cons of current hypotheses for the potential cell of origin of Merkel cell carcinoma (MCC)

Candidate	Pros	Cons
Merkel cell	Phenotypic similarities: (immunohistochemical profile: KRT8, KRT18, KRT20 + neuroendocrine markers+ultrastructural findings)	No mitotic activity No MCPyV infection No transformation by MCPyV antigens Lack of epidermal connection in almost all MCC cases
Epithelial progenitor	Ability to differentiate into Merkel cells Ability to generate combined MCC Most probable origin of neuroendocrine carcinoma in other sites	Exclusive dermal/hypodermal location of MCC No UV signature in MCPyV-positive cases Lack of epidermal connection in almost all MCC cases
Fibroblast and dermal stem cell	Site of replication of the MCPyV Ability of MCPyV antigens to induce transformation in these cell types Presence of SKP with reprogramming abilities	No proof of the ability of fibroblasts to acquire an MC-like phenotype Unexpected origin for a neuroendocrine carcinoma UV signature in MCPyV-negative MCCs
Pre/pro B cell	Epidemiologic association between MCC and B-cell neoplasia Expression of B-cell markers (PAX5, TdT and Immunoglobulins) Detection of MCPyV integration in B-cell neoplasia	No proof of the ability of B cells to acquire an MC-like phenotype Unexpected origin for a neuroendocrine carcinoma UV signature in MCPyV-negative MCCs

MC: Merkel cell; MCPyV: Merkel cell polyomavirus; SKP: skin-derived precursors

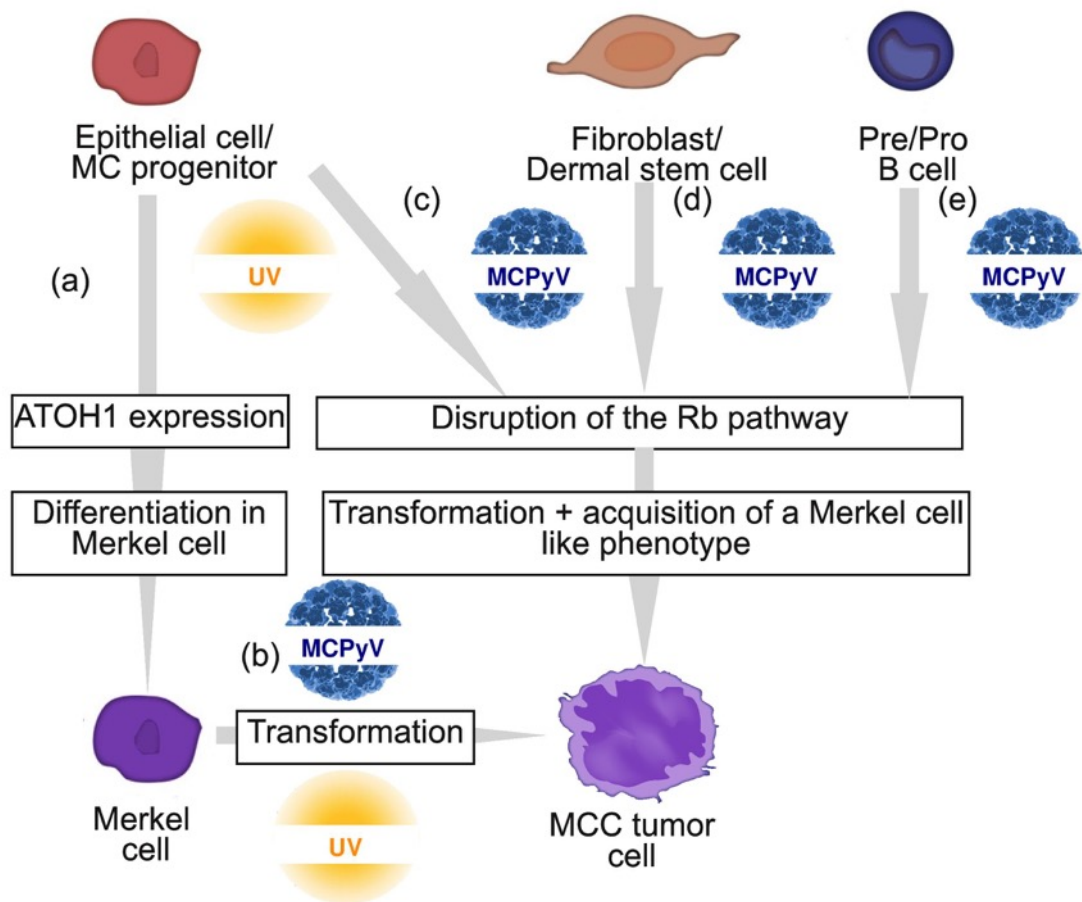


Figure 10. Graphic summary of the 4 putative cells of origin of Merkel cell carcinoma (MCC). (a) Physiological MC differentiation (b) First hypothesis: physiological MC as the cell of origin of MCC, suggesting that T antigens can induce transformation in this cell type. (c–e) Second hypothesis: oncogenic events occur in a non-MC and induce transformation and acquisition of an MC-like phenotype. Potential ancestries are epithelial progenitors (c), fibroblast/dermal stem cells (d) or pre/pro B cells (e) from the B cell lineage. Adapted from Kervarrec et al. 2019.

3. A non-MC epithelial origin

Whether MCs derive from the neural crest or epidermal lineage has been a matter of debate. Of note, both neural crest and epidermal lineages derive from the same embryologic structure, and this common ectodermal origin might explain the mixed neuroendocrine/epithelial phenotype observed in MCs. Indeed, ultrastructural studies of MC reveals on the one hand intracytoplasmic neuroendocrine granules suggesting a neural crest origin (Winkelman 1977) and on the other hand frequent desmosomes and cytokeratins, two hallmarks of the epithelial subset (Lucarz and Brand 2007). Accordingly, immunohistochemistry also demonstrated both expression of “neural crest” as well as epithelial markers. The neural crest origin hypothesis was further supported by chimeric chicken/quail models (Grim and Halata 2000; Halata et al. 1990). However, xenograft of human fetal skin free of neural crest progenitors in immunocompromised mice led to the development of human MCs, suggesting an epidermal origin of these cells (Moll et al. 1990). An epithelial origin of MCs in mammals was finally demonstrated in 2009 by two consecutive transgenic mouse studies (Morrison et al. 2009; Van Keymeulen et al. 2009). In both studies, deletion of *Atoh1* in epidermal progenitors resulted in a complete absence of MCs. Besides, Morrison and colleagues demonstrated that *Atoh1* deletion in the neural crest lineage did not affect the MC population (Morrison et al. 2009).

Additional studies in mouse models revealed that the acquisition of MC phenotype upon *Atoh1* expression was restricted to a specific subpopulation of keratinocyte progenitors, characterized by an activated Hedgehog pathway (Xiao et al. 2015; Xiao et al. 2014). Indeed, *Atoh1* expression failed to induce MC differentiation in other keratinocytic sub-populations (Van Keymeulen et al. 2009) and induced distinct differentiation towards other cell types (Aragaki et al. 2008; Mulvaney and Dabdoub 2012; Shi et al. 2014). MC differentiation regulation is controlled by redundant transcription factor networks (Perdigoto et al. 2014). While the Notch pathway (Logan et al. 2018) and the histone methyltransferases, *Ezh1* and *Ezh2* (Bardot et al. 2013; Perdigoto et al. 2016) act as repressors, the transcription factors *Sox2* (Bardot et al. 2013; Laga et al. 2010; Lesko et al. 2013) and *Isl1* (Perdigoto et al. 2014) cooperate with *Atoh1* to induce MC differentiation (Figures 11-12).

Limited data characterizing the MC progenitor population in humans are available (Moll et al. 1993). Therefore, our current knowledge on this cellular subset is mainly based on findings in mice. In this model, cells bearing MC differentiation potential are mainly located in the outer root sheet and hair follicle bulge region (Akiyama et al. 1995; Narisawa et al. 2015) but also in the interfollicular epidermis in specialized structures called touch domes (Xiao et al. 2014). The MC progenitors are expected to derive from Sox9-positive cells of the hair placode (Nguyen et al. 2018), and activation of the sonic hedgehog pathway is required for establishment of this population (Perdigoto et al. 2016). Additionally to the Gli1 positivity reflecting sonic hedgehog pathway activation, MCs progenitor are characterized by Krt17 positivity (Doucet et al. 2013; Wright et al. 2017; Xiao et al. 2015). Interestingly, these hair follicle- and touch- dome-derived stem cells have been determined as the preferential origin of basal cell carcinoma (Peterson et al. 2015). Therefore, their ability to acquire an MC phenotype and to proliferate, as well as their high sensitivity to oncogenic stimuli, could promote their transformation into MCC, rendering them *bona fide* candidates as cells of origin. Of note, MCC developing within follicular cysts (Requena et al. 2008) as well as preferential MCPyV infection of the dermal cells around hair follicles (Liu et al. 2016) support MCPyV(+) MCC as being derived from hair follicles.

A hair-follicle origin of MCC would also weaken one argument frequently used against an epithelial origin of MCC. Indeed, MCC cells are mostly found in the dermis and subcutis lacking a connection to the epidermis, making an epidermal origin unlikely (Zur Hausen et al. 2013a). However, some appendage tumours such as trichoblastoma (TB) and spiradenoma (Tellechea et al. 2015; Zheng et al. 2014) are well known to lack an epidermal connection (WHO 2018).

The observation of so-called combined MCC (or MCC with divergent differentiation) further supports an epithelial origin of MCC. Combined MCC represent 5% to 10% of cases and are characterized by the association of an MCC component with a tumour of another differentiation lineage (Busam et al. 2009; Martin et al. 2013). Although several divergent components have been described (sarcomatous, adnexal) (Martin et al. 2013; Pulitzer et al. 2015), MCC is most frequently associated with squamous/eccrine carcinoma (Walsh 2001). Shared genetic alterations have been reported for both components in some cases, which implies a common progenitor (Carter et al. 2017), whereas other cases gave proof of a collision

tumour (Falto Aizpurua et al. 2018). Furthermore, similar aberrant p53 expression is frequently observed in both components of combined MCC (Husein-ElAhmed et al. 2016). In some combined MCC cases, intra-epidermal neoplasia such as actinic keratosis or Bowen's disease (Walsh 2001) was detected close to the squamous cell carcinoma component. Since Bowen's disease originates from the epidermis, and invasive squamous cell carcinoma derive from Bowen's disease; hence, the clonality between squamous cell carcinoma and the MCC component (Carter et al. 2017) favours an epidermal origin of these typically MCPyV-negative MCC (Narisawa et al. 2015). Of note, hyperplasia of MCs in the squamous cell carcinoma component of combined tumours (Narisawa et al. 2018) might suggest that such component contains precursors with the ability to acquire an MC phenotype.

As mentioned before, such combined cases have been usually described to be typically UV-induced MCCs, displaying morphologic and immunohistochemical features distinct from MCPyV-positive MCC and carrying high mutational load (Carter et al. 2017; Martin et al. 2013; Pulitzer et al. 2015). Of note, low viral load of MCPyV in some cases is probably related to an episomal virus genome present in the skin. Hence, although combined cases imply that MCPyV-negative cases derive from some epidermal progenitors of the interfollicular epidermis, they provide no information about the origin of MCPyV-positive tumours (Sunshine et al. 2018).

In agreement with this observation, Sunshine et al. hypothesized that there might be two different cells of origin for the two MCC subtypes (Sunshine et al. 2018). They provided several arguments for this hypothesis. While the UV-mutation signature of virus-negative MCC favors an epidermal origin, the failure of epidermis targeted TA-expression to produce MCC tumors in mouse models (Shuda et al. 2015; Spurgeon et al. 2015; Verhaegen et al. 2015) suggests that other cells in the skin, such as dermal fibroblasts, may serve as origin of MCC (Sunshine et al. 2018). In line with this hypothesis, both UV- and virus-induced MCC occur in sun-exposed areas where frequent UV-induced mutations are observed in keratinocytes (Martincorena et al. 2015), whereas only MCPyV-negative cases are characterized by high mutational load and UV signature (Harms et al. 2015a; Sunshine et al. 2018). Sunshine and colleagues excluded an epithelial and instead proposed a fibroblastic origin of MCPyV(+) MCC (Sunshine et al. 2018). However, low mutational burden as well as lack of UV-signature in MCPyV(+) MCC might also

be explained by MCPyV integration into a cell from the hair follicle which, like dermal fibroblasts, is located deeper in the skin than epidermal keratinocytes.

In conclusion, and acting on the assumption that MCC generally has an epithelial origin, one could speculate that UV-induced MCC derives from a keratinocyte progenitor from the interfollicular epidermis that acquires the ability to differentiate into MCs during the oncogenic process, whereas MCPyV-driven oncogenesis is initiated in a progenitor cell from a hair follicle.

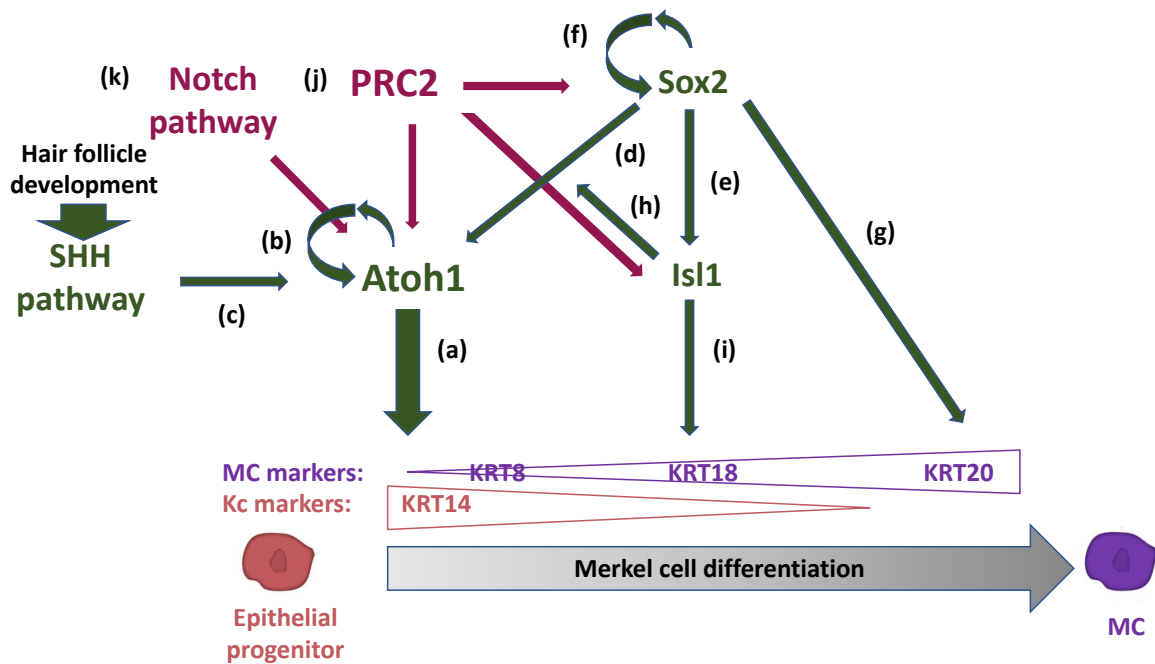


Figure 11. Graphic summary of Merkel cell differentiation in embryonic mice. KRT8, 18 and 20 expression arise sequentially during the MC differentiation process whereas markers of epithelial progenitors such as KRT14 are lost (Perdigoto, 2014). Transcription factors activating MC differentiation are depicted in green whereas repressors are in red. Atoh1, Sox2 and Isl1 are transcription factors involved in MC differentiation. a: Atoh1 is the most crucial transcription factor driving MC differentiation (Van Veymeulen, 2009; Morrison, 2009); b: Atoh1 protein binds to the promoter of Atoh1 1 gene inducing a positive feedback (Bardot 2013). c: Activation of the sonic hedgehog pathway (SHH) associated with hair follicle development is required for ATOH1 expression (Perdigoto 2016). Sox2 induces Atoh1 1 expression by acting on Atoh 1 enhancer (d) (Bardot 2013), moreover Sox2 increases Isl1 expression and interacts with its own promoter inducing a positive feedback loop (Bardot 2013), finally Sox2 is involved in the late MC differentiation and is necessary for KRT20 expression (Perdigoto 2014). Isl1 interacts with Sox2 to increase Atoh1 1 expression (h) (Perdigoto 2014) and contributes to the middle of MC differentiation process (i). The polycomb repressive complex 2 (PRC2) including EZH2 acts as a repressor of MC differentiation by adding a transcription repressive mark on Atoh1, Sox2 and Isl1 via H3K27 trimethylation (Bardot 2013, Perdigoto 2016). Notch pathway was also identified as a repressor of Atoh1 1 expression (Logan 2018). Kc: Keratinocytes, KRT: cytokeratins, MC: Merkel cell, SHH: sonic hedgehog

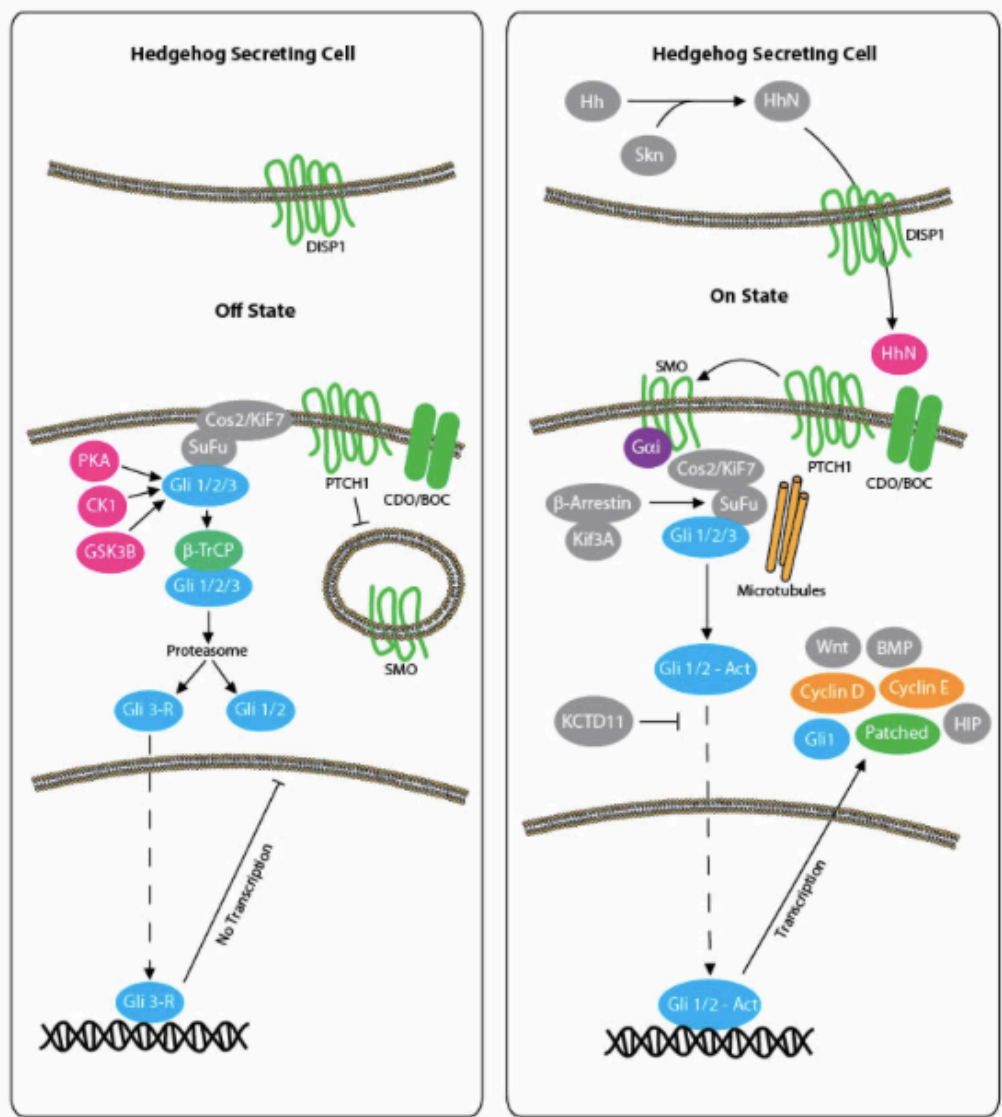


Figure 12. the sonic Hedgehog Pathway (adapted from Athar 2014).

In an off state, PTCH binds and subsequently inactivates SMO. By contrast, interaction of the Hedgehog (Hh) ligand with PTCH, leads to the release and the translocation of SMO in the cilium structure therefore resulting in transcriptional activation of GLI1. Indeed, SMO forms a complex with multiple cellular proteins which results in the dissociation of GLI factors from their endogenous inhibitor SuFu, translocation of GLI to the nucleus and transcription of GLI target genes. GLI: Glioma-associated oncogene homolog; Ptch1: patched 1; SMO: smoothed; SuFu: suppressor of fused homolog.

4. A fibroblastic origin

Another hypothesis is MCC developing from fibroblastic cells. This hypothesis might account for the quasi-exclusive dermal location of MCC, as discussed above. Furthermore, the fibroblastic origin of MCCs would be consistent with our knowledge of the MCPyV life cycle because fibroblasts of the papillary dermis have been identified as the main site of replicative infection (Liu et al. 2016). Although infectious MCPyV particles can enter several cell types including keratinocytes, with various efficiency rates (Liu et al. 2016; Schowalter et al. 2012), fibroblasts remain the only host evidencing early and late viral protein expression. One could argue that replication and transformation could occur in independent cell types, as previously demonstrated for the polyomavirus SV40 (Pipas 2009). However, the ability of fibroblasts to allow replication of the MCPyV genome increases the likelihood of accidental integration of the viral genome. Moreover, the *in vitro* transforming potential of sT antigen has until now been demonstrated only in fibroblasts (Pipas 2009; Shuda et al. 2015). Notably, ectopic expression of SV40 TAg in fibroblastic cells (Knapp and Franke 1989) triggered the induction of cytokeratin expression, which suggests that polyomavirus infection can influence a differentiation lineage. In such setting, acquisition of an MCC phenotype induced by viral protein expression could require a transient pluripotent stage. Indeed, fibroblasts are widely used for reprogramming to pluripotent cells. The resulting induced pluripotent stem cells (Takahashi and Yamanaka 2006) can be differentiated into epithelial cells *in vitro*. Furthermore, physiological stem cells of the papillar dermis [i.e., dermal skin precursors or skin-derived precursors (Naska et al. 2016)] share phenotypic similarities with induced pluripotent stem cells, such as expression of the stem cell factors c-Myc and Sox2 (Kwok et al. 2013), two markers also expressed by MCC (Azmahani et al. 2016; Kwun et al. 2013). These dermal skin precursors are able to differentiate into epithelial or neuronal cells *in vitro*. Hence, because of the close proximity of these cells to dermal fibroblasts, which can support productive MCPyV infection (Liu et al. 2016), as well as their expression of pluripotency factors and their differentiation abilities, MCPyV integration in such cells could lead to MCC oncogenesis and acquisition of an MCC phenotype.

5. A pre/pro or pre-B-cell origin

Because of the recurrent association between MCC and B-cell neoplasias (Brewer et al. 2012; Howard et al. 2006; Koljonen et al. 2015; Tadmor et al. 2011), the occasional integration of MCPyV in hematopoietic cells as well as phenotypic similarities between MCC and B cell precursors and, a lymphoid pre/pro B-cell origin is also discussed (Sauer et al. 2017; Zur Hausen et al. 2013a). Although no resident B-cells are observed in the skin, MCC might be derived from a circulating B-cell progenitor.

Indeed, chronic lymphocytic leukaemia (CLL) is the most frequent neoplasia associated with MCC development. Whether this is due to a common transforming event or the CLL creating an immunological microenvironment facilitating the development of the MCC or merely due to both tumours appearing in older immunocompromised people, has yet to be determined (Tadmor et al. 2011).

Moreover, MCC shares morphological features with other small round blue cell tumours, which explains why B-cell neoplasia must be considered as a differential diagnosis of MCC. In addition, the co-expression of terminal deoxy nucleotidyl transferase (TdT), paired box 5 (Pax5) and immunoglobulin chains, all markers expressed during B-cell differentiation, has been observed in MCC tumours (Sauer et al. 2017; Zur Hausen et al. 2013). Initially, the rates of TdT and Pax5 positivity were reported to reach about 65% (N=187) and 90% (N=143) of MCC cases (Sauer et al. 2017); however, recently observed rates were lower, 26% (N=217) or 23% (N=213) (Johansson et al. 2018). Of note, expression of immunoglobulin chains was restricted to the MCPyV(+) subset and detected in about 70% of cases (Murakami et al. 2014). In addition, rare observations of MCC with monoclonal immunoglobulin rearrangement of heavy chain as well as monoclonal expression of Kappa light chain were reported (Murakami et al. 2014). As already discussed, determination of the histogenesis based on phenotype similarities between terminally differentiated tumour and physiological cells does not account for phenotypic changes during oncogenesis (Fletcher 2006). In this regard, induction of immunoglobulin expression during the oncogenic process has been reported for several epithelial and soft-tissue neoplasias such as carcinoma, Ewing and osteosarcomas (Chen et al. 2011; Chen and Gu 2007) and may contribute to tumour aggressiveness (Yang et al. 2009). Furthermore, immunoglobulin rearrangement due to the expression of essential enzymes

required for gene rearrangement and class switch recombination has been described in non-hematopoietic neoplasia (Chen et al. 2011). Hence, immunoglobulin expression and rearrangement might result from the oncogenic process, and their occurrence in MCC cannot rule out a non-lymphoid cell origin. Induction of immunoglobulin expression in epithelial cells has been reported to result from Epstein-Barr virus infection (Liu et al. 2007) and was also observed in papillomavirus-induced neoplasia (Li et al. 2004). These findings, combined with the exclusive expression of immunoglobulins in MCPyV(+) MCC, led Murakami and colleagues to hypothesize that the immunoglobulin expression in MCC cells is induced by MCPyV oncoproteins (Murakami et al. 2014). In the same manner, the concomitant expression of TdT and Pax5, which is restricted to immature B cells and thymocytes under physiological conditions (Buscone et al. 2014) could be explained by an oncogene driven differentiation process. In this regard, positivity for one of these markers has also been demonstrated in several epithelial neoplasias (Dong et al. 2005; Mhawech-Fauceglia et al. 2007), which indicates that these markers can be acquired during the oncogenic process. Moreover, MCPyV genome integration (Hugg et al. 2011) associated with a deletion leading to a truncated LT antigen (Pantulu et al. 2010), the two hallmarks of MCC oncogenesis, have been evidenced in some cases of chronic lymphocytic leukaemia and tropism of other tumor viruses for the Pre-Pro B cells had been previously emphasized (Coleman et al. 2010). Although these findings demonstrate that MCPyV integration associated with transformation can occur in B cells, lack of acquisition of an MCC phenotype in these cases argue against a B-cell origin of MCC.

To conclude, our current knowledge on MCC histogenesis also challenges the basis of the current tumour classification system. Indeed, tumours are mostly classified according to their differentiation status and their level of similarities with physiological cells at the same location (Boyd et al. 2016). However, we should keep in mind that the final phenotype of a given tumour cell may result from strong differentiation changes occurring during oncogenesis and thus does not necessarily directly reflect the cell ancestry (Fletcher 2006). Accordingly, despite strong similarities, MCC likely does not derive from already differentiated MCs, which suggests that acquisition of an MC-like phenotype occurs during the carcinogenesis. From the observations of combined MCC tumours, and the high somatic mutation loads and detection of an UV signature in this subset, UV-induced MCC cases probably derive from a progenitor cell of the epidermis. By contrast, the nature of the cell in which MCPyV driven MCC

development occurs remains to be clarified. Use of experimental models in addition to phenotypic characterization of MCC to monitor phenotype changes induced by MCPyV in several cell types are needed to fully address this question.

Review Article

Histogenesis of Merkel Cell Carcinoma: A Comprehensive Review. [Kervarrec T](#), Samimi M, Guyétant S, Sarma B, Chéret J, Blanchard E, Berthon P, Schrama D, Houben R, Touzé A. *Front Oncol.* 2019
(see supplements)

CONTEXT AND OBJECTIVES

Briefly after the identification of the MCPyV genome into MCC tumor cells (Feng et al. 2008a), the virologist research team of *Dr. P. Coursaget/Prof. Antoine Touzé* (“Biologie des Infections à Polyomavirus” team (BIP) UMR INRA ISP 1282, University of Tours, France) started to investigate the specific association between MCPyV and MCC. For this purpose, a close collaboration was established with the Department of Dermatology (Prof. G. Lorette/Prof. M. Samimi) and the Department of Pathology (Prof. S. Guyétant) of the University Hospital center of Tours. This collaborative research group initially focused on MCPyV serological markers. Indeed they demonstrated that MCPyV seroconversion mainly occurs in childhood and accordingly observed high MCPyV seroprevalence in the healthy adult population (Martel-Jantin et al. 2014; Martel-Jantin et al. 2013). Moreover they identified that high level of anti-VP1 antibodies at the diagnosis time as associated with better survival in MCC patients (Touzé et al. 2011; Touzé et al. 2010), while, assessment of the TAg antibody titer by enzyme-linked immunosorbent assay (ELISA) was demonstrated as a useful technique for patient follow-up, and is currently routinely used in French Hospitals from the GCC (Groupe de Cancérologie Cutanée) network (Samimi et al. 2016).

With regards to the rarity of such tumors, extensive MCC tumor characterization required the establishment a multicentric cohort. To this end, under the supervision of Prof. Samimi, a network of physicians and pathologists was set up mostly in the West part of the France, currently including 8 Hospital centers (Angers, Besançon, Le Mans, Orléans, Poitiers, Nantes, Paris, Tours). The procedure was validated by the local ethical committee of Tours (no. ID RCB2009-A01056-51). MCC cases are included in the historical-prospective cohort after diagnosis confirmation by a pathologist expert in neuroendocrine pathology (Prof. S. Guyétant, from the TENPath network). Biological samples are collected after patients’ written consent. Clinical data regarding demographic characterization, staging and outcome are collected at the inclusion time and frequent follow-up updates are conducted. After microscopic selection of representative tumor area, FFPE tumor specimen are included in a tissue micro-array. This MCC collection currently includes currently more than 150 paraffin-embedded MCC tumors and already allowed to the investigation of tumor metabolism (Samimi et al. 2014), somatostatin receptor expression (Gardair et al. 2015) and immune responses (Kervarrec et al. 2018; Ollier et al. 2018; Zaragoza et al. 2016) in MCC patients.

In 2017, The BIP team and the research group of Dr. R. Houben and Dr. D. Schrama (Tumor Biology Forschung Laboratory (TBFL), University Hospital of Würzburg, Germany) established a collaboration in order to identify the cell of origin of MCC. As detailed before, TBFL members largely contributed to our understanding of oncogenic mechanisms in MCC tumors. Indeed they initially confirmed the presence of MCPyV in European MCC patients (Becker et al. 2009) and demonstrated the requirement of LT antigen expression for MCC tumor cell proliferation maintenance (Houben et al. 2010). Furthermore, they characterized LT functional domains (Houben et al. 2015) notably demonstrating the crucial role of the pRB binding site of the LT in such proliferation maintenance (Houben et al. 2012a). In addition, TBFL investigated several MCC aspects such as activation or inhibition of signaling pathways (Hafner et al. 2012; Houben et al. 2007), p53 contribution to the oncogenesis (Houben et al. 2013; Lill et al. 2011) and tumor immune response in MCC patients (Behr et al. 2014; Willmes et al. 2012). Taking advantage of their complementary expertise fields, TBFL and BIP team designed together a research collaborative project investigating MCC histogenesis, resulting in the present co-supervised PhD thesis.

Characterization of MCC tumors samples was considered by both teams as an essential preliminary step for working hypothesis establishment and subsequent *in vitro* experimental design. Indeed tumor cells phenotype is the result of two main factors combination: the nature of the primary cell hit and the phenotypic changes induced during the oncogenesis (Becker and Zur Hausen 2014; Visvader 2011). Therefore, any phenotypic variation between MCC tumors samples might reflect different oncogenic mechanisms, different cells of origin or combination of these two factors and accordingly some authors proposed different cells of origin for MCPyV-positive and negative tumors. In line with such considerations, the following questions were investigated on our MCC cohort: i) are MCC i.e. primary neuroendocrine carcinoma of the skin different from eNEC ii) should MCPyV-positive and -negative MCC be considered as the same tumor? iii) does MCC without cutaneous primary really belonging to the same tumor entity as cutaneous MCC and could this subset therefore provide indications regarding the cell of origin? iv) can the study of combined tumors further improve the understanding of MCC histogenesis?

Indeed, the WHO classification defined MCC as the eponymous name for primary neuroendocrine carcinoma of the skin underlining the similarities between MCC and other neuroendocrine carcinomas especially the small cell type. These findings further suggest that the neuroendocrine tumors of other locations might also provide clues regarding the pathogenesis of MCC. Of note, determination of the cell of origin was also a priority research question in this setting and lineage tracking experiments in transgenic mouse models demonstrated that lung extracutaneous neuroendocrine carcinoma (eNEC) derives either from epithelial progenitors or already differentiated neuro-endocrine cells (Park et al. 2011; Sutherland et al. 2011), a conclusion already suggested by combined tumors of the lung harboring a neuroendocrine component developed from adeno or squamous cell carcinoma (Oser et al. 2015). Although close phenotypic similarities between eNEC and MCC might although suggest an epithelial origin of the latter (Park et al. 2011; Sutherland et al. 2011), any phenotypic variations between the two groups should reflect differences either in the nature of the ancestry or the oncogenic mechanism. Therefore, in order to clarify the phenotypic variations between MCC and extracutaneous tumors and validate relevant discriminative criteria for diagnosis, we compared the immunohistochemical profiles of both subsets (**Article 1. Diagnostic accuracy of a panel of immunohistochemical and molecular markers to distinguish Merkel cell carcinoma from other neuroendocrine carcinomas**). Since phenotypic changes with acquisition of a MC-like phenotype during the oncogenesis is regarded as the most likely theory, the extensive characterization of the tumor phenotype performed in this study also represent a crucial preliminary step for later *in vitro* investigations of the differentiation processes induced by MCPyV TAGs.

The second objective of this work was to identify immunomorphological variations between MCPyV-positive and -negative tumors. Indeed, variations in morphology (Iwasaki et al. 2013; Kuwamoto et al. 2011), immunophenotype (Pasternak et al. 2018; Walsh 2001) and behavior (Moshiri et al. 2017) have been previously reported between the two groups and although these differences might be related to different oncogenic factors, they can alternatively be related to a different cell of origin as previously suggested (Sunshine et al. 2018). Therefore, clinical characteristics, morphologic and immunohistochemical features were compared between MCPyV-positive and -negative cases (**Article 2. Morphologic and**

immunophenotypical features distinguishing Merkel cell polyomavirus-positive and negative Merkel cell carcinoma).

Next, specific MCC subtypes were then investigated. MCC without a primary tumor represent 5 to 10% of all MCC cases and are characterized by a nodal metastasis without any detectable skin primary tumors (Fields et al. 2011; Haymerle et al. 2015; Kotteas and Pavlidis 2015; Reichgelt and Visser 2011). This tumor group might be considered as an independent tumor entity, primary developing from the lymph node (therefore suggesting a non-epithelial origin). On the other hand, they might alternatively represent a metastases derived from an occult and/or totally regressive skin primary tumors. Therefore, we first confirmed that these MCC without a primary tumor harbored all phenotypic hallmarks of cutaneous MCC (**Article 3. Differentiating Merkel cell carcinoma of lymph nodes without a detectable primary skin tumor from other metastatic neuroendocrine carcinomas: The ELECTHIP criteria**). We then assessed whether these tumors result from a metastatic process with spontaneous regression of the primary or from a primary tumor of the lymph node, by investigating expression of the epithelial-mesenchymal transition markers (**Article 4. Merkel cell carcinoma of lymph nodes without skin primary tumor are metastatic neoplasia associated with an efficient immune response**).

Finally, our investigations of tumor specimens focused on combined MCC cases, which also account for 5-10% of all MCC cases (Martin et al. 2013; Pulitzer et al. 2015; Walsh 2001). Combined MCCs are characterized by occurrence of an MCC in close association with another tumor type. Indeed, a large variety of differentiation subtypes (e. g. basal-cell-like, adnexal, melanocytic, glandular, sarcomatous and ganglioneuroblastic) of tumors associated with MCC have been reported (Lach et al. 2014; Martin et al. 2013a; Pulitzer et al. 2015b; Walsh 2001). The majority of the cases harbored squamous cell carcinoma component, sometimes associated with Bowen's disease (Walsh 2001). Since such Bowen's disease and related invasive squamous cell carcinoma are believed to derive from an epithelial cell, confirmation of the clonal filiation between the MCC and the squamous cell carcinoma component of such tumors might bring a clear demonstration of the epithelial origin of MCC, as suggested earlier and sequencing of such combined cases are actually on going in our team. However such combined cases have been reported to almost always belong to the MCPyV-negative subset

(Martin et al. 2013; Pulitzer et al. 2015). Therefore, we first identified the combined cases of our cohort, in order to determine the MCPyV viral status and characterize the immunohistochemical profile of these MCCs in comparison to pure cases (**Article 5. Detection of the Merkel cell polyomavirus in the neuroendocrine component of combined Merkel cell carcinoma**). We then focused our investigations on a MCPyV-positive combined MCC case, starting with an exceptional combined tumor consisting of a trichoblastoma (TB) and MCPyV-positive MCC (**Article 6. Polyomavirus-positive Merkel cell carcinoma derived from a TB suggests an epithelial origin of this Merkel cell carcinoma**). This exceptionally rare case provided us a model to understand the MCPyV induced MCC tumor development. The characterization of this tumor provided a clear proof that an MCPyV-positive MCC can derive from an epithelial cell and further suggests that MCPyV integration occurs in an MC progenitor cell of the hair follicle and induces acquisition of an MC-like phenotype by mimicking physiological differentiation process. Based on these findings, we consequently developed *in vitro* models to assess the respective contribution of the cell of origin and of the TAg expression in the final phenotype of MCPyV-positive tumor cells (**Article 7. Determinants of Human Merkel cell differentiation under physiologic and oncogenic conditions**)

RESULTS

Article 1. Diagnostic accuracy of a panel of immunohistochemical and molecular markers to distinguish Merkel cell carcinoma from other neuroendocrine carcinomas.

Modern Pathology 2019.

Article 2. Morphologic and immunophenotypical features distinguishing Merkel cell polyomavirus-positive and negative Merkel cell carcinoma.

Modern Pathology 2019.

Article 3. Differentiating Merkel cell carcinoma of lymph nodes without a detectable primary skin tumor from other metastatic neuroendocrine carcinomas: The ELECTHIP criteria. JAAD 2018.

Article 4. Merkel cell carcinoma of lymph nodes without skin primary tumor are metastatic neoplasia associated with an efficient immune response. Manuscript in preparation.

Article 5. Detection of the Merkel cell polyomavirus in the neuroendocrine component of combined Merkel cell carcinoma. Virchows Archiv 2018.

Article 6. Polyomavirus-positive Merkel cell carcinoma derived from a TB suggests an epithelial origin of this Merkel cell carcinoma. Accepted in J invest Dermatol.

Article 7. Merkel cell Polyomavirus T antigens promote Merkel cell differentiation in epithelial progenitors of the skin. Manuscript in preparation.

Name, Vorname: Kervarrec Thibault
Straße: 1 impasse de la Roquille
PLZ und Ort: 37250 Veigné, France
Tel.: +33611785648
E-Mail: thibaultkervarrec@yahoo.fr

Eidesstattliche Erklärungen nach §7 Abs. 2 Satz 3, 4, 5 der Promotionsordnung der Fakultät für Biologie

Eidesstattliche Erklärung

Hiermit erkläre ich an Eides statt, die Dissertation: „**Histogenesis of the Merkel cell carcinoma**“, eigenständig, d. h. insbesondere selbständig und ohne Hilfe eines kommerziellen Promotionsberaters, angefertigt und keine anderen, als die von mir angegebenen Quellen und Hilfsmittel verwendet zu haben.

Ich erkläre außerdem, dass die Dissertation weder in gleicher noch in ähnlicher Form bereits in einem anderen Prüfungsverfahren vorgelegen hat.

Weiterhin erkläre ich, dass bei allen Abbildungen und Texten bei denen die Verwertungsrechte (Copyright) nicht bei mir liegen, diese von den Rechtsinhabern eingeholt wurden und die Textstellen bzw. Abbildungen entsprechend den rechtlichen Vorgaben gekennzeichnet sind sowie bei Abbildungen, die dem Internet entnommen wurden, der entsprechende Hypertextlink angegeben wurde.

Affidavit

I hereby declare that my thesis entitled: „**Histogenesis of the Merkel cell carcinoma**“ is the result of my own work. I did not receive any help or support from commercial consultants. All sources and / or materials applied are listed and specified in the thesis.

Furthermore I verify that the thesis has not been submitted as part of another examination process neither in identical nor in similar form.

Besides I declare that if I do not hold the copyright for figures and paragraphs, I obtained it from the rights holder and that paragraphs and figures have been marked according to law or for figures taken from the internet the hyperlink has been added accordingly.

TOURS, den 18/08/2019

Signature PhD-student





Diagnostic accuracy of a panel of immunohistochemical and molecular markers to distinguish Merkel cell carcinoma from other neuroendocrine carcinomas

Thibault Kervarrec^{1,2,3} · Anne Tallet⁴ · Elodie Miquelestorena-Standley¹ · Roland Houben³ · David Schrama³ · Thilo Gambichler⁵ · Patricia Berthon² · Yannick Le Corre⁶ · Ewa Hainaut-Wierzbicka⁷ · Francois Aubin⁸ · Guido Bens⁹ · Flore Tabareau-Delalande¹⁰ · Nathalie Beneton¹¹ · Gaëlle Fromont¹² · Flavie Arbion¹² · Emmanuelle Leteurre¹³ · Antoine Touzé² · Mahtab Samimi^{2,14} · Serge Guyétant^{1,2}

Received: 14 July 2018 / Revised: 2 September 2018 / Accepted: 3 September 2018
© United States & Canadian Academy of Pathology 2018

Abstract

Merkel cell carcinoma is a rare neuroendocrine carcinoma of the skin mostly induced by Merkel cell polyomavirus integration. Cytokeratin 20 (CK20) positivity is currently used to distinguish Merkel cell carcinomas from other neuroendocrine carcinomas. However, this distinction may be challenging in CK20-negative cases and in cases without a primary skin tumor. The objectives of this study were first to evaluate the diagnostic accuracy of previously described markers for the diagnosis of Merkel cell carcinoma and second to validate these markers in the setting of difficult-to-diagnose Merkel cell carcinoma variants. In a preliminary set ($n = 30$), we assessed optimal immunohistochemical patterns (CK20, thyroid transcription factor 1 [TTF-1], atonal homolog 1 [ATOH1], neurofilament [NF], special AT-rich sequence-binding protein 2 [SATB2], paired box protein 5, terminal desoxynucleotidyl transferase, CD99, mucin 1, and Merkel cell polyomavirus-large T antigen) and Merkel cell polyomavirus load thresholds (real-time PCR). The diagnostic accuracy of each marker was then assessed in a validation set of 103 Merkel cell carcinomas (9 CK20-negative cases and 15 cases without a primary skin tumor) and 70 extracutaneous neuroendocrine carcinoma cases. The most discriminant markers for a diagnosis of Merkel cell carcinoma were SATB2, NF expression, and Merkel cell polyomavirus DNA detection (positive likelihood ratios: 36.6, 44.4, and 28.2, respectively). Regarding Merkel cell carcinoma variants, cases without a primary skin tumor retained a similar immunohistochemical profile and CK20-negative tumors displayed a different profile (decrease frequency of NF and SATB2 expression), but Merkel cell polyomavirus DNA remained detected (78% of cases by qPCR). Moreover, 8/9 (89%) CK20-negative Merkel cell carcinoma cases but only 3/61 (5%) CK20-negative extracutaneous neuroendocrine cases were positive for at least one of these markers. In conclusion, detection of SATB2 and NF expression and Merkel cell polyomavirus DNA helps distinguish between Merkel cell carcinoma classical and variant cases and extracutaneous neuroendocrine carcinomas.

These authors contributed equally: A. Tallet, E. Miquelestorena-Standley

These authors jointly supervised this work: M. Samimi, S. S. Guyétant

Electronic supplementary material The online version of this article (<https://doi.org/10.1038/s41379-018-0155-y>) contains supplementary material, which is available to authorized users.

✉ Serge Guyétant
serge.guyetant@univ-tours.fr

Extended author information available on the last page of the article.

Introduction

Merkel cell carcinoma is a rare primary carcinoma of the skin with both epithelial and neuroendocrine differentiation [1]. This tumor occurs essentially in older or immunosuppressed people and features aggressive behavior, with an overall 5-year survival estimated at 40%. In 2008, Feng et al. discovered the genome of a new polyomavirus in Merkel cell carcinoma tumors [2]. Indeed, genomic integration of the Merkel cell polyomavirus is observed in about 80% of Merkel cell carcinoma cases and is associated with mutations of the viral sequence that lead to truncation of the large T antigen (LTAg) [2, 3]. Besides the truncated

LTag, small T antigen is the only viral protein generally expressed in Merkel cell carcinoma; the expression of capsid proteins is frequently lost [4] and both T-antigens are considered the main oncogenic triggers in Merkel cell polyomavirus-positive Merkel cell carcinomas [5, 6].

Under microscopy examination, Merkel cell carcinoma appears as an undifferentiated, round, blue-cell neoplasm of the skin with high-grade neuroendocrine carcinoma features [1]. Immunohistochemical analysis reveals the expression of neuroendocrine markers, associated in most cases with cytokeratin 20 (CK20). Indeed, CK20 positivity and negativity for thyroid transcription factor 1 (TTF-1) are routinely used to distinguish Merkel cell carcinoma from metastasis of extracutaneous neuroendocrine carcinoma [1, 7]. However, Merkel cell carcinoma variants lacking CK20 expression [8, 9] or expressing TTF-1 [10] are observed in about 10% of cases. Furthermore, CK20 positivity has been reported in extracutaneous neuroendocrine carcinomas [7, 11], which led the World Health Organization to recommend a systematic whole-body imaging work-up in all suspected Merkel cell carcinoma cases to exclude metastasis of extracutaneous primary neuroendocrine carcinomas [1]. In addition, Merkel cell carcinoma may present as an isolated lymph node tumor without a detectable primary skin tumor [12, 13] and be misdiagnosed as lymph node metastasis of extracutaneous neuroendocrine carcinoma [13].

During the past few years, several immunohistochemical and molecular markers have been suggested as additional candidates for a positive diagnosis of Merkel cell carcinoma. Indeed, besides the expression of CK20 and neuroendocrine markers, Merkel cell carcinoma was found to express Merkel cell markers (e.g., neurofilament [NF] [14, 15], atonal homolog 1 [ATOH1] [16], and special AT-rich sequence-binding protein 2 [SATB2] [17]), lymphoid markers [18, 19] (e.g., paired box protein 5 [PAX5] and terminal desoxynucleotidyl transferase [TdT]), CD99 [20], and the cell surface-associated mucin 1 (MUC1) [21]. Because of Merkel cell polyomavirus-driven oncogenesis, detection of Merkel cell polyomavirus by immunochemistry [22, 23] and molecular procedures [2] has been suggested for Merkel cell carcinoma diagnosis. However, such markers were frequently assessed in small cohorts and without controlling for the main differential confounders of Merkel cell carcinoma, represented by neuroendocrine carcinoma metastasis. Therefore we have no comprehensive data on the accuracy of these markers for a positive diagnosis of Merkel cell carcinoma.

The aim of this study was to compare the diagnostic performance of these markers for distinguishing Merkel cell carcinoma from extracutaneous neuroendocrine carcinoma, with a focus on difficult-to-diagnose Merkel cell carcinoma variants such as CK20-negative cases and

Merkel cell carcinoma of the lymph node without a skin primary tumor.

Methods

Design and settings

Merkel cell carcinoma cases were selected from a historical/prospective multicentric French cohort of patients with a diagnosis of Merkel cell carcinoma established between 1998 and 2017 (Local Ethics Committee in Human Research, Tours, France; no. ID RCB2009-A01056-51). Inclusion criteria for the cohort were previously described [24, 25]. Briefly, tumors with available formalin-fixed and paraffin-embedded tissue samples were included as Merkel cell carcinoma cases if they displayed a compatible morphology, with the combination of CK20 positivity and at least one neuroendocrine marker (synaptophysin and chromogranin A) [1] or in the absence of CK20 positivity, expression of at least two neuroendocrine markers together with absence of deep neuroendocrine carcinoma confirmed by imaging work-up (CT scan or 18-FDG-TEP scan). Merkel cell carcinoma without a skin primary tumor cases were identified as previously described [13] as lymph node metastasis revealing the cancer, with no previous history of cutaneous Merkel cell carcinoma or deep neuroendocrine carcinoma and no evidence of cutaneous or extracutaneous primary neuroendocrine carcinoma after work-up consisting of cutaneous physical examination and imaging (CT scan and/or 18-FDG-TEP scan).

All extracutaneous neuroendocrine carcinomas registered between 1999 and 2017 in one department of pathology (Tours, France) were reviewed by using the following inclusion criteria: extracutaneous primary tumor, surgical biopsy or resection with available formalin-fixed and paraffin-embedded samples, high-grade and/or poorly differentiated features on pathological examination—classified as small-cell neuroendocrine carcinoma, large-cell neuroendocrine carcinoma, or mixed adenoneuroendocrine carcinoma—as well as immunohistochemical expression of pancytokeratin AE1–AE3 and at least two of the four following makers: chromogranin A, synaptophysin, CD56, and TTF-1 [26, 27].

The above inclusion criteria were considered the reference standards [28] for classification of Merkel cell carcinoma and neuroendocrine carcinoma.

Clinical data

Age, sex, and location of the primary tumor were collected from patient files. In addition, American Joint Committee on Cancer stage at the time of diagnosis, immune

suppression (HIV infection, organ transplant recipients, hematological malignancies) [29] and follow-up data were collected for Merkel cell carcinoma patients.

Tissue microarray and immunochemistry

All Merkel cell carcinoma and neuroendocrine carcinoma samples were included in a tissue microarray. Central intratumor areas without necrosis were selected on hematoxylin phloxin saffron (HPS)-stained sections to exclude non-specific staining. The selected areas were extracted by using a 1-mm tissue core, and cores were mounted in triplicate on the tissue microarray by using a semi-motorized tissue array system (MTA booster OI v2.00, Alphelys). Immunohistochemical staining for CK20, TTF-1, NF, PAX5, TdT, and CD99 involved using a BenchMark XT Platform as instructed. Staining was performed manually for ATOH1 [16], MUC1 [30], and CM2B4 [5] as described. Antibodies and dilutions are in Supplemental Method S1.

Interpretation of immunohistochemical staining

The staining of immunohistochemical markers was evaluated independently by two pathologists (EMS, TK) who were blinded to the clinical data, and discordant cases were reviewed together. The interpretation of immunohistochemistry (staining categories) was as follows: CK20 [1] and TTF-1 [10] staining was classified binarily as positive or negative, and CK20-negative cases detected on tissue microarray were confirmed by overall slide staining [31]; NF [15], and CD99 [20] staining was classified as negative, diffuse, or paranuclear dot pattern positive; ATOH1 [16], SATB2 [17], PAX5 [19], and MUC-1 [21] staining was classified by using a semiquantitative score: 0: lack of staining, 1: low/moderate or heterogenous expression, 2: diffuse, strong, and homogenous staining identified by low magnification ($\times 5$). Only cases with nuclear staining were classified as positive for TdT [32]. A semiquantitative Allred score was used for evaluating CM2B4 (LTA_g of Merkel cell polyomavirus); scores > 2 were considered Merkel cell polyomavirus-positive tumors, as described [22]. Representative illustrations of immunostainings are in Supplemental Method S1.

Detection and quantification of Merkel cell polyomavirus DNA

Detection and quantification of Merkel cell polyomavirus DNA were performed by a biologist (AT) who was blinded to the clinical and immunohistochemical data. Genomic DNA was isolated from tissue samples by use of the Maxwell 16 Instrument (Promega) with the Maxwell 16 formalin-fixed and paraffin-embedded Plus LEV DNA

purification kit (Promega). LTA_g real-time PCR assay was performed as described [23]. Briefly, 50 ng DNA was mixed with 0.2 μ M primers (Supplemental Method S2), 0.1 μ M DNA probe and Mix Life technologies (Applied) GoTaq Probe real-time PCR Master Mix 2 \times (Promega) in a final volume of 20 μ l. PCR reactions involved use of the LightCycler 480 II platform (Roche) with an initial denaturation at 95 $^{\circ}$ C \times 2 min, followed by 45 cycles at 95 $^{\circ}$ C \times 15 s and 58 $^{\circ}$ C \times 60 s. Normalization was with albumin as the reference gene and the Waga Merkel cell carcinoma cell line (RRID:CVCL_E998) included as a control. The Δ Ct method was used for quantification and results expressed as number of Merkel cell polyomavirus copies/cells. As negative controls, 37 non-Merkel cell carcinoma skin tumors (18 basal cell carcinomas, 9 squamous cell carcinomas, and 10 melanomas) were included, with no amplification observed in these cases.

Statistical analysis

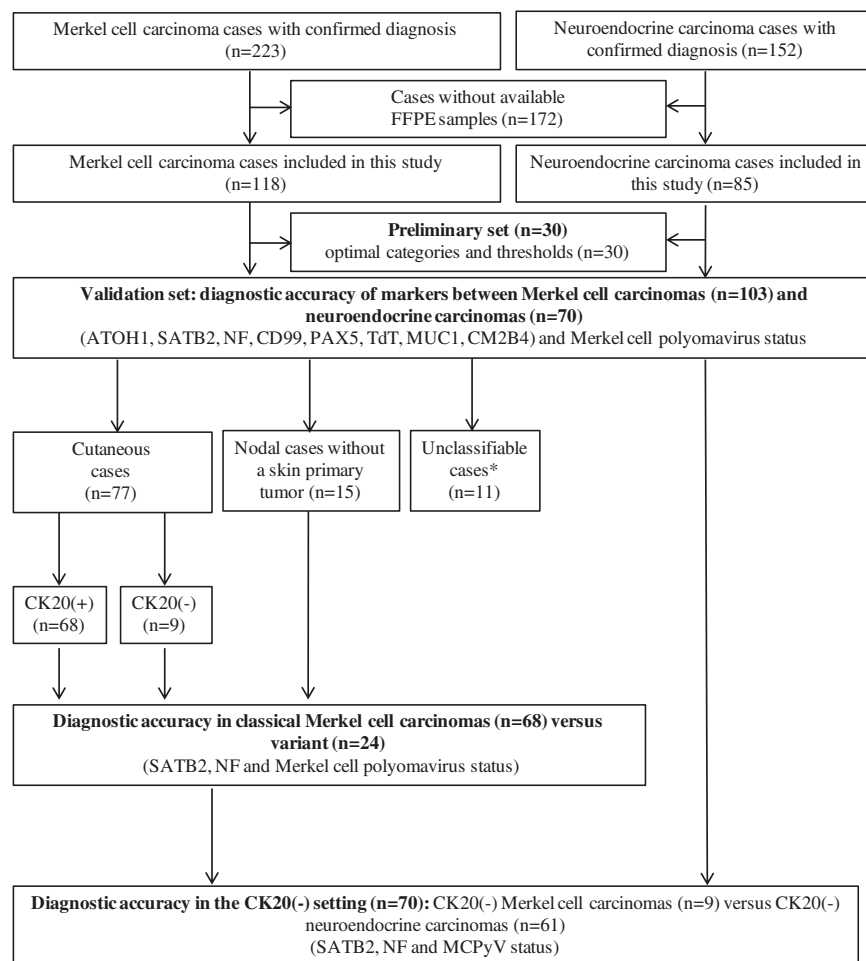
Continuous data are described with median (Q1–Q3) and categorical data with number (%) of interpretable cases. Categorical data were compared by two-tailed Fisher's exact test. $P < 0.05$ was considered statistically significant. Diagnostic accuracy of index tests was determined in accordance with the STARD guidelines [28]. The inclusion criteria described above (Methods section, data and settings criteria) were considered the reference standards. Categories and thresholds of index tests were determined with a preliminary set of 30 cases. The diagnostic accuracy of index tests was compared with the reference standard by using the positive likelihood ratio as a measure of accuracy combining sensitivity and specificity. Index tests with positive likelihood ratio > 10 were considered efficient [33]. Only markers with efficient diagnostic accuracy (positive likelihood ratio > 10) were considered for further analyses (validation step, subgroup analysis between classical and variant Merkel cell carcinomas and CK20-negative neuroendocrine carcinoma setting). Statistical analysis involved use of XL-Stat-Life (Addinsoft, Paris, France).

Results

Patient characteristics

Among the Merkel cell carcinoma cohort, 118 cases were included in this study (Fig. 1). Median age was 78 years (Q1–Q3: 70–84) and sex ratio was 1.35 (F/M: 66/49). Immunosuppression was identified in 13% of cases ($n = 11/83$). Tumors were diagnosed at American Joint Committee on Cancer stages I, II, III, and IV in 31, 26, 38, and 5% of cases, respectively. Most common primary tumor sites were

Fig. 1 Flow of cases in the study. ATOH1 atonal homolog 1, SATB2, special AT-rich sequence-binding protein 2, NF neurofilament, PAX5 paired box protein 5, TdT terminal deoxynucleotidyl transferase, MUC1 cell surface-associated mucin 1. (*) cases with insufficient data for determination of the primary site (cutaneous or superficial lymph node location)



lower limbs (39%) and head or neck (32%). Follow-up data were available for 85 Merkel cell carcinoma cases. Median duration of follow up was 16 months (ranges 1–209), and 34 recurrences and 30 deaths were reported during follow up. Fifteen cases (14%) were Merkel cell carcinomas without a skin primary tumor, 9 (8%) were CK20-negative cutaneous Merkel cell carcinomas, and 83 (78%) were CK20-positive cutaneous Merkel cell carcinomas. Thirteen cases (12%) showed TTF-1 expression. In 11 cases, clinical and imaging data did not allow for identification of the primary tumor site (skin or lymph node) and the cases were excluded from subgroup analysis (Fig. 1).

Among extracutaneous neuroendocrine carcinoma cases that met inclusion criteria (Fig. 1), median age was 65 (Q1–Q3: 55–72) and sex ratio 1.9 (F/M: 56/29). Primary tumor sites were lung ($n = 52$, 61%) and digestive ($n = 22$, 26%), urologic ($n = 7$, 8%), and gynecologic tract ($n = 4$, 5%). The histological subtype was small-cell neuroendocrine carcinoma in 49% of cases ($n = 42$), large-cell neuroendocrine carcinoma in 47% ($n = 40$) and mixed adenoneuroendocrine carcinomas in 4% ($n = 3$). Overall, 4 (5%) and 45 (58%) cases showed expression of CK20 and TTF-1, respectively.

Detailed immunohistochemical profiles of all Merkel cell carcinoma and neuroendocrine carcinoma cases by site of primary tumor and histological subtype are in supplemental Data S1.

Preliminary step: determining optimal categories and thresholds of index tests

Because several immunohistochemical markers were classified in three categories (semiquantitative score or expression by pattern) and lack of a consensual threshold for Merkel cell polyomavirus real-time PCR, optimal categories for a positive diagnosis of Merkel cell carcinoma versus neuroendocrine carcinoma were determined in an exploratory set of 30 cases. Fifteen Merkel cell carcinoma cases were randomly selected among the CK20-positive cutaneous Merkel cell carcinoma cases, considered the most representative, and compared with 15 neuroendocrine carcinoma cases from various anatomic sites randomly selected in each category (8 lung and 4 digestive, 2 urologic and 1 gynecologic tract). The detailed phenotype of these cases and representative illustrations of scoring are in supplemental Data S2-S3. In this preliminary analysis, NF and

CD99 “dot staining”; ATOH1, SATB2, and MUC1 high and diffuse staining (“score 2”) and Pax5 positivity (“scores 1–2”) showed optimal accuracy for a positive diagnosis of Merkel cell carcinoma (see Supplemental Data S2) and were then assessed in the validation step.

The optimal positive threshold of real-time PCR (Merkel cell polyomavirus copies/cell = 1.2) for a positive diagnosis of Merkel cell carcinoma was determined by the area under the receiver operating characteristic curve (AUC: 0.962; sensitivity: 0.93 (95% confidence interval [CI] 0.66–1; specificity: 1 (95% CI: 0.757–1) (Supplemental Data S4) and was then assessed in the validation step.

Validation step: diagnostic accuracy of histological and virological markers for a positive diagnosis of Merkel cell carcinoma

After excluding the 30 cases used in the preliminary step, the performance of markers was assessed by using the identified thresholds/categories. Comparison of immunohistochemical and virological features between Merkel cell carcinoma and neuroendocrine carcinoma cases is in Table 1 and representative illustrations are in Fig. 2.

All markers showed significant differential expression between Merkel cell carcinomas and neuroendocrine carcinomas (Fisher’s exact test: $p < 1 \times 10^{-5}$), except PAX5 ($p = 0.9$). Positive likelihood ratio > 10 , considered to provide substantial benefit for diagnostic accuracy [33], was observed for three index tests: detection of NF, SATB2, and Merkel cell polyomavirus (Table 1). Dot-pattern NF expression (Fig. 2c) was observed in 75% of Merkel cell carcinoma cases and only one small-cell bladder neuroendocrine carcinoma case (positive likelihood ratio: 44.4). In all, 64% of Merkel cell carcinoma cases and only one small-cell gallbladder neuroendocrine carcinoma case (positive likelihood ratio: 36.6) showed high and diffuse SATB2 expression (score 2) (Fig. 2d). However, both Merkel cell carcinoma (24%) and neuroendocrine carcinoma (18%) cases showed low and heterogenous SATB2 expression (score 1). Merkel cell polyomavirus detection, both by immunochemistry (LTA_g expression) and real-time PCR, demonstrated high specificity for Merkel cell carcinoma. With the cutoff determined in the preliminary set, real-time PCR (positive likelihood ratio: 28.2) was more sensitive (83% of positive Merkel cell carcinoma cases) than immunohistochemistry with LTA_g (64% positivity) ($p < 1 \times 10^{-3}$) (Table 1). In contrast, LTA_g immunohistochemistry was specific for Merkel cell carcinoma, whereas real-time PCR also detected Merkel cell polyomavirus above the pre-specified threshold in two extracutaneous neuroendocrine carcinoma cases: one large-cell colic case (Merkel cell polyomavirus copies/cell = 4)

and one small-cell bladder case previously described as NF-positive (Merkel cell polyomavirus copies/cell = 30). Neither of these two neuroendocrine carcinoma cases stained positive for LTA_g, CK20, or SATB2 on immunohistochemistry.

NF and SATB2 expression and Merkel cell polyomavirus detection in Merkel cell carcinoma variants

Because Merkel cell carcinoma phenotypic variants (CK20-negative and Merkel cell carcinoma without a skin primary tumor) are the most challenging Merkel cell carcinoma diagnoses in current practice, SATB2 and NF expression and Merkel cell polyomavirus detection were compared between classical cutaneous Merkel cell carcinoma cases and such variants (Fig. 1 and Table 2). Regarding Merkel cell carcinomas of the lymph node without a skin primary tumor, dot pattern NF expression, high and diffuse SATB2 expression (score 2), and Merkel cell polyomavirus detection above the pre-specified threshold were observed in 85%, 74%, and 93% of cases, respectively, and the diagnostic performance of these markers was similar to that for cutaneous Merkel cell carcinomas (Table 2) (positive likelihood ratios in Merkel cell carcinoma without a skin primary tumor: 51 (95% CI: 7–357), 41.8 (95% CI: 6–299), and 32 (95% CI: 8–124) respectively).

By contrast, CK20-negative Merkel cell carcinoma cases showed significantly lower dot pattern NF expression than classical Merkel cell carcinoma cases (44 vs 78%, $p = 0.03$) and lower, although not significantly, SATB2 (score 2) expression (37.5 vs 61%, $p = 0.25$) (Table 2). In total, 4 (50%) and 7 (78%) CK20-negative Merkel cell carcinoma cases featured LTA_g and Merkel cell polyomavirus genome detection, respectively (Table 2).

SATB2 and NF expression and Merkel cell polyomavirus detection in the CK20-negative neuroendocrine carcinoma setting

Because neuroendocrine carcinoma metastasis remains the main differential diagnosis to exclude when assessing a cutaneous CK20-negative tumor, we assessed the diagnostic accuracy of our markers in the restricted CK20-negative setting (Fig. 1 and Table 3). SATB2 and NF expression and Merkel cell polyomavirus real-time PCR remained accurate tools for Merkel cell carcinoma diagnosis in this setting (positive likelihood ratio: 20, 24, and 24, respectively). Accordingly, 8/9 (89%) CK20-negative Merkel cell carcinoma cases and only 3/61 (5%) extracutaneous neuroendocrine carcinoma cases were positive for at least one of these markers.

Table 1 Diagnostic accuracy of immunochemical and virological features between Merkel cell carcinoma and neuroendocrine carcinoma populations

Marker	Merkel cell carcinoma (n = 103)	Neuroendocrine carcinoma (n = 70)	<i>p</i> ^a	Sensitivity (95%CI)	Specificity (95%CI)	Positive likelihood ratio (95% CI)
Cytokeratin 20			<1 × 10 ⁻⁵	91% (84–95)	94% (85–98)	14.8 (6–38)
Positive	94 (91%)	4 (6%)				
Negative	9 (9%)	61 (94%)				
Uninterpretable cases	0	5				
TTF-1			<1 × 10 ⁻⁵	89% (81–95)	57% (44–69)	2.1 (1.6–2.8)
Positive	10 (11%)	37 (57%)				
Negative	85 (89%)	28 (43%)				
Uninterpretable cases	8	5				
ATOH1			<1 × 10 ⁻⁵	68% (58–78)	51% (38–64)	1.4 (1–1.9)
Score 2	65 (68%)	29 (49%)				
Score 1	29 (31%)	14 (24%)				
Score 0	1 (1%)	16 (27%)				
Uninterpretable cases	8	11				
NF			<1 × 10 ⁻⁵	75% (65–83)	98% (91–100)	44.4 (6–311)
Dot	73 (75%)	1 (2%)				
Diffus	0	2 (2%)				
Negative	24 (25%)	56 (96%)				
Uninterpretable cases	6	11				
SATB2			<1 × 10 ⁻⁵	64% (54–74)	98% (91–100)	36.6 (5–257)
Score 2	63 (64%)	1 (2%)				
Score 1	23 (24%)	10 (18%)				
Score 0	12 (12%)	46 (80%)				
Uninterpretable cases	5	13				
CD99			<1 × 10 ⁻⁵	65% (55–74)	83% (66–93)	3.8 (2–8)
Dot	63 (65%)	6 (17%)				
Diffus	19 (20%)	21 (60%)				
Negative	15 (15%)	8 (23%)				
Uninterpretable cases	6	35				
PAX5			0.9	23% (15–33)	76% (62–86)	0.9 (0.2–3.4)
Score 2	4 (5%)	3 (5%)				
Score 1	18 (18%)	11 (19%)				
Score 0	74 (77%)	43 (76%)				
Uninterpretable cases	7	13				
TdT			<1 × 10 ⁻⁵	20% (13–30)	100% (94–100)	—
Positive	20 (20%)	0				
Negative	78 (80%)	58 (100%)				
Uninterpretable cases	5	12				
MUC1						4.5 (2–11)

Table 1 (continued)

Marker	Merkel cell carcinoma (n = 103)	Neuroendocrine carcinoma (n = 70)	<i>p</i> ^a	Sensitivity (95%CI)	Specificity (95%CI)	Positive likelihood ratio (95% CI)
Score 2	45 (48%)	6 (10%)	<	48%	90%	
Score 1	26 (28%)	44 (73%)	1 ×	(37–58)	(79–96)	
Score 0	23 (24%)	10 (17%)	10 ⁻⁵			
Uninterpretable cases	9	10				
LTAg (CM2B4)			<	64%	100%	—
Positive	60 (64%)	0	1 ×	(53–73)	(94–100)	
Negative	34 (36%)	60 (100%)	10 ⁻⁵			
Uninterpretable cases	9	10				
Merkel cell polyomavirus qPCR			<	83%	97%	28.2
Positive	83 (83%)	2 (3%)	1 ×	(74–90)	(90–100)	(7–111)
Negative	17 (17%)	66 (97%)	10 ⁻⁵			
Uninterpretable cases	3	2				

Results are expressed in percentages of interpretable cases

Positive likelihood could not be determined for TdT and LTAg expression. Positive likelihood ratio > 10 indicated in bold were considered for further analysis. Merkel cell polyomavirus positive or negative status were determined by the Allred score and predetermined cutoff (Merkel cell polyomavirus copies/cell > 1.2) for immunochemistry and qPCR, respectively

ATOH1 atonal homolog 1, *CK20* cytokeratin 20, *LTAg* large T antigen, *MUC1* cell surface-associated mucin 1, *NF* neurofilament, *PAX5* paired box protein 5, *qPCR* quantitative PCR, *SATB2* special AT-rich sequence-binding protein 2, *TdT* terminal deoxynucleotidyl transferase, *TTF-1* thyroid transcription factor 1

^aFisher's exact test

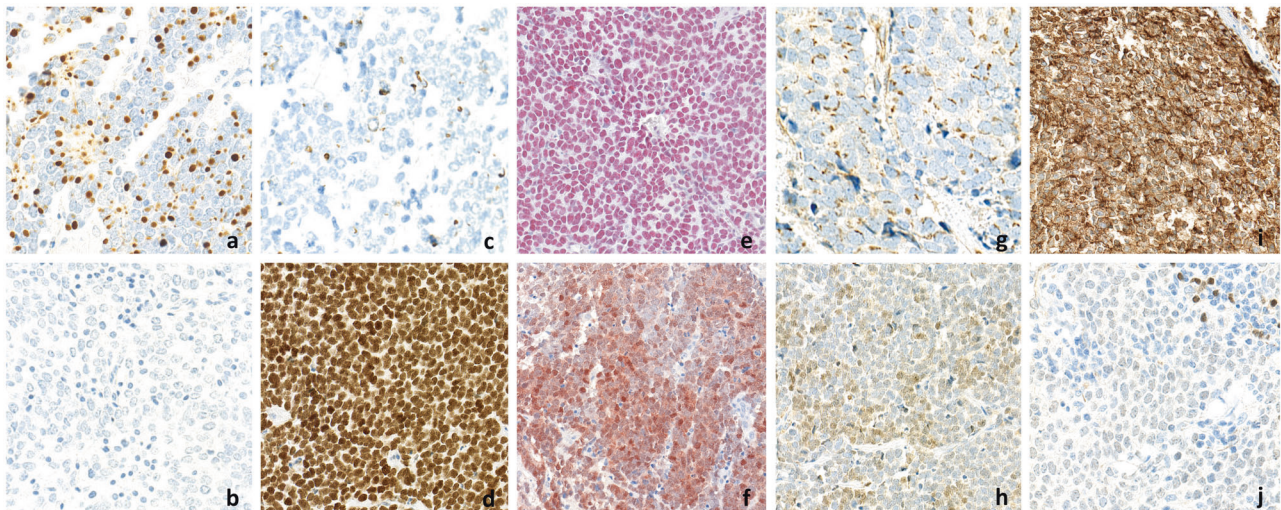


Fig. 2 Representative immunohistochemical staining of Merkel cell carcinoma tissue sections. **a** CK20 expression with paranuclear dot pattern, **b** lack of TTF-1 expression; **c** NF expression with a dot pattern; **d** high and diffuse nuclear expression of SATB2; **e** high and diffuse nuclear expression of ATOH1; **f** high and diffuse nuclear

expression of LTAg (Allred score = 8); **g** CD99 expression with paranuclear dot pattern; **h** low TdT expression; **i** high and diffuse expression of MUC1; **j** low expression of PAX5 with intratumor lymphocytes as positive controls

Table 2 Detection of the MCC markers NF, SATB2, and Merkel cell polyomavirus in classical MCC compared with MCC phenotypic variants

Marker	Classical Merkel cell carcinoma cases	Merkel cell carcinoma variants	
	Cutaneous CK20 (+) cases (<i>n</i> = 68)	Cutaneous CK20 (-) cases (<i>n</i> = 9)	Nodal cases without a skin primary tumor (<i>n</i> = 15)
CK20			
Positive	68 (100%)	0	15 (100%)
Negative	0	9 (100%)	0
Uninterpretable	0	0	0
cases			
NF			
Dot	50 (78%)	4 (44%)	12 (85%)
Diffuse	0	0	0
Negative	14 (22%)	5 (56%)	2 (15%)
Uninterpretable	4	0	1
cases			
SATB2			
Score 2	39 (61%)	3 (37.5%)	11 (74%)
Score 1	19 (30%)	2 (25%)	2 (13%)
Score 0	6 (9%)	3 (37.5%)	2 (13%)
Uninterpretable	4	1	0
cases			
LTA_g (CM2B4)			
Positive	38 (62%)	4 (50%)	10 (71%)
Negative	23 (38%)	4 (50%)	4 (29%)
Uninterpretable	7	1	1
cases			
Merkel cell polyomavirus qPCR			
Positive	54 (82%)	7 (78%)	13 (93%)
Negative	12 (18%)	2 (22%)	1 (7%)
Uninterpretable	2	0	1
cases			

The results are expressed in percentages of interpretable cases

Merkel cell polyomavirus positive or negative status were determined by the Allred score and predetermined cutoff (Merkel cell polyomavirus copies/cell > 1.2) for immunohistochemistry and qPCR, respectively

CK20 cytokeratin 20, LTA_g large T antigen, NF neurofilament, qPCR quantitative PCR, SATB2 special AT-rich sequence-binding protein 2

Discussion

The diagnosis of Merkel cell carcinoma is mainly based on the association of clinical data, microscopic features of high-grade neuroendocrine carcinoma, and CK20 positivity and TTF-1 negativity on immunohistochemistry. In current practice, distinguishing between Merkel cell carcinoma and

metastasis from a non-cutaneous neuroendocrine carcinoma may be challenging with some phenotypic variants of Merkel cell carcinoma, notably Merkel cell carcinoma without a skin primary tumor [12, 34] and CK20-negative cases [8, 9] (14 and 8% of our cases, respectively). The aim of this study was to evaluate the accuracy of additional markers in a large cohort of Merkel cell carcinoma cases in comparison with extracutaneous neuroendocrine carcinomas. Our results suggest that NF and SATB2 immunohistochemical expression as well as Merkel cell polyomavirus real-time PCR detection are accurate tools to distinguish Merkel cell carcinoma from extracutaneous neuroendocrine carcinoma metastasis. Regarding Merkel cell carcinoma variants, which remain the most challenging diagnostic issue, Merkel cell carcinoma of the lymph node without a skin primary tumor cases had frequent expression of these three markers (85, 74 and 93%, respectively). For CK20-negative cases, NF and SATB2 were less frequently expressed; however, the three markers still retained high diagnostic accuracy in this setting. Accordingly, at least one of these markers was positive in 89% of CK20-negative Merkel cell carcinoma cases and only 5% of extracutaneous CK20-negative neuroendocrine carcinoma cases.

A range of markers was previously reported to be expressed in Merkel cell carcinoma, but their diagnostic accuracy had not been compared to neuroendocrine carcinoma, which remains the main differential diagnosis of Merkel cell carcinoma.

In 1878, Sigmund Friedrich Merkel identified a new cellular type of cells located in the basal layer of the epidermis that frequently aggregated to form a specialized structure involved in proprioception—the touch dome [35]. Indeed, Merkel cells harbor a mechanoreceptor phenotype, form synaptic-like structures with afferent terminals [36] and express some neural-cell markers such as NF [37]. NF is frequently observed in Merkel cell carcinoma [14, 15], and we found that the “dot pattern” of NF expression is sensitive (75%) and highly specific (98%) for a positive diagnosis of Merkel cell carcinoma in the setting of neuroendocrine carcinoma.

SATB2 seems to be another useful marker of Merkel cell carcinoma [17]. SATB2 is a nuclear matrix-associated protein involved in chromatin remodeling and gene regulation [38]. In the skin, SATB2 expression is restricted to Merkel cells [17]. In extracutaneous tissues, SATB2 is involved in cell differentiation of neuronal [39] and colonic cells [40] and drives CK20 expression [39] in this latter, so it could also contribute to the Merkel cell phenotype in the skin. Recently Fukuhara et al. [17] reported SATB2 as a specific marker of Merkel cell carcinoma in comparison with 37 cutaneous tumors. In the present study, we confirmed the high specificity (98%) of SATB2 for the diagnosis of Merkel cell carcinoma among neuroendocrine

Table 3 Diagnostic accuracy of NF (dot pattern) and SATB2 (score 2) expression and Merkel cell polyomavirus detection (Merkel cell polyomavirus copie/cell > 1.2) for a positive diagnosis of Merkel cell carcinoma in the CK20-negative neuroendocrine carcinoma setting (70 cases)

Index test	No. of CK20 (-) Merkel cell carcinomas (n = 9)	No. of CK20(-) neuroendocrine carcinomas (n = 61)	Sensitivity (95%CI)	Specificity (95%CI)	Positive likelihood ratio (95%CI)
NF			44 (14–79)	98 (90–100)	24 (3–191)
Dot pattern	4 (44%)	1 (2%)			
Other	5 (56%)	53 (98%)			
Uninterpretable cases	0	7			
SATB2			37.5 (8.52–75)	98 (90–100)	20 (2–168)
Score 2	3 (37.5%)	1 (2%)			
Score 0–1	5 (62.5%)	52 (98%)			
Uninterpretable cases	1	8			
Merkel cell polyomavirus qPCR			78 (40–97)	97 (89–100)	24 (6–97)
Positive	7 (78%)	2 (3%)			
Negative	2 (22%)	59 (97%)			
Uninterpretable case	0	0			

The results are expressed in percentages of interpretable cases

Nine CK20-negative Merkel cell carcinoma and 61 CK20-negative neuroendocrine cases were analyzed. Merkel cell polyomavirus positive or negative status were determined by the Allred score and predetermined cutoff (Merkel cell polyomavirus copies/cell > 1.2) for immunohistochemistry and qPCR, respectively

NF neurofilament, SATB2 special AT-rich sequence-binding protein 2

carcinoma cases. Of note, in the spectrum of neuroendocrine tumors, well-differentiated tumors of the lower digestive tract showed SATB2 expression [41] and could be easily distinguished from Merkel cell carcinoma on morphology and tumor location.

ATOH1 did not show high diagnostic performance in our study. In mice, ATOH1 have been found the most important transcription factor driving Merkel cell differentiation [42]. In 2010, Heiskala et al. investigated ATOH1 expression in neuroendocrine neoplasia and observed ATOH1 positivity in Merkel cell carcinoma and in tumors of the digestive tract and parathyroid [43]. Accordingly, we found ATOH1 positivity in our extracutaneous neuroendocrine carcinoma cases, which rules out its use for Merkel cell carcinoma diagnosis. Similarly, other markers such as TdT and PAX5, CD99 or MUC1 did not seem relevant for Merkel cell carcinoma diagnosis because they were expressed in a few Merkel cell carcinoma cases and/or were expressed in other neuroendocrine carcinoma cases. Of note, INSM1 (Insulinoma-associated protein 1) was recently identified as a performant marker to confirm the neuroendocrine nature of Merkel cell carcinoma [44, 45]. Due to its lack of abilities to distinguish Merkel cell carcinoma from other neuroendocrine carcinoma cases, this marker was not tested in the present study but still remains an useful tool in combination with CK20, SATB2, NF, and Merkel cell polyomavirus

detection to confirm Merkel cell carcinoma diagnosis in current practice.

Assessing Merkel cell polyomavirus DNA as a marker of Merkel cell carcinoma has previously been debated. Merkel cell polyomavirus has been detected in a large range of non-Merkel cell carcinoma neoplasia [46] because this virus is ubiquitous in the papillary dermis of healthy people [47, 48] and can be detected in the environment if sufficiently sensitive methods are applied [49]. In a diagnosis context, the main issue is to distinguish Merkel cell polyomavirus episomal virus, which can be detected at very low levels in the skin of healthy people [48], from an integrated virus detected at higher levels, in at least each cell of Merkel cell polyomavirus-positive Merkel cell carcinomas. Thus, real-time PCR seems a relevant tool in this setting. Also, we determined an optimal threshold of Merkel cell polyomavirus load that allowed for accurately differentiating Merkel cell carcinomas from 100% of non-Merkel cell carcinoma cutaneous tumors included as negative controls and from 97% of extracutaneous neuroendocrine carcinoma tumors. Detection of Merkel cell polyomavirus-LTAG by immunohistochemistry with the commercial clone CM2B4 has recently been found have the best overall accuracy for classifying Merkel cell carcinomas as virus-positive or -negative [22]. However, with this technique, we and others [50] identified only 64% of viropositivity among Merkel

cell carcinoma cases as compared with 83% with molecular procedures [2]. Lower sensitivity of this antibody as compared with another non-commercial antibody was previously emphasized [23]. Of note, real-time PCR still detected Merkel cell polyomavirus in two neuroendocrine carcinoma cases, including a bladder neuroendocrine carcinoma tumor that also stained positive for the Merkel cell carcinoma marker NF. Merkel cell polyomavirus has been suggested to be involved as a carcinogenic agent in bladder carcinoma [51]. However, further investigations are needed to confirm the existence of Merkel cell polyomavirus (+) primary tumors of the bladder.

After having identified the most accurate markers in the overall Merkel cell carcinoma cases, we assessed them in the setting of difficult-to-diagnose cases, such as Merkel cell carcinomas without a skin primary tumor or CK20-negative Merkel cell carcinomas, which are the main challenge in practice. Indeed, Merkel cell carcinoma of the lymph node without a skin primary tumor, which represented 14% of our Merkel cell carcinoma cohort, can be misdiagnosed as lymph node metastases from other neuroendocrine carcinoma, with detrimental consequences on disease management. In a previous study, we reported that Merkel cell carcinoma without a skin primary tumor shared similar morphological and phenotypical features with cutaneous Merkel cell carcinoma but was accurately distinguished from other superficial neuroendocrine carcinoma lymph node metastasis by a spectrum of clinical, histological and virological criteria summarized as the ELECTHIP criteria (Elderly: ≥ 70 years, Location: inguinal or parotid, Extent restricted to the lymph node area, CK20 positivity, TTF-1 negativity, Histological type: small cell neuroendocrine carcinoma, Polyomavirus detection) [13]. Accordingly, NF and SATB2, the relevant immunohistochemical Merkel cell carcinoma markers assessed in the current study, were expressed in Merkel cell carcinoma without a skin primary tumor cases at similar levels as cutaneous primary Merkel cell carcinoma cases (NF, dot staining: 85%; SATB2 positivity, score 2: 74%) and therefore could be used as additional tools to confirm the Merkel cell carcinoma without a skin primary tumor diagnosis.

In contrast, we identified CK20-negative Merkel cell carcinoma cases (8% of the cases) as a distinct subgroup with decreased frequency of NF and SATB2 expression (44% and 37.5% of positive cases, respectively). Only few data are available on the phenotype of this Merkel cell carcinoma subset. TTF-1 negativity has been confirmed in this population [8, 52] and NF expression was previously detected in two of three investigated cases [8]. Although CK7 positivity has been observed [52], it was an infrequent finding in another study [8] and in our study ($n = 0/9$ cases, data not shown). In 2015, Miner et al. [8] reported 77% Merkel cell polyomavirus-negativity among CK20-negative

Merkel cell carcinoma cases. Additional analysis [9] revealed a high level of chromosomal anomalies and frequent somatic mutations with a UV signature, which suggested non-viral, UV-induced oncogenesis for CK20-negative cases and ruled out the relevance of Merkel cell polyomavirus detection as a diagnostic tool for this Merkel cell carcinoma subset. By contrast, in our study, Merkel cell polyomavirus detection was the most sensitive tool for Merkel cell carcinoma diagnosis (78% of real-time PCR positivity above predefined threshold—7/9 CK20-negative cases). However, considering that Merkel cell polyomavirus detection methods are only available in a few specialized centers and because of the widespread availability of SATB2 and NF markers, a first immunohistochemical investigation of NF and SATB2 status, which conferred a high positive likelihood ratio in this setting (24 and 20, respectively), followed by Merkel cell polyomavirus detection in a specialized center may represent an alternative approach in current practice.

To conclude, we provide evidence of NF and SATB2 protein expression and Merkel cell polyomavirus DNA detection as three relevant additional accurate markers for Merkel cell carcinoma. Moreover, regarding these three criteria, we demonstrate that Merkel cell carcinoma without a skin primary tumor shares a similar phenotype with other Merkel cell carcinoma, whereas CK20-negative Merkel cell carcinoma constitutes a distinct group, which nevertheless can be distinguished from other neuroendocrine carcinoma cases by using NF, SATB2 and Merkel cell polyomavirus detection.

Acknowledgements We sincerely thank Dr. C. Barbet, Dr. A.M. Bergemer-Fouquet, Dr. C. Collin, R. Gibon, Dr. M.C. Machet, Dr. A. de Muret, A.S. Neumann, Dr. I. Orain, Dr. C. Rousselot, I. Rüdell, and B. Sevin for their help and contributions.

Funding Fond de recherche de la société française de Pathologie 2016. Fondation ARC: "Aide individuelle 2017"

Compliance with ethical standards

Conflict of interest The authors declare that they have no conflict of interest.

Institutional review board The local Ethics Committee in Human Research of Tours (France) approved the study (no. ID RCB2009-A01056-51)

References

1. LeBoit PE, World Health Organization. Pathology and genetics of skin tumours. Lyon: IARC Press, 2007.
2. Feng H, Shuda M, Chang Y, et al. Clonal integration of a polyomavirus in human Merkel cell carcinoma. *Science*. 2008;319: 1096–100.
3. Shuda M, Guastafierro A, Geng X, et al. Merkel cell polyomavirus small T antigen induces cancer and embryonic merkel cell

- proliferation in a transgenic mouse model. *PLoS ONE*. 2015;10:e0142329.
4. Touzé A, Le Bidre E, Laude H, et al. High levels of antibodies against merkel cell polyomavirus identify a subset of patients with merkel cell carcinoma with better clinical outcome. *J Clin Oncol*. 2011;29:1612–9.
 5. Houben R, Adam C, Baeurle A, et al. An intact retinoblastoma protein-binding site in Merkel cell polyomavirus large T antigen is required for promoting growth of Merkel cell carcinoma cells. *Int J Cancer*. 2012;130:847–56.
 6. Verhaegen ME, Mangelberger D, Harms PW, et al. Merkel cell polyomavirus small T antigen initiates merkel cell carcinoma-like tumor development in mice. *Cancer Res*. 2017;77:3151–7.
 7. Cheuk W, Kwan MY, Suster S, et al. Immunostaining for thyroid transcription factor 1 and cytokeratin 20 aids the distinction of small cell carcinoma from Merkel cell carcinoma, but not pulmonary from extrapulmonary small cell carcinomas. *Arch Pathol Lab Med*. 2001;125:228–31.
 8. Miner AG, Patel RM, Wilson DA, et al. Cytokeratin 20-negative Merkel cell carcinoma is infrequently associated with the Merkel cell polyomavirus. *Mod Pathol*. 2015;28:498–504.
 9. Harms PW, Collie AMB, Hovelson DH, et al. Next generation sequencing of Cytokeratin 20-negative Merkel cell carcinoma reveals ultraviolet-signature mutations and recurrent TP53 and RB1 inactivation. *Mod Pathol*. 2016;29:240–8.
 10. Reddi DM, Puri PK. Expression of focal TTF-1 expression in a case of CK7/CK20-positive Merkel cell carcinoma. *J Cutan Pathol*. 2013;40:431–3.
 11. Nassar H, Albores-Saavedra J, Klimstra DS. High-grade neuroendocrine carcinoma of the ampulla of Vater: a clinicopathologic and immunohistochemical analysis of 14 cases. *Am J Surg Pathol*. 2005;29:588–94.
 12. Pan Z, Chen Y-Y, Wu X, et al. Merkel cell carcinoma of lymph node with unknown primary has a significantly lower association with Merkel cell polyomavirus than its cutaneous counterpart. *Mod Pathol*. 2014;27:1182–92.
 13. Kervarec T, Zaragoza J, Gaboriaud P, et al. Differentiating Merkel cell carcinoma of lymph nodes without a detectable primary skin tumor from other metastatic neuroendocrine carcinomas: the ELECTHIP criteria. *J Am Acad Dermatol*. 2018;78:964–72.
 14. McCalmont TH. Paranuclear dots of neurofilament reliably identify Merkel cell carcinoma. *J Cutan Pathol*. 2010;37:821–3.
 15. Schmidt U, Müller U, Metz KA, et al. Cytokeratin and neurofilament protein staining in Merkel cell carcinoma of the small cell type and small cell carcinoma of the lung. *Am J Dermatopathol*. 1998;20:346–51.
 16. Gambichler T, Mohtezabsade S, Wieland U, et al. Prognostic relevance of high atonal homolog-1 expression in Merkel cell carcinoma. *J Cancer Res Clin Oncol*. 2016;143:43–9.
 17. Fukuhara M, Agnarsdóttir M, Edqvist P-H, et al. SATB2 is expressed in Merkel cell carcinoma. *Arch Dermatol Res*. 2016;308:449–54.
 18. Kolhe R, Reid MD, Lee JR, et al. Immunohistochemical expression of PAX5 and TdT by Merkel cell carcinoma and pulmonary small cell carcinoma: a potential diagnostic pitfall but useful discriminatory marker. *Int J Clin Exp Pathol*. 2013;6:142–7.
 19. Zur Hausen A, Rennspiess D, Winnepenninckx V, et al. Early B-cell differentiation in Merkel cell carcinomas: clues to cellular ancestry. *Cancer Res*. 2013;73:4982–7.
 20. Rajagopalan A, Browning D, Salama S. CD99 expression in Merkel cell carcinoma: a case series with an unusual paranuclear dot-like staining pattern. *J Cutan Pathol*. 2013;40:19–24.
 21. Fernandez-Flores A, Suarez-Peñaranda JM. Expression of MUC1 by Merkel cell carcinoma is not dependent on merkel cell polyomavirus infection. *Appl Immunohistochem Mol Morphol*. 2016;24:e9–10.
 22. Moshiri AS, Doumani R, Yelistratova L, et al. Polyomavirus-negative Merkel cell carcinoma: a more aggressive subtype based on analysis of 282 cases using multimodal tumor virus detection. *J Invest Dermatol*. 2017;137:819–27.
 23. Rodig SJ, Cheng J, Wardzala J, et al. Improved detection suggests all Merkel cell carcinomas harbor Merkel polyomavirus. *J Clin Invest*. 2012;122:4645–53.
 24. Gardair C, Samimi M, Touzé A, et al. Somatostatin receptors 2A and 5 are expressed in Merkel cell carcinoma with no association with disease severity. *Neuroendocrinology*. 2015;101:223–35.
 25. Kervarec T, Gaboriaud P, Berthon P, et al. Merkel cell carcinomas infiltrated with CD33+myeloid cells and CD8+T cells are associated with improved outcome. *J Am Acad Dermatol*. 2018;78:973–82.
 26. Bosman FT, World Health Organization. WHO classification of tumours of the digestive system. Lyon: IARC Press, 2010.
 27. Travis WD, World Health Organization. Pathology and genetics of tumours of the lung, pleura, thymus and heart. Lyon: IARC Press, 2015.
 28. Bossuyt PM, Reitsma JB, Bruns DE, et al. STARD 2015: an updated list of essential items for reporting diagnostic accuracy studies. *BMJ*. 2015;351:h5527.
 29. Asgari MM, Sokil MM, Warton EM, et al. Effect of host, tumor, diagnostic, and treatment variables on outcomes in a large cohort with Merkel cell carcinoma. *JAMA Dermatol*. 2014;150:716–23.
 30. Renaud F, Gnemmi V, Devos P, et al. MUC1 expression in papillary thyroid carcinoma is associated with BRAF mutation and lymph node metastasis; the latter is the most important risk factor of relapse. *Thyroid*. 2014;24:1375–84.
 31. Beer TW. Merkel cell carcinomas with CK20 negative and CK7 positive immunostaining. *J Cutan Pathol*. 2009;36:385–6.
 32. Sidiropoulos M, Hanna W, Raphael SJ, et al. Expression of TdT in Merkel cell carcinoma and small cell lung carcinoma. *Am J Clin Pathol*. 2011;135:831–8.
 33. Harell FE, Califf RM, Pryor DB, et al. Evaluating the yield of medical tests. *JAMA*. 1982;247:2543–6.
 34. Haymerle G, Fochtmann A, Kunstfeld R, et al. Management of Merkel cell carcinoma of unknown primary origin: the Vienna Medical School experience. *Eur Arch OtorhinoLaryngol*. 2015;272:425–9.
 35. Halata Z, Grim M, Bauman KI. Friedrich Sigmund Merkel and his “Merkel cell”, morphology, development, and physiology: review and new results. *Anat Rec A Discov Mol Cell Evol Biol*. 2003;271:225–39.
 36. Nakatani M, Maksimovic S, Baba Y, et al. Mechanotransduction in epidermal Merkel cells. *Pflug Arch*. 2015;467:101–8.
 37. Narisawa Y, Hashimoto K, Kohda H. Immunohistochemical demonstration of the expression of neurofilament proteins in Merkel cells. *Acta Derm Venereol*. 1994;74:441–3.
 38. Zarate YA, Fish JL. SATB2-associated syndrome: mechanisms, phenotype, and practical recommendations. *Am J Med Genet A*. 2017;173:327–37.
 39. Leone DP, Heavner WE, Ferenczi EA, et al. Satb2 regulates the differentiation of both callosal and subcerebral projection neurons in the developing cerebral cortex. *Cereb Cortex* 1991. 2015;25:3406–19.
 40. Múnica JO, Sundaram N, Rankin SA, et al. Differentiation of human pluripotent stem cells into colonic organoids via transient activation of BMP signaling. *Cell Stem Cell*. 2017;21:51–64.e6.
 41. Li Z, Yuan J, Wei L, et al. SATB2 is a sensitive marker for lower gastrointestinal well-differentiated neuroendocrine tumors. *Int J Clin Exp Pathol*. 2015;8:7072–82.

42. Ostrowski SM, Wright MC, Bolock AM, et al. Ectopic Atoh1 expression drives Merkel cell production in embryonic, postnatal and adult mouse epidermis. *Dev Camb Engl*. 2015;142:2533–44.
43. Heiskala K, Arola J, Heiskala M, et al. Expression of Reg IV and Hath1 in neuroendocrine neoplasms. *Histol Histopathol*. 2010;25:63–72.
44. Lilo MT, Chen Y, LeBlanc RE. INSM1 is more sensitive and interpretable than conventional immunohistochemical stains used to diagnose merkel cell carcinoma. *Am J Surg Pathol*. 2018.
45. Rush PS, Rosenbaum JN, Roy M, et al. Insulinoma-associated 1: a novel nuclear marker in Merkel cell carcinoma (cutaneous neuroendocrine carcinoma). *J Cutan Pathol*. 2018;45:129–35.
46. Rollison DE, Giuliano AR, Messina JL, et al. Case-control study of Merkel cell polyomavirus infection and cutaneous squamous cell carcinoma. *Cancer Epidemiol Biomark Prev*. 2012;21:74–81.
47. Liu W, Yang R, Payne AS, et al. Identifying the target cells and mechanisms of merkel cell polyomavirus infection. *Cell Host Microbe*. 2016;19:775–87.
48. Martel-Jantin C, Pedergrana V, Nicol JTJ, et al. Merkel cell polyomavirus infection occurs during early childhood and is transmitted between siblings. *J Clin Virol*. 2013;58:288–91.
49. Di Bonito P, Libera SD, Petricca S, et al. Frequent and abundant Merkel cell polyomavirus detection in urban wastewaters in Italy. *Food Environ Virol*. 2015;7:1–6.
50. Leroux-Kozal V, Lévêque N, Brodard V, et al. Merkel cell carcinoma: histopathologic and prognostic features according to the immunohistochemical expression of Merkel cell polyomavirus large T antigen correlated with viral load. *Hum Pathol*. 2015;46:443–53.
51. Robles C, Viscidi R, Malats N, et al. Bladder cancer and seroreactivity to BK, JC and Merkel cell polyomaviruses: the Spanish bladder cancer study. *Int J Cancer*. 2013;133:597–603.
52. Calder KB, Coplowitz S, Schlauder S, et al. A case series and immunophenotypic analysis of CK20-/CK7 + primary neuroendocrine carcinoma of the skin. *J Cutan Pathol*. 2007;34:918–23.

Affiliations

Thibault Kervarrec^{1,2,3} · Anne Tallet⁴ · Elodie Miquelestorena-Standley¹ · Roland Houben³ · David Schrama³ · Thilo Gambichler⁵ · Patricia Berthon² · Yannick Le Corre⁶ · Ewa Hainaut-Wierzbicka⁷ · Francois Aubin⁸ · Guido Bens⁹ · Flore Tabareau-Delalande¹⁰ · Nathalie Beneton¹¹ · Gaëlle Fromont¹² · Flavie Arbion¹² · Emmanuelle Leteurre¹³ · Antoine Touzé² · Mahtab Samimi^{2,14} · Serge Guyétant^{1,2}

¹ Department of Pathology, Université de Tours, CHU de Tours, Avenue de la République, 37170 Chambray-les-tours, France

² “Biologie des infections à polyomavirus” team, UMR INRA ISP 1282, Université de Tours, 31, Avenue Monge, 37200 Tours, France

³ Department of Dermatology, Venereology and Allergology, University Hospital Würzburg, Josef-Schneider-Straße 2, 97080 Würzburg, Germany

⁴ Platform of Somatic Tumor Molecular Genetics, Université de Tours, CHU de Tours, Avenue de la République, 37170 Chambray-les-tours, France

⁵ Department of Dermatology, Venereology and Allergology, University Hospital Bochum, Gudrunstraße 5, 44791 Bochum, Germany

⁶ Dermatology Department, LUNAM Université, CHU Angers, 4 rue Larrey, 49933 Angers, France

⁷ Dermatology Department, Université de Poitiers, CHU de Poitiers,

2 rue de la Milétrie, 86021 Poitiers, France

⁸ Dermatology Department, Université de Franche Comté, CHU Besançon, EA3181, IFR133, 2 Boulevard Fleming, 25030 Besançon, France

⁹ Dermatology Department, CHR d’Orléans, 14 Avenue de l’hôpital, 45100 Orléans, France

¹⁰ Department of Pathology, CHR d’Orléans, 14 Avenue de l’hôpital, 45100 Orléans, France

¹¹ Dermatology Department, CHR Le Mans, 194 Avenue Rubillard, 72037 Le Mans Cedex 09, France

¹² Department of Pathology, Université de Tours, CHU de Tours, Boulevard Tonnellé, 37044 Tours, France

¹³ Univ. Lille, Inserm, CHU Lille, UMR-S 1172 - JPARC - Jean-Pierre Aubert Research Center-, F-59000 Lille, France

¹⁴ Dermatology Department, Université de Tours, CHU de Tours, Avenue de la République, 37170 Chambray-les-tours, France



Morphologic and immunophenotypic features distinguishing Merkel cell polyomavirus-positive and negative Merkel cell carcinoma

Thibault Kervarec^{1,2,3} · Anne Tallet⁴ · Elodie Miquelestorena-Standley¹ · Roland Houben³ · David Schrama³ · Thilo Gambichler⁵ · Patricia Berthon² · Yannick Le Corre⁶ · Ewa Hainaut-Wierzbicka⁷ · Francois Aubin⁸ · Guido Bens⁹ · Flore Tabareau-Delalande¹⁰ · Nathalie Beneton¹¹ · Gaëlle Fromont¹² · Flavie Arbion¹² · Emmanuelle Leteurre¹³ · Michael Herfs¹⁴ · Antoine Touzé² · Mahtab Samimi^{2,15} · Serge Guyétant^{1,2}

Received: 9 January 2019 / Revised: 6 May 2019 / Accepted: 7 May 2019
© United States & Canadian Academy of Pathology 2019

Abstract

In 2008, Feng et al. identified Merkel cell polyomavirus integration as the primary oncogenic event in ~80% of Merkel cell carcinoma cases. The remaining virus-negative Merkel cell carcinoma cases associated with a high mutational load are most likely caused by UV radiation. The current study aimed to compare the morphological and immunohistochemical features of 80 virus-positive and 21 virus-negative Merkel cell carcinoma cases. Microscopic evaluation revealed that elongated nuclei—similar to the spindle-shape variant of small cell lung cancer—were less frequent in Merkel cell polyomavirus-positive Merkel cell carcinoma compared to the virus-negative subset ($p = 0.005$). Moreover, virus-negative cases more frequently displayed a “large-cell neuroendocrine carcinoma” phenotype with larger cell size ($p = 0.0026$), abundant cytoplasm ($p = 4 \times 10^{-7}$) and prominent nucleoli ($p = 0.002$). Analysis of immunohistochemical data revealed frequent positivity for thyroid transcription factor 1 and cytokeratin 7, either absence or overexpression of p53, as well as frequent lack of neurofilament expression in virus-negative cases. By contrast, cytokeratin 8, 18 and 20 and a CD99 with a dot pattern as well as high EMA expression were identified as characteristic features of virus-positive Merkel cell carcinoma. In particular, the CD99 dot-like expression pattern was strongly associated with presence of the Merkel cell polyomavirus in Merkel cell carcinoma (sensitivity = 81%, specificity = 90%, positive likelihood ratio = 8.08). To conclude, virus-positive and -negative Merkel cell carcinoma are characterized by distinct morphological and immunohistochemical features, which implies a significant difference in tumor biology and behavior. Importantly, we identified the CD99 staining pattern as a marker indicating the virus status of this skin cancer.

These authors contributed equally: A. Tallet, E. Miquelestorena-Standley

These authors jointly supervised this work: M. Samimi, S. Guyétant

Institutional review board: The local Ethics Committee in Human Research of Tours (France) approved the study (no. ID RCB2009-A01056-51)

Supplementary information The online version of this article (<https://doi.org/10.1038/s41379-019-0288-7>) contains supplementary material, which is available to authorized users.

✉ Thibault Kervarec
thibaultkervarec@yahoo.fr

Extended author information available on the last page of the article

Introduction

Merkel cell carcinoma is a rare and aggressive neuroendocrine carcinoma of the skin with a 5-year overall survival rate of 40% [1]. The two main risk factors are immunosuppression [2] and sun exposure [1]. Whereas the incidence is still low, with 0.7 cases per 100,000 person-years in the United States in 2013, a dramatic increase of 95% was observed between 2000 and 2013, and a further rise in incidence has been predicted [3].

In 2008, Feng et al. identified a polyomavirus which they found integrated in the genome of Merkel cell carcinoma cells and accordingly named it Merkel cell polyomavirus (MCPyV) [4]. Currently, integration of this virus and the expression of viral oncoproteins named T antigens are established as the primary oncogenic events for

approximately 80% of Merkel cell carcinoma cases [4]. The remaining 20% of Merkel cell carcinoma cases lacking MCPyV integration are considered as a distinct tumor subset primarily caused by UV radiation [5, 6]. In line with this notion, substantial differences between the two subsets with respect to morphology [7], and immunohistochemical profiles [8] have been described. Moreover, virus-negative Merkel cell carcinomas are characterized by higher mutational burden with predominant UV signature [5, 6], and a worse outcome than their virus-positive counterparts [9].

In a previous study [10], to assess performance of a set of markers for Merkel cell carcinoma diagnosis, we characterized the expression of nine proteins by immunohistochemistry and determined the MCPyV status by quantitative PCR in a cohort of 118 patients with Merkel cell carcinoma in comparison to 85 with extra-cutaneous neuroendocrine carcinomas. To further exploit this dataset, the current study aimed to (1) compare the morphological and immunohistochemical features of MCPyV-positive and -negative Merkel cell carcinoma and (2) evaluate whether discriminative features could be used as surrogate markers for MCPyV status.

Methods

Patients and samples

Merkel cell carcinoma cases were selected from an historical/prospective cohort of Merkel cell carcinoma patients from 6 French hospital centers. Inclusion criteria for the cohort have been described previously [11]. Briefly, patients had a diagnosis of Merkel cell carcinoma established between 1998 and 2017 (local ethics committee, Tours, France; no. ID RCB2009-A01056-51) [12]. Among the cohort, only cases with sufficient available formalin-fixed paraffin-embedded tumors for representative hematein phloxin saffron (HPS) slide staining and previously determined MCPyV status [10] were included in the present analysis.

Clinical and follow-up data

Age, sex, immunosuppression (HIV infection, organ transplant recipient, hematological malignancies), American Joint Committee on Cancer (AJCC) stage at the time of surgery [13], location of the primary tumor and follow up (recurrence free and specific survival) were collected from patient files.

MCPyV status determination

MCPyV status was determined using real time PCR with a ROC curve validated cut-off as previously described [10].

The Merkel cell carcinoma cell line WaGa (RRID: CVCL_E998) [14] was used as positive control. To note, while immunohistochemical detection of Large T antigen has been proposed as an efficient method to determine MCPyV status [9], our previous study comparing the performances of both procedures to distinguish Merkel cell carcinoma from other neuroendocrine carcinoma, revealed higher sensitivity (83%) and high specificity (97%) of MCPyV genome detection by quantitative PCR [10]. Consequently, LT staining was performed but the classification into MCPyV-positive and negative was based on quantitative PCR results.

Morphologic study

For all specimens, one representative 4 µm thick, Hematein-phloxin-saffron stained section was reviewed by two pathologists (SG, TK) with blinding to diagnosis. Morphologic features were assessed by the following criteria: nuclear shape (0: regular, 1: elongated), presence of nucleoli (0: absent or inconspicuous, 1: present), cell size (0: small: <2 lymphocytic nuclei, 1: moderate: 2 to 3 lymphocytic nuclei, 2: large: >3 lymphocytic nuclei), cytoplasm volume (0: none/inconspicuous, 1: abundant), clear cytoplasm (0: no, 1: yes), rosette-like structure (0: no, 1: yes), intraepidermal component (0: no, 1: yes), divergent component (0: no, 1: yes) and associated intraepidermal neoplasia such as actinic keratosis or Bowen disease (0: no, 1: yes). All discordant cases were reviewed collegially.

Immunohistochemistry

We extracted data for the expression of the following markers from a previous study [10]: cytokeratin 20, thyroid transcription factor 1 (TTF-1), atonal homolog 1 (ATOH1), neurofilament (NF), special AT-rich sequence-binding protein 2 (SATB2), paired box protein 5 (PAX5), terminal desoxynucleotidyl transferase (TdT), CD99, epithelial membrane antigen (EMA) referred as MUC1 in the previous study, and large T antigen (CM2B4).

In addition, we analyzed cytokeratin 7 and p53 expression as well as the staining pattern (dot, diffuse or mixed) for cytokeratins 8, 18 and 20. All antibodies are available in supplementary method Table S1. A Benchmark platform was used for staining, except for cytokeratins 8, 18 and CM2B4 stainings, which were manually performed. p53 expression was evaluated according to the Allred score whereas 0, 7 and 8 are considered as abnormal expression, indicating loss of active p53 [15]. For all immunohistochemical analyses, the number of uninterpretable samples (mainly due to failure of tissue microarray inclusion) is mentioned in the corresponding figures.

Statistical analyses

Continuous data are described by medians (Q1–Q3) and categorical data with number and percentage of interpretable cases. Associations were assessed by Mann–Whitney and two-tailed Fisher’s exact tests for continuous and categorical data, respectively. $P < 0.05$ was considered statistically significant. MCPyV status was determined by qPCR with a previously validated cut-off (MCPyV load >1.2 copies/cell) [10]. Categories and thresholds of immunohistochemical markers were derived from previous studies [10, 16–18]. Since no thresholds were previously determined for cytokeratins 8, and 18, the same categories as for cytokeratin 20 were applied. The diagnostic accuracy of immunohistochemical markers to determine MCPyV status was compared with the reference standard (quantitative PCR) by using the positive likelihood ratio as a measure of accuracy combining sensitivity and specificity. Recurrence-free survival and specific survival related to patient MCPyV status were analyzed by log-rank test and presented as Kaplan–Meier curves. Univariate and multivariate Cox proportional-hazards regression was used to identify factors associated with Merkel cell carcinoma recurrence and death, estimating hazard ratios (HRs) and 95% confidence intervals (CIs). Specific deaths were considered events. Covariates were identified as potential prognostic confounders with $p \leq 0.25$ on Cox univariate regression analysis and then included in the multivariate Cox analysis. Statistical analysis involved use of XL-Stat-Life (Addinsoft, Paris, France).

Results

Patient characteristics and clinical outcome

For 101 Merkel cell carcinoma cases corresponding to 80 MCPyV-positive and 21 MCPyV-negative, sufficient material for morphologic examination allowed inclusion (Fig. 1/Flow Chart). To underline common and distinctive features of the two groups, clinical data are compared in Table 1. Virus-positive and -negative Merkel cell carcinoma did not differ with respect to age, sex, immune status, stage (American Joint Committee on Cancer), and location of the primary tumor. By contrast, Merkel cell polyomavirus-positivity was significantly associated with lower risk of recurrence (HR 0.36 CI 0.18–0.74, $P = 0.005$) and specific death (HR 0.37 CI 0.15–0.89), $P = 0.03$) on univariate analysis (Table 1/supplementary data S1) and was also statistically significant in multivariate Cox analysis (supplementary data S1). These results confirm virus-negative status as a negative prognostic marker for Merkel cell carcinoma [9].

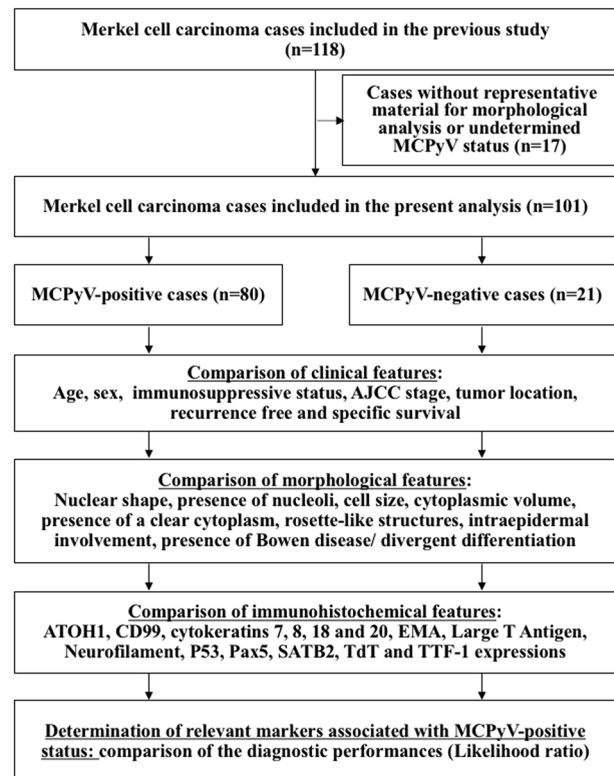


Fig. 1 Flow chart of the study

MCPyV-positive and -negative cases harbor distinct morphologic features

To evaluate the morphologic differences between the virus-positive and -negative Merkel cell carcinoma cases, assessment of nine microscopic criteria was conducted (Table 1/ Fig. 2). We identified nuclear roundness to be associated ($p = 0.005$) with virus-positivity, while elongated nuclei—similar to the spindle-shape variant of small cell lung cancer—were observed more frequently in virus-negative cases. Moreover, the latter samples more frequently displayed a “large cell neuroendocrine carcinoma” phenotype, with larger cell size ($p = 0.026$), abundant cytoplasm ($p = 4 \times 10^{-7}$) and clearly visible nucleoli ($p = 0.002$) (Table 1/ Fig. 2). The combination of elongated nuclei and abundant cytoplasm was observed in 19% ($n = 4$) and 1% ($n = 1$) of virus-negative and -positive cases, respectively. Furthermore, rosette-like structures (supplementary data S2) and clear cytoplasm (Fig. 2) were also associated with absence of Merkel cell polyomavirus ($p = 0.02$ and 2×10^{-6} respectively). To note, 100% of cases with clear cytoplasm have also an extended cytoplasmic size. Finally, only virus-negative Merkel cell carcinoma harbored intraepidermal Merkel cell carcinoma components and displayed Bowen-associated disease or divergent differentiation (supplementary data S2).

Table 1 Clinical, morphologic and immunohistochemical features of MCPyV-negative ($n = 21$) and -positive MCC ($n = 80$) cases. Characteristics of the two subsets were compared by non-parametric Mann Whitney and Fisher's exact tests for quantitative and qualitative data, respectively. For survival analyses, log rank test was used. Positive likelihood ratios for MCPyV positivity were assessed for markers that differed between the two groups ($p < 0.05$), by MCPyV status, by real-time PCR as the gold standard and predetermined cutoffs (underlined criteria vs rest) [4, 6, 11]

	Merkel cell carcinoma cases		<i>P</i> value*	Positive likelihood ratio (95% CI)
	MCPyV-negative ($n = 21$)	MCPyV-positive ($n = 80$)		
<i>Clinical features</i>				
Age, years			0.25	–
Median, quartiles	81 (76–85)	78 (69–84)		
Missing data	3	4		
Sex			0.8	–
F/M	12/8	45/35		
Missing data	1	0		
Immunosuppressive status			0.67	–
Yes	1 (7%)	9 (16%)		
No	13 (93%)	46 (84%)		
Missing data	7	25		
AJCC stage			0.45	–
I	7 (47%)	18 (27%)		
II	3 (20%)	22 (32%)		
III	5 (33%)	24 (36%)		
IV	0	2 (3%)		
Missing data	6	14		
Location			0.09	–
Head	9 (60%)	21 (30%)		
Trunk	0	4 (6%)		
Upper limb	0	5 (7%)		
Lower limb	5 (33%)	28 (39%)		
Unknown primary	1 (6.7%)	13 (18%)		
Missing data	6	9		
Recurrence free, month			0.005	–
Mean survival, 95% CI	11 (9–13)	66 (54–79)		
Missing data	8	13		
Specific death, month			0.027	–
Mean survival, 95% CI	30 (5–21)	88 (76–99)		
Missing data	8	13		
<i>Morphologic features</i>				
Nuclear shape			0.005	1.39
Regular	14 (67%)	74 (93%)		(1.02–1.89)
Elongated	7 (33%)	6 (7%)		
Uninterpretable cases	0	0		
Nucleoli			0.002	1.30
None/inconspicuous	16 (76%)	78 (99%)		(1.02–1.65)
Present	5 (24%)	1 (1%)		
Uninterpretable cases	0	1		
Cell size			0.026	1.20
Small (<2 Lc)	5 (24%)	17 (22%)		(0.97–1.49)
Moderate (2–3 Lc)	12 (57%)	58 (75%)		

Table 1 (continued)

	Merkel cell carcinoma cases		<i>P</i> value*	Positive likelihood ratio (95% CI)
	MCPyV-negative (<i>n</i> = 21)	MCPyV-positive (<i>n</i> = 80)		
Large (>3 Lc)	4 (19%)	2 (3%)		
Uninterpretable cases	0	3		
Cytoplasm volume			4 × 10⁻⁷	2.70
None/inconspicuous	7 (33%)	71 (90%)		(1.47–4.96)
Abundant	14 (67%)	8 (10%)		
Uninterpretable cases	0	1		
Clear cytoplasm			2 × 10⁻⁶	1.73
No	12 (57%)	78 (99%)		(1.19–2.50)
Yes	9 (43%)	1 (1%)		
Uninterpretable cases	0	1		
Rosette-like structure			0.02	1.35
No	14 (67%)	71 (90%)		(0.99–1.84)
Yes	7 (33%)	8 (10%)		
Uninterpretable cases	0	1		
Intraepidermal component			0.04	1.1
No	19 (90%)	80 (100%)		(0.96–1.27)
Yes	2 (10%)	0		
Uninterpretable cases	0	0		
Divergent differentiation			0.001	1.24
No	17 (81%)	80 (100%)		(1–1.52)
Yes	4 (19%)	0		
Uninterpretable cases	0	0		
Associated intraepithelial neoplasia			0.04	1.1 (0.96–1.27)
No	19 (90%)	80 (100%)		
Yes	2 (10%)	0		
Uninterpretable cases	0	0		
<i>Immunohistochemical profile</i>				
Cytokeratin 20			0.02	4.5
Negative	2 (10%)	6 (8%)		(0.64–31.63)
Diffuse	2 (10%)	0		
Mixed	14 (75%)	52 (68%)		
Dot-like pattern	1 (5%)	18 (23%)		
Uninterpretable cases	2	4		
Cytokeratin 8			0.02	1.73
Negative	0	0		(0.90–3.33)
Diffuse	0	0		
Mixed	10 (63%)	26 (35%)		
Dot-like pattern	6 (37%)	48 (65%)		
Uninterpretable cases	5	6		
Cytokeratin 18			0.006	2.18
Negative	1 (5%)	0		(1.01–4.70)
Diffuse	0	0		
Mixed	13 (69%)	28 (39%)		

Table 1 (continued)

	Merkel cell carcinoma cases		<i>P</i> value*	Positive likelihood ratio (95% CI)
	MCPyV-negative (<i>n</i> = 21)	MCPyV-positive (<i>n</i> = 80)		
Dot-like pattern	5 (26%)	43 (61%)		
Uninterpretable cases	2	9		
TTF-1			4 × 10⁻⁶	1.92
Negative	10 (40%)	72 (96%)		(1.24–2.98)
Positive	10 (50%)	3 (4%)		
Uninterpretable cases	1	5		
ATOH1			0.05	–
Negative	0	1 (1%)		
Low/heterogenous	3 (15%)	29 (38%)		
High and diffuse	17 (85%)	46 (61%)		
Uninterpretable cases	1	4		
Neurofilament			0.04	1.49
Negative	9 (47%)	17 (22%)		(0.95–2.31)
Dot-like pattern	10 (53%)	61 (78%)		
Uninterpretable cases	2	2		
SATB2			0.07	–
Negative	5 (25%)	6 (8%)		
Low/heterogenous	6 (30%)	19 (24%)		
High and diffuse	9 (45%)	54 (68%)		
Uninterpretable cases	1	1		
CD99			0.02	8.08
Negative	1 (5%)	12 (15%)		(2.16–30.21)
Dot-like pattern	2 (10%)	63 (81%)		
Diffus	17 (85%)	3 (4%)		
Uninterpretable cases	1	2		
PAX5			0.90	–
Negative	16 (80%)	57 (74%)		
Low/heterogenous	4 (20%)	16 (21%)		
High and diffuse	0	4 (5%)		
Uninterpretable cases	1	3		
TdT			0.34	–
Negative	16 (89%)	60 (76%)		
Positive	2 (11%)	19 (23%)		
Uninterpretable cases	3	1		
EMA			0.003	2.70
Negative	5 (25%)	22 (29%)		(1.10–6.64)
Low/heterogenous	11 (55%)	13 (17%)		
High and diffuse	4 (20%)	41 (54%)		
Uninterpretable cases	1	4		
Cytokeratin 7			0.006	1.36
Negative	12 (71%)	69 (96%)		(1–1.85)
Positive	5 (29%)	3 (4%)		
Uninterpretable cases	4	8		
p53			2 × 10⁻⁹	3.63
No expression	7 (37%)	2 (3%)		(1.71–7.7118)

Table 1 (continued)

	Merkel cell carcinoma cases		<i>P</i> value*	Positive likelihood ratio (95% CI)
	MCPyV-negative (<i>n</i> = 21)	MCPyV-positive (<i>n</i> = 80)		
Heterogenous expression	5 (26%)	63 (95%)		
Overexpression	7 (37%)	1 (2%)		
Uninterpretable cases	2	14		
Large T antigen			2 × 10⁻⁹	–
Negative	17 (100%)	17 (23%)		
Positive	0	58 (77%)		
Uninterpretable cases	4	5		

AJCC American Joint Committee on Cancer, *ATOH1* atonal homolog 1, *CI* 95 confidence interval 95%, *Lc* lymphocytes, *MUC1* cell surface-associated mucin 1, *PAX5* paired box protein 5, *qPCR* quantitative PCR, *SATB2* special AT-rich sequence-binding protein 2, *TdT* terminal deoxynucleotidyl transferase, *TTF-1* thyroid transcription factor 1. *quantitative and qualitative variables were compared by Mann Whitney and Fisher's tests, for survival analyses log rank test was used *p* values < 0.05 and subsequent positive likelihood ratios are in bold

These results confirmed that many Merkel cell polyomavirus-positive and -negative Merkel cell carcinoma can be distinguished based on morphological criteria [7, 18, 19] which probably reflects significant biological differences between the two groups. However, we also identified difficult-to-classify MCPyV-negative cases lacking prototypic morphologic features (supplementary data S2).

MCPyV-positive and -negative cases feature distinct immunohistochemical profiles

To determine whether also immunohistochemistry could discriminate between virus-positive and -negative Merkel cell carcinoma, we compared the two groups with respect to expression of a panel of diagnostic markers (Fig. 3/Table 1). Positivity for TTF1 and cytokeratin 7, lack of or overexpression of p53, and frequent lack of expression of neurofilament were hallmarks of the virus-negative cases (Table 1). By contrast, virus-positive cases not only featured large T antigen-positivity but also high EMA expression and more frequently a dot like staining pattern for the cytokeratins 8, 18 and 20, as well as for CD99. These findings demonstrate substantial variations in the immunohistochemical profiles of virus-positive and -negative Merkel cell tumors and additionally suggest a possible impact of the T antigens on cytoskeletal organization.

CD99 dot-like pattern as a marker of MCPyV-positive Merkel cell carcinoma

To compare the performances of all investigated markers to predict virus status, positive likelihood ratios were determined by using previously described cut-offs [7, 10, 16, 18] (Table 1). These analyses identified CD99 dot-like expression pattern as most highly associated with virus-positivity

of Merkel cell carcinoma (sensitivity = 81% [95% CI: 70–89], specificity = 90% [95% CI: 68–99], positive predictive value = 97% [95% CI: 89–99], negative predictive value 55% [95% CI: 43–66], positive likelihood ratio = 8.08 [95% CI: 2.16–30.21]). In line with this, such CD99 dot-like pattern was found in 86% (*n* = 49/57) of the cases which demonstrated large T antigen-expression in immunohistochemistry, as compared with only 35% (*n* = 12/34) of large T antigen-negative cases (supplementary data S3). Of interest, 10 MCPyV-positive cases lacking immunohistochemical large T antigen expression still showed a CD99 dot-like expression pattern (positive and negative predictive values of CD99 dot pattern for MCPyV status determination in the Large T non expressing cases: 83% [95% CI: 56–95] and 71% [95% CI: 56–82] respectively). These results suggest that the CD99 expression pattern might serve as an additional indicator to evaluate the Merkel cell carcinoma virus status.

Discussion

With respect to tumor cell morphology and immunophenotype, several differences between virus-positive and -negative Merkel cell carcinoma were assessed in the present study. In accordance with previous reports [7, 18], several distinctive microscopic features were observed between the two groups. Moreover, the virus-negative tumors differed from the others by a so called “aberrant” immunohistochemical profile [8] with reduced expression of the Merkel cell carcinoma marker i.e., neurofilament and a more prevalent positivity of those normally observed in extra-cutaneous neuroendocrine carcinomas such as TTF-1 and cytokeratin 7. Interestingly, dot-like expression patterns of cytokeratins and CD99 were more frequent in virus-

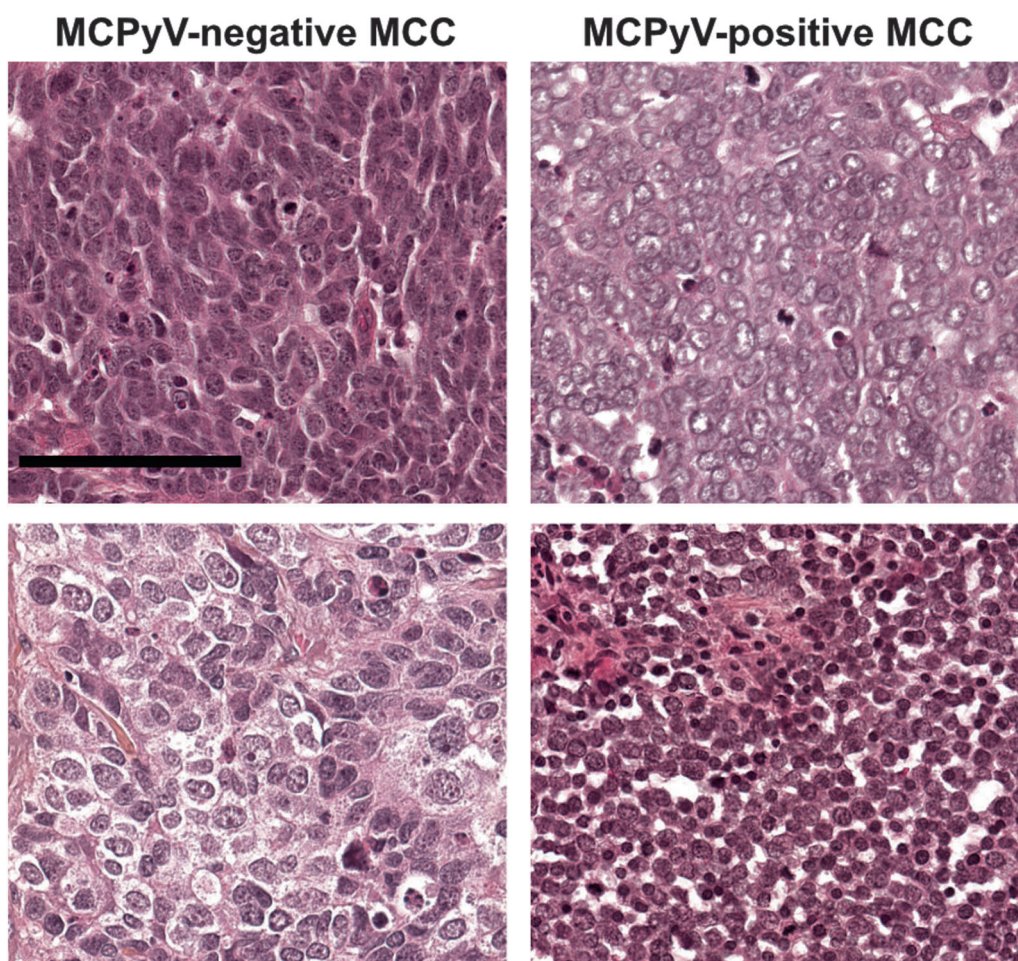


Fig. 2 Morphologic features of MCPyV-negative and -positive Merkel cell carcinoma cases (bar = 100 μ m): on standard examination, MCPyV-negative cases are characterized by more irregular, elongated nuclei as observed in small cell lung cancer. Additionally, some cases

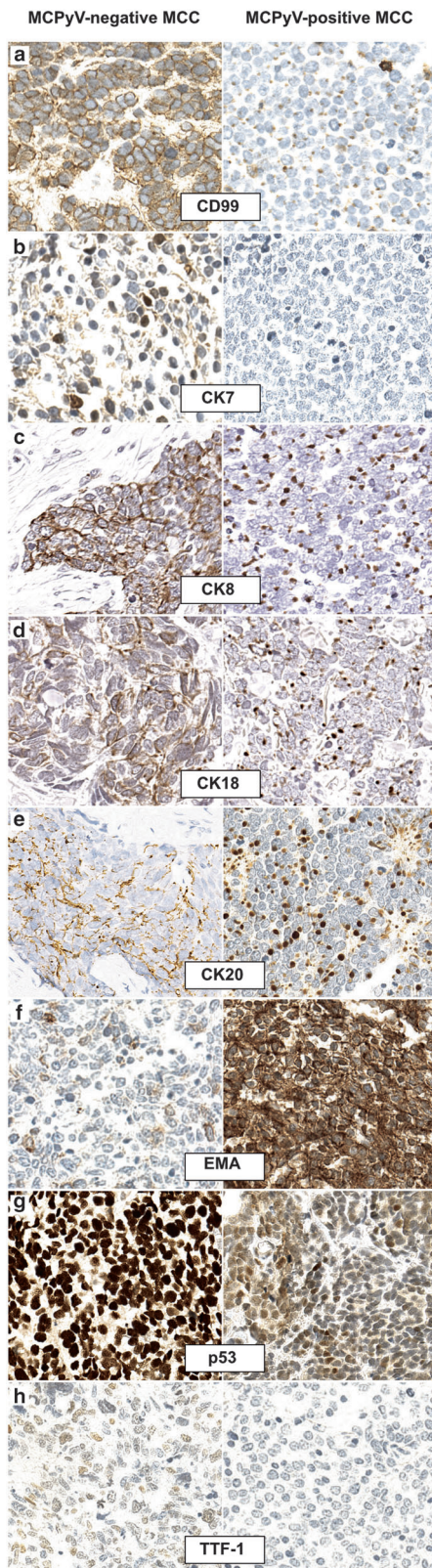
had large cell neuroendocrine carcinoma features with abundant and clear cytoplasm and predominant nuclei. By contrast, MCPyV-positive cases are composed of medium to small round tumor cells with scant cytoplasm and round nucleus. MCC: Merkel cell carcinoma

positive cases and accordingly, CD99 expression pattern was identified as suitable additional marker for the determination of the Merkel cell polyomavirus status of Merkel cell carcinoma.

Two viral oncoproteins i.e., small T and Large T are expressed in Merkel cell carcinoma tumor cells and are considered as the main oncogenic triggers for the development of virus-positive Merkel cell carcinoma [20, 21]. In contrast, UV-induced mutations are thought to drive carcinogenesis of virus-negative Merkel cell carcinoma [5, 6, 22, 23]. Targeting of the same oncogenic pathways (RB1 and p53) either by T antigens or somatic mutations, may account for the common neuroendocrine phenotype [24–26] observed in virus-positive and negative Merkel cell carcinomas. Nevertheless virus-negative tumors are now considered as a subset genetically distinct from the others [27] and characterized by a very high mutational burden (10 mutations per Mb) while very low mutation frequencies (0.4 mutations per Mb) were detected in Merkel cell

polyomavirus-positive Merkel cell carcinoma [5, 28–30]. Interestingly genomic complexity and cancer mutation burden have been demonstrated to correlate with microscopic features of tumor cells such as nuclear pleomorphism [31] and cytological atypia [32]. Indeed, in soft tissue tumors [33], “simple karyotype” neoplasias such as Ewing sarcoma with recurrent *EWSR1* rearrangement display uniform, regular cytology, while “complex karyotype” sarcoma feature more pronounced cytological atypia. Similarly, the degree of differentiation was directly related to genomic alteration level in cutaneous squamous cell carcinoma [34].

In line with such observations, substantial morphologic differences were observed between virus-positive and -negative Merkel cell carcinoma. Indeed, Katano et al. [19] reported that the 6 Merkel cell polyomavirus-positive cases investigated were characterized by round and vesicular nuclei with fine granular chromatin and small nucleoli whereas, by contrast, most of the five virus-negative samples had polygonal nuclei with clear cytoplasm. Applying



◀ **Fig. 3** Immunophenotypes of MCPyV-negative and -positive Merkel cell carcinoma cases (bar = 100 μ m): Immunohistochemical investigation of CD99 (a), cytokeratins 7 (b), 8 (c), 18 (d) and 20 (e), EMA (f), p53 (g) and TTF-1 (h) revealed several distinctive features between the two groups: MCPyV-positive status was associated with cytokeratins 8, 18 and 20 and CD99 dot-like expression pattern as well as high EMA expression, whereas MCPyV-negative cases frequently displayed expression of cytokeratin 7 and TTF-1 and abnormal p53 expression. MCC: Merkel cell carcinoma

series, investigating 101 Merkel cell carcinoma cases we provide further confirmation of these microscopy-studies.

Indeed, we found MCPyV-positive cases to be characterized by uniform round-ovoid nuclei, scant cytoplasm, and frequently displaying a morphology close that of Burkitt lymphoma or Ewing sarcoma, both neoplasias either induced by virus or chromosomal translocation [33, 35]. By contrast, more heterogeneous cytological features with marked atypia were observed in virus-negative Merkel cell carcinoma which, in our view, exhibited close similarities with extra-cutaneous neuroendocrine carcinoma. Indeed some virus-negative cases appeared as a dense proliferation of spindle cells with elongated dark nuclei similar to the spindle shape variant of small cell lung cancer [36] while others cases, comparable to the tumor previously reported as large cell neuroendocrine carcinoma of the skin [37], feature abundant cytoplasm and prominent nuclei as shown in Fig. 2. To note, intermediary phenotypes were also observed.

While virus-positive Merkel cell carcinoma is almost exclusively located in the dermis and subcutis, involvement of the epidermis has been mostly reported for virus-negative cases. Indeed, detection of an associated intra-epidermal neoplasia as well as a divergent differentiation are predictive of MCPyV-negative status [7, 38–40]. Although, intra-epidermal spreading of Merkel cell carcinoma was only observed in two cases in our study, both of them were virus-negative suggesting that epidermotropism as an additional –although rare- characteristic of virus-negative Merkel cell carcinoma.

Whereas cytokeratin 20-positivity and TTF-1 negativity are currently used in routine practice to distinguish Merkel cell carcinomas from extra-cutaneous carcinomas [10, 41], our study confirms the prevalence of so called “aberrant” immunohistochemical profiles in virus-negative cases [8]. Indeed, these latter differed from the viral induced tumors by a more frequent negativity of the Merkel cell carcinoma markers i.e., neurofilament [8, 42, 43], and more frequent positivity of TTF-1 [44] and cytokeratin 7 [8, 45] again underlining the phenotypic similarities between virus-negative Merkel cell carcinoma and extra-cutaneous neuroendocrine carcinomas. In addition, abnormal p53 expression probably due to loss of protein function by somatic mutations was frequently observed in UV-induced tumors as previously reported [46, 47].

morphometry, Kuwamoto et al. [7, 18] confirmed that virus-negative cases had more irregular nuclei and more abundant cytoplasm in a set of 26 Merkel cell carcinoma cases. In our

Interestingly, cytokeratins and CD99 “dot-like” patterns were associated with virus-positivity of Merkel cell carcinoma. In the interfollicular epidermis under physiological conditions, cytokeratins 8, 18 and 20 expression is restricted to the Merkel cell lineage [48–50] and accordingly, frequent positivity of Merkel cell carcinoma for these cytokeratins is observed [27]. In contrast to non-neoplastic Merkel cells that show a diffuse cytokeratin expression, Merkel cell carcinoma cells often harbor cytokeratins arranged in paranuclear dots. Of note, expression of cytokeratins 8 and 18 either in a diffuse or in a dot-like pattern can also be observed in extra-cutaneous high grade neuroendocrine carcinomas [51, 52]. Interestingly such cytokeratins dot-like pattern in virus-positive Merkel cell carcinoma not only renders this feature a useful additional marker for diagnosis but also suggests a potential involvement of the T antigens in cytokeratin “dot like” relocation. Indeed, using a transgenic mouse model, Verhaegen et al. [53] previously obtained similar cytokeratins 8 and 20 dot-like pattern upon ectopic expression of small T in Merkel cells and in line with such findings, capability of T antigens to disrupt cellular cytoskeletal organization has previously been emphasized [54, 55]. A possible explanation for these dots is entrapment of the Golgi apparatus in the cytokeratin aggregates which might explain why not only cytokeratins but also the membrane protein CD99 can be found in paranuclear dots. Indeed, CD99 is a transmembrane protein involved in a broad spectrum of physiological and pathological conditions such as cell migration and intracellular trafficking [56]. In Epstein Barr virus-related Hodgkin lymphoma, direct downregulation of CD99 by the latent membrane protein 1 (LMP1) affects tumor cell differentiation and contributes to immune escape via downregulation of major histocompatibility complex class 1 [57]. Therefore CD99 sequestration in cytoplasmic “dot”, might reduce the protein membrane delivery, and consequently contribute to the aggressiveness of virus positive-Merkel cell carcinoma.

While determination of the Merkel cell polyomavirus status is not yet recommended in the Merkel cell carcinoma guidelines, virus-negative cases constitute a subset of tumors phenotypically [8, 18] and genetically [5, 6] distinct from the others as described above and as underscored by the present study. In particular, increased aggressiveness and worse outcome [9] suggest a potential value of routine determination of the virus status in Merkel cell carcinoma patients. Although further confirmation in independent cohorts are needed, our results suggest that CD99 expression—with testing already available in pathology laboratories—might be used as a surrogate or associated with large T antigen immunohistochemistry to predict MCPyV status in clinical practice.

To conclude, our results confirm that MCPyV-positive and -negative Merkel cell carcinoma cases are characterized

by distinct morphological and immunohistochemical features that imply a significant difference in tumor biology and behavior. Importantly, we identified a dot-like pattern in CD99 expression as a relevant marker associated with MCPyV status.

Acknowledgements Fondation ARC pour la recherche contre le cancer.

Compliance with ethical standards

Conflict of interest The authors declare that they have no conflict of interest.

Publisher's note: Springer Nature remains neutral with regard to jurisdictional claims in published maps and institutional affiliations.




References

1. Becker JC, Stang A, DeCaprio JA, et al. Merkel cell carcinoma. *Nat Rev Dis Prim.* 2017;3:17077.
2. Cook M, Baker K, Redman M, et al. Differential outcomes among immunosuppressed patients with merkel cell carcinoma: impact of immunosuppression type on cancer-specific and overall survival. *Am J Clin Oncol.* 2019;42:82–8.
3. Paulson KG, Park SY, Vandeven NA, et al. Merkel cell carcinoma: Current US incidence and projected increases based on changing demographics. *J Am Acad Dermatol.* 2018;78:457–63.e2.
4. Feng H, Shuda M, Chang Y, et al. Clonal integration of a polyomavirus in human Merkel cell carcinoma. *Science.* 2008;319:1096–100.
5. Harms PW, Vats P, Verhaegen ME, et al. The Distinctive Mutational Spectra of Polyomavirus-Negative Merkel Cell Carcinoma. *Cancer Res.* 2015;75:3720–27.
6. Carter MD, Gaston D, Huang W-Y, et al. Genetic Profiles of Different Subsets of Merkel Cell Carcinoma Show Links between Combined and Pure MCPyV-negative Tumors. *Hum Pathol.* 2018;71:117–25.
7. Kuwamoto S, Higaki H, Kanai K, et al. Association of Merkel cell polyomavirus infection with morphologic differences in Merkel cell carcinoma. *Hum Pathol.* 2011;42:632–40.
8. Pasternak S, Carter MD, Ly TY, et al. Immunohistochemical profiles of different subsets of Merkel cell carcinoma. *Hum Pathol.* 2018;82:232–8.
9. Moshiri AS, Doumani R, Yelistratova L, et al. Polyomavirus-negative merkel cell carcinoma: a more aggressive subtype based on analysis of 282 cases using multimodal tumor virus detection. *J Invest Dermatol.* 2017;137:819–27.
10. Kervarrec T, Tallet A, Miquelestorena-Standley E, et al. Diagnostic accuracy of a panel of immunohistochemical and molecular markers to distinguish Merkel cell carcinoma from other neuroendocrine carcinomas. *Mod Pathol.* 2019;32:499–510.
11. Kervarrec T, Gaboriaud P, Berthon P, et al. Merkel cell carcinomas infiltrated with CD33+myeloid cells and CD8+T cells are associated with improved outcome. *J Am Acad Dermatol.* 2018;78:973–82.
12. Gardair C, Samimi M, Touzé A, et al. Somatostatin receptors 2A and 5 are expressed in merkel cell carcinoma with no association with disease severity. *Neuroendocrinology.* 2015;101:223–35.
13. Harms KL, Healy MA, Nghiem P, et al. Analysis of prognostic factors from 9387 Merkel cell carcinoma cases forms the basis for

- the New 8th Edition AJCC staging system. *Ann Surg Oncol*. 2016;23:3564–71.
14. Schrama D, Sarosi E-M, Adam C, et al. Characterization of six Merkel cell polyomavirus-positive Merkel cell carcinoma cell lines: Integration pattern suggest that large T antigen truncating events occur before or during integration. *Int J Cancer*. 2019.
 15. Watanabe G, Ishida T, Furuta A, et al. Combined Immunohistochemistry of PLK1, p21, and p53 for predicting TP53 status: an independent prognostic factor of breast cancer. *Am J Surg Pathol*. 2015;39:1026–34.
 16. Kervarrec T, Samimi M, Gaboriaud P, et al. Detection of the Merkel cell polyomavirus in the neuroendocrine component of combined Merkel cell carcinoma. *Virchows Arch Int J Pathol*. 2018;472:825–37.
 17. Murakami I, Takata K, Matsushita M, et al. Immunoglobulin expressions are only associated with MCPyV-positive Merkel cell carcinomas but not with MCPyV-negative ones: comparison of prognosis. *Am J Surg Pathol*. 2014;38:1627–35.
 18. Iwasaki T, Matsushita M, Kuwamoto S, et al. Usefulness of significant morphologic characteristics in distinguishing between Merkel cell polyomavirus-positive and Merkel cell polyomavirus-negative Merkel cell carcinomas. *Hum Pathol*. 2013;44:1912–7.
 19. Katano H, Ito H, Suzuki Y, et al. Detection of Merkel cell polyomavirus in Merkel cell carcinoma and Kaposi's sarcoma. *J Med Virol*. 2009;81:1951–8.
 20. Shuda M, Guastafierro A, Geng X, et al. Merkel cell polyomavirus small T antigen induces cancer and embryonic merkel cell proliferation in a transgenic mouse model. *PLoS ONE*. 2015;10:e0142329.
 21. Houben R, Adam C, Baeurle A, et al. An intact retinoblastoma protein-binding site in Merkel cell polyomavirus large T antigen is required for promoting growth of Merkel cell carcinoma cells. *Int J Cancer*. 2012;130:847–56.
 22. Goh G, Walradt T, Markarov V, et al. Mutational landscape of MCPyV-positive and MCPyV-negative Merkel cell carcinomas with implications for immunotherapy. *Oncotarget*. 2016;7:3403–15.
 23. Wong SQ, Waldeck K, Vergara IA, et al. UV-associated mutations underlie the etiology of MCV-negative merkel cell carcinomas. *Cancer Res*. 2015;75:5228–34.
 24. Kaplan-Lefko PJ, Chen T-M, Ittmann MM, et al. Pathobiology of autochthonous prostate cancer in a pre-clinical transgenic mouse model. *Prostate*. 2003;55:219–37.
 25. Syder AJ, Karam SM, Mills JC, et al. A transgenic mouse model of metastatic carcinoma involving transdifferentiation of a gastric epithelial lineage progenitor to a neuroendocrine phenotype. *Proc Natl Acad Sci USA*. 2004;101:4471–6.
 26. González-Vela MDC, Curiel-Olmo S, Derdak S, et al. Shared oncogenic pathways implicated in both virus-positive and UV-induced merkel cell carcinomas. *J Invest Dermatol*. 2017;137:197–206.
 27. Busam KJ, Walsh N, Wood BA, Merkel cell carcinoma. In Elder DE, Massi D, Scolyer R, Willemze R, editors. *WHO classification of skin tumours*, 4th edition. Lyon: International Agency for Research on Cancer, 2018. p48–9.
 28. Yarchoan M, Albacker LA, Hopkins AC, et al. PD-L1 expression and tumor mutational burden are independent biomarkers in most cancers. *JCI Insight*. 2019;4:126908.
 29. George J, Lim JS, Jang SJ, et al. Comprehensive genomic profiles of small cell lung cancer. *Nature*. 2015;524:47–53.
 30. Peifer M, Fernández-Cuesta L, Sos ML, et al. Integrative genome analyses identify key somatic driver mutations of small-cell lung cancer. *Nat Genet*. 2012;44:1104–10.
 31. Cancer Genome Atlas Research Network. Comprehensive and integrated genomic characterization of adult soft tissue sarcomas. *Cell*. 2017;171:950–65. e28.
 32. Budczies J, Bockmayr M, Denkert C, et al. Classical pathology and mutational load of breast cancer—integration of two worlds. *J Pathol Clin Res*. 2015;1:225–38.
 33. Mariño-Enríquez A, Bovée JVMG. Molecular pathogenesis and diagnostic, prognostic and predictive molecular markers in sarcoma. *Surg Pathol Clin*. 2016;9:457–73.
 34. Inman GJ, Wang J, Nagano A, et al. The genomic landscape of cutaneous SCC reveals drivers and a novel azathioprine associated mutational signature. *Nat Commun*. 2018;9:3667.
 35. Rochford R, Moormann AM. Burkitt's Lymphoma. *Curr Top Microbiol Immunol*. 2015;390:267–85.
 36. Travis W, Nicholson S, Hirsch RR et al. Small cell carcinoma. In Travis WD editor. *WHO classification of tumours of lung, pleura, thymus and heart*: [... reflects the views of a working group that convened for a consensus and editorial meeting at the International Agency for Research on Cancer, Lyon, April 24–26, 2014], 4th edition. Lyon: International Agency for Research on Cancer, 2015. p31–3.
 37. Nagase K, Kimura H, Yonekura N, et al. Large-cell neuroendocrine carcinoma of the skin: ultrastructural and immunohistochemical findings. *J Cutan Pathol*. 2016;43:1067–73.
 38. Martin B, Poblet E, Rios JJ, et al. Merkel cell carcinoma with divergent differentiation: histopathological and immunohistochemical study of 15 cases with PCR analysis for Merkel cell polyomavirus. *Histopathology*. 2013;62:711–22.
 39. Busam KJ, Jungbluth AA, Rekhman N, et al. Merkel cell polyomavirus expression in merkel cell carcinomas and its absence in combined tumors and pulmonary neuroendocrine carcinomas. *Am J Surg Pathol*. 2009;33:1378–85.
 40. Walsh NM. Primary neuroendocrine (Merkel cell) carcinoma of the skin: morphologic diversity and implications thereof. *Hum Pathol*. 2001;32:680–9.
 41. Cheuk W, Kwan MY, Suster S, et al. Immunostaining for thyroid transcription factor 1 and cytokeratin 20 aids the distinction of small cell carcinoma from Merkel cell carcinoma, but not pulmonary from extrapulmonary small cell carcinomas. *Arch Pathol Lab Med*. 2001;125:228–31.
 42. Miner AG, Patel RM, Wilson DA, et al. Cytokeratin 20-negative Merkel cell carcinoma is infrequently associated with the Merkel cell polyomavirus. *Mod Pathol*. 2015;28:498–504.
 43. Stanoszek LM, Chan MP, Palanisamy N, et al. Neurofilament is superior to cytokeratin 20 in supporting cutaneous origin for neuroendocrine carcinoma. *Histopathology*. 2019;74:504–13.
 44. Czapiewski P, Majewska H, Kutzner H, et al. TTF-1 and PAX5 are frequently expressed in combined merkel cell carcinoma. *Am J Derm*. 2016;38:513–6.
 45. Pulitzer MP, Brannon AR, Berger MF, et al. Cutaneous squamous and neuroendocrine carcinoma: genetically and immunohistochemically different from Merkel cell carcinoma. *Mod Pathol*. 2015;28:1023–32.
 46. Husein-ElAhmed H, Ramos-Pleguezuelos F, Ruiz-Molina I, et al. Histological Features, p53, c-Kit, and Poliovirus Status and Impact on Survival in Merkel Cell Carcinoma Patients. *Am J Derm*. 2016;38:571–9.
 47. Harms PW, Collie AMB, Hovelson DH, et al. Next generation sequencing of Cytokeratin 20-negative Merkel cell carcinoma reveals ultraviolet-signature mutations and recurrent TP53 and RB1 inactivation. *Mod Pathol*. 2016;29:240–8.
 48. Van Keymeulen A, Mascré G, Youseff KK, et al. Epidermal progenitors give rise to Merkel cells during embryonic development and adult homeostasis. *J Cell Biol*. 2009;187:91–100.
 49. Moll I, Roessler M, Brandner JM, et al. Human Merkel cells--aspects of cell biology, distribution and functions. *Eur J Cell Biol*. 2005;84:259–71.

50. Moll I, Paus R, Moll R. Merkel cells in mouse skin: intermediate filament pattern, localization, and hair cycle-dependent density. *J Invest Dermatol.* 1996;106:281–6.
51. Badzio A, Czapiewski P, Gorczyński A, et al. Prognostic value of broad-spectrum keratin clones AE1/AE3 and CAM5.2 in small cell lung cancer patients undergoing pulmonary resection. *Acta Biochim Pol.* 2019;66:111–4.
52. Jerome Marson V, Mazieres J, Groussard O, et al. Expression of TTF-1 and cytokeratins in primary and secondary epithelial lung tumours: correlation with histological type and grade. *Histopathology.* 2004;45:125–34.
53. Verhaegen ME, Mangelberger D, Harms PW, et al. Merkel cell polyomavirus small T antigen initiates merkel cell carcinoma-like tumor development in mice. *Cancer Res.* 2017;77:3151–7.
54. Knight LM, Stakaityte G, Wood JJ, et al. Merkel cell polyomavirus small T antigen mediates microtubule destabilization to promote cell motility and migration. *J Virol.* 2015;89:35–47.
55. Kwun HJ, Wendzicki JA, Shuda Y, et al. Merkel cell polyomavirus small T antigen induces genome instability by E3 ubiquitin ligase targeting. *Oncogene.* 2017;36:6784–92.
56. Manara MC, Pasello M, Scotlandi K. CD99: a cell surface protein with an oncojanus role in tumors. *Genes.* 2018;9:E159.
57. Lee EK, Chae JH, Kang M-S. Nuclear factor- κ B2 represses Sp1-mediated transcription at the CD99 promoter. *Mol Cells.* 2011;32:555–60.

Affiliations

Thibault Kervarrec ^{1,2,3} · Anne Tallet⁴ · Elodie Miquelstorena-Standley ¹ · Roland Houben ³ · David Schrama³ · Thilo Gambichler⁵ · Patricia Berthon² · Yannick Le Corre⁶ · Ewa Hainaut-Wierzbicka⁷ · Francois Aubin⁸ · Guido Bens⁹ · Flore Tabareau-Delalande¹⁰ · Nathalie Beneton¹¹ · Gaëlle Fromont¹² · Flavie Arbion¹² · Emmanuelle Leteurtre¹³ · Michael Herfs¹⁴ · Antoine Touzé² · Mahtab Samimi^{2,15} · Serge Guyétant^{1,2}

¹ Department of Pathology, Université François Rabelais de Tours, CHU de Tours, avenue de la République, 37170 Chambray-les-tours, France

² Biologie des infections à polyomavirus team, UMR INRA ISP 1282, Université François Rabelais de Tours, 31, avenue Monge, 37200 Tours, France

³ Department of Dermatology, Venereology and Allergology, University Hospital Würzburg, Josef-Schneider-Straße 2, 97080 Würzburg, Germany

⁴ Platform of Somatic Tumor Molecular Genetics, Université François Rabelais de Tours, CHU de Tours, avenue de la République, 37170 Chambray-les-tours, France

⁵ Department of Dermatology, Venereology and Allergology, University Hospital Bochum, Gudrunstraße 5, 44791 Bochum, Germany

⁶ Dermatology Department, LUNAM Université, CHU Angers, 4 rue Larrey, 49933 Angers, France

⁷ Dermatology Department, Université de Poitiers, CHU de Poitiers, 2 rue de la Milétrie, 86021 Poitiers, France

⁸ Dermatology Department, Université de Franche Comté, CHU Besançon, EA3181, IFR133, 2 boulevard Fleming, 25030 Besançon, France

⁹ Dermatology Department, CHR d'Orléans, 14 avenue de l'Hôpital, 45100 Orléans, France

¹⁰ Department of Pathology, CHR d'Orléans, 14 avenue de l'Hôpital, 45100 Orléans, France

¹¹ Dermatology Department, CHR Le Mans, 194 avenue Rubillard, 72037 Le Mans Cedex 09, France

¹² Department of Pathology, Université François Rabelais de Tours, CHU de Tours, Boulevard Tonnellé, 37044 Tours, France

¹³ Univ. Lille, Inserm, CHU Lille, UMR-S 1172—JPARC—Jean-Pierre Aubert Research Center, F-59000 Lille, France

¹⁴ Laboratory of Experimental Pathology, GIGA-Cancer, University of Liege, 4000 Liege, Belgium

¹⁵ Dermatology Department, Université François Rabelais, CHU de Tours, avenue de la République, 37170 Chambray-les-tours, France

Differentiating Merkel cell carcinoma of lymph nodes without a detectable primary skin tumor from other metastatic neuroendocrine carcinomas: The ELECTHIP criteria



Thibault Kervarrec, MD, MSc,^{a,b} Julia Zaragoza, MD,^c Pauline Gaboriaud,^b Amélie Le Gouge, MSc,^d Agnès Beby-Defaux, MD,^{e,f} Yannick Le Corre, MD,^g Ewa Hainaut-Wierzbicka, MD,^h Francois Aubin, MD, PhD,ⁱ Guido Bens, MD,^j Patrick Michenet, MD,^k Hervé Maillard, MD,^l Antoine Touzé, PhD,^b Mahtab Samimi, MD, PhD,^{b,c} and Serge Guyétant, MD, PhD^{a,b}
Tours, Poitiers, Angers, Besançon, Orléans, and Le Mans, France

Background: Merkel cell carcinoma (MCC) can present as a cutaneous tumor or a lymph node metastasis without a primary tumor. MCC presenting without a primary tumor (MCCWOPT) can be misinterpreted on histologic examination as lymph node metastasis (LNM) from another neuroendocrine carcinoma (LNMNEC). However, this distinction is crucial for therapeutic management.

Objective: To determine the discriminative criteria for the differential diagnosis of MCCWOPT, LNM from cutaneous MCC, and LNMNECs.

Methods: Clinical, morphologic, and immunohistochemical data (expression of cytokeratins AE1, AE3, 7, 19, and 20; chromogranin A, synaptophysin, thyroid transcription factor-1 [TTF-1]), as well as the presence of Merkel cell polyomavirus (by immunohistochemistry and PCR) were compared in patients with MCCWOPT (n = 17), LNM from a cutaneous MCC (n = 11), and LNMNEC (n = 20; 8 lung, 7 thyroid, 3 digestive tract, 2 other).

Results: MCC (including MCCWOPT and LNM from a cutaneous MCC) differed from LNMNEC by 7 discriminative criteria: 1) elderly age, 2) location of the tumor, 3) extent of the disease, 4) cytokeratin expression, 5) TTF-1 expression, 6) histologic type, and 7) Merkel cell polyomavirus detection, summarized under the acronym ELECTHIP. All MCC patients had ≥ 5 of the ELECTHIP criteria, whereas all patients with LNMNEC (except 1) had < 3 criteria.

Limitations: The discriminant ability of the ELECTHIP criteria should be validated in a second independent set.

From the Department of Pathology, Université Francois Rabelais, Centre Hospitalier Universitaire de Tours, Tours^a; Biologie des Infections à Polyomavirus Team Unite Mixte de Recherche 1282 Infectiologie et Santé Publique, Institut National de la Recherche Agronomique (INRA), Université Francois Rabelais, Tours^b; Dermatology Department, Université Francois Rabelais, Centre Hospitalier Universitaire de Tours, Tours^c; Centre Hospitalier Universitaire de Tours, Biometrical Department, Centre d'Investigation Clinique - Institut National de la Santé et de la Recherche Médicale Centres d'Investigation Clinique 1415^d; Virology Department, Université de Poitiers, Centre Hospitalier Universitaire de Poitiers^e; Récepteurs et Régulation des Cellules Tumorales Team, Poitiers^f; Dermatology Department, LUNAM (L'Université-Nantes-Angers-Le-Mans), Centre Hospitalier Universitaire d'Angers^g; Dermatology Department, Université de Poitiers, Centre Hospitalier Universitaire de Poitiers^h; Dermatology Department, Université de Franche Comté, Centre Hospitalier Universitaire de Besançonⁱ; Dermatology Department, Centre

Hospitalier Régional d'Orléans^j; Department of Pathology, Centre Hospitalier Régional d'Orléans^k; and Dermatology Department, Centre Hospitalier Régional du Mans.^l

Drs Samimi and Guyétant contributed to this work equally.

Funding sources: Supported by project POCAME, Axe Immunothérapies, and Cancéropole Grand Ouest-Région Centre Val de Loire.

Conflicts of interest: None disclosed.

Accepted for publication November 7, 2017.

Reprints not available from the authors.

Correspondence to: Mahtab Samimi, MD, PhD, Dermatology Department, Hospital of Tours, Avenue de la République, 37170, Chambray-les-tours, France. E-mail: mahtab.samimi@univ-tours.fr.

Published online November 24, 2017.

0190-9622/\$36.00

© 2017 by the American Academy of Dermatology, Inc.

<https://doi.org/10.1016/j.jaad.2017.11.037>

Conclusion: MCCWOPT can be distinguished from other LNMNEC by the ELECTHIP criteria. (J Am Acad Dermatol 2018;78:964-72.)

Key words: CK20; differential diagnosis; lymph nodes; MCPyV; Merkel cell carcinoma; metastasis; neuroendocrine carcinoma; TTF-1.

Merkel cell carcinoma (MCC) is a rare aggressive cutaneous neoplasm with a 5-year overall survival rate of 40%.¹ It occurs essentially in elderly patients, and the main risk factors are sun exposure and immunosuppression. Histologic examination reveals infiltration of the dermis or hypodermis by small cells with neuroendocrine features. Immunochemical stainings show the expression of both epithelial and neuroendocrine markers in tumor cells.

Cytokeratin (CK) 20 expression is observed in 92% of MCC cases²; thyroid transcription factor-1 (TTF-1) expression is rare.²

Merkel cell polyomavirus (MCPyV) is a ubiquitous human polyomavirus with seroprevalence reaching 90% in adults.³ In 2008, Feng et al⁴ identified integration of the MCPyV genome in tumor cells of most MCCs. MCPyV DNA is detected by PCR in ~80% of cutaneous MCC cases, and the large T antigen, a major viral oncoprotein, is detected by immunochemical staining in 60% of cases.^{2,5}

Approximately 5%-15% of MCC cases present as a lymph node metastasis (LNM) without a primary skin tumor.⁶⁻⁸ In such cases, superficial lymph nodes are removed and standard histologic examination reveals features of high-grade neuroendocrine carcinoma (NEC) indistinguishable from LNM of an unidentified (non-Merkel cell) NEC (LNMNEC). However, the distinction between MCC without a primary skin tumor (MCCWOPT) and LNMNEC is crucial because of significant differences in therapeutic management and outcome.⁸ Indeed, treatment of MCCWOPT requires lymph node dissection combined with radiotherapy,⁸ and treatment of LNMNEC requires chemotherapy. The outcome for patients with MCCWOPT is worse with chemotherapy alone than with surgery and radiotherapy,⁹ which highlights the need for accurate differential diagnosis of MCCWOPT from LNMNEC.

CK20 and TTF-1 expression profiles, which enable a differential diagnosis between cutaneous

CAPSULE SUMMARY

- Merkel cell carcinoma can initially present in lymph nodes without an evident primary skin tumor.
- When this occurs the tumor might be misdiagnosed as lymph node metastasis from other neuroendocrine carcinomas.
- The ELECTHIP criteria assists in differentiating between these diagnoses and might facilitate the classification of patients with lymph node metastasis from neuroendocrine tumors.

MCC and small-cell NEC from other sites,¹⁰⁻¹² are currently used as diagnostic criteria for a positive diagnosis of MCC. Although features of MCCWOPT have been compared with those from cutaneous MCC,^{13,14} no study has investigated the diagnostic accuracy of any marker for the differential diagnosis of MCCWOPT, LNM from a cutaneous MCC, and LNMNEC.

We aimed to compare the clinical, histologic, and virologic features of these

3 conditions to establish relevant criteria for their differential diagnosis.

METHODS

Design and settings

MCC cases diagnosed in the dermatology departments from 6 hospital centers were considered for inclusion in the historical prospective MCC cohort¹⁵ (local ethics committee, Tours, France, no. ID RCB2009-A01056-51). Formalin-fixed paraffin-embedded (FFPE) tumor samples were reviewed by a pathologist from the French TENPath network (Dr Guyétant) and were included as MCC cases if they displayed a morphology compatible with MCC, together with positive immunostaining for CK20 and ≥ 1 neuroendocrine marker (eg, synaptophysin and chromogranin A). CK20-negative tumors were also considered if the morphology was compatible and ≥ 2 neuroendocrine markers were expressed. Cases of LNMNECs were retrieved from the database of 1 department of pathology (Tours, France) by a search of samples registered during 1999-2015.

Inclusion criteria

MCC cases. For the specific needs of our study, all MCC cases included in our cohort that had available FFPE samples had their medical history and clinical and imaging data reviewed. A diagnosis of MCCWOPT was retained with LNM revealing the cancer, no history of cutaneous MCC or deep NEC, no evidence of cutaneous or extracutaneous primary

Abbreviations used:

CK:	cytokeratin
CT:	computed tomography
ELECTHIP:	elderly age, location of tumor, extent of the disease, cytokeratin expression, TTF-1 expression, histologic type, and MCPyV detection
FFPE:	formalin-fixed paraffin-embedded
LNM:	lymph node metastasis
LNMNEC:	lymph node metastasis from neuroendocrine carcinoma
MANEC:	mixed adenoneuroendocrine carcinoma
MCC:	Merkel cell carcinoma
MCCWOPT:	Merkel cell carcinoma of lymph nodes without skin primary tumor
MCPyV:	Merkel cell polyomavirus
NEC:	neuroendocrine carcinoma
TTF-1:	thyroid transcription factor 1

NEC after exhaustive work-up consisting of cutaneous physical examination and extensive imaging (whole-body computed tomography [CT] scan, 18-fluorodeoxyglucose positron emission tomography CT scan, or both). The samples from patients with LNM from cutaneous MCC were included on the basis of the following criteria: LNM with confirmation of cutaneous MCC primary tumor.

Cases of LNMNEC. MCCWOPT occurs mostly in superficial lymph nodes,⁸ so only patients with superficial LNMs originating from other NECs were included in this group. From our database, we retrieved data of patients with LNMs from any NEC histologic subtype in a superficial location (parotid, cervical, supraclavicular, axillary, or groin areas) and with a lymph node revealing cancer or relapsed cancer, presence of histologic NEC features, and immunohistochemical expression of both neuroendocrine (chromogranin A or synaptophysin) and epithelial (CKAE1-CKAE3) markers.

Exclusion criteria

We excluded data for patients without available tissue samples or insufficient samples to perform molecular analysis.

Clinical and follow-up data

Age, sex, history of cancer, and lymph node location were collected from patient files. Disease extent at the time of diagnosis was classified as localized (restricted to the primary skin and/or one superficial lymph node area) or systemic (extension beyond the skin and the lymph node). Regarding LNMNECs, the primary tumor location was classified as proved (diagnosis on the basis of histologic examination of primary tumor sample), possible (diagnosis on the basis of strong clinical and imaging

arguments without biopsy of the primary tumor sample), or undetermined.

Histology and immunohistochemistry

Histologic classification of tumors was assessed by a pathologist (Dr Guyétant) according to the World Health Organization classification,¹⁶⁻¹⁸ which distinguishes 3 NEC subtypes (small cell, large cell, well-differentiated) on the basis of cytologic features and proliferation rate. Briefly, cases of poorly differentiated NEC shared features of high proliferative activity and frequent necrosis; they were subclassified as small cell NEC when composed of small- to medium-sized cells with a high nucleocytoplasmic ratio, salt-and-pepper chromatin, and inconspicuous nucleoli or subclassified as large cell NEC when composed of larger cells with more abundant cytoplasm and apparent nucleoli. Well-differentiated NECs showed a more prominent nested or trabecular pattern (often with the absence of necrosis), bland cytology, and low proliferation rate.

Tissue samples were included in a tissue microarray with a semimotorized tissue arrayer (tissue microarray booster OI v2.00, ALPHELYS, Westburg, The Netherlands). Triplicate spots were obtained for all patients. Immunohistochemical staining was performed according to the manufacturer's instructions on a BenchMark XT platform (Ventana Medical Systems Inc, Basel, Switzerland). Tumors were screened with relevant markers for NEC (pan-CKAE1-AE3, chromogranin A, synaptophysin), MCC (CK19, CK20, large T antigen) and other NEC markers (TTF-1, CK7). Antibodies and dilutions are in [Supplemental Table I](#) (available at <http://www.jaad.org>). CKAE1-AE3- and CK20-positive cases were classified as dot-like or diffuse according to the staining pattern. Chromogranin A and synaptophysin positive cases were classified as low or high according a arbitrary threshold of 30% of stained cells. Positivity for MCPyV-specific antibody CM2B4 was assessed using the Allred score as previously described.¹⁹

Detection of MCPyV DNA

Genomic DNA was isolated from tissue samples by using the Maxwell 16 Instrument (Promega, Madison, WI) with the Maxwell 16 FFPE Plus LEV DNA Purification Kit (Promega). PCR assays were performed as described.²⁰ Briefly, 15 ng of DNA was mixed with 0.2 μ M primers ([Supplemental Table II](#), available at <http://www.jaad.org>), 0.1 μ M DNA probe, and Mix Life technologies Taqman Universal PCR Master Mix (2X) (Applied Biosystems, Foster City, CA) in a final volume of 25 μ L. PCR reactions

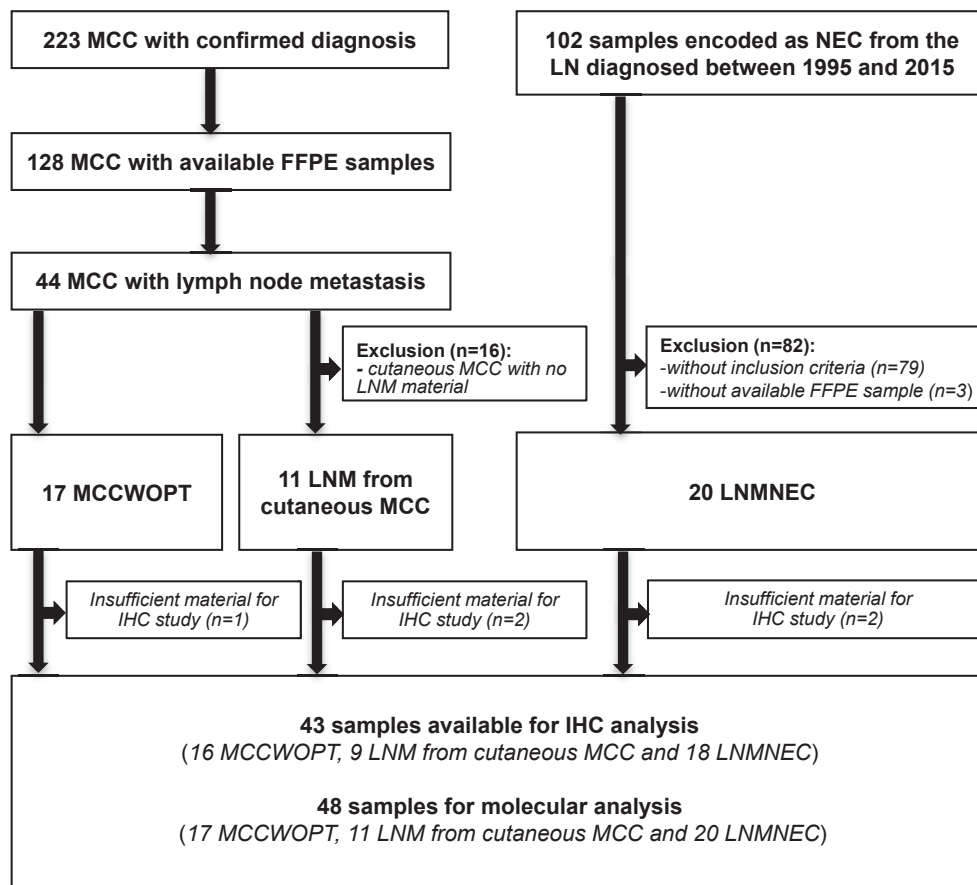


Fig 1. Flow of patients in this study. *FFPE*, Formalin-fixed paraffin-embedded; *IHC*, immunohistochemical; *LN*, lymph node; *LNM*, lymph node metastasis; *MCC*, Merkel cell carcinoma; *MCCWOPT*, Merkel cell carcinoma of lymph node without primary tumor; *NEC*, neuroendocrine carcinoma.

were performed with the Applied Biosystems 7500 Real-Time PCR Systems platform programmed with an initial denaturation at 95°C for 15 min, followed by 45 cycles at 95°C for 15 sec and 60°C for 60 sec.

Statistical analysis

Data involving continuous variables are described with median and quartiles 1-3, and categorical variables with number and percentages of the interpretable cases. Categorical variable data were compared between groups by using the 2-tailed Fisher's exact test. *P* values <.05 were considered statistically significant.

RESULTS

Patient characteristics

Among the 223 patients included in the MCC cohort, FFPE samples were available for 128 cases, including 44 with LNM at the time of diagnosis (Fig 1). Among these, 17 met our criteria for

MCCWOPT and 11 for LNM from cutaneous MCC (Fig 1). Among the 17 patients with MCCWOPT, a dermatologist had performed a skin examination to exclude a primary tumor of the skin or mucosae for 16, and an oncologist had performed multiple physical examinations for 1 (patient 9). Extracutaneous primary NEC was excluded in all 17 cases by imaging (8 with 18-fludeoxyglucose positron emission tomography CT scan, 4 with whole body CT scan, and 5 with both). Two patients underwent endoscopy and indium-111 somatostatin analog scintigraphy (Octreoscan) (patients 1 and 17). Among the 102 patients with NEC and LNM retrieved from our database, 23 with LNMNEC met our inclusion criteria and 3 were excluded because of unavailable samples (Fig 1). Patients had primary LNMNEC tumors of the lung (*n* = 8; 5 with small cell carcinoma and 3 with large cell NEC); thyroid (*n* = 7), or gastrointestinal tract (*n* = 3; 1 with small cell carcinoma and 2 with large cell neuroendocrine

Table I. Characteristics of patients with MCC without primary tumor, LNM from cutaneous MCC, and LNM from neuroendocrine carcinoma

Characteristic	MCCWOPT, n = 17	LNM from cutaneous MCC, n = 11	LNMNEC, n = 20	P value
Age, y, n (%)				<.001
<70	8 (47)	1 (9)	16 (80)	
≥70	9 (53)	10 (91)	4 (20)	
Sex ratio (male/female)	8/9	4/7	11/9	NS
Lymph node location, n (%)				<.01
Parotid	2 (12)	1 (9)	0 (0)	
Cervical	0 (0)	1 (9)	10 (50)	
Supraclavicular	0 (0)	0 (0)	6 (30)	
Axillar	0 (0)	2 (18)	3 (15)	
Inguinal	15 (88)	7 (64)	1 (5)	
Disease extent, n (%)				<.02
Localized	16 (94)	11 (100)	9 (45)	
Systemic	1 (6)	0 (0)	11 (55)	

LNM, Lymph node metastasis; LNMNEC, lymph node metastasis from neuroendocrine carcinoma; MCC, Merkel cell carcinoma; MCCWOPT, Merkel cell carcinoma without primary tumor; NS, not significant.

component of mixed adenoneuroendocrine carcinoma [MANEC]); atypical carcinoid tumor of the arytenoid (n = 1); and unknown cancer (n = 1; large cell NEC).

Clinical data

Clinical features of patients are described in Table I. The median age was 70 (63-79) years. At the time of diagnosis, most of the MCC cases were limited to the inguinal area (15 MCCWOPT and 7 LNM from cutaneous MCC). In contrast, LNMNEC patients with a pulmonary primary tumor (n = 8) had advanced metastatic disease at diagnosis (large mediastinal tumor bulk, extensive lymph-node involvement, and visceral metastases) with no history of NEC. Patients with a gastrointestinal primary tumor (n = 3) had a previous history of NEC and showed aggressive relapse (2 had generalized disease and 1 had localized disease with fast disease progression and death). All patients with primary thyroid (n = 7) and arytenoid (n = 1) cancer showed localized lymph node recurrence. One patient with an unknown primary site (patient 27) had extensive metastatic disease and died a few days after lymph node biopsy.

Immunomorphologic and virologic data

The 3 groups showed close morphological similarities, as illustrated by representative microscopic features of MCCWOPT, LNM from cutaneous MCC and LNMNEC cases in Fig 2. All cases of MCCWOPT and LNM from cutaneous MCC were classified as small cell carcinoma, whereas LNMNEC cases displayed small cell (n = 6), large cell (n = 6), or well-differentiated NEC (n = 8) features.

Comparative immunostaining data for the 43 tumors analyzed is reported in Table II. Marker expression by histologic type and primary tumor site is reported in Supplemental Table III (available at <http://www.jaad.org>). MCPyV DNA was detected in 15 of 17 (88%) patients with MCCWOPT, all patients (100%) with LNM from cutaneous MCC, and 1 patient (5%) with LNM from a large cell NEC of the lung.

Determining diagnostic features — the ELECTHIP criteria

We were able to identify 7 features that differed significantly among MCCWOPT, LNM from cutaneous MCC, and LNMNEC. MCCWOPT and LNM from cutaneous MCC differed from LNMNEC by age (≥70 years vs <70 years, $P < .001$), location of the lymph node (inguinal or parotid vs other locations, $P < .01$), disease extent (localized vs systemic, $P < .01$), histologic type (small cell carcinoma vs large cell carcinoma and well-differentiated tumors, $P < .01$), CK expression (CK20 positive vs CK20 negative, $P < .01$), TTF-1 expression (absent vs present, $P < .01$), and MCPyV detection (present vs absent, $P < .01$). These 7 features can be summarized using the abbreviation ELECTHIP (elderly: ≥70 years, location: inguinal or parotid, extent restricted to the lymph node area, CK20 positivity, TTF-1 negativity, histological type: small cell carcinoma, polyomavirus detection) criteria. In contrast, no differences were observed with sex ratio, CKAE1-CKAE3 expression, and neuroendocrine marker expression between the MCC and LNMNEC groups.

The classification of patients by their diagnosis and number of positive ELECTHIP criteria (0-7) is

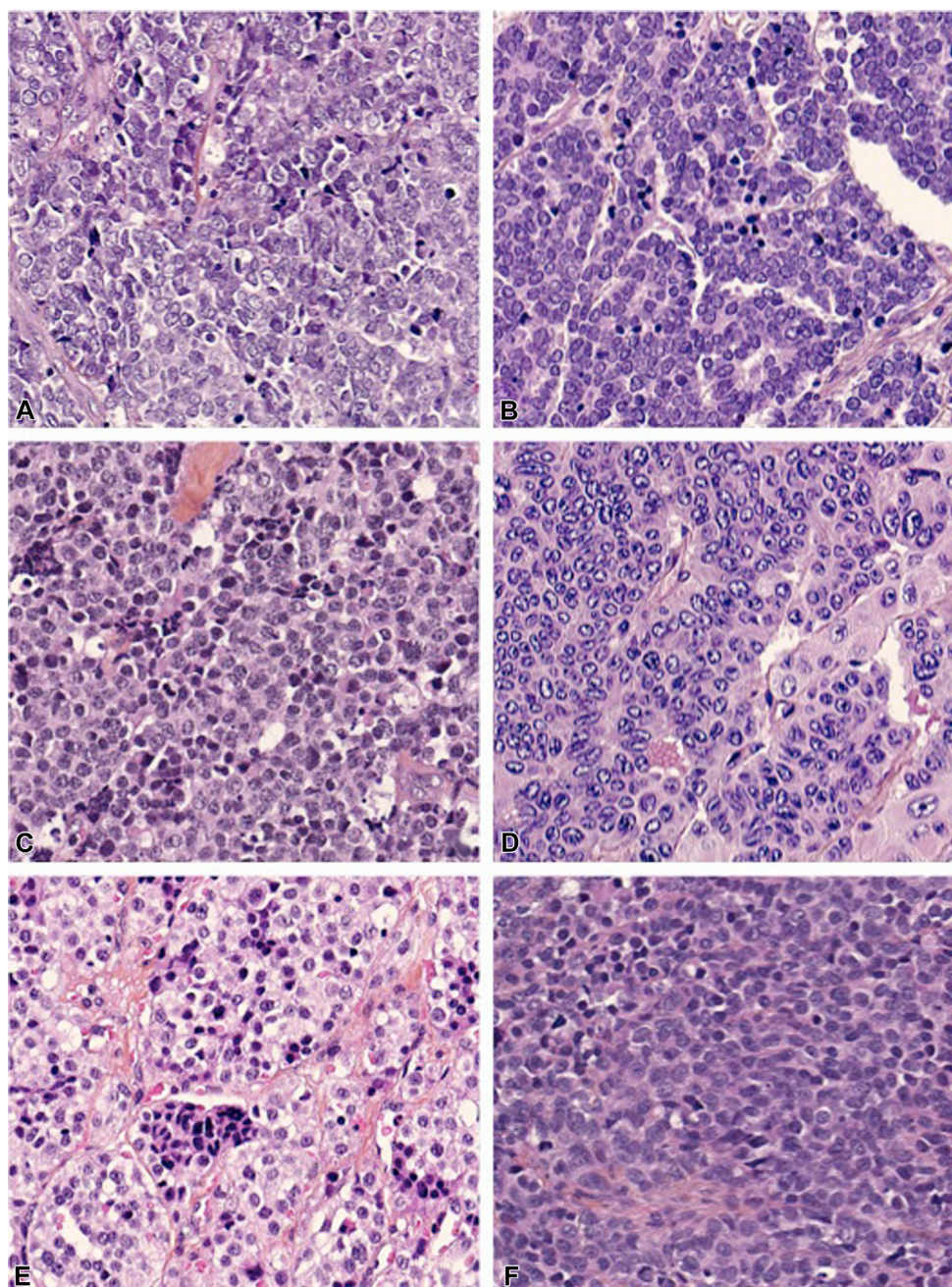


Fig 2. Microscopic features of Merkel cell carcinoma of lymph node without primary tumor (MCCWOPT) (**A**), lymph node metastasis (LNM) from cutaneous MCC (**B**), and LNM from other neuroendocrine carcinomas (NECs) (**C-F**). **C**, Small cell carcinoma of the lung. **D**, Large cell carcinoma of the lung. **E**, Well-differentiated neuroendocrine tumor of the thyroid (medullary thyroid carcinoma). **F**, Neuroendocrine component of mixed adenoneuroendocrine carcinoma from the digestive tract. On morphologic examination, all high-grade NEC cases shared a similar architectural pattern, forming islands and ribbons of uniform tumor cells. Tumors classified as small cell carcinoma (**A, B, C**) displayed a high nucleocytoplasmic ratio, salt-and-pepper chromatin, and a high number of mitoses; large cell NEC (**D, F**) were characterized by abundant cytoplasm and apparent nuclei. Well-differentiated neuroendocrine tumors (**E**: medullary thyroid carcinoma) showed few mitosis and a more obvious nested pattern. (**A-F**, Hematoxylin-eosin staining; original magnifications: $\times 200$.)

Table II. Histologic, immunohistochemical, and virologic features of patients with MCCWOPT, LNM from cutaneous MCC, and LNMNEC

Feature	MCCWOPT, n = 17	LNM from cMCC, n = 11	LNMNEC, n = 20	P value
Histologic features				
Histologic subtypes				<.01
Small cell carcinoma	17 (100)	11 (100)	6 (30)	
Large cell carcinoma	0 (0)	0 (0)	6 (30)	
Well-differentiated tumor	0 (0)	0 (0)	8 (40)	
Immunochemical features				
Cytokeratin expression				
AE1 and AE3				
Dot staining	14 (88)	7 (78)	3 (17)	NS
Diffuse staining	2 (13)	2 (22)	15 (83)	
CK7	0 (0)	0 (0)	8 (44)	<.01
CK19	10 (63)	1 (11)	3 (17)	<.01
CK20				<.01
Dot staining	5 (31)	6 (67)	0 (0)	
Diffuse staining	11 (69)	2 (22)	1 (6)	
Neuroendocrine marker expression				
Chromogranin A expression				
High	14 (88)	7 (78)	14 (78)	NS
Low	2 (13)	2 (22)	4 (22)	
Synaptophysin expression				
High	9 (56)	2 (22)	11 (61)	NS
Low	3 (19)	6 (67)	5 (22)	
Other markers				
TTF-1	1 (6)	0 (0)	14 (78)	<.01
MCPyV detection by immunocytochemistry	8 (50)	4 (44)	0 (0)	<.01
Virologic features				
MCPyV detection by PCR	15 (88)	11 (100)	1 (5)	<.01

CK, Cytokeratin; LNM, lymph node metastasis; LNMNEC, lymph node metastasis from neuroendocrine carcinoma; MCC, Merkel cell carcinoma; MCCWOPT, Merkel cell carcinoma without primary tumor; MCPyV, Merkel cell polyomavirus; NS, not significant; TTF-1, thyroid transcription factor 1.

shown in Fig 3. Among patients with MCCWOPT and LNM from cutaneous MCC, the 7 criteria were assessable in 16 of 17 and 9 of 10 patients, respectively. All of these patients had ≥5 criteria (4 patients had 5 criteria, 12 had 6 criteria, and 9 had 7 criteria). In contrast, 19 of 20 patients with LNM from NEC had <3 criteria (2 patients had 0 criteria, 13 had 1 criterion, and 4 had 2 criteria), except for 1 patient with metastatic digestive MANEC (patient 28), who had 5 criteria.

DISCUSSION

In this study, we examined the diagnostic markers for MCCWOPT, LNM from cutaneous MCC, and LNMNEC to establish criteria for the differential diagnosis of these cancers. MCCWOPT shared similar morphologic and phenotypic features as LNM from cutaneous MCC but were accurately distinguished from other superficial LNMNEC by a spectrum of clinical, histologic, and virologic criteria that were summarized as the ELECTHIP criteria

(elderly: ≥ 70 years, location: inguinal or parotid, extent restricted to the lymph node area, CK20 positivity, TTTF-1 negativity, histological type: small cell carcinoma, polyomavirus detection).

Although MCCWOPT features have been compared with those from cutaneous MCC tumors,^{13,14} the biologic connection between MCCWOPT and cutaneous MCC is still unclear: whether MCCWOPT primarily originates in nodal lymph nodes or occurs after a metastatic process is unknown. In current practice, superficial LNMNEC represents the main differential diagnosis of MCCWOPT and must be distinguished from MCCWOPT because of different therapeutic management and outcome.⁸ It must be emphasized that there is no current gold standard for the positive diagnosis of MCCWOPT. In our study, the classification of cases involved multiple pathology reviewing, as well as a multidisciplinary approach to develop criteria that could be easily used in routine practice.

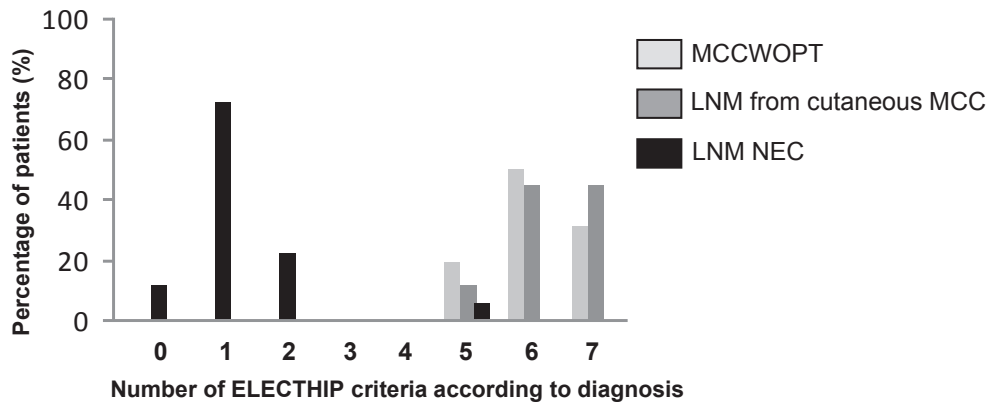


Fig 3. Patient diagnoses by ELECTHIP criteria. All patients with MCCWOPT and LNM from cutaneous MCC had ≥ 5 ELECTHIP criteria, whereas 19 of 20 patients with LNM from NEC had < 3 criteria, except for 1 patient with metastatic digestive mixed adenoneuroendocrine carcinoma, who had 5 criteria. *ELECTHIP*, elderly: ≥ 70 years, location: inguinal or parotid, extent restricted to the lymph node area, CK20 positivity, TTF-1 negativity, histologic type: small cell carcinoma, polyomavirus detection; *LNM*, lymph node metastasis; *MCC*, Merkel cell car; *MCCWOPT*, Merkel cell carcinoma of lymph nodes without skin primary tumor; *NEC*, neuroendocrine carcinoma.

The ELECTHIP criteria include 3 clinical features: age, disease extent, and LNM location. Indeed, MCCWOPT mainly affects older people (median age at onset, 81 years²¹) and is often confined to a single lymph node area.¹⁴ However, LNMNEC, especially small cell carcinoma of the lung,²² occurs in younger patients, often in a setting of extensive disease.

The ELECTHIP criteria include the tumoral CK20 expression, which appears as a robust but not specific marker for MCC. In our study, all patients with MCCWOPT expressed CK20, as did 1 patient with LNMNEC, a large cell NEC component of a metastatic digestive MANEC (patient 28). Although CK20 expression is rare among patients with NEC,^{10,11,23} it can be expressed in patients with MANEC, who have a nonneuroendocrine component (mainly adenocarcinoma) associated with their disease in the primary tumor.¹⁷ Therefore, 1 patient with LNM from MANEC in our series had 5 ELECTHIP criteria, which indicates that LNM from MANEC remains a major diagnostic pitfall in the differential diagnosis of MCCWOPT. Similarly, TTF-1 expression was rarely detected in MCC,² but 1 of our patients with MCCWOPT showed moderate nuclear TTF-1 expression (patient 12). In our experience, as in others,²⁴ moderate nuclear expression of TTF-1 is not an infrequent feature of MCC (15% of our MCC cohort, data not shown) and moderate expression of TTF-1 should not by itself exclude the diagnosis of MCC.

The last ELECTHIP criterium was detection of MCPyV DNA by PCR in tumor samples. Indeed,

MCPyV DNA was detected in 15 of 17 patients with MCCWOPT, all with LNM from cutaneous MCC, and only 1 with LNMNEC. Previously, De Biase et al¹³ detected MCPyV DNA by PCR in 5 of 5 patients with MCCWOPT as compared with 7 of 22 with MCCWOPT by Pan et al.¹⁴ Using immunohistochemistry, Haymerle et al²⁵ detected MCPyV in 4 of 6 patients with MCCWOPT. Such discrepancies have been observed for cutaneous MCC² and probably reflect heterogenous technical procedures (DNA fragmentation in FFPE tissue samples, PCR amplicon size, primer sets, and CM2B4 antibody immunostaining sensitivity). Altogether, our results suggest that MCPyV prevalence in MCCWOPT is probably the same as in its cutaneous counterpart. However, we also detected MCPyV DNA in a large cell NEC of the lung, which is consistent with previous detection of MCPyV in non-Merkel cell neoplasms.²⁶

Because none of the markers we describe allow for accurate discrimination between MCC and LNMNEC when used alone, we suggest combining them into the 7 ELECTHIP criteria. In our cohort, all patients with assessable MCC had ≥ 5 of the 7 criteria, whereas all patients with other metastatic NEC except 1 (with MANEC, discussed previously) showed < 3 criteria. When considering the ELECTHIP criteria as a 7-point diagnostic score, an ELECTHIP score ≥ 3 would be associated with a MCCWOPT diagnosis with sensitivity of 100% (95% confidence interval 84%-100%) and a specificity of 95% (95% confidence interval 75%-100%) in our study sample. Although this score

should be validated in a second independent set of patients before drawing definite conclusions regarding its accuracy, we assessed our tool with 19 additional MCCWOPT patients, with all available items retrieved from the literature,^{13,14} and confirmed ELECTHIP scores of ≥ 3 in all patients: 1 patient had a ELECTHIP score of 3, four score 4, three score 5, seven score 6, and 4 score 7.

To conclude, MCCWOPT represents a well-defined entity in the MCC tumor spectrum. MCCWOPT can be discriminated from LNMNEC by a body of clinical, radiologic, morphologic, and biologic criteria. We suggest the use of the ELECTHIP criteria to optimize classification of these cancers and thus management in current practice.

The authors sincerely thank the patients who gave their approval for the study. They also thank Pr Gaëlle Fromont (Tours, France), Roseline Guibon (Tours, France), Dr Micheline Chargeboeuf (Lons le Saunier, France), Dr Christine Collin (Tours, France), Dr Benjamin Linot (Angers, France), and Dr Isabelle Valo (Angers, France) for their help and contributions to the study.

REFERENCES

- Lemos BD, Storer BE, Iyer JG, et al. Pathologic nodal evaluation improves prognostic accuracy in Merkel cell carcinoma: analysis of 5823 cases as the basis of the first consensus staging system. *J Am Acad Dermatol*. 2010;63:751-761.
- Kuwamoto S. Recent advances in the biology of Merkel cell carcinoma. *Hum Pathol*. 2011;42:1063-1077.
- Nicol JT, Robinot R, Carpentier A, et al. Age-specific seroprevalences of Merkel cell polyomavirus, human polyomaviruses 6, 7, and 9, and trichodysplasia spinulosa-associated polyomavirus. *Clin Vaccin Immunol*. 2013;20:363-368.
- Feng H, Shuda M, Chang Y, Moore PS. Clonal integration of a polyomavirus in human Merkel cell carcinoma. *Science*. 2008;319:1096-1100.
- Shuda M, Arora R, Kwun HJ, et al. Human Merkel cell polyomavirus infection I. MCV T antigen expression in Merkel cell carcinoma, lymphoid tissues and lymphoid tumors. *Int J Cancer J Int Cancer*. 2009;125:1243-1249.
- Reichgelt BA, Visser O. Epidemiology and survival of Merkel cell carcinoma in the Netherlands. A population-based study of 808 cases in 1993-2007. *Eur J Cancer Oxf Engl*. 1990. 2011;47:579-585.
- Fields RC, Busam KJ, Chou JF, et al. Five hundred patients with Merkel cell carcinoma evaluated at a single institution. *Ann Surg*. 2011;254:465-473. discussion 473-475.
- Kotteas EA, Pavlidis N. Neuroendocrine Merkel cell nodal carcinoma of unknown primary site: management and outcomes of a rare entity. *Crit Rev Oncol Hematol*. 2015;94:116-121.
- Deneve JL, Messina JL, Marzban SS, et al. Merkel cell carcinoma of unknown primary origin. *Ann Surg Oncol*. 2012;19:2360-2366.
- Cheuk W, Kwan MY, Suster S, Chan JK. Immunostaining for thyroid transcription factor 1 and cytokeratin 20 aids the distinction of small cell carcinoma from Merkel cell carcinoma, but not pulmonary from extrapulmonary small cell carcinomas. *Arch Pathol Lab Med*. 2001;125:228-231.
- Chan JK, Suster S, Wenig BM, Tsang WY, Chan JB, Lau AL. Cytokeratin 20 immunoreactivity distinguishes Merkel cell (primary cutaneous neuroendocrine) carcinomas and salivary gland small cell carcinomas from small cell carcinomas of various sites. *Am J Surg Pathol*. 1997;21:226-234.
- Bobos M, Hytiroglou P, Kostopoulos I, Karkavelas G, Papadimitriou CS. Immunohistochemical distinction between merkel cell carcinoma and small cell carcinoma of the lung. *Am J Dermatopathol*. 2006;28:99-104.
- de Biase D, Ragazzi M, Asioli S, Eusebi V. Extracutaneous Merkel cell carcinomas harbor polyomavirus DNA. *Hum Pathol*. 2012;43:980-985.
- Pan Z, Chen YY, Wu X, et al. Merkel cell carcinoma of lymph node with unknown primary has a significantly lower association with Merkel cell polyomavirus than its cutaneous counterpart. *Mod Pathol*. 2014;27:1182-1192.
- Gardair C, Samimi M, Touzé A, et al. Somatostatin receptors 2A and 5 are expressed in Merkel cell carcinoma with no association with disease severity. *Neuroendocrinology*. 2015;101:223-235.
- International Agency for Research on Cancer. In: Travis WD, Brambilla E, Burke AP, Marx A, Nicholson AG, eds. *WHO classification of tumours of lung, pleura, thymus and heart*. Geneva: World Health Organization; 2015.
- International Agency for Research on Cancer. In: Bosman FT, Carneiro F, Hruban RH, Theise ND, eds. *WHO classification of tumours of the digestive system*. Geneva: The World Health Organization; 2010.
- International Agency for Research on Cancer. In: DeLellis R, Lloyd RV, Heitz P, Eng C, eds. *Pathology and genetics of tumours of endocrine organs*. Geneva: World Health Organization; 2004.
- Moshiri AS, Doumani R, Yelistratova L, et al. Polyomavirus-negative Merkel cell carcinoma: a more aggressive subtype based on analysis of 282 cases using multimodal tumor virus detection. *J Invest Dermatol*. 2017;137(4):819-827.
- Rodig SJ, Cheng J, Wardzala J, et al. Improved detection suggests all Merkel cell carcinomas harbor Merkel polyomavirus. *J Clin Invest*. 2012;122:4645-4653.
- Zaar O, Gillstedt M, Lindelöf B, Wennberg-Larkö A-M, Paoli J. Merkel cell carcinoma incidence is increasing in Sweden. *J Eur Acad Dermatol Venereol*. 2016;30(10):1708-1713.
- Dores GM, Qubaiah O, Mody A, Ghabach B, Devesa SS. A population-based study of incidence and patient survival of small cell carcinoma in the United States, 1992-2010. *BMC Cancer*. 2015;15:185.
- Ordóñez NG. Value of thyroid transcription factor-1 immunostaining in distinguishing small cell lung carcinomas from other small cell carcinomas. *Am J Surg Pathol*. 2000;24:1217-1223.
- Reddi DM, Puri PK. Expression of focal TTF-1 expression in a case of CK7/CK20-positive Merkel cell carcinoma. *J Cutan Pathol*. 2013;40:431-433.
- Haymerle G, Fochtmann A, Kunstfeld R, Pammer J, Erovic BM. Management of Merkel cell carcinoma of unknown primary origin: the Vienna Medical School experience. *Eur Arch Oto-rhinolaryngol*. 2015;272:425-429.
- Andres C, Ihrler S, Puchta U, Flaig MJ. Merkel cell polyomavirus is prevalent in a subset of small cell lung cancer: a study of 31 patients. *Thorax*. 2009;64:1007-1008.

Supplemental Table I. Antibodies used for immunohistochemistry*

Antigen	Clone	Provider	Dilution
CKAE1–AE3	M3515	Dako	1/200
CK7	M7018	Dako	1/200
CK19	M8880	Dako	1/100
CK20	M7019	Dako	1/100
Chromogranin A	A0430	Dako	1/2000
Synaptophysin	RBK011	Zytomed	1/200
TTF-1	SP141	Roche	Prediluted
Large T antigen	sc-136172	Santa Cruz	1/50

CK, Cytokeratin; *TTF-1*, thyroid transcription factor-1.

*Kit used for all antibodies was Ultraview Universal DAB Detection Kit (ref 760-500; Ventana Medical Systems Inc, Basel, Switzerland).

Supplemental Table II. Large T-antigen primer sequences for Merkel cell polyomavirus detection by PCR

Primer or probe	Sequence
LT3F	5'-TCG-CCA-GCA-TTG-TAG-TCT-AAA-AAC-3'
LT3R	5'-CCA-AAC-CAA-AGA-ATA-AAG-CAC-TGA-3'
LT3S	6-FAM 5'-AGC-AAA-AAC-AAC-ACT-CTC-CCC-ACG-TCA-GAC-AG-3' BHQ

BHQ, Black hole quencher; 6-FAM, 6-carboxyfluorescein.

Supplemental Table III. Detailed immunohistochemical features of MCCWOPT, LNM from MCC and LNMNEC

Tumors	Cases, N	CKAE1 and CKAE3 positivity			Chromogranine			Synaptophysine		TTF-1	CDX2	Large T antigen	
		Dot staining	Diffuse staining	CK7	CK19	CK20	High staining	Low staining	High staining				Low staining
MCCWOPT	16	14	2	0	10	16	14	2	9	3	1	0	8
LNM from MCC	9	6	2	0	1	8	7	2	2	6	0	0	4
LNMNEC, total	18	3	15	8	3	1	14	4	11	5	14	0	0
Lung NEC													
Small cell carcinoma	5	3	2	0	0	0	3	2	3	1	5	0	0
Large cell carcinoma	1	0	1	1	0	0	1	0	1	0	1	0	0
Digestive NEC													
Small cell carcinoma	1	0	1	0	1	1	1	1	1	0	0	0	0
MANEC	2	0	2	1	0	0	0	1	1	0	1	0	0
MTC	7	0	7	5	2	0	7	0	3	4	7	0	0
Arytenoid carcinoid	1	0	1	0	0	0	1	0	1	0	0	0	0
Unknown	1	0	1	1	0	0	1	0	1	0	0	0	0

CK, Cytokeratin; LNM, lymph node metastasis; LNMNEC, lymph node metastasis from neuroendocrine carcinoma; MANEC, mixed adenoneuroendocrine carcinoma; MCC, Merkel cell carcinoma; MCCWOPT, Merkel cell carcinoma without primary tumor; MTC, medullar thyroid carcinoma; NEC, neuroendocrine carcinoma; NS, not significant; TTF-1, thyroid transcription factor 1.

Merkel cell carcinoma of lymph nodes without a skin primary tumor: a metastatic neoplasia associated with marked immune response ?

Thibault Kervarrec, MD, MSc^{1,2}, Julia Zaragoza, MD³, Pauline Gaboriaud², Patricia Berthon, PhD², Gaëlle Fromont, MD, PhD⁴, Yannick Le Corre, MD⁵, Eva Hainaut-Wierzbicka, MD⁶, Francois Aubin, MD, PhD⁷, Guido Bens, MD³, Patrick Michenet, MD⁸, Hervé Maillard, MD⁹, Antoine Touzé, PhD², Serge Guyétant, MD, PhD(*)^{1,2}, Mahtab Samimi, MD, PhD(*)^{2,10}

- (1) Department of Pathology, Université de Tours, CHU de Tours, avenue de la République, 37170, Chambray-les-tours, France
- (2) “Biologie des infections à polyomavirus” team, UMR INRA ISP 1282, Université de Tours, 31, avenue Monge 37200 Tours, France
- (3) Dermatology Department, CHR d’Orléans, 14 avenue de l’Hôpital, 45100 Orléans, France
- (4) Department of Pathology, Université de Tours, CHU de Tours, Boulevard Tonnelé, 37000, Tours, France
- (5) Dermatology Department, LUNAM Université, CHU Angers, 4 rue Larrey 49933 Angers, France
- (6) Dermatology Department, Université de Poitiers, CHU de Poitiers, 2 rue de la Milétrie, 86021 Poitiers, France
- (7) Dermatology Department, Université de Franche Comté, CHU Besançon, EA3181, IFR133, 2 boulevard Fleming 25030 Besançon, France
- (8) Department of Pathology, CHR d’Orléans, 14 avenue de l’Hôpital, 45100 Orléans, France
- (9) Dermatology Department, CHR Le Mans, 194 avenue Rubillard 72037 Le Mans Cedex 09, France
- (10) Dermatology Department, Université Francois Rabelais, CHU de Tours, avenue de la République, 37170, Chambray-les-tours, France

(*) M. Samimi and S. Guyétant contributed equally to the present study.

Disclosure/Conflict of Interest: The authors declare no conflict of interest.

Grant numbers and sources of support: project POCAME, Axe Immunothérapies, Cancéropole Grand Ouest-Région Centre Val de Loire (France), Fond de recherche de la Société Française de Pathologie.

Institutional review board: The local Ethics Committee of Tours (France) approved the study (N° ID RCB2009-A01056-51)

Manuscript Word count (up to 3000) (Excluding capsule summary, abstract, references, figures, and tables): **2415**

Abstract word count: **250**

Bulleted statement: word count: **81**

References: **38**

Figures: **2**

Supplementary Figure: **1**

Tables: **4**

Supplementary Method: **1**

Key words: Merkel cell carcinoma; Merkel cell carcinoma without primary; lymph node; CD8; CD33; ZEB1; epithelial–mesenchymal transition; metastasis

Abstract

Background: Overall, 5% to 15% of Merkel cell carcinoma (MCC) cases appear as isolated adenopathy and have been reported as MCC without primary tumor (MCCWOP). However whether this tumor results from a metastatic process with regression of a primary skin tumor or either constitutes itself a primary tumor is debated.

Objective: To determine the metastatic or primitive nature of MCCWOP.

Methods: Cases from an MCC cohort were classified as primary cutaneous tumors (n=60), lymph node metastasis (LNM) from primary cutaneous tumors (n=18) or MCCWOP (n=15). Immunohistochemistry was used to compare the expression of 4 potential metastatic markers related to the epithelial–mesenchymal transition (E-cadherin, N-cadherin, zinc finger E-box binding homeobox 1 [ZEB1], vimentin) among the three groups. Because high immune response may explain the regression of an occult primary tumor, density of intratumoral immune cells, which have been associated with improved outcome (CD8 and CD33 cells), was evaluated.

Results: Among MCC cases with identified primary, high and diffuse expression of ZEB1 was more frequently observed in LNM (74%) than in primary MCC (36%) ($p=0.017$), and could be therefore considered as indicative of the metastatic nature. Accordingly high and diffuse expression of ZEB1 was observed in the majority of MCCWOP cases (67%). Moreover, MCCWOP were characterized by more frequent CD8 and CD33^{brisk}/CD8^{positive} intratumoral immune infiltrate than MCC with cutaneous primary (both primary MCC and LNM) ($p=0.03$ and $p=0,0012$ respectively).

Conclusion: Frequent ZEB1 expression and high immune infiltrate suggest that MCCWOP results from a metastatic process associated with an efficient immune response.

Bulleted statement

What's already known about this topic?

Whether Merkel cell carcinoma without a primary results from a metastatic process with regression of a primary skin tumour or constitutes itself a primary tumor is debated.

What does this study add?

Frequent expression of the transcription factor ZEB1, one of the main regulator of the epithelial–mesenchymal transition, and high density of CD8 and CD33 immune cells are observed in Merkel cell carcinoma lymph nodes without a cutaneous primary.

What is the translational message ?

Merkel cell carcinoma without a primary result from a metastatic process associated with marked immune response.

Introduction

Merkel cell carcinoma (MCC) is a rare and aggressive neuroendocrine cutaneous carcinoma occurring mainly in elderly. The two identified risk factors are sun exposure and immunosuppression¹. In 2008, Feng et al.² reported genomic integration of a new polyomavirus (MCPyV) into MCC tumor cells. Additional studies confirmed Merkel cell polyomavirus (MCPyV) DNA detection in approximately 80% of cutaneous MCC cases while the remaining 20% of MCPyV-negative MCC cases are thought to be due to UV exposure³.

In current practice, MCC diagnosis is supported by microscopic examination, revealing infiltration of the dermis and/or subcutaneous tissues by tumor cells harboring high-grade neuroendocrine carcinoma features and frequent immunohistochemical expression of the cytokeratin 20⁴. However, in approximately 5% to 15% of cases, MCC presents as lymph-node metastasis (LNM) without a primary skin tumor (MCCWOP)⁴⁻⁷. We and others⁸⁻¹² confirmed that MCCWOP share a common phenotype with their cutaneous counterparts while being distinct from other neuroendocrine carcinomas. However biological connections between MCCWOP and cutaneous MCC have been, nevertheless, a matter of debate. In one hand, MCCWOP might be nodal metastatic location deriving from an occult, infraclinical, and/or totally regressive skin MCC¹³, and accordingly detection of an UV signature in MCCWOP genome¹⁴, argues in favor of an cutaneous origin of such specimens. On the other hand, MCCWOP might alternatively derive from intranodal nests of MCC cell precursors¹³, as reported for nodal melanocytic naevi¹⁵, and therefore constitute a primitive, non-metastatic process.

To note, metastatic evolution is closely related to the tumor cells invasion abilities and to epithelial–mesenchymal transition (EMT)^{16,17}. EMT is characterized by a loss of epithelial

markers such as E-cadherin and acquisition of a mesenchymal phenotype with abnormal expression of N-cadherin or vimentin. EMT depends on a few transcription factors that are common to most neoplasias^{16,17}. Among these, zinc finger E-box binding homeobox 1 (ZEB1)¹⁶ is an crucial determinant of the EMT in many solid cancers¹⁶. In the current study, we hypothesize that investigating markers of EMT in MCCWOP would help to determine either they constitute a primary neoplasia or result from a metastatic process. The metastatic nature of MCCWOP would imply a complete regression of a skin primary tumor. Indeed, complete spontaneous regression of both localized and metastatic MCC has previously been reported¹³. Inoue et al. identified increased apoptosis as well as high cytotoxic T-cell-mediated responses^{18,19} as major determinants of this regression. Accordingly, the significant impact of immune infiltrates on MCC behavior has been demonstrated in non-regressive tumors. Notably, brisk CD8 lymphocytic infiltrate in the intratumoral area of MCC cases are associated with improved outcome²⁰⁻²². Additionally, CD33-expressing myeloid cells were also found to be associated with an efficient immune response²³.

In this context, to clarify whether MCCWOP could represent a metastatic process associated with a robust immune response which could account for regression, this aim of this study was to assess the epithelial–mesenchymal transition status and intratumor immune infiltrates in such tumors.

Methods

Design and settings

MCC cases were selected from an ongoing historical/prospective cohort of MCC patients from 5 French hospital centers. Inclusion criteria of the cohort were previously described²⁴. Briefly, patients had a diagnosis of MCC established between 1998 and 2016 (local ethics committee, Tours, France, no. ID RCB2009-A01056-51). Only cases with available formalin-fixed paraffin-embedded (FFPE) samples were considered for inclusion in the present study.

Among these cases, MCCWOP cases were identified as previously described¹¹

MCC cases with identified cutaneous primary tumor were included as cutaneous primary tumor or LNM, according to the location of the available FFPE sample. In cases with available FFPE samples from both the primary tumor and metastasis were available, only the metastasis was included. Cases in which the primitive or metastatic nature of the FFPE tumor specimen available could not be clarify were excluded from the study.

Clinical and follow-up data

Age, sex, immunosuppression (HIV infection, organ transplant recipients, hematological malignancies)²⁵ and American Joint Committee on Cancer (AJCC) stage²⁶ at the time of surgery were collected from patient files.

Immunohistochemistry

Tumor samples were included in a tissue microarray as previously described²⁷.

Immunohistochemistry for CD8, E-cadherin and vimentin staining was performed on a BenchMark XT Platform as instructed. Staining was performed manually for ZEB1, N-cadherin

and CD33 as previously described²⁸. Antibodies and dilutions are summarized in supplementary **Method S1**.

Interpretation of immunohistochemical staining

E-cadherin, N-cadherin and vimentin expression was considered positive or negative²⁹. Because of significant variations in expressing cells proportion and staining intensity, ZEB1 expression was evaluated with a semiquantitative score: 0, lack of expression; 1, low staining of tumor cells or high staining of less than 50% of the tumor cells; 2, high staining of more than 50% of tumor cells, as shown in **supplementary Method S1**. CD8 infiltration was scored according to Paulson et al.²², considering only intratumor cells. CD33 infiltrates were assessed as previously described²⁷. The representativeness of this TMA regarding assessment of immune infiltrates was previously validated²³. In order to validate the representativeness of this TMA for the four epithelial-mesenchymal transition markers assessed in the current study, 9 randomly selected MCC cases were included in an independent TMA and evaluated for E-cadherin, N-cadherin, ZEB1 and vimentin expression. Concordance between the two evaluations was assessed using a Kappa test, as shown **Supplementary Method S1**.

Statistical Analysis

Continuous data are described with medians (ranges) and categorical data with number (percentage of the population with available data). Continuous data were compared by Non-parametric Mann Whitney test and categorical data by two-tailed Fisher exact test. $P < 0.05$ was considered statistically significant. Statistical analysis involved use of XL-Stat-Life (Addinsoft, Paris, France).

Results

Patient characteristics

Among the whole MCC cohort (n=242), FFPE tumor samples were available for 103 patients which were considered for inclusion in this study. The nature of the FFPE tumor (primitive tumor or metastasis) could not be determined in 10 cases, which were excluded from further analysis. The 93 remaining cases consisted of 60 cutaneous primary MCC, 18 LNM from cutaneous MCC and 15 MCCWOP (**Flow chart/Figure 1**). Clinical features of the 3 groups are reported in **Table 1**.

MCCWOP frequently harbored high and diffuse ZEB1 expression suggesting a metastatic process

To determine whether MCCWOP might constitute a primary neoplasia or result from a metastatic process, we first investigate EMT markers expression among the MCC cohort. Overall, loss of E-cadherin expression, aberrant positivity of N-cadherin and vimentin were observed in 91% (n=82), 88% (n=75) and 6% (n=5) of interpretable cases respectively (**supplementary Figure 1**). Moreover, ZEB1 expression was evaluated as score 0, 1 and 2 in 25.5% (n=21), 25.5% (n=21) and 49% (n=42) of the cases (**Figure 2**).

EMT markers were then assessed in MCC cases with an identified primary, to select those with a differential expression among primary tumors and LNM. As reported in **Table 2**, only transcription factor ZEB1 was found to be overexpressed in LNM compared to primary tumours (p= 0.047) (**Table 2**). In line with this, 74% of the LNM (n=11/15) but only 36% of primary tumours (n=19/52) showed high and diffuse expression of ZEB1 (score 2) (p=0.017). Therefore, we considered high and diffuse ZEB1 staining (score 2) as the most relevant marker of metastatic process in MCC. In line with these findings, such profile of Zeb 1 expression

(score 2) was found for 38%, 56%, 58% and 100% of MCC cases with AJCC stage I, II, III and IV, respectively (p=0.22). In addition, MCC tumors with score 2 ZEB1 expression more frequently displayed aberrant N-cadherin expression (97%, n=37) compared to others (75%, n=30) (p=0.007), arguing in favour of an on-going EMT process in these cases.

After validation of ZEB1 as a marker of metastatic process, the latter was investigated among the MCCWOP group. In this setting, 67% of cases (n=10/15) displayed high and diffuse expression of ZEB1 (score 2) (Table 3). Therefore, more frequent detection of high and diffuse ZEB1 expression in LNM from cutaneous MCCs (74%) as well as in MMCWOP (67%) compared to primary cutaneous MCCs (**Table 3**) (p=0.014) might suggest that MCCWOP results from a metastatic process.

Frequent detection of intratumoral immune infiltrates in MCCWOP suggest that immune response contribute to the natural history of such tumors.

To investigate whether an efficient immune response might contribute to MCCWOP natural history, we subsequently focused on intra-tumoral immune cells (CD8 and CD33 infiltrates) in primary and metastatic MCC cases. Among the 87 MCC cases with interpretable staining, 34 cases did not harbor any tumor-infiltrating CD8 lymphocytes (score 0, 39%). In other cases (n=53), most displayed low CD8 infiltrates (score 1, n=45) whereas brisk infiltrates (scores 2-5) were found in only 8 cases (9%) (**Table 4**). Of note, only primary cutaneous MCC displayed such brisk CD8⁺ infiltrates. We had previously reported that the subgroup of MCC cases with CD33^{brisk}/CD8⁺ immune infiltrates experimented better outcome²³; such profile of immune infiltrates was identified in 32 of our cases (42%) (**Table 4**).

Among the 78 MCC cases with a known primary, intratumor CD8-infiltrates (scores 1-5) were more frequently observed in primary cutaneous MCC than LNM (66% vs 31%, $p=0.04$), as was CD33/CD8^{high} infiltrate (48% vs 7%, $p=0.005$) (**Table 4**). However, such MCC cases with a known primary were less frequently immune-infiltrated than MCCWOP, as intratumoral CD8 and combined CD33^{brisk}/CD8⁺ infiltrates were observed in 73% and 69% of MCCWOP respectively ($p=0.03$ and 0.001 respectively) (**Table 4/Figure 2**). Therefore, more frequent detection of intratumor immune infiltrates in MCCWOP than in LNM from cutaneous MCCs might indicate that MCCWOP are associated with marked immune response.

Discussion

While MCCWOP belonging to the MCC spectrum is supported by the close phenotype similarities between such tumours and their cutaneous counterpart^{8–10}, whether MCCWOP constitutes a primary nodal tumor or results from the metastasis of an infraclinical skin MCC, remains a matter of debate. In our study, analysis of ZEB1, one of the main regulators of EMT, revealed a common high and diffuse expression profile shared by MCCWOP and LNM from cutaneous MCC, and mainly lacking from cutaneous primary MCC tumors. Moreover, we evidenced more frequent intratumoral immune infiltration by both CD8 lymphocytes and CD33^{brisk}/CD8⁺ infiltrates within MCCWOP when compared to primary MCC and LNM from cutaneous MCC. Altogether, our data might suggest MCCWOP consist in a metastatic neoplasia associated with marked immune response.

Metastasis results from complex biological mechanisms implying invasion, migration, preparation of the pre-metastatic niche and metastatic tumor development. EMT, occurring during such metastatic process, is defined as the ability of the carcinoma to lose its epithelial phenotype, and to acquire mesenchymal features required for invasion^{16,17} and the N-cadherin/E-cadherin couple has notably been used to reflect this balance¹⁷. As previously described²⁹, our study revealed frequent positivity of N-cadherin and frequent lack of E-cadherin expression in MCC, confirming such tumour as an aggressive neoplasia. Interestingly, molecular determinants driving EMT seem to be common in most carcinomas¹⁶ and depend on a few transcription factors — ZEB1, ZEB2, SNAIL, SLUG and TWIST. In the neuroendocrine carcinoma setting, frequent EMT features were demonstrated in small-cell lung carcinomas^{30,31}, mainly related to ZEB1 expression³².

In line with such findings, frequent ZEB1 positivity in MCC tumors, notably in metastases suggests ZEB1 as a new unexplored determinant of aggressiveness in MCC. Of note, in addition to its key role in EMT, ZEB1 has been associated with other aggressiveness mechanisms such as “cancer stem-cell” ability, and cisplatin chemotherapy resistance¹⁶.

In this context, frequent ZEB1 expression in MCCWOP and LNM from cutaneous MCC, supported the concept that MCCWOP are metastatic neoplasia. However, in comparison with other metastatic MCC cases, MCCWOP show better outcome¹⁴, which led to its reclassification as AJCC stage IIIa²⁶. Recently, Vandeven et al.¹⁴ confirmed increased survival in a cohort of 72 MCCWOP cases in comparison with other stage III MCC and evidenced elevated level of tumor immunogenicity in this setting¹⁴. Tumor mutation burden was notably higher in the MCCWOP compared to metastatic MCC cases suggesting that neoantigen formation might enhance immunogenicity in MCCWOP. Interestingly, high mutation burden was previously reported as the hallmark of MCPyV(-) MCC cases³³, a tumor subset associated with poor outcome³⁴. Therefore, high tumor mutational burden appears as a double edge sword with both positive and negative impact on behavior. Similarly, MCCWOP cases harbored an unexpected association of the EMT marker, ZEB1, involved tumor immune escape³⁵ with high intratumor CD8 and CD33 infiltrates. Altogether these findings supported the notion that MCCWOP results from the balance between tumor aggressiveness and marked immune response which could induce regression of an occult primary.

While fewer than 40 cases of total regression of cutaneous primary MCC have been reported, always after biopsy¹³, MCCWOP represents up to 15% of all MCC cases^{4,5,7}. However such discrepancies might be explained by under-reported incidence of spontaneous regression.

Moreover, spontaneous regression might occur in the skin at a subclinical, undetectable tumor stage.

Biological determinants of the MCC regression were investigated by Inoue et al¹⁸, who showed marked lymphocytic CD8 infiltrates on prior biopsies of MCC before spontaneous regression. Indeed, specific CD8 cells targeted against viral and cellular antigens have been detected in the MCC microenvironment, and intratumoral CD8 density is also associated with better outcome in non-spontaneous MCC²¹. However, in a large portion of MCC, CD8 populations are excluded from the intratumor area and are confined to the fibrous septa surrounding the tumor^{22,36}. Moreover, CD8 populations show expression of anergy markers, probably because of the expression of immune checkpoints. Here we observed frequent infiltration of CD8 cells in MCCWOP, probably related to an effective lymphocyte response, which could be responsible for the spontaneous regression of an undetectable cutaneous primary tumor and for the better outcome of MCCWOP as compared with other AJCC stage III tumors⁵. In addition, we identified a frequent CD33^{brisk}/CD8⁺ infiltrate in MCCWOP which have also been associated with better outcome²³. In a previous study, comparing primary cutaneous tumors with MCC lymph node locations (both MCCWOP and MCC with LNM), we did not find any difference concerning the immune infiltrate density. In this present work, separating MCCWOP from LNM from cutaneous MCC, we revealed specificity of both entities. Indeed, MCCWOP appeared as a high immune-infiltrating cell tumor, in contrast to MCC with LNM, which lacked relevant immune infiltrates. Our study shows some limitations essentially the low number of MCCWOP and LNM from cutaneous, due to the low incidence of the disease.

To conclude, our study favors the view of MCCWOP as a metastatic process associated with a specific high and efficient immune response rather than a primitive LN tumor. ZEB1 appears

as a potential marker of the metastatic process in MCC. Further investigations are needed to define the specific molecular pathway triggered by this factor in MCC.

Acknowledgments:

The authors sincerely thank the patients who gave their approval for the study. They also thank Roseline Guibon (Tours, France), Dr Micheline Chargeboeuf (Lons le Saunier, France), Dr Benjamin Linot (Angers, France), and Dr Isabelle Valo (Angers, France) for their help and contributions to the study.

Abbreviation and acronym list:

AJCC: American Joint Committee on Cancer

CD: Cluster of differentiation

DNA: Desoxyribonucleic acid

EMT: Epithelial-mesenchymal transition

HES: Hematein-eosin safran

LNМ: Lymph node metastasis

MCC: Merkel cell carcinoma

MCCWOP: Merkel cell carcinoma of lymph nodes without skin primary tumor

MCPyV: Merkel cell polyomavirus

PCR: Polymerase chain reaction

TMA: Tissue micro array

ZEB1: Zinc Finger E-Box Binding Homeobox 1

References

1. *Pathology and genetics of skin tumours: [... reflects the views of a working group that convened for an editorial and consensus conference in Lyon, France, September 22 - 25, 2003]*. (IARC Press, 2007).
2. Feng, H., Shuda, M., Chang, Y. & Moore, P. S. Clonal integration of a polyomavirus in human Merkel cell carcinoma. *Science* **319**, 1096–1100 (2008).
3. González-Vela, M. D. C. *et al.* Shared Oncogenic Pathways Implicated in Both Virus-Positive and UV-Induced Merkel Cell Carcinomas. *J. Invest. Dermatol.* **137**, 197–206 (2017).
4. Fields, R. C. *et al.* Five hundred patients with Merkel cell carcinoma evaluated at a single institution. *Ann. Surg.* **254**, 465–473; discussion 473-475 (2011).
5. Kotteas, E. A. & Pavlidis, N. Neuroendocrine Merkel cell nodal carcinoma of unknown primary site: management and outcomes of a rare entity. *Crit. Rev. Oncol. Hematol.* **94**, 116–121 (2015).
6. Zaar, O., Gillstedt, M., Lindelöf, B., Wennberg-Larkö, A.-M. & Paoli, J. Merkel cell carcinoma incidence is increasing in Sweden. *J. Eur. Acad. Dermatol. Venereol. JEADV* (2016). doi:10.1111/jdv.13698
7. Haymerle, G., Fochtmann, A., Kunstfeld, R., Pammer, J. & Erovic, B. M. Management of Merkel cell carcinoma of unknown primary origin: the Vienna Medical School experience. *Eur. Arch. Oto-Rhino-Laryngol. Off. J. Eur. Fed. Oto-Rhino-Laryngol. Soc. EUFOS Affil. Ger. Soc. Oto-Rhino-Laryngol. - Head Neck Surg.* **272**, 425–429 (2015).
8. Pan, Z. *et al.* Merkel cell carcinoma of lymph node with unknown primary has a significantly lower association with Merkel cell polyomavirus than its cutaneous counterpart. *Mod. Pathol. Off. J. U. S. Can. Acad. Pathol. Inc* **27**, 1182–1192 (2014).
9. de Biase, D., Ragazzi, M., Asioli, S. & Eusebi, V. Extracutaneous Merkel cell carcinomas harbor polyomavirus DNA. *Hum. Pathol.* **43**, 980–985 (2012).
10. Deneve, J. L. *et al.* Merkel cell carcinoma of unknown primary origin. *Ann. Surg. Oncol.* **19**, 2360–2366 (2012).
11. Kervarrec, T. *et al.* Differentiating Merkel cell carcinoma of lymph nodes without a detectable primary skin tumor from other metastatic neuroendocrine carcinomas: The ELECTHIP criteria. *J. Am. Acad. Dermatol.* **78**, 964-972.e3 (2018).
12. Kervarrec, T. *et al.* Diagnostic accuracy of a panel of immunohistochemical and molecular markers to distinguish Merkel cell carcinoma from other neuroendocrine carcinomas. *Mod. Pathol. Off. J. U. S. Can. Acad. Pathol. Inc* **32**, 499–510 (2019).
13. Walsh, N. M. Complete spontaneous regression of Merkel cell carcinoma (1986-2016): a 30 year perspective. *J. Cutan. Pathol.* **43**, 1150–1154 (2016).
14. Vandeven, N. A. *et al.* Merkel cell carcinoma patients presenting without a primary lesion have elevated markers of immunity, higher tumor mutation burden and improved survival. *Clin. Cancer Res. Off. J. Am. Assoc. Cancer Res.* (2017). doi:10.1158/1078-0432.CCR-17-1678
15. Ribero, S. *et al.* Lymph nodes' capsular naevi are associated with high naevus count in melanoma patients: a case-control study. *Melanoma Res.* **27**, 274–276 (2017).
16. Zhang, P., Sun, Y. & Ma, L. ZEB1: at the crossroads of epithelial-mesenchymal transition, metastasis and therapy resistance. *Cell Cycle Georget. Tex* **14**, 481–487 (2015).
17. De Craene, B. & Berx, G. Regulatory networks defining EMT during cancer initiation and progression. *Nat. Rev. Cancer* **13**, 97–110 (2013).
18. Inoue, T., Yoneda, K., Manabe, M. & Demitsu, T. Spontaneous regression of merkel

cell carcinoma: a comparative study of TUNEL index and tumor-infiltrating lymphocytes between spontaneous regression and non-regression group. *J. Dermatol. Sci.* **24**, 203–211 (2000).

19. Pang, C., Sharma, D. & Sankar, T. Spontaneous regression of Merkel cell carcinoma: A case report and review of the literature. *Int. J. Surg. Case Rep.* **7C**, 104–108 (2015).
20. Sihto, H. *et al.* Tumor infiltrating immune cells and outcome of Merkel cell carcinoma: a population-based study. *Clin. Cancer Res. Off. J. Am. Assoc. Cancer Res.* **18**, 2872–2881 (2012).
21. Paulson, K. G. *et al.* Transcriptome-wide studies of merkel cell carcinoma and validation of intratumoral CD8+ lymphocyte invasion as an independent predictor of survival. *J. Clin. Oncol. Off. J. Am. Soc. Clin. Oncol.* **29**, 1539–1546 (2011).
22. Paulson, K. G. *et al.* CD8+ lymphocyte intratumoral infiltration as a stage-independent predictor of Merkel cell carcinoma survival: a population-based study. *Am. J. Clin. Pathol.* **142**, 452–458 (2014).
23. Kervarrec, T. *et al.* Merkel cell carcinomas infiltrated with CD33+ myeloid cells and CD8+ T cells are associated with improved outcome. *J. Am. Acad. Dermatol.* (2017). doi:10.1016/j.jaad.2017.12.029
24. Gardair, C. *et al.* Somatostatin Receptors 2A and 5 Are Expressed in Merkel Cell Carcinoma with No Association with Disease Severity. *Neuroendocrinology* **101**, 223–235 (2015).
25. Asgari, M. M. *et al.* Effect of host, tumor, diagnostic, and treatment variables on outcomes in a large cohort with Merkel cell carcinoma. *JAMA Dermatol.* **150**, 716–723 (2014).
26. Harms, K. L. *et al.* Analysis of Prognostic Factors from 9387 Merkel Cell Carcinoma Cases Forms the Basis for the New 8th Edition AJCC Staging System. *Ann. Surg. Oncol.* **23**, 3564–3571 (2016).
27. Kervarrec, T. *et al.* Merkel cell carcinomas infiltrated with CD33+ myeloid cells and CD8+ T cells are associated with improved outcome. *J. Am. Acad. Dermatol.* **78**, 973–982.e8 (2018).
28. Figiel, S. *et al.* Clinical significance of epithelial-mesenchymal transition markers in prostate cancer. *Hum. Pathol.* **61**, 26–32 (2017).
29. Vlahova, L. *et al.* P-cadherin expression in Merkel cell carcinomas is associated with prolonged recurrence-free survival. *Br. J. Dermatol.* **166**, 1043–1052 (2012).
30. Meredith, S. L. *et al.* Irradiation Decreases the Neuroendocrine Biomarker Pro-Opiomelanocortin in Small Cell Lung Cancer Cells In Vitro and In Vivo. *PloS One* **11**, e0148404 (2016).
31. Krohn, A. *et al.* Tumor cell heterogeneity in Small Cell Lung Cancer (SCLC): phenotypical and functional differences associated with Epithelial-Mesenchymal Transition (EMT) and DNA methylation changes. *PloS One* **9**, e100249 (2014).
32. Goscinski, M. A. *et al.* Nuclear, cytoplasmic, and stromal expression of ZEB1 in squamous and small cell carcinoma of the esophagus. *APMIS Acta Pathol. Microbiol. Immunol. Scand.* **123**, 1040–1047 (2015).
33. Carter, M. D. *et al.* Genetic Profiles of Different Subsets of Merkel Cell Carcinoma Show Links between Combined and Pure MCPyV-negative Tumors. *Hum. Pathol.* (2017). doi:10.1016/j.humpath.2017.10.014
34. Moshiri, A. S. *et al.* Polyomavirus-Negative Merkel Cell Carcinoma: A More Aggressive Subtype Based on Analysis of 282 Cases Using Multimodal Tumor Virus Detection. *J. Invest.*

Dermatol. (2016). doi:10.1016/j.jid.2016.10.028

35. Chockley, P. J. & Keshamouni, V. G. Immunological Consequences of Epithelial-Mesenchymal Transition in Tumor Progression. *J. Immunol. Baltim. Md 1950* **197**, 691–698 (2016).

36. Afanasiev, O. K. *et al.* Vascular E-selectin expression correlates with CD8 lymphocyte infiltration and improved outcome in Merkel cell carcinoma. *J. Invest. Dermatol.* **133**, 2065–2073 (2013).

Figures and tables:

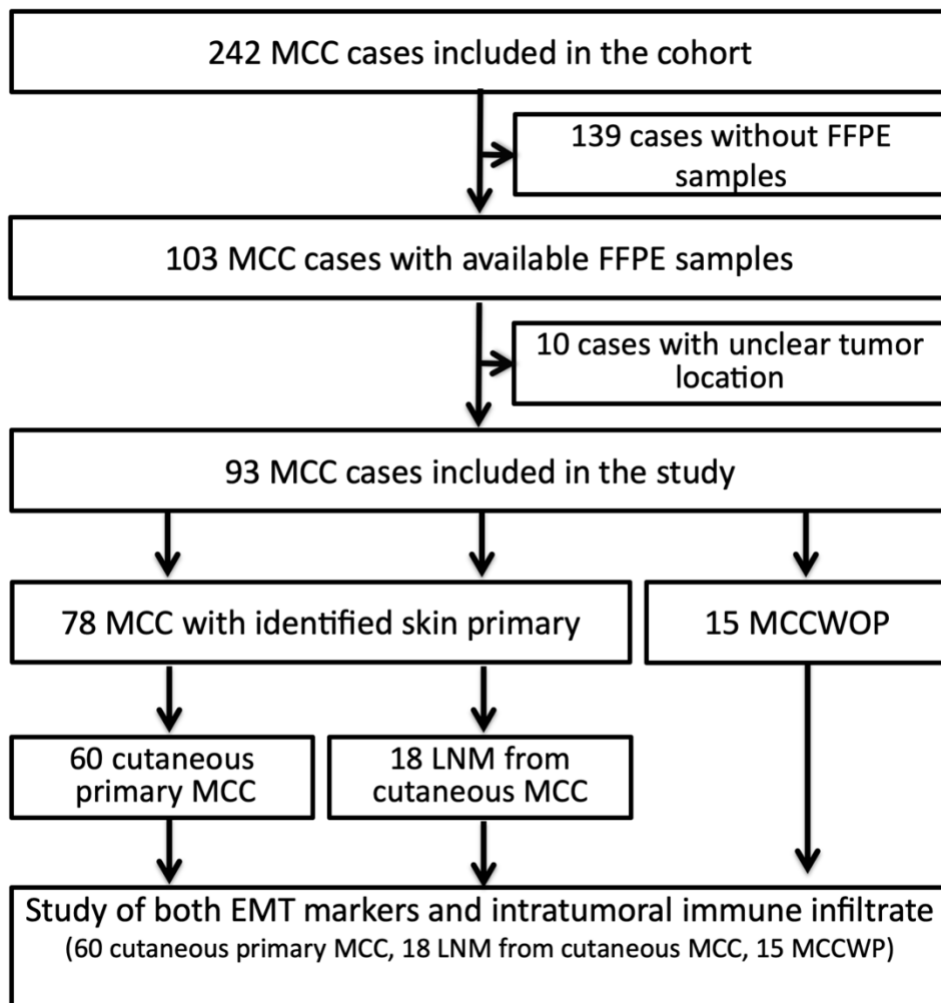


Figure 1. Flow chart.

EMT: Epithelial-mesenchymal transition; FFPE: Formalin-Fixed Paraffin-Embedded; LNM: lymph node metastasis; MCC: Merkel cell carcinoma; MCCWOP: Merkel cell carcinoma of lymph node without primary tumor.

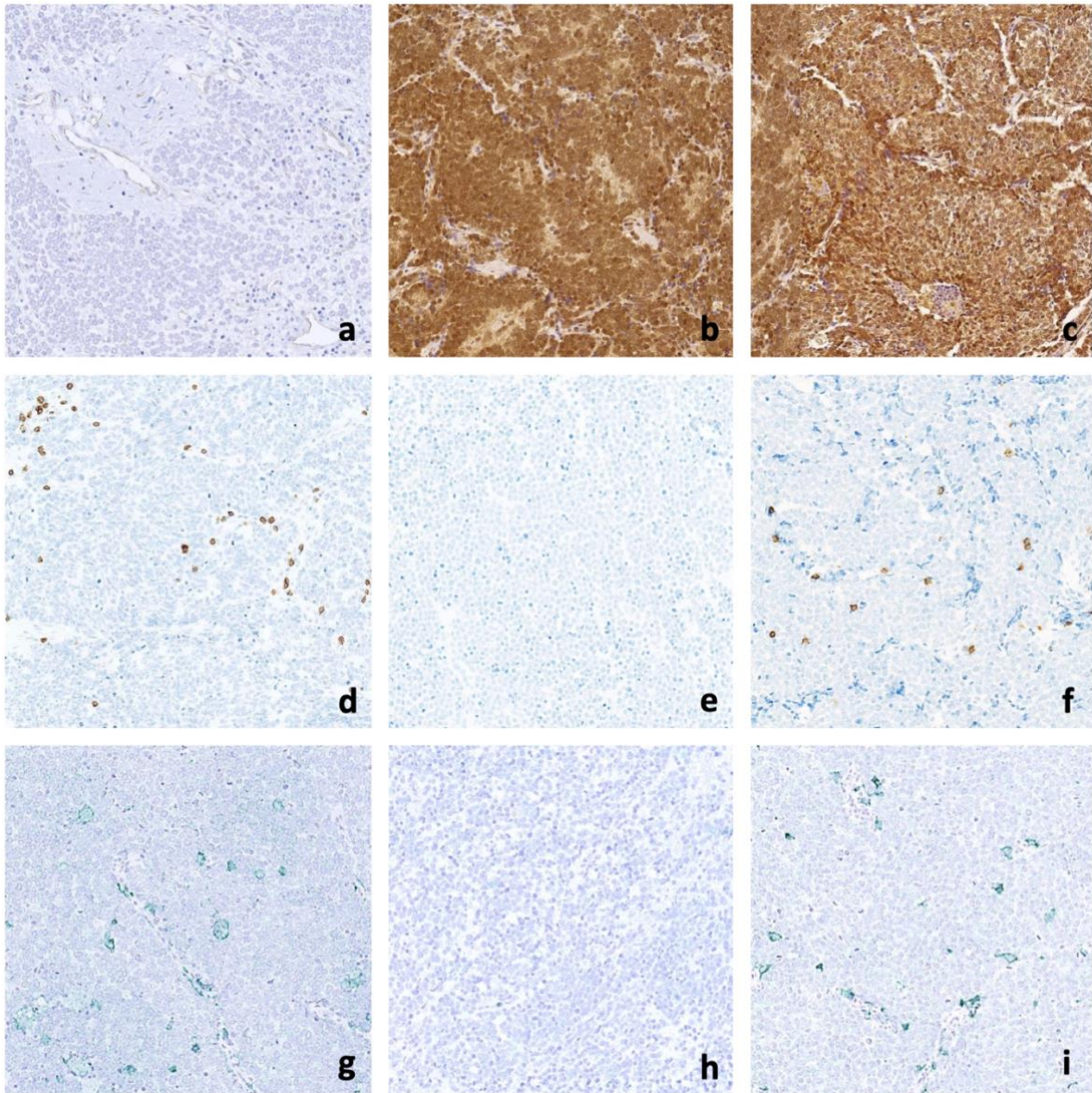


Figure 2. Representative immunochemical stainings of ZEB1 (a, b,c), CD8 (d,e,f) and CD33 (g,h,i) in the primary cutaneous tumor (a,d,g), metastasis of cutaneous MCC (b,e,h) and MCCWOP (c,f,i)

Table 1. Clinical characteristics of the 3 groups: primary cutaneous Merkel cell carcinoma (MCC), lymph-node metastasis (LNM) from cutaneous MCC and MCC of the lymph node without primary tumor (MCCWOP).

Clinical data	Primary MCC (n=60)	LNM from cutaneous MCC (n=18)	MCCWOP (n=15)
Age:			
Median, range	82 (49-100)	74 (54-90)	70 (59-84)
Missing data	4	0	0
Sex:			
F/M	37/19	10/8	6/9
Missing data	4	0	0
Stage:			
I	16 (37%)	0	0
II	18 (42%)	0	0
III	9 (21%)	16 (89%)	14 (93%)
IV	0	2 (11%)	1 (7%)
Missing data	17	0	0
Immunosuppression:			
Yes	7 (17%)	1 (6%)	0
No	34 (83%)	15 (94%)	15 (100%)
Missing data	19	2	0

Table 2. Immunohistochemical expression of epithelial–mesenchymal transition (EMT) markers in primary cutaneous MCC and LNM from cutaneous MCC.

EMT markers	Primary MCC (n=60)	LNM from cutaneous MCC (n=18)	p
E-cadherin:			0.30
Yes	6 (10%)	0	
No	52 (90%)	18 (100%)	
Missing data	2	0	
N-cadherin:			0.67
Yes	47 (85%)	14 (93%)	
No	8 (15%)	1 (7%)	
Missing data	5	3	
ZEB1:			0.047
Score 0	17 (33%)	2 (13%)	
Score 1	16 (31%)	2 (13%)	
Score 2	19 (36%)	11 (74%)	
Missing data	8	3	
Vimentin:			0.56
Yes	4 (8%)	0	
No	47 (92%)	14 (100%)	
Missing data	9	4	

ZEB1 score: 0, lack of expression; 1, low staining of tumor cells or high staining of less than 50% of the tumor cells; 2, high staining of more than 50% of tumor cells.

Table 3. Immunohistochemical expression of ZEB1 in primary cutaneous MCC, LNM from cutaneous MCC and MCCWOP.

ZEB1	Primary MCC (n=60)	LNM from cutaneous MCC (n=18)	MCCWOP (n=15)	p
Score 0-1	33 (64%)	4 (26%)	5 (33%)	0.001
Score 2	19 (36%)	11 (74%)	10 (67%)	
Missing data	8	3	0	

Score 0, lack of expression; 1, low staining of tumor cells or high staining of less than 50% of the tumor cells; 2, high staining of more than 50% of tumor cells.

Table 4. Immune infiltrates in primary cutaneous MCC, LNM from cutaneous MCC and MCCWOP

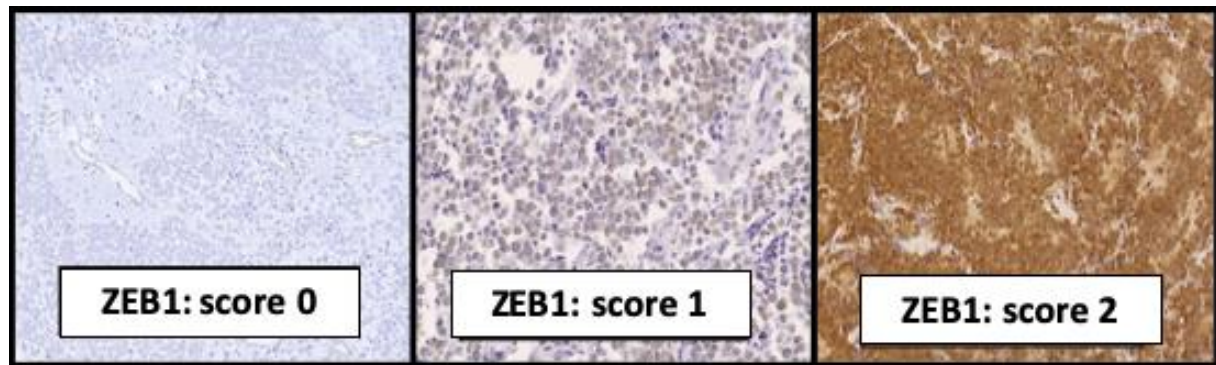
Immune infiltrate	All MCC cases	Primary MCC (n=60)	LNM from cutaneous MCC (n=18)	MCCWOP (n=15)	p
CD8 score:					0.03
Absent	34	19 (34%)	11 (69%)	4 (27%)	
Present	53	37 (66%)	5 (31%)	11 (73%)	
Missing data	6	4	2	0	
CD33^{brisk}/CD8⁺ infiltrate:					0.001
No	42	24 (52%)	14 (93%)	4 (31%)	
Yes	32	22 (48%)	1 (7%)	9 (69%)	
Missing data	19	14	3	2	

Supplemental Method S1. Protocol of the immunochemical study.

a. Antibodies used and dilutions

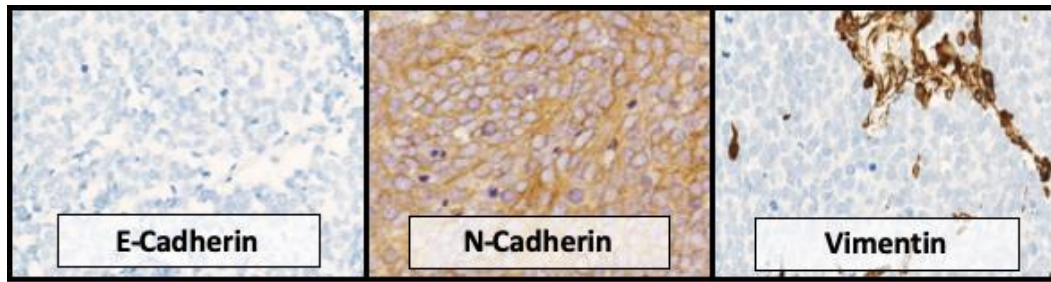
Target	Clone/provider	dilution
E-cadherin	NCH-38 / Dako	1/100
N-cadherin	13A9 /Novus Biological	1/100
Vimentin	V9/Dako	1/1000
Zeb1	PAB19268/Abnova	1/500
CD8	C8/144B/Dako	1/50
CD33	SP266/Ventana	ready to use solution

b. Representative illustrations of the Zeb1 score



c. Validation of EMT markers evaluation in a cohort of 9 cases included twice in two independent tissue microarray (Kappa test).

Marker	Kappa test
E-cadherin	0.94
N-cadherin	0.94
Vimentin	1
ZEB1	0.83



Supplementary Figure 1. Representative pictures of E-cadherin, N-cadherin and vimentin expression in MCC.



Detection of the Merkel cell polyomavirus in the neuroendocrine component of combined Merkel cell carcinoma

Thibault Kervarrec^{1,2,3} · Mahtab Samimi^{2,4} · Pauline Gaboriaud² · Tarik Gheit⁵ · Agnès Beby-Defaux^{6,7} · Roland Houben³ · David Schrama³ · Gaëlle Fromont¹ · Massimo Tommasino⁴ · Yannick Le Corre⁸ · Eva Hainaut-Wierzbicka⁹ · Francois Aubin¹⁰ · Guido Bens¹¹ · Hervé Maillard¹² · Adeline Furudoï¹³ · Patrick Michenet¹⁴ · Antoine Touzé² · Serge Guyétant^{1,2}

Received: 13 November 2017 / Revised: 15 February 2018 / Accepted: 19 March 2018 / Published online: 28 March 2018
© Springer-Verlag GmbH Germany, part of Springer Nature 2018

Abstract

Merkel cell carcinoma (MCC) is an aggressive neuroendocrine carcinoma of the skin. The main etiological agent is Merkel cell polyomavirus (MCPyV), detected in 80% of cases. About 5% of cases, called combined MCC, feature an admixture of neuroendocrine and non-neuroendocrine tumor cells. Reports of the presence or absence of MCPyV in combined MCC are conflicting, most favoring the absence, which suggests that combined MCC might have independent etiological factors and pathogenesis. These discrepancies might occur with the use of different virus identification assays, with different sensitivities. In this study, we aimed to determine the viral status of combined MCC by a multimodal approach. We histologically reviewed 128 cases of MCC and sub-classified them as “combined” or “conventional.” Both groups were compared by clinical data (age, sex, site, American Joint Committee on Cancer [AJCC] stage, immunosuppression, risk of recurrence, and death during follow-up) and immunochemical features (cytokeratin 20 and 7, thyroid transcription factor 1 [TTF1], p53, large T antigen [CM2B4], CD8 infiltrates). After a first calibration step with 12 conventional MCCs and 12 cutaneous squamous cell carcinomas as controls, all eight cases of combined MCC were investigated for MCPyV viral status by combining two independent molecular procedures. Furthermore, on multiplex genotyping assay, the samples were examined for the presence of other polyoma- and papillomaviruses. Combined

Electronic supplementary material The online version of this article (<https://doi.org/10.1007/s00428-018-2342-0>) contains supplementary material, which is available to authorized users.

✉ Thibault Kervarrec
thibaultkervarrec@yahoo.fr

¹ Department of Pathology, Université de Tours, Centre Hospitalier Universitaire de Tours, 37044 Tours Cedex 09, France

² Biologie des infections à polyomavirus team, UMR INRA ISP 1282, Université de Tours, 31, Avenue Monge, 37200 Tours, France

³ Department of Dermatology, Venereology and Allergology, University Hospital Würzburg, Josef-Schneider-Straße 2, 97080 Würzburg, Germany

⁴ Department of Dermatology, Université François Rabelais, Centre Hospitalier Universitaire de Tours, 37044 Tours Cedex 09, France

⁵ Infections and Cancer Biology Group, International Agency for Research on Cancer, 150 Cours Albert Thomas, 69008 Lyon, France

⁶ Université de Poitiers, 2RCT “Récepteurs et régulation des cellules tumorales” team, 1 rue Georges Bonnet, 86073 Poitiers, France

⁷ Department of Virology, Université de Poitiers, Centre Hospitalier Universitaire de Poitiers, 2 rue de la Milétrie, 86021 Poitiers, France

⁸ Department of Dermatology, LUNAM Université, Centre Hospitalier Universitaire d’Angers, 4 rue Larrey, 49933 Angers, France

⁹ Department of Dermatology, Université de Poitiers, Centre Hospitalier Universitaire de Poitiers, 2 rue de la Milétrie, 86021 Poitiers, France

¹⁰ Department of Dermatology, Université de Franche Comté, Centre Hospitalier Universitaire de Besançon, EA3181, IFR133, 2 boulevard Fleming, 25030 Besançon, France

¹¹ Department of Dermatology, Centre Hospitalier Régional d’Orléans, 14 avenue de l’Hôpital, CS 86709, 45067 Orléans cedex 2, France

¹² Department of Dermatology, Centre Hospitalier Régional du Mans, 194 avenue Rubillard, 72037 Le Mans, France

¹³ Department of Pathology, Université de Bordeaux, Centre Hospitalier Universitaire de Bordeaux, Avenue de Magellan, 33604 Pessac, France

¹⁴ Department of Pathology, Centre Hospitalier Régional d’Orléans, 14 avenue de l’Hôpital, CS 86709, 45067 Orléans cedex 2, France

MCC differed from conventional MCC in earlier AJCC stage, increased risk of recurrence and death, decreased CD8 infiltrates, more frequent TTF1 positivity (5/8), abnormal p53 expression (8/8), and frequent lack of large T antigen expression (7/8). With the molecular procedure, half of the combined MCC cases were positive for MCPyV in the neuroendocrine component. Beta papillomaviruses were detected in 5/8 combined MCC cases and 9/12 conventional MCC cases. In conclusion, the detection of MCPyV DNA in half of the combined MCC cases suggests similar routes of carcinogenesis for combined and conventional MCC.

Keywords Merkel cell carcinoma · Merkel cell polyomavirus · Combined merkel cell carcinoma · Squamous carcinoma · Polyomavirus · Papillomavirus

Introduction

Merkel cell carcinoma (MCC) is a rare tumor of the skin that features an aggressive course, with overall 5-year survival estimated at 40% [1]. MCC occurs essentially in older people and the two main risk factors are sun exposure and immunodeficiency [1]. The diagnosis is based on histology, which reveals high-grade neuroendocrine morphological features close to small cell carcinoma and expression of neuroendocrine markers and/or cytokeratin 20 [2].

In 2008, Moore et al. described Merkel cell polyomavirus (MCPyV) as the major etiological agent of MCC [3]. MCPyV establishes a latent chronic infection in the dermis of most healthy individuals, and the mechanisms leading to oncogenesis are still under investigation. In about 80% of cases, tumor cells harbor integrated virus. Of note, MCPyV large T antigen in tumor cells is characterized by non-sense mutations leading to the loss of replicative abilities of the virus and the lack of late protein synthesis [4]. MCPyV genome expression in tumors is restricted to the early oncogenic proteins (small and large T antigens), and expression of T antigens is required for tumor proliferation [5]. These two viral proteins are probably the main early determinants of MCC oncogenesis.

Whether MCPyV-negative tumors should be considered a specific biological entity is debated. Indeed, MCPyV-negative MCC is thought to be essentially due to UV exposure [6] because the rates of somatic genetic mutations with a predominant UV signature are higher than in MCPyV-positive tumors. Moreover, levels of intratumoral CD8 infiltrates are lower, which suggests decreased immunogenicity [7] and a worse outcome [8].

Combined MCC involves rare MCC variants that represent 5 to 10% of MCC cases [9]. Combined MCC cases are characterized by the association of a main component of MCC with one or more other tumor components harboring non-neuroendocrine differentiation, including an epidermic orthologous component [2] (squamous, basal-cell-like, adnexial, and melanocytic) or a heterologous component [10] (glandular and sarcomatous).

Three main studies detected no MCPyV in combined MCC [9–11]. Conversely, a few recent case reports have demonstrated the presence of MCPyV in the MCC component of combined MCC [12], associated with papillomavirus infection in one case [13].

Papillomaviruses and polyomaviruses are closely related double-strand DNA viruses with similar oncogenic abilities. Indeed, beta human papillomaviruses are involved in the oncogenesis of cutaneous squamous cell carcinoma, and alpha-human papillomaviruses involved in cutaneous Bowen disease and combined tumors in the oropharynx (associating neuroendocrine and squamous components) [14]. Hence, human papillomavirus might be an etiological agent of combined carcinomas.

Whether combined MCC belongs to the spectrum of virus-induced tumors or should be considered a non-MCPyV MCC induced by an alternative oncogenetic pathway remains unclear. In this study, we compared the clinical features of conventional and combined MCC and determined the viral status of combined MCC by systematic assessment of MCPyV, 9 other polyomaviruses and 46 papillomaviruses.

Methods

Study period, data, and settings

MCC cases were selected from an ongoing historical/prospective cohort of 223 patients with MCC from six French hospital centers. The diagnosis of MCC was established between 1998 and 2015 (local ethics committee approval, Tours, France, no. RCB2009-A01056-51). The cohort inclusion criteria were previously reported [15]. All tumors were submitted to histological review by an endocrine pathologist (SG), based on the identification of morphological features of high-grade neuroendocrine carcinoma and immunohistochemical expression of epithelial and neuroendocrine markers. Only cases with available formalin-fixed paraffin-embedded (FFPE) samples and sufficient tumor material for tissue microarray inclusion were included in the study ($n = 107$).

Design of the study

Tumors were classified as combined MCC when the following criteria were met on pathological examination: presence in the same tumor mass of a conventional MCC component and an additional subpopulation of tumor cells showing non-neuroendocrine differentiation in contact with MCC. Both

conventional and combined MCC were compared on clinical and immunochemical features.

All cases of combined MCC, 12 randomly selected conventional MCC cases from the cohort and 12 cutaneous squamous cell carcinoma cases from the pathology department of the hospital center of Tours were considered for molecular analysis.

Clinical and histological data

The following data were collected from patient files: age, sex, tumor site, tumor extension at the time of diagnosis (reported in accordance with American Joint Committee on Cancer [AJCC] staging), immunosuppression (HIV infection, organ transplant recipients, hematological malignancies) [16], and follow-up data. On histology, the characteristics of the non-MCC component were noted: histological type confirmed by immunochemistry, notable expression of squamous cell carcinoma markers, degree of cytological atypia, and presence of keratinization. In addition, the relation between the two tumoral components was investigated: the tumor was considered admixed when one component surrounded multiple small foci of another component and distinct when the two components were located in two distinct areas of the tumor. Finally, the characteristics of the epidermis (connection with the tumor or not, presence of an ulceration) were noted.

Immunohistochemistry

FFPE tumor samples were included in a tissue microarray. Briefly, representative areas were selected on hematoxylin/eosin-stained sections (representative of the two tumor components in combined MCC), extracted by using a 1-mm tissue core and mounted by using a semi-motorized tissue arrayer (MTA booster OI v2.00, Alphelys). For each patient, five tumor cores were placed adjacent to each other on the tissue microarray.

Tumors were screened with a panel of antibodies including conventional MCC markers used for diagnosis (pan-cytokeratin AE1-AE3, chromogranin A, synaptophysin, cytokeratin 20), several markers rarely expressed by MCC (thyroid transcription factor 1 (TTF-1), cytokeratin 7), squamous differentiation markers (cytokeratin 5/6, p40), MCPyV large T antigen, and p53. Antibodies and dilutions are available in Supplemental Table S1. Staining was performed on a Benchmark platform, except for CM2B4 staining, which was manually performed, as previously described [5]. Immunohistochemical viral status was interpreted by using the Allred score [8]: intensity and percentage of positive cells were assessed by an 8-point semi-quantitative score. A score > 2 was considered MCPyV-positive. In the same way, p53 expression was evaluated according to the Allred score, considering scores 0, 7, and 8 as abnormal expression, predictive

for loss of active p53 [17]. Intratumor CD8 infiltrate was scored as previously described [7]. For all immunohistochemical analyses, the number of uninterpretable samples (mainly due to failure of tissue microarray inclusion) is mentioned in the figures.

DNA extraction

Three 10- μ m-thick FFPE sections of representative tumor areas were used for molecular analysis. In addition, for MCPyV-positive combined MCC cases showing “distinct patterns” (defined as a large distinct area of both components), each component underwent specific sample coring, followed by a morphological control on HE slides. Genomic DNA was isolated from FFPE tissue samples by using a Maxwell 16 instrument (Promega) with the Maxwell 16 FFPE Plus LEV DNA purification kit (Promega) according to the manufacturer’s instructions.

VP1 gene PCR assay

MCPyV VP1 coding sequence was detected by nested PCR as previously described [4]. Primer sequences are listed in Supplemental Table S2.

Large T antigen quantitative PCR assay

Quantitative PCR assay was performed as reported previously [18]. Briefly, 100 ng DNA was mixed with 0.2 μ M primers (Supplemental Table S2), 0.1 μ M DNA probe, and 2xTaqman Universal PCR Master Mix (Applied Biosystems) in a final volume of 25 μ l. PCR reaction involved use of Applied Biosystems 7500 Real-Time PCR Systems programmed for 50 °C \times 2 min with an initial denaturation at 95 °C \times 15 min, followed by 45 cycles at 95 °C \times 15 s and 60 °C \times 60 s. Normalization was to human albumin gene level under the same conditions. DNA range was determined by using the MKL-1 cell line as a reference (6 points: 100 copies to 10,000,000 copies).

MCPyV viral status determination

Because MCPyV is a ubiquitous virus of the skin infecting a large part of the population and the papillary dermis is the site of replication of wild-type episomal MCPyV [19], low viral load detection may be expected in the dermis of healthy people in the absence of MCC and in non-MCC skin neoplasms when using ultrasensitive methods [19–21]. To avoid detection of wild-type episomal MCPyV of the dermis unrelated to MCC tumors, a first validation step of the MCPyV detection procedures (VP1 PCR, large T antigen quantitative PCR) was performed with 12 conventional MCC and 12 non-MCC tumor samples as positive and negative controls, which

confirmed the high sensitivity and specificity of the procedures. Therefore, MCPyV-positive status was retained only in cases positive with both validated molecular procedures.

Type-specific multiplex genotyping assays

In total, 76 different polyomaviruses and papillomaviruses were investigated by type-specific multiplex genotyping (TS-MPG) assay, a validated, highly sensitive procedure [22] designed to detect low load of episomal viruses in the skin [23] and the environment [24].

The procedure combines multiplex PCR and bead-based Luminex technology (Luminex Corp., Austin, TX, USA), as previously described [22, 25]. Multiplex type-specific PCR involved use of specific primers for detecting 9 polyomaviruses (BKV, KIV, JCV, WUV, TSV, HPyV6, HPyV7, HPyV9, and SV40), 19 high-risk alpha-human papillomaviruses (types 16, 18, 26, 31, 33, 35, 39, 45, 51, 52, 53, 56, 58, 59, 66, 68a, 68b, 70, 73, and 82), 2 low-risk alpha-human papillomaviruses (types 6, 11), and 46 beta human papillomaviruses (types 5, 8, 9, 12, 14, 15, 17, 19, 20, 21, 22, 23, 24, 25, 36, 37, 38, 47, 49, 75, 76, 80, 92, 93, 96, 98, 99, 100, 104, 105, 107, 110, 111, 113, 115, 118, 120, 122, 124, 143, 145, 150, 151, 152, 159 and 174). Two primers for amplifying beta-globin were added to provide a positive control for determining quality of the template DNA. Of note, the original set of primers included MCPyV sequences, which were excluded from the present study because of detection of the episomal virus in healthy skin as well as non-MCC tumors [21] as described previously.

Statistical analysis

Continuous data are described as median and range and categorical data as number and percentage of cases for which data were available. Proportional analysis was assessed by two-tailed Fisher's exact test. Continuous variables were compared by non-parametric Mann-Whitney *U* test. Recurrence-free survival and overall survival related to patient characteristics were analyzed by log-rank test and represented by Kaplan-Meier curves. Univariate and multivariate Cox proportional-hazards regression was used to identify factors associated with MCC recurrence and death, estimating hazard ratios (HRs) and 95% confidence intervals (CIs). Overall deaths were considered as events and living patients were censored on the date of last follow-up. AJCC stage [26], immunosuppression [16] and covariates with $p \leq 0.20$ on Cox univariate analysis were included in the multivariate Cox analysis as potential prognostic confounders. Statistical analysis involved use of XL-Stat-Life (Addinsoft, Paris, France). $p < 0.05$ was considered statistically significant.

Results

Characterization of the MCC population

Among 128 MCC cases with available FFPE samples, 8 (6%) met combined MCC criteria (Fig. 1), exhibiting squamous cell carcinoma differentiation in all cases. Characteristics of these cases are shown in Table 1. The 120 other tumors were classified as conventional MCC; the 8 combined MCC and 99 conventional cases could be included in the tissue microarray and were considered in this study.

Comparison between combined and conventional MCC

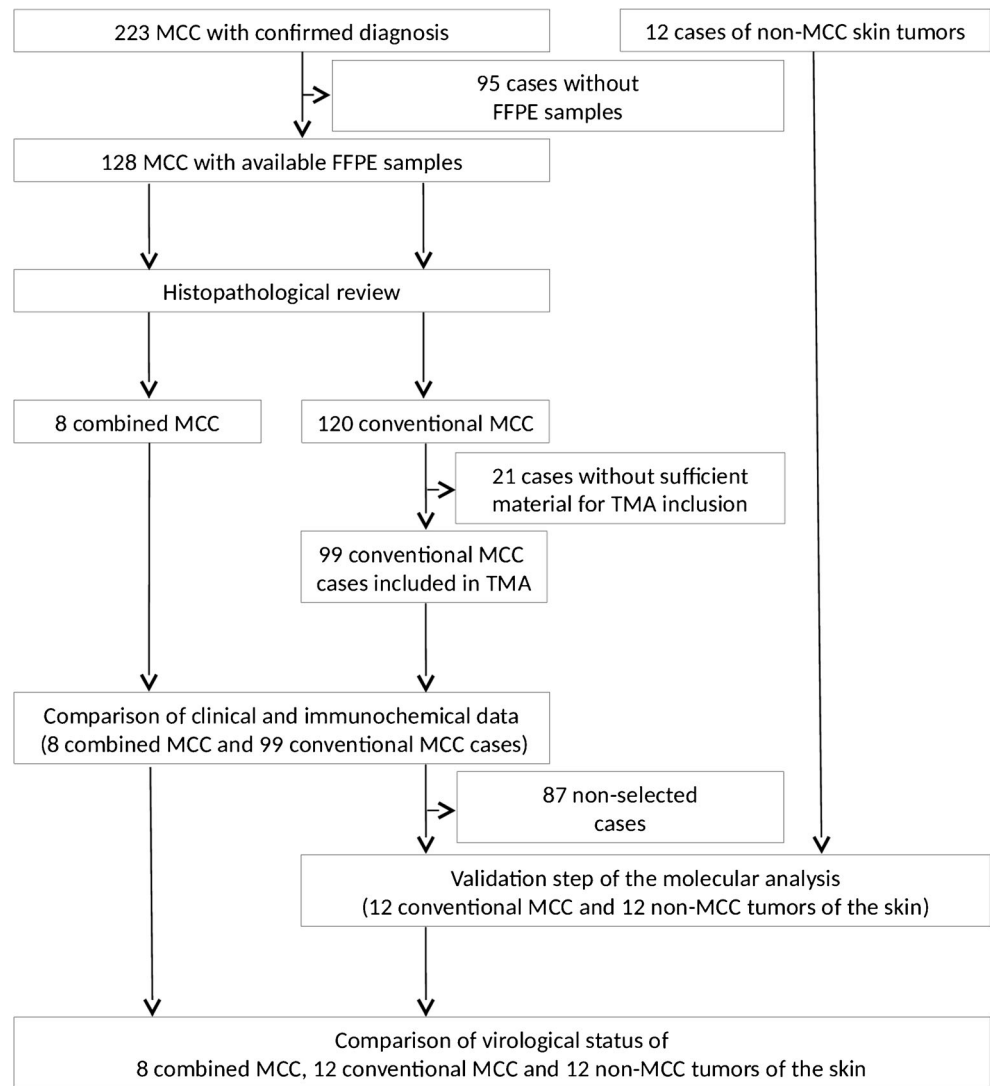
Clinical and immunohistochemical data of both groups are summarized in Table 2.

Combined MCC cases were more often diagnosed at localized stages (stage I: $n = 5$, 63%; stage II: $n = 3$, 37%) than conventional MCC cases (stage I: $n = 23$, 28%; stage II: $n = 26$, 32%, stage III: $n = 29$, 36%; stage IV: $n = 3$, 4%; localized (stages I–II) vs metastatic diseases (stages III–IV), $p = 0.046$). In addition, most combined MCC cases ($n = 5$, 62%) occurred in the head and neck area, with no significant difference from conventional MCC cases ($n = 27$, 34%) ($p = 0.3$).

On immunohistochemistry, combined MCC cases showed frequent expression of TTF1 ($n = 5$, 62%), which was rarely expressed in the other tumors ($n = 10$, 11%; $p = 2.10^{-3}$). Furthermore, all combined MCC cases but only 15 (16%) conventional MCC cases demonstrated abnormal p53 staining, possibly reflecting p53-inactivating mutation ($p = 3.10^{-6}$). Intratumoral CD8 infiltrates were absent in 6 (75%) combined MCC cases and was brisk (score 1) in the other cases. In contrast, CD8 intratumoral cells were observed in 64 (67%) conventional MCC cases ($p = 0.03$), with high density (scores 2–5) in 12 (13%). Representative illustrations of immunohistochemical staining are in Fig. 2. Only one combined MCC case presented weak large T antigen positivity (Fig. 3), whereas the viral protein was detectable by immunohistochemistry in 56 (62%) conventional MCC cases ($p = 0.01$).

Follow-up data were available for 86 patients including 7 combined MCC cases. Median duration of follow-up was 17 months (ranges 2–209) and 36 recurrences and 33 deaths were reported during follow-up. On univariate analysis, combined MCC patients harbored a trend towards increased risk of recurrence (HR 2.44, 95% CI 0.95–6.29, $p = 0.065$) as shown in Fig. 4. Only male sex was associated with a decreased risk of recurrence (HR 2.83, 95% CI 1.44–5.56, $p = 0.002$) (Supplemental Table S3) whereas male sex and older age were associated with death (HR 2.27, 95% CI 1.13–4.58, $p = 0.022$ and HR 2.07, 95% CI 1.02–4.19, $p = 0.043$, respectively).

Fig. 1 Flow chart of cases in the study. *MCC* Merkel cell carcinoma, *FFPE* formalin-fixed paraffin-embedded, *TMA* tissue microarray



A multivariate Cox analysis model including age, sex, immunosuppression, and AJCC stage (Table 3) revealed increased risk of recurrence (HR 4.15, 95% CI 1.37–12.57, $p = 0.012$) and death (HR 4.15, 95% CI 1.22–14.16, $p = 0.023$) with combined MCC.

MCPyV genome detection

The preliminary validation step of the MCPyV detection procedures (VP1 PCR, Large T antigen quantitative PCR) allowed us to detect MCPyV in all 12 conventional MCC cases except one by quantitative PCR (Table 2). All non-MCC tumors were negative for MCPyV with the two procedures, which led to the validation of this bimodal strategy for MCPyV status characterization.

This bimodal approach revealed MCPyV-positive status in 4/8 combined MCC cases, as shown in Table 2. Median MCPyV load was lower in combined MCC than MCC control cases (5.7 [range 0.13–28] vs 58 [4–313] copies/cell) ($p =$

0.04). Three of the four MCPyV-positive combined tumors were eligible for specific sampling independently targeting the two tumor components, and the remaining case consisted of closely intermixed components, which ruled out reliable specific separation. MCPyV DNA could be detected in the MCC component of the three tumors but was consistently absent in the other non-MCC part of the tumor.

Clinical, histological, and immunochemical features of MCPyV-positive and MCPyV-negative combined MCC cases are summarized in Table 1, and representative histological features of both subgroups are in Fig. 5. MCPyV was detected in combined MCC cases with basaloid squamous cell carcinoma ($n = 2$) and conventional squamous cell carcinoma ($n = 2$).

Other polyomaviruses and papillomaviruses

Beta papillomavirus DNA was detected in 5/8 combined MCC cases (63%), 9/12 conventional MCC cases (75%), and 9/12 (75%) squamous cell carcinoma cases. No

Table 1 Features of combined Merkel cell carcinoma (MCC) cases

Case number	Case 1	Case 2	Case 3	Case 4	Case 5	Case 6	Case 7	Case 8
Clinical data								
Age	85	95	81	80	68	88	92	79
Sex	M	F	F	F	F	F	F	M
Tumor location	Neck	Ear	Leg	Leg	Eyelid	Face	Leg	Lip
AJCC stage	II	II	I	I	I	I	II	I
Immunosuppression	–	UD	–	–	–	–	–	–
Morphologic features SCC component								
Morphology	Basaloid	Basaloid	Conventional	Conventional	Conventional	Bowen	Bowen	Conventional
Atypia	+	+++	++	+++	++	++	++	++
Keratinization	–	–	+	+	+	–	+	+
Architecture epidermis	Admixed	Distinct	Distinct	Distinct	Admixed	Distinct	Distinct	Admixed
Connection	+	+	+	+	+	+	+	UD
Ulceration	+	–	+	+	–	–	+	UD
References (Fig. 5)	a	b	c	d	e	f	g	h
Immunohistochemical features: MCC component								
CK20	+	+	+	+	–	+	+	+
CK7	–	–	–	–	–	–	–	–
TTF1	–	–	Low	Low	Low	High	Low	–
p53 (status/Allred score)	PMS/0	PMS/8	PMS/8	PMS/0	PMS/0	PMS/8	PMS/8	PMS/8
LTA _g	–	+	–	–	–	–	–	–
CD8 (score)	0	1	0	0	0	1	0	0
SCC component								
CK5/6	+	+	+	+	+	+	+	+
p40	+	+	+	+	+	+	+	+
Virologic features polyomavirus detection								
VP1 PCR	+	+	+	+	–	–	–	–
qPCR (Nb of copy/cell)	0,13	11	28	0,38	–	–	–	–
Other HPyV	–	–	–	–	–	–	–	–
Papillomavirus detection								
α type	–	–	–	–	–	–	–	–
β type	–	–	98	9/12/98/110	–	5/38	107	21/122

AJCC American Joint Committee on Cancer, CK cytokeratin, LTA_g large T antigen, MCC Merkel cell carcinoma, + positive, – negative, MCPyV Merkel cell polyomavirus, PCR polymerase chain reaction, PMS predicted mutated status (i.e., Allred score = 0, 7, or 8), PWTs predicted wild-type status (i.e., Allred score = 1 to 6), SCC squamous cell carcinoma, TTF1 thyroid transcription factor, UD unavailable data

recurrence considering genotypes was observed in the combined MCC group, except for human papillomavirus 98, which was present in 2 cases (Supplemental Table S4). In addition, we detected human polyomavirus 6 in one conventional MCC case and human papillomavirus 16 in 2 squamous cell carcinoma cases.

Discussion

We identified 8 cases of combined MCC in a series of 128 MCC tumors. Combined MCC often expressed TTF1, which is almost always absent in conventional MCC cases and often showed p53-aberrant expression. In addition, multivariate

analysis revealed an increased risk of recurrence and death in this population. Using two independent validated molecular procedures, we detected MCPyV in half of our combined MCC cases, only in the MCC component. Moreover, combined MCC cases showed lower MCPyV load as compared with conventional MCC tumors and frequent large T antigen negativity on immunohistochemistry. Finally, beta papillomaviruses were frequent in combined and conventional MCC and non-MCC tumor samples.

In accordance with previous reports, our series shows that combined MCC is a rare tumor, representing 6% of our cohort. Combined MCC tumors occurred preferentially on the head, the main sun-exposed area in our country. On immunohistochemistry, the neuroendocrine component of these

Table 2 Clinical, immunochemical, and virological features of combined and conventional MCC cases

Clinical data	Combined MCC (n = 8)	Conventional MCC (n = 99)	p value
Age, y, median, range	83 (68–95)	76 (45–96)	0.4
Sex			0.5
Female	6	50	
Male	2	35	
Missing data	0	14	
Location			0.3
Head	5	27	
Trunk	0	7	
Upper limb	0	8	
Lower limb	3	24	
Unknown primary	0	13	
Missing data	0	20	
Disease extension at diagnosis			0.046
Localized (stages I–II)	8	49	
Metastatic (stages III–IV)	0	32	
Missing data	0	18	
Immunodepression			0.9
Yes	0	9	
No	7	68	
Missing data	1	22	
Immunochemical features (n = 8) (n = 99)			p value
Cytokeratin 20			0.12
Positive	6	89	
Negative	2	6	
Uninterpretable cases	0	4	
Cytokeratin 7			0.9
Positive	0	9	
Negative	8	80	
Uninterpretable cases	0	10	
TTF1			2.10 ⁻³
Positive	5 (4 low)	10	
Negative	3	80	
Uninterpretable cases	0	9	
p53			3.10 ⁻⁶
PMS	8	15	
PWTS	0	76	
Uninterpretable cases	0	8	
Large T antigen (CM2B4)			0.01
Positive	1	56	
Negative	7	35	
Uninterpretable cases	0	8	
CD8			0.03
Absent (score 0)	6	31	
Present (score 1–5)	2	64	
Uninterpretable cases	0	4	
Virological features (n = 8) (n = 12)			p value
MCPyV detection (VP1 PCR)			0.01
Positive cases	4	12	
Negative cases	4	0	
Uninterpretable cases	0	0	
MCPyV detection (LTAq qPCR)			0.1
Positive cases	4	11	
Negative cases	4	1	
Uninterpretable cases	0	0	
Other polyomavirus detection			0.9

Table 2 (continued)

Clinical data	Combined MCC (n = 8)	Conventional MCC (n = 99)	p value
Positive cases	0	0	
Negative cases	8	12	
Uninterpretable cases	0	0	
Papillomavirus detection			0.6
Positive cases	5	9	
Negative cases	3	3	
Uninterpretable cases	0	0	

AJCC American Joint Committee on Cancer, *CMCC* combined MCC, *LTA* large T antigen, *MCC* classical MCC, + positive, – negative, *MCPyV(+)* Merkel cell polyomavirus-positive MCC, *MCPyV(-)* Merkel cell polyomavirus-negative MCC, *PMS* predicted mutated status (i.e., Allred score = 0, 7, or 8), *PWTS* predicted wild-type status (i.e., Allred score = 1 to 6), *SCC* squamous cell carcinoma, *TTF1* thyroid transcription factor 1

tumors harbored the same phenotypical markers as conventional MCC, notably cytokeratin 20, but with unusual expression of TTF1 [27]. In addition, aberrant expression of p53, suggesting p53 mutation [9, 28], was common. This finding agrees with genomic analysis performed by Pullitzer et al. reporting higher somatic gene mutation rate in combined than conventional MCC [29].

In accordance with the Martin et al. study, which found 61% mortality³, we found combined MCC an aggressive neoplasm with decreased recurrence-free survival ($p = 0.012$) and overall survival ($p = 0.023$) as compared with conventional MCC, which highlights the importance of this morphological distinction in current practise.

Three studies [9–11] by Busam (in 2009), Martin (in 2013), and Carter (in 2017) reported the absence of MCPyV in combined MCC (7 and 15 cases, respectively). As a result, the authors proposed that combined MCCs should be included in the MCPyV-negative cutaneous tumor group. However, two case reports have given contradictory results, identifying MCPyV in two combined MCC cases by molecular biology [13, 30]. In addition, MCPyV was identified in the neuroendocrine component of a combined MCC case by high-sensitive immunofluorescence staining [12] and in another case by conventional immunochemistry [31]. Here, using a multimodal approach for MCPyV detection, we confirm these findings in a large series of combined MCC.

Weak expression of MCPyV large T antigen was detectable by immunochemistry in only one case with high MCPyV viral load (11 copies/cell), and MCPyV DNA was identified in half of the cases with a lower viral load. Variations in viral load offer an explanation for the previous discordant results. Indeed, immunochemical procedures used in most studies have a sensitivity of 80% as compared with amplification techniques, which probably reflects the influence of viral load on the sensitivity of the different identification approaches [32].

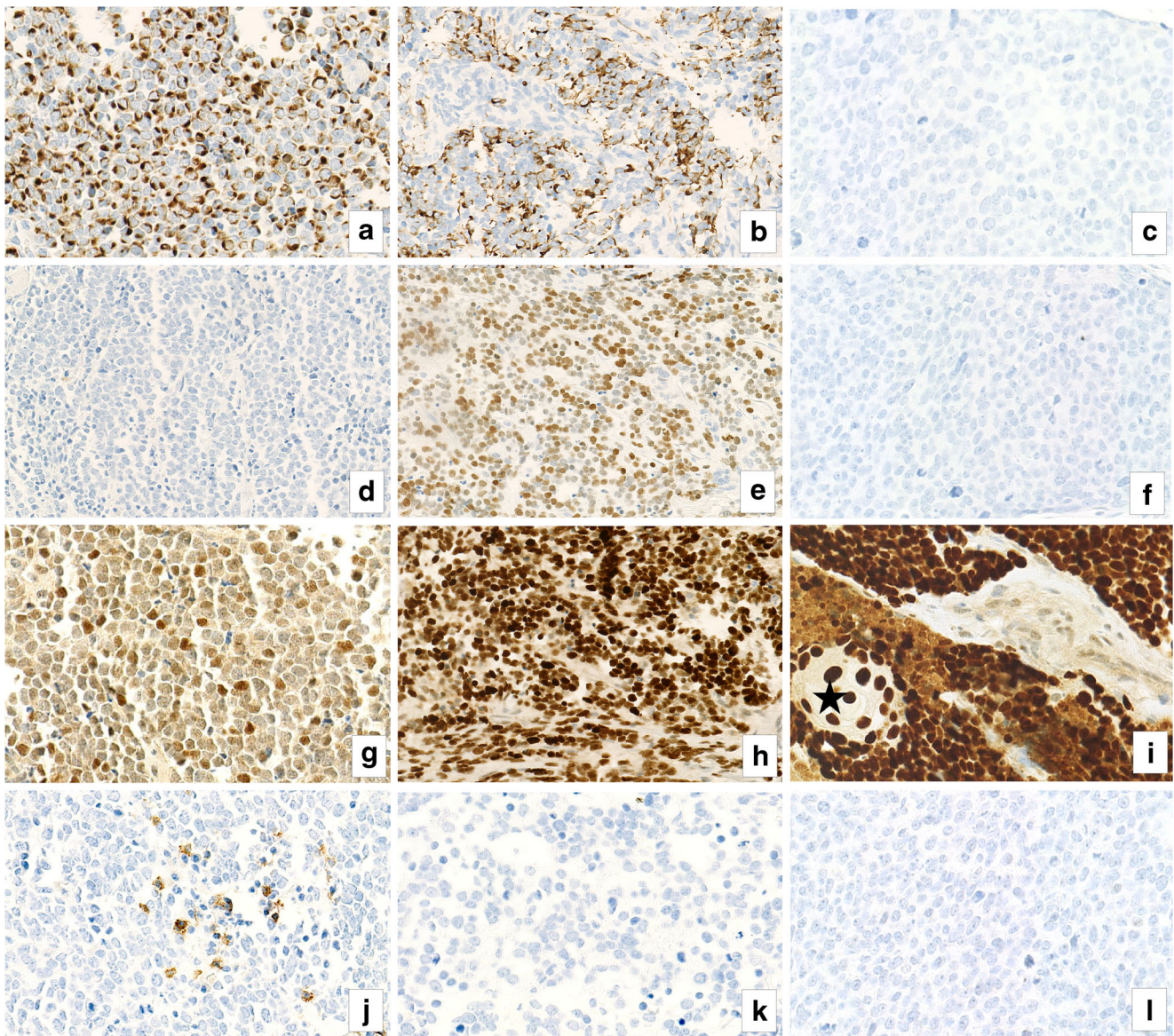


Fig. 2 Representative microphotographs of the immunohistochemical study for cytokeratin 20 (a–c), TTF-1 (d–f), p53 (g–i), and CD8 immune infiltrate (j–l) in conventional (a, d, g, j) and combined MCC (MCC (b, e, h, k) and squamous (c, f, i, l)

components of combined cases harbored same immunochemical p53 profile as illustrate in (i): overexpression of p53 in a small islet of squamous carcinoma (black star) surrounding by the MCC component

Fig. 3 Immunohistochemical detection of Merkel cell polyomavirus (MCPyV) large T antigen in a combined MCC sample: **a** moderate nuclear large T antigen expression in the MCC component and **b** lack of large T antigen expression in the squamous carcinoma component

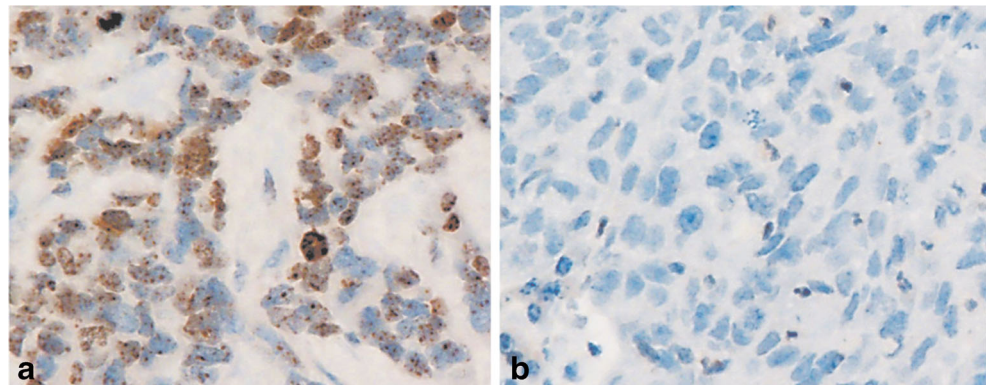
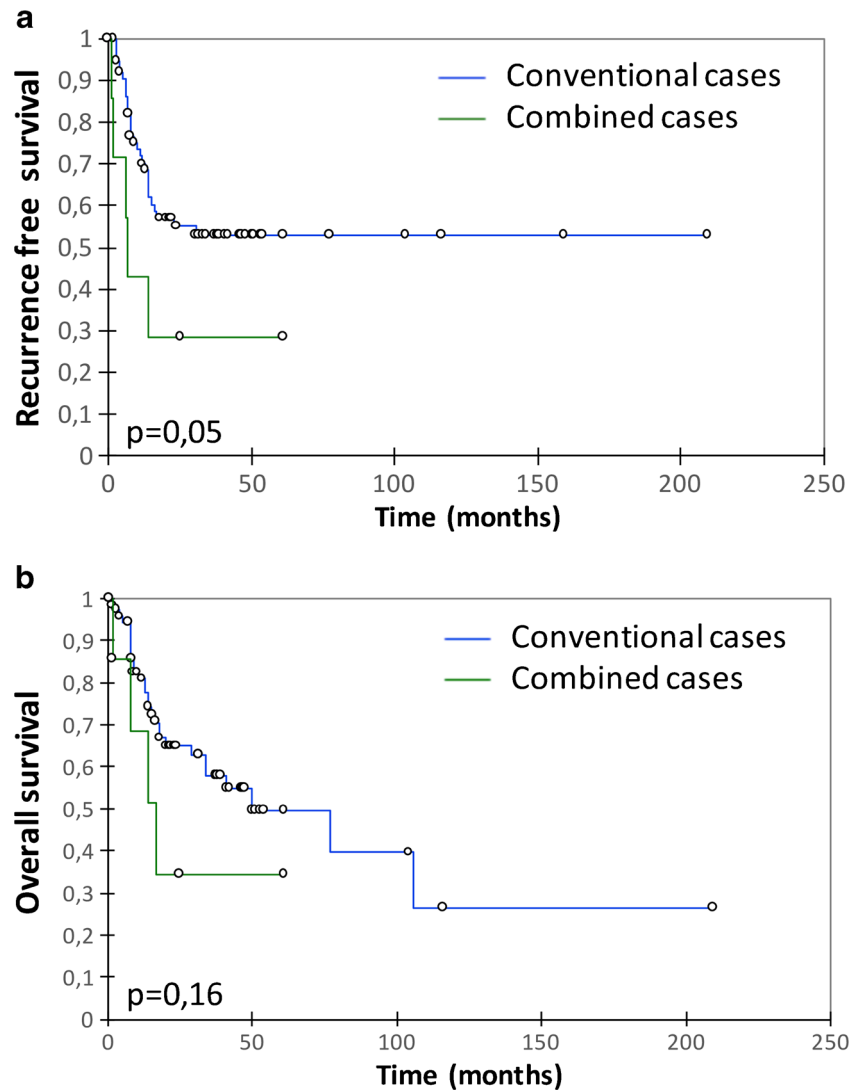


Fig. 4 Kaplan-Meier survival curves for the Merkel cell carcinoma population by the MCC type (combined vs conventional cases): **a** recurrence-free survival and **b** overall survival



Considering the high prevalence of the MCPyV in normal skin, the use of highly sensitive molecular biology procedures might represent a pitfall in the identification of an MCPyV-related tumor, introducing a risk of false-positive results, which justifies our multimodal approach. Although MCPyV is considered a hallmark of MCC, episomal MCPyV can be detected with

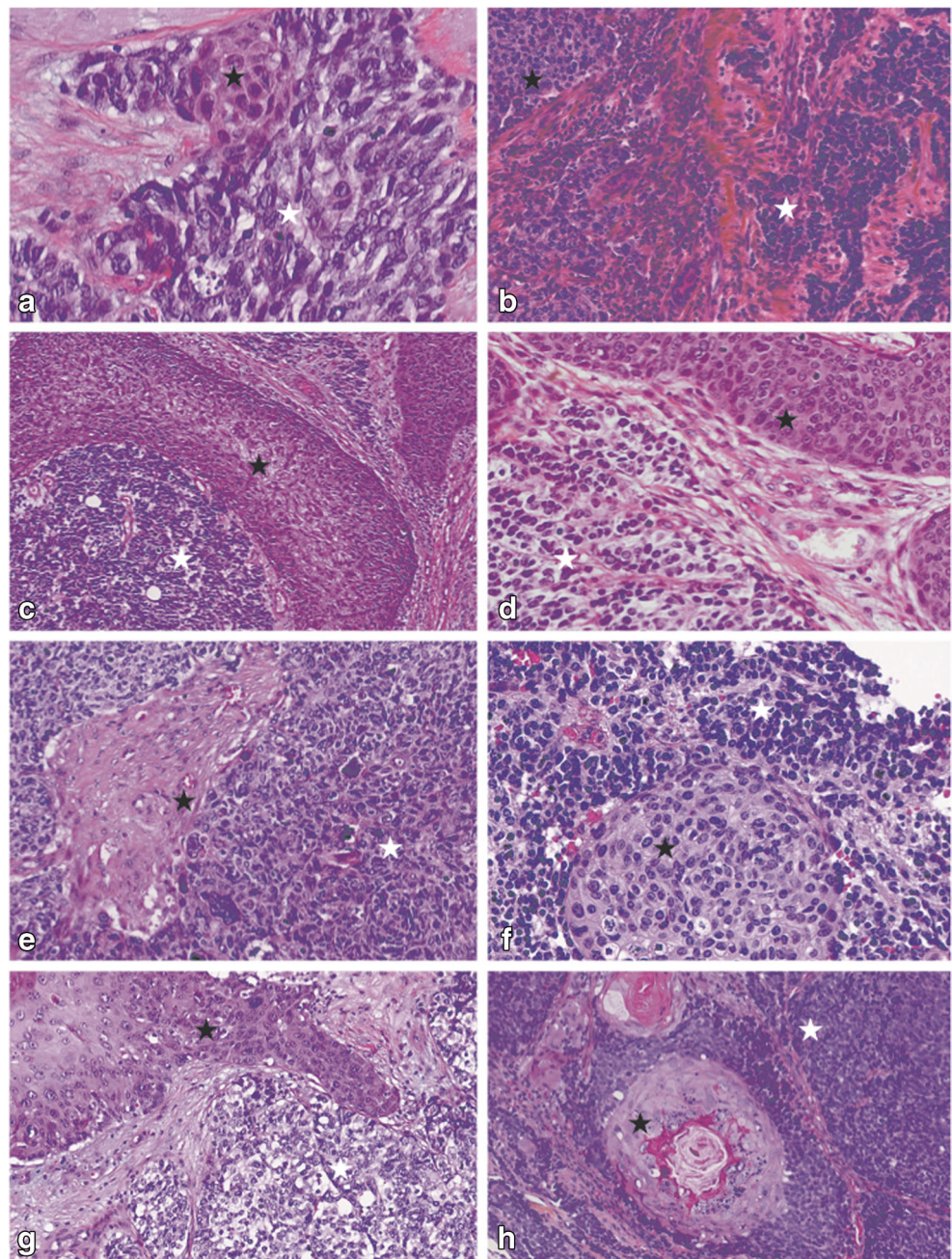
very low load in the papillary dermis of normal skin in many healthy adults [19] and in non-MCC skin tumors [20]. With the lack of an international gold standard for MCPyV quantification, arbitrary cutoffs have been used [33] to distinguish MCPyV-negative from MCPyV-positive tumors. To avoid this bias, we introduced a first step of calibration of our molecular MCPyV

Table 3 Multivariate Cox proportional-hazard analysis of factors associated with MCC recurrence and death

Covariate	Recurrence		Death	
	Adjusted HR (95% CI)	<i>p</i>	Adjusted HR (95% CI)	<i>p</i>
Age (≥ 77 vs < 77 years)	2.14 (1.04–4.41)	0.040	2.87 (1.27–6.52)	0.011
Sex (male vs female)	4.67 (2.12–10.32)	0.0001	5.53 (2.26–13.57)	0.0002
AJCC stages (3–4 vs 1–2)	1.64 (0.76–3.52)	0.206	2.10 (0.96–4.60)	0.065
Immunosuppression (yes vs no)	0.93 (0.32–2.73)	0.901	2.23 (0.93–5.34)	0.072
MCC status (combined vs conventional)	4.15 (1.37–12.57)	0.012	4.15 (1.22–14.16)	0.023

HR hazard ratio, CI confidence interval, MCC Merkel cell carcinoma

Fig. 5 Representative microphotographs of MCPyV-positive (**a–d**) and MCPyV-negative (**e–h**) combined MCC samples. The neuroendocrine component is characterized by sheet of small uniform cells with high nucleocytoplasmic ratio (white star). It is associated with another carcinomatous component (black star): basaloid squamous cell carcinoma (**a, b**), conventional squamous cell carcinoma (**c, d, e, h**), and Bowen disease (**f, g**)



detection test in the study, using conventional MCC and non-MCC skin tumors as controls. Indeed in our setting, the sensitivity of the MCPyV detection was carefully managed to detect only significant MCPyV loads associated with MCC.

The significance of MCPyV detection in tumors and its relation with somatic mutations is still unclear. According to the “hit and run” phenomenon [34], MCC could feature loss of large T antigen dependence. Indeed, accumulation of somatic mutations—notably p53 mutations—could cause an empowerment process and might finally cause loss of MCPyV sequence by a selection process. In this way, the low viral load that we detected in combined MCC cases could

be due to the presence of a minor MCPyV-positive tumor subpopulation. The divergent differentiation component that we found was squamous cell carcinoma in all cases. Because squamous cell carcinoma is related to papillomavirus infection [35], papillomaviruses could represent a possible etiological agent for combined MCC. Beta human papillomaviruses were detected in 63% of our combined MCC cases and 75% of conventional MCC cases, which rules out the possibility of a specific association between human papillomavirus and combined MCC. However, the frequent detection of cutaneous human papillomavirus in MCC in our study raises the question of their potential impact as a co-carcinogen.

Because specific morphological features—notably non-keratinizing basaloid morphology—have been described in virus-induced tumors [36], we compared morphological features of MCPyV-positive and MCPyV-negative tumors (data not shown). Although we found no statistically significant difference because of the small number of cases, we detected MCPyV in the two tumors containing squamous components with basaloid morphology, which suggests possible interactions between viral status and morphology.

MCPyV integration has been found in the main oncogenic event in MCC, but the nature of the cell in which this integration occurs is unknown. Of note, in contrast to conventional MCC, combined MCC with squamous differentiation showed an epidermal connection in all of our cases. The development of combined tumors implicates a common progenitor cell; as previously mentioned, Bowen's disease is an epidermic intraepithelial neoplasm often present in combined MCC. Considering these two findings, combined MCC might originate from an epidermal cell. In addition, keratinocytes have been suggested as precursors of Merkel cells [37]. These considerations led us to hypothesize that MCPyV infection in a keratinocyte could be the first oncogenic event in combined MCC. Premature occurrence and accumulation of UV-induced somatic mutations could secondarily lead to the loss of the virus in a portion of the cell population and to squamous differentiation in the intraepithelial component. At the same time, the MCC component could invade the dermis and further undergo progressive loss of MCPyV. Hence, advanced combined MCC would feature very low load or lack of MCPyV, high somatic mutation rate, lack of T cell response and impaired outcome. In this way, our results do not rule out that combined MCC shares the same genetic background and behavior as other MCC types with negative-status or low-load MCPyV but may improve our understanding of their oncogenesis.

Our study has some limitations, owing to the low number of combined MCC cases, which is inherent to the low incidence of the tumor. The frequent MCPyV negativity found on immunostaining in combined MCC—currently considered the main tool for viral status determination [8]—led us to use molecular detection procedures, which implies sensitivity bias management, as discussed previously. Nonetheless, our results were validated by bimodal molecular procedures and positive and negative relevant controls.

To conclude, we detected MCPyV in half of our combined MCC cases, with a lower viral load than with conventional MCC, which suggests a shared oncogenesis between both MCC variants. The impact of MCPyV on the oncogenesis and behavior of the tumor remains to be determined.

Funding This work was funded by project POCAME, Axe Immunothérapies, Cancéropole Grand Ouest-Région Centre Val de Loire (France) and by the Fond de recherche de la société française de Pathologie 2016.

Compliance with ethical standards

Conflict of interest The authors declare no conflict of interest.

Institutional review board The local Ethics Committee of Tours (France) approved the study (no. RCB2009-A01056-51)

References

- Lemos BD, Storer BE, Iyer JG, Phillips JL, Bichakjian CK, Fang LC, Johnson TM, Liegeois-Kwon NJ, Otley CC, Paulson KG, Ross MI, Yu SS, Zeitouni NC, Byrd DR, Sondak VK, Gershenwald JE, Sober AJ, Nghiem P (2010) Pathologic nodal evaluation improves prognostic accuracy in Merkel cell carcinoma: analysis of 5823 cases as the basis of the first consensus staging system. *J Am Acad Dermatol* 63:751–761. <https://doi.org/10.1016/j.jaad.2010.02.056>
- LeBoit PE, World Health Organisation, International Agency for Research on Cancer (eds) (2007) Pathology and genetics of skin tumours: [... reflects the views of a working group that convened for an editorial and consensus conference in Lyon, France, September 22 - 25, 2003]. Reprinted. IARC Press, Lyon
- Feng H, Shuda M, Chang Y, Moore PS (2008) Clonal integration of a polyomavirus in human Merkel cell carcinoma. *Science* 319:1096–1100. <https://doi.org/10.1126/science.1152586>
- Touzé A, Gaitan J, Maruani A, Le Bidre E, Doussinaud A, Clavel C et al (2009) Merkel cell polyomavirus strains in patients with Merkel cell carcinoma. *Emerg Infect Dis* 15:960–962. <https://doi.org/10.3201/eid1506.081463>
- Houben R, Adam C, Baeurle A, Hesbacher S, Grimm J, Angermeyer S, Henzel K, Hauser S, Elling R, Bröcker EB, Gaubatz S, Becker JC, Schrama D (2012) An intact retinoblastoma protein-binding site in Merkel cell polyomavirus large T antigen is required for promoting growth of Merkel cell carcinoma cells. *Int J Cancer* 130:847–856. <https://doi.org/10.1002/ijc.26076>
- González-Vela MDC, Curriel-Olmo S, Derdak S, Beltran S, Santibañez M, Martínez N et al (2017) Shared oncogenic pathways implicated in both virus-positive and UV-induced Merkel cell carcinomas. *J Invest Dermatol* 137:197–206. <https://doi.org/10.1016/j.jid.2016.08.015>
- Paulson KG, Iyer JG, Tegeder AR, Thibodeau R, Schelter J, Koba S, Schrama D, Simonson WT, Lemos BD, Byrd DR, Koelle DM, Galloway DA, Leonard JH, Madeleine MM, Argenyi ZB, Disis ML, Becker JC, Cleary MA, Nghiem P (2011) Transcriptome-wide studies of merkel cell carcinoma and validation of intratumoral CD8+ lymphocyte invasion as an independent predictor of survival. *J Clin Oncol Off J Am Soc Clin Oncol* 29:1539–1546. <https://doi.org/10.1200/JCO.2010.30.6308>
- Moshiri AS, Doumani R, Yelistratova L, Blom A, Lachance K, Shinohara MM, Delaney M, Chang O, McArdle S, Thomas H, Asgari MM, Huang ML, Schwartz SM, Nghiem P (2016) Polyomavirus-negative Merkel cell carcinoma: a more aggressive subtype based on analysis of 282 cases using multimodal tumor virus detection. *J Invest Dermatol* 137:819–827. <https://doi.org/10.1016/j.jid.2016.10.028>
- Busam KJ, Jungbluth AA, Rektman N, Coit D, Pulitzer M, Bini J, Arora R, Hanson NC, Tassello JA, Frosina D, Moore P, Chang Y (2009) Merkel cell polyomavirus expression in merkel cell carcinomas and its absence in combined tumors and pulmonary neuroendocrine carcinomas. *Am J Surg Pathol* 33:1378–1385. <https://doi.org/10.1097/PAS.0b013e3181aa30a5>
- Martin B, Poblet E, Rios JJ, Kazakov D, Kutzner H, Brenn T, Calonje E (2013) Merkel cell carcinoma with divergent differentiation: histopathological and immunohistochemical study of 15

- cases with PCR analysis for Merkel cell polyomavirus. *Histopathology* 62:711–722. <https://doi.org/10.1111/his.12091>
11. Carter MD, Gaston D, Huang W-Y, Greer WL, Pasternak S, Ly TY, Walsh NM (2017) Genetic profiles of different subsets of Merkel cell carcinoma show links between combined and pure MCPyV-negative tumors. *Hum Pathol* 71:117–125. <https://doi.org/10.1016/j.humpath.2017.10.014>.
 12. Chou T-C, Tsai K-B, Wu C-Y, Hong C-H, Lee C-H (2016) Presence of the Merkel cell polyomavirus in Merkel cell carcinoma combined with squamous cell carcinoma in a patient with chronic arsenism. *Clin Exp Dermatol* 41:902–905. <https://doi.org/10.1111/ced.12954>
 13. Mitteldorf C, Mertz KD, Fernández-Figueras MT, Schmid M, Tronnier M, Kempf W (2012) Detection of Merkel cell polyomavirus and human papillomaviruses in Merkel cell carcinoma combined with squamous cell carcinoma in immunocompetent European patients. *Am J Dermatopathol* 34:506–510. <https://doi.org/10.1097/DAD.0b013e31823b9b4e>
 14. Bishop JA, Westra WH (2011) Human papillomavirus-related small cell carcinoma of the oropharynx. *Am J Surg Pathol* 35:1679–1684. <https://doi.org/10.1097/PAS.0b013e3182299cde>
 15. Gardair C, Samimi M, Touzé A, Coursaget P, Lorette G, Caille A et al (2015) Somatostatin receptors 2A and 5 are expressed in Merkel cell carcinoma with no association with disease severity. *Neuroendocrinology* 101:223–235. <https://doi.org/10.1159/000381062>
 16. Asgari MM, Sokil MM, Warton EM, Iyer J, Paulson KG, Nghiem P (2014) Effect of host, tumor, diagnostic, and treatment variables on outcomes in a large cohort with Merkel cell carcinoma. *JAMA Dermatol* 150:716–723. <https://doi.org/10.1001/jamadermatol.2013.8116>
 17. Watanabe G, Ishida T, Furuta A, Takahashi S, Watanabe M, Nakata H, Kato S, Ishioka C, Ohuchi N (2015) Combined immunohistochemistry of PLK1, p21, and p53 for predicting TP53 status: an independent prognostic factor of breast cancer. *Am J Surg Pathol* 39:1026–1034. <https://doi.org/10.1097/PAS.0000000000000386>
 18. Rodig SJ, Cheng J, Wardzala J, DoRosario A, Scanlon JJ, Laga AC, Martinez-Fernandez A, Barletta JA, Bellizzi AM, Sadasivam S, Holloway DT, Cooper DJ, Kupper TS, Wang LC, DeCaprio JA (2012) Improved detection suggests all Merkel cell carcinomas harbor Merkel polyomavirus. *J Clin Invest* 122:4645–4653. <https://doi.org/10.1172/JCI64116>
 19. Liu W, Yang R, Payne AS, Schowalter RM, Spurgeon ME, Lambert PF, Xu X, Buck CB, You J (2016) Identifying the target cells and mechanisms of Merkel cell polyomavirus infection. *Cell Host Microbe* 19:775–787. <https://doi.org/10.1016/j.chom.2016.04.024>
 20. Rollison DE, Giuliano AR, Messina JL, Fenske NA, Cherpelis BS, Sondak VK, Roetzheim RG, Iannacone MR, Michael KM, Gheit T, Waterboer T, Tommasino M, Pawlita M (2012) Case-control study of Merkel cell polyomavirus infection and cutaneous squamous cell carcinoma. *Cancer Epidemiol Biomark Prev Publ Am Assoc Cancer Res Cosponsored Am Soc Prev Oncol* 21:74–81. <https://doi.org/10.1158/1055-9965.EPI-11-0764>
 21. Hampras SS, Michel A, Schmitt M, Waterboer T, Kranz L, Gheit T, Fisher K, Sondak VK, Messina J, Fenske N, Cherpelis B, Tommasino M, Pawlita M, Rollison DE (2015) Merkel cell polyomavirus (MCV) T-antigen seroreactivity, MCV DNA in eyebrow hairs, and squamous cell carcinoma. *Infect Agent Cancer* 10:35. <https://doi.org/10.1186/s13027-015-0030-0>
 22. Gheit T, Billoud G, de Koning MNC, Gemignani F, Forslund O, Sylla BS, Vaccarella S, Franceschi S, Landi S, Quint WGV, Canzian F, Tommasino M (2007) Development of a sensitive and specific multiplex PCR method combined with DNA microarray primer extension to detect Betapapillomavirus types. *J Clin Microbiol* 45:2537–2544. <https://doi.org/10.1128/JCM.00747-07>
 23. Iannacone MR, Gheit T, Pfister H, Giuliano AR, Messina JL, Fenske NA, Cherpelis BS, Sondak VK, Roetzheim RG, Silling S, Pawlita M, Tommasino M, Rollison DE (2014) Case-control study of genus-beta human papillomaviruses in plucked eyebrow hairs and cutaneous squamous cell carcinoma. *Int J Cancer* 134:2231–2244. <https://doi.org/10.1002/ijc.28552>
 24. Di Bonito P, Libera SD, Petricca S, Iaconelli M, Accardi L, Muscillo M et al (2015) Frequent and abundant Merkel cell polyomavirus detection in urban wastewaters in Italy. *Food Environ Virol* 7:1–6. <https://doi.org/10.1007/s12560-014-9168-y>.
 25. Gheit T, Landi S, Gemignani F, Snijders PJF, Vaccarella S, Franceschi S, Canzian F, Tommasino M (2006) Development of a sensitive and specific assay combining multiplex PCR and DNA microarray primer extension to detect high-risk mucosal human papillomavirus types. *J Clin Microbiol* 44:2025–2031. <https://doi.org/10.1128/JCM.02305-05>
 26. Harms KL, Healy MA, Nghiem P, Sober AJ, Johnson TM, Bichakjian CK, Wong SL (2016) Analysis of prognostic factors from 9387 Merkel cell carcinoma cases forms the basis for the new 8th edition AJCC staging system. *Ann Surg Oncol* 23:3564–3571. <https://doi.org/10.1245/s10434-016-5266-4>
 27. Czapiewski P, Majewska H, Kutzner H, Kazakov D, Renkielska A, Biernat W (2016) TTF-1 and PAX5 are frequently expressed in combined Merkel cell carcinoma. *Am J Dermatopathol* 38:513–516. <https://doi.org/10.1097/DAD.0000000000000464>
 28. Lai JH, Fleming KE, Ly TY, Pasternak S, Godlewski M, Doucette S, Walsh NM (2015) Pure versus combined Merkel cell carcinomas: immunohistochemical evaluation of cellular proteins (p53, Bcl-2, and c-kit) reveals significant overexpression of p53 in combined tumors. *Hum Pathol* 46:1290–1296. <https://doi.org/10.1016/j.humpath.2015.05.008>
 29. Pulitzer MP, Brannon AR, Berger MF, Louis P, Scott SN, Jungbluth AA, Coit DG, Brownell I, Busam KJ (2015) Cutaneous squamous and neuroendocrine carcinoma: genetically and immunohistochemically different from Merkel cell carcinoma. *Mod Pathol Off J U S Can Acad Pathol Inc* 28:1023–1032. <https://doi.org/10.1038/modpathol.2015.60>
 30. Chen C-H, Wu Y-Y, Kuo K-T, Liao J-Y, Liang C-W (2015) Combined squamous cell carcinoma and Merkel cell carcinoma of the vulva: role of human papillomavirus and Merkel cell polyomavirus. *JAAD Case Rep* 1:196–199. <https://doi.org/10.1016/j.jdc.2015.04.005>
 31. Iwasaki T, Kodama H, Matsushita M, Kuroda N, Yamasaki Y, Murakami I, Yamamoto O, Hayashi K (2013) Merkel cell polyomavirus infection in both components of a combined Merkel cell carcinoma and basal cell carcinoma with ductal differentiation; each component had a similar but different novel Merkel cell polyomavirus large T antigen truncating mutation. *Hum Pathol* 44:442–447. <https://doi.org/10.1016/j.humpath.2012.08.022>
 32. Leroux-Kozal V, Lévêque N, Brodard V, Lesage C, Dudev O, Makeieff M, Kanagaratnam L, Diebold MD (2015) Merkel cell carcinoma: histopathologic and prognostic features according to the immunohistochemical expression of Merkel cell polyomavirus large T antigen correlated with viral load. *Hum Pathol* 46:443–453. <https://doi.org/10.1016/j.humpath.2014.12.001>
 33. Eid M, Nguyen J, Brownell I (2017) Seeking standards for the detection of Merkel cell polyomavirus and its clinical significance. *J Invest Dermatol* 137:797–799. <https://doi.org/10.1016/j.jid.2016.12.024>
 34. Houben R, Grimm J, Willmes C, Weinkam R, Becker JC, Schrama D (2012) Merkel cell carcinoma and Merkel cell polyomavirus: evidence for hit-and-run oncogenesis. *J Invest Dermatol* 132:254–256. <https://doi.org/10.1038/jid.2011.260>

35. Tommasino M (2017) The biology of beta human papillomaviruses. *Virus Res* 2016. <https://doi.org/10.1016/j.virusres.2016.11.013>
36. Mehrad M, Carpenter DH, Chernock RD, Wang H, Ma X-J, Luo Y, Luo J, Lewis JS Jr, el-Mofly SK (2013) Papillary squamous cell carcinoma of the head and neck: clinicopathologic and molecular features with special reference to human papillomavirus. *Am J Surg Pathol* 37:1349–1356. <https://doi.org/10.1097/PAS.0b013e318290427d>
37. Ostrowski SM, Wright MC, Bolock AM, Geng X, Maricich SM (2015) Ectopic Atoh1 expression drives Merkel cell production in embryonic, postnatal and adult mouse epidermis. *Dev Camb Engl* 142:2533–2544. <https://doi.org/10.1242/dev.123141>

Polyomavirus-positive Merkel cell carcinoma derived from a trichoblastoma suggests an epithelial origin of this Merkel cell carcinoma

Accepted in J Invest Dermatol.

Thibault Kervarrec^{1,2,3*,**}, Mohanad Aljundi^{4**}, Silke Appenzeller^{5**}, Mahtab Samimi^{2,6}, Eve Maubec⁴, Bernard Cribier⁷, Lydia Deschamps⁸, Bhavishya Sarma³, Eva-Maria Sarosi³, Patricia Berthon², Annie Levy⁹, Guilhem Bousquet¹⁰, Anne Tallet¹¹, Antoine Touzé², Serge Guyétant^{1,2}, David Schrama^{3***} & Roland Houben^{3***}

- (1) Department of Pathology, Université de Tours, Centre Hospitalier Universitaire de Tours, 37044 Tours Cedex 09, France
- (2) “Biologie des infections à polyomavirus” team, UMR INRA ISP 1282, Université de Tours, 31, Avenue Monge 37200 TOURS, France
- (3) Department of Dermatology, Venereology and Allergology, University Hospital Würzburg, Josef-Schneider-Straße 2, 97080 Würzburg, Germany
- (4) Department of Dermatology, Avicenne University Hospital, 125 rue de Stalingrad, 97000 Bobigny, France
- (5) Core Unit Bioinformatics, Comprehensive Cancer Center Mainfranken, University Hospital of Würzburg, Josef-Schneider-Straße 6, 97080 Würzburg, Germany
- (6) Département de Dermatologie, Université de Tours, Centre Hospitalier Universitaire de Tours, 37044 Tours Cedex 09, France
- (7) Dermatology Clinic, Hôpitaux Universitaires & Université de Strasbourg, Hôpital Civil, 1 Place de l’Hôpital, 67000 Strasbourg, France
- (8) Department of Pathology Bichat Hospital, 45 rue Henri Huchard, 75018 Paris, France
- (9) Department of Pathology, Avicenne University Hospital, 125 rue de Stalingrad, 97000 Bobigny, France
- (10) Department of Medical Oncology, Avicenne University Hospital, 125 rue de Stalingrad, 97000 Bobigny, France
- (11) Platform of Somatic Tumor Molecular Genetics, Université de Tours, Centre Hospitalier Universitaire de Tours, 37044 Tours Cedex 09, France

Disclosure/Conflict of Interest: The authors declare no conflict of interest.

(*) T. Kervarrec is the corresponding author. (**) T. Kervarrec, M. Aljundi and S. Appenzeller contributed equally to the present study. (***) D. Schrama and R. Houben contributed equally to the present study.

Grant numbers and sources of support: Fondation ARC pour la recherche contre le cancer, Interdisziplinäres Zentrum für Klinische Forschung Würzburg (IZKF B-343) and LEO Foundation Award to DS. Ligue nationale contre le cancer, Comités 16, 18, 28.

Institutional review board: The local Ethics Committee of Tours (France) approved the study (no. RCB2009-A01056-51)

Corresponding author:

Dr Thibault Kervarrec

Department of Pathology, Hôpital Trousseau, CHRU de Tours, 37044 TOURS Cedex 09 France. Tel: +33 (2) 47 47 80 69/Fax: +33 (2) 47 47 46 22

Email: thibaultkervarrec@yahoo.fr

Word count (Excluding abstract and references): 3552

List of attachments: Figures: 4 / Supplements consisting of 5 Tables, 4 Figures and 3 Supplementary Materials)

Abstract

Merkel cell carcinoma (MCC), an aggressive neuroendocrine carcinoma of the skin, is to date the only human cancer known to be frequently caused by a polyomavirus. However, it is a matter of debate which cells are targeted by the Merkel cell polyomavirus (MCPyV) to give rise to the phenotypically multifaceted MCC cells.

To assess the lineage of origin of MCPyV-positive MCC, genetic analysis of a very rare tumor combining benign trichoblastoma and MCPyV-positive MCC was conducted by massive parallel sequencing. Although MCPyV was found to be integrated only in the MCC part, six somatic mutations were shared by both tumor components. The mutational overlap between trichoblastoma and MCPyV-positive MCC part of the combined tumor implies that MCPyV integration occurred in an epithelial tumor cell prior to MCC development. Therefore, our report demonstrates that MCPyV-positive MCC can derive from the epithelial lineage.

Introduction

Merkel cell carcinoma (MCC) is a rare, aggressive neoplasm of the skin with a 5-year overall survival rate of 40% (Becker et al. 2017). In about 80% of MCC cases the Merkel cell polyomavirus (MCPyV), an ubiquitous virus causing asymptomatic infections in the general population, is integrated into the genome of the tumor cells (Feng et al. 2008). In addition to the random integration of MCPyV, alterations of the viral sequence resulting in a truncated Large T antigen (LT) devoid of replicative abilities seem to be essential for MCC oncogenesis. Together with the truncated LT a viral small T antigen (sT) with multiple oncogenic properties is expressed in MCC cells, and both oncoproteins are considered as the main drivers for development and growth of MCPyV-positive MCC (Becker et al. 2017).

Although it is well established that MCPyV is a crucial oncogenic trigger in MCC pathogenesis, the nature of the cell in which virus integration occurs is unknown. Despite close phenotypic similarities with MCC such as expression of keratin (KRT) 20 and neuroendocrine markers, the eponym Merkel cell (MC) is considered as an unlikely candidate because this mechanoreceptor cell is post-mitotic (Van Keymeulen et al. 2009), insensitive to oncogenic stimuli in mice (Shuda et al. 2015), and - while MCCs are predominantly dermal or hypodermal (Pulitzer 2017) - resides in the basal layer of the epidermis (Halata et al. 2003). Alternatively, MCPyV integration could occur in a non-MC, and an MC-like phenotype might be acquired during tumorigenesis (Sunshine et al. 2018). In this respect, epithelial, fibroblastic, lymphoid as well as a neural crest origin of MCC have been discussed as potential candidates for MCC origin (Liu et al. 2016; Sunshine et al. 2018; Tilling and Moll 2012; Zur Hausen et al. 2013). Here, analysis of a rare combined tumor consisting of trichoblastoma and MCC parts, suggests that an MCPyV-positive MCC can arise from an epithelial cell.

Results

An MCPyV-positive MCC within a benign epithelial follicular tumor

In this study, a case of combined trichoblastoma/MCC tumor was subjected to extensive analyses. Details of the case are available in **Supplementary Table S1** and **Supplementary Figures S1-2**. Briefly, morphological examination revealed a well-delimited tumor located in the subcutis, without connection to the epidermis and harboring two different components (**Figure 1a and b**). On the borders, the combined tumor displayed typical trichoblastoma features with epithelial follicular germinative cells arranged in nodules or anastomotic strands entrapped in a prototypic stroma mimicking the dermal papillae (**Figure 1a-b** and **Supplementary Figure S1**). By contrast, the MCC part, located in the center of the combined tumor, was composed of sheets of round, medium-sized tumor cells with scant cytoplasm, round nucleus and dusty clear chromatin (**Figure 1a-b**). Immunohistochemical investigations (**Figure 1c-e/Supplementary Figure S2**) confirmed the diagnosis, notably revealing co-expression of KRT20 and neuroendocrine markers in all MCC cells and scattered KRT20-positive MCs in the trichoblastoma, a hallmark of this entity (Kurzen et al. 2001).

It has been suggested that MCPyV is not involved in the development of combined MCCs (Martin et al. 2013) which account for 5-10% of all MCCs (Kervarrec et al. 2018a). However, quantitative PCR demonstrated a substantial MCPyV viral load (20 copies/cell) in the MCC component, and staining for MCPyV-LT (**Figure 1c**) revealed moderate expression in the MCC cells suggesting an MCPyV-driven oncogenesis. In contrast, most of the trichoblastoma stained negative, and only in one restricted area a fraction of cells expressed LT (**Figure 1c**). It could, however, not be concluded whether these cells represented MCPyV-infected trichoblastoma cells or disseminated cells from the adjacent MCC tumor (**Figure 1b**). Interestingly, an increased number of cells expressing the MC differentiation markers SOX2, KRT8 and KRT20 was present in this area, with KRT8 and KRT20 frequently displaying a distinct paranuclear

dot-like pattern dissimilar from the diffuse cytoplasmic KRT20-distribution in normal MCs in the rest of the trichoblastoma component (**Figure 1d-e/Supplementary Figure S3a-c**). Furthermore, co-expression of KRT20 and LT in about 50% and KRT20 and the proliferation marker MKi67 in about 10% of the KRT20-expressing cells was observed (**Supplementary Figure S3a, c-d**).

In summary, the morphological and immunohistochemical analyses of the combined tumor revealed presence of MCPyV in specific trichoblastoma areas and widespread presence of MCPyV in the MCC part suggesting a virus-induced MCC oncogenesis.

MCPyV integration and LT truncation in the MCC

Two molecular features characterize MCPyV-associated MCC. First, the virus genome is clonally integrated into the genome of the tumor cells (Feng et al. 2008) and second, the LT antigen coding sequence is always affected in a way leading to expression of a truncated protein (Shuda et al. 2008). Applying combination of whole genome and Sanger sequencing onto DNA isolated from the MCC part, we could detect and confirm integration of MCPyV in chromosome 3 of the tumor genome (**Figure 2a-b**). Moreover, the presence of MCPyV sequences beyond the unique break points suggest integration of a concatemer consisting of one or more viral copies in addition to the sequence between the break points. Sequencing further indicates that even two differently truncated LT proteins may be expressed in the MCC part. One truncation caused by the integration break point at 1956, the other by a deletion spanning base pairs 2248 – 2542 (both according to GenBank EU375803) (**Fig. 2b**). In conclusion, the genetic analysis of MCPyV in the MCC part of the combined tumor revealed that this carcinoma harbors the hallmarks of an MCPyV-positive MCC.

Importantly, amplification of the insertion sites and a fragment specific for the LT-truncating deletion was only achieved with DNA from the MCC while from the trichoblastoma DNA only

wild type LT sequence could be amplified (**Figure 2c**). These results clearly indicate that the trichoblastoma tumor cells do not harbor the integrated form of the virus found in the MCC.

Shared mutations in trichoblastoma and MCC component

In order to prove a genetic relationship between the MCPyV-positive MCC and the trichoblastoma part of the combined tumor, DNA isolated from the different tumor components and healthy tissue was analyzed by whole exome sequencing and somatic mutations were identified (**Supplementary Tables S2-4**). Several acquired variants were present in only one of the tumor samples indicating that each tumor component partly experienced its own genetic history. Strikingly, however, the six acquired non-synonymous variants detected with the highest allelic frequencies in the trichoblastoma were also present in the MCC part (**Supplementary Table S2**). This was confirmed by Sanger sequencing (**Figure 3**) thus suggesting a common origin of the two tumor parts. Since integrated MCPyV could only be detected in the MCC part (**Fig. 2c**), these results imply that upon MCPyV integration occurring in an epithelial cell of the trichoblastoma component the MCC developed. In line with this, allelic frequencies of approximately 50% for the shared somatic mutations in the MCC part (lacking significant stroma (**Figure 1**)) are in accordance with heterozygous mutations being present in all MCC tumor cells. Measured allelic frequencies of 21-32% in the trichoblastoma part (**Figure 3 and Supplementary Table S2**), which harbors more extensive stroma (**Figure 1**), may reflect heterozygotic presence of the shared mutations in most if not all trichoblastoma cells. Interestingly, all further mutations detected in the trichoblastoma part were less frequent (**Supplementary Table S2**) suggesting that they are not present in all trichoblastoma cells. This is in line with a scenario where MCPyV integration has occurred in a trichoblastoma cell lacking these mutations. Among the somatic variants present in only the MCC part there are some which were detected with frequencies close to those of the shared mutations (e.g. GRIK4

and FAM219A) (**Supplementary Table S2**). They either may represent (i) mutations, present below the detection limit in the trichoblastoma but, nevertheless existent in the specific “MCC cell of origin”, or (ii) may have been acquired early during MCPyV-mediated oncogenesis. Finally, the low number of mutations lacking any UV-signature (**Supplementary Table S4**) confirms that the MCC part of the combined tumor matches also these attributes of MCPyV-positive MCC (Becker et al. 2017).

In conclusion, the data provided so far, clearly indicate that an MCPyV-positive MCC can arise from an epithelial cell.

Analogy between trichoblastoma and MC progenitor

Next, we asked whether the analyses of the combined tumor would allow further conclusions regarding the cellular origin of this MCPyV-positive MCC. As expected, an epithelial lineage descendance was confirmed by widespread expression of cytokeratins in trichoblastoma cells. Moreover, trichoblastoma cells characteristically bear intrinsic MC-differentiation capability and phenotypically resemble hair follicle stem cells (Kurzen et al. 2001) (**Figure 4a-c**) which have been demonstrated to be essential for MC development (Nguyen et al. 2018; Perdigoto et al. 2016). In particular, GLI1 activation in the hair follicle and the surrounding touch domes is critical for the maintenance of the MC lineage (Perdigoto et al. 2016; Xiao et al. 2015). Interestingly, we could demonstrate in the trichoblastoma part of the combined tumor, like in normal hair follicles, widespread expression of KRT17 and SOX9, two markers shared by hair follicle and MC-progenitors as well as GLI1 nuclear localization (**Figure 4c-e**) (Brownell et al. 2011; Larouche et al. 2008; Moll et al. 1993; Nguyen et al. 2018; Nguyen et al. 2018; Xiao et al. 2015) in association with the interspersed presence of KRT8- and KRT20-positive MCs (**Figures 1c and 4f, Supplementary Figure S3b-d**). Therefore, the trichoblastoma cell in which MCPyV integration occurred as demonstrated by genomic analyses could be either a cell resembling an epithelial progenitor cell of the hair follicle or an already differentiated MC.

A second case of MCPyV-positive MCC arising within a trichoblastoma

Our study has limitations and most prominent, our conclusions are based on only one case. Due to the exceedingly low incidence of combined trichoblastoma/MCC, we could identify only one additional case published previously (Battistella et al. 2011). Analyses of this second combined MCC by immunohistochemistry confirmed a further case of MCPyV-positive MCC arising within a trichoblastoma composed of KRT17- and SOX9-positive MC-precursor-like cells and interspersed KRT20- and KRT-8 expressing MCs (**Supplementary Figure S4/Supplementary Table S5**). Unfortunately, additional molecular analyses could not be performed due to very poor DNA quality related to Bouin fixation.

Discussion

Identification of the cellular origin of MCPyV-positive and virus-negative MCC are considered as high-priority research questions not only to improve our understanding of the initiation of this disease, but also for developing appropriate models and possibly new therapeutic approaches (Harms et al. 2018; Sauer et al. 2017; Sunshine et al. 2018). Due to close phenotypic similarities with MCC, MC – a highly specialized mechanoreceptor, and a descendant from KRT14-positive epidermal progenitors (Halata et al. 2003; Van Keymeulen et al. 2009) - was historically regarded as the cell of origin of MCC. Proposed alternatives as potential MCC origin include pre/pro-B cells, dermal fibroblasts, dermal mesenchymal stem cells and epithelial progenitor cells (Becker and Zur Hausen 2014; Kervarrec et al. 2019; Lemasson et al. 2012; Liu et al. 2016; Tilling and Moll 2012; Verhaegen et al. 2017; Woo et al. 2010; Zur Hausen et al. 2013).

Although investigating only a single case belonging to an exceptionally rare tumor entity, the results presented here provide a clear proof that MCPyV-positive MCC can arise from the epithelial lineage, i.e., either from already differentiated MCs or their progenitors. Moreover, while an alternative histogenesis either in mesenchymal or lymphoid cells could not formerly be excluded for other MCPyV-positive MCC cases such scenario appears unlikely because a tumor cell phenotype is determined by both, the tumorigenic alterations and by the primary nature of the cell of origin (Bailleul et al. 1990; Brown et al. 1998; Visvader 2011). This concept referred to as “oncogene lineage-addiction” (Garraway and Sellers 2006) was proven for MCPyV oncoproteins using transgenic mice. Indeed, in such model, ectopic expression of the T antigens (sT alone or in combination with LT) failed to generate tumors with an MCC-like phenotype in all tested compartments (Shuda et al. 2015; Spurgeon et al. 2015; Verhaegen et al. 2015) except for the Merkel cell lineage (Verhaegen et al. 2017). In light of these findings,

while trichoblastoma tumors could not be considered as a frequent site of MCPyV integration, it is conceivable that MCPyV induced carcinogenesis occurs in a similar cellular context i.e. an epithelial cell of the MC lineage being either an hair follicle progenitor or an already differentiated MC.

Indeed, we confirmed trichoblastoma as a benign epithelial tumor phenotypically resembling progenitor cells of the hair follicle (Kurzen et al. 2001) and bearing MC differentiation ability (Katona et al. 2008; Kurzen et al. 2001; Leblebici et al. 2018). Under physiological conditions, the hair follicle is a privileged niche for MC differentiation and accordingly, abrogation of hair follicle development in transgenic mice resulted in complete MC loss (Perdigoto et al. 2016). Furthermore, Sox9- and Fgfr2-expressing cells in the embryonic hair follicle were identified as MC progenitors, and active Sonic hedgehog signaling was shown to be critical for establishment of this population, and for subsequent MC differentiation (Nguyen et al. 2018; Perdigoto et al. 2016). Interestingly, all these features can also be found in the trichoblastoma germinative cells of the presented combined tumor and accordingly sparse MCs were detected. Therefore our results suggest that hair follicles with potential for MC differentiation might represent a major cellular origin of MCPyV-positive MCC. This notion has been suggested earlier (Tilling and Moll 2012), and is also corroborated by rare cases of MCC found within follicular cysts (Requena et al. 2008; Su et al. 2008). Furthermore, frequent connections between MCC tumors and hair follicles have been described (Walsh 2001) although one might also argue that collision with a hair follicle is an inevitable consequence when a dermal tumor reaches a certain size.

Of note, while the lineage from which tumor cells derived have been identified for several solid cancers, the precise differentiation degree of the cell in which transformation occurs remains

elusive in most cases (Visvader 2011). In the analyzed tumor, oncogenic virus integration may have occurred in one of the differentiated MCs present in the trichoblastoma. On the other hand, arguments against the possibility that MCCs arise from already differentiated MCs include i) lack of mitotic activity of MCs (Moll et al. 1996), although a recent publication demonstrated some proliferative activity (Narisawa et al. 2019), ii) poor MCPyV infectibility (Liu et al. 2016) and iii) insusceptibility of these cells to oncogenic stimuli (including T antigens) in mice (Shuda et al. 2015; Van Keymeulen et al. 2009). Alternatively, MCC could derive from MC progenitors (Tilling and Moll 2012) which can arise from GLI1-expressing hair follicle stem cells. Interestingly, this population has been demonstrated to be highly susceptible to tumorigenic stimuli, and can serve as an important cellular origin in the development of other skin cancers (Peterson et al. 2015). In such a scenario phenotypic changes may arise during oncogenesis (Fletcher 2006). In this regard, it has been suggested that TA expression can induce an MC-like differentiation process (Sunshine et al. 2018). Indeed, expression of LT of the polyomavirus simian virus 40 in gastric or prostate murine epithelial cells can induce an epithelial to neuroendocrine differentiation (Kaplan-Lefko et al. 2003; Syder et al. 2004). Moreover, in human prostate cancer as well as mouse models, inactivation of RB1 and TP53 – both expected outcomes of MCPyV-TA expression (Houben et al. 2012; Park et al. 2019) – have been demonstrated to induce the epigenetic reprogramming factors SOX2 and EZH2 (Ku et al. 2017), i.e. two critical actors involved in Merkel cell differentiation. In line with these published results, we observed an increase in cells positive for the MC markers KRT8, SOX2 and KRT20 in a trichoblastoma region containing MCPyV-LT expression. Although a metastatic spreading of the MCC tumor cells with “small cell morphology” into the trichoblastoma might explain these findings, it could alternatively be the result of LT-induced MC proliferation, or indicate a differentiation process promoted by MCPyV oncoproteins. This notion is supported by more frequent cells expressing SOX2 and KRT8 which appear earlier

during MC differentiation than the less frequently expressed KRT20 (**Supplementary Figure 3**) (Perdigoto et al. 2014). Taken together, it is conceivable that MCPyV-TAs contribute to the development of a MC-like phenotype upon expression in an epithelial precursor cell.

Irrespective of these more speculative considerations, the mutational overlap between a benign epithelial tumor and a MCPyV-positive MCC provides a clear proof that an MCPyV-positive MCC can evolve from an epithelial cell. Moreover, close similarities between trichoblastoma and MC progenitors suggest that cells of the MC lineage might represent a prominent cellular target of MCPyV in MCC carcinogenesis.

Methods

Ethics

This study was approved by the local ethics committee (Tours, France, N° ID RCB2009-A01056-51), and consent of the patient was obtained.

Immunohistochemistry

Immunohistochemical staining for CD274, CHGA, pan-KRT (AE1/AE3), KRT14, KRT20, MKI67, MCPyV-LT, TP53, SOX9, TDT and TTF1 as well as double staining for KRT20/MCPyV-LT and KRT/MKI67 was performed using a BenchMark XT Platform as instructed (Kervarrec et al. 2018b; Kervarrec et al. 2018a). Immunohistochemical staining for GLI1, KRT8, KRT15, KRT17 and SOX2 was performed manually. Antibodies and dilutions are provided in **Supplementary Materials**. TP53 as well as MCPyV-LT were analyzed using an Allred score (Moshiri et al. 2016). Quantification of LT, KRT8 and -20, SOX2 and MKI67 positive cells in MCPyV(+) and (-) trichoblastoma areas was performed by counting cells in 8 independent fields (0.027 mm²) and compared using a Mann-Whitney test.

DNA isolation and MCPyV quantitative PCR

After microdissection of the two tumor components and of the healthy tissue under a binocular magnifier, genomic DNA was isolated by use of the Maxwell 16 Instrument (Promega) with the Maxwell 16 formalin-fixed and paraffin-embedded Plus LEV DNA purification kit (Promega). MCPyV-LT real-time PCR was performed as described (Kervarrec et al. 2018b). Of note, dissection of the trichoblastoma was performed in areas devoid of LT expression. Briefly, 50 ng DNA was mixed with primers (0.2 µM), probe (0.1 µM) and Mix Life technologies GoTaq Probe real-time PCR Master Mix 2X (Promega) in a final volume of 20 µl. PCR reactions were performed with the LightCycler 480 II (Roche) with an initial denaturation at 95°C × 2 min, followed by 45 cycles at 95°C × 15 sec and 58°C × 60 sec. Albumin was used as reference gene for normalization. The $2^{-\Delta\Delta C_t}$ method was used for

quantification, and results expressed as number of MCPyV copies per cell (Kervarrec et al. 2018b). Sequences of the primers used for quantitative PCR are available in **Supplementary Materials**.

PCR amplification and Sanger sequencing.

Nested PCRs with primers listed in **Supplementary Materials** were performed to amplify the respective regions. PCR reactions were carried out in a total volume of 20 μ l containing 1x HF buffer, 1 μ M of each primer, 200 μ M dNTPs, 1 unit Q5 Phusion (NEB) and 1 μ l of template. After an initial denaturation at 98°C for 1 min, the thermal profile consisted of denaturation at 98°C for 10 sec, annealing at the optimal temperature for 30 sec and elongation at 72°C for 1 min (30 cycles for pre-amplification and 40 cycles for amplification). After PCR purification the amplicons were sent to SeqLab (Microsynth) for sequencing.

Next Generation Sequencing

For the library preparation of the exomes the SureSelectXT Library Prep Kit (Agilent) was used. Enrichment was performed using Agilent's SureSelectXT Human All Exon V6 Kit. The genomic library was prepared using TruSeq Nano DNA (Illumina). Paired end sequencing with a read length of 100 bps (exomes) and 150 bps (genome) was performed on a NovaSeq 6000 (Illumina).

Data analysis

Demultiplexing of the sequencing reads was performed with Illumina bcl2fastq (v2.19). Adapters were trimmed with Skewer, v0.2.25 (Jiang et al. 2014). An initial quality assessment was performed using FastQC, v0.11.5 (Andrews S., 2010. Available online at: <http://www.bioinformatics.babraham.ac.uk/projects/fastqc>). Low-quality reads were trimmed with TrimGalore, v0.4.0 (Krueger, F., 2012: Available online at: http://www.bioinformatics.babraham.ac.uk/projects/trim_galore/) powered by Cutadapt, v1.86

(Martin 2011). The trimmed reads were mapped to the human reference genome (hg19) using BWA mem, v0.7.127 (Li and Durbin 2009) and sorted and indexed using Picard, v1.125 (available online at: <http://broadinstitute.github.io/picard/>) and SAMtools, v1.38 (Li et al. 2009) respectively. Duplicates were marked with Picard. For the exomes local realignment around indels was executed with GATK, v3.59 (McKenna et al. 2010). GATK was also used for coverage calculations.

Somatic variant calling

MuTect1, v 1.1.410 (Cibulskis et al. 2013) and VarScan2, v2.4.111 (Koboldt et al. 2012) were used to identify somatic single nucleotide variants (SNVs). Samtools (mpileup) with VarScan2 and Scalpel, v0.5.312 (Fang et al. 2016) were applied to identify small somatic insertions or deletions. All variants were annotated with ANNOVAR, v2017-06-0113 (Wang et al. 2010). Six somatic variants shared by the trichoblastoma and the MCC were visually examined using the Integrative Genomics Viewer, v2.3.6814 (Thorvaldsdóttir et al. 2013) and confirmed with Sanger sequencing if they have an impact on the protein sequence or affect a splice site, are rare in the population (below a frequency of 2 % in 1000g2015aug_all, ExAC_nontcga_ALL, gnomAD_exome_ALL and gnomAD_genome_ALL) and the position is covered by at least 20 reads and the alternative allele is covered by at least 8 reads and comprised at least 5 %. Mutational signatures were identified using MuSiCa (Díaz-Gay et al. 2018) investigating somatic variants comprised at least 10%.

Detection of the virus integration site

Seeksv, v1.2.315 (Liang et al. 2017) was used with the human reference genome sequence (hg19) and the MCPyV MCC350 genome sequence (GenBank EU375803) to detect the virus integration site.

Data availability statement

The datasets generated during and/or analysed during the current study are available in European Genome-phenome Archive (ID: EGAS00001003784).

Acknowledgements

The authors thank Dr A. Balaton, Dr L. Durand, Dr J Mabile and Dr S. Manela for their help and contribution.

Competing interests

The authors declare no competing interests.

Contributions

T.K., D.S. and R.H. designed the study, contributed to acquisition, analysis and interpretation of data and drafted and substantively revised the manuscript. M.A. and S.A. contributed to data acquisition and interpretation as well as writing of the manuscript. M.S., E.M., B.C., S.G., L.D., B.S., P.B., A.L., E.-M. S., G.B., A.T. contributed to data acquisition and revision of the manuscript.

Corresponding author

Correspondence to Thibault Kervarrec.

References

- Bailleul B, Surani MA, White S, Barton SC, Brown K, Blessing M, et al. Skin hyperkeratosis and papilloma formation in transgenic mice expressing a ras oncogene from a suprabasal keratin promoter. *Cell*. 1990;62(4):697–708
- Battistella M, Durand L, Jouary T, Peltre B, Cribier B. Primary cutaneous neuroendocrine carcinoma within a cystic trichoblastoma: a nonfortuitous association? *Am. J. Dermatopathol*. 2011;33(4):383–7
- Becker JC, Stang A, DeCaprio JA, Cerroni L, Lebbé C, Veness M, et al. Merkel cell carcinoma. *Nat. Rev. Dis. Primer*. 2017;3:17077
- Becker JC, Zur Hausen A. Cells of origin in skin cancer. *J. Invest. Dermatol*. 2014;134(10):2491–3
- Brown K, Strathdee D, Bryson S, Lambie W, Balmain A. The malignant capacity of skin tumours induced by expression of a mutant H-ras transgene depends on the cell type targeted. *Curr. Biol. CB*. 1998;8(9):516–24
- Brownell I, Guevara E, Bai CB, Loomis CA, Joyner AL. Nerve-derived sonic hedgehog defines a niche for hair follicle stem cells capable of becoming epidermal stem cells. *Cell Stem Cell*. 2011;8(5):552–65
- Cibulskis K, Lawrence MS, Carter SL, Sivachenko A, Jaffe D, Sougnez C, et al. Sensitive detection of somatic point mutations in impure and heterogeneous cancer samples. *Nat. Biotechnol*. 2013;31(3):213–9
- Díaz-Gay M, Vila-Casadesús M, Franch-Expósito S, Hernández-Illán E, Lozano JJ, Castellví-Bel S. Mutational Signatures in Cancer (MuSiCa): a web application to implement mutational signatures analysis in cancer samples. *BMC Bioinformatics*. 2018;19(1):224
- Fang H, Bergmann EA, Arora K, Vacic V, Zody MC, Iossifov I, et al. Indel variant analysis of short-read sequencing data with Scalpel. *Nat. Protoc*. 2016;11(12):2529–48
- Feng H, Shuda M, Chang Y, Moore PS. Clonal integration of a polyomavirus in human Merkel cell carcinoma. *Science*. 2008;319(5866):1096–100
- Fletcher CDM. The evolving classification of soft tissue tumours: an update based on the new WHO classification. *Histopathology*. 2006;48(1):3–12
- Garraway LA, Sellers WR. Lineage dependency and lineage-survival oncogenes in human cancer. *Nat. Rev. Cancer*. 2006;6(8):593–602
- Halata Z, Grim M, Bauman KI. Friedrich Sigmund Merkel and his “Merkel cell”, morphology, development, and physiology: review and new results. *Anat. Rec. A. Discov. Mol. Cell. Evol. Biol*. 2003;271(1):225–39
- Harms PW, Harms KL, Moore PS, DeCaprio JA, Nghiem P, Wong MKK, et al. The biology and treatment of Merkel cell carcinoma: current understanding and research priorities. *Nat. Rev. Clin. Oncol*. 2018;
- Houben R, Adam C, Baeurle A, Hesbacher S, Grimm J, Angermeyer S, et al. An intact retinoblastoma protein-binding site in Merkel cell polyomavirus large T antigen is required for promoting growth of Merkel cell carcinoma cells. *Int. J. Cancer*. 2012;130(4):847–56
- Iwasaki T, Kodama H, Matsushita M, Kuroda N, Yamasaki Y, Murakami I, et al. Merkel cell polyomavirus infection in both components of a combined Merkel cell carcinoma and basal cell carcinoma with ductal differentiation; each component had a similar but different novel Merkel cell polyomavirus large T antigen truncating mutation. *Hum. Pathol*. 2013;44(3):442–7
- Jiang H, Lei R, Ding S-W, Zhu S. Skewer: a fast and accurate adapter trimmer for next-generation sequencing paired-end reads. *BMC Bioinformatics*. 2014;15:182
- Kaplan-Lefko PJ, Chen T-M, Ittmann MM, Barrios RJ, Ayala GE, Huss WJ, et al. Pathobiology of autochthonous prostate cancer in a pre-clinical transgenic mouse model. *The*

Prostate. 2003;55(3):219–37

Katona TM, Perkins SM, Billings SD. Does the panel of cytokeratin 20 and androgen receptor antibodies differentiate desmoplastic trichoepithelioma from morpheiform/infiltrative basal cell carcinoma? *J. Cutan. Pathol.* 2008;35(2):174–9

Kervarrec T, Samimi M, Gaboriaud P, Gheit T, Beby-Defaux A, Houben R, et al. Detection of the Merkel cell polyomavirus in the neuroendocrine component of combined Merkel cell carcinoma. *Virchows Arch. Int. J. Pathol.* 2018a;

Kervarrec T, Samimi M, Guyétant S, Sarma B, Chéret J, Blanchard E, et al. Histogenesis of Merkel cell carcinoma: a comprehensive review. *Front. Oncol.* Accepted Manuscript. 2019;

Kervarrec T, Tallet A, Miquelstorena-Standley E, Houben R, Schrama D, Gambichler T, et al. Diagnostic accuracy of a panel of immunohistochemical and molecular markers to distinguish Merkel cell carcinoma from other neuroendocrine carcinomas. *Mod. Pathol. Off. J. U. S. Can. Acad. Pathol. Inc.* 2018b;

Koboldt DC, Zhang Q, Larson DE, Shen D, McLellan MD, Lin L, et al. VarScan 2: somatic mutation and copy number alteration discovery in cancer by exome sequencing. *Genome Res.* 2012;22(3):568–76

Ku SY, Rosario S, Wang Y, Mu P, Seshadri M, Goodrich ZW, et al. Rb1 and Trp53 cooperate to suppress prostate cancer lineage plasticity, metastasis, and antiandrogen resistance. *Science.* 2017;355(6320):78–83

Kurzen H, Esposito L, Langbein L, Hartschuh W. Cytokeratins as markers of follicular differentiation: an immunohistochemical study of trichoblastoma and basal cell carcinoma. *Am. J. Dermatopathol.* 2001;23(6):501–9

Larouche D, Tong X, Fradette J, Coulombe PA, Germain L. Vibrissa hair bulge houses two populations of skin epithelial stem cells distinct by their keratin profile. *FASEB J. Off. Publ. Fed. Am. Soc. Exp. Biol.* 2008;22(5):1404–15

Leblebici C, Bambul Sığircı B, Kelten Talu C, Koca SB, Huq GE. CD10, TDAG51, CK20, AR, INSM1, and Nestin Expression in the Differential Diagnosis of Trichoblastoma and Basal Cell Carcinoma. *Int. J. Surg. Pathol.* 2018;1066896918781719

Lemasson G, Coquart N, Lebonvallet N, Boulais N, Galibert MD, Marcorelles P, et al. Presence of putative stem cells in Merkel cell carcinomas. *J. Eur. Acad. Dermatol. Venereol. JEADV.* 2012;26(6):789–95

Li H, Durbin R. Fast and accurate short read alignment with Burrows-Wheeler transform. *Bioinforma. Oxf. Engl.* 2009;25(14):1754–60

Li H, Handsaker B, Wysoker A, Fennell T, Ruan J, Homer N, et al. The Sequence Alignment/Map format and SAMtools. *Bioinforma. Oxf. Engl.* 2009;25(16):2078–9

Liang Y, Qiu K, Liao B, Zhu W, Huang X, Li L, et al. Seeksv: an accurate tool for somatic structural variation and virus integration detection. *Bioinforma. Oxf. Engl.* 2017;33(2):184–91

Liu W, Yang R, Payne AS, Schowalter RM, Spurgeon ME, Lambert PF, et al. Identifying the Target Cells and Mechanisms of Merkel Cell Polyomavirus Infection. *Cell Host Microbe.* 2016;19(6):775–87

Martin M. Cutadapt removes adapter sequences from high-throughput sequencing reads. *EMBnet.journal.* 2011;17(1):10

Martin B, Poblet E, Rios JJ, Kazakov D, Kutzner H, Brenn T, et al. Merkel cell carcinoma with divergent differentiation: histopathological and immunohistochemical study of 15 cases with PCR analysis for Merkel cell polyomavirus. *Histopathology.* 2013;62(5):711–22

McKenna A, Hanna M, Banks E, Sivachenko A, Cibulskis K, Kernytsky A, et al. The Genome Analysis Toolkit: a MapReduce framework for analyzing next-generation DNA sequencing data. *Genome Res.* 2010;20(9):1297–303

Moll I, Troyanovsky SM, Moll R. Special program of differentiation expressed in

keratinocytes of human haarscheiben: an analysis of individual cytokeratin polypeptides. *J. Invest. Dermatol.* 1993;100(1):69–76

Moll I, Zieger W, Schmelz M. Proliferative Merkel cells were not detected in human skin. *Arch. Dermatol. Res.* 1996;288(4):184–7

Moshiri AS, Doumani R, Yelistratova L, Blom A, Lachance K, Shinohara MM, et al. Polyomavirus-Negative Merkel Cell Carcinoma: A More Aggressive Subtype Based on Analysis of 282 Cases Using Multimodal Tumor Virus Detection. *J. Invest. Dermatol.* 2016;

Narisawa Y, Inoue T, Nagase K. Evidence of proliferative activity in human Merkel cells: implications in the histogenesis of Merkel cell carcinoma. *Arch. Dermatol. Res.* 2019;311(1):37–43

Nguyen MB, Cohen I, Kumar V, Xu Z, Bar C, Dauber-Decker KL, et al. FGF signalling controls the specification of hair placode-derived SOX9 positive progenitors to Merkel cells. *Nat. Commun.* 2018;9(1):2333

Park DE, Cheng J, Berrios C, Montero J, Cortés-Cros M, Ferretti S, et al. Dual inhibition of MDM2 and MDM4 in virus-positive Merkel cell carcinoma enhances the p53 response. *Proc. Natl. Acad. Sci. U. S. A.* 2019;116(3):1027–32

Perdigoto CN, Bardot ES, Valdes VJ, Santoriello FJ, Ezhkova E. Embryonic maturation of epidermal Merkel cells is controlled by a redundant transcription factor network. *Dev. Camb. Engl.* 2014;141(24):4690–6

Perdigoto CN, Dauber KL, Bar C, Tsai P-C, Valdes VJ, Cohen I, et al. Polycomb-Mediated Repression and Sonic Hedgehog Signaling Interact to Regulate Merkel Cell Specification during Skin Development. *PLoS Genet.* 2016;12(7):e1006151

Peterson SC, Eberl M, Vagnozzi AN, Belkadi A, Veniaminova NA, Verhaegen ME, et al. Basal cell carcinoma preferentially arises from stem cells within hair follicle and mechanosensory niches. *Cell Stem Cell.* 2015;16(4):400–12

Pulitzer M. Merkel Cell Carcinoma. *Surg. Pathol. Clin.* 2017;10(2):399–408

Requena L, Jaqueti G, Rütten A, Mentzel T, Kutzner H. Merkel cell carcinoma within follicular cysts: report of two cases. *J. Cutan. Pathol.* 2008;35(12):1127–33

Sauer CM, Hagg AM, Chteinberg E, Rennspiess D, Winnepeninckx V, Speel E-J, et al. Reviewing the current evidence supporting early B-cells as the cellular origin of Merkel cell carcinoma. *Crit. Rev. Oncol. Hematol.* 2017;116:99–105

Shuda M, Feng H, Kwun HJ, Rosen ST, Gjoerup O, Moore PS, et al. T antigen mutations are a human tumor-specific signature for Merkel cell polyomavirus. *Proc. Natl. Acad. Sci. U. S. A.* 2008;105(42):16272–7

Shuda M, Guastafierro A, Geng X, Shuda Y, Ostrowski SM, Lukianov S, et al. Merkel Cell Polyomavirus Small T Antigen Induces Cancer and Embryonic Merkel Cell Proliferation in a Transgenic Mouse Model. *PloS One.* 2015;10(11):e0142329

Spurgeon ME, Cheng J, Bronson RT, Lambert PF, DeCaprio JA. Tumorigenic activity of merkel cell polyomavirus T antigens expressed in the stratified epithelium of mice. *Cancer Res.* 2015;75(6):1068–79

Su W, Kheir SM, Berberian B, Cockerell CJ. Merkel cell carcinoma in situ arising in a trichilemmal cyst: a case report and literature review. *Am. J. Dermatopathol.* 2008;30(5):458–61

Sunshine JC, Jahchan NS, Sage J, Choi J. Are there multiple cells of origin of Merkel cell carcinoma? *Oncogene.* 2018;

Syder AJ, Karam SM, Mills JC, Ippolito JE, Ansari HR, Farook V, et al. A transgenic mouse model of metastatic carcinoma involving transdifferentiation of a gastric epithelial lineage progenitor to a neuroendocrine phenotype. *Proc. Natl. Acad. Sci. U. S. A.* 2004;101(13):4471–6

Thorvaldsdóttir H, Robinson JT, Mesirov JP. Integrative Genomics Viewer (IGV): high-

performance genomics data visualization and exploration. *Brief. Bioinform.* 2013;14(2):178–92

Tilling T, Moll I. Which are the cells of origin in merkel cell carcinoma? *J. Skin Cancer.* 2012;2012:680410

Van Keymeulen A, Mascré G, Youseff KK, Harel I, Michaux C, De Geest N, et al. Epidermal progenitors give rise to Merkel cells during embryonic development and adult homeostasis. *J. Cell Biol.* 2009;187(1):91–100

Verhaegen ME, Mangelberger D, Harms PW, Eberl M, Wilbert DM, Meireles J, et al. Merkel Cell Polyomavirus Small T Antigen Initiates Merkel Cell Carcinoma-like Tumor Development in Mice. *Cancer Res.* 2017;77(12):3151–7

Verhaegen ME, Mangelberger D, Harms PW, Vozheiko TD, Weick JW, Wilbert DM, et al. Merkel cell polyomavirus small T antigen is oncogenic in transgenic mice. *J. Invest. Dermatol.* 2015;135(5):1415–24

Visvader JE. Cells of origin in cancer. *Nature.* 2011;469(7330):314–22

Walsh NM. Primary neuroendocrine (Merkel cell) carcinoma of the skin: morphologic diversity and implications thereof. *Hum. Pathol.* 2001;32(7):680–9

Wang K, Li M, Hakonarson H. ANNOVAR: functional annotation of genetic variants from high-throughput sequencing data. *Nucleic Acids Res.* 2010;38(16):e164

Woo S-H, Stumpfova M, Jensen UB, Lumpkin EA, Owens DM. Identification of epidermal progenitors for the Merkel cell lineage. *Dev. Camb. Engl.* 2010;137(23):3965–71

Xiao Y, Thoresen DT, Williams JS, Wang C, Perna J, Petrova R, et al. Neural Hedgehog signaling maintains stem cell renewal in the sensory touch dome epithelium. *Proc. Natl. Acad. Sci. U. S. A.* 2015;112(23):7195–200

Zur Hausen A, Rennspiess D, Winnepenninckx V, Speel E-J, Kurz AK. Early B-cell differentiation in Merkel cell carcinomas: clues to cellular ancestry. *Cancer Res.* 2013;73(16):4982–7

Figures and Tables:

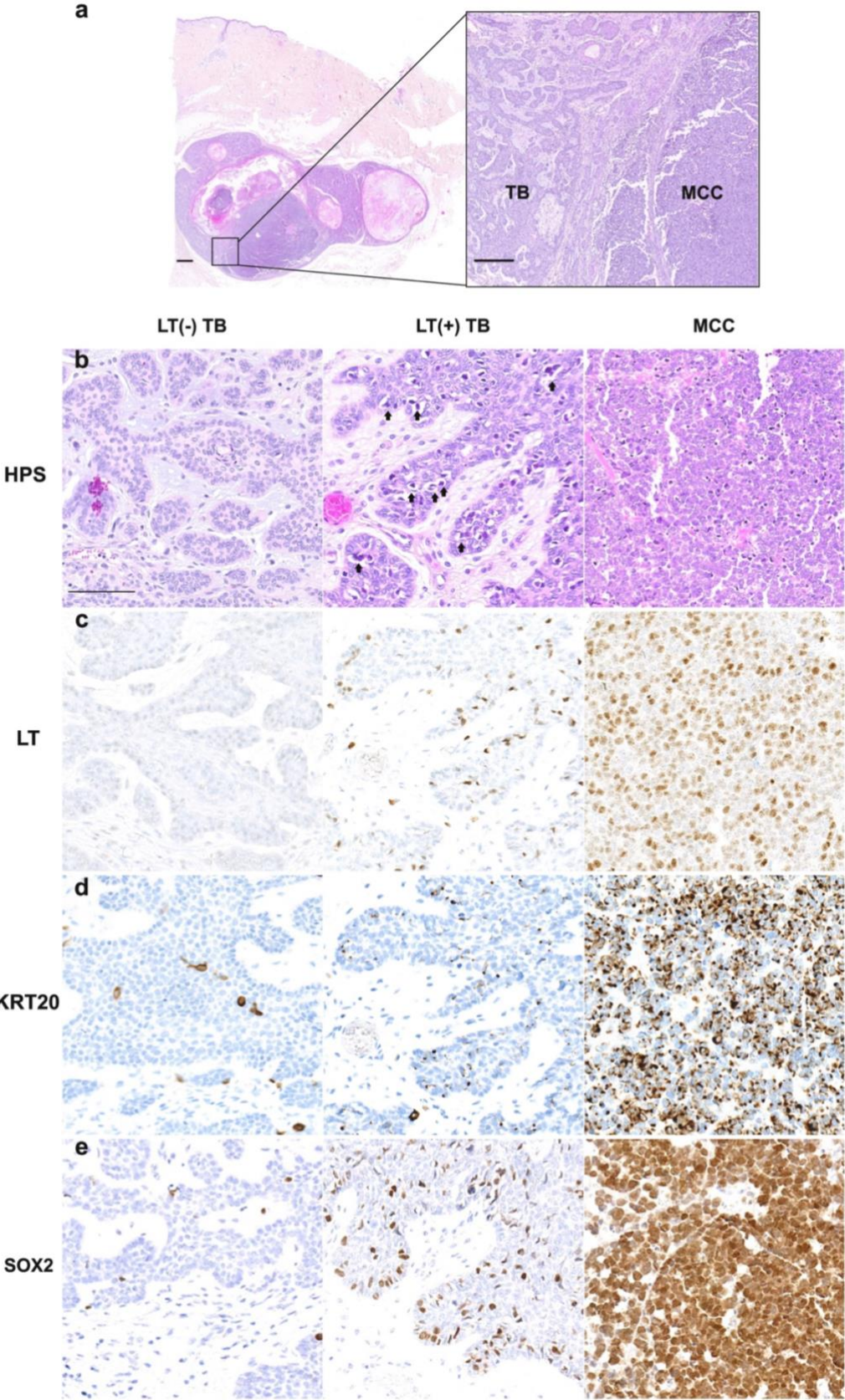
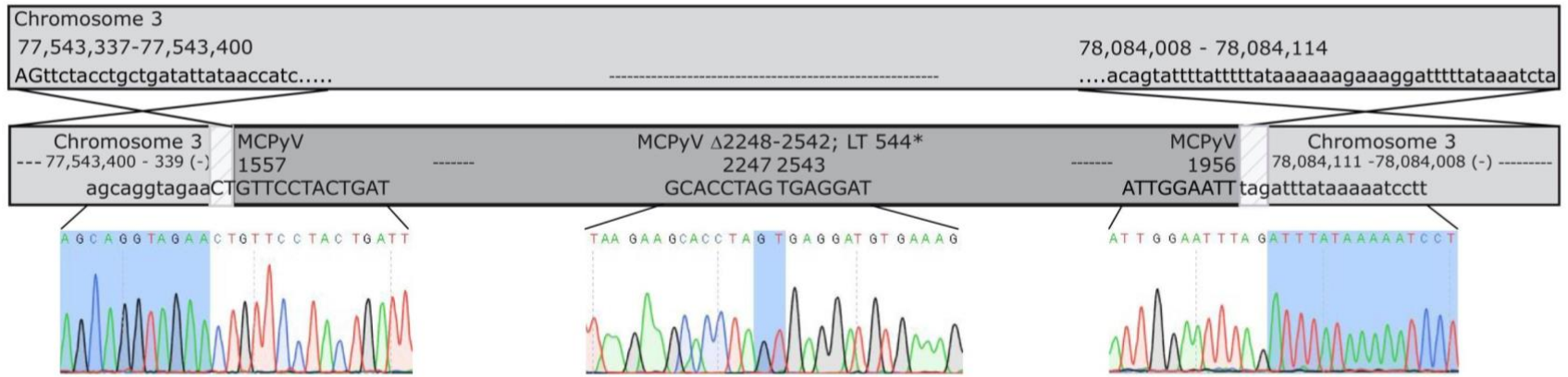


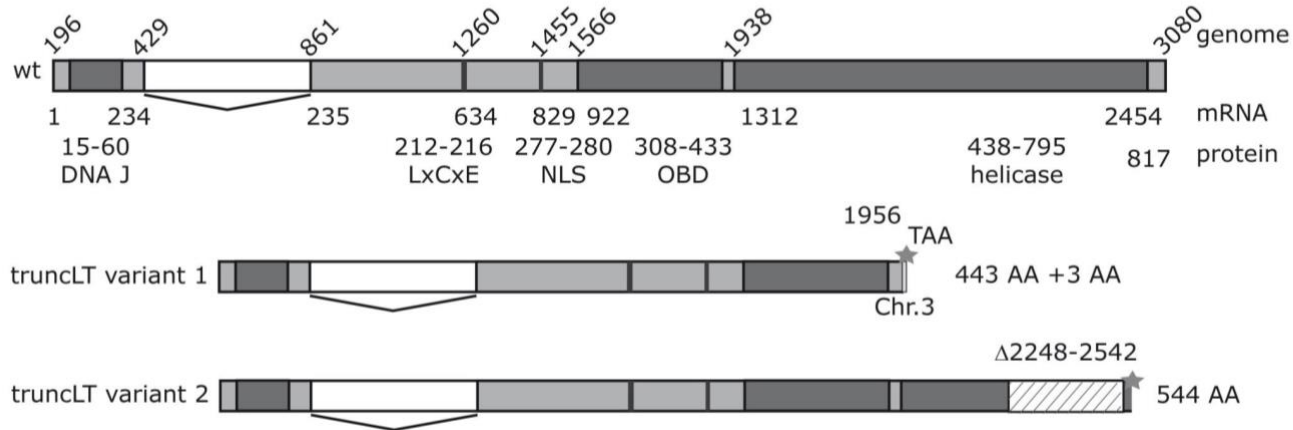
Figure 1. (See legends below).

Figure 1. Microscopic and immunohistochemical features of the trichoblastoma/MCC combined tumor. (a) Morphological features of the case (hematein-phloxin-saffron staining (HPS)). Low magnification revealed a well delimited tumor mainly located in the subcutis without connection to the epidermis (bar=1 mm); higher magnification shows the MCC in close association with the trichoblastoma (TB; bar=250 μ m). Indeed, the trichoblastoma was composed of clusters and anastomotic strands of basaloid epithelial cells surrounded by a clear stroma containing mucin deposits whereas the MCC was characterized by sheets of small to medium sized cells with scant cytoplasm, round nucleus, dusty chromatin, and a high mitotic rate. (b-e) Microscopic and immunohistochemical details of the case (bar=100 μ m). Two regions from the trichoblastoma part, representing either the majority of TB area without LT expression (LT(-) TB) or an TB area with occasional LT expression (LT(+) TB), as well as one representative region from the MCC part are displayed. In the LT-positive area of the trichoblastoma, a population of clear cells with coarse chromatin morphologically distinct from the other cells of the trichoblastoma but also from the MCC tumor cells (black arrows) was evident in the HPS staining. While KRT20 stained with a diffuse pattern in virus-negative parts of the trichoblastoma, in MCPyV-LT-expressing areas a KRT20 dot-like pattern was observed comparable to MCC. The LT expressing area was additionally characterized by an increased number of SOX2-expressing cells compared to the rest of the trichoblastoma, while the MCC cells generally displayed nuclear positivity for this marker.

a



b



c

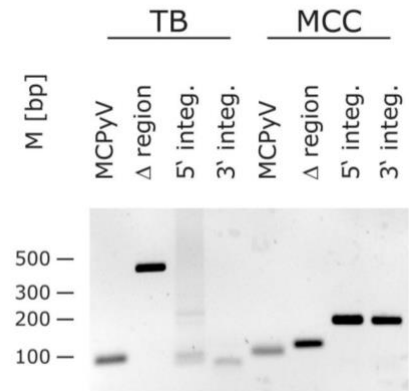


Figure 2. (See legends below).

Figure 2. The MCC part of the combined tumor fulfills the hallmarks of MCPyV-positive MCC. (a) Integration of MCPyV in chromosome 3 of the MCC genome. DNA isolated from the MCC part of the combined tumor was analyzed by whole genome sequencing (WGS) and confirmed by Sanger sequencing. The integration break points in the viral genome (Genbank EU375803) as well as in chromosome 3 (GRCh37; NC000003.11) are depicted. To note, human sequences adjacent to the integration break points were found to be swapped. Moreover, sequencing revealed a deletion in the viral genome (Δ 2248-2542). Frequently, MCPyV integrates as head to tail concatemer. In this case, nucleotides 1557-1956 are followed by one or more full length copies (1957-1956) which is predicted to lead to **(b)** one or two different truncated Large T antigen proteins expressed in the MCC part. One premature stop codon is caused by the integration break point at nucleotide 1956 in the final MCPyV genome of the concatemer and will lead to expression of the 443 N-terminal amino acids of LT followed by 3 additional amino acids. A second larger truncated LT is encoded in case that the concatemer encompasses more than two full copies of the MCPyV genome. The Δ 2248-2542 deletion leads to an LT sequence coding for the 540 N-terminal amino acids followed by three frame shifted amino acid codons prior to a stop codon. **(c)** PCR was performed with primers for general MCPyV detection (MCPyV; product size = 84 bp), flanking Δ 2248-2542 (Δ region), or for the 5' (5' integ.; product size = 171 bp) and 3' (3' integ.; product size = 172 bp) integration sites, respectively. For MCPyV wt the Δ region PCR will produce a PCR product of 398 bp, while it will be only 103 bp when the MCPyV contains the deletion. Notice a faint band for the 5' integration site with DNA from the trichoblastoma part at around 200 bp. Sanger sequencing, however, confirmed it to be an unspecific product.

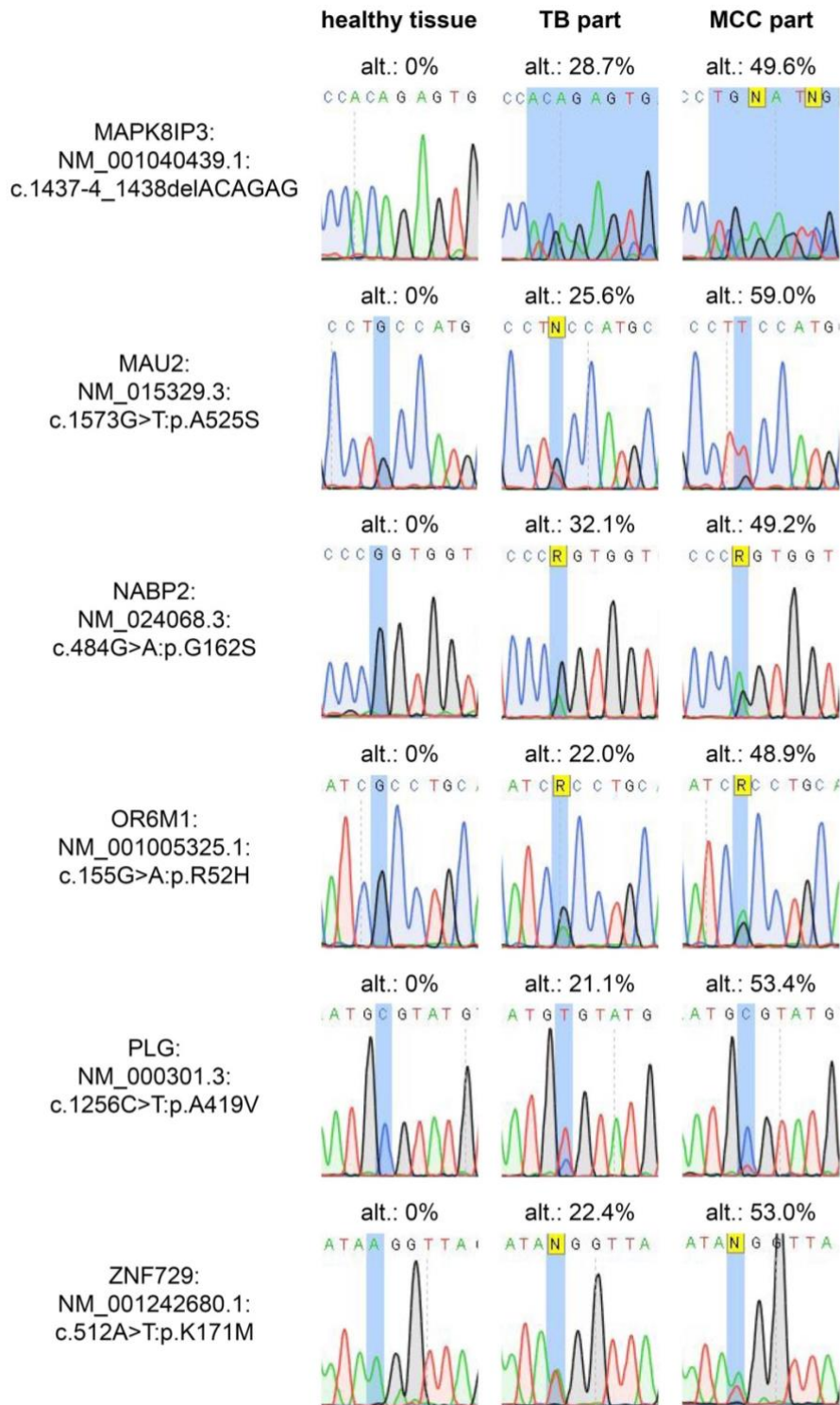


Figure 3. Trichoblastoma and MCC cells of the combined tumor share six protein-altering somatic variants. Whole exome sequencing identified six variants shared by trichoblastoma and MCC (**Supplementary Table S2**). The variant as well as the allelic frequency for the alternative sequence (alt.) derived from the massive parallel sequencing are given in the figure. DNA obtained from PBMC or any of the two tumor components were amplified by primers specific for the respective variants. The results of the direct sequencing are depicted. Blue shading indicates the position of the variant or the frame shift region caused by deletion, respectively.

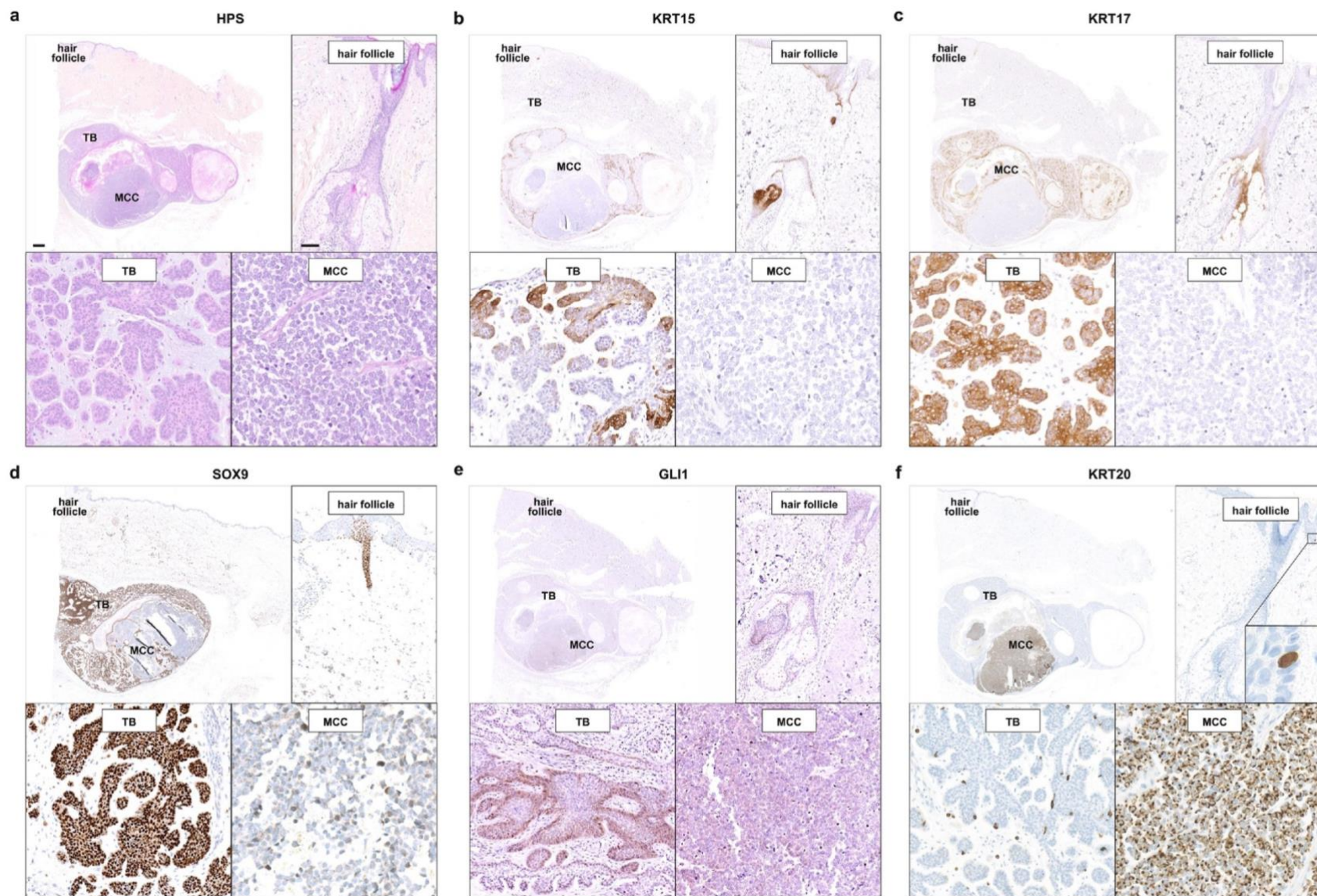


Figure 4. (See legends below).

Figure 4. Shared morphologic and immunohistochemical features of MC progenitors in the hair follicle and trichoblastoma cells. Overview photographs (bar = 1 mm) of the complete specimen containing the combined TB/MCC and a hair follicle as well as details of each component (bars = 100 mm) are displayed. **(a)** Morphological examination (hematein-phloxin saffron (HPS) staining) revealed clusters of basaloid cells displaying focal palisading in the trichoblastoma periphery, similar to the germinative cells of the hair follicle. In line with these findings, expression of **(b)** KRT15, a marker expressed by the outer root sheath of the hair follicle, was observed also in the trichoblastoma periphery. Furthermore, in TB as well as in the hair follicle cells, the progenitor markers **(c)** KRT17 and **(d)** SOX9 are frequently present. The same applies to nuclear localization of GLI1 **(e)** indicating activation of the sonic hedgehog pathway which is known to be critical for the maintenance of MC progenitors and their subsequent MC differentiation. In accordance with the presence of many markers indicating MC differentiation capability in the hair follicle and TB KRT20-positive MCs **(f)** can be found in both tissues.

Supplements

Supplementary Table S1. Clinical features of the combined trichoblastoma/MCC case analyzed in this study as well as a second case described by Battistella and colleagues.

Supplementary Table S2. Somatic mutations detected by whole exome sequencing in the trichoblastoma and the MCC part of the combined tumor.

Supplementary Table S3. Read statistics.

Supplementary Table S4. Distribution of the COSMIC signatures in the trichoblastoma and the MCC part of the combined tumor.

Supplementary Table S5. Immunohistochemical profil of a second trichoblastoma/MCC combined tumor previously described by Battistella and colleagues

Supplementary Figure S1. Further microscopic characterization of the trichoblastoma/MCC combined tumor (hematein-phloxin-saffron staining).

Supplementary Figure S2. Immunohistochemical profiles of TB and MCC component of the combined tumor.

Supplementary Figure S3. MCPyV-LT-positive areas of the trichoblastoma part differ from LT-negative areas also with respect to cytokeratins-8 and -20, SOX2 and KI-67 expression.

Supplementary Figure S4. MCPyV-positivity in a second trichoblastoma/MCC combined tumor previously described by Battistella and colleagues

Supplementary Material S1. Antibodies used for Immunohistochemistry.

Supplementary Material S2. DNA isolation and MCPyV quantitative PCR.

Supplementary Material S3. PCR amplification and Sanger sequencing.

Supplementary Table S1. Clinical features of the combined trichoblastoma/MCC case analyzed in this study as well as a second case described by Battistella and colleagues.

characteristics	Battistella et al.	present case
age (year)	84	70
sex	female	male
medical history	-	myocardial infarction, cardiac arrhythmia, coma, diabetes, tuberculosis
tumor location	left forearm	chest wall
clinical presentation	rapidly growing mass appeared 4 months ago	recurrence of a trichoblastoma partially excised 3 years earlier
tumor size (cm)	1.5	4
tumor spread at the time of diagnosis	localized	regional nodal metastases (2 axillary lymph-node)
initial treatment	surgery	surgery & radiotherapy
follow up (months)	-	16
recurrence	-	metastatic spreading (subcutaneous and pancreatic metastases)
additional treatment	-	avelumab

Supplementary Table S2. Description of the somatic mutations detected by whole exome sequencing in the trichoblastoma and the MCC part of the combined tumor. Genomic DNA derived from the two tumor components (TB and MCC) and healthy tissue (HT) was analyzed by whole exome sequencing to identify acquired variants in the tumor exomes using three detection methods (M – MuTect1, V – VarScan2, S – Scalpel).

chromosome	start (hg19)	end (hg 19)	ref	alt	type	amino acid change (or splice site change)	depth TB	frequency TB [%]	depth MCC	frequency MCC [%]	depth HT	frequency HT [%]	detection method
chr6	161143599	161143599	C	T	exonic	PLG :NM_000301.3:c.1256C>T:p.A419V	57	21.1	58	53.4	67	0	M+V
chr11	123676903	123676903	C	T	exonic	OR6M1 :NM_001005325.1:c.155G>A:p.R52H	97	21.6	73	46.6	116	0	M+V
chr12	56622845	56622845	G	A	exonic	NABP2 :NM_024068.3:c.484G>A:p.G162S	97	32	84	50	83	0	M+V
chr16	1811221	1811226	ACAGAG	'	exonic	MAPK8IP3 :NM_001040439.1:c.1437-4_1438delACAGAG	94	28.7	117	49.6	92	0	S
chr19	19465188	19465188	G	T	exonic	MAU2 :NM_015329.3:c.1573G>T:p.A525S	153	26.8	158	56.3	92	0	M+V
chr19	22496731	22496731	A	T	exonic	ZNF729 :NM_001242680.1:c.512A>T:p.K171M	74	20.3	58	56.9	72	0	M+V
chr1	214557127	214557127	G	A	exonic	PTPN14 :NM_005401.4:c.2071C>T:p.Q691X	295	5.1	201	0	128	0	M
chr12	80890100	80890100	C	T	exonic	PTPRQ :NM_001145026.1:c.1546C>T:p.P516S	142	19.7	116	0	127	0	M+V
chr13	88329882	88329882	C	A	exonic	SLITRK5 :NM_015567.1:c.2239C>A:p.H747N	273	6.2	269	0	87	0	M
chr17	48538171	48538171	C	T	exonic	ACSF2 :NM_025149.4:c.262C>T:p.R88X	183	4.4	177	0.6	120	0	M
chr1	2125325	2125342	TGGGCTCCG GGCCGCACC	'	exonic	FAAP20 :NM_001256945.1: c.70_87delTGGGCTCCGGCCGCACC:p.G24_P29del	311	0	266	23.7	159	0	S+V
chr3	46007863	46007863	C	T	exonic	FYCO1 :NM_024513.3:c.2963G>A:p.R988Q	123	0	92	25	100	1	M+V
chr9	34402397	34402397	A	G	exonic	FAM219A :NM_001184940.1:c.332T>C:p.L111P	133	0	127	44.1	121	0	M+V
chr10	7786884	7786884	C	A	exonic	ITIH2 :NM_002216.2:c.2539C>A:p.P847T	93	0	67	31.3	95	0	M+V
chr10	93811989	93811989	C	G	exonic	CPEB3 :NM_001178137.1:c.2035G>C:p.V679L	127	1.6	115	38.3	118	0	M+V
chr11	68318588	68318588	G	A	exonic	PPP6R3 :NM_001164161.1:c.553-1G>A	120	0.8	108	39.8	119	0	M+V
chr11	120769341	120769341	C	A	exonic	GRIK4 :NM_014619.2:c.1265C>A:p.T422N	188	0	186	55.4	98	0	M+V
chr19	389915 77	38991577	G	A	exonic c	RYR1 :NM_000540.2:c.7561G>A:p.V2521M	205	0.5	160	23.1	96	0	M+V

Supplementary Table S3. Read statistics.

sample	total number of reads	total number of trimmed reads	trimmed reads [%]	coverage
healthy exome	219 216 275	217 252 084	99.1	130.2
MCC exome	95 912 676	94 824 350	98.9	134.8
TB exome	103 181 911	101 966 983	98.8	146.4
MCC genome	397 893 750	393 199 816	98.8	18.41

Supplementary Table S4. Distribution of the COSMIC signatures in the trichoblastoma and the MCC part of the combined tumor.

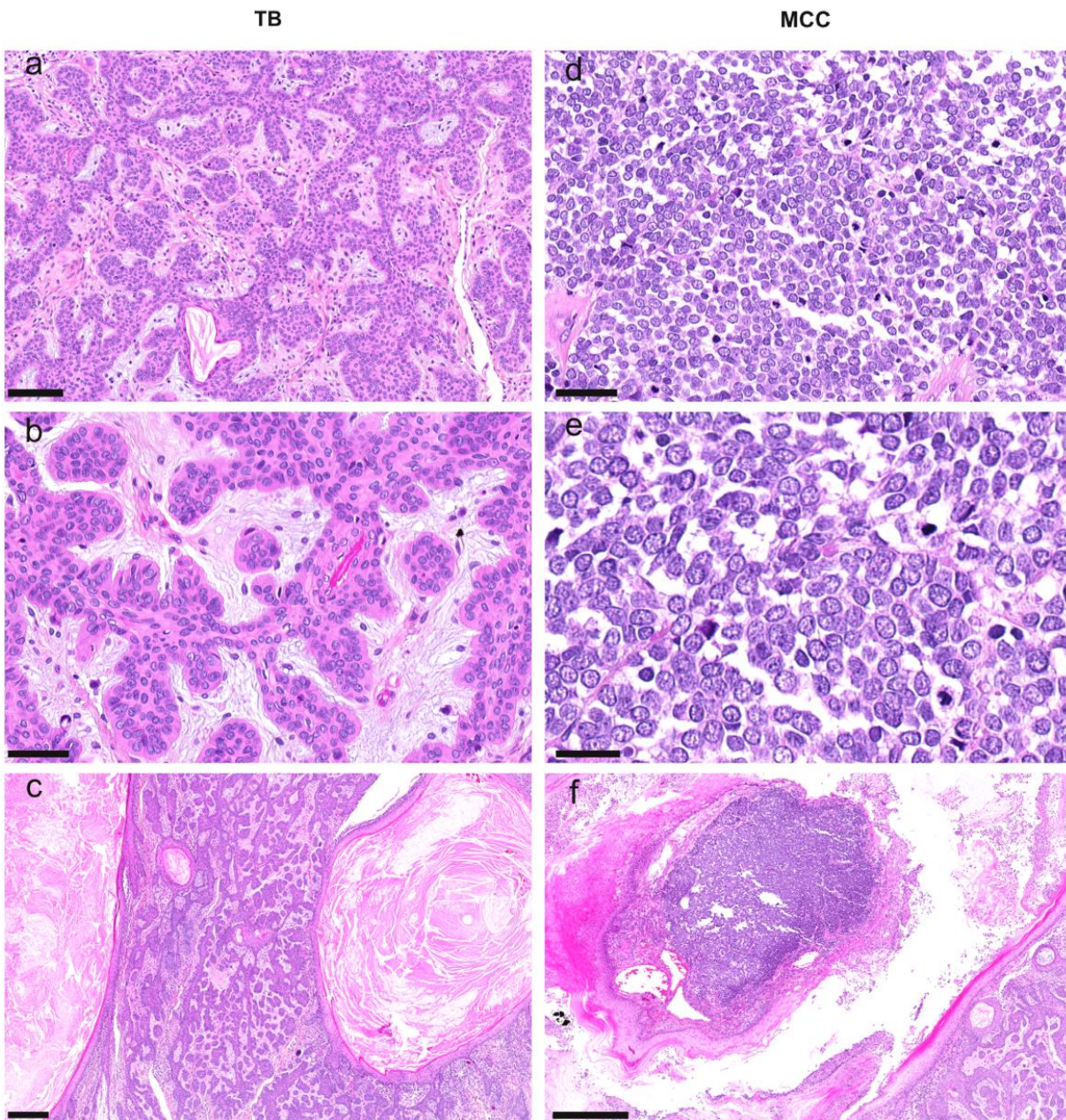
Signature	Proposed_Etiology	TB (%)	MCC (%)
1	Age	0.31	0.07
2	APOBEC	0	0
3	BRCA1 / BRCA2 (failure of DNA DSB repair / large INDELS)	0	0
4	Smoking	0	0
5	Unknown (all cancer types)	0	0
6	Defective DNA MMR / MSI (small INDELS)	0.47	0.583
7	UV light	0	0
8	Unknown (breast cancer and medulloblastoma)	0.083	0
9	POLH (CLL, BCL)	0	0
10	POLE (ultra-hypermutation)	0	0
11	Alkylating agents	0	0
12	Unknown (liver cancer)	0	0
13	APOBEC	0	0
14	Unknown (uterine cancer and glioma / hypermutation)	0	0
15	Defective DNA MMR (small INDELS)	0	0.209
16	Unknown (liver cancer)	0	0
17	Unknown (different cancers)	0.034	0
18	Unknown (different cancers)	0	0.101
19	Unknown (pilocytic astrocytoma)	0	0
20	Defective DNA MMR (small INDELS)	0	0
21	Unknown (stomach cancer / MSI)	0	0
22	Aristolochic acid	0.007	0.037
23	Unknown (liver cancer)	0	0
24	Aflatoxin	0	0

25	Unknown (Hodgkin lymphoma)	0	0
26	Defective DNA MMR (small INDELS)	0	0
27	Unknown (kidney cancer / small INDELS)	0	0
28	Unknown (stomach cancer)	0	0
29	Tobacco chewing	0.095	0
30	Unknown (breast cancer)	0	0

Analyses were conducted on 19 (trichoblastoma) and 8 (MCC) somatic mutations respectively.

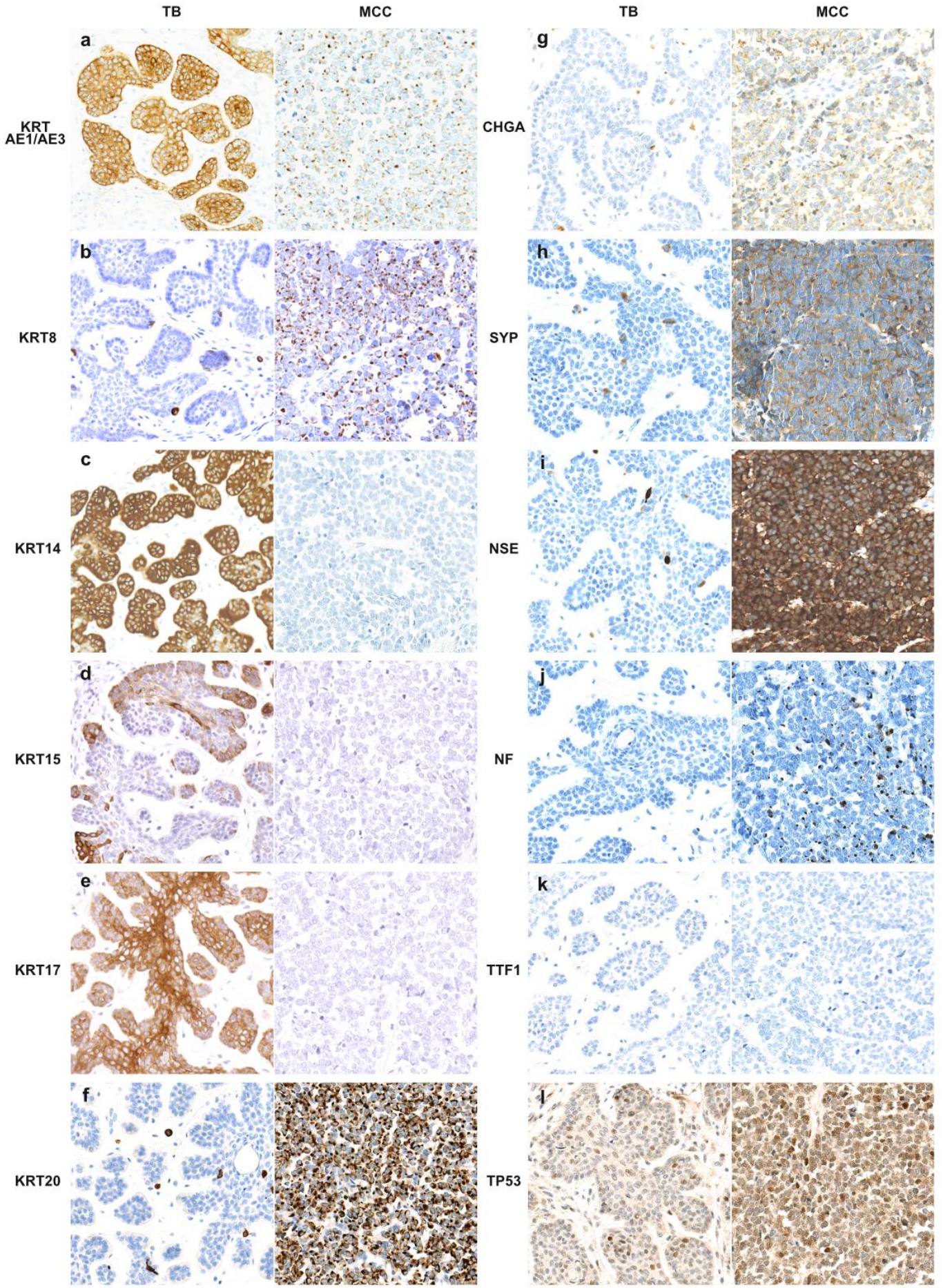
Supplementary Table S5. Immunohistochemical profil of a second trichoblastoma/MCC combined tumor previously described by Battistella and colleagues.

Differentiation markers	Expression in healthy skin	Location and level of expression in the TB part	Location and level of expression in the MCC part
GLI1	Hair follicle progenitors Touch dome progenitors	Intense, nuclear	Weak
KRT15	Outer root sheath	Intense, cytoplasmic In the external part of the nodules	None
KRT17	Companion layer of the hair follicle Touch dome progenitors	Intense, cytoplasmic	None
SOX9	Hair follicle Sweat gland Touch dome progenitor	Intense, nuclear	None
SOX2	Merkel cells Melanocytes	Intense, nuclear In Merkel cells	Intense, nuclear
KRT8	Merkel cells Sweat glands	Intense, cytoplasmic in Merkel cells	Intense, cytoplasmic with a dot like pattern
KRT20	Merkel cells	Intense, cytoplasmic In Merkel cells	Intense, cytoplasmic with a dot like pattern

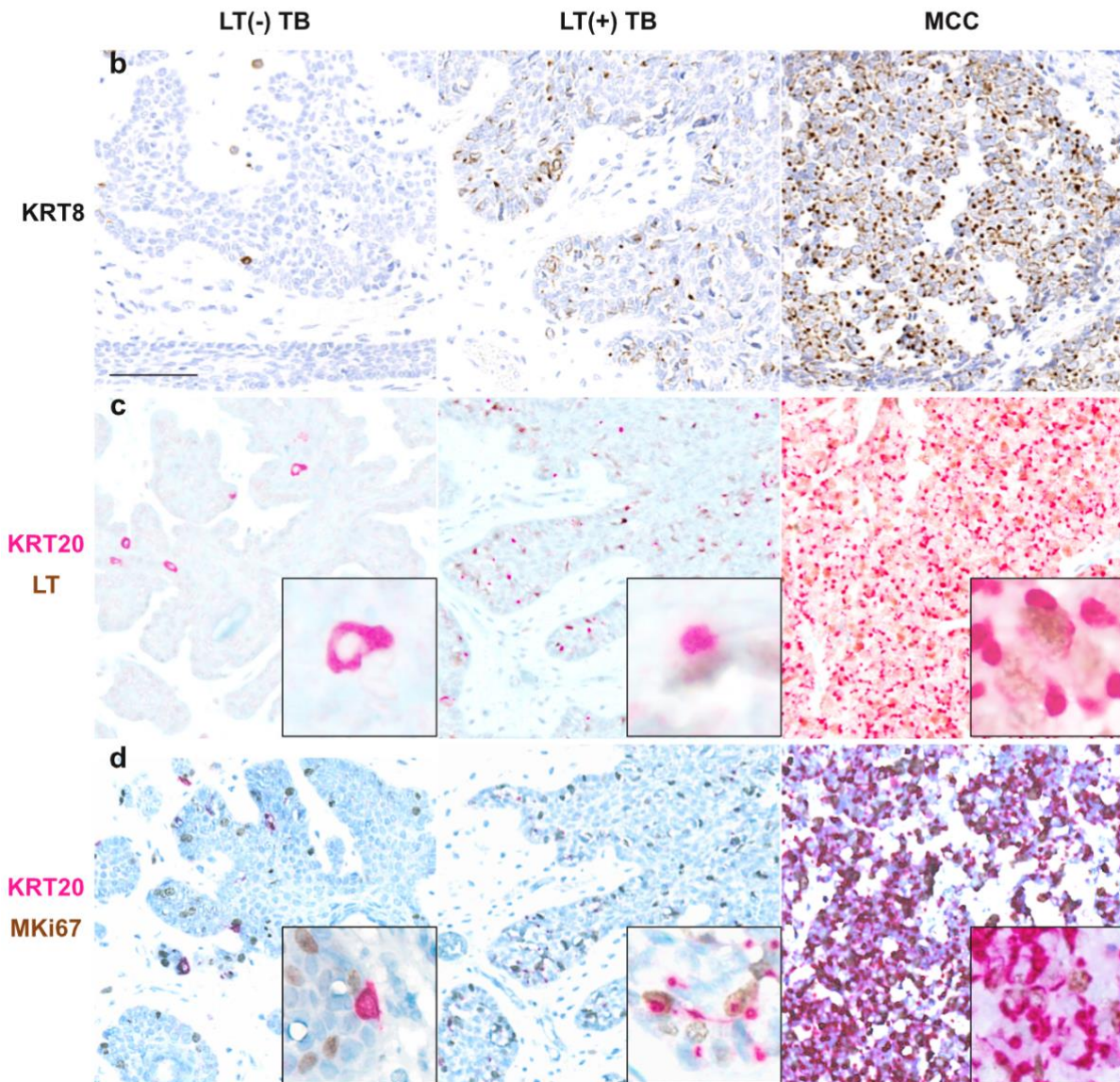
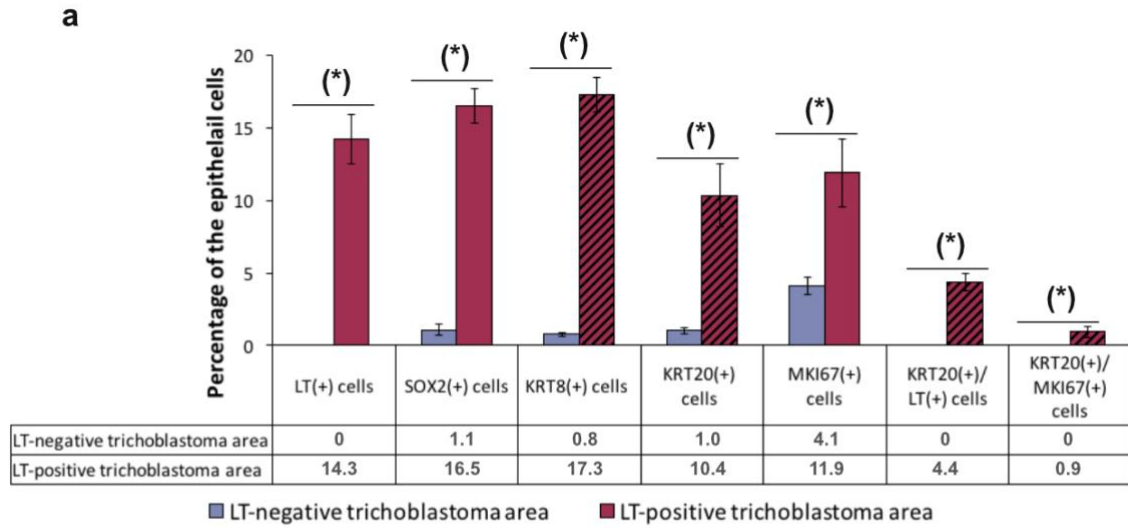


Supplementary Figure S1. Further microscopic characterization of the trichoblastoma/MCC combined tumor (hematein-phloxin-saffron staining).

The trichoblastoma part (a-c) of the tumor was composed of epithelial nests or anastomotic strands of basaloid cells surrounded by a particularly clear stroma containing mucin deposits. In some areas (c) also cystic dilatations containing keratin deposits were present in the epithelial component (a: bar=100 μ m, b: bar = 50 μ m, c: bar = 250 μ m). The MCC part (d-f) consisted of sheets of tumors cells with few cytoplasm, round nuclei and clear chromatin. Moreover, several mitotic figures were observed (d). At some locations (f), invasion of MCC cells into the epithelial cyst was noticed (d: bar=50 μ m, e: bar = 25 μ m, f: bar = 500 μ m).

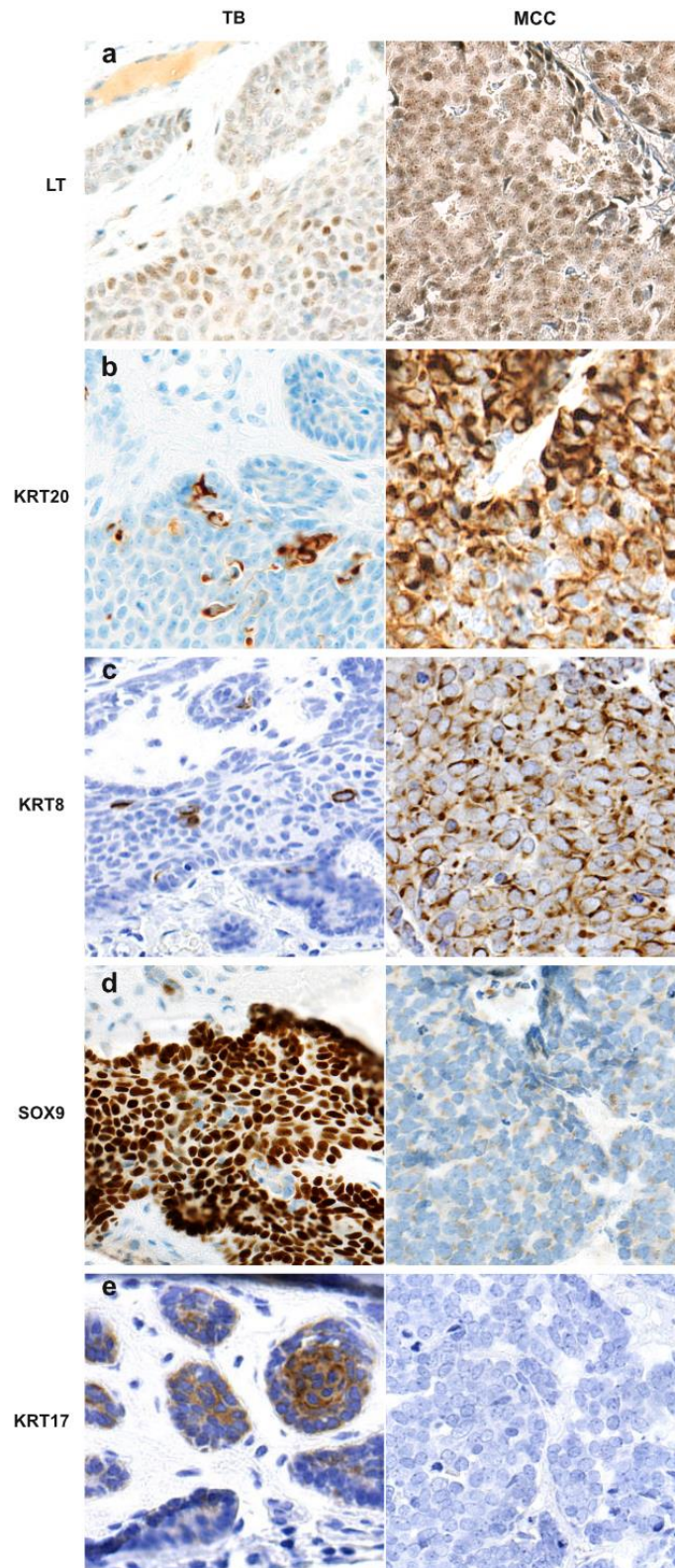


Supplementary Figure S2. Immunohistochemical profiles of TB and MCC component of the combined tumor. Expression of pan-Keratin(AE1/AE3) **(a)**, KRT8 **(b)**, KRT14 **(c)**, KRT15 **(d)**, KRT17 **(e)**, KRT20 **(f)**, chromogranin A (CHGA) **(g)**, synaptophysin (SYN) **(h)**, neuron specific enolase (NSE) **(i)**, neurofilament (NF) **(j)**, TTF1 **(k)**, TP53 **(l)** was analyzed in the trichoblastoma and the MCC part. Epithelial trichoblastoma cells displayed diffuse keratins expression (AE1/AE3) whereas a dot pattern was observed in the MCC part **(a)**. Immunohistochemical staining for the MC markers KRT8, KRT20, CHGA, SYN, NSE, and NF revealed in the trichoblastoma part rare scattered Merkel cells whereas all MCC tumor cells were positive for both markers **(b,f,g-j)**. Neither TTF1-positivity **(k)** nor TP53-overexpression **(l)**, both hallmarks of UV-induced MCC₂ were observed in the MCC part. Trichoblastoma epithelial cells expressed KRT 14,15 and 17, these two latter hallmarks of the outer root sheet and the companion layer of the hair follicle, whereas negativity for these markers was observed in the MCC part **(c-e)**.



Supplementary Figure 3. (See legends below)

Supplementary Figure 3. Areas of the trichoblastoma with occasional LT expression (LT+) TB) differ from areas without Large T expression also with respect to KRT8, KRT20, SOX2 and MKI67 expression. Comparison of trichoblastoma areas without or with occasional LT expression **(a)** revealed significantly increased numbers of SOX2-, KRT8 and KRT20-positive cells ($p=5.10^{-4}$, 2.10^{-4} and 1.10^{-3} respectively). Moreover KRT20(+)/LT(+) and KRT20(+)/MKI67(+) co-expressing cells were only observed in the LT-positive area ($p= 5.10^{-4}$ and $p=2.10^{-3}$, respectively). Counts were performed on eight independent microscopic fields of 0.027 mm^2 . Results are expressed in percentage of epithelial cells (mean \pm standard error of the mean); (*): $p<0.05$ (Mann-Whitney test); hatched bars indicate cells expressing Keratins with a dot pattern. Representative details for KRT8 mono- **(b)** as well as KRT20 (red)/LT- (brown) **(c)** and KRT20 (red)/MKI67 (brown) **(d)** double-stainings in MCPyV-negative and MCPyV-positive trichoblastoma areas as well as in the MCC part (bar= $50 \mu\text{m}$) are depicted. KRT20/LT as well as KRT20/MKI67 double positive cells could be identified in the LT-positive area of the TB and the MCC but not in the LT-negative regions of the TB. , as well as one representative region from the MCC part are displayed.



Supplementary Figure 4. MCPyV-positivity in a second trichoblastoma/MCC combined tumor previously described by Battistella and colleagues. Immunohistochemical staining for MCPyV-LT (a) and cytoke­ratin-20 (b) in the second trichoblastoma /MCC combined tumor. MCPyV-LT-positivity was observed in both tumor components (a). Intermixture of dot and diffuse cytoke­ratin-20 and cytoke­ratin-8 expression was observed in the trichoblastoma whereas only dot pattern was observed in the MCC part (b-c). Expressions of SOX9 and cytoke­ratin 17 were observed in the trichoblastoma but not in the MCC part (d-e).

Supplementary Material S1. Antibodies used for Immunohistochemistry.

antigen	clone	company	dilution
CHGA	polyclonal (#A0430)	Dako	1/2000
KRT8	M20	Santa Cruz	1/50
KRT14	SP53	Dako	pre-diluted
KRT15	LHK15	Santa Cruz	1/200
KRT17	Ks17.E3	Santa Cruz	1/200
KRT20	Ks20.8	Dako	1/100
Pan-Keratin	AE1/AE3	Dako	1/200
GLI1	C68H3	Ozyme	1/200
MKI67	30-9	Ventana	pre-diluted
MCPyV-LT	CM2B4	Santa Cruz	1/50
PAX5	SP34	Ventana	pre-diluted
CD274	22-C3	Dako	1/50
TP53	DO-7	Dako	1/50
SOX2	EPR3131	Abcam	1/50
SOX9	AB5535	Merck	1/1000
TdT	760-26710	Cell Marque	pre-diluted
TTF1	SP141	Roche	pre-diluted

GLI1: GLI family zinc finger 1, PAX5: paired box protein 5, SOX2: SRY-box 2, SOX9 : SRY-box 9, TdT: terminal deoxynucleotidyl transferase, TTF-1: thyroid transcription factor.

Supplementary Material S2. Primers used for MCPyV quantitative PCR.

primer	sequence (5'-3')
LT3F	TCG CCA GCA TTG TAG TCT AAA AAC
LT3R	CCA AAC CAA AGA ATA AAG CAC TGA
LT3S (Probe)	6-FAM-CTG TCT GAC GTG GGG AGA GTG TTT TTG CT
ALBF	CCA AAC CAA AGA ATA AAG CAC TG
ALBR	TGT CTC TCC TTC TCA GAA AGT GT
AlbuminS (Probe)	VIC-ACA TTC ACC TTC CAT GCA GA

Supplementary Material S3. Primers used for Sanger sequencing.

target ¹	type ²	sense	antisense	size [bp] ³	temp. [°C] ⁴
MAPK8IP3	pre	GCA CAG AGG CAA GGA CAC A	CTG CTT ACA TCC TCC GCC TC	166	69
	amp	CAG AGG CAA GGA CAC AGG TT	TCC GCC TCT TCT TTG GGT TC	151	68
MAU2	pre	GGG CTG GGT TCG GCA AGT GG	AGG CTG GGG CTG GGG AAG AGG	192	72
	amp	CTC CCC CTT GCT GCT CTT GGT TGA	TGG CCA TTG CAC TCA CCT CTC AGC	134	72
NABP2	pre	TGT GCA TGG TGA AGA CTG TG	TGC TAT CTC TTG CTG CTC CTC	310	66
	amp	ATG GAG ACA GGC CTT GGG ATG GAC	TCC TCC GGG TTT CTT TGC CGT TAC	260	72
OR6M1	pre	TTA ACA GC AAC AGG AAA CAT CAC C	TAG GAG GCA GGC CAA CAA CTT	150	66
	amp	TCA TCT CCC TGA TAT GGA TTG AT	CAA CAA CTT TGG GGT AAT GAC A	113	63
PLG	pre	ACA GAG CTA CCG AGG CAC AT	CAG GCC CTT TCT TCA AAA GC	275	65
	amp	GAG CTA CCG AGG CAC ATC CT	ATG CCC CTC TTA CAG TAA AAA TCA	141	65
ZNF729	pre	AGT GCC AAT GAG GGT AAG ATG	GCA TGA AAA ATG ATT TGC TAC AT	193	60
	amp	GCA GGA CAG CTA CCC AGA G	ATT TGC TAC ATT TTA TAC ATT TGA	129	56
MCPyV	amp	TTT TTG AGA GGG CTT TTG AGG TC	GCC CCA GCA GCA GTA ACA TTC	84	60
MCPyV Δ-region	pre	AGC CAA AAG GAG GTT AGA GAT G	TTA TTT ATT CCT TGC CCT GGT T	432/137	62
	amp	AGC CAA AAG GAG GTT AGA GAT G	TTA GGC TAT TTT GCC CTT TCA	398/103	62
MCPyV 5' integ.	pre	TGC AGG CAG TAA TTG GAG AA	TCAACTTAAATTTCTCAATCTTATCA	196	59
	amp	TGC AGG CAG TAA TTG GAG AA	CATATAACTCTATAGCTTTATCAGAAG	171	59
MCPyV 3' integ.	pre	AAA GGA GTG AAT AAG ATG CCT GA	TTG TCC ATT AAT GTT TTA TTT GTT TCA	210	60
	amp	ATG CAA GCC CCC TTA CA	TTG TCC ATT AAT GTT TTA TTT GTT TCA	172	60

¹Primer pairs were designed to amplify the regions containing the shared pathological variants, general MCPyV (MCPyV), the MCPyV region containing the deletion (Δ-region), or the 5' or 3' integration sites (5' or 3'integ.).

²For most targets a nested approach with pre-amplification (pre) and amplification (amp) was pursued.

³The size of the PCR product for MCPyV Δ-region depends on whether wildtype or MCPyV with deletion is present in the sample. ⁴Annealing temperature (temp.) for each primer pair is given.

Merkel cell Polyomavirus T antigens promote Merkel cell differentiation in epithelial progenitors of the skin.

T Kervarrec MD MSc^{1,2,3}, M Samimi MD PhD^{2,4}, S Hesbacher PhD³, P Berthon PhD², M Wobser MD³, A Sallot MD⁵, B Laure MD, PhD⁶, B Sarma MSc³, S Schweinitzer³, T Gandon MSc², C Destrieux MD PhD⁷, C Pascalín PharmD PhD⁸, S Guyétant MD PhD^{1,2}, A Touzé PhD², R Houben PhD³, D Schrama PhD³

- (1) Department of Pathology, Université François Rabelais, CHU de Tours, avenue de la République, 37170, Chambray-les-tours, France
- (2) "Biologie des infections à polyomavirus" team, UMR INRA ISP 1282, Université François Rabelais, 31 avenue Monge, 37200, Tours, France
- (3) Department of Dermatology, Venereology and Allergology, University Hospital Würzburg, Josef-Schneider-Straße 2, 97080 Würzburg, Germany.
- (4) Dermatology Department, Université François Rabelais, CHU de Tours, avenue de la République, 37170, Chambray-les-tours, France
- (5) Plastic surgery Department, Université François Rabelais, CHU de Tours, avenue de la République, 37170, Chambray-les-tours, France
- (6) Head surgery Department, Université François Rabelais, CHU de Tours, avenue de la République, 37170, Chambray-les-tours, France
- (7) Neurosurgery Department, Université François Rabelais, CHU de Tours, Boulevard tonnelé, 37044, Tours, France
- (8) CNRS ERL 7368, Signalisation et Transports Ioniques Membranaires, Equipe Transferts Ioniques et Rythmicité Cardiaque, Groupe Physiologie des Cellules Cardiaques et Vasculaires, Tours, France

Abstract:

Merkel cell carcinoma (MCC) is a rare, and aggressive cutaneous neoplasia frequently caused by a polyomavirus. However, the nature of the cell in which viral integration and subsequent MCC development occur was for a long time unknown. Recently, we demonstrated that virus-positive MCC can be derived from trichoblastomas, a benign epithelial neoplasia harboring hair follicle differentiation and bearing Merkel cell differentiation abilities. Accordingly, we hypothesized that viral-positive MCC can be derived from MC progenitors of the hair follicle.

To confirm these findings, phenotypic comparison of trichoblastomas and physiologic human MC progenitors was conducted and revealed common expression of the GLI1, KRT17 and SOX9 in both subsets. Interestingly, ectopic GLI1 expression in keratinocytes induced transcription of the MC lineage marker SOX2 suggesting GLI1 as a molecular determinant of MC differentiation under physiologic and tumor conditions.

To assess a potential contribution of the T antigens to the tumor phenotype, the viral oncoproteins were transduced in human keratinocytes. While this experiment only led to induction of KRT8, a marker appearing early during Merkel cell differentiation, combined GLI1 and TA ectopic expressions gave rise to the development of a cell population expressing several MC markers (SOX2, KRT8 and KRT20). Moreover, ectopic T antigen expression in hair follicles induced formation of tumor cell clusters with “small cell carcinoma” features. Finally we demonstrated that Large T Antigen prevents the degradation of the transcription factor ATOH1, the master regulator driving Merkel cell differentiation. Therefore our report suggests that under a specific cellular context, T antigens contribute to the acquisition of a Merkel cell like phenotype.

Introduction

Merkel cell carcinoma (MCC) is a rare, and aggressive cutaneous neoplasm with a 5-year overall survival rate of 40%¹. Microscopically, MCC appears as a proliferation of tumor cells harboring small cell carcinoma features and expressing both neuroendocrine and epithelial markers. In 2008, Feng et al. detected the sequences of a new polyomavirus integrated in most MCC tumor cell genome². Indeed, 80% of MCC cases are Merkel cell polyomavirus (MCPyV) positive and expression of the two viral T antigens (TA) (small T (sT) and Large T Antigen (LT)) are considered as the main drivers for carcinogenesis and growth of such tumors³.

Based on close phenotypic similarities between tumor cells and the eponym Merkel cell (MC), the latter was initially regarded as the most probable cell of origin of MCC. Indeed, MCs are located in the appendages or in the basal layer of the epidermis, and have been shown to function as mechanoreceptors capable of transforming tactile stimuli into Ca²⁺-action potentials⁴ and serotonin release⁵, and passing these signals onto A β -afferent nerve endings⁴. In mice and humans, MCs can be distinguished immunohistochemically from other intraepidermal cells by positivity for SOX2, and cytokeratins (KRT) 8, 18 and 20, which sequentially appear during MC differentiation and are additionally observed in MCC tumors⁶⁻¹⁰.

For a long time, it was a matter of debate whether MCs develop from the epidermal or neural crest lineage¹¹. Now, it is widely accepted, that MCs derive from epidermal progenitors^{10,12,13}, and that the transcription factor *Atonal homolog 1* (Atoh1) is the master regulator of this differentiation process^{10,14,15}. While ectopic Atoh1 expression induces MC differentiation in the complete epidermis of transgenic mice¹⁶, physiological MCs development preferentially occurs in epithelial progenitors located in hair follicles and in specialized structures named “touch domes”^{17,18}. A critical step for MC differentiation in mice hairy skin is that epidermal progenitors come into contact with dermal nerves leading to induction of Sonic Hedgehog pathway (SHH) activation and subsequent Gli1 expression^{17,18}. Markers characterizing these Gli1-expressing progenitors are Krt17^{17,19}, Sox9²⁰, and CD200²¹. Notably, a high tumorigenic potential for this population has been demonstrated²². In contrast, due to the lack of

proliferative activity²³ and insensitiveness to oncogenic stimuli including TA ectopic expression²⁴, differentiated MCs are regarded as an unlikely cellular origin for malignant transformation²⁵ and accordingly alternative MCC ancestries such as epithelial progenitors, fibroblasts and B-cells have been recently proposed^{16,25-27}.

Besides MCC, a second tumor entity known as Trichoblastoma (TB) harbors cells with MC phenotype. TB, as a benign epithelial skin tumor displaying hair follicle differentiation²⁸, is mainly composed of germinative basaloid cells similar to the hair follicle precursors. However, TB is also characterized by sparse intra-tumoral MCs, probably reflecting a preserved potential of follicular germinative tumor cells to differentiate into MCs²⁹⁻³¹, although the molecular determinants of such process still needs to be determined³¹.

Recently, applying massive parallel sequencing on a combined tumor, we demonstrated that MCPyV integration in a TB cell gave rise to an MCPyV-positive MCC³². This report provides a clear demonstration that MCPyV-positive MCC can arise from epithelial cells. Moreover, the close similarities between TB and physiologic hair follicles, strongly suggest epithelial progenitors of the hair follicle with intrinsic MC differentiation as main MCC ancestry. Furthermore, LT expression observed in the TB part was associated with enhanced MC differentiation³². Therefore, our current working hypothesis is, that in a specific cellular context, i.e. an epithelial progenitor with intrinsic MC differentiation, T antigens may be able to support development of an MC phenotype.

Accordingly, using the observation of the combined TB/MCPyV-positive tumor case as a model, the main objective of the present study is to determine the relative contribution of the cell of origin and the T antigens to MCC phenotype.

Method

Human samples

Healthy cutaneous tissues were obtained from dead peoples who signed a body donation procedure. Skin from 5 anatomic sites (scalp, face, trunk, finger, lower limb) were collected using 6 mm diameter punch in the 24 h following death, and then immediately fixed in Formalin and then paraffin embedded. 15 TB cases were extracted from the archives of the Dermatology department of Würzburg (Local Ethics Committee in Human Research, 196/12). After histological diagnosis confirmation by two pathologists (MW, TK), only cases containing MCs were selected based on KRT20 immunostainings. MCC cases enrolled in the present work were already included in a tissue microarray used in a previous study³³. Briefly, cases were selected from a historical/prospective multicentric French cohort of patients with a diagnosis of MCC established between 1998 and 2017 (Local Ethics Committee in Human Research, Tours, France; no. ID RCB2009-A01056-51). Inclusion criteria for the cohort were previously described^{34,35}. MCPyV status of the MCC cases were previously determined using a validated real time PCR³³.

Immunohistochemistry

Protein immunochemical detection were performed on formalin-fixed, paraffin embedded (FFPE) samples (tissue, hair follicle), paraformalin-fixed (cytospin) or living cells. Immunohistochemical staining for KRT20, MCPyV-LT, Neurofilament and SOX9 were performed using a BenchMark XT Platform as instructed^{33,36}. Immunohistochemical staining for GLI1, KRT8, KRT17, KRT18 and SOX2 as well as all cytospin stainings were performed manually. Antibodies and dilutions are provided in **Supplementary Method S1**. Microscopic evaluation was performed by a Pathologist (TK).

Samples management and interpretation of immunohistochemical staining

To determine MC densities, 250 consecutives 5 µm-thick sections were cut from FFPE healthy cutaneous tissues (6 µm-diameter skin punches cut in two equal parts). Every 10th slide, a KRT20 immunohistochemical staining allowing the detection of MC was performed, i.e., one KRT20 stained slide every 50 µm. Unstained slides were preserved for further analyses. MC number and location (interfollicular epidermis, hair follicle (infundibulum or isthmus), sebaceous or sweat glands) was then assessed by a pathologist (TK). Since MC are frequently

located in the connection area between epidermis and an appendage, i.e., either hair follicles or sweat glands, all MC located in front of an appendage structure (hair follicle, ostium of a sweat gland or sweat gland duct) were considered to belong to this appendage. In addition, MC hotspot were defined as areas with more than 3 MCs in one microscopic field at high magnification. Densities of MCs and related hotspots were estimated taking account cut thickness and length of the skin sample. Unstained slides adjacent to the hotspots were consequently investigated for MC progenitor markers.

Primary keratinocytes culture and cell lines

Normal human epidermal keratinocytes (NHEK) and Hair follicles were extracted from abdominal and scalp human samples respectively obtained from the plastic and Head surgery departments of the university hospital center of Tours using previously described protocols³⁷⁻⁴⁰. The use of skin samples was approved by the Ethical Committee of the Tours Hospital, and they were collected after informed consent (Local Ethics Committee in Human Research, Tours, France; no. ID RCB2009-A01056-512016 064). NHEK were cultured in Keratinocyte Serum-Free Medium (K-SFM; Invitrogen Life Technologies), supplemented with epidermal growth factor (5 ng/ml) and bovine pituitary extract (50 µg/ml; all purchased from Invitrogen Life Technologies) at 37°C, 5% CO₂ in a humidified incubator. Human scalp samples were used for microdissecting anagen hair follicles as previously described^{39,40}. Isolated hair follicles were cultured in minimal media of Wiliam's E media supplemented with L-glutamine (2 mM), hydrocortisone (10 ng/ml), insulin (10 µg/ml) and 1% penicillin/streptomycin. HEK293 (RRID:CVCL_0045) and U2OS (RRID:CVCL_0045) were used for co-transfection experiments; HEK293T (RRID:CVCL_0063), i.e., HEK293 expression SV40 T antigens, were used for lentiviral vector production. The MCC cell line WaGa (RRID:CVCL_E998) was included as positive control for immunostaining of MC markers⁴¹. All cell lines were cultivated in RPMI 1640 supplemented with 10% FCS, 100 U/ml penicillin and 0.1 mg/ml streptomycin.

Plasmids and lentiviral vectors

pFLAG-CMV-4-GLI1 plasmid was kindly provided by Dr J. Vachtenheim (Czech Republic)⁴². *GLI1* was introduced into pCDH backbone (System Biosciences) containing puromycin resistance by classical cloning. Phosphosites mutations (S331, S337, S341) were introduced in ATOH1 sequence using the quick change mutagenesis kit (Stratagene) as previously

described⁴³. All TA and LT expressing pCDH vectors were previously described⁴⁴. GLI-IRES-TA sequences were introduced in a pCDH backbone.

Transient transfection and ATOH1 half-life evaluation

Transient transfections were done using 2 µg of DNA with Polyethylenimine (PEI), and protein expression was analyzed 24 h after transfection. For ATOH1 half-life determination, 24 h after transfection cells were exposed to cycloheximide (0.3 mg/mL) in a time course experiment. After harvesting, protein expression was then investigated by immunoblotting, and quantification was performed using ImageJ software.

Lentivirus production

Lentiviral supernatants were produced in HEK293T cells as previously described⁴⁵. Harvested virus supernatant was sterile filtered (0.45 µm) and polybrene (1 µg/ml) was added for infection. Lentiviral transduction of NHEK was performed after 7 days of culture. Human hair follicles were exposed to concentrated lentiviral vectors (centricon technology) immediately after isolation. 14-20 h after infection target cells were washed with medium. NHEK were then subjected to antibiotic selection (puromycin). NHEK were analyzed 2 weeks after transduction, while analyze of the hair follicles was done after 7 days, the maximum culture duration in this setting³⁹.

Gene expression analyses

Total cellular RNA was isolated by using the peqGOLD total RNA kit (Peqlab, Germany) with a subsequent DNaseI digestion step according to the manufacturer's instructions. For cDNA synthesis the Superscript II RT First Strand Kit (Invitrogen GmbH, Karlsruhe) was used. PCR primer sequences used to detect *ATOH1*, *GLI1*, *KRT8*, *14*, *17*, *18*, *20*, *RPLP0*, *SOX2* and *SOX9* are given in **Supplementary Method 2**. Thermal profile for the PCR using the Takyon Low Rox Sybr MasterMix (Eurogentec; Cologne, Germany) contained an initial denaturation step at 95°C for 10 min, followed by 40 cycles of three-step PCR including 15 sec at 95°C, 60 sec at 60°C and 30 sec at 95°C. Evaluation was performed in three independent experiments.

Immunoblot

Cells were lysed in 0.6% SDS, 1 mM EDTA, 10 mM Tris- HCl (pH 8.0), 2 mM NaF, 2 mM NaVO₃ supplemented with a protease inhibitor cocktail (Roche Diagnostics, Basel, Switzerland). Samples were resolved by SDS-PAGE, transferred to nitrocellulose membrane, blocked for 1 h with PBS containing 0.05% Tween 20 and 5% powdered skim milk, then incubated overnight with anti-HA (ab18181, Abcam, 1/1000), LT (CM2B4, Santa Cruz, 1/200), anti-GLI1 (C68H3, Ozyme, 1/200), anti-SOX2 (EPR3131, Abcam, 1/200) or anti-Actin antibody (A5441, Sigma, 1/1000), washed three times with PBS with 0.05% Tween 20 (PBS/Tween), then incubated for 1 h with a peroxidase conjugated secondary antibody. Finally, following three washes with PBS/Tween, immunoreactive proteins were detected by using a chemiluminescence detection procedure.

Image Analysis and Expression score determination

Cell morphology was analyzed on adherent living cells. After acquisition of 5 adjacent microscopic fields, cell contouring was performed on 100 cells per conditions (3 independent experiments), and cell size was then analyzed using ImageJ software. For Protein expression evaluation, $2 \cdot 10^5$ cells were fixed in formalin, spotted on slides and submitted to immunohistochemical staining. Stained slides were scanned by using NanoZoomer (Hamamatsu, Hamamatsu City, Japan). Computation of the expression score after transduction was performed with a custom software written in ImageJ Macro Language. Briefly, color range for each staining was first defined from the whole image data set, then, cells were segmented in each image. For each cell related area, the percentage of each type of viral protein staining: low, medium and high was computed. H-score was finally calculated for each cell with the following formula:

$$Hscore = \frac{(lowstainingarea \times 1) + (mediumstainingarea \times 2) + (highstainingarea \times 3)}{totalcellarea}$$

Analyses was initially performed on 10 consecutive fields (magnification x10). In case in which less than 1000 cells per conditions were analyzed, new acquisitions were performed in order to reach this minimal limit of analyzed cells. Results were subsequently expressed as median,

quartiles Q1-Q3 and 1st-99rd percentiles of the complete cell population analyzed. Protein quantification on immunoblot was performed by ImageJ using the “gel analysis” function.

Statistical analysis

Continuous data are described as median with quantile range, and categorical data with number and as per cent. Associations were assessed by two-tailed Fisher exact test for categorical data and Mann–Whitney test for continuous data. Paired t test was used for RNA expression analysis. $P < 0.05$ was considered statistically significant. Statistical analysis involved use of XL-Stat-Life (Addinsoft, Paris, France).

Results

Cells with an MC progenitor phenotype characterized by active GLI1 are found in close proximity of MCs in human hairy skin

To compare MC differentiation process under physiological and tumor conditions, we first characterized physiological MC lineage in human. To this aim, we first analyzed density and location of MCs in a set of 15 samples from three autopsy specimens (**Figure 1A-B/Supplementary Figure 1/ supplementary Table 1**). Mean MC density regardless of the location was 168 cells/mm², and head and neck as well as acral skin were enriched in MCs compared to the other sites (density =244 and 418 MCs/mm² respectively). Moreover, MCs were often located in appendage structures (74% of all observed MCs), i.e. either hair follicles or sweat glands as depicted in **Figure 1B / Supplementary Figure 1**. Of note, contrary to previous reports, some dermal MCs were observed (**Supplementary Figure 1**).

Since MCs progenitors are expected to be located in close contact with MCs, areas enriched in MCs were selected on the basis of KRT20 positivity, subsequently stained for the MCs progenitor markers GLI1, SOX9 and KRT17 (**Figure 1C**) and compared to adjacent skin area without MCs. Such MCs hotspots were mostly observed in hair follicles (52% of the cases regardless of the anatomic site) or in the junction between eccrine sweat ducts and the overlying epidermis (36%). In this latter place, MCs were surrounded by clusters of verticalized basal keratinocytes similar to those reported as “touch domes” (**Figure 1C/ supplementary Figure 1/supplementary Table 1**). Immunohistochemical investigation of MCs hotspots in hairy skin revealed that epidermal cells surrounding MCs – in contrast to the rest of the epidermis - were characterized by GLI1 nuclear expression and positivity for the stem cell markers KRT17 and SOX9 (**Figure 1B/Supplementary Figure 1**). In contrast, no nuclear positivity of GLI1 was observed in MC hotspots in acral skin, while expression of KRT17 and SOX9 was still detected, in such areas. Therefore, molecular mechanisms leading to MC differentiation might vary according to the anatomic location. However, since GLI1-expressing keratinocytes have been identified as MC progenitors in mice^{15,17,18,20}, our results suggests that such a population mostly located in the hair follicle might also bear the ability to differentiate into MCs in human hairy skin.

GLI1 expression in keratinocytes induces MC lineage markers

To evaluate whether GLI1 expression might be able to induce an MC progenitor phenotype, we used primary normal human epidermal keratinocytes (NHEK) as model system (**Supplementary Figure 2**). These cells were transduced with a lentiviral vector encoding GLI1 (**Figure 1C**). Indeed, gene expression analysis after 14 days revealed an increase of the MC lineage markers *SOX2* (80-fold compared to the empty vector control; $p=0.0003$) and *KRT8* (5-fold; $p=0.03$) (**Figure 1C**). Moreover, in GLI1-transduced cells *KRT17* and *SOX9* mRNA were found to be slightly elevated (1.7; $p=0.08$ and 1.8 fold; $p=0.05$, respectively). On protein level, we observed increased expression levels of *SOX2* upon GLI1 expression by immunocytochemistry and immunoblot (**Figure 1D/Supplementary Figure 2**). Moreover, additional immunostainings suggested enhanced *KRT17* and *SOX9* expression in GLI1-transduced NHEK, while no expression of the additional MC markers *KRT8* or *KRT20* was observed. Together, these results suggested that GLI1, the executor of the sonic hedgehog pathway, is capable of initiating MC-like differentiation steps in human keratinocytic cells via *SOX2* expression.

GLI1 expression may contribute to the MC differentiation observed in TB

To assess if a similar process might contribute to MC differentiation in TB, expression of GLI1, *KRT17*, *SOX9* and *SOX2* was assessed for this tumor entity. In line with active hedgehog pathway signaling being crucial for MC differentiation in human epithelial cells, nuclear GLI1 expression was detectable in 7 of 8 TB specimens, in which immunohistochemical staining for *KRT8*, 18 and/or 20 allowed detection of scattered MCs (**Table 1, Supplementary Figure 3**). Furthermore, expression of the GLI1 targets, *SOX9* and *KRT17*, was also observed in all TB cases, and *SOX2* positive intratumoral cells expected to be MCs were detected in all cases except one. Therefore, it is likely that in TB activation of SHH pathway induces MC differentiation in a similar manner to that observed under physiological conditions^{7,17}. Consequently, these results underline the similarities between TB and MC progenitors of the hair follicles and further suggest the latter cells as a probable origin of MCC.

Of note, while in TB a mixture of cells with either MC progenitor or MC phenotype is present, almost all MCC tumor cells display MC differentiation. Indeed, in a previous study⁴⁶, we observed 100, 99 and 92% of positivity for the MC markers *KRT8*, 18 and 20, respectively.

Accordingly, in the present work, strong nuclear positivity for SOX2 was detected in almost all analyzed MCC tumors (98%). While the MC progenitor marker KRT17 was not detectable (**Table 1, Supplementary Figure 3**), GLI1 and SOX9 nuclear expression, representing the active forms of these transcription factors, were detected in 33% and 28% of the cases, respectively. Moreover, such findings were more frequently observed in MCPyV-negative than in MCPyV-positive cases (GLI1: 52 versus 24%, $p < 0.03$; SOX9 nuclear positivity: 81 versus 10%, $p < 10^{-9}$, respectively) (**Supplementary Figure 3/Supplementary Table 2**) suggesting that MCPyV presence is associated with a more matured MC phenotype.

T antigens can trigger early MC differentiation in epidermal cells

To investigate a possible contribution of the MCPyV TA to the development of an MC phenotype, sT and truncated large T were ectopically expressed in NHEK (**Figure 2A**). Notably, while cells could not be immortalized by the viral proteins, significant morphologic changes with reduction of cell size were observed upon TA expression (**Figure 2A**). Gene expression analysis after two weeks revealed an increase of mRNAs coding for early MC differentiation markers (*KRT8*; $p = 0.02$ and *KRT18*; $p = 0.02$) while *KRT14* mRNA, coding for a marker of basal keratinocytes was slightly reduced upon TA expression ($p = 0.09$) (**Figure 2B**). Moreover, although not statistically significant ($p = 0.08$), a slight increase in *ATOH1* expression was observed upon TA expression in NHEK. Induction of KRT8 upon TA expression in NHEKs was confirmed by immunoblot and immunocytochemical staining while no expression of SOX2 or KRT20 was observed (**Figure 2C-D/Supplementary Figure 2**). Of note, in accordance with morphological changes previously described, KRT8 staining of adherent TA-expressing NHEK further demonstrated that expression of this marker was observed in a subpopulation of cells with small-medium size and round shape (**Figure 2C**).

Combination of GLI1 and T antigens expression induces a MC-like differentiation in NHEK.

To assess the impact of TA expression in GLI1-expressing progenitors, we then induced ectopic expression of GLI1 and TA in NHEK using a bicistronic lentiviral construct. As recently observed for TA-expressing fibroblasts⁴⁷, this transduction of the vector encoding GLI1 and TA in NHEK led after antibiotic selection to the formation of a population of non-adherent living cells. Therefore, both non-adherent and adherent cells were investigated by immunocytochemistry. This analysis revealed induction of the MC markers SOX2, KRT8 and to

a lesser extent KRT20 in a subpopulation of cells harboring reduced size and round shape while such a population was lacking in the control (**Figure 3**). Notably, however, independent analyses of non-adherent and adherent cells revealed expression of MC markers in both populations (**supplementary Figure 4**). Together, these findings demonstrate that combined GLI1 and TA expression induces an MC-like phenotype in NHEK with KRT20 expression restricted to only a few cells.

Ectopic T antigen expression in hair follicles induce formation of tumor with “small cell carcinoma” features

To further confirm the impact of TA expression on MC progenitors of the hair follicles, TA ectopic expression was induced in human hair follicles using concentrated lentiviral vectors. Immunohistochemical analyses revealed ectopic TA expression in the external part of the outer root sheath and in the infundibular region, whereas the inner part of the structure and the bulb region remained negative (**supplementary Figure 5**). No expression of KRT8, KRT18 or KRT20 was observed in Large T-expressing cells of the hair follicles. However, detached from the hair follicle structures clusters of presumably transformed cells with “small cell carcinoma” morphology similar to the one observed in MCC were observed (**Figure 5/supplementary Figure 5**). Immunohistochemical investigation of these clusters revealed Epcam expression while cytokeratin expression was largely absent. Accordingly, no expression of KRT 8, 18 or 20 was observed in the transformed cells. Additional stainings, however, demonstrated synaptophysin and chromogranin A expression, two well established neuroendocrine markers, in a few cells . These findings additionally demonstrate that TA bear the ability to induce a “small cell carcinoma” morphology and partial expression of some neuroendocrine markers in hair follicle cells. Our results obtained for NHEK and hair follicles suggest that TA can induce the acquisition of a Merkel cell-like phenotype when expressed in epithelial progenitors.

T antigens prevent ATOH1 degradation

Since ATOH1 is considered as the master regulator of MC differentiation, we then hypothesized that TA expression might have an impact on ATOH1. To test this hypothesis, we performed co-transfections of U2OS cells with a constant amount of *ATOH1* encoding plasmid

(0.3 μg) and increasing amounts of TA encoding plasmid (0-1.4 μg) (**Figure 5A-B**). These experiments revealed that while *ATOH1* transcription was not affected, immunoblot analyses demonstrated an accumulation of ATOH1 indicating that TA either enhances translation and/or stability of ATOH1. To test whether TA affects ATOH1 stability, cycloheximide chase assays were performed allowing to assess ATOH1 protein decay in the presence or absence of TA (**Figure 5C**). This analysis revealed an increased ATOH1 half-life in the presence of TA compared to the control (half-life = 9 vs 2 h).

In mice, Atoh1 degradation has been shown to be controlled by phosphorylation of 3 carboxy-terminal serine residues (S331, S337, S341) leading to Atoh1 ubiquitinylation and subsequent targeting to the proteasome^{48,49}. Hence, we assumed that TA-dependent stabilization might also involve such sites. Consequently, we generated human ATOH1 constructs lacking one to three of the corresponding phosphorylation sites as previously described^{48,49}. As expected, these modified ATOH1 proteins displayed extended half-life in cycloheximide chase assays (**Figure 5D/supplementary Figure 6**). More importantly, however, while T antigens still stabilized ATOH1 proteins harboring single phosphosite mutations (**supplementary Figure 6**), no stabilization effect was observed with the triple mutant protein (**Figure 5**). This result suggests that ATOH1 is stabilized by T antigens by either impacting phosphorylation of several serine residues or a subsequent step in proteasome targeting.

Next, we analyzed which of the two T antigens are involved in ATOH1 stabilization. Hence, we assessed ATOH1 protein levels after co-transfection of ATOH1 with either sT or LT, respectively. These experiments identified LT as the main effector of ATOH1 stability (**supplementary Figure 6**). To scrutinize which functional domain of the large T might affect ATOH1 degradation, another series of co-transfections was performed combining ATOH1 with Large T mutants either devoid of specific interaction sites or defined regions. Accumulation of ATOH1 was observed in presence of all Large T constructs except the one encoding an LT with deleted MCPyV unique Region 1(MUR1) region (**supplementary Figure 6**) one of two domains distinguishing MCPyV LT from many other known polyomavirus LT proteins.

In conclusion, these results suggest that MCPyV LT is able to stabilize the MC master regulator ATOH1.

Discussion

Whether MCC is derived from MC or from another skin lineage is since a long time a matter of debate. In this regard, we recently demonstrated that MCPyV integration in a TB gave rise to an MCPyV-positive MCC. Since TB is a benign tumor harboring hair follicle differentiation but also bearing the ability to differentiate into MC, we consequently postulated that MCC tumorigenesis can be initiated by MCPyV integration in MC progenitors of the hair follicle. In the present work, we confirmed the close similarities between TB tumors cells and follicular MC progenitors evident by expression of GLI1 and its related downstream targets, i.e. KRT17 and SOX9, in both settings. Moreover, ectopic expression of GLI1 in NHEK induced SOX2 expression, one of the identified start point of MC differentiation¹⁵. Therefore, since activation of the SHH pathway has been demonstrated as a mandatory step for subsequent MC differentiation in murine hairy skin^{17,18}, it is likely that the same process is involved in MC differentiation in human skin as well as in TB tumors. While a mixture of cells with either MC progenitor phenotype or already differentiated MCs was observed in TB, almost all MCC tumor cells display a fully-differentiated MC phenotype. Consequently, we assessed if TA could contribute to the acquisition of an MC phenotype. Indeed, this hypothesis was supported by our observation that ectopic TA expression in NHEK led to induction of early MC markers while concomitant induction of SOX2, KRT8, and KRT20 were only achieved upon co-expression of TA and GLI1. Moreover, clusters of transformed cells with “small cell carcinoma morphology” arised from hair follicle cells upon ectopic TA expression. Therefore, combination of changes observed in NHEK and hair follicles strongly suggest that TA can induce acquisition of Merkel cell-like phenotype when expressed in epithelial progenitors. Accordingly, since Large T antigen extends ATOH1 half-life, ATOH1 stabilization by MCPyV oncoproteins might further contribute to the MC-like phenotype observed in MCC.

In hairy skin, MCs preferential locate in hair follicles as well as in touch dome structures initially referred as “Haarscheiben”^{50,51}. However, the filiation link between MCs and the surrounding epidermal cells was for a long time unclear, and an alternative neural crest origin was discussed^{52,53}. Engrafting embryonic human skin on immunocompromised mice, Moll. et al. first demonstrated that MCs derive from the epidermal component in mammals¹³. Accordingly, specific deletion of *Atoh1*, the main transcription factor driving MC

differentiation^{54,55}, in the epidermal compartment of transgenic mice resulted in complete MCs loss^{10,12}. Vice versa, ectopic expression of this factor in the epidermis resulted in increased MCs number^{14,16}. Of note, MC differentiation preferentially arises in specific epidermal progenitors located in the hair follicles and in touch domes in murine hairy skin^{21,56}. Indeed, under physiological conditions, the hair follicle is a privileged niche for MC differentiation. Hence, impairment of hair follicle development resulted in complete MC loss⁵⁷. Furthermore, Sox9-expressing cells in the embryonic murine hair follicle were identified as MC progenitors. For establishment of this population⁵⁸ and subsequent MC differentiation^{57,58} SHH signaling is critical. Similarly, SHH pathway has also been demonstrated in touch dome progenitor establishment in mice^{17,18}. These touch dome progenitors express KRT17^{19,59}, an intermediary filament normally restricted to the appendages⁶⁰, and are expected to be an alternative origin of MCs with abilities to generate both keratinocytes and MCs²¹.

While MC progenitors have been extensively characterized in mice, only few corresponding studies in humans are available¹⁹. In the present study, we describe MC hotspots in contact with dermal nerves. In these areas, GLI1-expressing keratinocytes surrounded MCs (either in hair follicles or touch dome structures). In line with previous reports identifying SOX9⁶¹ and KRT17⁶² as downstream targets of GLI1, we confirmed expression of these two markers upon GLI1-expression in NHEK and physiologically in GLI1-expressing MC progenitor cells. Of note, KRT17 expression is normally restricted to the companion layer of the outer root sheet in the hair follicle and absent in the interfollicular epidermis. We, however, observed positivity in the external infundibular cells in hair follicles enriched in MCs (**Figure 1C**). As described for other cell lineages^{63,64}, we demonstrated that ectopic expression of GLI1 led to a prominent induction of SOX2 in NHEK. Since SOX2 can drive ATOH1 expression and subsequent MC differentiation⁶⁵ by binding to *ATOH1* enhancer¹⁵ or *ATOH1* promoter⁶⁶ SOX2 induction appears as a potential mechanism by which GLI1 promotes ATOH1-driven MC development. Moreover, impaired ATOH1 degradation by SHH pathway activation has been previously reported in medulloblastoma⁴⁸ and might also contribute to MC differentiation in GLI1-expressing cells.

We wondered if similar MC differentiation mechanisms are present in TB tumors. In this regard, presence of scattered Merkel cells is a diagnostic criteria of TB^{28,30,31} is in line with their close similarities with MC progenitors of the hair follicle. The molecular determinants of such an MC differentiation process, however, are unknown. Interestingly, activation of SHH has been demonstrated in a set of 4 TB cases⁶⁷, and accordingly we could confirm nuclear GLI1 positivity and related downstream targets SOX9 and KRT17²⁸ expression in our TB cases. These observations suggest that GLI1 expression might contribute to the MC differentiation in such tumors. Of note, SHH pathway activation and subsequent GLI1 expression are not restricted to TB, but are also evidenced in skin tumors lacking MCs such as basal cell carcinoma⁶⁷. Hence, other factors are additionally necessary to drive MC differentiation.

Interestingly, we recently reported a MCPyV-positive MCC arising from a TB and consequently hypothesized that MCPyV integration and subsequent oncoprotein expression are able to induce acquisition of a Merkel cell-like phenotype in a GLI1-expressing epithelial cell. Indeed, TA expression in NHEK reduced cell size, triggered KRT8 protein expression and enhanced *KRT18* transcription level, while we did not observed expression of KRT20, a marker appearing latter during the MC differentiation process⁷.

Although, *Atoh1* alone is able to initiate MC differentiation during embryonic mice development, *Sox2* expression is required for *Krt20* expression⁷. Accordingly, in our cohort, the two MCC tumors lacking SOX2 expression were also KRT20 negative (data not shown). Hence, to test if the lack of KRT20 expression was due to a lack of SHH activation in NHEK, and subsequent lack of SOX2 expression, we co-expressed GLI1 and TA in these cells. This additional experiment led to the formation of a cell population characterized by a reduced size, expression of SOX2 and KRT8 and to a lesser extent KRT20 positivity. Since these observations suggested GLI1-expressing epithelial progenitors as a potential source of MCC, we tested this conclusion by ectopically expressing TA in hair follicles, a preferential niche for such progenitor population. While this experiment harbors several limitations, i.e. limited culture duration (restricted to 7 days), low transduction rate, restriction to the external part of the hair follicle and uncertainty which cell are transduced, we observed formation of presumably tumor cell clusters displaying “small cell carcinoma” morphology and partial expression of neuroendocrine markers. Therefore, altogether, these findings seem to indicate that TA are able to induce MC-like phenotype when expressed in epithelial progenitors.

Interestingly, the recently reported induction of ATOH1 upon Large T expression might explain these findings⁴⁷. Although we only detected slight, non-statistically significant increased *ATOH1* mRNA levels upon TA expression in NHEKs, we observed that ATOH1 degradation is impaired in presence of LT. Indeed, T antigens are known to hijack many cellular process⁶⁸, and stabilization of the LT by sT via inhibition of the ubiquitin ligase SCF^{Fbw7} has been proposed⁶⁹. In mice, phosphorylation of the Atoh1 serine residues S328, S334 and S339^{48,49} equivalent to the amino acids S331, S337, S342 in human, led to the ubiquitination of the protein by HUWE1 ubiquitin ligase and subsequent targeting to the proteasome. Accordingly, human ATOH1 lacking the respective phosphorylation sites harbored an extended half-life in our study. Notably, while LT impaired degradation of wild type ATOH1, it had no effect on mutant ATOH1. Hence, LT appears to affect the degradation process of ATOH1, either by interfering with the phosphorylation or ubiquitination step. Of note, wild spread ATOH1 expression on both mRNA and proteins levels have been confirmed in MCC tumors^{70,71}.

To conclude, recent demonstration that MCPyV-positive MCC can arise from TB, suggests GLI1-expressing epithelial progenitors of the hair follicle as a potential cell of origin of MCC. In the present study, we bring further arguments in favor of such hypothesis. After confirming GLI1 involvement in human MC progenitors establishment, our study identify GLI1 as a potential contributor to MC differentiation in TB tumor cells. Accordingly, the independent and combined abilities of GLI1 and TA to induce Merkel cell-like differentiation *in vitro* was demonstrated in NHEK and in hair follicles. In line with these observations, stabilization of ATOH1 by LT might also contribute to this process.

Acknowledgment:

We thank Dr JF Jégou and Dr J Vachtenheim for their help and assistance. In addition, we thank Daniel Sage (EPFL) for the color segmentation imageJ plugin.

References:

1. Lemos, B. D. *et al.* Pathologic nodal evaluation improves prognostic accuracy in Merkel cell carcinoma: analysis of 5823 cases as the basis of the first consensus staging system. *J. Am. Acad. Dermatol.* **63**, 751–761 (2010).
2. Feng, H., Shuda, M., Chang, Y. & Moore, P. S. Clonal integration of a polyomavirus in human Merkel cell carcinoma. *Science* **319**, 1096–1100 (2008).
3. Feng, H., Shuda, M., Chang, Y. & Moore, P. S. Clonal integration of a polyomavirus in human Merkel cell carcinoma. *Science* **319**, 1096–1100 (2008).
4. Ikeda, R. *et al.* Merkel cells transduce and encode tactile stimuli to drive A β -afferent impulses. *Cell* **157**, 664–675 (2014).
5. Chang, W. *et al.* Merkel disc is a serotonergic synapse in the epidermis for transmitting tactile signals in mammals. *Proc. Natl. Acad. Sci. U. S. A.* **113**, E5491–5500 (2016).
6. Laga, A. C. *et al.* Expression of the embryonic stem cell transcription factor SOX2 in human skin: relevance to melanocyte and merkel cell biology. *Am. J. Pathol.* **176**, 903–913 (2010).
7. Perdigoto, C. N., Bardot, E. S., Valdes, V. J., Santoriello, F. J. & Ezhkova, E. Embryonic maturation of epidermal Merkel cells is controlled by a redundant transcription factor network. *Dev. Camb. Engl.* **141**, 4690–4696 (2014).
8. Moll, R., Moll, I. & Franke, W. W. Identification of Merkel cells in human skin by specific cytokeratin antibodies: changes of cell density and distribution in fetal and adult plantar epidermis. *Differ. Res. Biol. Divers.* **28**, 136–154 (1984).
9. Moll, I., Paus, R. & Moll, R. Merkel cells in mouse skin: intermediate filament pattern, localization, and hair cycle-dependent density. *J. Invest. Dermatol.* **106**, 281–286 (1996).
10. Van Keymeulen, A. *et al.* Epidermal progenitors give rise to Merkel cells during embryonic development and adult homeostasis. *J. Cell Biol.* **187**, 91–100 (2009).
11. Halata, Z., Grim, M. & Bauman, K. I. Friedrich Sigmund Merkel and his ‘Merkel cell’, morphology, development, and physiology: review and new results. *Anat. Rec. A. Discov. Mol. Cell. Evol. Biol.* **271**, 225–239 (2003).
12. Morrison, K. M., Miesegaes, G. R., Lumpkin, E. A. & Maricich, S. M. Mammalian Merkel cells are descended from the epidermal lineage. *Dev. Biol.* **336**, 76–83 (2009).
13. Moll, I., Lane, A. T., Franke, W. W. & Moll, R. Intraepidermal formation of Merkel cells in xenografts of human fetal skin. *J. Invest. Dermatol.* **94**, 359–364 (1990).
14. Ostrowski, S. M., Wright, M. C., Bolock, A. M., Geng, X. & Maricich, S. M. Ectopic Atoh1 expression drives Merkel cell production in embryonic, postnatal and adult mouse epidermis. *Dev. Camb. Engl.* **142**, 2533–2544 (2015).
15. Bardot, E. S. *et al.* Polycomb subunits Ezh1 and Ezh2 regulate the Merkel cell differentiation program in skin stem cells. *EMBO J.* **32**, 1990–2000 (2013).
16. Verhaegen, M. E. *et al.* Merkel cell polyomavirus small T antigen initiates Merkel cell carcinoma-like tumor development in mice. *Cancer Res.* **77**, 3151–3157 (2017).
17. Xiao, Y. *et al.* Neural Hedgehog signaling maintains stem cell renewal in the sensory touch dome epithelium. *Proc. Natl. Acad. Sci. U. S. A.* **112**, 7195–7200 (2015).
18. Xiao, Y. *et al.* A Cascade of Wnt, Eda, and Shh Signaling Is Essential for Touch Dome Merkel Cell Development. *PLoS Genet.* **12**, e1006150 (2016).
19. Moll, I., Troyanovsky, S. M. & Moll, R. Special program of differentiation expressed in keratinocytes of human haarscheiben: an analysis of individual cytokeratin polypeptides. *J. Invest. Dermatol.* **100**, 69–76 (1993).
20. Nguyen, M. B. *et al.* FGF signalling controls the specification of hair placode-derived

- SOX9 positive progenitors to Merkel cells. *Nat. Commun.* **9**, 2333 (2018).
21. Woo, S.-H., Stumpfova, M., Jensen, U. B., Lumpkin, E. A. & Owens, D. M. Identification of epidermal progenitors for the Merkel cell lineage. *Dev. Camb. Engl.* **137**, 3965–3971 (2010).
 22. Peterson, S. C. *et al.* Basal cell carcinoma preferentially arises from stem cells within hair follicle and mechanosensory niches. *Cell Stem Cell* **16**, 400–412 (2015).
 23. Moll, I., Zieger, W. & Schmelz, M. Proliferative Merkel cells were not detected in human skin. *Arch. Dermatol. Res.* **288**, 184–187 (1996).
 24. Shuda, M. *et al.* Merkel Cell Polyomavirus Small T Antigen Induces Cancer and Embryonic Merkel Cell Proliferation in a Transgenic Mouse Model. *PloS One* **10**, e0142329 (2015).
 25. Tilling, T. & Moll, I. Which are the cells of origin in merkel cell carcinoma? *J. Skin Cancer* **2012**, 680410 (2012).
 26. Becker, J. C. & Zur Hausen, A. Cells of origin in skin cancer. *J. Invest. Dermatol.* **134**, 2491–2493 (2014).
 27. Visvader, J. E. Cells of origin in cancer. *Nature* **469**, 314–322 (2011).
 28. Kurzen, H., Esposito, L., Langbein, L. & Hartschuh, W. Cytokeratins as markers of follicular differentiation: an immunohistochemical study of trichoblastoma and basal cell carcinoma. *Am. J. Dermatopathol.* **23**, 501–509 (2001).
 29. Leblebici, C., Bambul Sığircı, B., Kelten Talu, C., Koca, S. B. & Huq, G. E. CD10, TDAG51, CK20, AR, INSM1, and Nestin Expression in the Differential Diagnosis of Trichoblastoma and Basal Cell Carcinoma. *Int. J. Surg. Pathol.* **27**, 19–27 (2019).
 30. McNiff, J. M., Eisen, R. N. & Glusac, E. J. Immunohistochemical comparison of cutaneous lymphadenoma, trichoblastoma, and basal cell carcinoma: support for classification of lymphadenoma as a variant of trichoblastoma. *J. Cutan. Pathol.* **26**, 119–124 (1999).
 31. Collina, G., Eusebi, V., Capella, C. & Rosai, J. Merkel cell differentiation in trichoblastoma. *Virchows Arch. Int. J. Pathol.* **433**, 291–296 (1998).
 32. Kervarrec, T. *et al.* Polyomavirus-positive Merkel cell carcinoma derived from a trichoblastoma suggests an epithelial origin of this Merkel cell carcinoma. *accepted in J invest Dermatol* (2019).
 33. Kervarrec, T. *et al.* Diagnostic accuracy of a panel of immunohistochemical and molecular markers to distinguish Merkel cell carcinoma from other neuroendocrine carcinomas. *Mod. Pathol. Off. J. U. S. Can. Acad. Pathol. Inc* **32**, 499–510 (2019).
 34. Gardair, C. *et al.* Somatostatin Receptors 2A and 5 Are Expressed in Merkel Cell Carcinoma with No Association with Disease Severity. *Neuroendocrinology* **101**, 223–235 (2015).
 35. Kervarrec, T. *et al.* Merkel cell carcinomas infiltrated with CD33+ myeloid cells and CD8+ T cells are associated with improved outcome. *J. Am. Acad. Dermatol.* (2017). doi:10.1016/j.jaad.2017.12.029
 36. Kervarrec, T. *et al.* Detection of the Merkel cell polyomavirus in the neuroendocrine component of combined Merkel cell carcinoma. *Virchows Arch. Int. J. Pathol.* (2018). doi:10.1007/s00428-018-2342-0
 37. Boniface, K. *et al.* IL-22 inhibits epidermal differentiation and induces proinflammatory gene expression and migration of human keratinocytes. *J. Immunol. Baltim. Md 1950* **174**, 3695–3702 (2005).
 38. Couderc, E. *et al.* Interleukin-17A-induced production of acute serum amyloid A by keratinocytes contributes to psoriasis pathogenesis. *PloS One* **12**, e0181486 (2017).
 39. Langan, E. A., Philpott, M. P., Kloepper, J. E. & Paus, R. Human hair follicle organ culture: theory, application and perspectives. *Exp. Dermatol.* **24**, 903–911 (2015).
 40. Chéret, J. *et al.* Olfactory receptor OR2AT4 regulates human hair growth. *Nat.*

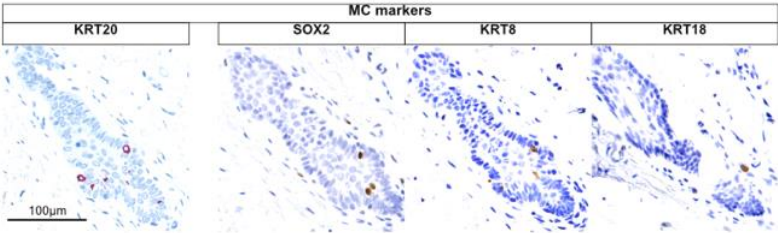
Commun. **9**, 3624 (2018).

41. Schrama, D. *et al.* Characterization of six Merkel cell polyomavirus-positive Merkel cell carcinoma cell lines: Integration pattern suggest that large T antigen truncating events occur before or during integration. *Int. J. Cancer* (2019). doi:10.1002/ijc.32280
42. Vlčková, K. *et al.* Survivin, a novel target of the Hedgehog/GLI signaling pathway in human tumor cells. *Cell Death Dis.* **7**, e2048 (2016).
43. Houben, R. *et al.* An intact retinoblastoma protein-binding site in Merkel cell polyomavirus large T antigen is required for promoting growth of Merkel cell carcinoma cells. *Int. J. Cancer* **130**, 847–856 (2012).
44. Houben, R. *et al.* Characterization of functional domains in the Merkel cell polyoma virus Large T antigen. *Int. J. Cancer* **136**, E290-300 (2015).
45. Angermeyer, S., Hesbacher, S., Becker, J. C., Schrama, D. & Houben, R. Merkel cell polyomavirus-positive Merkel cell carcinoma cells do not require expression of the viral small T antigen. *J. Invest. Dermatol.* **133**, 2059–2064 (2013).
46. Kervarrec, T. *et al.* Morphologic and immunophenotypical features distinguishing Merkel cell polyomavirus-positive and -negative Merkel cell carcinoma. *Modern Pathology: An Official Journal of the United States and Canadian Academy of Pathology, Inc* (2019).
47. Fan, K. *et al.* MCPyV Large T antigen induced atonal homolog 1 (ATOH1) is a lineage-dependency oncogene in Merkel cell carcinoma. *J. Invest. Dermatol.* (2019). doi:10.1016/j.jid.2019.06.135
48. Forget, A. *et al.* Shh signaling protects Atoh1 from degradation mediated by the E3 ubiquitin ligase Huwe1 in neural precursors. *Dev. Cell* **29**, 649–661 (2014).
49. Cheng, Y.-F., Tong, M. & Edge, A. S. B. Destabilization of Atoh1 by E3 Ubiquitin Ligase Huwe1 and Casein Kinase 1 Is Essential for Normal Sensory Hair Cell Development. *J. Biol. Chem.* **291**, 21096–21109 (2016).
50. Nurse, C. A., Mearow, K. M., Holmes, M., Visheau, B. & Diamond, J. Merkel cell distribution in the epidermis as determined by quinacrine fluorescence. *Cell Tissue Res.* **228**, 511–524 (1983).
51. Pinkus, F. XIX. Ueber einen bisher unbekanntem Nebenapparat am Haarsystem des Menschen: Haarscheiben. *Dermatology* **9**, 465–469 (1902).
52. Grim, M. & Halata, Z. Developmental origin of avian Merkel cells. *Anat. Embryol. (Berl.)* **202**, 401–410 (2000).
53. Halata, Z., Grim, M. & Christ, B. Origin of spinal cord meninges, sheaths of peripheral nerves, and cutaneous receptors including Merkel cells. An experimental and ultrastructural study with avian chimeras. *Anat. Embryol. (Berl.)* **182**, 529–537 (1990).
54. Maricich, S. M. *et al.* Merkel cells are essential for light-touch responses. *Science* **324**, 1580–1582 (2009).
55. Ben-Arie, N. *et al.* Functional conservation of atonal and Math1 in the CNS and PNS. *Dev. Camb. Engl.* **127**, 1039–1048 (2000).
56. Vielkind, U., Sebzda, M. K., Gibson, I. R. & Hardy, M. H. Dynamics of Merkel cell patterns in developing hair follicles in the dorsal skin of mice, demonstrated by a monoclonal antibody to mouse keratin 8. *Acta Anat. (Basel)* **152**, 93–109 (1995).
57. Perdigoto, C. N. *et al.* Polycomb-Mediated Repression and Sonic Hedgehog Signaling Interact to Regulate Merkel Cell Specification during Skin Development. *PLoS Genet.* **12**, e1006151 (2016).
58. Nguyen, M. B. *et al.* FGF signalling controls the specification of hair placode-derived SOX9 positive progenitors to Merkel cells. *Nat. Commun.* **9**, 2333 (2018).
59. Doucet, Y. S., Woo, S.-H., Ruiz, M. E. & Owens, D. M. The Touch Dome Defines an Epidermal Niche Specialized for Mechanosensory Signaling. *Cell Rep.* **3**, 1759–1765 (2013).
60. Troyanovsky, S. M., Guelstein, V. I., Tchipysheva, T. A., Krutovskikh, V. A. &

- Bannikov, G. A. Patterns of expression of keratin 17 in human epithelia: dependency on cell position. *J. Cell Sci.* **93** (Pt 3), 419–426 (1989).
61. Vidal, V. P. I., Ortonne, N. & Schedl, A. SOX9 expression is a general marker of basal cell carcinoma and adnexal-related neoplasms. *J. Cutan. Pathol.* **35**, 373–379 (2008).
 62. Mikami, Y. *et al.* GLI-mediated Keratin 17 expression promotes tumor cell growth through the anti-apoptotic function in oral squamous cell carcinomas. *J. Cancer Res. Clin. Oncol.* **143**, 1381–1393 (2017).
 63. Jia, Y. *et al.* The role of GLI-SOX2 signaling axis for gemcitabine resistance in pancreatic cancer. *Oncogene* **38**, 1764–1777 (2019).
 64. Santini, R. *et al.* SOX2 regulates self-renewal and tumorigenicity of human melanoma-initiating cells. *Oncogene* **33**, 4697–4708 (2014).
 65. Lesko, M. H., Driskell, R. R., Kretzschmar, K., Goldie, S. J. & Watt, F. M. Sox2 modulates the function of two distinct cell lineages in mouse skin. *Dev. Biol.* **382**, 15–26 (2013).
 66. Harold, A. *et al.* Conversion of Sox2-dependent Merkel cell carcinoma to a differentiated neuron-like phenotype by T antigen inhibition. *Proc. Natl. Acad. Sci. U. S. A.* (2019). doi:10.1073/pnas.1907154116
 67. Tanese, K., Emoto, K., Kubota, N., Fukuma, M. & Sakamoto, M. Immunohistochemical visualization of the signature of activated Hedgehog signaling pathway in cutaneous epithelial tumors. *J. Dermatol.* **45**, 1181–1186 (2018).
 68. Starrett, G. J. *et al.* Merkel Cell Polyomavirus Exhibits Dominant Control of the Tumor Genome and Transcriptome in Virus-Associated Merkel Cell Carcinoma. *mBio* **8**, (2017).
 69. Kwun, H. J. *et al.* Merkel cell polyomavirus small T antigen controls viral replication and oncoprotein expression by targeting the cellular ubiquitin ligase SCFFbw7. *Cell Host Microbe* **14**, 125–135 (2013).
 70. Kervarrec, T. *et al.* Diagnostic accuracy of a panel of immunohistochemical and molecular markers to distinguish Merkel cell carcinoma from other neuroendocrine carcinomas. *Mod. Pathol. Off. J. U. S. Can. Acad. Pathol. Inc* (2018). doi:10.1038/s41379-018-0155-y
 71. Gambichler, T. *et al.* Prognostic relevance of high atonal homolog-1 expression in Merkel cell carcinoma. *J. Cancer Res. Clin. Oncol.* **143**, 43–49 (2017).
 72. Moll, I. Merkel cell distribution in human hair follicles of the fetal and adult scalp. *Cell Tissue Res.* **277**, 131–138 (1994).

Figures and Tables:

A



B

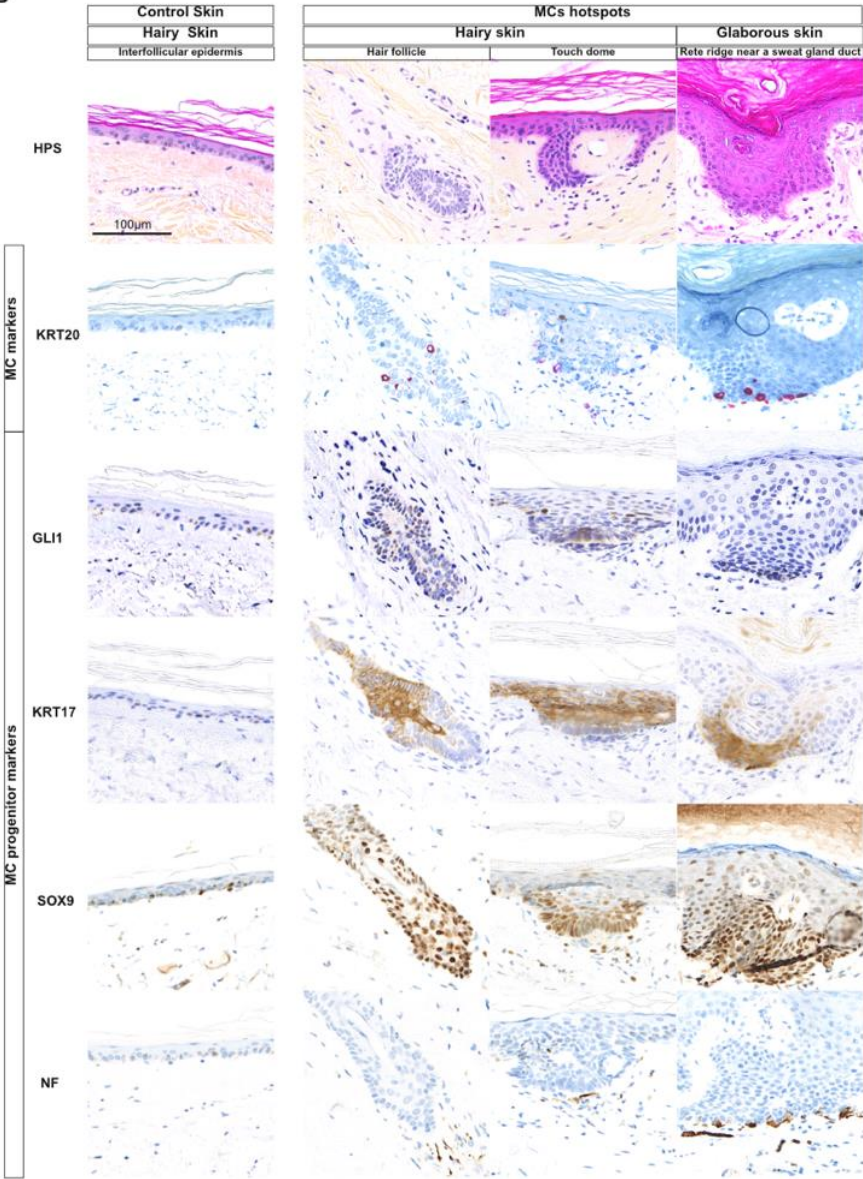


Figure 1. (continued).

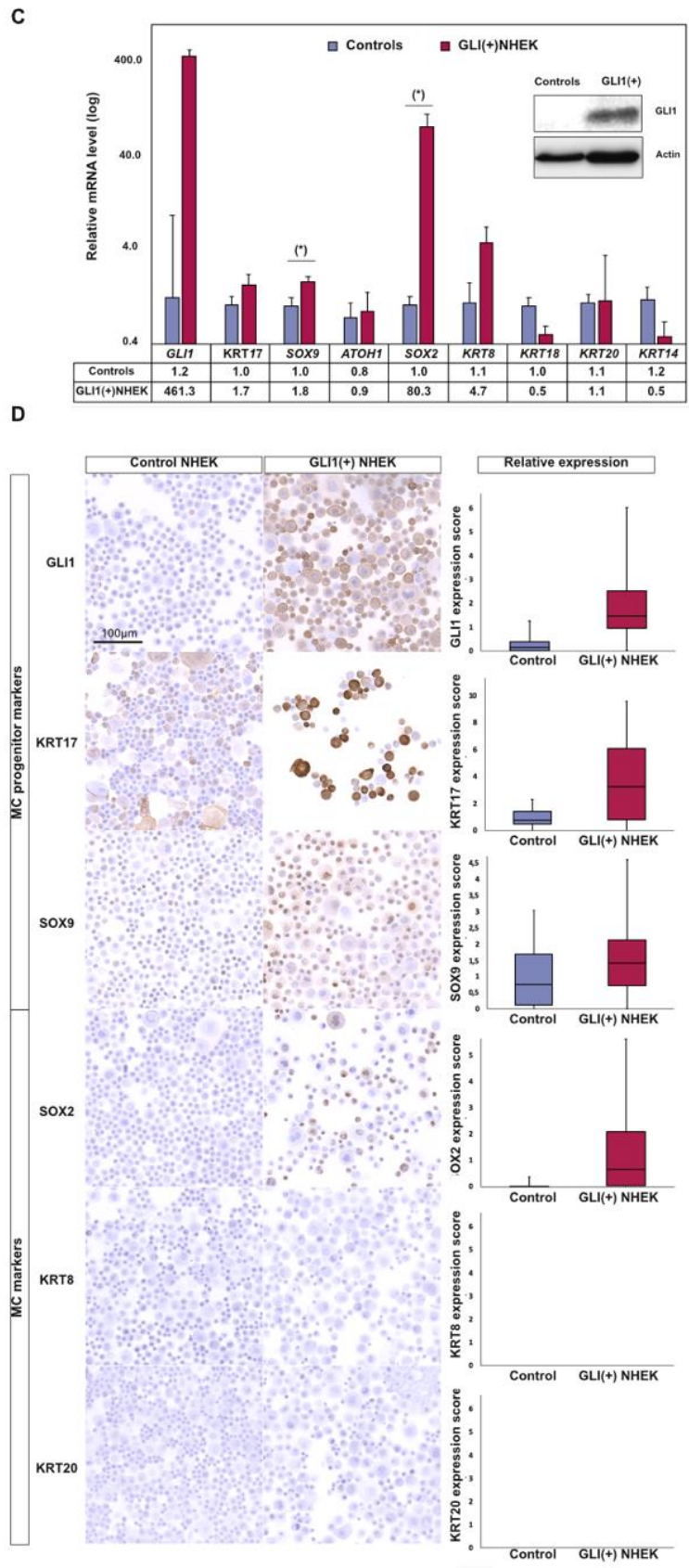


Figure 1. (See legends below).

Figure 1. Merkel cell lineage in human skin. **A:** Detection of Merkel cells in human. KRT20 staining was used to identify MCs, but other MC markers like SOX2, KRT8 and 18 were also expressed by these cells (bar=100 μ m). Merged analysis is presented in supplementary Figure 1B. **B:** Characterization of the MC progenitors in human: three Merkel cell hotspots and control interfollicular epidermis are depicted (bar=100 μ m). Immunohistochemical staining reveals KRT17 and SOX9 expression in the epidermal cells surrounding differentiated MC suggesting that these cells are MC progenitors. Moreover, detection of GLI1 was only achieved in hairy skin. Of note, dermal nerves were observed in contact with the MCs. **C-D: Impact of GLI1 expression on Normal human epidermal keratinocytes.** **C:** relative mRNA expression of the Merkel Cell lineage markers upon ectopic GLI1 expression (results are median +/-SEM)(*p value < 0.05, paired t test). Expression of GLI1 protein in transduced Normal human epidermal keratinocytes (NHEK) was confirmed by immunoblot as shown in the inset. **D:** Immunohistochemical assessment of progenitors (KRT17, SOX9) and MC (SOX2, KRT8 and KRT20) marker expression levels in GLI1-expressing NHEK and controls. Relative protein expression quantification was performed on at least 1000 cell /condition using ImageJ software. Horizontal line indicates the median, box edges the quantiles and whiskers 1st and 99th percentiles. Results are representative of two independent experiments (immunostaining and immunoblot repetitions are shown in **Supplementary Figure 2**).

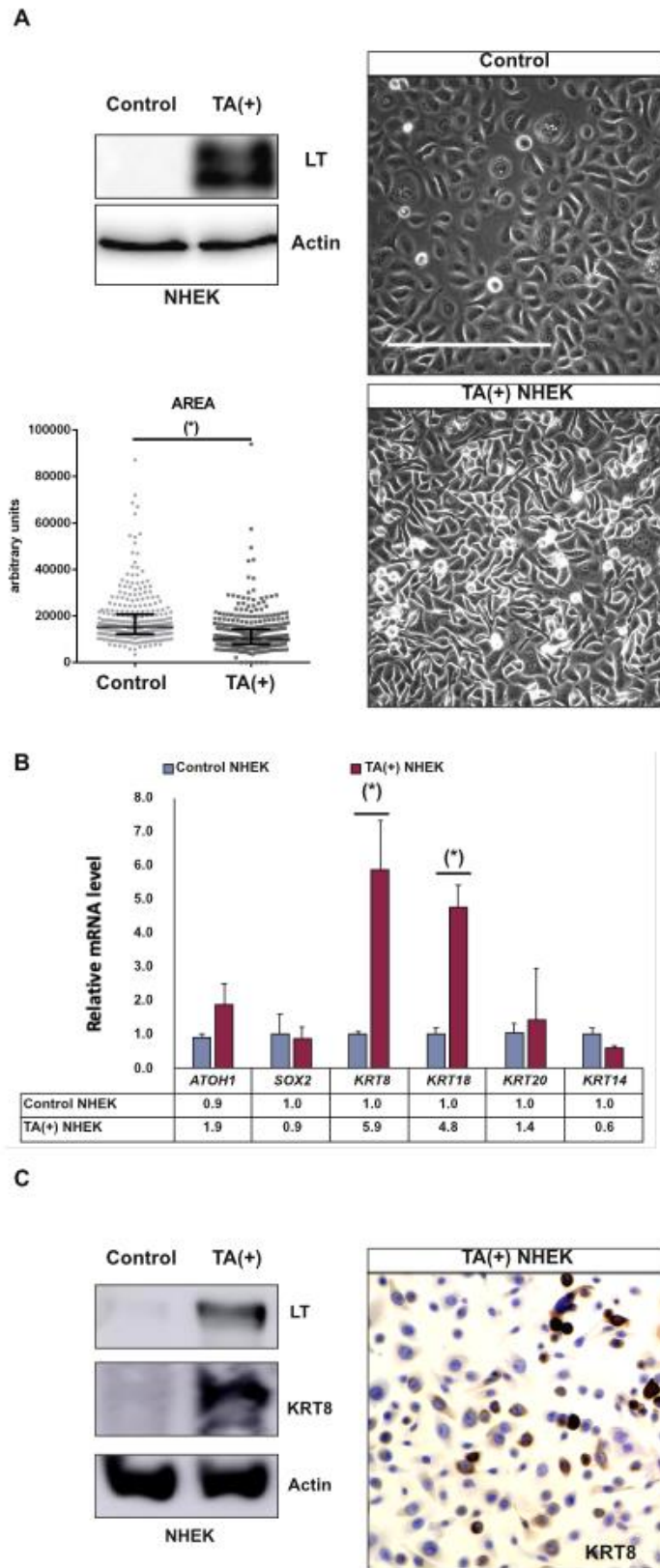


Figure 2. (continued)

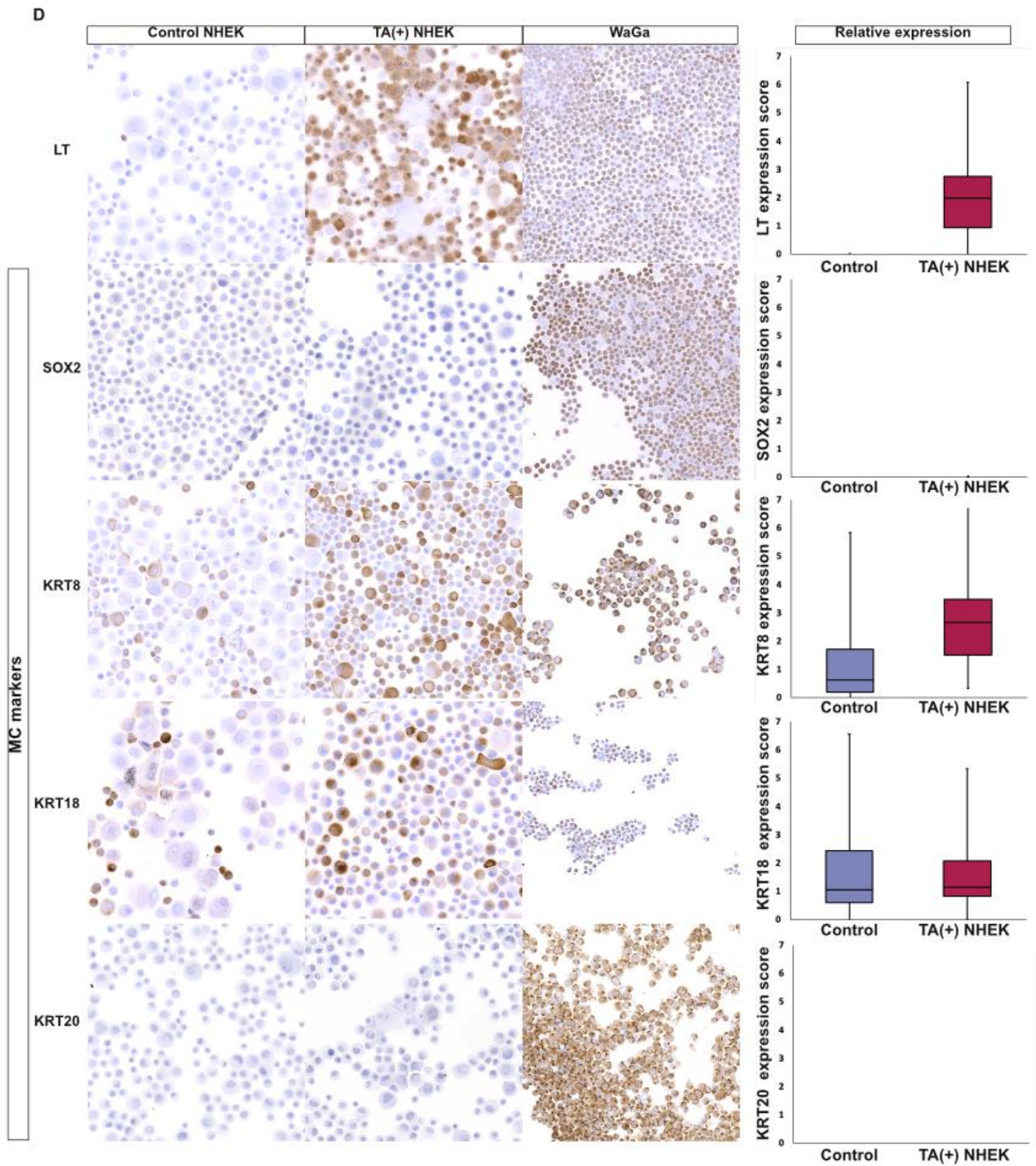


Figure 2. (See legends below).

Figure 2. Impact of T antigen expression on Normal human epidermal keratinocytes.

A: Ectopic expression of T antigens (TA) was associated with reduced cell size in Normal human epidermal keratinocytes (NHEK). After antibiotic selection, immunoblot analysis confirmed truncated Large T expression in transduced NHEK. Under microscopic examination, such cells harbored reduced cytoplasmic size compared to the controls which was evaluated using imageJ software (* p value < 0.05, Mann-Whitney U test). **B:** Relative mRNA levels of the Merkel cell differentiation markers (* p value < 0.05, paired t test), **C:** Ectopic TA expression in NHEK triggers KRT8 expression as revealed by immunoblot. Furthermore, in accordance to the previous observations, KRT8 immunocytochemical staining on adherent cells revealed that KRT8 expression is restricted to a population of small round cells. In addition, some “dot like” expression pattern was observed. **D.** Immunohistochemical assessment of Merkel cell markers (SOX2, KRT8, KRT18 and KRT20) expression levels in TA-expressing NHEK, control NHEK and WaGa MCC cell line. Relative protein expression quantification was performed on at least 1000 cell /condition using ImageJ software. Horizontal line indicated the median, box edges the quantiles and whiskers 1st and 99th percentiles. These results were confirmed in two independent experiments as shown in **Supplementary Figure 2.**

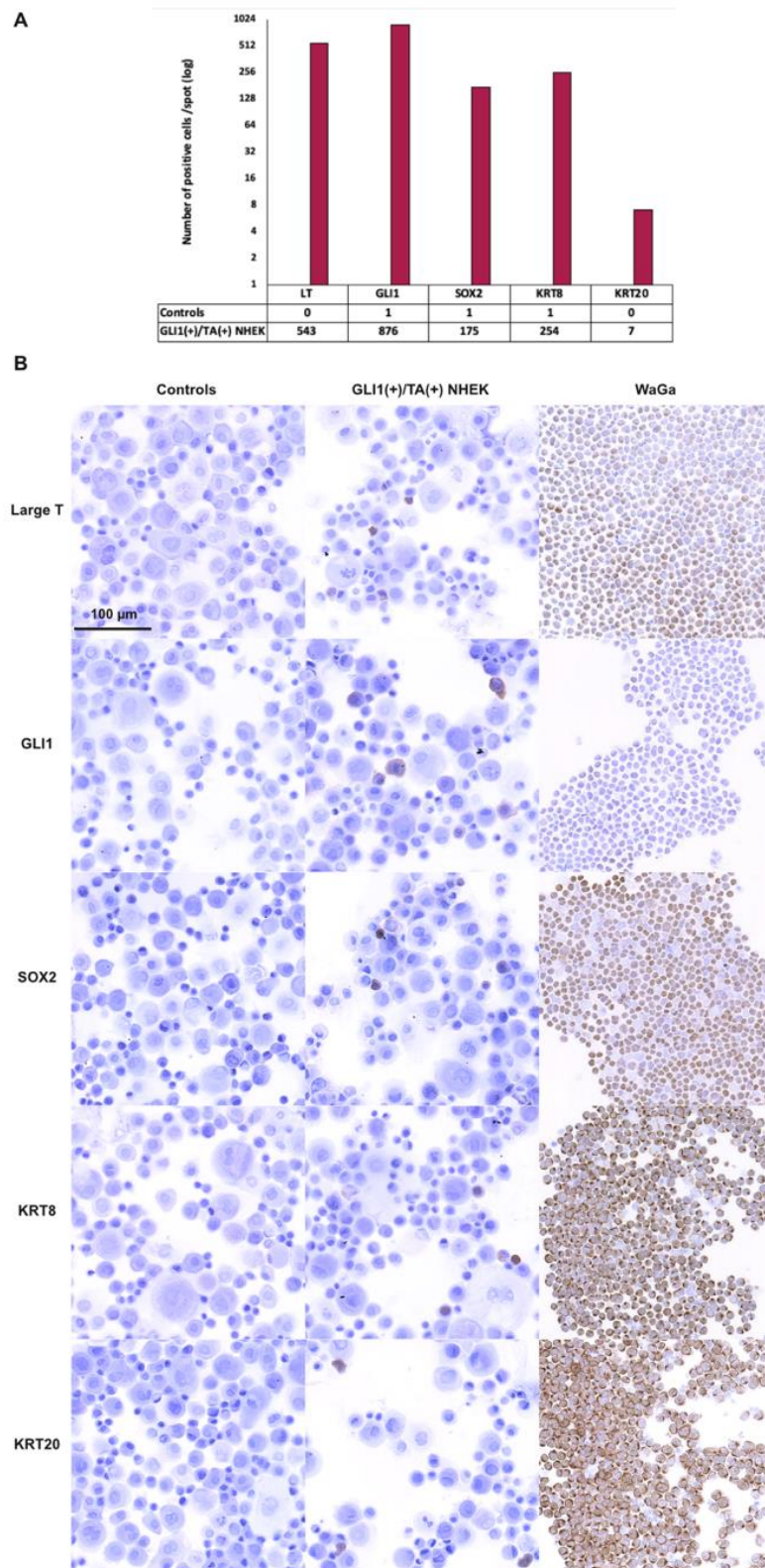


Figure 3. Immunohistochemical assessment of Merkel cell marker (SOX2, KRT8 and KRT20) expression in GLI1/T antigen-expressing Normal human epidermal keratinocytes and controls. After transduction and subsequent antibiotic selection, Normal human epidermal keratinocytes (NHEK) were spotted on slides ($2 \cdot 10^5$ cells / condition) and immunostained. **A.** Frequency of cells expressing the Merkel cell markers (cell number /spot) in GLI1/ T Antigens (TA)-expressing NHEK and controls. **B.** Representative illustration of SOX2, KRT8, KRT18 and KRT20 expression in GLI1/TA-expressing NHEK, control NHEK and the MCC cell line WaGa.

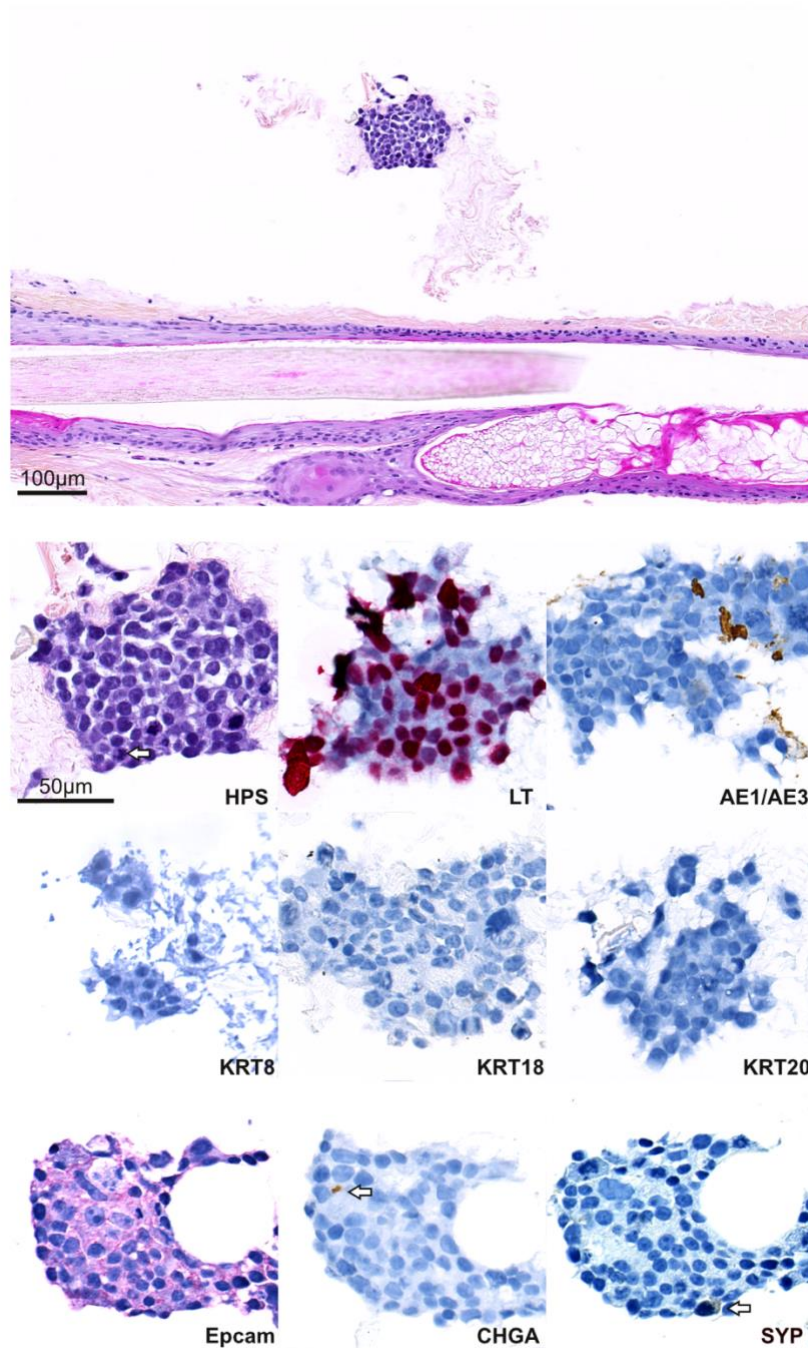


Figure 4. T Antigen-transduction in hair follicles led to the formation of transformed cell clusters displaying small cell carcinoma features. Microscopic examination (Hematein phloxin saffran staining (HPS)) of the T Antigen (TA)-transduced hair follicle revealed the presence of clusters of transformed cells in the connective tissue surrounding the hair follicle (bar=100 µm). Higher magnification revealed a cluster of cells with high nucleocytoplasmic ratio, scant cytoplasm and hyperchromatic nuclei (bar=50 µm). Formation of clusters, and detection of several mitotic figures (white arrows) suggest an oncogenic transformation of these cells. Immunohistochemical stainings confirmed large T (LT) expression by these clusters. Moreover, TA-expressing cells in the clusters demonstrated a partial loss of expression of the keratins when assessed by pancyokeratins detection (AE1/AE1) while EPCAM expression is preserved. Accordingly, no positivity for the keratins (KRT) 8, 18 and 20 was observed. By contrast, in a limited number of cells, expression of neuroendocrine markers chromogranin A: CHGA and synaptophysine (SYP) was detected (white arrow).

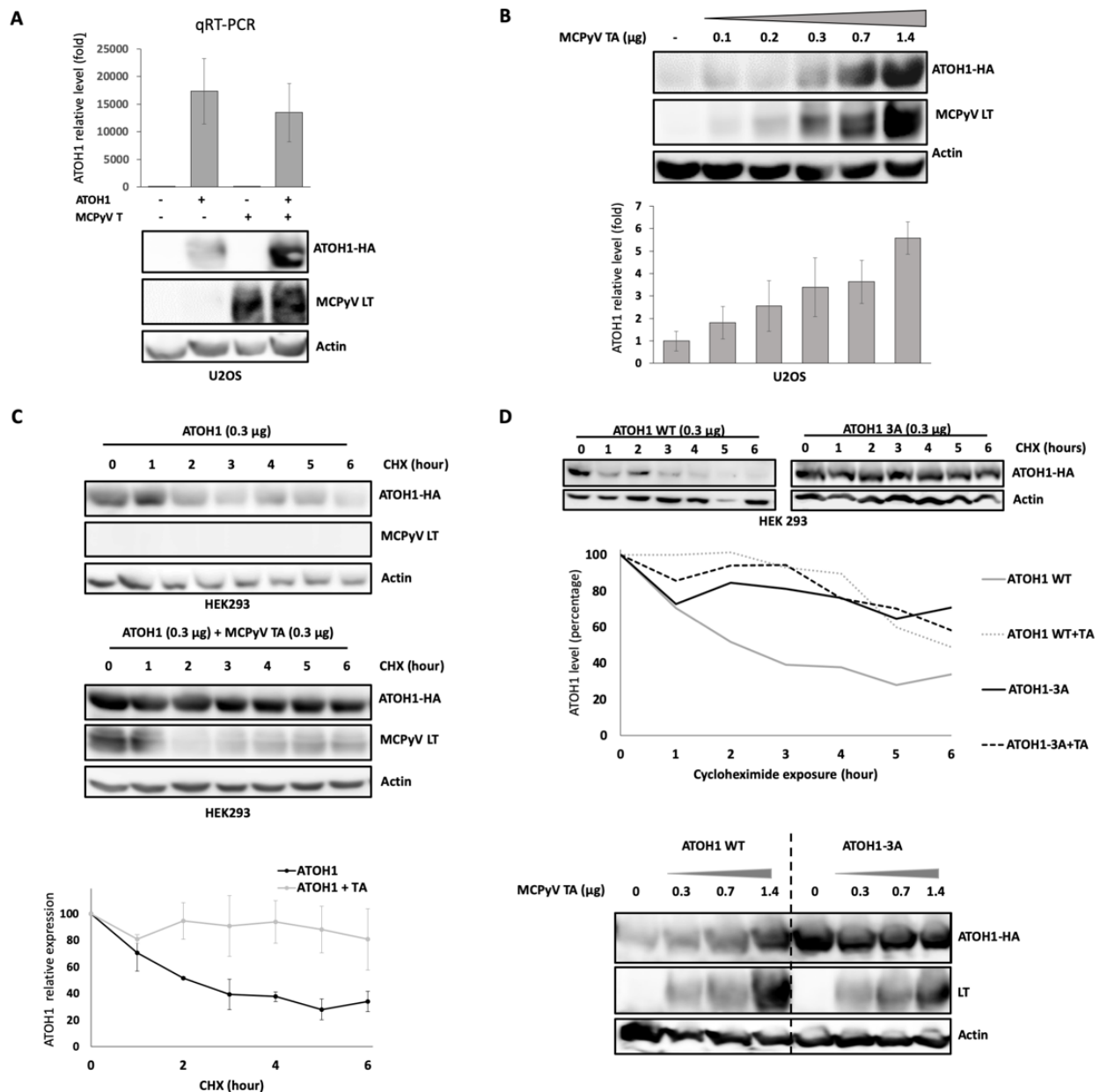


Figure 5. Increased ATOH1 levels upon T Antigen co-expression. **A-B:** Expression of T Antigens (TA) led to ATOH1 protein accumulation in U2OS. **A:** Impact of TA on ATOH1 expression on both RNA and protein levels. No induction of *ATOH1* transcription was observed in presence of TA when evaluated by real time PCR (three independent experiments, results are expressed as median \pm SEM). On protein level, however, immunoblot revealed ATOH1-HA accumulation in presence of TA. **B:** Ectopic expression of TA resulted in gradual accumulation of ATOH1-HA protein. U2OS cells were transfected with constant amount of ATOH1-HA construct (0.3 μ g) and increased amount of TA (0-1.4 μ g). Quantification of ATOH1-HA protein expression was performed using Image J Software (results are expressed as median \pm SEM on three independent experiments). **C:** Evaluation of ATOH1 half-life in absence or presence of T antigens. 24 hours after transfection, HEK293 cells were exposed to cycloheximide (CHX) for variable duration (0-6 h), and ATOH1-HA expression was then evaluated using immunoblot and quantified via Image J Software (results of three independent experiments are depicted as median \pm SEM). **D:** Impact of TA on ATOH1-HA wild type and ATOH1-HA-3A expression. Half-life of ATOH1 wild type and 3A-mutant proteins were

evaluated in absence or presence of T antigens using cycloheximide (CHX) as previously described. These experiments confirmed that TA increases ATOH1 wild type half-life whereas no effect was observed for the already stabilized ATOH1-3A mutant lacking the phosphorylation sites S331, S337, S342. Indeed, co-transfection of ATOH1-HA-3A even with increasing amounts of TA did not affect protein expression level.

Table 1. Expression of Merkel cell progenitor markers in Trichoblastoma and Merkel cell carcinoma tumors.

MC progenitors markers	TB (n=8)	MCC (n=103)
GLI1		
Negative	1 (13%)	60 (67%)
Positive	7 (87%)	29 (33%)
Unavailable data	0	14
KRT17		
Negative	0	94 (100%)
Positive	8 (100%)	0
Unavailable data	0	9
SOX9		
Negative	0	7 (8%)
Dot like	0	59 (64%)
Patchy	0	26 (28%)
Diffuse	8 (100%)	0
Unavailable data	0	11
MC markers	TB	MCC
SOX2		
Negative	1 (17%)	2 (2%)
Positive	5 (83%)	94 (98%)
Unavailable data	2	7
KRT20		
Negative	0	8
Diffuse	8 (100%)	2
Mixed	0	66
Dot-like pattern	0	19
Unavailable data	0	8

KRT: keratin; GLI1: GLI family zinc finger 1, MC: Merkel cell, MCC: Merkel cell carcinoma, SOX2: SRY-box 2, SOX9 : SRY-box 9, TB: Trichoblastoma. Representative illustrations of SOX9 expression patterns are available in supplementary Figure 3. Results are expressed in numbers and percentage of the interpretable cases

Supplements.

Supplementary Method 1. Antibodies used for Immunohistochemistry.

Supplementary Method 2. Primer sequences.

Supplementary Table 1. MCs density and location depending of the anatomic site.

Supplementary Table 2. Expression of GLI1 and SOX9 according to the Merkel cell Polyomavirus status in Merkel cell carcinoma tumors.

Supplementary Figure 1. Further characterization of Merkel cells and related progenitors in human.

Supplementary Figure 2. Further characterization of native and transduced normal human epidermal keratinocytes.

Supplementary Figure 3. Expression of the Merkel cell progenitor markers in tumors.

Supplementary Figure 4. Further characterization of KRT8 and KRT20 expression in GLI(+)/T Antigens (TA)(+) adherent and non adherent Normal human epidermal keratinocytes.

Supplementary Figure 5. Impact of ectopic expression of T antigens in Human Hair follicles.

Supplementary Figure 6. Further characterization of factors involved in ATOH1 stabilization.

Supplementary Method 1. Antibodies used for Immunohistochemistry.

antigen	clone	company	dilution
Large T	CM2B4	Santa Cruz	1/50
KRT8	M20	Santa Cruz	1/50
KRT14	SP53	Dako	pre-diluted
KRT17	Ks17.E3	Santa Cruz	1/200
KRT18	DC-10	Santa Cruz	1/100
KRT20	Ks20.8	Dako	1/100
GLI1	C68H3	Ozyme	1/200
Neurofilament	2F11	Dako	Pre-diluted
SOX2	EPR3131	Abcam	1/50
SOX9	AB5535	Merck	1/1000

KRT: keratin; GLI1: GLI family zinc finger 1, SOX2: SRY-box 2, SOX9 : SRY-box 9

Supplementary Method 2. Primers used.

Primename indicting gene	sequence
ATOH1 fw	ACTTGCCTCATCCGAGTCAC
ATOH1 rv	GCAGGAGGAAAACAGCAAAA
GLi1 fw	CCTTCAGCAATGCCAGTG
GLi1 rv	GCTTACATACATACGGCTTCTC
KRT8 fw	TGGAGCAGCAGAACAAGATG
KRT8 rv	CCGCCTAAGGTTGTTGATGT
KRT14 fw	AGAGGACGCCACCTTTC
KRT14 rv	TTAGTTCTGGTGCGCAG
KRT17 fw	CCCACTTGGTGGCCTATAAA
KRT17 rv	GTCATCAGGCAAGGAAGCAT
KRT18 fw	TAGATGCCCCCAAATCTCAG
KRT18 rv	CACTGTGGTGCTCTCCTCAA
KRT20 fw	GGACGACACCCAGCGTTTAT
KRT20 rv	CGCTCCCATAGTTCACCGTG
RPLP0 fw	CCATCAGCACCACAGCCTTC
RPLP0 rv	GGCGACCTGGAAGTCCAAC
SOX2 fw	GCTTAGCCTCGTCGATGAAC
SOX2 rv	AACCCCAAGATGCACAAC
SOX9 fw	GGAGATGAAATCTGTTCTGGGAATG
SOX9 rv	TTGAAGGTTAACTGCTGGTGTCTG

ATOH1: Atonal homolog 1; KRT: keratin; GLI1: GLI family zinc finger 1; RPLP0: ribosomal protein lateral stalk subunit P0; SOX2: SRY-box 2, SOX9 : SRY-box 9.

Supplementary Table 1. Merkel cell distribution according to anatomic site.

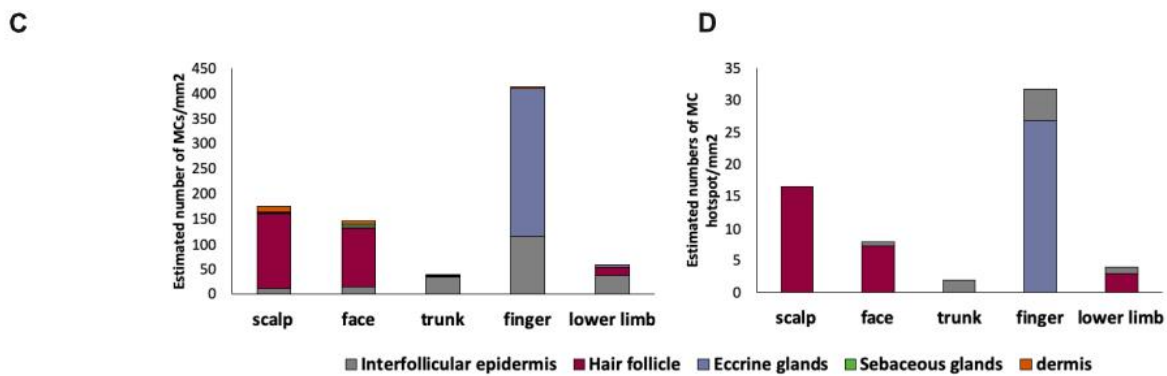
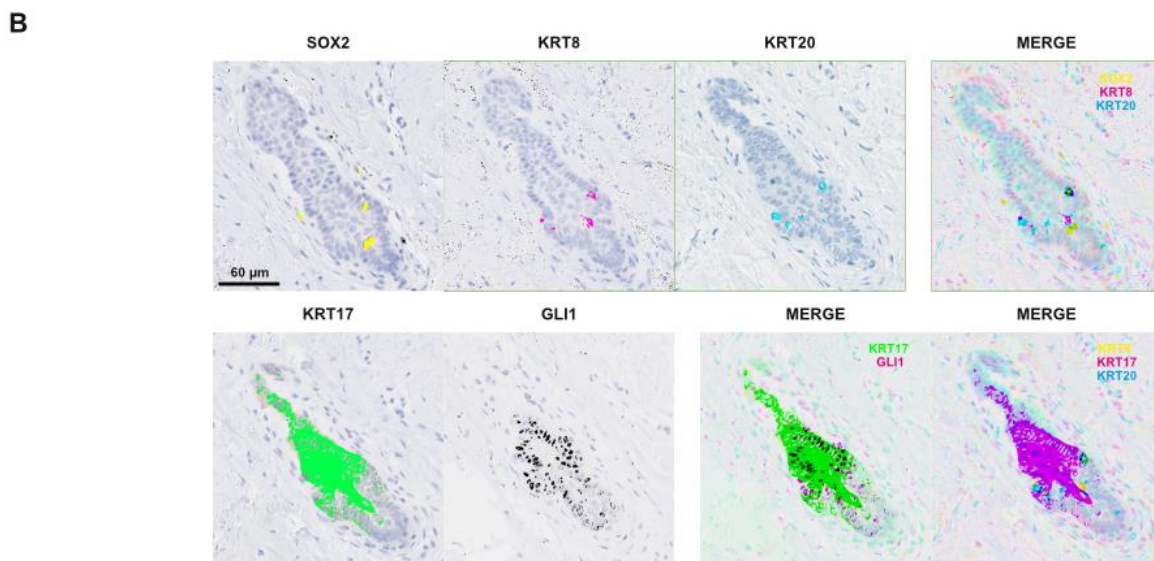
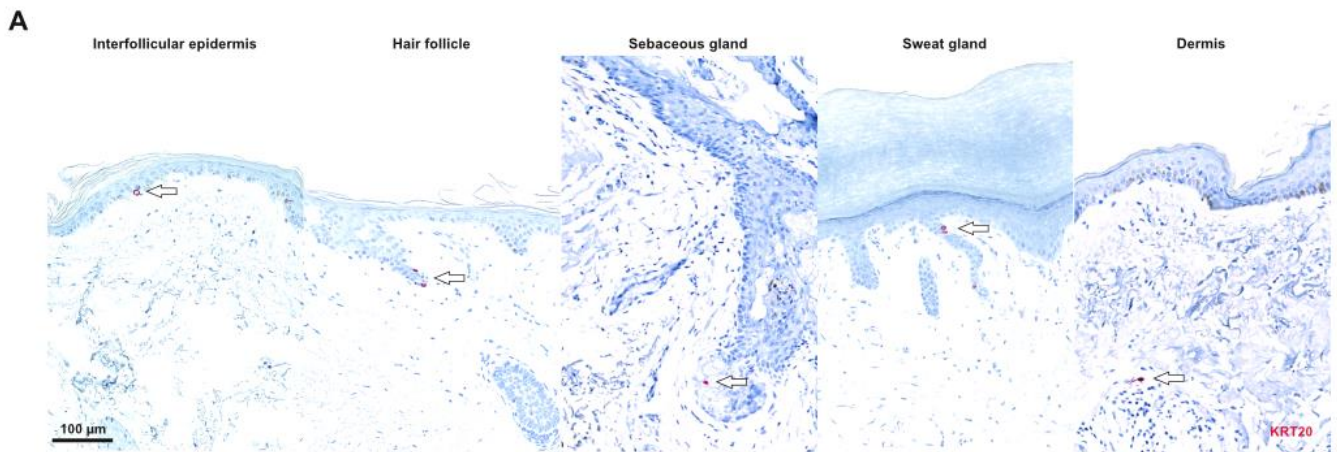
Subject	Anatomic site	MCs counts (50 sections)	Estimated MC density (nb/mm ²)	MCs hotspot count	Estimated MCs hotspot density (nb/mm ²)
N°1	Scalp	133	263	14	28
	Face	40	79	2	4
	Trunk	36	71	2	4
	Finger	146	289	11	22
	Legs	54	106	4	8
N°2	Scalp	94	186	10	20
	Face	62	122	1	2
	Trunk	7	14	0	0
	Finger	272	538	23	46
	Legs	12	23	0	0
N°3	Scalp	39	77	3	6
	Face	120	237	9	18
	Trunk	on going	on going	on going	on going
	Finger	on going	on going	on going	on going
	Legs	on going	on going	on going	on going

MC: Merkel cell, nb: number

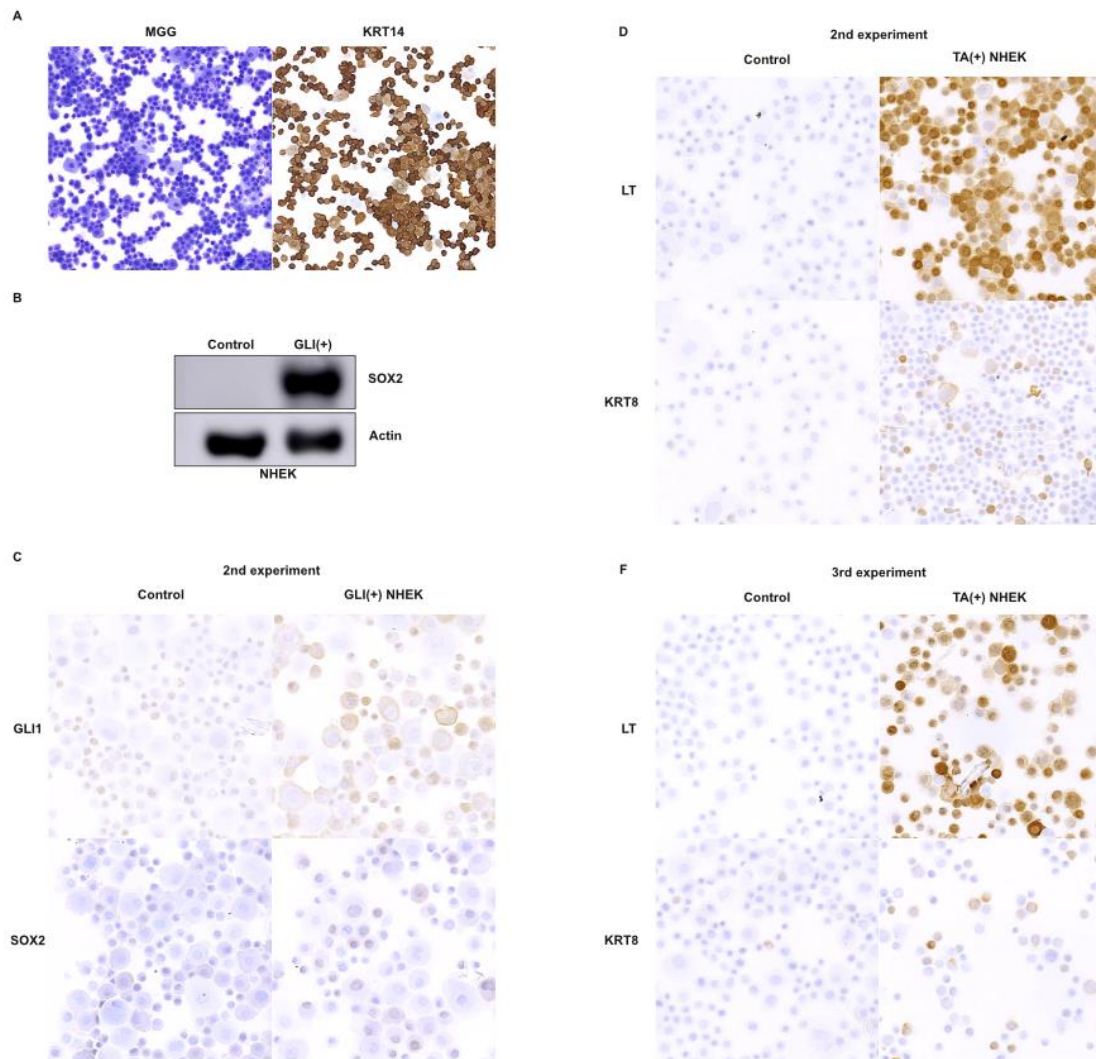
Supplementary Table 2. Expression of GLI1 and SOX9 according to the Merkel cell polyomavirus status in Merkel cell carcinoma tumors.

	MCPyV(-) MCC	MCPyV(+) MCC	Unavailable data	p*
GLI1				
Negative (n=60)	10 (48%)	50 (76%)	0	0.028
Positive (N=29)	11 (52%)	16 (24%)	2	
Unavailable data	1	12	1	
SOX9				
Negative	1 (5%)	6 (9%)	0	<1.10 ⁻⁹
Dot like	3 (14%)	56 (81%)	2	
Patchy	17 (81%)	7 (10%)	0	
Unavailable data	1	10	1	

GLI1: GLI family zinc finger 1, MCC: Merkel cell carcinoma, MCPyV: Merkel cell Polyomavirus, SOX9 : SRY-box 9, * variables were compared by Fisher's tests, and p values < 0.05 were considered as significant.



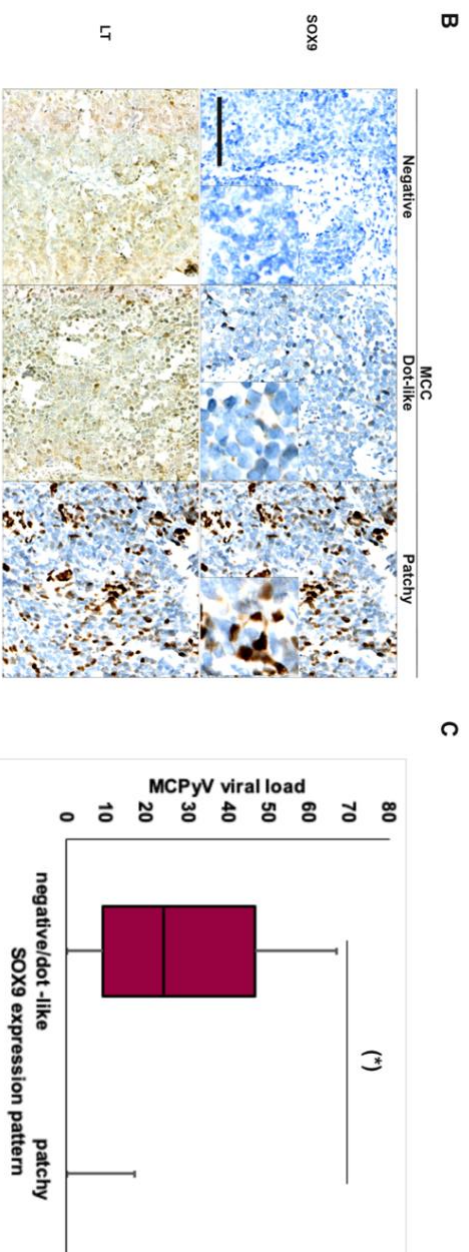
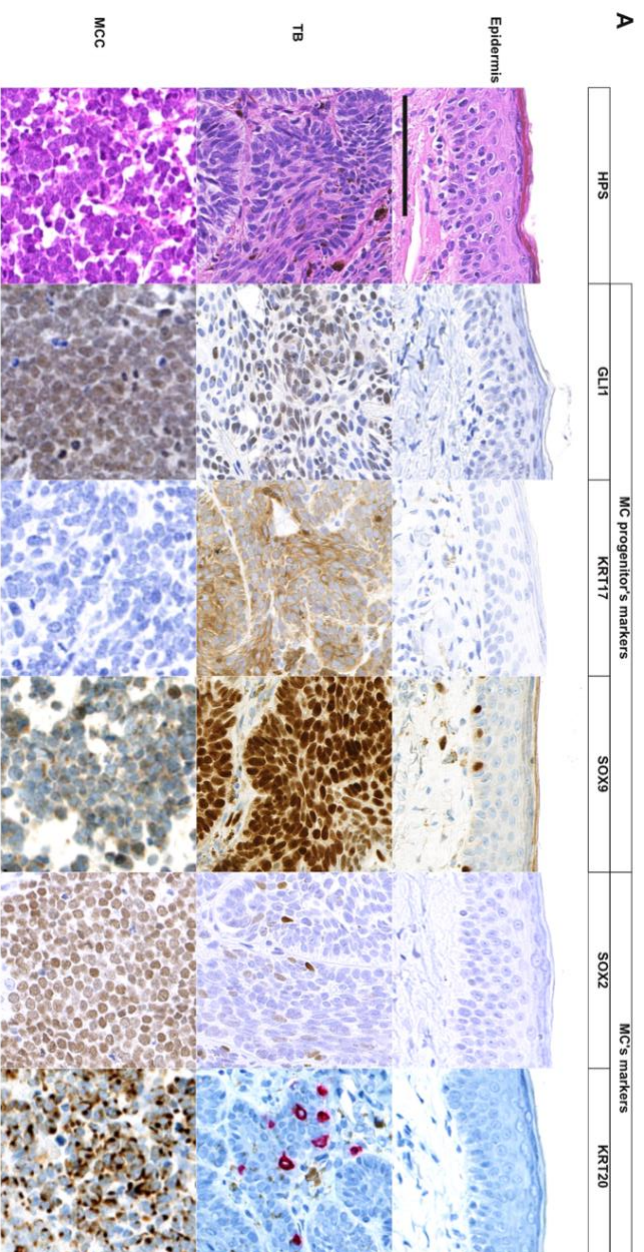
Supplementary Figure 1. Further characterization of Merkel cells and related progenitors in human: **A:** Merkel cell (MC) locations in human. KRT20-expressing MCs were observed in the interfollicular epidermis, in appendages structures and in few cases in the dermis (bar=100 µm). MCs were mostly located in hair follicles (43% of the observed MCs). There, MCs were detected in infundibulum (80%) or in the isthmus part (20%). The proximal part of the eccrine sweat gland duct was also a MC niche predominantly detected in acral skin. Of note, by contrast to previous report⁷² some MCs were also observed in the papillary dermis, frequently in close proximity to the hair follicle. These findings suggest that MCs might experiment an epithelia-mesenchymal transition process. **B:** MC markers in human: merged analyses confirmed colocalisation of the MC markers (KRT8, KRT20 and SOX2). Moreover, colocalisation of GLI1 and KRT17 expression could also be detected. Of note, expression of the MC progenitors' markers GLI1 and KRT17 seems to be reduced in MCs. **C:** MCs density according to the anatomic sites and microscopic location. **D:** MC hotspot densities per location and anatomic sites.



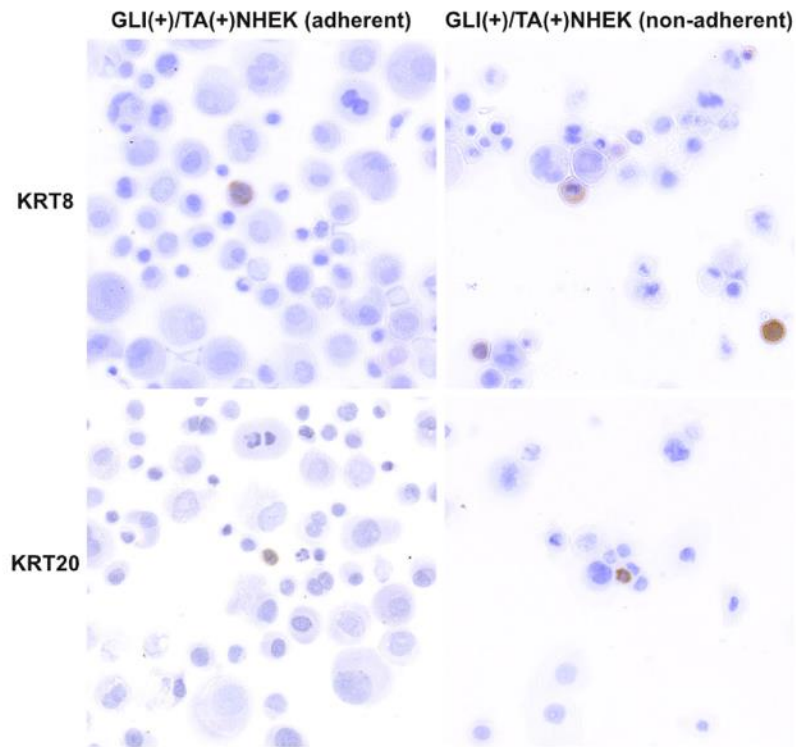
Supplementary Figure 2. Further characterization of native and transduced normal human epidermal keratinocytes. **A:** After isolation from surgical piece, morphology of normal human epidermal keratinocytes (NHEK) were assessed by May Grunwald Giemsa staining (MGG), and expression of KRT14, a basal keratinocyte marker, was confirmed these preparations.

B: Detection of SOX2 expression by immunoblot in GLI-transduced NHEK and control.

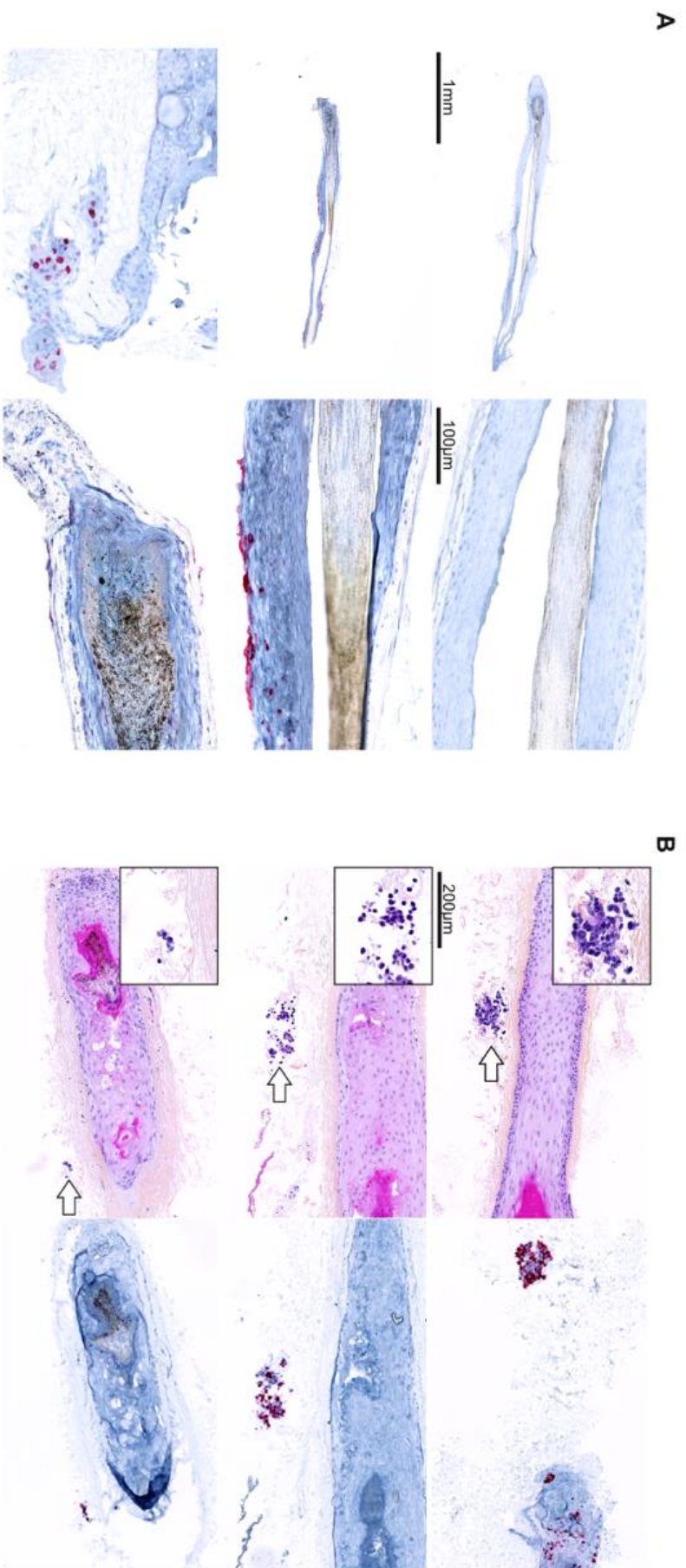
C: Immunohistochemical assessment of GLI1 and SOX2 expression levels in GLI1-expressing NHEK and control (second independent experiment). **D:** Immunohistochemical assessment of Large T (LT) and keratin 8 (KRT8) in T antigens (TA)-expressing NHEK and controls in a second and a third experiment.



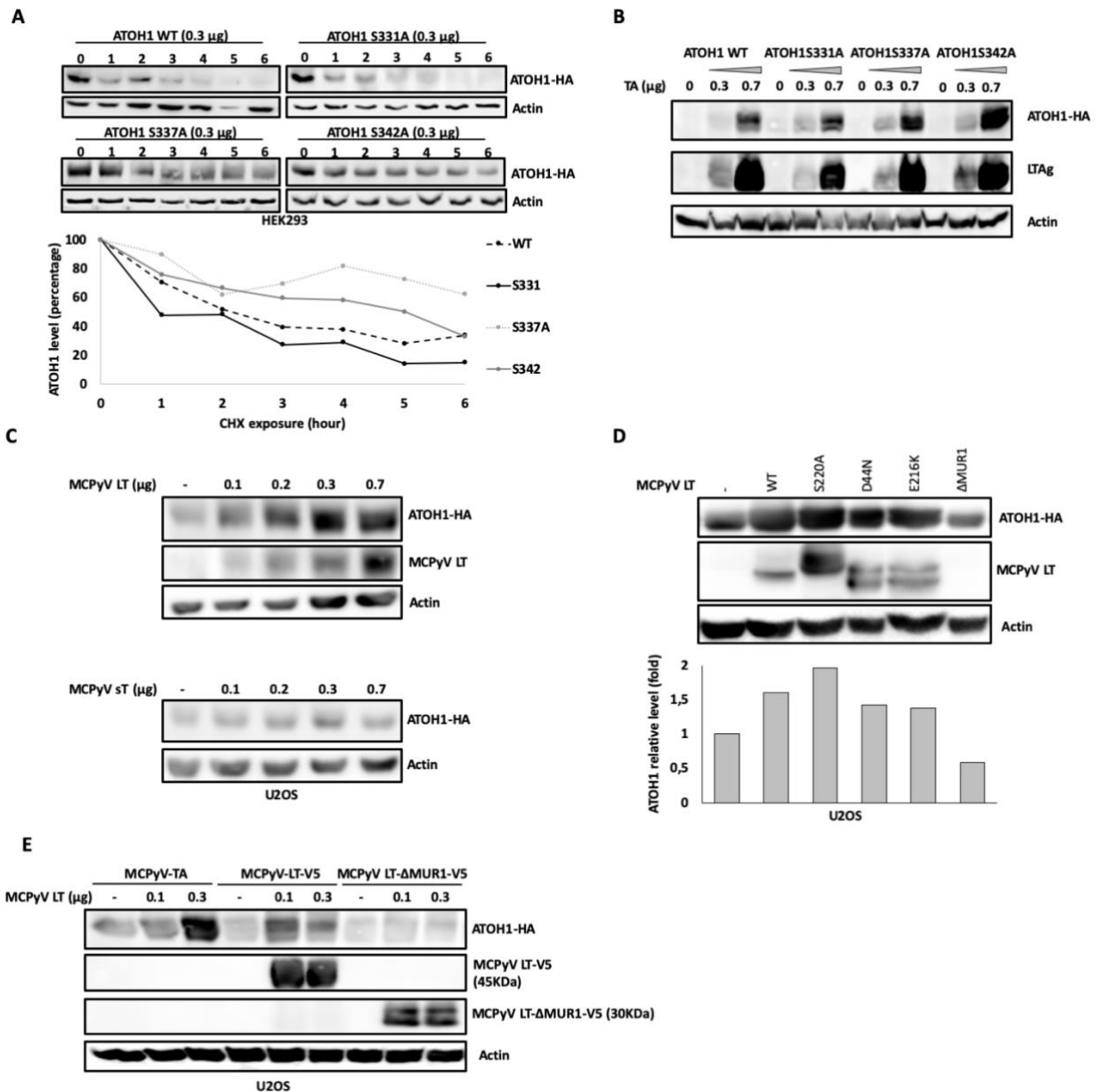
Supplementary Figure 3. Expression of Merkel cell progenitor markers in tumors. A: microscopic and immunophenotypic features of Trichoblastoma (TB) and Merkel cell carcinoma (MCC) tumors: Morphology (hematein-phloxin-saffran staining), expression of the progenitor markers GLI1, KRT17 and SOX9 as well as the Merkel cell markers SOX2 and KRT20 in TB and MCC are depicted. Surrounding epidermis was used as control (bar=100 μ m). **B:** Expression pattern of SOX9 in Merkel cell polyomavirus (MCPyV)-positive and negative MCC (bar=100 μ m). While nuclear positivity for GLI1 was always homogenous, a patchy pattern consisting of a mixture of tumor cells without and with nuclear expression was observed for SOX9 (Figure 3) suggesting that in such cases only in a subpopulation of tumor cells SOX9 was activated. Of note, most of the cases without SOX9 nuclear positivity were characterized by a hitherto undescribed paranuclear dot like SOX9 staining (64%) suggesting a potential sequestration of this factor in the cytoplasm or the Golgi apparatus. Since it has been previously postulated that MCPyV-negative cases harbor a subpopulation of pluripotent progenitor cells explaining why divergent differentiation only occurs in aMCC subset^{2,3}, we investigated expression of GLI1 and SOX9 according to the MCPyV status. In line with this hypothesis, SOX9 nuclear positivity (81 versus 10%) was more frequently observed in MCPyV-negative MCC ($p < 10^{-9}$) (supplementary Table 2). **C:** MCPyV viral load of the MCC cases dichotomized by their SOX9 expression pattern ($p < 0.05$).



Supplementary Figure 4. KRT8 and KRT20 expression in GLI(+)/T Antigen (TA)(+) adherent and non adherent Normal human epidermal keratinocytes (NHEK). After transduction and antibiotic selection, adherent and non adherent cells were analyzed independently. This analysis demon



Supplementary Figure 5. Impact of ectopic T antigen expression in human hair follicles. Seven days after transduction, hair follicles were fixed in formalin, paraffin embedded and then investigated for morphology and expression of different markers. A: Immunohistochemical detection of large T in T antigen (TA)-transduced hair follicles and controls (bars= 1 mm and 100 μ m respectively). Use of highly concentrated lentiviral vectors allowed to induce TA expression in the external (outer root sheath) and proximal (infundibulum) part of the hair follicle while the inner part (inner root sheath and hair shaft) and bulbe region remained unstained. B: Further illustrations of TA-transformed cell clusters (bar=200 μ m). Microscopic examination (Hematein phloxin saffran staining) of the TA-transduced hair follicle revealed the presence of clusters of transformed cells in the connective tissue surrounding the hair follicle (white arrows). Immunohistochemical investigation revealed large T expression by these clusters



Supplementary Figure 6. LT containing MUR1 region is required for ATOH1 stabilization. **A:** Evaluation of ATOH1 mutated protein half-lives in comparison to the wild type form. Phosphorylation of the serine residues S331, S337, S342 of the ATOH1 protein are expected to control protein degradation. Therefore, these serine residues were changed to alanine in three independent constructs in order to remove the phosphorylation site. Half-lives of the obtained constructs were evaluated by cycloheximide experiments. An increased half-life was observed for S337 and S342 ATOH1 mutants. **B:** Impact of T antigens (TA) on protein level of ATOH1-HA wild type and single mutants. **C:** Evaluation of the effect of truncated Large T (LT) or small T (sT) on ATOH1-HA protein levels in U2OS cells. ATOH1-HA protein levels were assessed by immunoblot after transfection of increasing amounts of LT or sT encoding vectors. These experiments identified LT as the main contributor of ATOH1-HA stabilization. **D:** Evaluation of the ability of mutated forms of truncated Large T antigen resulting in specific inactivated sites (S220A : mutant lacking LT phosphosite, D44N: mutant with inactivated Hsc binding site, E216K: mutant with inactivated RB1 binding site, ΔMUR1: mutant deleted for the Merkel unique 1 region (MUR1)) to stabilize ATOH1-HA. Quantification of ATOH1-HA expression level was performed using ImageJ software. Of note, since the antibody used for LT detection (clone: CM2B4) recognizes an epitope located in MUR1, no signal was obtained with the LT-ΔMUR1 mutant. **E:** further confirmation of the lack of ATOH1-HA stabilization by LT-ΔMUR1 mutant. ATOH1-HA construct was transfected in absence or presence of increasing amounts of TA, a V5-tagged LT wild type and V5-tagged LT-ΔMUR1 encoding vector. Evaluation of ATOH1 amount by immunoblot revealed an accumulation of the ATOH1-HA protein in presence of wild type Large T while no effect was observed for the LT-ΔMUR1 mutant.

DISCUSSION

MCC was first described in 1972. Despite being the most aggressive skin cancer, MCC was for a long time only noticed in the field of dermatology. Recent years, however, boosted the awareness level for this tumor entity. From the clinical point of view, treatment of MCC patients with immune checkpoint inhibitors is a prime example of efficacy of this therapeutic approach (Samimi 2019). More important, MCC was the first human cancer shown to be induced by a polyomavirus (Feng et al. 2008a). Indeed, in approximately 80% of MCC cases integration of the MCPyV into the host genome appears to be the crucial causal event for MCC tumorigenesis. However, the nature of the cell in which virus integration occurs is unknown. Indeed, quite diverging hypotheses have been suggested. While some provide evidence for a lymphoid origin (Zur Hausen et al. 2013), others propose that MCPyV-positive MCCs derive from dermal fibroblasts (Sunshine et al. 2018), neuronal progenitors (Harold et al. 2019) and furthermore, it has been suggested that MCC evolves from epidermal cells (Tilling and Moll 2012). Accordingly, during the International Workshop on MCC Research in March 2018, determination of the cell of origin of MCC was considered as a high-priority research question (Harms et al. 2018). Indeed, determining the cells of origin in cancer not only answers academic questions but also has important diagnostic and therapeutic implications (Becker and Zur Hausen 2014; Harms et al. 2018; Zur Hausen et al. 2013).

I. Conclusions on the origin of MCC based on the phenotypic characterization of the tumors

To determine the cell of origin of MCC, we started with phenotypic characterization of MCC tumors. Although such approach constituted the start-point of our demonstration, it is however crucial to bear in mind how this strategy might help to determine the cell of origin. Indeed, direct comparison of the tumor cell phenotype with healthy tissue initially led Tang and others (Tang and Toker 1978) to propose MC as a probable MCC ancestry due to similarities in morphology, immunohistochemical profile and ultrastructural features. More recently, Zur Hausen et al. proposed a B-cell origin based on the morphological similarities between B-cell and MCC tumor cells, as well as co-expression of B-cell markers and immunoglobulin rearrangements in MCC tumor cells (Zur Hausen et al. 2013). However, these conclusions are challenged by the fact that phenotypic changes may occur during the oncogenic process (Fletcher 2006), and such findings have been proved for MCC since ectopic

expression of TAGs induces phenotypic changes (Fan et al. 2019). In line with this conclusion, MCC tumor features have to be considered as the result from the combination of a physiological cell (i.e. the cell of origin) together with oncogenic alterations inducing phenotypic changes.

1. Do morphological differences reflect the nature of the oncogenic factors driving MCC development?

In this context, comparisons of MCC with extracutaneous neuroendocrine carcinomas (**Article 1.**) and comparisons between MCPyV-positive and -negative cases (**Article 2.**) allowed us to confirm that MCPyV-positive MCCs are a distinct subset of tumors while close similarities are observed between MCPyV-negative MCCs and extra-cutaneous neuroendocrine carcinomas. In line with such findings, genetic characterization of MCPyV-negative MCC and small cell lung cancer cases demonstrated high tumor mutation burden in both subsets (Carter et al. 2018; Goh et al. 2016; Starrett et al. 2017; Sunshine et al. 2018; Yarchoan et al. 2019) (around 10 mutations /Mb) (Goh et al. 2016). In addition, common mutations in *TP53* and *RB1* were observed (Carter et al. 2013; Goh et al. 2016; Starrett et al. 2017), although these genetic alterations are related to different etiological agents (UV vs smoking) (Carter et al. 2018; Goh et al. 2016; Starrett et al. 2017; Testa et al. 2018). By contrast, only low mutation burden (around 0.40 mutations/Mb) (Harms et al. 2015a) were detected in MCPyV-positive cases, a finding reflecting the crucial role of MCPyV integration in MCPyV-positive MCC oncogenesis.

In accordance with these genomic analyses, tumor cell morphology might reflect the genetic tumor background in MCC as well known in soft tissue tumors (Mariño-Enríquez and Bovée 2016). Indeed, as previously suggested (Iwasaki et al. 2013; Kuwamoto et al. 2011), we demonstrated that MCPyV-negative cases harbored prototypic neuroendocrine carcinoma features, either similar to those observed in small cell lung cancers or in large cell neuroendocrine carcinomas (Nagase et al. 2016). By contrast, MCPyV-positive prototypic features consist in monomorphous proliferation of round tumor cells with scant cytoplasm and clear chromatin. As discussed in the **Article 2.**, such kind of bland morphology is observed in tumors caused by a unique genetic alteration, which might be translocation (ex: Ewing sarcoma) or viral integration (Burkitt's lymphoma). Therefore, these findings strongly suggest that MCPyV-MCC tumor cell morphology is induced by the viral proteins in cases of MCPyV-

positive MCC. It is still important to note that MCPyV-positive and negative cases harbor a distinct but close morphology, which does not always allow a correct determination of the viral status on the sole basis of morphology. Such close similarities are probably related to the fact that both MCPyV TAg and UV induced mutations act on the same signaling pathways (Harms et al. 2018; Starrett et al. 2017).

2. Do immunohistochemical differences reflect the nature of the oncogenic factors driving MCC development?

In line with our morphological characterization of MCC, significant variations in immunohistochemical profiles support the hypothesis of distinct differentiation between the two subsets. Indeed, MCPyV-negative cases are characterized by a so called “aberrant” phenotype with frequent expression of markers observed in extracutaneous carcinoma but not in MCPyV-positive MCC, such as TTF-1 and KRT7 (**Article 2.**) (Czapiewski et al. 2016; Pasternak et al. 2018). In addition, MCPyV-negative tumors frequently harbor a distinct pattern of high p53 expression, probably reflecting inactivating mutation of the tumor suppressor gene (**Article 2. and 5.**). Finally, MCPyV-negative MCC cells frequently do not express “typical” MCC markers such as KRT20 (Harms et al. 2016; Miner et al. 2015), Neurofilament (Pasternak et al. 2018) and SATB2 (**Article 2.**). By contrast, a fully differentiated and homogenous state is observed in MCPyV-positive cases.

Interestingly, in contradiction to previous reports (Harms et al. 2016; Miner et al. 2015; Pasternak et al. 2018), no statistically significant difference was observed in our cohort regarding KRT20-positivity among MCPyV-positive and -negative MCC (**Article 2.**). However, cytokeratin expression patterns were distinct between the two subsets. Indeed, a cytokeratin dot-like pattern, defined as aggregation of the cytokeratins on one side of the cytoplasm, is a hallmark of MCC. By contrast, a diffuse distribution of these intermediary filaments is observed in physiological MCs (Verhaegen et al. 2017). In the current work, we demonstrated that MCPyV-positive cases more frequently harbor exclusive “dot-like pattern” expression of KRT8, 18 and 20 whereas a mixed pattern is observed in MCPyV-negative cases. Of note, a cytokeratin dot-like expression pattern is not specific for MCC but can also be observed in extracutaneous neuroendocrine carcinoma (Badzio et al. 2019). Accordingly, investigation of KRT8 and 18 expression in our eNEC cohort also revealed presence of a mixed (diffuse and

dot-like) expression pattern in more than half of the cases (unpublished data). Indeed, the cytokeratins dot-like expression appears as a feature shared by all neuroendocrine carcinomas while more pronounced in MCPyV-positive cases, therefore suggesting a potential TAg contribution to this phenotype. This hypothesis is supported by the impact of Atoh1 expression, with or without the TAg, in a transgenic mouse model. In this setting, Atoh1 expression alone leads to MC differentiation in the epidermis and subsequent expression of the Krt8 and 20 in a diffuse manner (Verhaegen et al. 2017). By contrast, coexpression of sT and Atoh1 induces cytokeratins aggregation and a dot-like pattern.

To investigate the biological mechanism of this dot-like pattern, we recently performed electron microscopy on MCC cell lines (ongoing collaboration with Pr E. Blanchard, IBI SA platform, Tours, France). First analyses confirmed that aggregation of the intermediary filaments is located in the cytoplasm and colocalize with the microtubule organizing center at one pole of the cells. Interestingly, almost all organelles are also restricted to this area in MCC tumor cells. Therefore, the observations of dot-like pattern expression of membranous markers such as CD99 or CD56 (**Article 2.**), might be explained by sequestration of these proteins in the Golgi apparatus. Although molecular determinants of the “dot” are poorly understood, Isaac Brownell recently proposed that such aggregates are due to impairment in protein ubiquitination and degradation. Such mechanisms might result in cytokeratin accumulation and aggregation, a mechanism which might contribute to resistance to TNF- α and apoptosis (Brownell, 2019) as described in other cancers (Caulin et al. 2000).

3. Do prognostic differences reflect the nature of the oncogenic factors driving MCC development?

In line with the genetic and phenotypic variations observed between the two groups there is also a difference with respect to clinical outcome. Patients in our cohort with MCPyV-negative MCC experience a worse clinical outcome compared to patients with to virus-positive tumors (Article 2.). Although discordant reports can be found in the literature (Moshiri et al. 2017; Schrama et al. 2011), our results are in accordance with the results of the largest series published (Moshiri et al. 2017), which also strongly suggests that MCPyV-negative tumors are the more aggressive subgroup of MCC. Since currently approved therapeutic strategies (surgery and radiotherapy, immune check point inhibitors) seem to be effective in both

subsets of MCC patients, determination of the MCPyV status is not required for therapeutic decision in current practice. However, regarding the biological variation between the two populations, MCPyV status evaluation would be of great interest in clinical trials since some new therapeutic options might be efficient in one subset and not in the other.

To conclude on our characterization of MCC tumors according to the virus status, MCPyV-positive and -negative MCC cases appear as two distinct subsets with significant differences with respect to morphology, immunohistochemical profiles and clinical outcome. Moreover, they might have a different cellular ancestry (Sunshine et al. 2018) and this conclusion may challenge the current classification of both entities in the same category by the WHO classification i.e. neuroendocrine carcinoma of the skin. Indeed, based on the detection of high mutational burden, prominent UV-signature and the observation of combined cases associated with epidermal involvement, MCPyV-negative cases are likely to derive from an epidermal cell. By contrast, deep location of the MCPyV-positive cases without any connection to the interfollicular epidermis as well as lack of UV signature indicate that the cell of origin of such cases are located deeper in the skin, and could be either appendages epithelial cells, mesenchymal, neuronal or hematopoietic cells.

II. Conclusions on the origin of MCC based on the characterization of combined tumors

1. Are Squamous cell carcinoma/MCC combined tumors indicative of the cell of origin of MCPyV-negative MCC?

MCPyV-negative cases frequently harbor a divergent component, a finding also observed in small cell lung cancer (Oser et al. 2015). Although we and others (Chou et al. 2016; Mitteldorf et al. 2012) were able to detect MCPyV sequences using molecular tools in combined squamous carcinoma/MCC tumors, these results have to be interpreted with caution. Indeed, employing three independent very sensitive methods (**Article 5.**), we detected MCPyV sequences in half of the combined cases, which is more than the frequency observed in non MCC skin cancer. However, these combined cases differed from classical non combined MCC cases in various respects: i) viral load was very low ii) truncating LT mutations were not

detectable and iv) immunohistochemistry could not demonstrate LT expression. Therefore, MCPyV-positivity is most likely due only to presence of episomal wild type virus and not to MCC-typical integration of a mutated MCPyV.

Generally, MCPyV-negative “combined MCC tumors” also termed “MCC with divergent differentiation” could result from three different biological processes: i) collision of two tumors, i.e. two independent but spatially associated tumors without a clonal link, ii) acquisition of a neuroendocrine differentiation of some cells from a non-neuroendocrine skin neoplasia, iii) dedifferentiation of MCC cells leading to an undifferentiated (so-called sarcomatous) tumor component (Figure 13).

Although, a final proof is still pending, several points argue in favor of a clonal filiation of the combined tumors components. First, the over-representation of combined tumors among the MCPyV-negative MCC subsets (around 40% in our cohort), and rarity of such a phenotype among MCPyV-positive cases argues against an incidental association of two different components. Second, although not observed in all combined tumors investigated (Falto Aizpurua et al. 2018), shared genetic alterations have been reported in both components of MCC combined with invasive squamous cell carcinoma components in some cases (Carter et al. 2017). In order to confirm the clonal filiation of MCPyV-negative combined MCCs, the genomic analysis of several combined cases by our group is currently on-going.

Interestingly, combined MCC tumors sometimes also harbor intraepithelial neoplasias such as actinic keratosis or Bowen's disease and an invasive squamous cell component. In light of the arguments detailed above, consecutive differentiation steps are conceivable leading from Bowen' disease to an intermediate squamous cell carcinoma and finally to MCC. Accordingly, Narisawa et al. recently described proliferative MCs in the Bowen's component of a MCPyV-negative combined MCC, which therefore might be already neoplastic epidermal cells acquiring neuroendocrine differentiation (Narisawa et al. 2018). The possibility that UV-induced combined MCC can derive from the epidermis is further supported by the observation of intra-epidermal MCCs. Indeed, we recently reported that intra-epidermal MCC involvement is only observed in MCPyV-negative cases (**Article 2.**).

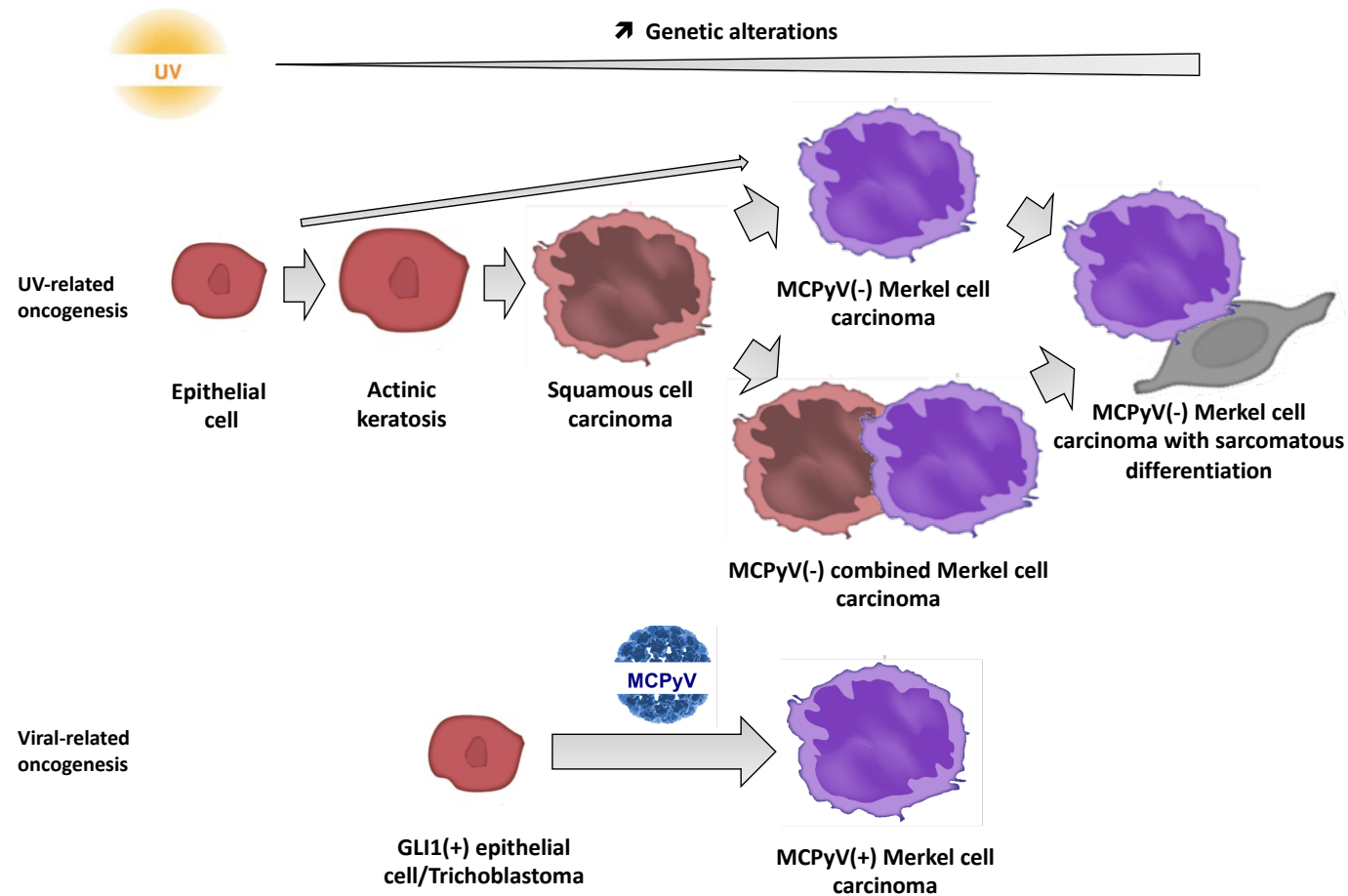


Figure 13: Graphic abstract of the putative mechanisms of MCC development according to the etiologic factors. UV-induced MCC are likely to arise from an epithelial cell hit by UV-radiations. Accumulation of DNA damages in such cells finally cause neuroendocrine differentiation in a part (combined cases) or in the complete tumor. Undifferentiated so called sarcomatous component can arise from such MCPyV(-) cases. By contrast, MCPyV(+) cases depend on a unique oncogenetic event i.e. MCPyV integration and our results suggests that GLI1(+) progenitors of the hair follicle as the main cell hit by the virus. Cells in red and purple harbor keratinocytic and neuroendocrine phenotype respectively while differentiation is lacking from cells in grey.

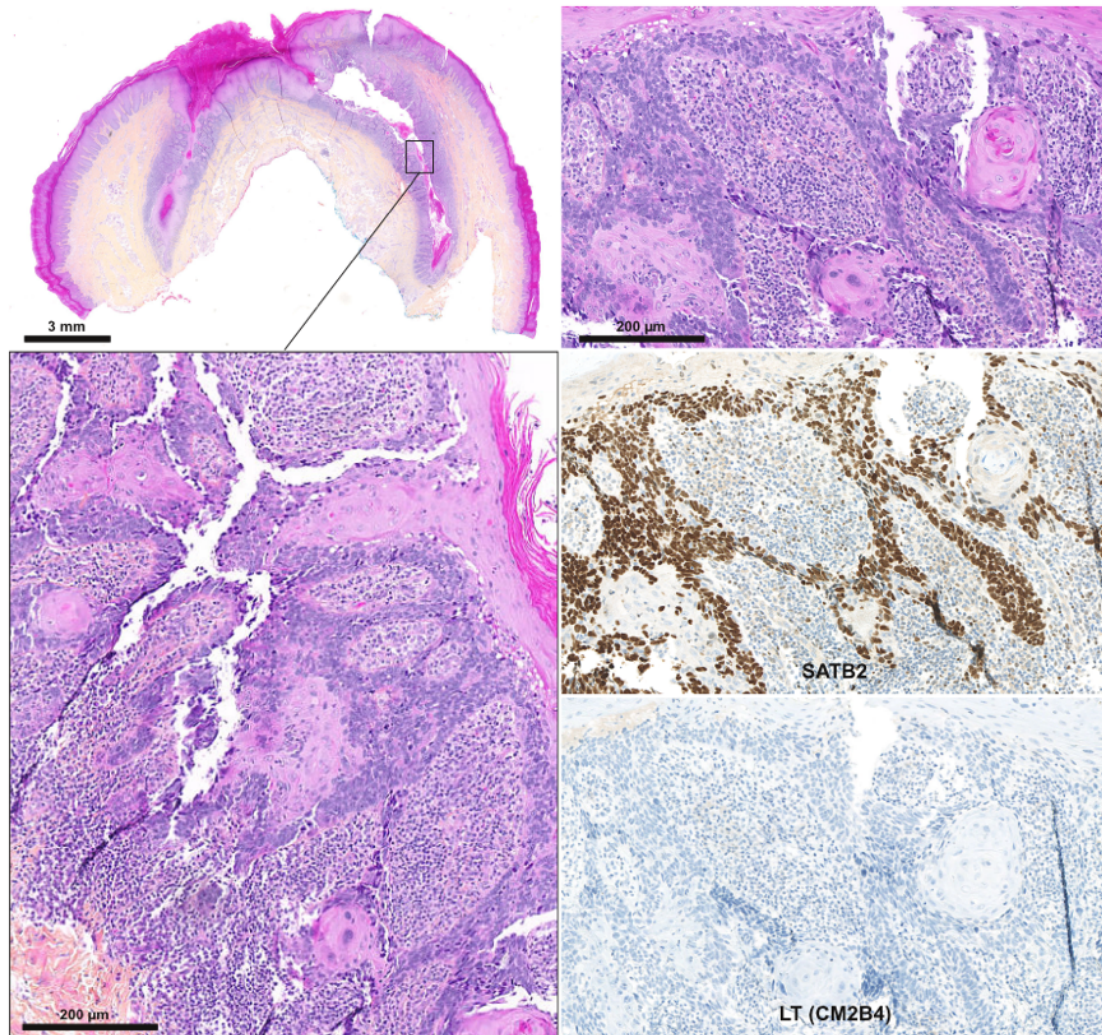


Figure 14. Intra epidermal MCC without dermal involvement. This exceptional case was kindly provided by Dr E. Calonje, London, UK. A surgical specimen of an intraepidermal MCC located in nail bed is depicted (hematein-phloxin-saffron staining). Microscopic examination reveals a massive infiltration of the epithelium by a proliferation of atypical tumor cells harboring dark and elongated nucleus, and few cytoplasm. In some places, foci of squamous differentiation were evidenced in the tumor proliferation. These tumor cells harbored all MCC markers including KRT20 and SATB2. MCPyV was no detected in this tumor either by immunohistochemistry or by implying molecular procedure.

Accordingly, recent analysis of an extremely rare intra-epidermal MCC without any dermal involvement (kindly provided by Dr E. Calonje, Figure 14) revealed it as MCPyV-negative.

In summary, these findings argue in favor of an epidermal origin of MCPyV-negative MCC cases, which might frequently derive from already neoplastic cells (actinic keratosis, Bowen's disease) and acquire neuroendocrine differentiation during the oncogenic process.

Several divergent differentiation patterns such as basal-cell-like, adnexal, melanocytic, glandular, sarcomatous and ganglioneuroblastic have been reported in combined MCC (Carter et al. 2018; Martin et al. 2013; Walsh 2001). While Narisawa et al. proposed that these findings reflect the stem cell properties of the primary cell of origin, this might alternatively result from the acquisition of stem cell-like properties during tumor development (Koba et al. 2015; Narisawa et al. 2015). This latter is suggested by the presence of a SOX9 expressing cells in MCPyV-negative cases (**Article. 7**).

Indeed, some findings actually suggest that MCPyV-negative MCCs harbor properties of dedifferentiation, which may be related to such stem-cell like cells. A special case is MCC combined with a sarcomatous spindle cell component, which is thought to result from dedifferentiation process. Similar to the so called carcinoma with sarcomatoid differentiation which represents dedifferentiated cutaneous basal cell or squamous cell carcinomas, it is likely that loss of epithelial and neuroendocrine differentiation of MCC cells in these MCC with sarcomatous differentiation result in an anaplastic form of MCC (Clark et al. 2017). Accordingly, the term "Merkel cell carcinosarcoma" has been proposed for such tumors (Lau et al. 2012). In our experience (unpublished data), some MCPyV-negative cutaneous primary tumors lack neuroendocrine differentiation but still harbor a morphology of small cell carcinoma, and express some MCC markers. These tumors could represent the cutaneous counterpart of the non-neuroendocrine small cell lung cancer. Indeed expression of the neuroendocrine markers is lacking in about 5 to 10% of small cell carcinoma of the lung, while such cases are still belonging to the same entity than neuroendocrine tumors. Various degrees of neuroendocrine differentiation have been observed between MCC tumors (Fernández-Figueras et al. 2007; Koljonen et al. 2005), but a correlation between the level of expression of neuroendocrine markers and MCPyV status is still lacking, and would be an interesting issue

in order to investigate whether such differentiation might be reduced in MCPyV-negative cases. Nevertheless, regarding the phenotypic heterogeneity probably reflecting genetic heterogeneity, MCPyV-negative MCC appears as a dynamic tumor state which is likely to derive from skin intraepidermal neoplasia and might additionally harbor a subpopulation of tumor cells with stem cell-like properties allowing divergent differentiation/anaplasia. Interestingly, all these features are lacking in MCPyV-positive MCC, which appear as a monomorphic population of tumor cells without divergent differentiation.

2. Are Trichoblastoma/MCC combined tumors indicative of the cell of origin of MCPyV-positive MCC?

Based on tumor cell morphology, we identified an exceptional case of TB/MCPyV-positive MCC combined tumor (**Article 6.**). Detailed genetic analysis of this case demonstrated for the first time that a prototypic MCPyV-positive MCC can arise following integration of a MCPyV genome into the genome of epithelial cell. It is important to note that the developmental history of TB tumor drastically differs from the UV-induced combined cases. Indeed, UV-induced neoplasias such as squamous cell carcinoma are highly mutated tumors (around 3000 pathologic variations/genomes in SCC (Inman et al. 2018)). Accumulation of genetic alterations over the time might drive the natural history by improving aggressiveness and invasiveness of these neoplasias (Inman et al. 2018). Therefore accumulation of mutations is likely to be the main determinant of the neuroendocrine phenotype acquisition in MCPyV-negative combined tumors.

By contrast, TB is a benign epithelial tumor characterized by a hair follicle differentiation and a benign behavior with only extremely rare malignant transformation (Fusumae et al. 2019). While *CYLD* mutations have been identified in TBs in the context of Brooke Spiegler's syndrome (Kazakov 2016), only few genetic data are available on sporadic TBs, with only *HRAS* mutation reported in tumors arising on naevus sebaceus (Saraggi et al. 2017; Shen et al. 2015). In this context, the whole exome sequencing of the TB component of our combined case, an analysis which, in our knowledge, has never been performed before, revealed very few genetic alterations (10 pathologic variants/genome). Moreover, we did not find mutations in classical

oncogenes. Although we found a few additional mutations only present in the MCC component, these were also not affecting known oncogenes and the allelic frequencies suggests that most of them are only present in a fraction of the MCC tumor cells. Therefore, occurrence of the MCC component in the TB was not related to a progressive accumulation of mutations over time but resulted most likely from a single oncogenic event i.e. integration of MCPyV with mutant LT coding sequence. This “on/off” induction of MCPyV-positive MCC was also supported by the patient's clinical history. Indeed, the patient experienced a partial excision one year before and pathological examination of the biopsy revealed a benign TB at that time. Several months later, a fast growing and inflammatory tumor appeared on a scar at the surgical site leading to excision of the combined tumor. This sequence suggests that MCPyV integration in the TB tumor residue contributed to this aggressive clinical presentation.

Interestingly, TB is composed of so-called “germinative” tumor cells (Collina et al. 1998; Goyal et al. 2016; Kurzen et al. 2001; Leblebici et al. 2019; McNiff et al. 1999) which mimic the hair germ i.e. an embryonic structure giving rise to the hair follicle (Perdigoto et al. 2016). In addition, the sparse MCs frequently observed in TB are considered as a diagnostic criterion of this entity. While colonization of the TB tumors by such MCs might be hypothesized, several arguments favoring a differentiation process from the germinative tumor cells into MCs can be presented: i) the sparse distribution of MCs in TBs lobules (Collina et al. 1998); ii) the frequent lack of connection of the TB with the surrounding epidermis in which the physiological MCs are located (WHO 2018); iii) the high density of MCs in the TB whereas the physiological MCs are rare in the epidermis and post mitotic (Moll et al. 2005); iv) the phenotypic similarities between TB germinative cells and MC progenitors with activation of the Sonic Hedgehog pathway and expression of KRT17 and SOX9 (**Article 7**). To prove the neoplastic nature of these TB associated MCs, a microdissection approach, using laser capture of these MCs in the TB part will be performed to confirm that the same pathologic variants are present in MCs and germinative cells of the TB.

Interestingly, in one restricted area of the TB, some LT-expressing cells were detected by immunohistochemistry. This area was additionally characterized by an increased number of cells expressing the MCs markers and moreover by cytokeratin expression with the dot-like pattern. While these findings might be explained by disseminated MCC tumor cells presents

in this part of the TB, it might alternatively be the result of TB cells infected with the wild type virus. The latter conclusion is supported by several points: i) the random single cells distribution of the LT positive cells in the TB without clusters argues against a metastatic spreading and subsequent cells proliferation, ii) the difference in morphology between LT expressing cells and adjacent MCC tumor cells with cytoplasm vacuolization which was more indicative of cellular damages than oncogenic transformation, iii) more frequent immunohistochemical expression of the early MC differentiation markers SOX2 and KRT8 than KRT20 in LT-expressing TB area suggests an ongoing differentiation process; iv) the very few KRT20-positive Ki67 positive cells (<10% of the KRT20 positive cells) argue against these cells being MCC tumor cells; v) the lack of physiological MCs with a diffuse cytokeratin expression pattern suggests that already differentiated MCs of the TB were affected by the virus; vi) high MCPyV viral load was detected in both TB and MCC part of the combined tumor, whereas deletion of LT and insertion sites sequences could only be detected in the MCC part. To finally confirm the presumed nature of the above described LT-expressing cells in the trichoblastoma, microdissection and subsequent genetic analysis will be performed. In case these are really not MCC tumor cells this would allow important conclusions regarding the capability of the MCPyV Tags to induce acquisition of a Merkel cell like phenotype upon expression in epithelial cells similar to hair follicle cells.

The analysis of the combined TB/MCC case clearly demonstrated that a MCPyV-positive MCC can arise from an epithelial cell. However, one main limitation is obviously that we could analyzed only one such case due to the rarity of this entity. In the literature, we identified two further specimens. The first one was a TB/ MCC case published by Battistella et al. . With the support of Prof. Bernard Cribier (Dermatology department, Strasbourg, France), we were able to confirm LT expression in the MCC and TB part of this tumor as depicted in **Article 6**. However, molecular analysis was not possible due to Bouin fixation. Of note, a second case of combined tumor of combined tumor harboring MCPyV-positive MCC and basal cell carcinoma with ductal differentiation component has been reported by the Hayashi group in 2013 (Iwasaki et al. 2013). While the authors did not diagnose the second part as TB, the non MCC-component of this combined tumor clearly displays adnexal and follicular differentiation. These findings were additionally proved by the detection of normal MCs in the “basal cell carcinoma” component suggesting that the non MCC components of MCPyV-positive

combined tumor frequently harbor MC differentiation ability. By contrast to our case, immunohistochemical analysis of the Japanese tumor revealed a diffuse expression of LT in both MCC and basal cell carcinoma parts. In addition, the authors observed two different truncated LT for each component, suggesting that MCPyV integration has although occurred in cells of the TB part. Interestingly, high MCPyV viral load has also been detected in some trichoblastoma tumors lacking MCC components (Kassem et al. 2010) suggesting a potential MCPyV tropism for such tumors.

Of note, an additional case of TB/MCPyV-positive case was recently identified (Dr. Marie-Laure Jullié, Bordeaux, France) which is depicted in Figure 15. Although, this case appears to be similar to our initial report, one additional feature is the presence of widespread expression of MCPyV LT in areas of the TB lacking MC-like differentiation. Whether this LT expression is due to an episomal or integrated form of the virus has to be clarified (molecular analysis of this case is ongoing). However morphologic and immunohistochemical features of the case again suggest that a MCPyV-positive MCC can derive from a TB tumor cells i.e. an epithelial cell harboring hair follicle differentiation and bearing the ability to differentiate into MCs.

Interestingly, almost all of our knowledge about the MC lineage derive from transgenic mice models (Morrison et al. 2009; Ostrowski et al. 2015; Van Keymeulen et al. 2009; Xiao et al. 2015). In humans, some early reports using human skin xenograft in immunocompromised mice suggested that human MCs derive from epithelial cells of the epidermis (Moll et al. 1990; Tilling et al. 2014). Furthermore, based on the hypothesis that MC progenitors are located close to the MCs, the same group identified a population of KRT17-expressing MC progenitor cells located in the touch dome (Moll et al. 1993). Investigating healthy skin from cadavers, we were able to confirm that epidermal cells located in MC hotspots either in hair follicles or in touch dome area harbor a common phenotype with co-expression of GLI1, KRT17 and SOX9 (**Article 7.**), three markers absent from the interfollicular epidermis and already described in mouse models (Doucet et al. 2013; Nguyen et al. 2018; Xiao et al. 2015). In addition, expression of these three markers was also evidenced in TBs confirming that MCPyV integration is likely to occur in an epithelial cell expressing GLI1, KRT17 and SOX9, a crucial key finding for development of immunocompetent mouse models of MCC.

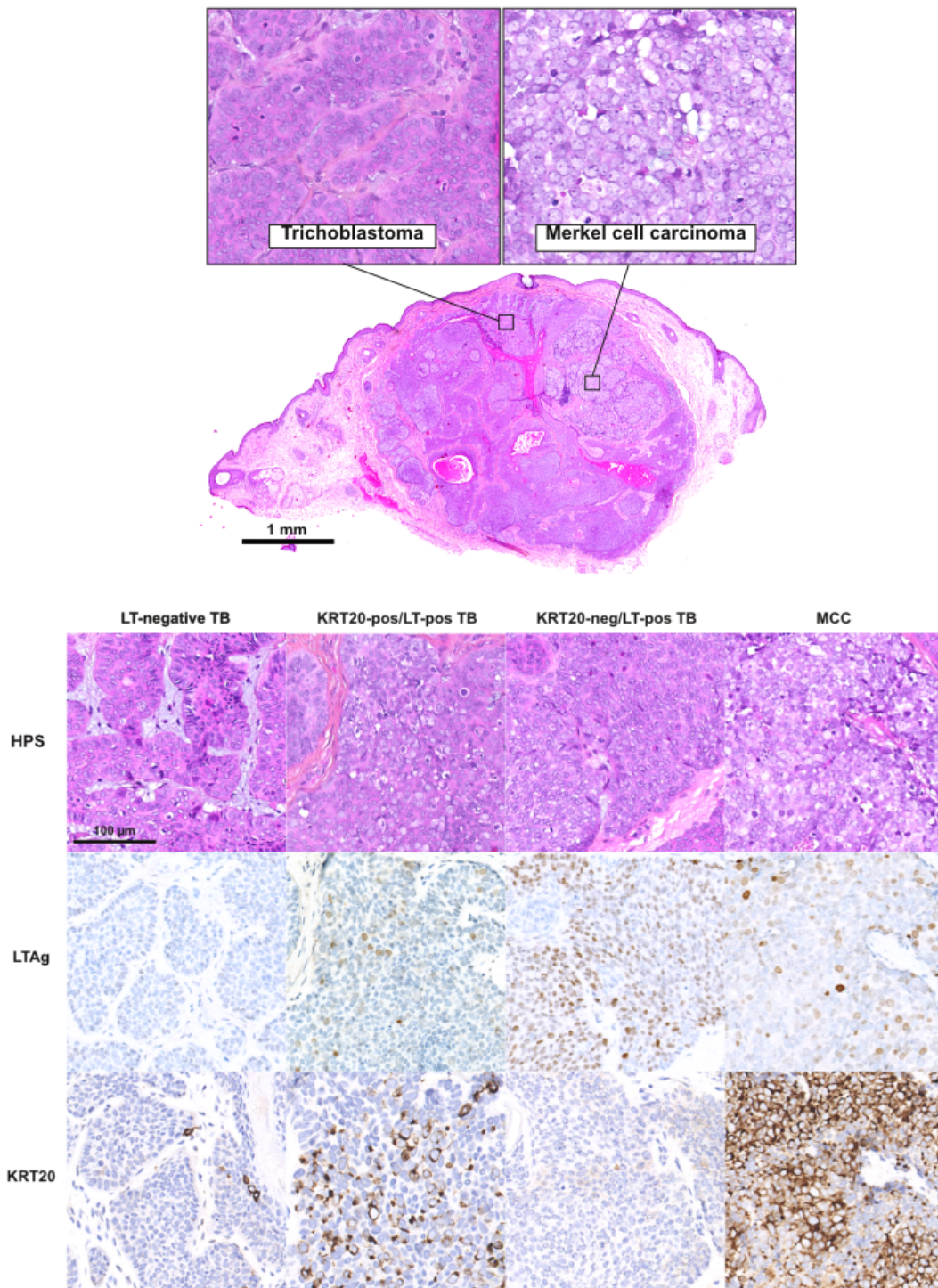


Figure 15. A third MCPyV-positive/Trichoblastoma combined tumor This exceptional case was provided by *Dr. Marie-Laure Jullié*, Bordeaux, France. In accordance with our previous report, this tumor harbors a trichoblastoma and an MCPyV-positive MCC. Large T expression was also detected in the trichoblastoma part and this LT positivity was frequently associated with an increased number of cells expressing MC markers. However, one crucial finding distinguishes this case from our first report: diffuse expression of the Large T was observed in a TB area lacking MC differentiation.

During the last decade, several mouse models tried to reproduce MCC development. In the epidermis, ectopic expression of sT alone or in combination with LT (using KRT5 or KRT14 promoters) led to the development of intraepidermal neoplasia lacking MCC-like features (Spurgeon et al. 2015; Verhaegen et al. 2015). Moreover, ubiquitous sT expression induced hyperplasia in both epidermal and dermal components while combination of sT expression and p53 knock-down induced anaplastic tumors (Shuda et al. 2015). Regarding the MC lineage, sT expression led to the proliferation of embryonic MCs without tumor formation (Shuda et al. 2015), whereas no MC mitotic activity was observed in adults (Shuda et al. 2015). Finally, in a preterm mouse model, combined expression of sT and ATOH1, i.e., the main transcription factor driving MC differentiation, in epithelial cells (K5 promotor) induced formation of MCC-like aggregates in the epidermis, a site where human virus-positive MCC is, almost never located (Verhaegen et al. 2017).

Our conclusion that specialized hair follicle cells may be the main source for MCPyV-induced MCC development might explain why these models had failed. First, Cre recombination inducing oncoproteins expression was performed using KRT14 or KRT5 promoters. Although expression of these KRT are observed in the basal layer of the epidermis and in the appendages, it has been previously shown that “K14 driven recombinase displays robust activity in the interfollicular epidermis, but minimal activity in the hair follicle” (Peterson et al. 2015). Similarly, the same pattern was described for K5 driven recombination (Grachtchouk et al. 2011). In addition, most of the failed MCC models only included sT expression or demonstrated that additional LT expression did not affect tumorigenesis (Shuda et al. 2015; Verhaegen et al. 2017; Verhaegen et al. 2015). In contrast, the strict dependency of human MCC cells on LT expression and the MCC characteristic mutations in LT abolishing its replicative but always preserving its oncogenic function strongly suggest an essential role of LT in MCC carcinogenesis (Houben et al. 2015; Houben et al. 2010).

III. Are the MCPyV T Antigens capable of promoting Merkel cell like differentiation?

As described above our results do not exclude that MCPyV driven carcinogenesis may occur in an already differentiated MC. However, we regard as much more likely that TAg expression in epithelial cells contributes to the acquisition of a Merkel cell like phenotype. Therefore, ectopic expression of sT and truncated LT was performed in primary normal human epidermal keratinocytes (NHEK). This did not induce cell transformation but several changes in phenotypes. First, TAg-expressing NHEK have a reduced size and underwent changes in their shape. Second, enhanced expression of KRT8, one of the earlier marker expressed during the MC differentiation (Perdigoto et al. 2014), was observed in association with slight KRT18 increase (enhance RNA level) and KRT14 decrease, two characteristic changes of the early phase of MC differentiation. By contrast, induction of KRT20 expression was not observed. Interestingly an ability to induce KRT8 and 18 expression as well as KRT14 downregulation were already reported for other polyomaviruses (Knapp and Franke 1989; Royal et al. 1992).

Of note, TAg transduction experiments were initially performed in HaCaT cells, i.e. immortalized human keratinocytes harboring p53 and multiple further mutations (Henseleit et al. 1997). In these cells, no phenotypic changes were observed upon TAg expression underlining again the importance of the cellular context. Therefore, aiming to resemble MC progenitor cells closer in an *in vitro* model, we transduced primary keratinocytes with a key factor of MC progenitor differentiation, i.e. GLI1. Upon lentiviral infection with a bicistronic vector allowing GLI1 or combined GLI1/Tag expression, we were able i) to confirm the involvement of GLI1 in development of an MC progenitor phenotype and ii) to evaluate the effect of TAg in GLI1-expressing cells.

In line with previous reports identifying SOX9 (Vidal et al. 2008) and KRT17 (Mikami et al. 2017) as downstream targets of GLI1, we confirmed an enhanced transcription of these two markers upon GLI1-expression in NHEK. Moreover, as described in other cell lineages (Jia et al. 2019; Santini et al. 2014), we demonstrated that ectopic expression of GLI1 led to a prominent induction of SOX2 in NHEK. Since SOX2 can drive *ATOH1* expression and subsequent MC differentiation (Lesko et al. 2013) by binding to the *ATOH1* enhancer (Bardot et al. 2013) or promoter (Harold et al. 2019), SOX2 induction appears as a potential mechanism by which GLI1 promotes ATOH1-driven MC development. Moreover, impaired ATOH1 degradation by

SHH pathway activation has been previously reported in medulloblastoma (Forget et al. 2014) and might also contribute to MC differentiation in GLI1-expressing cells.

Combined expression of the GLI1 and TAgS led to more pronounced induction of Merkel cell features compared to GLI1 alone. Indeed, a subpopulation of cells expressing the MC markers SOX2, KRT8, KRT18 and KRT20 was induced. Furthermore, in accordance to a previous report describing a population of floating cells with neuroendocrine features upon the ectopic expression of TAgS in fibroblast (Fan et al. 2019), small and floating but still living cells arose from NHEK upon ectopic coexpression of GLI1 and TAgS. Although no proof of transformation was observed in this model, these results demonstrated the ability of MCPyV TAgS to induce a MC-like phenotype in GLI1-expressing epithelial cells.

To further confirm that MCPyV oncogenes impact on MC progenitors, we induced ectopic expression of TAgS in primary human hair follicles (Langan et al. 2015) (Collaboration with Dr. J. Chéret / Prof. R. Paus, Münster, Germany). While this model is highly representative of hair follicle biology, it also harbors evident limitations. First, lentiviral transduction only allowed us to hit the external part of the hair follicle, mainly the infundibular cells. More importantly, the duration of the experiment was restricted to 7 days (Langan et al. 2015) whereas NHEK could be grown for one month. Based on the transgenic mouse models (Perdigoto et al. 2014), acquisition of a MC phenotype is expected to be a long term process, a finding which might explain why expression of KRT8, 18 and 20 was not observed in hair follicle, seven days after transduction. Indeed, ectopic TAgS expression in hair follicle cells induced a population of transformed cells with small cell carcinoma morphology. While no expression of KRT8, 18 and 20 was observed, a partial loss of the other cytokeratins expression was observed in association with sporadic synaptophysin and chromogranin A positivities might indicate first steps of an MC differentiation process.

.

IV. How could the MCPyV T Antigens promote Merkel cell like differentiation?

In situ observations in TB/MCC combined tumors and the phenotypic changes observed upon ectopic TAg expression *in vitro* suggest ability capability of the MCPyV oncoproteins to promote the development of an MC-like phenotype in a specific cellular context. Of note, inactivation of pRB and p53 are well known determinants of neuroendocrine phenotype acquisition in tumors (Gazdar et al. 2017; Klöppel 2017; Meder et al. 2016; Park et al. 2011), therefore targeting of these two tumor suppressor proteins by sT and truncated LT respectively (Houben et al. 2012; Park et al. 2019) might contribute to the neuroendocrine features in MCC. Furthermore Rb1 has been described to affect Atoh1 in intestinal tissue, (Haigis et al. 2006). Accordingly, Fan et al. evidenced an induction of ATOH1 in presence of the TAgS (Fan et al. 2019) and although we did not confirm this finding in HEK293 cells, a slight increase of ATOH1 expression was observed in TAg transduced keratinocytes. Although, pRB1 sequestration by truncated LT might contribute to this process, our experiments revealed that LT antigen additionally affects ATOH1 in a post translational manner by preventing its degradation. Since ATOH1 binds its own enhancer inducing a positive feed-back loop (Bossuyt et al. 2009), stabilization of ATOH1 by LT might also contribute to the high level of expression observed in MCC tumors and cell lines (Fan et al. 2019; Gambichler et al. 2016).

A role of ATOH1 is not restricted to MCs and MCC. In intestinal tissue, central nervous system and development of inner ear, Atoh1 functions to determine a specific cellular phenotype (Forget et al. 2014; Ishibashi et al. 2018; Mulvaney and Dabdoub 2012). In these settings, several translational repressors like the Notch pathway and EZH2, as well as post translational regulation mechanisms have been reported (Cheng 2019; Cheng et al. 2016). Indeed, ATOH1 half-life is regulated by phosphorylation of the C-terminally located serine residues (S331, S337, S342), leading to protein ubiquitination by the ubiquitin ligase HUWE1 (HECT, UBA and WWE domain containing E3 ubiquitin protein ligase 1) and subsequent degradation by the proteasome (Cheng et al. 2016; Forget et al. 2014). Although the residue S337 might be phosphorylated by the Casein kinase 1 (CK1) (Cheng et al. 2016), the kinases recognizing the two other phosphorylation sites are unknown. Our results demonstrate that MCPyV LT stabilizes ATOH1 by affecting this pathway, however whether LT blocks phosphorylation or the subsequent ubiquitination has still to be determined. MCPyV sT has been described to affect cellular protein degradation by interacting with the cellular ubiquitin ligases SCFFbw7.

However this ligase is not expected to be a privileged partner of ATOH1 (Cheng et al. 2016). Moreover, sT was recently identified as an activator of the CK1 transcription which might limit ATOH1 expression (Park et al. 2019). Although interaction of LT with ubiquitin ligases have been demonstrated (Kwun et al. 2017), no direct interaction with HUWE1 has been reported and in our hands co-immunoprecipitation failed to evidence such an interaction.

Interestingly although several lines of evidence suggest that LT can increase ATOH1 protein expression, a possible contribution of ATOH1 to tumor behavior is unclear. While Bossuyt et al. described ATOH1 as a tumor suppressor protein (Bossuyt et al. 2009), Gambichler observed an increased expression in advanced cases (Gambichler et al. 2016) and inactivation of ATOH1 seems to not affect MCC tumor cell proliferation *in vitro* (Fan et al. 2019). Interestingly in medulloblastoma and colonic carcinoma, Atoh1 promotes metastatic spreading and progression (Grausam et al. 2017) (Ishibashi et al. 2018). Therefore, evaluation of the impact of ATOH1 knock-down *in vivo* in a mouse model of MCC would be of interest.

CONCLUSION

According to the current WHO classification, MCC is the “eponym name of primary neuroendocrine carcinoma of the skin” and MCPyV as well as UV-radiations are regarded as two different etiologic factors for this tumor entity. However, the current works and recent data from the literature clearly demonstrate that MCPyV-negative MCC are highly similar to extracutaneous NEC while MCPyV-positive MCCs differ from both groups with respect to morphology, immunohistochemical profile, genetics, origin and behavior.

Indeed, morphological features of MCPyV-positive tumor cells are evocative of a neoplasia driven by a unique genetic alteration whereas more typical eNEC features are displayed by MCPyV-negative MCC. Using immunohistochemistry, MCPyV-negative cases are hardly distinguishable from eNEC whereas MCPyV-positive cases displays distinct features including more prominent expression of the MCs markers. In light of our results, it seems worth to reconsider Boyd’s statement that “rare cancers have been divided into two groups: cancers defined by their unusual histogenesis (cell of origin or differentiation state) or histologically defined subtypes of common cancers”. Indeed, inclusion of MCPyV-negative MCC i.e. neuroendocrine skin carcinoma in the second category is justified by the similarities with eNEC. By contrast, MCPyV-positive MCC, in our view, belongs to the first group i.e. tumors with unusual histology, due to a distinct very characteristic MC differentiation. In line with such considerations, Boyd also pointed out that “genomic investigation has led to the discovery of pathognomonic (i.e. defining) mutations in many of the cancers defined in the pre-molecular era by unusual histogenesis” (Boyd et al. 2016). In this respect, MCPyV genomic integration has to be considered as defining genetic alteration for MCPyV-positive MCC.

In addition, the two MCC subsets are likely to differ with respect to the cell of origin. In the present work, we provide clear evidence that MCPyV can arise from an epithelial cell. The detailed genetic analysis of a combined tumor comprising a TB and a MCPyV-positive MCC part demonstrated that the MCC derived from a TB cell following integration of a mutated MCPyV genome into the genome of the host cell. Because of the close similarity of TB cells with germinative cells from the hair follicle which can give rise to Merkel cells, our observation suggests that MCC generally develops from cells of the MC lineage. Candidates are either

already differentiated MCs or the hair follicle MC progenitor cells. Although alternative ancestries cannot formerly be excluded by our results, they appear unlikely in light of the “lineage-addiction” concept, which suggests that the capability of the MCPyV oncoproteins to induce MCC is restricted to a specific cellular context. In line with a scenario in which MCPyV hits a cell with MC differentiation potential and drives the development of an MC-like phenotype, we provide *in vitro* data demonstrating that TAgS can induce MC-markers and repress markers of MC progenitor cells when overexpressed in epithelial cells. Furthermore, we demonstrate that MCPyV LT is able to stabilize the transcription factor ATOH1 which is known to be the master regulator of MC differentiation. This might be one of the biological mechanisms contributing to the characteristic phenotype of MCPyV-positive MCC.

Observation of combined MCC tumors also appears helpful to determine the origin of the MCPyV-negative subset. Indeed, our observations as well as data provided by others suggest that MCPyV-negative cases frequently arise from an already neoplastic cell in the epidermis. In such a scenario of multistep carcinogenesis, accumulation of genetic alterations over the time would finally lead to the acquisition of a neuroendocrine phenotype in parallel with an increase in tumor aggressiveness.

Although mainly of importance for basic science, determination of the cell of origin provides also research opportunities, which might contribute to improved patient’s management. Indeed, immunotherapy is actually the gold standard for patients with unresectable metastatic MCC, resulting in a clear survival benefit (Samimi 2019). However, in about 40% of the cases the tumors do not respond to these treatments and sustained response is only observed in half of the patients with initial tumor regression (Kaufman et al. 2018; Samimi 2019). Therefore, development of new therapeutic options remains of high priority, and establishment of an immunocompetent MCC mouse model - requiring knowledge on the cell of origin - would be very useful for preclinical evaluation of new therapeutic approaches.

SUPPLEMENTS: OTHER PUBLICATIONS OF THE CANDIDATE DURING THE PhD

Histogenesis of Merkel Cell Carcinoma: A Comprehensive Review.

VEGF-A Inhibition as a Potential Therapeutic Approach in Merkel Cell Carcinoma.

Merkel cell carcinomas infiltrated with CD33(+) myeloid cells and CD8(+) T cells are associated with improved outcome.



Histogenesis of Merkel Cell Carcinoma: A Comprehensive Review

Thibault Kervarrec^{1,2,3}, Mahtab Samimi^{2,4}, Serge Guyétant^{1,2}, Bhavishya Sarma³, Jérémy Chéret⁵, Emmanuelle Blanchard^{1,6}, Patricia Berthon², David Schrama³, Roland Houben³ and Antoine Touzé^{2*}

¹ Department of Pathology, Centre Hospitalier Universitaire de Tours, Tours, France, ² ISP "Biologie des infections à polyomavirus" team, UMR INRA 1282, University of Tours, Tours, France, ³ Department of Dermatology, Venereology and Allergology, University Hospital Würzburg, Würzburg, Germany, ⁴ Departement of Dermatology, Centre Hospitalier Universitaire de Tours, Tours, France, ⁵ Monasterium Laboratory, Skin and Hair Research Solutions GmbH, Münster, Germany, ⁶ Plateforme IBISA de Microscopie Electronique, INSERM 1259, Université de Tours, Tours, France

OPEN ACCESS

Edited by:

Axel zur Hausen,
Maastricht University Medical
Centre, Netherlands

Reviewed by:

Giuseppe Palma,
National Cancer Institute G. Pascale
Foundation (IRCCS), Italy
Anca Maria Cimpean,
Victor Babes University of Medicine
and Pharmacy, Romania

*Correspondence:

Antoine Touzé
antoine.touze@univ-tours.fr

Specialty section:

This article was submitted to
Molecular and Cellular Oncology,
a section of the journal
Frontiers in Oncology

Received: 07 December 2018

Accepted: 13 May 2019

Published: 10 June 2019

Citation:

Kervarrec T, Samimi M, Guyétant S,
Sarma B, Chéret J, Blanchard E,
Berthon P, Schrama D, Houben R and
Touzé A (2019) Histogenesis of Merkel
Cell Carcinoma: A Comprehensive
Review. *Front. Oncol.* 9:451.
doi: 10.3389/fonc.2019.00451

Merkel cell carcinoma (MCC) is a primary neuroendocrine carcinoma of the skin. This neoplasia features aggressive behavior, resulting in a 5-year overall survival rate of 40%. In 2008, Feng et al. identified Merkel cell polyomavirus (MCPyV) integration into the host genome as the main event leading to MCC oncogenesis. However, despite identification of this crucial viral oncogenic trigger, the nature of the cell in which MCC oncogenesis occurs is actually unknown. In fact, several hypotheses have been proposed. Despite the large similarity in phenotype features between MCC tumor cells and physiological Merkel cells (MCs), a specialized subpopulation of the epidermis acting as mechanoreceptor of the skin, several points argue against the hypothesis that MCC derives directly from MCs. Alternatively, MCPyV integration could occur in another cell type and induce acquisition of an MC-like phenotype. Accordingly, an epithelial as well as a fibroblastic or B-cell origin of MCC has been proposed mainly based on phenotype similarities shared by MCC and these potential ancestries. The aim of this present review is to provide a comprehensive review of the current knowledge of the histogenesis of MCC.

Keywords: merkel cell polyomavirus (MCPyV), epithelial, fibroblast, B cell, Merkel cell carcinoma (MCC), histogenesis, origin

INTRODUCTION

Merkel cell carcinoma (MCC) is an aggressive neoplasm defined as a primary neuroendocrine carcinoma of the skin. The incidence is still low, with for example 0.7 cases per 100,000 person-years in the United States in 2013, but has increased by 95% from 2000 to 2013, and a further increase in incidence has been predicted (1). MCC occurs essentially in older people, with known risk factors being sun exposure (2) and immunosuppression (3, 4). MCC is characterized by aggressive behavior resulting in a 5-year overall survival rate of 40% (5). Combined radiotherapy and surgery is considered the mainstay of treatment for patients with localized disease, but until recently, those with advanced, inoperable disease received various regimens of cytotoxic chemotherapy, without a significant effect on survival (6). Recently, restoration of T-cell responses by inhibitors targeting programmed cell death 1 (PD-1) and its ligand (PD-L1) checkpoints has been identified as an effective approach in such patients (7). Indeed, after failure of first-line chemotherapy, treatment

with avelumab resulted in objective tumoral responses in 32% of MCC patients with advanced disease (7), and avelumab has been approved for advanced MCC both in the United States and European Union (7, 8). Avelumab is being investigated as first-line therapy in this setting, with objective responses in approximately 60% of patients in preliminary reports (9).

MCC is diagnosed on the basis of histological examination, which reveals infiltration of the dermis or hypodermis by proliferating tumor cells harboring high-grade neuroendocrine carcinoma features (10) (**Figure 1**). Blastic lymphomas as well as other small round blue cell tumors must be considered in the differential diagnosis. Immunohistochemical investigation of MCC cases (**Figure 1**) reveals the expression of both epithelial (pancytokeratin AE1/AE3) and neuroendocrine markers such as chromogranin A (11), synaptophysin (11), CD56 (10) and INSM1 (insulinoma-associated 1) (12). In addition, the combination of cytokeratin 20 (CK20) positivity with thyroid transcription factor-1 negativity (13) is currently used to distinguish MCC from other metastatic neuroendocrine carcinomas. Neurofilament and special AT-rich sequence-binding protein 2 (SATB2) have been proposed as additional markers providing high diagnostic accuracy (14, 15).

Significant progress in understanding the MCC pathogenesis occurred in 2008, when Feng et al. reported a yet undescribed virus, the Merkel cell polyomavirus (MCPyV), whose genome was integrated in 80% of MCC tumors (16). MCPyV was further found to be an ubiquitous virus responsible for an asymptomatic life-long infection, because the episomal genome of MCPyV can be detected in the skin flora of most healthy people (17) and antibodies directed against the viral capsid are highly prevalent in the general population (18, 19).

Despite the high population prevalence of MCPyV, viral integration probably occurs very rarely, which accounts for the rarity of MCC tumors, and constitutes the main oncogenic event leading to MCC oncogenesis. MCPyV integration together with mutations of the viral sequence (20) result in loss of replicative abilities of the virus before MCC development. As a consequence, MCPyV-positive MCC tumors do not produce MCPyV virions but are characterized by permanent nuclear expression of the viral T-antigen proteins (small T [sT] and large T [LT] antigen in a truncated form). Both sT and LT antigens bear oncogenic properties, by targeting various host cell proteins involved in cell cycle control and proliferation, and are now considered as the key actors of oncogenesis in MCPyV-positive MCC (21). By contrast, MCPyV-negative MCC, which accounts for approximately 20% of MCC cases, have a high mutational burdens, with a prominent UV signature, which affects various oncogenes. Among these, mutations of the tumor suppressor genes *RBI* and *TP53* appear to be critical oncogenic events (22).

Despite identification of both viral and UV-induced oncogenic triggers in MCC, the nature of the cell where MCC oncogenesis occurs remains unknown (23). Actually, several hypotheses have been advanced. The aim of this article is to provide a comprehensive review of current knowledge of the histogenesis of MCC.

The Merkel Cell: the Historical Candidate

According to Boyd et al. rare cancer types identified before the molecular biology era were “either tumors presumed to originate from or resemble a cell type that infrequently gave rise to cancer, or histologically defined subsets within a more common type of cancer” (24). MCC, a perfect illustration of the first group, was classified according to its similarities with skin physiological Merkel cells (MCs). MCs are highly specialized epithelial cells located in the basal layer of the epidermis and in the external part of the hair follicle (**Figure 2**). They have been shown to act as mechanoreceptors by transforming tactile stimuli into Ca^{2+} -action potentials (25) and serotonin release (26) and pass these signals on to $A\beta$ -afferent nerve endings. The protein allowing transformation of mechanic into electric signals is the ion channel Piezo2 (25), which is also highly expressed by MCC cells [(27), unpublished data]. Expression of this MC-characteristic molecule is only one of many features shared by MCs and MCC cells. Originally described as “trabecular carcinomas of the skin” by Toker (28), ultrastructural studies of such cases revealed numerous neuroendocrine dense cores neuroendocrine granules, which are hallmarks of MCs (28, 29) (**Figure 2**). Hence, these “trabecular carcinomas” were suggested to derive from MCs, leading to their reclassification as MCC (29). Further immunohistochemical studies corroborated these initial findings by revealing a shared expression of many common markers in MCs and MCC (10, 30) but only a limited number of markers distinguishing them from each other (**Table 1**; **Figures 1, 2**). Indeed, both MCs and MCC express cytokeratin 20 (CK20) (13, 15, 31), neuroendocrine markers chromogranin A and synaptophysin (11, 37) and neuropeptides (30, 47). In contrast, the expression of vasoactive intestinal peptide and metenkephalin (44) are specific to MCs, whereas CD117 and CD171 are detected in only MCC cells (49, 61).

Despite the large similarity in phenotypic features, several points argue against MCC deriving directly from MCs. First, in other organs such as lung, strong data suggest that neuroendocrine carcinoma derives more from epithelial progenitors rather than an neuroendocrine cell (66, 67). Second, MCs are mainly post-mitotic cells (31) and thus have low sensitivity to oncogenic stimuli. Accordingly, ectopic expression of sT antigen in MCs failed to induce cell proliferation or transformation in a transgenic mouse model (68). Of note, hyperplasia of MCs as well as mitotic activity in keratin 20-positive cells has been reported in pathologic conditions (69, 70); however, whether these observations are due to proliferation of already differentiated MCs or MC precursor cells is still unclear. Third, MCs are most frequently present in the palm and sole in humans (71, 72), whereas MCC occurs mainly in sun-exposed areas [head and neck, legs (2, 73)]. Moreover, no infection of MCs by MCPyV has been reported (74). Finally, in an *in vitro* model, MCPyV pseudovirions could barely infect CK20-positive cells obtained from the fetal scalp (0.8%) (75), which argues against an efficient MCPyV infection triggering MCC oncogenesis in an already differentiated MC.

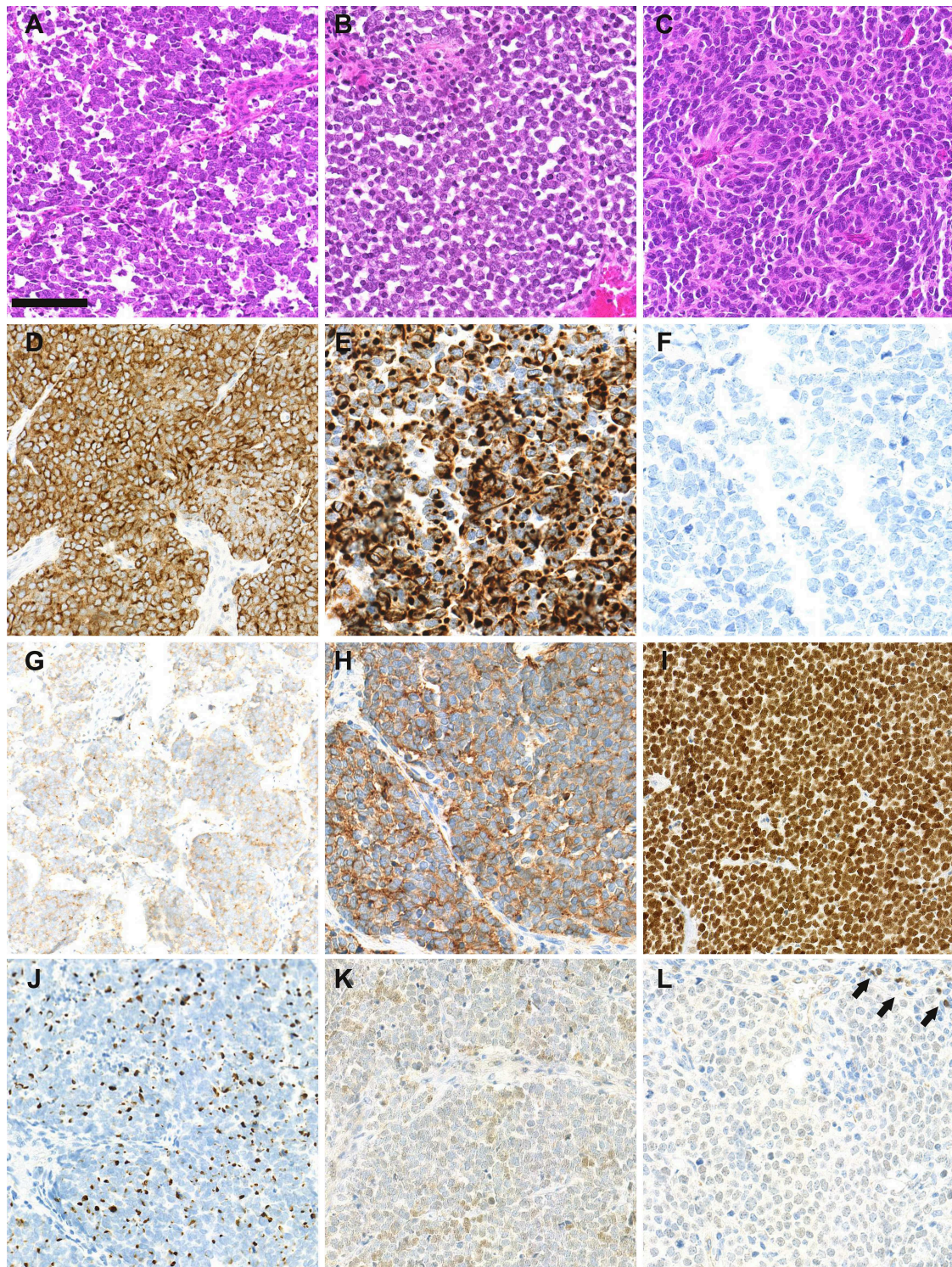


FIGURE 1 | Morphological and immunohistochemical features of Merkel cell carcinoma: **(A–C)**: hematein-phloxin-saffron staining revealed sheet of tumor cells with high mitotic activity (bar = 100 μ m). Whereas, MCPyV-positive MCC **(A,B)** harbor scant cytoplasm, round nucleus and dusty chromatin, MCPyV negative tumor cells have more abundant clear cytoplasm and irregular nucleus **(C)**. **(D)** chromogranin A cytoplasmic positivity, **(E)** cytokeratin 20 expression with paranuclear dot-pattern; **(F)** thyroid transcription factor-1 negativity; **(G)** membranous synaptophysin expression; **(H)** membranous CD56 expression; **(I)** special AT-rich sequence-binding protein 2 (SATB2) nuclear expression; **(J)** neurofilament expression with a dot-pattern; **(K)** terminal deoxy nucleotidyl transferase weak/moderate expression, **(L)** paired box 5 weak expression in tumor cells in comparison with intratumor lymphocytes (arrows).

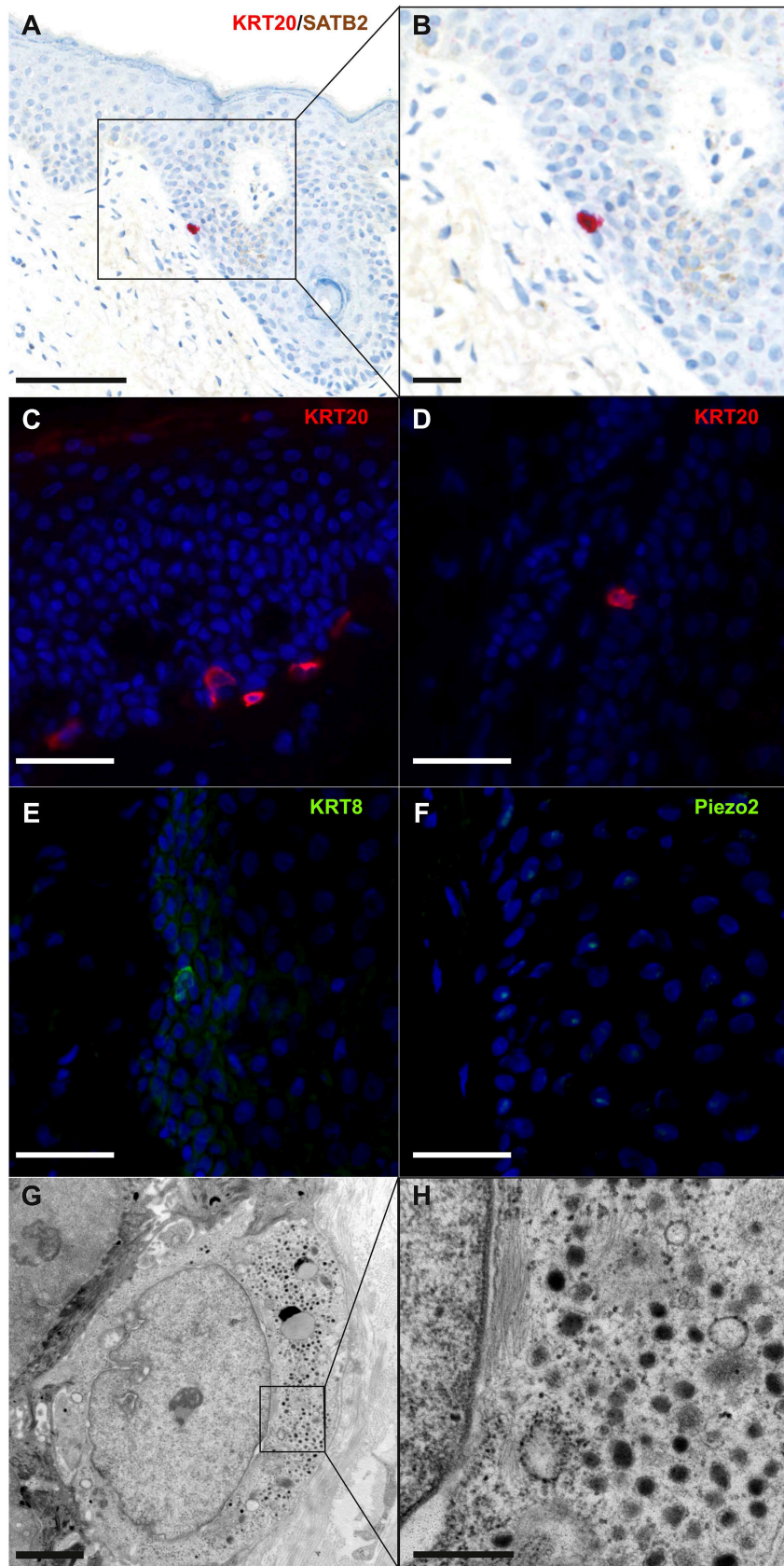


FIGURE 2 | Continued.

FIGURE 2 | Immunohistochemical and ultrastructural features of physiological Merkel cells: immunohistochemical staining of normal skin (**A,B**) revealed one Merkel cell located in the infundibulum of a hair follicle and coexpressing cytokeratin 20 (cytoplasmic expression in red) and SATB2 (nuclear expression in brown) (bar = 100 and 50 μm for **A,B**). Immunofluorescence staining of healthy skin revealed some Merkel cells expressing cytokeratin 20 (**C,D**), cytokeratin 8 (**E**) and Piezo2 (**F**) in the epidermis (**C**) and in hair follicles (**D–F**) (bar = 40 μm for **C–F**). Electron microscopy of a Merkel cell (**G,H**) revealed numerous dense-core granules (bars = 2 and 0.5 μm for **G,H**, respectively). A cropped region is shown in the inset (**H**).

Putative Mechanism of a “Non-MC” Origin for MCC

The tumor classification system is based on tumor differentiation and should not be considered a direct indicator of tumor histogenesis (76). Indeed, several phenotypic changes occurring during the oncogenic process contribute to the final differentiation profile of tumor cells, which consequently differ from the primary cell in which the first oncogenic event took place (76). Accordingly, acquisition of an MC-like phenotype including neuroendocrine differentiation (77) during MCC oncogenesis could explain the similarities between MCs and MCC (23). In MCC, both UV and virus-induced oncogenic triggers are thought to act on shared molecular pathways, accounting for the similar phenotype between MCPyV-positive and -negative tumors (78). In this respect, disruption of pRB function occurs by somatic mutations and repression of protein expression in virus-negative tumors (22), whereas sequestration by MCPyV LT antigen inactivates pRB1 in virus-positive MCC cells (79). Interestingly, disruption of this pathway has been identified as a main contributor driving acquisition of a neuroendocrine phenotype in tumors of other organs (80–82).

In the skin, MC differentiation occurs in specific epithelial precursors upon expression of one main transcription factor, atonal homolog 1 (ATOH1) (31). Under physiologic conditions, ATOH1 expression in the skin is restricted to MCs (31). Because ATOH1 is also observed in MCC, its expression could explain the shared phenotype between MCs and MCC (83). Moreover, genetic ablation of Rb1 and the related Rb-family protein p130 in the intestinal epithelium in a mouse model led to increased expression of Atoh1 (84), which suggests that Atoh1 induction could occur during an oncogenic process associated with Rb inactivation.

Considering these findings, a non-MC could also be candidate for the ancestry of MCC, and an epithelial non-MC as well as a fibroblastic and B-cell origin has been proposed (Figure 3; Table 2).

A Non-MC Epithelial Origin

For quite some time it has been a matter to debate whether MCs derive from the neural crest or epidermal lineage. Of note both neural crest and epidermal lineages derived from the same embryologic structure and this common ectodermal origin might explain the mixed phenotype observed in Merkel cell. Indeed, ultrastructural studies of MC revealed on the one hand intracytoplasmic neuroendocrine granules suggesting a neural crest origin (85) and on the other hand frequent desmosomes and cytokeratins, two hallmarks of the epithelial subset (86). Accordingly, also immunohistochemistry demonstrated both expression of “neural crest” as well as epithelial markers

(Table 1). Although the neural crest origin hypothesis was additionally supported by chimeric chicken/quail models (87, 88), xenograft of human fetal skin free of neural crest progenitors in immunocompromised mice led to the development of human Merkel cell suggesting an epidermal origin of this population (89).

An epithelial origin of Merkel cells in mammals was finally demonstrated in 2009 by two consecutive transgenic mouse studies (31, 90). In both studies it was shown that deletion of *Atoh1* in epidermal progenitors resulted in a complete absence of MCs. Additionally, Morrison and colleagues demonstrated that *Atoh1* deletion in the neural crest lineage did not affect the MC population (90).

Additional studies in mice models revealed that MC phenotype acquisition upon *Atoh1* expression seems to be restricted to a specific subpopulation of keratinocyte progenitors characterized by an activated Sonic Hedgehog pathway (91, 92). Indeed, *Atoh1* expression failed to induce MC differentiation in other keratinocyte populations (31) and gave rise to distinct differentiation in other cell types (93–95).

A thorough characterization of the MC progenitor population in humans is still missing (96). Therefore, our current knowledge of this cellular subset is mainly based on findings in mice, in which cells bearing MC differentiation potential are mainly located in the outer root sheath and bulge region of the hair follicle (97, 98) but are also present in the interfollicular epidermis in specialized structures called touch domes (92). Interestingly, these hair follicle- and touch- dome-derived stem cells have been found as preferentially the origin of basal cell carcinomas (99). Therefore, their ability to acquire an MC phenotype and to proliferate, as well as their high sensitivity to oncogenic stimuli, should promote their transformation into MCC, rendering them likely candidates as cells of origin. Of note, MCC developing within follicular cysts (100) as well as preferential MCPyV infection of the dermal cells around hair follicles (75) support MCPyV(+) MCC as being derived from hair follicles.

A hair-follicle origin of MCC would also weaken one argument frequently used against an epithelial origin of MCC. Because MCC cells are mostly found in the dermis and subcutis lacking a connection to the epidermis, an epidermal origin is unlikely (62). However, some appendage tumors such as trichoblastoma and spiradenoma (101, 102) are well known to lack an epidermal connection (10).

The observation of so-called combined MCC or MCC with divergent differentiation further supports an epithelial origin of MCC. Combined MCC represents 5 to 10% of cases and is characterized by the association of an MCC component with a tumor of another differentiation lineage (103–105). Although several divergent additional components have been described

TABLE 1 | Markers expressed by physiological Merkel cells and Merkel cell carcinoma.

Markers	Merkel cells	Merkel cell carcinoma
EPITHELIAL MARKERS		
Cytokeratin 20	+(31, 32)	+(10, 15)
Cytokeratin 8	+(31, 32)	+(33)
Cytokeratin 18	+(31, 32)	+(34, 35)
β1 integrin	+(36)	
LRIG1	+(36)	
CSPG4	+(36)	
NEUROENDOCRINE MARKERS		
Chromogranin A	+(37, 38)	+(10, 11)
Synaptophysin	+(37, 38)	+(10, 11)
CD56	+(39, 40)	+(10, 41)
ISL1	+(42)	+(43)
INSM1	Lacking data	+(12)
Vasoactive intestinal peptide	+(44, 45)	-(44, 45)
Metenkephalin	+(44, 45)	-(44, 45)
MAO A and B	+(46)	Lacking data
NEUROGENIC/ MECHANORECEPTOR MARKERS		
Neuropeptides	+(30)	+(47)
Neurofilament	-(48)+	+(14, 15)
CD171	-(49)	+(49)
SATB2	+(50)	+(15, 50)
PIEZO2	+(38)	+(unpublished data)
PGP9.5	+(51)	+(52, 53)
SOX2	+(42)	+(54, 55)
WNT1	+(56)	Lacking data
TUBB3	+(51)	+(57)
p75NTR	+(58)	Lacking data
TrkC	+(58)	Lacking data
NT-3	+(58)	Lacking data
Advillin	+(59)	Lacking data
B CELL MARKERS		
CD117 (c-KIT)	-(60)	+(61)
PAX5	Lacking data	+(15, 62, 63)
TDT	Lacking data	+(15, 62, 63)
Immunoglobulins	Lacking data	+(64, 65)

(+), positivity of the marker; (-), negativity of the marker; CSPG4, chondroitin sulfate proteoglycan 4; INSM1, insulinoma associated 1; ISL1, Islet-1; LRIG1, leucine rich repeats and immunoglobulin like domains 1; MAO, monoamine oxidase; NT-3, neurotrophin 3; p75NTR, neurotrophin receptor p75; PAX5, paired box 5; PGP9.5, ubiquitin C-terminal hydrolase L1; SATB2, special AT-rich sequence binding site 2; SOX2, SRY-box2; TDT, terminal deoxynucleotidyltransferase; TRKC, neurotrophic tyrosine kinase receptor type 3; TUBB3, tubulin beta 3 class III; WNT1, Wnt family member 1.

(sarcomatous, adnexal) (104, 106), MCC is most frequently found associated with squamous/eccrine carcinoma (105, 107) (Figure 4). For individual cases, the same genetic alterations have been reported for both components, which implies a common progenitor (108), whereas other cases gave proof of a collision tumor (109). Furthermore, similar aberrant p53 expression is frequently observed in both components of combined MCC (105). In some combined MCC cases, intra-epidermal neoplasia

such as actinic keratosis or Bowen's disease (107) was detected close to the squamous cell carcinoma component. Bowen's disease originates from the epidermis, and invasive squamous cell carcinoma can derive from Bowen's disease; hence, the clonality between squamous cell carcinoma and the MCC component (108) favors an epidermal origin of MCC (97). Of note, the hyperplasia of MCs in the squamous cell carcinoma component of combined tumors (70) might suggest that such components contain precursors with the ability to acquire an MC phenotype.

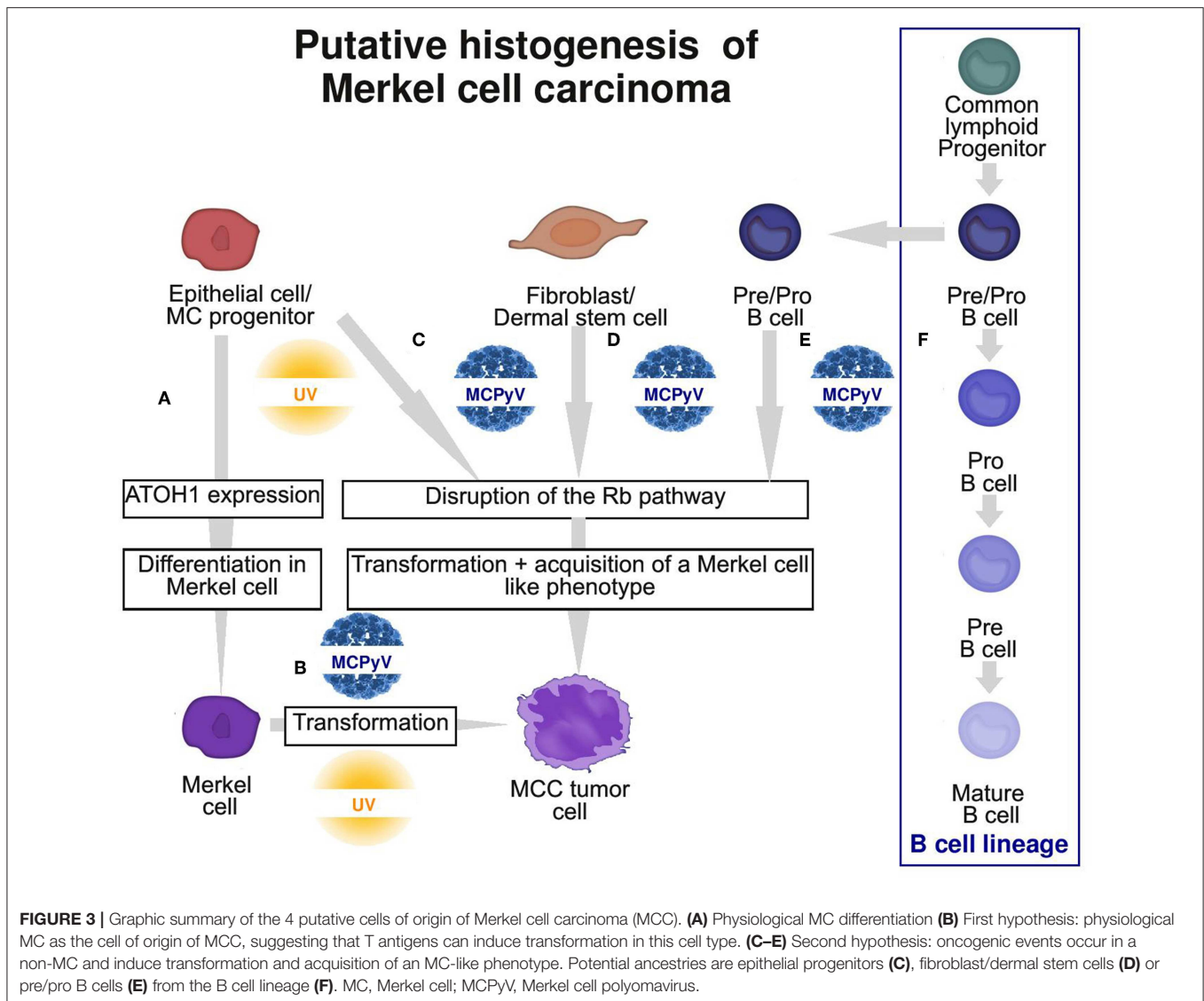
Importantly, such combined cases have been described to be usually typical UV-induced MCCs, harboring morphologic and immunohistochemical features distinct from MCPyV-positive MCC and high mutational load (104, 106, 108) as depicted in Table 3. Of note low viral load of MCPyV in some cases is probably related to an episomal viral genome present in the skin (105). In our experience [(118), Figure 4], rare cases of MCC with intra-epidermal involvement [2% in our previously reported cohort (73)] are also related to the UV-induced subset. Hence, although combined cases imply that MCPyV-negative cases derive from some epidermal progenitors of the interfollicular epidermis, they provide no information about MCPyV-induced tumors (119).

In agreement with this observation, Sunshine et al. hypothesized that there might be two different cells of origin for the two MCC subtypes (119). They provided several arguments for this conclusion. For example while the UV-mutation signature of virus-negative MCC favors an epidermal origin the failure of epidermis targeted TA-expression to produce tumors resembling human MCC in mouse models (68, 120, 121) suggests that other cells in the skin such as dermal fibroblast may serve as origin of MCC (119). Since both UV- and virus-induced MCC occur in sun-exposed areas where frequent UV-induced mutations are observed in keratinocytes (122), but only MCPyV-negative cases are characterized by high mutational load and UV signature (22, 119) Sunshine and colleagues excluded an epithelial and instead proposed a fibroblastic origin of MCPyV(+) MCC (119). However, low mutational burden as well as lack of UV-signature in MCPyV(+) MCC might also be explained by MCPyV integration into a cell from the hair follicle which like dermal fibroblasts is located deeper in the skin than normal epidermal keratinocytes.

In conclusion and acting on the assumption that MCC generally has an epithelial origin, one could speculate that UV-induced MCC derives from a keratinocytic progenitor from the interfollicular epidermis that acquires the ability to differentiate into MCs during the oncogenic process, whereas MCPyV-driven oncogenesis is initiated in a progenitor from a hair follicle.

A Fibroblastic Origin

Another hypothesis is MCC developing from fibroblastic cells. This hypothesis might account for the quasi-exclusive dermal location of MCC, discussed above. Furthermore, the fibroblastic origin of MCCs would be consistent with our knowledge of the MCPyV cycle because fibroblasts of the papillary dermis have



been identified as the main site of replicative MCPyV infection (75). Although infectious MCPyV particles can enter several cell types including keratinocytes with various efficiency rates (75, 123), fibroblasts remain the only host cell evidencing early and late viral protein expression. One could argue that replication and transformation can occur in independent cell types, as was previously demonstrated for polyomavirus SV40 (124); however, the ability of fibroblasts to allow replication of the MCPyV genome increases the likelihood of accidental integration of the viral genome. Moreover, the *in vitro* transforming potential of sT antigen has until now been demonstrated only in fibroblasts (68, 124, 125). Notably, ectopic expression of SV40T antigens in fibroblastic cells (126) triggered the induction of cytokeratin expression, which suggests that polyomavirus infection can influence a differentiation lineage. In such a setting, acquisition of an MCC phenotype induced by viral protein expression could require a transient pluripotent stage. Indeed, fibroblasts are widely used for reprogramming to pluripotent cells. The resulting induced pluripotent stem cells (127) can be differentiated into

epithelial cells *in vitro*. Furthermore, physiological stem cells of the papillar dermis [i.e., dermal skin precursors or skin-derived precursors (128)] share phenotypic similarities with induced pluripotent stem cells, such as expression of the stem cell factors *c-Myc* and *Sox2* (129), two markers also expressed by MCC (54, 130). These dermal skin precursors are able to differentiate into epithelial or neuronal cells *in vitro*. Hence, because of the close proximity of these cells to dermal fibroblasts, which can support productive MCPyV infection (75), as well as their expression of pluripotent factors and their differentiation abilities, MCPyV integration in such cells could lead to MCC oncogenesis and acquisition of an MCC phenotype.

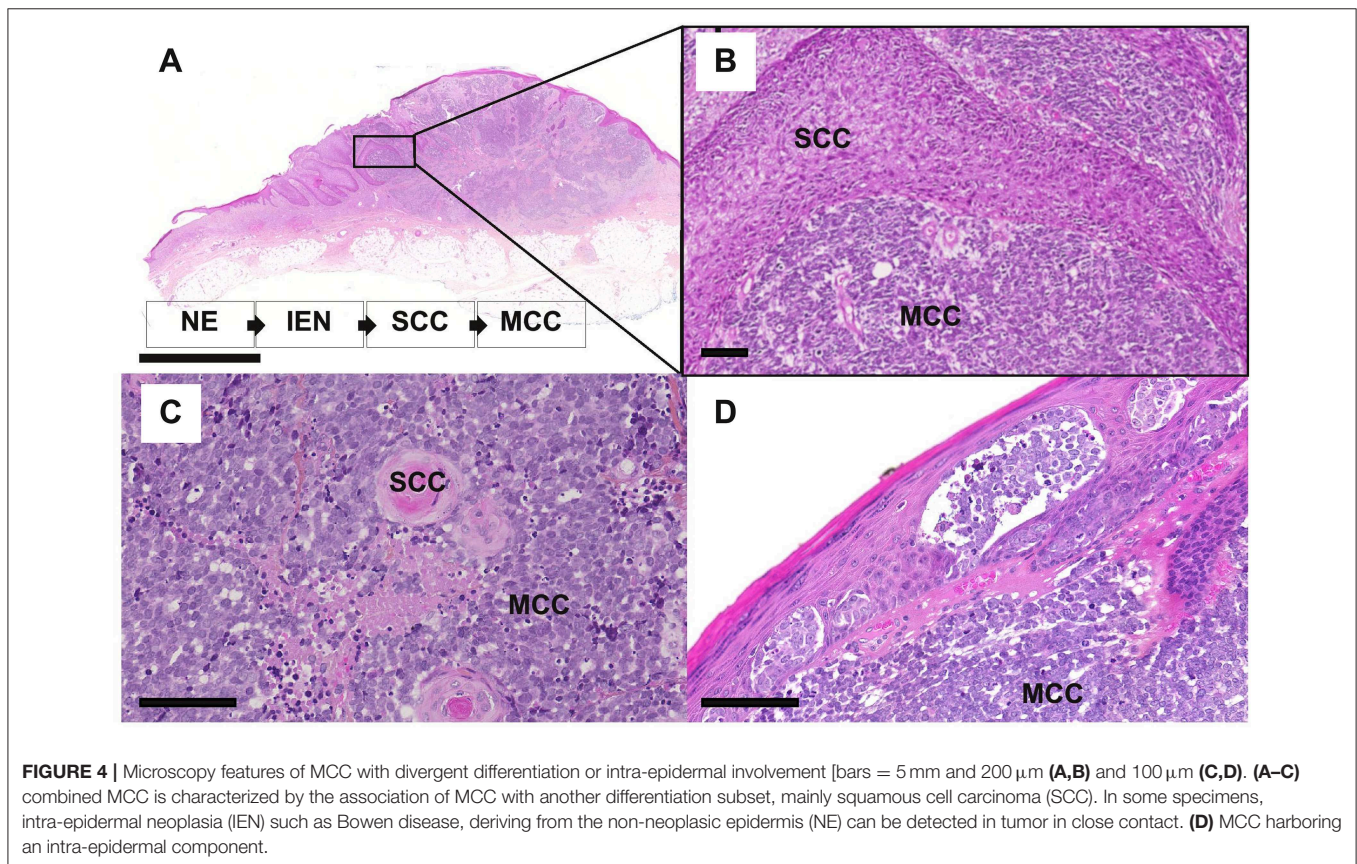
A Pre/Pro or Pre-B-Cell Origin

Because of the recurrent association between MCC and B-cell neoplasias (131–134) as well as phenotypic similarities and the occasional integration of MCPyV in hematopoietic cells, a lymphoid pre/pro B-cell origin is also discussed (62, 64).

TABLE 2 | Pros and cons of current hypotheses for the potential cell of origin of Merkel cell carcinoma (MCC).

Candidate	Pros	Cons
Merkel cell	Phenotypic similarities: (immunohistochemical profile: CK8, CK18, CK20 + neuroendocrine markers+ultrastructural findings)	No mitotic activity No demonstrated MCPyV demonstration No transformation by MCPyV antigens Lack of epidermal connection in almost all MCC cases
Epithelial progenitor	Ability to differentiate into Merkel cells Ability to generate combined MCC Most probable origin of neuroendocrine carcinoma in other sites	Exclusive dermal/hypodermal location of MCC No UV signature Lack of epidermal connection in almost all MCC cases
Fibroblast and dermal stem cell	Site of replication of the MCPyV Ability of MCPyV antigens to induce transformation in these cell types Presence of SKP with reprogramming abilities	No proof of the ability of fibroblasts to acquire an MC-like phenotype Unexpected origin for a neuroendocrine carcinoma
Pre/pro B cell	Epidemiologic association between MCC and B-cell neoplasia Co-expression of B-cell markers (PAX5, TdT and Immunoglobulins) Detection of MCPyV integration in B-cell neoplasia	No proof of the ability of B cells to acquire an MC-like phenotype Unexpected origin for a neuroendocrine carcinoma

MC, Merkel cell; MCPyV, Merkel cell polyomavirus; SKP, skin-derived precursors.



Indeed, chronic lymphocytic leukemia is the most frequent neoplasia associated with MCC development. Whether this is due to a common transforming event or the first tumor creating an immunological microenvironment facilitating the development of the second tumor or merely due to both tumors

appearing in older immunocompromised subject has yet to be determined (131).

Moreover, MCC shares morphological features with other small round blue cell tumors, which explains why B-cell neoplasia must be considered a differential diagnosis of MCC. In addition,

TABLE 3 | Distinct features of MCPyV-positive and -negative MCC cases.

Features	MCPyV(+) Merkel cell carcinoma	MCPyV(-) Merkel cell carcinoma
MORPHOLOGY		
Nucleus	Round (110, 111)	Irregular/spindle (110, 111)
Cytoplasm	Few (110, 111)	More abundant (110, 111)
Divergent differentiation	No (103, 104)	Yes (103, 104)
IMMUNOHISTOCHEMICAL MARKERS		
CK20	+(112, 113)	+/(112, 113)
CK7	-(112)	+/(112)
TTF1	-(112, 114)	+/(112, 114)
Neurofilament	+(14, 106, 112)	+/(14, 106, 112)
Oncogenic triggers	MCPyV T antigens (16, 68, 79, 115)	UV induced genetic alteration (22, 116, 117)
Mutation load	Low (22, 116, 117)	High (22, 116, 117)

(+), frequent positivity of the marker; (-), frequent negativity of the marker; (+/-) increased or decrease expression frequency of this marker compared to the MCPyV(+) subset. Compared to the MCPyV-positive MCC cells MCPyV-negative MCC tumor cells have been described to harbor more irregular nuclei, more abundant cytoplasm and display more frequently so called divergent differentiation.. Moreover, MCPyV-negative cases are characterized by an specific immunohistochemical profile with frequent lack of expression of CK20 and neurofilaments, and more frequent positivity for TTF1 and CK7. Finally, very high mutational burden with UV signature are observed only in MCPyV-negative cases.

the coexpression of terminal deoxy nucleotidyl transferase (TdT), paired box 5 (Pax5) and immunoglobulin chains, all markers expressed during B-cell differentiation, has been observed in MCC tumors (62, 64). Initially, the frequency of TdT and Pax5 positivity was reported to be about 65% ($N = 187$) and 90% ($N = 143$) of MCC cases (64); however, recently observed rates were lower, 26% ($N = 217$) or 23% ($N = 213$) (15, 63). Of note, expression of immunoglobulin chains was restricted to the MCPyV(+) subset and detected in about 70% of cases (65). In addition, rare observations of MCC cases with monoclonal immunoglobulin rearrangement of heavy chain as well as monoclonal expression of Kappa light chain were reported (62, 65). As already discussed, determination of the histogenesis based on phenotype similarities between terminally differentiated tumor and physiological cells does not account for phenotypic changes during oncogenesis (76). In this regard, induction of immunoglobulin expression during the oncogenic process has been reported for several epithelial and soft-tissue neoplasias (135, 136) and may contribute to tumor aggressiveness (137). Furthermore, immunoglobulin rearrangement due to the expression of essential enzymes required for gene rearrangement and class switch recombination has been described in non-hematopoietic neoplasia (136). Hence, immunoglobulin expression and rearrangement might result from the oncogenic process, and their occurrence in MCC cannot rule out a non-lymphoid cell origin. Induction of immunoglobulin expression in epithelial cells has been reported to result from Epstein-Barr virus infection (138) and was also observed in papillomavirus-induced neoplasia (139).

These findings, combined with the exclusive expression of immunoglobulins in MCPyV(+) MCC, led Murakami and colleagues to hypothesize that the immunoglobulin expression in MCC cells is induced by MCPyV oncoproteins (65). In the same manner, the concomitant expression of TdT and Pax5 is restricted to immature B cells and thymocytes under physiological conditions (140) and is also observed in MCC. While co-expression have not yet been described positivity of one of these markers has also been demonstrated in several epithelial neoplasias (141, 142), which indicates that these markers can be acquired during the oncogenic process. Moreover, MCPyV genome integration (143) associated with a deletion leading to a truncated LT antigen (144), the two hallmarks of MCC oncogenesis, have been evidenced in some cases of chronic lymphocytic leukemia and tropism of other tumor viruses for the Pre-Pro B cells has been previously emphasized (145). Although these findings demonstrate that MCPyV integration associated with transformation can occur in B cells, lack of acquisition of an MCC phenotype in these cases argue against a B-cell origin of MCC.

SUMMARY

To conclude, reviewing the current knowledge of MCC histogenesis allows for also underlining the basis of the current tumor classification system. Indeed, tumors are mostly classified according to their differentiation status and their level of similarities with physiological cells at the same location (24). However, we should keep in mind that the final phenotype of a given tumor cell may result from strong differentiation changes occurring during oncogenesis and thus does not necessarily directly reflect the cell ancestry (76). Accordingly, despite strong similarities, MCC likely does not derive from already differentiated MCs, which suggests that acquisition of an MC-like phenotype occurs during the oncogenic process (**Figure 3**). From the observations of combined MCC tumors, high somatic pathologic variant loads and detection of an UV signature in this subset, UV-induced MCC cases probably derive from a progenitor cell of the epidermis. By contrast, the nature of the cell in which MCPyV integration occurs remains to be clarified. The lack of connection between tumor cells and the epidermis as well as lack of a UV signature could favor a non-epithelial origin but alternatively could be explained by integration of MCPyV in cutaneous appendage enriched with MC precursors. Use of experimental models in addition to phenotypic characterization of MCC to monitor phenotype changes induced by MCPyV in several cell types are needed to fully address this question.

AUTHOR CONTRIBUTIONS

All authors listed have made a substantial, direct and intellectual contribution to the work, and approved it for publication.

FUNDING

This work was supported by the Foundation ARC and the Ligue nationale contre le cancer, Comités 16, 18, 28.

REFERENCES

- Paulson KG, Park SY, Vandeven NA, Lachance K, Thomas H, Chapuis AG, et al. Merkel cell carcinoma: current US incidence and projected increases based on changing demographics. *J Am Acad Dermatol.* (2018) 78:457–63 e2. doi: 10.1016/j.jaad.2017.10.028
- Miller RW, Rabkin CS. Merkel cell carcinoma and melanoma: etiological similarities and differences. *Cancer Epidemiol Biomark Prev.* (1999) 8:153–8.
- Asgari MM, Sokil MM, Warton EM, Iyer J, Paulson KG, Nghiem P. Effect of host, tumor, diagnostic, and treatment variables on outcomes in a large cohort with Merkel cell carcinoma. *JAMA Dermatol.* (2014) 150:716–23. doi: 10.1001/jamadermatol.2013.8116
- Cook M, Baker K, Redman M, Lachance K, Nguyen MH, Parvathaneni U, et al. Differential outcomes among immunosuppressed patients with Merkel cell carcinoma: impact of immunosuppression type on cancer-specific and overall survival. *Am J Clin Oncol.* (2019) 42:82–8. doi: 10.1097/COC.0000000000000482
- Lemos BD, Storer BE, Iyer JG, Phillips JL, Bichakjian CK, Fang LC, et al. Pathologic nodal evaluation improves prognostic accuracy in Merkel cell carcinoma: analysis of 5823 cases as the basis of the first consensus staging system. *J Am Acad Dermatol.* (2010) 63:751–61. doi: 10.1016/j.jaad.2010.02.056
- Nghiem P, Kaufman HL, Bharmal M, Mahnke L, Phatak H, Becker JC. Systematic literature review of efficacy, safety and tolerability outcomes of chemotherapy regimens in patients with metastatic Merkel cell carcinoma. *Future Oncol Lond Engl.* (2017) 13:1263–79. doi: 10.2217/fon-2017-0072
- Kaufman HL, Russell J, Hamid O, Bhatia S, Terheyden P, D'Angelo SP, et al. Avelumab in patients with chemotherapy-refractory metastatic Merkel cell carcinoma: a multicentre, single-group, open-label, phase 2 trial. *Lancet Oncol.* (2016) 17:1374–85. doi: 10.1016/S1470-2045(16)30364-3
- Colunga A, Pulliam T, Nghiem P. Merkel cell carcinoma in the age of immunotherapy: facts and hopes. *Clin Cancer Res.* (2018) 24:2035–43. doi: 10.1158/1078-0432.CCR-17-0439
- D'Angelo SP, Russell J, Lebbé C, Chmielowski B, Gambichler T, Grob J-J, et al. Efficacy and safety of first-line avelumab treatment in patients with stage IV metastatic Merkel cell carcinoma: a preplanned interim analysis of a clinical trial. *JAMA Oncol.* (2018) 4:e180077. doi: 10.1001/jamaoncol.2018.0077
- World Health Organization. *Who Classification of Skin Tumours.* Lyon: IARC (2018).
- Koljonen V, Haglund C, Tukiainen E, Böhling T. Neuroendocrine differentiation in primary Merkel cell carcinoma—possible prognostic significance. *Anticancer Res.* (2005) 25:853–8.
- Lilo MT, Chen Y, LeBlanc RE. INSM1 is more sensitive and interpretable than conventional immunohistochemical stains used to diagnose Merkel cell carcinoma. *Am J Surg Pathol.* (2018) 42:1541–48. doi: 10.1097/PAS.0000000000001136
- Cheuk W, Kwan MY, Suster S, Chan JK. Immunostaining for thyroid transcription factor 1 and cytokeratin 20 aids the distinction of small cell carcinoma from Merkel cell carcinoma, but not pulmonary from extrapulmonary small cell carcinomas. *Arch Pathol Lab Med.* (2001) 125:228–31. doi: 10.1043/0003-9985(2001)125<0228:IFTTFA>2.0.CO;2
- Stanoszek LM, Chan MP, Palanisamy N, Carskadon S, Siddiqui J, Patel RM, et al. Neurofilament is superior to cytokeratin 20 in supporting cutaneous origin for neuroendocrine carcinoma. *Histopathology.* (2019) 74:504–3. doi: 10.1111/his.13758
- Kervarrec T, Tallet A, Miquelostorena-Standley E, Houben R, Schrama D, Gambichler T, et al. Diagnostic accuracy of a panel of immunohistochemical and molecular markers to distinguish Merkel cell carcinoma from other neuroendocrine carcinomas. *Mod Pathol.* (2019) 32:499–510. doi: 10.1038/s41379-018-0155-y
- Feng H, Shuda M, Chang Y, Moore PS. Clonal integration of a polyomavirus in human Merkel cell carcinoma. *Science.* (2008) 319:1096–100. doi: 10.1126/science.1152586
- Foulongne V, Kluger N, Dereure O, Mercier G, Molès JP, Guillot B, et al. Merkel cell polyomavirus in cutaneous swabs. *Emerg Infect Dis.* (2010) 16:685–7. doi: 10.3201/eid1604.091278
- Martel-Jantin C, Pederghana V, Nicol JTJ, Leblond V, Tréguouët D-A, Tortevoye P, et al. Merkel cell polyomavirus infection occurs during early childhood and is transmitted between siblings. *J Clin Virol.* (2013) 58:288–91. doi: 10.1016/j.jcv.2013.06.004
- Tolstov YL, Knauer A, Chen JG, Kensler TW, Kingsley LA, Moore PS, et al. Asymptomatic primary Merkel cell polyomavirus infection among adults. *Emerg Infect Dis.* (2011) 17:1371–80. doi: 10.3201/eid1708.110079
- Shuda M, Feng H, Kwun HJ, Rosen ST, Gjoerup O, Moore PS, et al. T antigen mutations are a human tumor-specific signature for Merkel cell polyomavirus. *Proc Natl Acad Sci USA.* (2008) 105:16272–7. doi: 10.1073/pnas.0806526105
- Houben R, Angermeyer S, Haferkamp S, Aue A, Goebeler M, Schrama D, et al. Characterization of functional domains in the Merkel cell polyoma virus Large T antigen. *Int J Cancer.* (2015) 136:E290–300. doi: 10.1002/ijc.29200
- Harms PW, Vats P, Verhaegen ME, Robinson DR, Wu Y-M, Dhanasekaran SM, et al. The distinctive mutational spectra of polyomavirus-negative Merkel cell carcinoma. *Cancer Res.* (2015) 75:3720–7. doi: 10.1158/0008-5472.CAN-15-0702
- Harms PW, Harms KL, Moore PS, DeCaprio JA, Nghiem P, Wong MKK, et al. The biology and treatment of Merkel cell carcinoma: current understanding and research priorities. *Nat Rev Clin Oncol.* (2018) 15:763–76. doi: 10.1038/s41571-018-0103-2
- Boyd N, Dancy JE, Gilks CB, Huntsman DG. Rare cancers: a sea of opportunity. *Lancet Oncol.* (2016) 17:e52–61. doi: 10.1016/S1470-2045(15)00386-1
- Ikeda R, Cha M, Ling J, Jia Z, Coyle D, Gu JG. Merkel cells transduce and encode tactile stimuli to drive Aβ-afferent impulses. *Cell.* (2014) 157:664–75. doi: 10.1016/j.cell.2014.02.026
- Chang W, Kanda H, Ikeda R, Ling J, DeBerry JJ, Gu JG. Merkel disc is a serotonergic synapse in the epidermis for transmitting tactile signals in mammals. *Proc Natl Acad Sci USA.* (2016) 113:E5491–500. doi: 10.1073/pnas.1610176113
- Harms PW, Patel RM, Verhaegen ME, Giordano TJ, Nash KT, Johnson CN, et al. Distinct gene expression profiles of viral- and nonviral-associated merkel cell carcinoma revealed by transcriptome analysis. *J Invest Dermatol.* (2013) 133:936–45. doi: 10.1038/jid.2012.445
- Toker C. Trabecular carcinoma of the skin. *Arch Dermatol.* (1972) 105:107–10. doi: 10.1001/archderm.1972.01620040075020
- Tang CK, Toker C. Trabecular carcinoma of the skin: an ultrastructural study. *Cancer.* (1978) 42:2311–21. doi: 10.1002/1097-0142(197811)42:5<2311::AID-CNCR2820420531>3.0.CO;2-L
- Godlewski J, Kowalczyk A, Koziol Z, Pidsudko Z, Kmieć A, Siedlecka-Kroplewska K. Plasticity of neuroepithelial neoplasm cells in the primary and metastatic Merkel cell carcinoma. *Folia Histochem Cytobiol.* (2013) 51:168–73. doi: 10.5603/FHC.2013.0015
- Van Keymeulen A, Mascré G, Youseff KK, Harel I, Michaux C, De Geest N, et al. Epidermal progenitors give rise to Merkel cells during embryonic development and adult homeostasis. *J Cell Biol.* (2009) 187:91–100. doi: 10.1083/jcb.200907080
- Perdigoto CN, Dauber KL, Bar C, Tsai P-C, Valdes VJ, Cohen I, et al. Polycomb-mediated repression and sonic hedgehog signaling interact to regulate Merkel cell specification during skin development. *PLoS Genet.* (2016) 12:e1006151. doi: 10.1371/journal.pgen.1006151
- Baudoin C, Meneguzzi G, Portier MM, Demarchez M, Bernerd F, Pisani A, et al. Peripherin, a neuronal intermediate protein, is stably expressed by neuroendocrine carcinomas of the skin, their xenograft on nude mice, and the corresponding primary cultures. *Cancer Res.* (1993) 53:1175–81.
- Kontochristopoulos GJ, Stavropoulos PG, Krasagakis K, Goerdts S, Zouboulis CC. Differentiation between merkel cell carcinoma and malignant melanoma: an immunohistochemical study. *Dermatol Basel Switz.* (2000) 201:123–6. doi: 10.1159/000018454
- Li Z, Yang J-J, Wu M. Collision tumor of primary merkel cell carcinoma and chronic lymphocytic leukemia/small lymphocytic lymphoma, diagnosed on ultrasound-guided fine-needle aspiration biopsy: a unique case report and review of literature. *Diagn Cytopathol.* (2015) 43:66–71. doi: 10.1002/dc.23127
- Tilling T, Wladykowski E, Failla AV, Houdek P, Brandner JM, Moll I. Immunohistochemical analyses point to epidermal origin of human Merkel cells. *Histochem Cell Biol.* (2014) 141:407–21. doi: 10.1007/s00418-013-1168-8

37. Moll I, Kuhn C, Moll R. Cytokeratin 20 is a general marker of cutaneous Merkel cells while certain neuronal proteins are absent. *J Invest Dermatol.* (1995) 104:910–5. doi: 10.1111/1523-1747.ep12606183
38. García-Mesa Y, García-Piqueras J, García B, Feito J, Cabo R, Cobo J, et al. Merkel cells and Meissner's corpuscles in human digital skin display Piezo2 immunoreactivity. *J Anat.* (2017) 231:978–89. doi: 10.1111/joa.12688
39. Mouchet N, Coquart N, Lebonvallet N, Le Gall-Ianotto C, Mogha A, Fautrel A, et al. Comparative transcriptional profiling of human Merkel cells and Merkel cell carcinoma. *Exp Dermatol.* (2014) 23:928–30. doi: 10.1111/exd.12546
40. Boulais N, Pereira U, Lebonvallet N, Gobin E, Dorange G, Rougier N, et al. Merkel cells as putative regulatory cells in skin disorders: an *in vitro* study. *PLoS ONE.* (2009) 4:e6528. doi: 10.1371/journal.pone.0006528
41. Fernández-Figueras M-T, Puig L, Musulén E, Gilaberte M, Lerma E, Serrano S, et al. Expression profiles associated with aggressive behavior in Merkel cell carcinoma. *Mod Pathol.* (2007) 20:90–101. doi: 10.1038/modpathol.3800717
42. Perdigoto CN, Bardot ES, Valdes VJ, Santoriello FJ, Ezhkova E. Embryonic maturation of epidermal Merkel cells is controlled by a redundant transcription factor network. *Dev Camb Engl.* (2014) 141:4690–6. doi: 10.1242/dev.112169
43. Agaimy A, Erlenbach-Wünsch K, Konukiewicz B, Schmitt AM, Rieker RJ, Vieth M, et al. ISL1 expression is not restricted to pancreatic well-differentiated neuroendocrine neoplasms, but is also commonly found in well and poorly differentiated neuroendocrine neoplasms of extrapancreatic origin. *Mod Pathol.* (2013) 26:995–1003. doi: 10.1038/modpathol.2013.40
44. Nguyen BD, McCullough AE. Imaging of Merkel cell carcinoma. *Radiogr Rev.* (2002) 22:367–76. doi: 10.1148/radiographics.22.2.g02mr14367
45. Hoefler H, Kerl H, Rauch HJ, Denk H. New immunocytochemical observations with diagnostic significance in cutaneous neuroendocrine carcinoma. *Am J Dermatopathol.* (1984) 6:525–30. doi: 10.1097/00000372-198412000-00002
46. Vitalis T, Alvarez C, Chen K, Shih JC, Gaspar P, Cases O. Developmental expression pattern of monoamine oxidases in sensory organs and neural crest derivatives. *J Comp Neurol.* (2003) 464:392–403. doi: 10.1002/cne.10804
47. Halata Z, Grim M, Bauman KI. Friedrich Sigmund Merkel and his “Merkel cell”, morphology, development, and physiology: review and new results. *Anat Rec A Discov Mol Cell Evol Biol.* (2003) 271:225–39. doi: 10.1002/ar.a.10029
48. Narisawa Y, Hashimoto K, Kohda H. Immunohistochemical demonstration of the expression of neurofilament proteins in Merkel cells. *Acta Derm Venereol.* (1994) 74:441–3. doi: 10.2340/0001555574441443
49. Deichmann M, Kurzen H, Egner U, Altevogt P, Hartschuh W. Adhesion molecules CD171 (L1CAM) and CD24 are expressed by primary neuroendocrine carcinomas of the skin (Merkel cell carcinomas). *J Cutan Pathol.* (2003) 30:363–8. doi: 10.1034/j.1600-0560.2003.00073.x
50. Fukuhara M, Agnarsdóttir M, Edqvist P-H, Coter A, Ponten F. SATB2 is expressed in Merkel cell carcinoma. *Arch Dermatol Res.* (2016) 308:449–54. doi: 10.1007/s00403-016-1655-6
51. Sebastian A, Volk SW, Halai P, Colthurst J, Paus R, Bayat A. Enhanced neurogenic biomarker expression and reinnervation in human acute skin wounds treated by electrical stimulation. *J Invest Dermatol.* (2017) 137:737–47. doi: 10.1016/j.jid.2016.09.038
52. McCluggage WG, Kennedy K, Busam KJ. An immunohistochemical study of cervical neuroendocrine carcinomas: neoplasms that are commonly TTF1 positive and which may express CK20 and P63. *Am J Surg Pathol.* (2010) 34:525–32. doi: 10.1097/PAS.0b013e3181d1d457
53. Inoue T, Shimono M, Takano N, Saito C, Tanaka Y. Merkel cell carcinoma of palatal mucosa in a young adult: immunohistochemical and ultrastructural features. *Oral Oncol.* (1997) 33:226–9. doi: 10.1016/S0964-1955(96)00078-4
54. Azmahani A, Nakamura Y, Ishida H, McNamara KM, Fujimura T, Haga T, et al. Estrogen receptor β in Merkel cell carcinoma: its possible roles in pathogenesis. *Hum Pathol.* (2016) 56:128–33. doi: 10.1016/j.humpath.2016.06.005
55. Lasithiotaki I, Tsitoura E, Koutsopoulos A, Lagoudaki E, Koutoulaki C, Pitsidianakis G, et al. Aberrant expression of miR-21, miR-376c and miR-145 and their target host genes in Merkel cell polyomavirus-positive non-small cell lung cancer. *Oncotarget.* (2017) 8:112371–83. doi: 10.18632/oncotarget.11222
56. Szeder V, Grim M, Halata Z, Sieber-Blum M. Neural crest origin of mammalian Merkel cells. *Dev Biol.* (2003) 253:258–63. doi: 10.1016/S0012-1606(02)00015-5
57. Jirásek T, Matej R, Pock L, Knotková I, Mandys V. Merkel cell carcinoma—immunohistochemical study in a group of 11 patients. *Cesk Patol.* (2009) 45:9–13.
58. Sieber-Blum M, Szeder V, Grim M. The role of NT-3 signaling in Merkel cell development. *Prog Brain Res.* (2004) 146:63–72. doi: 10.1016/S0079-6123(03)46004-4
59. Hunter DV, Smaila BD, Lopes DM, Takatoh J, Denk F, Ramer MS. Advillin is expressed in all adult neural crest-derived neurons. *eNeuro.* (2018) 5:e0077-18. doi: 10.1523/ENEURO.0077-18.2018
60. Kritchik JM, Ali WN, Burch JA, Byers JD, Garcia CA, Clark RE, et al. KIT expression reveals a population of precursor melanocytes in human skin. *J Invest Dermatol.* (1996) 106:967–71. doi: 10.1111/1523-1747.ep12338471
61. Su LD, Fullen DR, Lowe L, Uherova P, Schnitzer B, Valdez R. CD117 (KIT receptor) expression in Merkel cell carcinoma. *Am J Dermatopathol.* (2002) 24:289–93. doi: 10.1097/00000372-200208000-00001
62. Zur Hausen A, Rennspiess D, Winnepeninckx V, Speel E-J, Kurz AK. Early B-cell differentiation in Merkel cell carcinomas: clues to cellular ancestry. *Cancer Res.* (2013) 73:4982–7. doi: 10.1158/0008-5472.CAN-13-0616
63. Johansson B, Sahi H, Koljonen V, Böhlhag T. The expression of terminal deoxynucleotidyl transferase and paired box gene 5 in Merkel cell carcinomas and its relation to the presence of Merkel cell polyomavirus DNA. *J Cutan Pathol.* (2018). doi: 10.1111/cup.13372
64. Sauer CM, Haugg AM, Chteinberg E, Rennspiess D, Winnepeninckx V, Speel E-J, et al. Reviewing the current evidence supporting early B-cells as the cellular origin of Merkel cell carcinoma. *Crit Rev Oncol Hematol.* (2017) 116:99–105. doi: 10.1016/j.critrevonc.2017.05.009
65. Murakami I, Takata K, Matsushita M, Nonaka D, Iwasaki T, Kuwamoto S, et al. Immunoglobulin expressions are only associated with MCPyV-positive Merkel cell carcinomas but not with MCPyV-negative ones: comparison of prognosis. *Am J Surg Pathol.* (2014) 38:1627–35. doi: 10.1097/PAS.0000000000000279
66. Yoshimoto T, Motoi N, Yamamoto N, Nagano H, Ushijima M, Matsuura M, et al. Pulmonary carcinoids and low-grade gastrointestinal neuroendocrine tumors show common MicroRNA expression profiles, different from adenocarcinomas and small cell carcinomas. *Neuroendocrinology.* (2018) 106:47–57. doi: 10.1159/000461582
67. Yazawa T. Recent advances in histogenesis research of lung neuroendocrine cancers: evidence obtained from functional analyses of primitive neural/neuroendocrine cell-specific transcription factors. *Pathol Int.* (2015) 65:277–85. doi: 10.1111/pin.12267
68. Shuda M, Guastafierro A, Geng X, Shuda Y, Ostrowski SM, Lukianov S, et al. Merkel cell polyomavirus small T antigen induces cancer and embryonic merkel cell proliferation in a transgenic mouse model. *PLoS ONE.* (2015) 10:e0142329. doi: 10.1371/journal.pone.0142329
69. Kanitakis J, Bourchany D, Faure M, Claudy A. Merkel cells in hyperplastic and neoplastic lesions of the skin. An immunohistochemical study using an antibody to keratin 20. *Dermatol Basel Switz.* (1998) 196:208–12. doi: 10.1159/000017900
70. Narisawa Y, Inoue T, Nagase K. Evidence of proliferative activity in human Merkel cells: implications in the histogenesis of Merkel cell carcinoma. *Arch Dermatol Res.* (2019) 311:37–43. doi: 10.1007/s00403-018-1877-x
71. Vela-Romera A, Carriel V, Martín-Piedra MA, Aneiros-Fernández J, Campos F, Chato-Astrain J, et al. Characterization of the human ridged and non-ridged skin: a comprehensive histological, histochemical and immunohistochemical analysis. *Histochem Cell Biol.* (2019) 151:57–73. doi: 10.1007/s00418-018-1701-x
72. Fradette J, Godbout MJ, Michel M, Germain L. Localization of Merkel cells at hairless and hairy human skin sites using keratin 18. *Biochem Cell Biol.* (1995) 73:635–9. doi: 10.1139/o95-070
73. Kervarrec T, Gaboriau P, Berthon P, Zaragoza J, Schrama D, Houben R, et al. Merkel cell carcinomas infiltrated with CD33⁺ myeloid cells and CD8⁺ T cells are associated with improved outcome. *J Am Acad Dermatol.* (2018) 78:973–82. doi: 10.1016/j.jaad.2017.12.029
74. Tilling T, Moll I. Which are the cells of origin in merkel cell carcinoma? *J Skin Cancer.* (2012) 2012:680410. doi: 10.1155/2012/680410

75. Liu W, Yang R, Payne AS, Schowalter RM, Spurgeon ME, Lambert PF, et al. Identifying the target cells and mechanisms of Merkel cell polyomavirus infection. *Cell Host Microbe*. (2016) 19:775–87. doi: 10.1016/j.chom.2016.04.024
76. Fletcher CDM. The evolving classification of soft tissue tumours: an update based on the new WHO classification. *Histopathology*. (2006) 48:3–12. doi: 10.1111/j.1365-2559.2005.02284.x
77. Chteinberg E, Sauer CM, Rennspiess D, Beumers L, Schifferers L, Eben J, et al. Neuroendocrine key regulator gene expression in Merkel cell carcinoma. *Neoplasia*. (2018) 20:1227–35. doi: 10.1016/j.neo.2018.10.003
78. González-Vela MDC, Curriel-Olmo S, Derdak S, Beltran S, Santibañez M, Martínez N, et al. Shared oncogenic pathways implicated in both virus-positive and uv-induced Merkel cell carcinomas. *J Invest Dermatol*. (2017) 137:197–206. doi: 10.1016/j.jid.2016.08.015
79. Houben R, Adam C, Baeurle A, Hesbacher S, Grimm J, Angermeyer S, et al. An intact retinoblastoma protein-binding site in Merkel cell polyomavirus large T antigen is required for promoting growth of Merkel cell carcinoma cells. *Int J Cancer*. (2012) 130:847–56. doi: 10.1002/ijc.26076
80. Shamir ER, Devine WP, Pekmezci M, Umetsu SE, Krings G, Federman S, et al. Identification of high-risk human papillomavirus and Rb/E2F pathway genomic alterations in mutually exclusive subsets of colorectal neuroendocrine carcinoma. *Mod Pathol*. (2019) 32:290–305. doi: 10.1038/s41379-018-0131-6
81. Meder L, König K, Ozretić L, Schultheis AM, Ueckerth F, Ade CP, et al. NOTCH, ASCL1, p53 and RB alterations define an alternative pathway driving neuroendocrine and small cell lung carcinomas. *Int J Cancer*. (2016) 138:927–38. doi: 10.1002/ijc.29835
82. Syder AJ, Karam SM, Mills JC, Ippolito JE, Ansari HR, Farook V, et al. A transgenic mouse model of metastatic carcinoma involving transdifferentiation of a gastric epithelial lineage progenitor to a neuroendocrine phenotype. *Proc Natl Acad Sci USA*. (2004) 101:4471–6. doi: 10.1073/pnas.0307983101
83. Gambichler T, Mohtezabsade S, Wieland U, Silling S, Höh A-K, Dreißigacker M, et al. Prognostic relevance of high atonal homolog-1 expression in Merkel cell carcinoma. *J Cancer Res Clin Oncol*. (2017) 143:43–9. doi: 10.1007/s00432-016-2257-6
84. Haigis K, Sage J, Glickman J, Shafer S, Jacks T. The related retinoblastoma (pRb) and p130 proteins cooperate to regulate homeostasis in the intestinal epithelium. *J Biol Chem*. (2006) 281:638–47. doi: 10.1074/jbc.M509053200
85. Winkelmann RK. The Merkel cell system and a comparison between it and the neurosecretory or APUD cell system. *J Invest Dermatol*. (1977) 69:41–6. doi: 10.1111/1523-1747.ep12497864
86. Lucarz A, Brand G. Current considerations about Merkel cells. *Eur J Cell Biol*. (2007) 86:243–51. doi: 10.1016/j.ejcb.2007.02.001
87. Halata Z, Grim M, Christ B. Origin of spinal cord meninges, sheaths of peripheral nerves, and cutaneous receptors including Merkel cells. An experimental and ultrastructural study with avian chimeras. *Anat Embryol (Berl)*. (1990) 182:529–37. doi: 10.1007/BF00186459
88. Grim M, Halata Z. Developmental origin of avian Merkel cells. *Anat Embryol (Berl)*. (2000) 202:401–10. doi: 10.1007/s004290000121
89. Moll I, Lane AT, Franke WW, Moll R. Intraepidermal formation of Merkel cells in xenografts of human fetal skin. *J Invest Dermatol*. (1990) 94:359–64. doi: 10.1111/1523-1747.ep12874488
90. Morrison KM, Miesegaes GR, Lumpkin EA, Maricich SM. Mammalian Merkel cells are descended from the epidermal lineage. *Dev Biol*. (2009) 336:76–83. doi: 10.1016/j.ydbio.2009.09.032
91. Xiao Y, Thoresen DT, Williams JS, Wang C, Perna J, Petrova R, et al. Neural Hedgehog signaling maintains stem cell renewal in the sensory touch dome epithelium. *Proc Natl Acad Sci USA*. (2015) 112:7195–200. doi: 10.1073/pnas.1504177112
92. Xiao Y, Williams JS, Brownell I. Merkel cells and touch domes: more than mechanosensory functions? *Exp Dermatol*. (2014) 23:692–5. doi: 10.1111/exd.12456
93. Mulvaney J, Dabdoub A. Atoh1, an essential transcription factor in neurogenesis and intestinal and inner ear development: function, regulation, and context dependency. *J Assoc Res Otolaryngol*. (2012) 13:281–93. doi: 10.1007/s10162-012-0317-4
94. Shi X, Zhang Z, Zhan X, Cao M, Satoh T, Akira S, et al. An epigenetic switch induced by Shh signalling regulates gene activation during development and medulloblastoma growth. *Nat Commun*. (2014) 5:5425. doi: 10.1038/ncomms6425
95. Aragaki M, Tsuchiya K, Okamoto R, Yoshioka S, Nakamura T, Sakamoto N, et al. Proteasomal degradation of Atoh1 by aberrant Wnt signaling maintains the undifferentiated state of colon cancer. *Biochem Biophys Res Commun*. (2008) 368:923–9. doi: 10.1016/j.bbrc.2008.02.011
96. Moll I, Troyanovsky SM, Moll R. Special program of differentiation expressed in keratinocytes of human haarscheiben: an analysis of individual cytokeratin polypeptides. *J Invest Dermatol*. (1993) 100:69–76. doi: 10.1111/1523-1747.ep12354535
97. Narisawa Y, Koba S, Inoue T, Nagase K. Histogenesis of pure and combined Merkel cell carcinomas: an immunohistochemical study of 14 cases. *J Dermatol*. (2015) 42:445–52. doi: 10.1111/1346-8138.12808
98. Akiyama M, Dale BA, Sun TT, Holbrook KA. Characterization of hair follicle bulge in human fetal skin: the human fetal bulge is a pool of undifferentiated keratinocytes. *J Invest Dermatol*. (1995) 105:844–50. doi: 10.1111/1523-1747.ep12326649
99. Peterson SC, Eberl M, Vagnozzi AN, Belkadi A, Veniaminova NA, Verhaegen ME, et al. Basal cell carcinoma preferentially arises from stem cells within hair follicle and mechanosensory niches. *Cell Stem Cell*. (2015) 16:400–12. doi: 10.1016/j.stem.2015.02.006
100. Requena L, Jaqueti G, Rütten A, Mentzel T, Kutzner H. Merkel cell carcinoma within follicular cysts: report of two cases. *J Cutan Pathol*. (2008) 35:1127–33. doi: 10.1111/j.1600-0560.2007.00919.x
101. Tellechea O, Cardoso JC, Reis JP, Ramos L, Gameiro AR, Coutinho I, et al. Benign follicular tumors. *An Bras Dermatol*. (2015) 90:780–96; quiz 797–8. doi: 10.1590/abd1806-4841.20154114
102. Zheng Y, Tian Q, Wang J, Dong X, Jing H, Wang X, et al. Differential diagnosis of eccrine spiradenoma: a case report. *Exp Ther Med*. (2014) 8:1097–101. doi: 10.3892/etm.2014.1906
103. Busam KJ, Jungbluth AA, Rektman N, Coit D, Pulitzer M, Bini J, et al. Merkel cell polyomavirus expression in merkel cell carcinomas and its absence in combined tumors and pulmonary neuroendocrine carcinomas. *Am J Surg Pathol*. (2009) 33:1378–85. doi: 10.1097/PAS.0b013e3181aa30a5
104. Martin B, Poblet E, Rios JJ, Kazakov D, Kutzner H, Brenn T, et al. Merkel cell carcinoma with divergent differentiation: histopathological and immunohistochemical study of 15 cases with PCR analysis for Merkel cell polyomavirus. *Histopathology*. (2013) 62:711–22. doi: 10.1111/his.12091
105. Kervarrec T, Samimi M, Gaboriaud P, Gheit T, Beby-Defaux A, Houben R, et al. Detection of the Merkel cell polyomavirus in the neuroendocrine component of combined Merkel cell carcinoma. *Virchows Arch Int J Pathol*. (2018) 472:825–37. doi: 10.1007/s00428-018-2342-0
106. Pulitzer MP, Brannon AR, Berger MF, Louis P, Scott SN, Jungbluth AA, et al. Cutaneous squamous and neuroendocrine carcinoma: genetically and immunohistochemically different from Merkel cell carcinoma. *Mod Pathol*. (2015) 28:1023–32. doi: 10.1038/modpathol.2015.60
107. Walsh NM. Primary neuroendocrine (Merkel cell) carcinoma of the skin: morphologic diversity and implications thereof. *Hum Pathol*. (2001) 32:680–9. doi: 10.1053/hupa.2001.25904
108. Carter MD, Gaston D, Huang W-Y, Greer WL, Pasternak S, Ly TY, et al. Genetic profiles of different subsets of Merkel cell carcinoma show links between combined and pure MCPyV-negative tumors. *Hum Pathol*. (2017). doi: 10.1016/j.humpath.2017.10.014
109. Falto Aizpurua LA, Wang M, Ruiz HA, Sánchez JL, Chan MP, Andea AA, et al. A case of combined Merkel cell carcinoma and squamous cell carcinoma: molecular insights and diagnostic pitfalls. *JAAD Case Rep*. (2018) 4:996–9. doi: 10.1016/j.jidcr.2018.08.004
110. Kuwamoto S, Higaki H, Kanai K, Iwasaki T, Sano H, Nagata K, et al. Association of Merkel cell polyomavirus infection with morphologic differences in Merkel cell carcinoma. *Hum Pathol*. (2011) 42:632–40. doi: 10.1016/j.humpath.2010.09.011
111. Iwasaki T, Matsushita M, Kuwamoto S, Kato M, Murakami I, Higaki-Mori H, et al. Usefulness of significant morphologic characteristics in distinguishing between Merkel cell polyomavirus-positive and Merkel cell polyomavirus-negative Merkel cell carcinomas. *Hum Pathol*. (2013) 44:1912–7. doi: 10.1016/j.humpath.2013.01.026
112. Pasternak S, Carter MD, Ly TY, Doucette S, Walsh NM. Immunohistochemical profiles of different subsets of Merkel cell carcinoma. *Hum Pathol*. (2018) 82:232–8. doi: 10.1016/j.humpath.2018.07.022

113. Harms PW, Collie AMB, Hovelson DH, Cani AK, Verhaegen ME, Patel RM, et al. Next generation sequencing of Cytokeratin 20-negative Merkel cell carcinoma reveals ultraviolet-signature mutations and recurrent TP53 and RB1 inactivation. *Mod Pathol.* (2016) 29:240–8. doi: 10.1038/modpathol.2015.154
114. Czapiewski P, Majewska H, Kutzner H, Kazakov D, Renkielska A, Biernat W. TTF-1 and PAX5 are frequently expressed in combined Merkel cell carcinoma. *Am J Dermatopathol.* (2016) 38:513–6. doi: 10.1097/DAD.0000000000000464
115. Shuda M, Kwun HJ, Feng H, Chang Y, Moore PS. Human Merkel cell polyomavirus small T antigen is an oncoprotein targeting the 4E-BP1 translation regulator. *J Clin Invest.* (2011) 121:3623–34. doi: 10.1172/JCI46323
116. Goh G, Walradt T, Markarov V, Blom A, Riaz N, Doumani R, et al. Mutational landscape of MCPyV-positive and MCPyV-negative Merkel cell carcinomas with implications for immunotherapy. *Oncotarget.* (2016) 7:3403–15. doi: 10.18632/oncotarget.6494
117. Wong SQ, Waldeck K, Vergara IA, Schröder J, Madore J, Wilmott JS, et al. UV-associated mutations underlie the etiology of MCV-negative Merkel cell carcinomas. *Cancer Res.* (2015) 75:5228–34. doi: 10.1158/0008-5472.CAN-15-1877
118. Thibault K, Anne T, Elodie M-S, Roland H, David S, Thilo G, et al. Morphologic and immunophenotypic features distinguishing Merkel cell polyomavirus-positive and -negative Merkel cell carcinoma. *Modern Pathol.* (accepted).
119. Sunshine JC, Jahchan NS, Sage J, Choi J. Are there multiple cells of origin of Merkel cell carcinoma? *Oncogene.* (2018) 37:1409–16. doi: 10.1038/s41388-017-0073-3
120. Spurgeon ME, Cheng J, Bronson RT, Lambert PF, DeCaprio JA. Tumorigenic activity of merkel cell polyomavirus T antigens expressed in the stratified epithelium of mice. *Cancer Res.* (2015) 75:1068–79. doi: 10.1158/0008-5472.CAN-14-2425
121. Verhaegen ME, Mangelberger D, Harms PW, Vozheiko TD, Weick JW, Wilbert DM, et al. Merkel cell polyomavirus small T antigen is oncogenic in transgenic mice. *J Invest Dermatol.* (2015) 135:1415–24. doi: 10.1038/jid.2014.446
122. Martincorena I, Roshan A, Gerstung M, Ellis P, Van Loo P, McLaren S, et al. Tumor evolution. High burden and pervasive positive selection of somatic mutations in normal human skin. *Science.* (2015) 348:880–6. doi: 10.1126/science.aaa6806
123. Schowalter RM, Reinhold WC, Buck CB. Entry tropism of BK and Merkel cell polyomaviruses in cell culture. *PLoS ONE.* (2012) 7:e42181. doi: 10.1371/journal.pone.0042181
124. Pipas JM. SV40: Cell transformation and tumorigenesis. *Virology.* (2009) 384:294–303. doi: 10.1016/j.virol.2008.11.024
125. Angermeyer S, Hesbacher S, Becker JC, Schrama D, Houben R. Merkel cell polyomavirus-positive Merkel cell carcinoma cells do not require expression of the viral small T antigen. *J Invest Dermatol.* (2013) 133:2059–64. doi: 10.1038/jid.2013.82
126. Knapp AC, Franke WW. Spontaneous losses of control of cytokeratin gene expression in transformed, non-epithelial human cells occurring at different levels of regulation. *Cell.* (1989) 59:67–79. doi: 10.1016/0092-8674(89)90870-2
127. Takahashi K, Yamanaka S. Induction of pluripotent stem cells from mouse embryonic and adult fibroblast cultures by defined factors. *Cell.* (2006) 126:663–76. doi: 10.1016/j.cell.2006.07.024
128. Naska S, Yuzwa SA, Johnston APW, Paul S, Smith KM, Paris M, et al. Identification of drugs that regulate dermal stem cells and enhance skin repair. *Stem Cell Rep.* (2016) 6:74–84. doi: 10.1016/j.stemcr.2015.12.002
129. Kwok CK-M, Tam PK-H, Ngan ES-W. Potential use of skin-derived precursors (SKPs) in establishing a cell-based treatment model for Hirschsprung's disease. *J Pediatr Surg.* (2013) 48:619–28. doi: 10.1016/j.jpedsurg.2012.08.026
130. Kwun HJ, Shuda M, Feng H, Camacho CJ, Moore PS, Chang Y. Merkel cell polyomavirus small T antigen controls viral replication and oncoprotein expression by targeting the cellular ubiquitin ligase SCFFbw7. *Cell Host Microbe.* (2013) 14:125–35. doi: 10.1016/j.chom.2013.06.008
131. Tadmor T, Aviv A, Polliack A. Merkel cell carcinoma, chronic lymphocytic leukemia and other lymphoproliferative disorders: an old bond with possible new viral ties. *Ann Oncol.* (2011) 22:250–6. doi: 10.1093/annonc/mdq308
132. Brewer JD, Shanafelt TD, Otley CC, Roenigk RK, Cerhan JR, Kay NE, et al. Chronic lymphocytic leukemia is associated with decreased survival of patients with malignant melanoma and Merkel cell carcinoma in a SEER population-based study. *J Clin Oncol.* (2012) 30:843–9. doi: 10.1200/JCO.2011.34.9605
133. Howard RA, Dores GM, Curtis RE, Anderson WF, Travis LB. Merkel cell carcinoma and multiple primary cancers. *Cancer Epidemiol Biomark Prev.* (2006) 15:1545–9. doi: 10.1158/1055-9965.EPI-05-0895
134. Koljonen V, Rantanen M, Sahi H, Mellekjær L, Hansen BT, Chen T, et al. Joint occurrence of Merkel cell carcinoma and non-Hodgkin lymphomas in four Nordic countries. *Leuk Lymphoma.* (2015) 56:3315–9. doi: 10.3109/10428194.2015.1040010
135. Chen Z, Gu J. Immunoglobulin G expression in carcinomas and cancer cell lines. *FASEB J.* (2007) 21:2931–8. doi: 10.1096/fj.07-8073.com
136. Chen Z, Li J, Xiao Y, Zhang J, Zhao Y, Liu Y, et al. Immunoglobulin G locus events in soft tissue sarcoma cell lines. *PLoS ONE.* (2011) 6:e21276. doi: 10.1371/journal.pone.0021276
137. Yang S-B, Chen X, Wu B-Y, Wang M-W, Cai C-H, Cho D-B, et al. Immunoglobulin kappa and immunoglobulin lambda are required for expression of the anti-apoptotic molecule Bcl-xL in human colorectal cancer tissue. *Scand J Gastroenterol.* (2009) 44:1443–51. doi: 10.3109/00365520903369953
138. Liu H, Zheng H, Li M, Hu D, Tang M, Cao Y. Upregulated expression of kappa light chain by Epstein-Barr virus encoded latent membrane protein 1 in nasopharyngeal carcinoma cells via NF-kappaB and AP-1 pathways. *Cell Signal.* (2007) 19:419–27. doi: 10.1016/j.cellsig.2006.07.012
139. Li M, Feng D-Y, Ren W, Zheng L, Zheng H, Tang M, et al. Expression of immunoglobulin kappa light chain constant region in abnormal human cervical epithelial cells. *Int J Biochem Cell Biol.* (2004) 36:2250–7. doi: 10.1016/j.biocel.2004.03.017
140. Buscone S, Garavello W, Pagni F, Gaini RM, Cattoretto G. Nasopharyngeal tonsils (adenoids) contain extrathymic corticothymocytes. *PLoS ONE.* (2014) 9:e98222. doi: 10.1371/journal.pone.0098222
141. Dong HY, Liu W, Cohen P, Mahle CE, Zhang W. B-cell specific activation protein encoded by the PAX-5 gene is commonly expressed in merkel cell carcinoma and small cell carcinomas. *Am J Surg Pathol.* (2005) 29:687–92. doi: 10.1097/01.pas.0000155162.33044.4f
142. Mhaweck-Fauceglia P, Saxena R, Zhang S, Terracciano L, Sauter G, Chadhuri A, et al. Pax-5 immunoreexpression in various types of benign and malignant tumours: a high-throughput tissue microarray analysis. *J Clin Pathol.* (2007) 60:709–14. doi: 10.1136/jcp.2006.039917
143. Haugg AM, Speel E-JM, Pantulu ND, Pallasch C, Kurz AK, Kvasnicka HM, et al. Fluorescence *in situ* hybridization confirms the presence of Merkel cell polyomavirus in chronic lymphocytic leukemia cells. *Blood.* (2011) 117:5776–7. doi: 10.1182/blood-2011-03-339895
144. Pantulu ND, Pallasch CP, Kurz AK, Kassem A, Frenzel L, Sodenkamp S, et al. Detection of a novel truncating Merkel cell polyomavirus large T antigen deletion in chronic lymphocytic leukemia cells. *Blood.* (2010) 116:5280–4. doi: 10.1182/blood-2010-02-269829
145. Coleman CB, Nealy MS, Tibbetts SA. Immature and transitional B cells are latency reservoirs for a gammaherpesvirus. *J Virol.* (2010) 84:13045–52. doi: 10.1128/JVI.01455-10

Conflict of Interest Statement: The authors declare that the research was conducted in the absence of any commercial or financial relationships that could be construed as a potential conflict of interest.

Copyright © 2019 Kervarrec, Samimi, Guyétant, Sarma, Chéret, Blanchard, Berthon, Schrama, Houben and Touzé. This is an open-access article distributed under the terms of the Creative Commons Attribution License (CC BY). The use, distribution or reproduction in other forums is permitted, provided the original author(s) and the copyright owner(s) are credited and that the original publication in this journal is cited, in accordance with accepted academic practice. No use, distribution or reproduction is permitted which does not comply with these terms.

VEGF-A Inhibition as a Potential Therapeutic Approach in Merkel Cell Carcinoma

Journal of Investigative Dermatology (2018) ■, ■-■; doi:10.1016/j.jid.2018.08.029

TO THE EDITOR

Merkel cell carcinoma (MCC) is an aggressive carcinoma of the skin with frequent metastases and fatal outcomes (Lemos et al., 2010). Until recently, despite rapid chemoresistance, platinum salt-based chemotherapy remained the first-line therapy for stage IV disease (Nghiem et al., 2017). Tumor progression is related to escape from the immune system and restoration of the T-cell response by inhibitors targeting the PD-1/PD-L1 checkpoint is an emerging approach (Colunga et al., 2017; Kaufman et al., 2016). Thus, avelumab has recently been approved as second-line therapy in refractory advanced MCC (Colunga et al., 2017; Kaufman et al., 2016).

However, MCC tumor progression is also related to interactions with nonimmune microenvironment components, notably by promoting angiogenesis. In this respect, high vascular density has been associated with decreased recurrence-free survival (Bob et al., 2017) and overall survival (Ng et al., 2008) in MCC. Indeed, vascular endothelial growth factor A (VEGF-A), a proangiogenic factor involved in the development of a wide range of neoplasms (Veeravagu et al., 2007), was previously detected in more than 90% of MCC tumors (Brunner et al., 2008). In addition, high intratumoral level of VEGF-A predicts metastasis (Fernández-Figueras et al., 2007). From these observations, we hypothesized that VEGF-A could represent a therapeutic target in MCC.

In a first validation step, VEGF-A expression was assessed by immunohistochemistry on a tissue microarray assay of 97 MCC patients from a French cohort previously described (Kervarrec

et al., 2017), which were scored semiquantitatively (null, low, or high expression). The institutional review board of the local ethics committee of Tours (France) approved the study (no. RCB2009-A01056-51) and patients gave written, informed consent. VEGF-A staining was observed in 92 patients (95%), showing high VEGF-A expression in 38 patients (39%), low VEGF-A expression in 54 patients (56%), and no expression in 5 patients (5%). Patients with absent/low or high VEGF-A expression did not differ in age, sex, American Joint Committee on Cancer stage, tumor sample (primary vs. metastases), or immunosuppression (data not shown). However, we found an association between high VEGF-A level and presence of the Merkel cell polyomavirus (MCPyV), considered the main trigger in MCPyV-positive MCC oncogenesis. Indeed, high VEGF-A expression was observed in 27/57 patients (47%) showing immunohistochemical expression of large T antigen (LTag), evaluated as described (Kervarrec et al., 2017), and only 8 of 34 patients (24%) showing no LTag expression (Figure 1a and b) (Fisher exact test: $P = 0.027$). Accordingly, quantitative PCR (primer specific for LTag sequence) showed higher viral loads in patients with high VEGF-A expression compared with the others: median = 16 copies/cell (quartile [Q] 1–Q3 = 9.25–28.75) versus median = 9 copies/cell (Q1–Q3 = 0–16) (Mann-Whitney U test, $P < 0.001$) (Figure 1c). These results show increased VEGF-A levels in MCPyV-positive tumors, but further investigations are required to clarify whether VEGF-A production is primarily driven by MCPyV oncoproteins.

Next, we investigated VEGF-A production by MCC tumor cells. The VEGF-A expression was assessed in five MCPyV-positive MCC cell lines by reverse transcription-PCR and Western blot analysis, and VEGF-A concentration was quantified in supernatants by ELISA (all described in the Supplementary Materials online). In accordance with our previous results, VEGF-A expression was detected at the RNA and protein levels in all investigated MCC cell lines and in supernatants (Figure 1d–f), thereby confirming VEGF-A production by MCC tumor cells. Notably, VEGF-A expression was generally higher than in HaCaT cells (see Supplementary Figure S1 online), an established VEGF-A-expressing cell culture system (Cai et al., 2018).

In a second step, we investigated VEGF-A as a potential therapeutic target. Because of its high specificity for tumor-human derived VEGF-A and no recognition of the mouse counterpart (Liang et al., 2006), its acceptable toxicity, and its potential use in combination with immunotherapy (Manegold et al., 2017), we selected the humanized monoclonal antibody bevacizumab for VEGF-A inhibition in MCC. In vitro experiments confirmed that bevacizumab did not have a direct effect on MCC cell line viability (data not shown). We then tested the anti-tumor growth effect of bevacizumab on the previously established xenotransplantation mouse model using the MCPyV⁺ MCC cell line WaGa (Houben et al., 2012). Briefly, tumors were induced by subcutaneous injection of 10^7 tumor cells in 16 female NOD SCID mice (local ethics committee: Apafis 3973, 2016-020410139630-V2). The general state of each animal and tumor volume were monitored every 2 days during the entire procedure. When tumor volume reached 25 mm^3 , mice were randomly assigned to the experimental ($n = 8$) or control group ($n = 8$) and received an intraperitoneal

Abbreviations: LTag, large T antigen; MCC, Merkel cell carcinoma; MCPyV, Merkel cell polyomavirus; Q, quartile; VEGF-A, vascular endothelial growth factor A

Accepted manuscript published online 22 October 2018; corrected proof published online XXX

© 2018 The Authors. Published by Elsevier, Inc. on behalf of the Society for Investigative Dermatology.

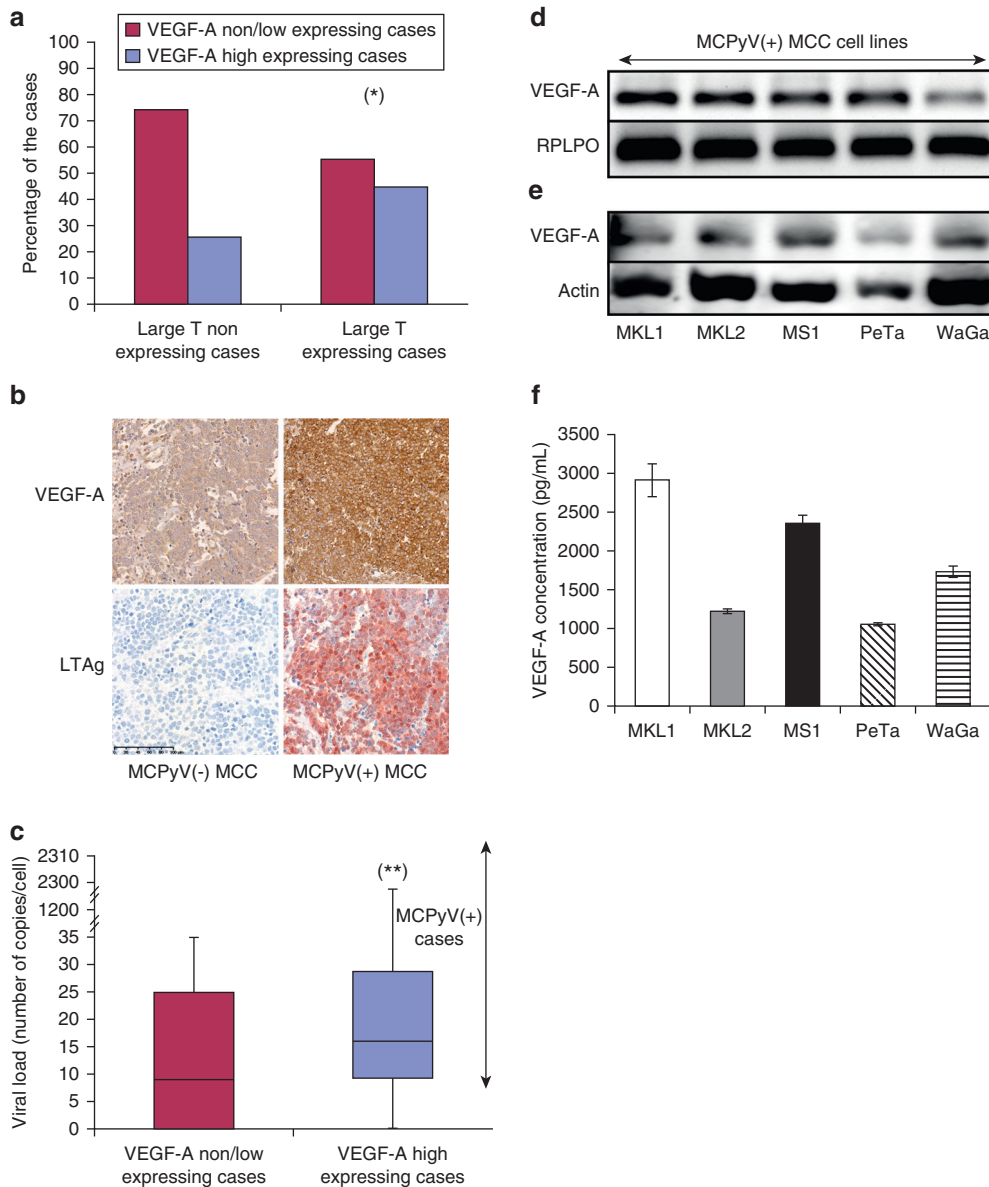


Figure 1. VEGF-A expression in MCC tumor samples and MCC cell lines (MKL-1, MKL-2, MS-1, WaGa, and PeTa). (a) Expression of VEGF-A in LTAg-expressing and nonexpressing MCC tissue. VEGF-A expression was assessed semiquantitatively and dichotomized as VEGF-A low (absent or low) and VEGF-A high expression. In parallel, an Allred score for MCPyV-LTAg expression was determined. Only patients with score greater than 2 were considered to be LTAg expressing. Data are expressed as percentage of VEGF-A-expressing and non-/low-expressing patients. $*P = 0.027$ comparing LTAg-expressing and nonexpressing patients by Fisher exact test. (b) Representative immunochemical detection of MCPyV LTAg (CM2B4) and VEGF-A protein in MCPyV⁻ and MCPyV⁺ tumor tissue (scale bar = 100 μ m). (c) MCPyV viral load in VEGF-A non-/low- and high-expressing MCC groups. Viral load was determined by quantitative PCR with WaGa cells as a control (Rodig et al., 2012). Horizontal line is the median, and box edges are Q1–Q3 and whiskers are range. $**P < 0.001$, Mann-Whitney *U* test. (d) VEGF-A mRNA level in MCC cell lines. Reverse transcription-PCR analysis of VEGF-A and RPLPO levels (the latter used as a control). (e) VEGF-A protein level in MCC cell lines: Western blot analysis of VEGF-A protein level (expected size = 22 kDa). (f) VEGF-A protein level in supernatant of MCC cell lines. ELISA of VEGF-A secretion in conditioned culture media from 3×10^5 cells/ml cultured for 6 days. Nonconditioned culture media was used for normalization. Data are mean \pm standard deviation of three independent experiments. All procedures are described in the [Supplementary Materials](#). LTAg, large T antigen; MCC, Merkel cell carcinoma; MCPyV, Merkel cell polyomavirus; Q, quartile; RPLPO, ribosomal protein lateralstalk subunit P0; VEGF-A, vascular endothelial growth factor A.

injection of bevacizumab three times per week (2 mg/kg, injected volume = 0.2 ml) (experimental group) or an equivalent volume of phosphate buffered saline (control group).

Tumor growth rates were significantly lower in the experimental than control mice (growth curve slope: median = 0.8

mm³/day [Q1–Q3 = 0.7–4.1] vs. 130 mm³/day [Q1–Q3 = 107–144]; Mann-Whitney *U* test, $P = 1.5 \times 10^{-4}$) (Figure 2a and b, and see [Supplementary Figure S2](#) online). Accordingly, final median tumor weight was significantly lower in the experimental than control mice (median = 0.4

g [Q1–Q3 = 0.2–0.5] vs. 2.4 g [Q1–Q3 = 2.1–2.6]; Mann-Whitney *U* test, $P = 3 \times 10^{-4}$). Intratumor vascular density, assessed by CD31 immunohistochemical staining, was significantly lower in experimental than control mice (mean value of vascular density = 0.49% [Q1–Q3 = 0.43–0.51] vs.

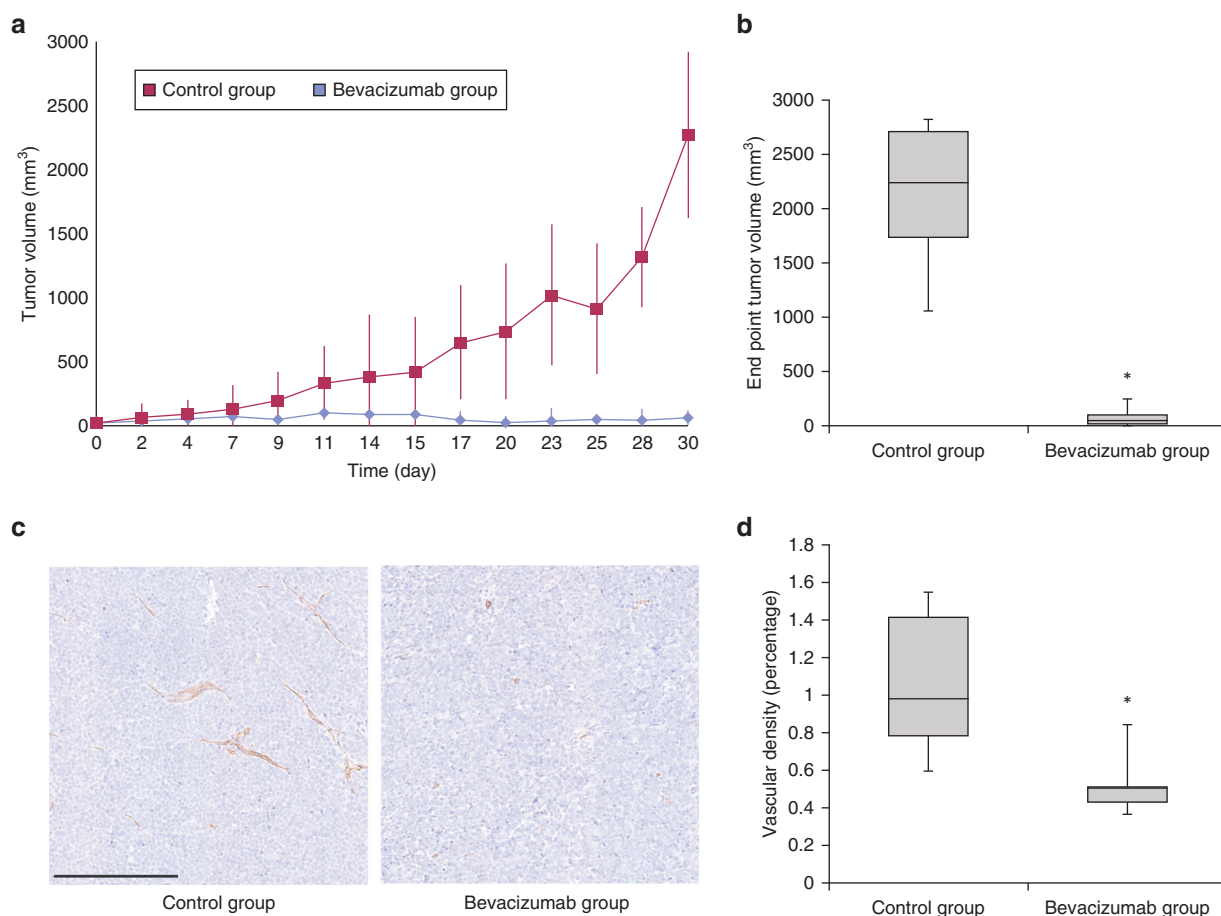


Figure 2. Efficacy of bevacizumab treatment on growth of WaGa xenotransplantation tumors in mice. (a) Tumor growth in bevacizumab and control groups (mean \pm standard deviation tumor volume in mm³). Tumors were induced by subcutaneous injection of 10⁷ WaGa MCC cells with 100 μ g Matrigel (Benson Dickinson, France) in a final volume of 0.2 ml DMEM medium into mice. Mice received intraperitoneal injections of bevacizumab three times per week (2 mg/kg, injected volume 0.2 ml) (bevacizumab group, n = 8) or an equivalent volume of phosphate buffered saline (controls, n = 8). (b) End-point tumor volume (mm³) in bevacizumab and control groups. * $P < 0.001$, Mann-Whitney U test. (c) Representative CD31 immunohistochemical staining of tumors in bevacizumab and control groups showing lower vascular density ($P < 0.001$, Mann-Whitney U test) and smaller vessel size ($P < 0.01$, Mann-Whitney U test) in bevacizumab- versus control-treated tumors. Scale bar = 250 μ m. (d) Vascular density at the end point in the bevacizumab and control groups. ** $P < 0.001$ Mann-Whitney U test.

0.98% [Q1–Q3 = 0.78–1.42]; Mann-Whitney U test, $P = 3 \times 10^{-4}$), showing a direct inhibition of blood vessel growth by bevacizumab (Figure 2c and d). We observed no liver or lung metastasis in either group and no difference in necrosis ($P = 0.5$).

One major limitation of MCC pre-clinical studies is the lack of an available tumor model with immunocompetent mice. Indeed, VEGF-A also acts on immune cells by inhibiting both lymphocytic and dendritic cell maturation (Ohm et al., 2003). Thus, bevacizumab could reduce these immunosuppressive effects in combination with immunotherapy (Manegold et al., 2017). In addition, inclusion of an VEGF-A non-expressing cell line to exclude a stromal VEGF-A targeting by bevacizumab

and a MCPyV-negative MCC cell line in a xenograft model would be suitable but was not performed in this study because of lack of appropriate or representative cell lines (Guastafierro et al., 2013).

To conclude, our results suggest VEGF-A as a potential therapeutic target in MCC. VEGF-A is frequently highly expressed in tumor cells, especially in MCPyV⁺ patients. Because bevacizumab was found efficient for tumor growth inhibition in a preclinical model, it may be a promising therapeutic option in metastatic MCC, as an alternative or combined with current treatments.

ORCIDiS

Thibault Kervarrec: <http://orcid.org/0000-0002-2201-6914>

Roland Houben: <http://orcid.org/0000-0003-4538-2324>

CONFLICT OF INTEREST

The authors state no conflict of interest.

ACKNOWLEDGMENTS

The authors express their sincerest thanks to the patients who gave their approval for use of their data in the study. We also thank Yannick Le Corre (Angers), Ewa Hainaut-Wierzbicka (Poitiers), Francois Aubin (Besançon), Guido Bens (Orléans), and Hervé Maillard (Le Mans) for their help and contributions. This study was supported by a grant from project POCAME, Cancéropole Grand Ouest-Région Centre Val de Loire (France) and a grant from the Société Française de Recherche Dermatologique.

Thibault Kervarrec^{1,2,3},
Pauline Gaboriau², Anne Tallet⁴,
Valérie Leblond², Françoise Arnold²,
Patricia Berthon²,
Sophie Schweinitzer³,
Thibaut Larcher⁵, Serge Guyétant^{1,2},

T Kervarrec et al.

VEGF-A Inhibition in Merkel Cell Carcinoma

David Schrama³, Roland Houben³,
Mahtab Samimi^{2,6,7,*} and
Antoine Touze^{2,7}

¹Department of Pathology, Université de Tours, CHU de Tours, Chambray-les-tours, France; ²Biologie des infections à polyomavirus team, INRA ISP 1282 Université de Tours, Tours, France; ³Department of Dermatology, Venereology and Allergology, University Hospital Würzburg, Würzburg, Germany; ⁴Molecular Biology Platform, Université de Tours, CHU de Tours, Chambray-les-tours, France; ⁵APEX, INRA, ONIRIS, ENVN, Université de Nantes, Ecole vétérinaire de Nantes, Nantes, France; and ⁶Dermatology Department, Université de Tours, CHU de Tours, Chambray-les-tours, France

⁷These authors contributed equally to this work.

*Corresponding author e-mail: mahtab.samimi@univ-tours.fr

SUPPLEMENTARY MATERIAL

Supplementary material is linked to the online version of the paper at www.jidonline.org, and at <https://doi.org/10.1016/j.jid.2018.08.029>.

REFERENCES

- Bob A, Nielsen F, Krediet J, Schmitter J, Freundt D, Terhorst D, et al. Tumor vascularization and clinicopathologic parameters as prognostic factors in Merkel cell carcinoma. *J Cancer Res Clin Oncol* 2017;143:1999–2010.
- Brunner M, Thurnher D, Pammer J, Geleff S, Heiduschka G, Reinisch CM, et al. Expression of VEGF-A/C, VEGF-R2, PDGF-alpha/beta, c-kit, EGFR, Her-2/Neu, Mcl-1 and Bmi-1 in Merkel cell carcinoma. *Mod Pathol* 2008;21:876–84.
- Cai W, Salvador-Reyes LA, Zhang W, Chen Q-Y, Matthew S, Ratnayake R, et al. Apratyramide, a marine-derived peptidic stimulator of VEGF-A and other growth factors with potential application in wound healing. *ACS Chem Biol* 2018;13:91–9.
- Colunga A, Pulliam T, Nghiem P. Merkel cell carcinoma in the age of immunotherapy: facts and hopes. *Clin Cancer Res* 2017;24:2035–43.
- Fernández-Figueras M-T, Puig L, Musulén E, Gilaberte M, Lerma E, Serrano S, et al. Expression profiles associated with aggressive behavior in Merkel cell carcinoma. *Mod Pathol* 2007;20:90–101.
- Guastafierro A, Feng H, Thant M, Kirkwood JM, Chang Y, Moore PS, et al. Characterization of an early passage Merkel cell polyomavirus-positive Merkel cell carcinoma cell line, MS-1, and its growth in NOD scid gamma mice. *J Virol Methods* 2013;187:6–14.
- Houben R, Adam C, Baeurle A, Hesbacher S, Grimm J, Angermeyer S, et al. An intact retinoblastoma protein-binding site in Merkel cell polyomavirus large T antigen is required for promoting growth of Merkel cell carcinoma cells. *Int J Cancer* 2012;130:847–56.
- Kaufman HL, Russell J, Hamid O, Bhatia S, Terheyden P, D'Angelo SP, et al. Avelumab in patients with chemotherapy-refractory metastatic Merkel cell carcinoma: a multicentre, single-group, open-label, phase 2 trial. *Lancet Oncol* 2016;17:1374–85.
- Kervarrec T, Gaboriaud P, Berthon P, Zaragoza J, Schrama D, Houben R, et al. Merkel cell carcinomas infiltrated with CD33⁺ myeloid cells and CD8⁺ T cells are associated with improved outcome. *J Am Acad Dermatol* 2017;78:973–82.
- Lemos BD, Storer BE, Iyer JG, Phillips JL, Bichakjian CK, Fang LC, et al. Pathologic nodal evaluation improves prognostic accuracy in Merkel cell carcinoma: analysis of 5823 cases as the basis of the first consensus staging system. *J Am Acad Dermatol* 2010;63:751–61.
- Liang W-C, Wu X, Peale FV, Lee CV, Meng YG, Gutierrez J, et al. Cross-species vascular endothelial growth factor (VEGF)-blocking antibodies completely inhibit the growth of human tumor xenografts and measure the contribution of stromal VEGF. *J Biol Chem* 2006;281:951–61.
- Manegold C, Dingemans A-MC, Gray JE, Nakagawa K, Nicolson M, Peters S, et al. The potential of combined immunotherapy and antiangiogenesis for the synergistic treatment of advanced NSCLC. *J Thorac Oncol* 2017;12:194–207.
- Ng L, Beer TW, Murray K. Vascular density has prognostic value in Merkel cell carcinoma. *Am J Dermatopathol* 2008;30:442–5.
- Nghiem P, Kaufman HL, Bharmal M, Mahnke L, Phatak H, Becker JC. Systematic literature review of efficacy, safety and tolerability outcomes of chemotherapy regimens in patients with metastatic Merkel cell carcinoma. *Future Oncol* 2017;13:1263–79.
- Ohm JE, Gabrilovich DI, Sempowski GD, Kisseleva E, Parman KS, Nadaf S, et al. VEGF inhibits T-cell development and may contribute to tumor-induced immune suppression. *Blood* 2003;101:4878–86.
- Rodig SJ, Cheng J, Wardzala J, DoRosario A, Scanlon JJ, Laga AC, et al. Improved detection suggests all Merkel cell carcinomas harbor Merkel polyomavirus. *J Clin Invest* 2012;122:4645–53.
- Veeravagu A, Hsu AR, Cai W, Hou LC, Tse VCK, Chen X. Vascular endothelial growth factor and vascular endothelial growth factor receptor inhibitors as anti-angiogenic agents in cancer therapy. *Recent Pat Anticancer Drug Discov* 2007;2:59–71.

Merkel cell carcinomas infiltrated with CD33⁺ myeloid cells and CD8⁺ T cells are associated with improved outcome



Thibault Kervarrec, MD, MSc,^{a,b,c} Pauline Gaboriaud,^b Patricia Berthon, PhD,^b Julia Zaragoza, MD,^d David Schrama, PhD,^c Roland Houben, PhD,^c Yannick Le Corre, MD,^e Ewa Hainaut-Wierzbicka, MD,^f Francois Aubin, MD, PhD,^g Guido Bens, MD,^h Jorge Domenech, PhD,ⁱ Serge Guyétant, MD, PhD,^{a,b} Antoine Touzé, PhD,^b and Mahtab Samimi, MD, PhD^{b,d}
Tours, Angers, Poitiers, Besançon, and Orléans, France; and Würzburg, Germany

Background: Merkel cell carcinoma (MCC) is a rare tumor of the skin that has an aggressive behavior. Immunity is the main regulator of MCC development, and many interactions between lymphocytes and tumor cells have been proven. However, the impact of tumor-infiltrating myeloid cells needs better characterization.

Objective: To characterize tumor-infiltrating myeloid cells in MCC and their association with other immune effectors and patient outcome.

Methods: MCC cases were reviewed from an ongoing prospective cohort study. In all, 103 triplicate tumor samples were included in a tissue microarray. Macrophages, neutrophils, and myeloid-derived suppressor cells were characterized by the following markers: CD68, CD33, CD163, CD15, CD33, and human leukocyte antigen-DR. Associations of these cell populations with programmed cell death ligand 1 expression, CD8 infiltrates, and vascular density were assessed. Impact on survival was analyzed by log-rank tests and a Cox multivariate model.

Results: The median density of macrophages was 216 cells/mm². CD68⁺ and CD33⁺ macrophage densities were associated with CD8⁺ T-cell infiltrates and programmed cell death ligand 1 expression. In addition, MCC harboring CD8⁺ T cell infiltrates and brisk CD33⁺ myeloid cell infiltrates were significantly and independently associated with improved outcomes (recurrence-free and overall survival).

Limitations: Sampling bias and the retrospective design were potential study limitations.

Conclusion: Infiltration of CD33⁺ myeloid cells and CD8⁺ T lymphocytes defines a subset of MCC associated with improved outcome. (J Am Acad Dermatol 2018;78:973-82.)

Key words: CD33; immune infiltrate; macrophages; Merkel cell carcinoma; myeloid cells; PD-L1.

Merkel cell carcinoma (MCC) is a rare and aggressive tumor of the skin, and the main risk factors are age, ultraviolet light

exposure, and immunosuppression. The diagnosis of MCC relies on the association of histologic features of small cell neuroendocrine carcinoma and

From the Department of Pathology, Centre Hospitalier Universitaire (CHU) de Tours, Université Francois Rabelais^a; Biologie des Infections à Polyomavirus Team, Unité Mixte de Recherche 1282 Infectiologie et Santé Publique INRA, Université Francois Rabelais^b; Department of Dermatology, Venereology and Allergology, University Hospital Würzburg^c; Department of Dermatology, CHU de Tours, Université Francois Rabelais^d; Department of Dermatology, CHU de Angers, Université d'Angers^e; Department of Dermatology, CHU de Poitiers, Université de Poitiers^f; Department of Dermatology, CHU de Besançon, Université de Franche Comté^g; Department of Dermatology, Centre Hospitalier Régional d'Orléans^h; and Department of Hematology, CHU de Tours, Université Francois Rabelais.ⁱ

Funding sources: Supported by a grant to project POCAME, Cancéropole Grand Ouest-Région Centre Val de Loire (France). Conflicts of interest: None disclosed.

Accepted for publication December 7, 2017.

Correspondence to: Mahtab Samimi, MD, PhD, Dermatology Department, Hospital of Tours, Avenue de la République, 37170, Chambray-lès-Tours, France. E-mail: mahtab.samimi@univ-tours.fr.

Published online December 19, 2017.

0190-9622/\$36.00

© 2017 by the American Academy of Dermatology, Inc.

<https://doi.org/10.1016/j.jaad.2017.12.029>

immunohistochemical expression of cytokeratin 20 or neuroendocrine markers.¹ In 2008, Feng et al discovered Merkel cell polyomavirus (MCPyV) integration in a large proportion of MCC tumors,² and MCPyV is currently considered the main etiologic agent of MCC.

Increasing evidence supports that cellular immune responses play a crucial role controlling MCC progression. Brisk intratumoral CD8⁺ lymphoid infiltrates have been associated with improved outcomes for MCC cohorts,³⁻⁵ which suggests effective antitumor-specific cytotoxic responses in at least some MCC cases. However, most MCC cases displayed immune evasion from antitumoral effectors, with lymphocytes excluded at the periphery of the tumor (the stalling phenomenon) and cytotoxic responses inhibited.⁴⁻⁷

Tumor-infiltrating myeloid cells (TIMs) have been suggested to be involved in such immune regulation in MCC.^{8,9} Indeed, TIMs can affect tumor development by modulating immune responses and enhancing vascular density.¹⁰⁻¹² Recruited, immune efficient M1-polarized macrophages are progressively replaced during tumor development by tumor-associated macrophages closely related to the M2 tolerogenic subset. Tumor-secreted factors can block the differentiation process of myeloid progenitors, thereby leading to the development of an immunosuppressive myeloid subset, the myeloid-derived suppressor cells (MDSCs).¹³

In MCC, TIMs (previously characterized by immunohistochemical stainings^{5,14,15} assessing CD68⁺ and CD163⁺ macrophages) were found to be major components of the tumoral microenvironment and the main source of programmed cell death (PD) ligand 1 (PD-L1), a component of the tolerogenic PD-1/PD-L1 pathway currently targeted by avelumab immunotherapy.¹⁶ One recent study⁸ of 12 MCC samples revealed that MCC tumors were also infiltrated by CD33-expressing cells, suspected to be tumor-infiltrating MDSCs.

In this study, we investigated TIMs in a cohort of MCC patients by using the pan-macrophage marker CD68, the M2 macrophage marker CD163, and the early differentiation myeloid marker CD33. CD15 was used as a neutrophil marker, and an innovative combination of immunostaining was developed to

identify tumor-infiltrating MDSCs. Tumor characteristics; intratumoral microenvironment composition (CD8 infiltration, PD-L1 expression, tumoral vascular density, and MCPyV detection); and patient outcomes (MCC recurrence and death) were investigated for the TIM subsets.

METHODS

Study period, data, and settings

MCC cases were recruited from an ongoing prospective cohort of MCC patients who had an MCC diagnosis established during 1998-2015 from 5 French hospital centers (local ethics committee, Tours, France, no. ID RCB2009-A01056-51). Cohort inclusion criteria were previously reported.¹⁷ Only cases with sufficient available formalin-fixed paraffin-embedded (FFPE) samples

were included.

Clinical and follow-up data

Age and sex; American Joint Committee on Cancer (AJCC) 2010 stage at time of surgery¹⁸; location of samples (primary tumors or metastases); information relating to immunosuppression (HIV infection, organ transplant, and hematologic malignancies)¹⁹; and follow-up data were collected from patient files.

Tissue microarray establishment

Inflammatory immune cells are localized in peritumoral or intratumoral areas of the tumor microenvironment, but prognosis is related mostly to the intratumoral components.^{3,4} Therefore, we focused the study on intratumoral areas. In brief, these areas were selected on hematoxylin phloxine saffron-stained sections by using the following criteria: central intratumoral area, lack of necrosis or fibrous septa, and representative immune infiltrates after overall slide evaluation on hematoxylin phloxine saffron staining. The selected areas were extracted as a 1-mm tissue core and mounted in triplicate by using a semi-motorized tissue arrayer (MTA booster OI v2.00, Alphelys).

Immunohistochemistry

Immunohistochemical stainings involved the use of the BenchMark XT Platform (Ventana Medical Systems Inc, Basel, Switzerland) as instructed.

CAPSULE SUMMARY

- Brisk infiltration of CD8⁺ T lymphocytes represents an efficient immune response in patients with Merkel cell carcinoma.
- In this study, tumors with brisk infiltration of both CD33⁺ myeloid cells and CD8⁺ T lymphocytes were associated with an improved outcome.
- Patients with tumors lacking brisk CD33 infiltration may be considered to be at higher risk.

Abbreviations used:

AJCC:	American Joint Committee on Cancer
CI:	confidence interval
FFPE:	formalin-fixed paraffin-embedded
HLA-DR:	human leukocyte antigen-DR
HR:	hazard ratio
MCC:	Merkel cell carcinoma
MCPyV:	Merkel cell polyomavirus
MDSC:	myeloid-derived suppressor cell
PD:	programmed cell death
PD-L1:	programmed cell death ligand 1
Q:	quartile
TIM:	tumor-infiltrating myeloid cells

The target population markers, antibodies, and dilutions used are summarized in [Supplemental Table I](#) (available at <http://www.jaad.org>).

Assessment of tumor-infiltrating immune cells

Myeloid cells were counted on 5 high-power fields of the intratumor area (0.785 mm^2) defined as the tumor area with few fibrous septa and no necrosis. Only immune cells with obvious nuclei and adequate morphology (macrophages or neutrophils) in contact with tumor cells and not within vessels were considered in the analysis.⁴ The representativeness of our counts were validated on the first set of overall slides as shown in [Supplemental Table II](#) (available at <http://www.jaad.org>). Second, cells on tissue microarray slides were counted by 2 pathologists (Drs Guyétant and Kervarrec). When cell counts differed by >10%, a third count was performed by the 2 pathologists together. Mean cell count was used for further analysis. Density of CD8⁺ T lymphocytes was graded as described.⁴ Cases with <5 representative high-power foci were excluded as not interpretable.

Assessment of MDSCs by double-staining immunocytochemistry

MDSCs were previously investigated by flow cytometry and found to have the phenotype CD33⁺CD11b⁺HLA-DR (human leukocyte antigen-DR)^{-low}.¹³ Because CD33 and CD11b are both myeloid lineage markers, with CD33 being expressed earlier,²⁰ we performed double staining for CD33 and HLA-DR. To detect cells expressing CD33 without HLA-DR, we used a strong dark chromogenic component for HLA-DR staining. This chromogen, 5-bromo-4-chloro-3-indolyl-1-phosphate with nitro-blue tetrazolium, masks other colors in colocalization stains and allows for exclusion of all cells expressing HLA-DR. The procedures and controls used in these stainings are described in the

[Supplementary Appendix](#) and [Supplemental Fig 1](#) (available at <http://www.jaad.org>).

To investigate MDSC location, all cases with positive CD33⁺HLA-DR⁻ cell were reviewed on overall slide staining, and cells were counted on 3 fields of the intratumor area, area of necrosis, and fibrous septa.

Assessment of vascular density

After CD34 immunostaining, slides were scanned by using NanoZoomer (Hamamatsu, Hamamatsu City, Japan), and digitalized slides were analyzed by using ImageJ software²¹ as described in the [Supplementary Appendix](#) and [Supplemental Fig 1](#) (available at <http://www.jaad.org>).

Assessment of MCPyV status

MCPyV status of the tumors was assessed by the expression of the large T antigen by using CM2B4 antibody and the Allred score as described.^{22,23} In brief, a semiquantitative score was used to assess intensity and proportion of large T-antigen-expressing cells; tumors with scores >2 were considered MCPyV positive.²³

Statistical analyses

Continuous data were described with medians and quartiles 1-3 (Q1-Q3). Categorical data were described with numbers and percentages of interpretable cases. Associations were assessed by two-tailed Fisher's exact test for categorical data and nonparametric Mann-Whitney U test for continuous data. The relationship between patient characteristics and survival (recurrence-free and overall) were analyzed by log-rank test and presented on Kaplan-Meier curves. Univariate and multivariate Cox proportional-hazards regression was used to estimate hazard ratios (HRs) and 95% confidence intervals (CIs) and identify factors associated with MCC recurrence and death. Overall deaths were considered events, and living patients were censored on the date of last follow-up. Covariates with $P \leq .20$ on Cox univariate regression analysis were identified as potential prognostic confounders and then included in the multivariate Cox analysis. Statistical analysis involved use of XL-Stat-Life (Addinsoft, Paris, France). $P < .05$ was considered statistically significant, except with multiple testing, when only $P < .01$ was considered significant.

RESULTS

Density of TIM populations in MCC tumors

Among the 242 MCC patients included in the cohort, 103 cases with sufficient available FFPE samples were included ([Fig 1](#)). The number of interpretable cases per myeloid marker is listed in

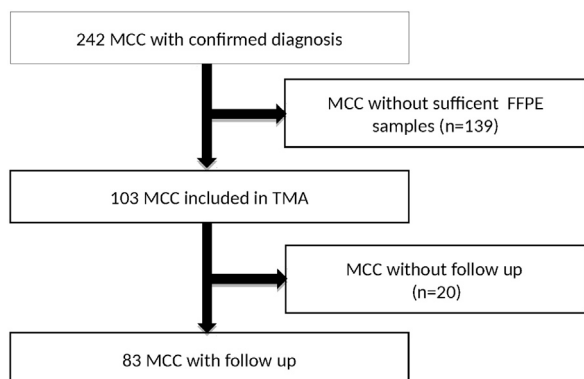


Fig 1. Flow chart of MCC samples excluded and included in study. *FFPE*, Formalin-fixed paraffin-embedded; *MCC*, Merkel cell carcinoma; *TMA*, tissue microarray.

Table I. The median cell densities of CD68⁺, CD163⁺, and CD33⁺ myeloid cells were 216 (Q1-Q3 131-323) cells/mm², 120 (Q1-Q3 76-191) cells/mm², and 83 (Q1-Q3 31-213) cells/mm², respectively. Overall, 66 of 95 (69%) interpretable samples showed tumor-infiltrating, CD15-expressing neutrophils median density 2.5 [Q1-Q3 0-4] cells/mm². Only 5 of 84 (7%) interpretable MCC samples showed CD33⁺/HL-DR⁻ cells, with a median of 5 (Q1-Q3 3-5) cells/mm² in positive cases. On overall slide examination of these latter cases, MDSCs were only rarely located in intratumor areas without necrosis (median 2.8 [Q1-Q3 0-5] cells/mm²) compared with intratumor areas with necrosis (median 66 [Q1-Q3 39-81] cells/mm²; $P < .01$) or with the fibrous septa surrounding the tumor (median 57 [Q1-Q3 11-112] cells/mm²; $P < .01$) as shown in Fig 2.

Association of TIMs with baseline clinical characteristics

The median age of patients was 77 (Q1-Q3, 69-84) years, 42% (42/100) of the population was male, and 14% (10/72) was immunosuppressed. Regarding AJCC staging at diagnosis, patients were classified as having stage 1 (25%, 21/85); stage 2 (26%, 22/85); stage 3 (45%, 39/85); or stage 4 disease (4%, 3/85).

Patient baseline clinical characteristics by density of TIMs (macrophages, neutrophils, and MDSCs) are provided in Supplemental Table III (available at <http://www.jaad.org>). In brief, TIM infiltrates were dichotomized as brisk and nonbrisk by median count, except for MDSCs, which were dichotomized as MDSC-positive ($n = 5$) or MDSC-negative tumors ($n = 79$). TIMs were not associated with clinical baseline characteristics or MCPyV status, except for the neutrophil infiltrates, which were more frequent in advanced tumor stage samples (Supplemental Table III).

TIMs are closely associated with other components of the tumor microenvironment

The association between TIM density and relevant components of the MCC microenvironment is shown in Table I and Fig 3.

MCC tumors with CD8⁺ T-cell infiltrates (scores 1-5, $n = 62$, 63% of cases) harbored brisker TIM infiltrates than CD8-negative tumors (score 0, $n = 36$, 37% of cases) ($P < .001$ for CD68⁺, CD163⁺, and CD33⁺ myeloid cells; Table I). MCC cases with the most CD8⁺ T-cell infiltrates (scores 2-5, $n = 11$, 11%) were significantly associated with brisk CD68⁺, CD163⁺, and CD33⁺ myeloid-cell infiltration (Fisher's exact test, $P = .0002$, .02, and .001, respectively).

Most MCC tumors (61 cases, 78%) showed PD-L1⁺ myeloid cells within their microenvironment (Fig 3). Cases were dichotomized as brisk or nonbrisk according to the median PD-L1⁺ myeloid cell count. MCC tumors with brisk CD68⁺ and CD33⁺ infiltrates frequently showed brisk PD-L1⁺ cells in their microenvironment (Fisher's exact test, $P = 9.10^{-3}$ and $P = 3.10^{-3}$, respectively; Table I). The vascular area occupied 1.5% (Q1-Q3 0.9%-1.9%) of the tumor surface, with no significant association with TIM infiltrate density (Table I).

Association between density of tumor immune infiltrates and patient outcome

Factors associated with survival on univariate analysis are reported in Table II. On univariate analysis, only female sex, as previously reported,²⁴⁻²⁷ and CD33⁺ TIM density were associated with decreased risk for recurrence (female: HR 0.39, 95% CI 0.19-0.83, $P = .014$; CD33⁺ TIM: HR 0.35, 95% CI 0.15-0.83, $P = .016$) and death (female: HR 0.40, 95% CI 0.19-0.82, $P = .012$; CD33⁺ TIM: HR 0.44, 95% CI 0.20-0.99, $P = .047$) (Table II). Covariates identified as potential prognostic confounders (with $P \leq .20$) on Cox univariate regression analysis were included in the multivariate Cox analysis. In this model (Supplemental Table IV; available at <http://www.jaad.org>), only AJCC stage was associated independently with death (HR 3.90, 95% CI 1.20-12.70, $P = .024$). Interestingly, among myeloid infiltrates, brisk CD33⁺ infiltrates showed a trend toward association, with a decreased risk for recurrence (HR 0.35, 95% CI 0.11-1.00, $P = .051$) and death (HR 0.40, 95% CI 0.14-1.25, $P = .083$).

MCCs infiltrated with CD33⁺ myeloid cells and CD8⁺ T cells are associated with improved outcome

Intratumoral infiltration with CD8⁺ T cells has previously been shown to be associated with MCC

Table I. MCC microenvironmental characteristics by tumor-infiltrating myeloid cell density

Characteristic	Myeloid cell, median intratumoral cell density											
	CD68 ⁺ macrophages, N = 93, 216 cells/mm ²		CD163 ⁺ macrophages, N = 89, 120 cells/mm ²		CD33 ⁺ macrophages, N = 82, 83 cells/mm ²		CD15 ⁺ neutrophils, N = 95, 2.5 cells/mm ²		MDSC, N = 84		P	
	Nonbrisk density, N = 47, n (%)	Brisk density, N = 46, n (%)	Nonbrisk density, N = 45, n (%)	Brisk density, N = 44, n (%)	Nonbrisk density, N = 41, n (%)	Brisk density, N = 41, n (%)	Nonbrisk density, N = 47, n (%)	Brisk density, N = 48, n (%)	Negative, N = 79, n (%)	Positive, N = 5, n (%)		
CD8 infiltration												
Absent (score 0)	24 (51)	11 (24)	26 (58)	8 (18)	21 (51)	6 (15)	20 (44)	15 (31)	27 (35)	0 (0)		
Low (score 1)	23 (49)	24 (52)	17 (38)	27 (62)	20 (49)	25 (61)	21 (47)	26 (54)	41 (53)	3 (60)		
Moderate to robust (score 2-5)	0 (0)	11 (24)	2 (4)	9 (20)	0 (0)	10 (24)	4 (9)	7 (15)	9 (12)	2 (40)		
Unknown status	0	0	0	0	0	0	2	0	2	0		
PD-L1 expression												
Brisk	12 (32)	23 (64)	16 (44)	21 (54)	10 (31)	24 (69)	11 (31)	26 (65)	32 (51)	3 (60)		
Nonbrisk	26 (68)	13 (36)	20 (56)	18 (36)	23 (69)	11 (31)	25 (69)	14 (35)	31 (49)	2 (40)		
Unknown status	9	10	9	5	8	6	11	8	16	0		
Vascularization*												
High	19 (41)	28 (62)	21 (47)	22 (55)	18 (45)	24 (60)	23 (52)	24 (52)	40 (53)	3 (60)		
Low	27 (59)	17 (38)	24 (53)	20 (45)	22 (55)	16 (40)	21 (48)	22 (48)	36 (47)	2 (40)		
Unknown status	1	1	0	2	1	1	3	1	3	0		
Viral status												
Positive	28 (61)	26 (62)	27 (61)	25 (61)	23 (59)	28 (74)	25 (57)	31 (69)	49 (67)	2 (40)		
Negative	18 (39)	16 (38)	17 (39)	16 (39)	16 (41)	10 (26)	19 (43)	14 (31)	24 (33)	3 (60)		
Unknown status	1	4	1	3	2	3	3	3	6	0		

Data are expressed as numbers and percentages of interpretable cases.

CD68⁺, CD163⁺, and CD33⁺ macrophages and CD15⁺ neutrophils were dichotomized into the brisk or nonbrisk categories according to their median intratumoral cell densities.

Association between tumor-infiltrating myeloid cell infiltrates and MCC microenvironment components were assessed with Fisher's exact test.

MCC, Merkel cell carcinoma; MDSCs, myeloid-derived suppressor cells; PD-L1, programmed cell death ligand 1.

*Vascularization dichotomized as low and high according to the median percentage of the vascularized area.

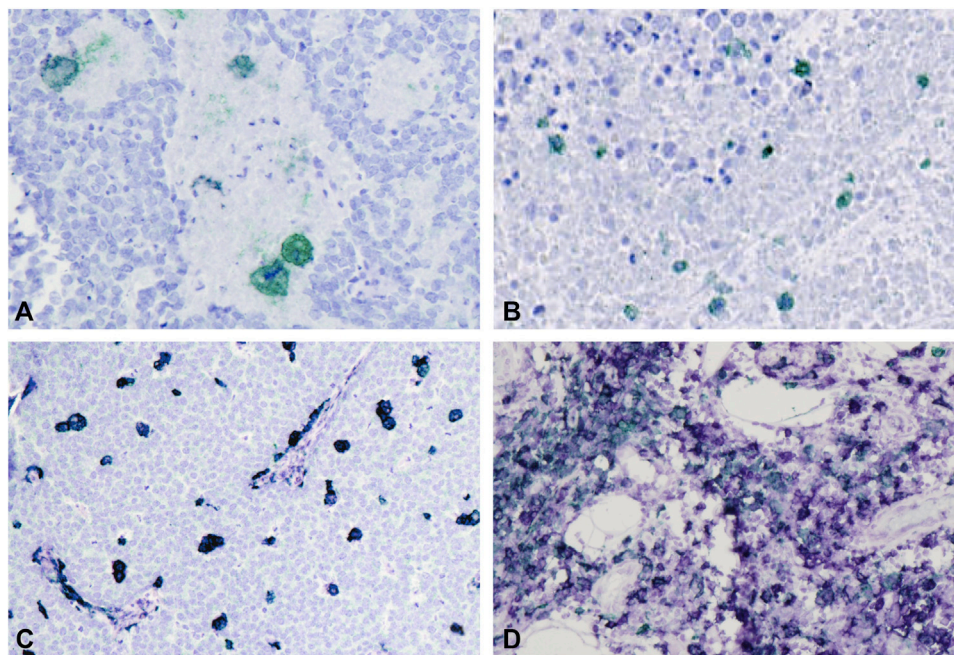


Fig 2. Myeloid-derived suppressor cell immunostaining in Merkel cell carcinoma. **A**, CD33⁺HLA-DR⁻ (green) cells. **B**, Presence of CD33⁺HLA-DR⁻ (green) cells in areas of necrosis. **C**, HLA-DR-expressing tumor-infiltrating myeloid cells in the intratumoral area. **D**, Admixture of CD33⁺HLA-DR⁻ and HLA-DR-expressing cells in fibrous septa surrounding the tumor. HLA-DR, Human leukocyte antigen—antigen D related. (**A-D**, Immunochemical staining [HRP/Emerald-AP/NBTBCIP].)

outcome.⁵⁻⁷ Although we did not find evidence of such an association in our study (Fig 4), we observed a strong correlation between infiltrating CD8⁺ T-cell infiltrates and CD33⁺ myeloid cells (Table D) as well as an impact of CD33⁺ myeloid cells on outcome (Fig 4). We therefore hypothesized that concomitant intratumoral infiltration by these 2 cell populations would affect outcome. Thirty-five MCC cases (43% of interpretable cases) harbored both brisk CD33⁺ infiltrates (ie, CD33⁺ infiltrates with a density greater than the median CD33⁺ infiltrate density) together with CD8⁺ T-cell infiltrates (scores 1-5). Characteristics of this population are reported in Supplemental Table V (available at <http://www.jaad.org>). These cases had a mean time to death of 97.5 ± 16.4 months (vs 32.3 ± 3.7 months for other patients, $P = .049$, log-rank test) and mean time to recurrence of 120.3 ± 15.0 months (vs 30.3 ± 4.6 months for other patients, $P = .007$, log-rank test) (Fig 4). This subset was, therefore, assessed by using a Cox multivariate model that included covariates previously identified in the univariate analysis (age, sex, AJCC stage, immunosuppression, and MCPyV status). In this model, such subset of MCC cases were associated with both decreased risk for recurrence (HR 0.22,

95% CI 0.008-0.61, $P = .004$) and decreased risk for death (HR 0.28, 95% CI 0.1-0.83, $P = .022$; Table III).

DISCUSSION

We investigated intratumoral infiltrating myeloid cells in 103 MCC tumors, together with CD8⁺ T-cell infiltrates, vascular density, and PD-L1 expression in the microenvironment. All MCC tumors were infiltrated with macrophages. CD8⁺ T-cell infiltration and PD-L1 expression were associated with intratumoral CD68⁺ and CD33⁺ myeloid infiltrates. These recently described intratumoral CD33⁺ cells were not found to be MDSCs but are likely to yield clinical relevance. Indeed, the subset of MCC cases with both CD8⁺ T-cell and brisk CD33⁺ infiltrates showed improved outcome.

Previous reports have described the presence of CD68⁺ macrophages in the same proportion or even exceeding that of lymphoid cells in most MCC cases.^{5,14,15,28,29} CD68⁺ macrophages were found located at the periphery of the tumor and in intratumoral areas,^{15,29} and we focused on the intratumoral spots, which are considered areas of privileged immune responses.⁴ In this setting, infiltrating myeloid cells consisted of CD68⁺ and CD163⁺ cells, as previously described,^{5,14,15,28,29} but

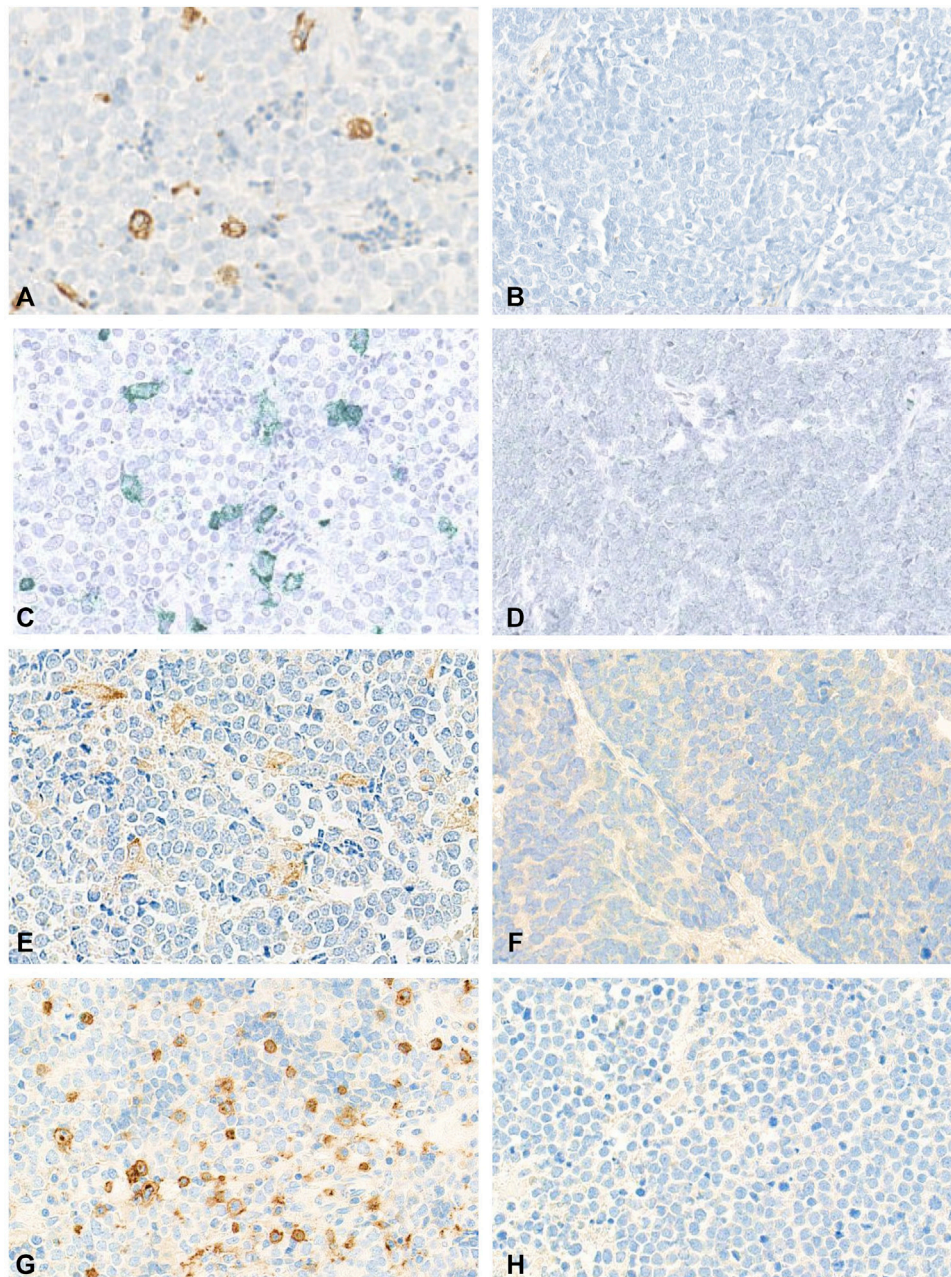


Fig 3. Representative immunostainings of both high-infiltrated (**A, C, E, G**) and noninfiltrated (**B, D, F, H**) Merkel cell carcinoma tumors. Staining for CD68 macrophages (**A, B**), CD33 macrophages (**C, D**), programmed cell death ligand 1-expressing tumor-infiltrating myeloid cells (**E, F**), and CD8 infiltrates (**G, H**). (**A-H**, Immunohistochemical staining [HRP/Emerald-AP/NBTBCIP].)

also a high number of CD33⁺ myeloid cells. Such CD33⁺ myeloid cells were recently reported in the MCC microenvironment in an immunohistochemistry study of 14 tumor samples.⁸ CD33 is a transmembranous protein that belongs to the sialic acid receptor family (sialic acid-binding immunoglobulin-type lectins). This protein is used as an early myeloid differentiation marker²⁰ that is

expressed at various levels by both neutrophil and monocyte precursors and is down regulated during cell maturation in peripheral tissues.^{30,31} CD33 has also been suggested as an MDSC marker,³² thus leading to the hypothesis that CD33⁺ cells infiltrating MCC tumors were actually MDSCs.⁸ Indeed, a putative role that was previously suggested for MDSCs was acting to exclude lymphocytes from

Table II. Univariate analysis of factors associated with Merkel cell carcinoma recurrence and death

Covariates	Recurrence		Death	
	HR (95% CI)	P	HR (95% CI)	P
Age, ≥77 vs <77 years	1.33 (0.64-2.75)	.448	1.94 (0.94-4.00)	.073
Sex, female versus male	0.39 (0.19-0.83)	.014	0.40 (0.19-0.82)	.012
AJCC stages, 3-4 vs 1-2	1.34 (0.62-2.92)	.458	1.51 (0.73-3.13)	.264
Immunosuppression, yes vs no	0.68 (0.24-1.97)	.481	1.81 (0.80-4.12)	.157
MCPyV status, positive vs negative	0.58 (0.26-1.28)	.175	0.56 (0.27-1.19)	.130
CD8 ⁺ infiltrates, score 0 vs 1-5	1.72 (0.82-3.63)	.152	1.27 (0.60-2.68)	.601
CD68 ⁺ infiltrates, brisk vs nonbrisk*	0.78 (0.36-1.68)	.530	1.22 (0.59-2.52)	.590
CD163 ⁺ infiltrates, brisk vs nonbrisk*	0.63 (0.28-1.41)	.260	0.91 (0.43-1.93)	.820
CD33 ⁺ infiltrates, brisk vs nonbrisk*	0.35 (0.15-0.83)	.016	0.44 (0.20-0.99)	.047
CD15 ⁺ infiltrates, brisk vs nonbrisk*	0.90 (0.41-1.96)	.790	1.06 (0.51-2.20)	.850

Covariates identified as potential prognostic confounders with $P \leq .20$ on Cox univariate regression analysis were included in the multivariate Cox analysis.

AJCC, American Joint Committee on Cancer; CI, confidence interval; HR, hazard ratio; MCPyV, Merkel cell polyomavirus.

*Brisk and nonbrisk defined by the median intratumoral cell density of the appropriate cell type: CD68⁺, CD163⁺, or CD33⁺ macrophages or CD15⁺ neutrophils.

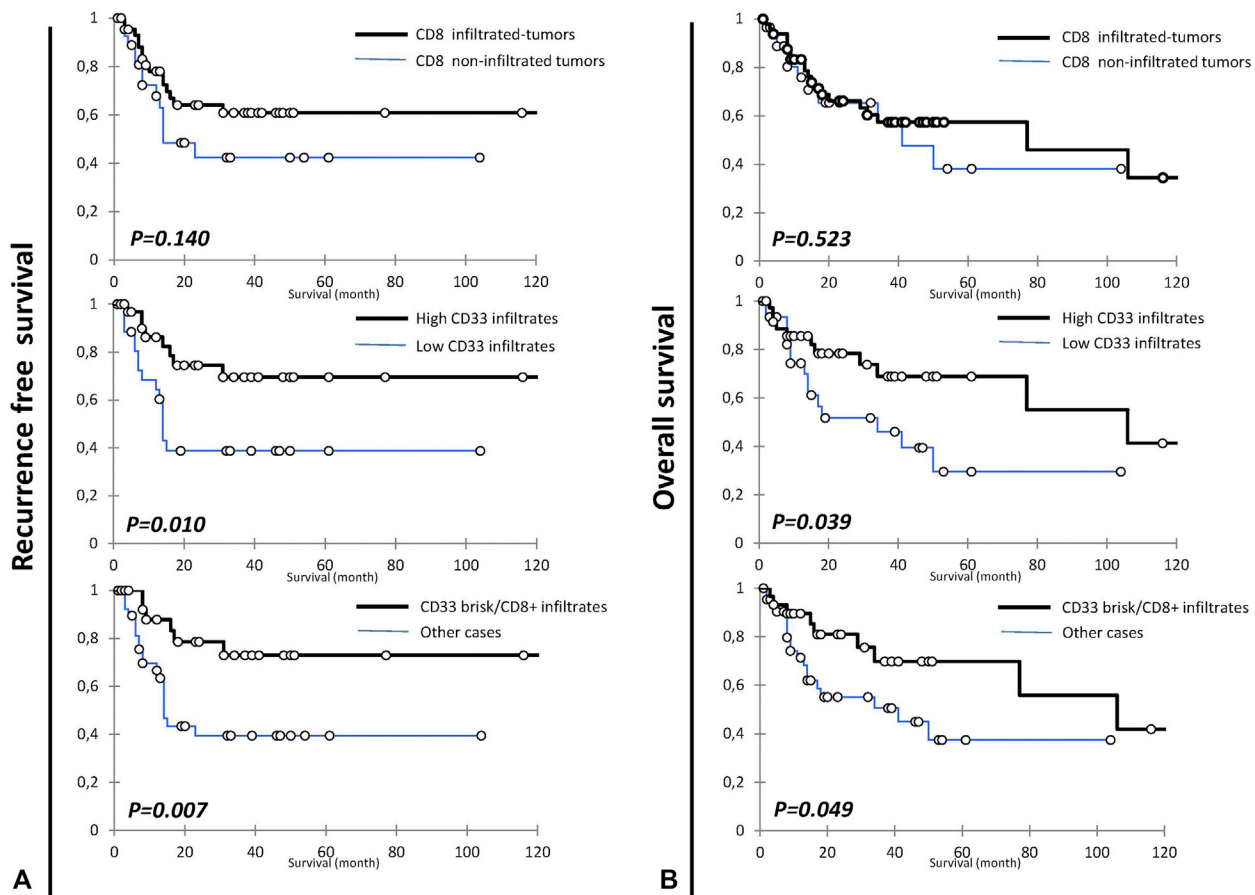


Fig 4. Kaplan-Meier survival curves for the Merkel cell carcinoma population by level of CD8⁺, CD33⁺, and CD33⁺CD8⁺ infiltrates. **A.** Recurrence-free survival. **B.** Overall survival.

MCC intratumoral areas (the stalling phenomenon).⁶ Therefore, we expected to observe an inverse relationship between myeloid infiltrates, especially CD33⁺ myeloid cells, and CD8⁺ T-lymphocyte

infiltrates in the intratumoral MCC micro-environment. By contrast, we found that CD33⁺, CD68⁺, and CD163⁺ infiltrates were closely associated with CD8⁺ T-cell infiltrates.

Table III. Multivariate Cox proportional-hazard analysis of factors associated with Merkel cell carcinoma recurrence and death

Covariate	Recurrence		Death	
	Adjusted HR (95% CI)	P	Adjusted HR (95% CI)	P
Age, ≥77 years vs <77 years	1.37 (0.52-3.62)	.525	2.70 (0.98-7.43)	.055
Sex, female vs male	0.36 (0.15-0.9)	.028	0.42 (0.17-1.03)	.058
AJCC stages, 3-4 vs 1-2	2.08 (0.81-5.34)	.130	3.80 (1.32-10.90)	.013
Immunosuppression, yes vs no	0.65 (0.21-2.01)	.458	2.50 (0.99-6.36)	.053
MCPyV status, positive vs negative	0.94 (0.37-2.42)	.902	0.91 (0.35-2.33)	.842
Brisk CD33 and CD8 infiltrate—positive,* yes vs no	0.22 (0.008-0.61)	.004	0.28 (0.1-0.83)	.022

AJCC, American Joint Committee on Cancer; CI, confidence interval; HR, hazard ratio; MCC, Merkel cell carcinoma; MCPyV, Merkel cell polyomavirus.

*Brisk CD33 was defined as tumor CD33 infiltrates with a cell density greater than the median CD33 intratumoral cell density, and CD8 infiltrate—positive was defined as having a score of 1-5.

To characterize this CD33 subset further, we developed an innovative immunohistochemistry staining protocol to visualize MDSCs. Previously, MDSC identification in FFPE tissues was proposed with only CD33³³ or the association of several slide stainings.³² Here, we used an immunohistochemical approach based on a double enzymatic staining in a uniquely cut FFPE sample with no colocalization required. This procedure allowed us to identify putative MDSCs having a CD33⁺/HLA-DR⁻ phenotype in only 5 MCC cases. Variations in MDSC nature between peripheral and intratumoral areas have been demonstrated.¹¹ Indeed, overall staining of these 5 MCC cases revealed fibrous septa distant from the tumor areas as privileged sites for CD33⁺/HLA-DR⁻ cells. Regarding intratumoral areas, MDSCs were identified in areas with necrosis, and their characteristic large cell monocytoïd morphology allowed us to rule out artifactual staining due to necrosis (Fig 2). In contrast, most of the tumor-infiltrating CD33⁺ cells in the nonnecrotic intratumoral areas actually expressed HLA-DR and, thus, were not likely to be MDSCs. Accordingly, these tumor-infiltrating CD33⁺ cells are not likely to exert immunosuppressive effects because they were found to be associated with a subset of MCC cases with improved outcome.

Previous studies failed to reveal a relationship between myeloid populations and MCC outcome.^{5,14} Here, we reveal the prognostic relevance of the concomitant intratumoral infiltration by brisk CD33⁺ myeloid cells and CD8⁺ T lymphocytes. Taken together, their close correlation with CD8⁺ T-cell infiltrates; their expression of HLA-DR, part of the class II major histocompatibility complex; and their positive impact on outcome led us to hypothesize that such CD33-expressing tumor-infiltrating macrophages contribute to an efficient antitumoral immune response.

The subset of MCC cases with brisk CD33⁺ TIMs and CD8⁺ T-lymphocyte infiltrates identified in our study did not display other specific clinical features and were not associated with MCPyV status but did have frequent PD-L1 expression in the microenvironment. CD33⁺HLA-DR⁻infiltrating myeloid cells, therefore, appear as a potential component of the PD-L1-expressing immune infiltrates. This observation led us to distinguish 2 classes of tumors: 1) CD33^{high}CD8⁺infiltrating tumors associated with improved outcome that could be targeted by PD1/PD-L1 blockage therapy and 2) other tumors with low immune infiltrates and few therapeutic targets.

The authors express their sincerest thanks to the patients who gave their approval for use of their data in the study. We also thank Professor G Fromont (Tours, France) and Roseline Guibon (Tours, France) for their help and contributions.

REFERENCES

1. Kuwamoto S. Recent advances in the biology of Merkel cell carcinoma. *Hum Pathol.* 2011;42:1063-1077.
2. Feng H, Shuda M, Chang Y, Moore PS. Clonal integration of a polyomavirus in human Merkel cell carcinoma. *Science.* 2008;319:1096-1100.
3. Paulson KG, Iyer JG, Tegeder AR, et al. Transcriptome-wide studies of Merkel cell carcinoma and validation of intratumoral CD8+ lymphocyte invasion as an independent predictor of survival. *J Clin Oncol.* 2011;29:1539-1546.
4. Paulson KG, Iyer JG, Simonson WT, et al. CD8+ lymphocyte intratumoral infiltration as a stage-independent predictor of Merkel cell carcinoma survival: a population-based study. *Am J Clin Pathol.* 2014;142:452-458.
5. Sihto H, Böbling T, Kavola H, et al. Tumor infiltrating immune cells and outcome of Merkel cell carcinoma: a population-based study. *Clin Cancer Res.* 2012;18:2872-2881.
6. Afanasiev OK, Nagase K, Simonson W, et al. Vascular E-selectin expression correlates with CD8 lymphocyte infiltration and improved outcome in Merkel cell carcinoma. *J Invest Dermatol.* 2013;133:2065-2073.
7. Dowlatshahi M, Huang V, Gehad AE, et al. Tumor-specific T cells in human Merkel cell carcinomas: a possible role for

- Tregs and T-cell exhaustion in reducing T-cell responses. *J Invest Dermatol.* 2013;133:1879-1889.
8. Mitteldorf C, Berisha A, Tronnier M, Pfaltz MC, Kempf W. PD-1 and PD-L1 in neoplastic cells and the tumor microenvironment of Merkel cell carcinoma. *J Cutan Pathol.* 2017.
 9. Vandeven N, Nghiem P. Rationale for immune-based therapies in Merkel polyomavirus-positive and -negative Merkel cell carcinomas. *Immunotherapy.* 2016;8:907-921.
 10. Elliott LA, Doherty GA, Sheahan K, Ryan EJ. Human tumor-infiltrating myeloid cells: phenotypic and functional diversity. *Front Immunol.* 2017;8:86.
 11. Kumar V, Patel S, Tcyganov E, Gabrilovich DI. The nature of myeloid-derived suppressor cells in the tumor microenvironment. *Trends Immunol.* 2016;37:208-220.
 12. Granot Z, Jablonska J. Distinct functions of neutrophil in cancer and its regulation. *Mediators Inflamm.* 2015;2015:701067.
 13. Talmadge JE, Gabrilovich DI. History of myeloid-derived suppressor cells. *Nat Rev Cancer.* 2013;13:739-752.
 14. Lipson EJ, Vincent JG, Loyo M, et al. PD-L1 expression in the Merkel cell carcinoma microenvironment: association with inflammation, Merkel cell polyomavirus and overall survival. *Cancer Immunol Res.* 2013;1:54-63.
 15. Walsh NM, Fleming KE, Hanly JG, et al. A morphological and immunophenotypic map of the immune response in Merkel cell carcinoma. *Hum Pathol.* 2016;52:190-196.
 16. Kaufman HL, Russell J, Hamid O, et al. Avelumab in patients with chemotherapy-refractory metastatic Merkel cell carcinoma: a multicentre, single-group, open-label, phase 2 trial. *Lancet Oncol.* 2016;17:1374-1385.
 17. Gardair C, Samimi M, Touzé A, et al. Somatostatin receptors 2A and 5 are expressed in Merkel cell carcinoma with no association with disease severity. *Neuroendocrinology.* 2015;101:223-235.
 18. Harms KL, Healy MA, Nghiem P, et al. Analysis of prognostic factors from 9387 Merkel cell carcinoma cases forms the basis for the new 8th edition AJCC staging system. *Ann Surg Oncol.* 2016;23:3564-3571.
 19. Paulson KG, Iyer JG, Blom A, et al. Systemic immune suppression predicts diminished Merkel cell carcinoma-specific survival independent of stage. *J Invest Dermatol.* 2013;133:642-646.
 20. Ferlazzo G, Spaggiari GM, Semino C, Melioli G, Moretta L. Engagement of CD33 surface molecules prevents the generation of dendritic cells from both monocytes and CD34+ myeloid precursors. *Eur J Immunol.* 2000;30:827-833.
 21. Ozerdem U, Wojcik EM, Barkan GA, Duan X, Erşahin Ç. A practical application of quantitative vascular image analysis in breast pathology. *Pathol Res Pract.* 2013;209:455-458.
 22. Houben R, Adam C, Baeurle A, et al. An intact retinoblastoma protein-binding site in Merkel cell polyomavirus large T antigen is required for promoting growth of Merkel cell carcinoma cells. *Int J Cancer.* 2012;130:847-856.
 23. Moshiri AS, Doumani R, Yelistratova L, et al. Polyomavirus-negative Merkel cell carcinoma: a more aggressive subtype based on analysis of 282 cases using multimodal tumor virus detection. *J Invest Dermatol.* 2016.
 24. Iyer JG, Storer BE, Paulson KG, et al. Relationships among primary tumor size, number of involved nodes, and survival for 8044 cases of Merkel cell carcinoma. *J Am Acad Dermatol.* 2014;70:637-643.
 25. Harrington C, Kwan W. Outcomes of Merkel cell carcinoma treated with radiotherapy without radical surgical excision. *Ann Surg Oncol.* 2014;21:3401-3405.
 26. Bhatia S, Storer BE, Iyer JG, et al. Adjuvant radiation therapy and chemotherapy in Merkel cell carcinoma: survival analyses of 6908 cases from the National Cancer Data Base. *J Natl Cancer Inst.* 2016;108.
 27. Albores-Saavedra J, Batich K, Chable-Montero F, et al. Merkel cell carcinoma demographics, morphology, and survival based on 3870 cases: a population based study. *J Cutan Pathol.* 2010;37:20-27.
 28. Werchau S, Toberer F, Enk A, Dammann R, Helmbold P. Merkel cell carcinoma induces lymphatic microvessel formation. *J Am Acad Dermatol.* 2012;67:215-225.
 29. Wheat R, Roberts C, Waterboer T, et al. Inflammatory cell distribution in primary Merkel cell carcinoma. *Cancers.* 2014;6:1047-1064.
 30. Forsyth RG, De Boeck G, Baeide JJ, et al. CD33+ CD14- phenotype is characteristic of multinuclear osteoclast-like cells in giant cell tumor of bone. *J Bone Miner Res.* 2009;24:70-77.
 31. Lock K, Zhang J, Lu J, Lee SH, Crocker PR. Expression of CD33-related siglecs on human mononuclear phagocytes, monocyte-derived dendritic cells and plasmacytoid dendritic cells. *Immunobiology.* 2004;209:199-207.
 32. Liu WR, Tian MX, Yang LX, et al. PKM2 promotes metastasis by recruiting myeloid-derived suppressor cells and indicates poor prognosis for hepatocellular carcinoma. *Oncotarget.* 2015;6:846-861.
 33. Cui TX, Kryczek I, Zhao E, et al. Myeloid-derived suppressor cells enhance stemness of cancer cells by inducing microRNA101 and suppressing the corepressor CtBP2. *Immunity.* 2013;39:611-621.

SUPPLEMENTARY APPENDIX. METHODS

Assessment of the reproducibility of the immune cell count in a validation cohort of overall slide stained cases

In order to assess the representativeness of our tissue microarray approach, studies of the CD68, CD163, CD33, and CD15 markers were performed on overall slides for 20 cases. Evaluation was performed in the intratumoral area as described in the Methods section. For each case, counts of cells were performed with 2 distinctive areas using 5 high-power fields each. The obtained counts were compared for each case by using the Pearson correlation ([Supplemental Table II](#)).

Protocol for CD33 and HLA-DR immunostaining and associated controls

The procedure was performed as follows: 4- μ m sections of paraffin-embedded Merkel cell carcinoma (MCC) tissues were dried at 37°C overnight and deparaffinized by a graded alcohol series according to standard protocols. Subsequent heat-induced antigen retrieval was performed in EDTA buffer pH 8.4 for 20 min at 121°C. Slides were stained with antibodies for CD33 and human leukocyte antigen-DR (HLA-DR) ([Supplemental Table I](#)). Antigen-bound primary antibodies were visualized by appropriate horseradish-peroxidase-coupled anti-rabbit and alkaline phosphatase-coupled anti-mouse polymer secondary antibodies (N-Histofine, Nichirei Biosciences Inc, Tokyo, Japan) associated with appropriate enzymatic substrates (NBT/BCIP [Vector Laboratories, Burlingame, CA] and Emerald [GBI Labs, Bothell, WA]) followed by Papanicolaou counterstaining. U-mount mounting medium (GBI Labs) was used.

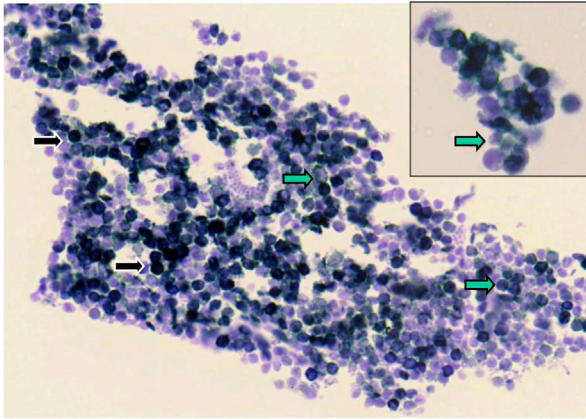
Five technical controls were added: single CD33 or HLA-DR antibodies associated with appropriate secondary antibody, single CD33 or HLA-DR antibodies associated with the other secondary antibody (CD33 antibody with the secondary

anti-mouse antibody, and HLA-DR antibody with the secondary anti-rabbit antibody) and secondary antibodies alone.

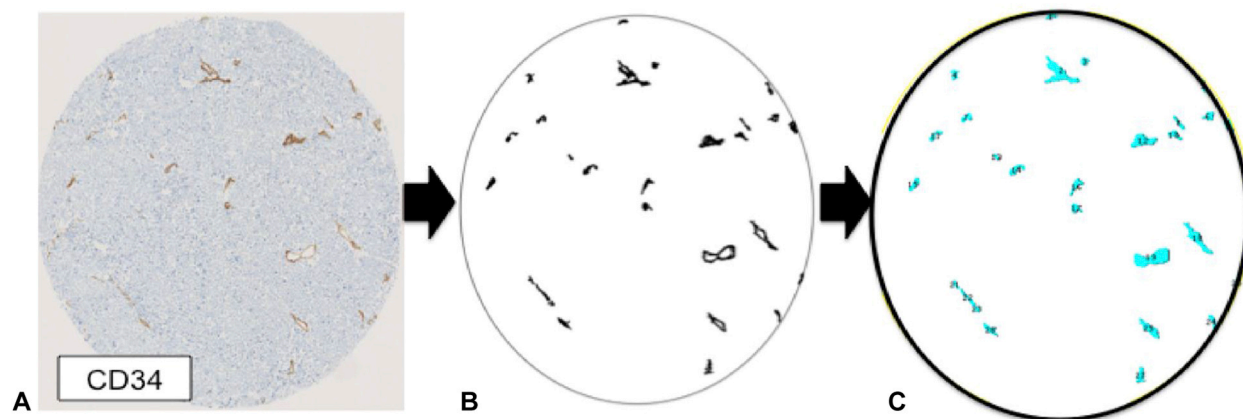
In addition, to test our procedure on immature myeloid cells, bone marrow blood precursors were used as biologic positive controls and investigated by immunochemistry. Bone marrow mobilization of hematopoietic precursors is currently used during the monitoring of patients with a history of acute leukemia and bone marrow transplant. These patients receive granulocyte colony-stimulating factor inducing activation and degranulation of neutrophils in bone marrow and finally the release of bone marrow precursors into blood circulation. At this time, cytopheresis is performed to isolate nucleated cells, which are analyzed to check the quality of the transplant. With the consent of the patients and local committee agreement (OPTICYTE protocol), 2 anonymized samples were included in our study. After centrifugation, cells were formalin-fixed and paraffin-embedded (FFPE). Immunochemical staining was performed as described in the Methods section. Microscopy reveals green staining of numerous bone marrow precursors associated with few mature blood-circulating monocytes showing HLA-DR expression ([Supplemental Figure 1](#)), thereby validating our strategy.

Measurement of vascular density

Analyses involved use of ImageJ. Tumor areas were first delineated using the CROP function. Adjust color was then used to exclude the blue counterstaining color. Size of the picture was then restricted to 8 bits and the staining was underlined by using the following functions: binary and dilate. Area measurement was performed by the Analyse particle function with the following parameters: size: 30-infinity; sphericity: 0-0.9. Finally, morphology of the delineated areas was assessed by a pathologist who used the overlying mask function.



Supplemental Fig 1. CD33/HLA-DR immunostaining on FFPE cytopheresis sample after bone marrow precursor mobilization. Myeloid precursors are stained green (*green arrow*) and circulating monocytes are stained black (*black arrow*). (Immunostain; original magnification: $\times 200$.)



Supplemental Fig 2. Representative images of the vascular measurement: CD34 immunostaining (A), delineated vascular areas (B), assessment using the overlying mask function (C).

Supplemental Table I. Antibodies and dilutions used

Antigen	Antibody, clone/manufacturer (location)	Dilution	Targeted population
CD68	PGM1/Dako (Glostrup, Denmark)	1/400	Pan monocyte-macrophages
CD163	10D6/Novocastra	1/200	Tumor-associated macrophages
CD33	SP166/Ventana Medical Systems	Ready to use	Early differentiation myeloid population
HLA-DR	TAL.1B5/Dako	1/400	Macrophages and dendritic cells
CD15	MMA/Roche (Basel, Switzerland)	Ready to use	Neutrophils
CD8	M7103/Dako	1/50	CD8 lymphocytes
CD34	QBEnd10/Dako	1/50	Endothelial cells
PD-L1	E1L3N/Cell Signaling Technology (Beverly, MA)	1/200	Not appropriate
MCPyV-LT	CM2B4/Santa Cruz Biotechnology (Dallas, TX)	1/200	Tumor cells

HLA-DR, Human leukocyte antigen–DR; *MCPyV-LT*, Merkel cell polyomavirus large T-antigen; *PD-L1*, programmed cell death ligand 1.

Supplemental Table II. Myeloid populations:
Reproducibility of count between areas

Myeloid populations	R²	P value
CD68	0.93	7.10 ⁻⁷
CD163	0.98	2.10 ⁻¹⁰
CD33	0.90	4.10 ⁻⁶
CD15	0.5	.03

R², Pearson correlation coefficient.

Supplemental Table III. Baseline clinical characteristics of patients with Merkel cell carcinoma by tumor-infiltrating myeloid cell density

Clinical characteristics	Myeloid cell type; median intratumoral cell density												
	CD68 macrophages, N = 93, 216 cells/mm ²		CD163 macrophages, N = 89, 120 cells/mm ²		CD33 macrophages, N = 82, 83 cells/mm ²		CD15 neutrophils, N = 95, 2.5 cells/mm ²		MDSC, N = 84		P		
	Nonbrisk density, N = 47, n (%)	Brisk density, N = 46, n (%)	Nonbrisk density, N = 45, n (%)	Brisk density, N = 44, n (%)	Nonbrisk density, N = 41, n (%)	Brisk density, N = 41, n (%)	Nonbrisk density, N = 47, n (%)	Brisk density, N = 48, n (%)	Negative, N = 79, n (%)	Positive, N = 5, n (%)			
Age, y*													
≤77.3	20 (52)	16 (39)	22 (54)	13 (37)	15 (44)	17 (46)	16 (39)	21 (51)	30 (45)	1 (25)			
>77.3	18 (48)	25 (61)	19 (46)	22 (63)	19 (56)	20 (54)	23 (61)	20 (49)	37 (55)	3 (75)			
Unknown status	9	5	4	9	7	4	8	7	12	1			
Sex													
Female	24 (53)	28 (62)	24 (55)	27 (64)	24 (60)	21 (54)	31 (67)	22 (48)	44 (58)	3 (60)			
Male	21 (47)	17 (38)	20 (45)	15 (36)	16 (40)	18 (46)	15 (33)	24 (52)	32 (42)	2 (40)			
Unknown status	2	1	1	2	1	2	1	2	3	0			
Immunosuppression													
Yes	7 (23)	3 (9)	4 (11)	5 (19)	7 (24)	2 (7)	4 (13)	6 (18)	9 (17)	0			
No	24 (77)	30 (91)	31 (89)	21 (81)	22 (76)	27 (93)	27 (87)	28 (82)	45 (83)	4 (100)			
Unknown status	16	13	10	18	12	12	16	14	25	1			
AJCC stage													
I	9 (24)	11 (28)	8 (20)	12 (38)	9 (26)	10 (29)	16 (43)	4 (10)	18 (28)	1 (25)			
II	13 (34)	7 (18)	16 (39)	4 (13)	10 (29)	6 (18)	8 (22)	14 (34)	15 (23)	2 (50)			
III	15 (39)	19 (49)	16 (39)	15 (46)	13 (39)	17 (50)	13 (35)	20 (48)	28 (44)	1 (25)			
IV	1 (3)	2 (5)	1 (2)	1 (3)	2 (6)	1 (3)	0	3 (8)	3 (5)	0			
Unknown status	9	7	4	12	7	7	10	7	15	1			
Location of sample													
Primary tumors	29 (70)	27 (64)	27 (66)	27 (71)	27 (73)	23 (60)	31 (74)	26 (60)	48 (67)	3 (80)			
Head	14	9	15	8	13	9	10	14	21	2			
Trunk	1	0	0	1	1	1	2	0	2	0			
Upper limb	2	4	1	4	2	3	3	3	5	0			
Lower limb	12	14	11	14	11	10	16	9	20	1			
Metastasis	12 (30)	15 (36)	14 (34)	11 (29)	10 (27)	15 (40)	11 (26)	17 (40)	23 (33)	1 (20)			
Unknown status	6	4	4	6	4	3	5	5	8	1			

Data are expressed as number and percentages of interpretable cases.

CD68⁺, CD163⁺, and CD33⁺ macrophages and CD15⁺ neutrophils were dichotomized into the brisk or nonbrisk categories according to their median intratumoral cell densities.

Associations between tumor-infiltrating myeloid cell infiltrates and clinical characteristics were assessed with Fisher's exact test.

Significant value is in bold.

AJCC, American Joint Committee on Cancer; MDSC, myeloid-derived suppressor cells.

*Dichotomized by median age (77.3 years).

Supplemental Table IV. Multivariate Cox proportional-hazard analysis of factors associated with MCC recurrence and death

Covariate	Recurrence		Death	
	Adjusted HR (95% CI)	P	Adjusted HR (95% CI)	P
Age, y, ≥ 77 vs < 77	1.39 (0.50-3.89)	.529	2.42 (0.85-6.85)	.09
Sex, male vs female	2.42 (0.93-6.29)	.070	2.12 (0.81-5.52)	.126
AJCC score, 3-4 vs 1-2	2.75 (0.94-8.08)	.065	3.90 (1.20-12.70)	.024
Immunosuppression, yes vs no	0.84 (0.27-2.60)	.775	2.40 (0.86-6.66)	.096
MCPyV status, positive vs negative	0.75 (0.247-2.10)	.582	0.88 (0.30-2.55)	.808
CD8 infiltrate score, 0 vs 1-5	1.65 (0.63-4.38)	.315	1.30 (0.48-3.53)	.601
CD33 infiltrate, brisk versus nonbrisk*	0.35 (0.11-1)	.051	0.40 (0.14-1.25)	.083

AJCC, American Joint Committee on Cancer; CI, confidence interval; HR, hazard ratio; MCC, Merkel cell carcinoma; MCPyV, Merkel cell polyomavirus.

*CD33⁺ infiltrates were dichotomized into brisk or nonbrisk on the basis of median intratumoral cell density.

Supplemental Table V. Characteristics of the Merkel cell carcinoma subset with CD33 brisk and CD8⁺ T-cell infiltrates

Characteristics	CD33 brisk, CD8 ⁺ infiltrates		P value
	No, N = 47, n (%)	Yes, N = 35, n (%)	
Age, y*			.8
≤77.3	19 (48)	13 (58)	
>77.3	21 (52)	18 (42)	
Unknown status	7	4	
Sex			.8
Female	25 (56)	20 (59)	
Male	20 (44)	14 (41)	
Unknown status	2	1	
Immunosuppression			.17
Yes	7 (22)	2 (8)	
No	25 (78)	24 (92)	
Unknown status	15	9	
AJCC stage			.9
I	10 (25)	9 (32)	
II	10 (25)	6 (21)	
III	18 (45)	12 (43)	
IV	2 (5)	1 (4)	
Unknown status	7	7	
Location of the sample			.8
Primary tumors	28 (65)	22 (69)	
Head	14	8	
Trunk	1	1	
Upper limb	2	3	
Lower limb	11	10	
Metastasis	15 (35)	10 (31)	
Unknown status	4	3	
PD-L1 expression [†]			6 × 10⁻³
Brisk	13 (34)	21 (70)	
Nonbrisk	25 (66)	9 (30)	
Unknown status	9	5	
Vascularization [‡]			.9
High	24 (52)	17 (50)	
Low	22 (48)	17 (50)	
Unknown status	1	1	
Viral status			.2
Positive	27 (60)	24 (75)	
Negative	18 (40)	8 (25)	
Unknown status	2	3	

Significant value is in bold.

AJCC, American Joint Committee on Cancer; PD-L1, programmed cell death ligand 1.

*Dichotomized by median age (77.3 years).

[†]Brisk and nonbrisk defined by median count of intratumoral CD33-expressing macrophages.[‡]High and low vascularized cases defined by the median density of vascular area (1.5%).

REFERENCES

- Abdul-Sada H, Müller M, Mehta R, Toth R, Arthur JSC, Whitehouse A, et al. The PP4R1 sub-unit of protein phosphatase PP4 is essential for inhibition of NF- κ B by merkel polyomavirus small tumour antigen. *Oncotarget*. 2017;8(15):25418–32
- Adam C, Baeurle A, Brodsky JL, Wipf P, Schrama D, Becker JC, et al. The HSP70 modulator MAL3-101 inhibits Merkel cell carcinoma. *PloS One*. 2014;9(4):e92041
- Agaimy A, Erlenbach-Wünsch K, Konukiewitz B, Schmitt AM, Rieker RJ, Vieth M, et al. ISL1 expression is not restricted to pancreatic well-differentiated neuroendocrine neoplasms, but is also commonly found in well and poorly differentiated neuroendocrine neoplasms of extrapancreatic origin. *Mod. Pathol. Off. J. U. S. Can. Acad. Pathol. Inc.* 2013;26(7):995–1003
- Akazawa Y, Terada Y, Yamane T, Tanaka S, Aimoto M, Koh H, et al. Fatal BK virus pneumonia following stem cell transplantation. *Transpl. Infect. Dis. Off. J. Transplant. Soc.* 2012;14(6):E142-146
- Akiyama M, Dale BA, Sun TT, Holbrook KA. Characterization of hair follicle bulge in human fetal skin: the human fetal bulge is a pool of undifferentiated keratinocytes. *J. Invest. Dermatol.* 1995;105(6):844–50
- Albores-Saavedra J, Batich K, Chable-Montero F, Sagy N, Schwartz AM, Henson DE. Merkel cell carcinoma demographics, morphology, and survival based on 3870 cases: a population based study. *J. Cutan. Pathol.* 2010;37(1):20–7
- Angermeyer S, Hesbacher S, Becker JC, Schrama D, Houben R. Merkel cell polyomavirus-positive Merkel cell carcinoma cells do not require expression of the viral small T antigen. *J. Invest. Dermatol.* 2013;133(8):2059–64
- Aragaki M, Tsuchiya K, Okamoto R, Yoshioka S, Nakamura T, Sakamoto N, et al. Proteasomal degradation of Atoh1 by aberrant Wnt signaling maintains the undifferentiated state of colon cancer. *Biochem. Biophys. Res. Commun.* 2008;368(4):923–9
- Asgari MM, Sokil MM, Warton EM, Iyer J, Paulson KG, Nghiem P. Effect of host, tumor, diagnostic, and treatment variables on outcomes in a large cohort with Merkel cell carcinoma. *JAMA Dermatol.* 2014;150(7):716–23
- Atkin SJL, Griffin BE, Dilworth SM. Polyoma virus and simian virus 40 as cancer models: history and perspectives. *Semin. Cancer Biol.* 2009;19(4):211–7
- Azmahani A, Nakamura Y, Ishida H, McNamara KM, Fujimura T, Haga T, et al. Estrogen receptor β in Merkel cell carcinoma: its possible roles in pathogenesis. *Hum. Pathol.* 2016;56:128–33
- Badzio A, Czapiewski P, Gorczyński A, Szczepańska-Michalska K, Haybaeck J, Biernat W, et al. Prognostic value of broad-spectrum keratin clones AE1/AE3 and CAM5.2 in small cell lung cancer patients undergoing pulmonary resection. *Acta Biochim. Pol.* 2019;66(1):111–4
- Bandino JP, Purvis CG, Shaffer BR, Gad A, Elston DM. A Comparison of the Histopathologic Growth Patterns Between Non-Merkel Cell Small Round Blue Cell Tumors and Merkel Cell Carcinoma. *Am. J. Dermatopathol.* 2018;40(11):815–8
- Bardot ES, Valdes VJ, Zhang J, Perdigoto CN, Nicolis S, Hearn SA, et al. Polycomb subunits Ezh1 and Ezh2 regulate the Merkel cell differentiation program in skin stem cells. *EMBO J.* 2013;32(14):1990–2000
- Baudoin C, Meneguzzi G, Portier MM, Demarchez M, Bernerd F, Pisani A, et al. Peripherin, a neuronal intermediate protein, is stably expressed by neuroendocrine carcinomas of the skin, their xenograft on nude mice, and the corresponding primary cultures. *Cancer Res.* 1993;53(5):1175–81
- Becker M, Dominguez M, Greune L, Soria-Martinez L, Pfliederer MM, Schowalter R, et al. Infectious Entry of Merkel Cell Polyomavirus. *J. Virol.* 2019a;93(6)
- Becker JC, Eigentler T, Frerich B, Gambichler T, Grabbe S, Höller U, et al. S2k guidelines for Merkel cell carcinoma (MCC, neuroendocrine carcinoma of the skin) - update 2018. *J. Dtsch. Dermatol. Ges. J. Ger. Soc. Dermatol. JDDG.* 2019b;17(5):562–76
- Becker JC, Houben R, Ugurel S, Trefzer U, Pföhler C, Schrama D. MC polyomavirus is frequently present in Merkel cell carcinoma of European patients. *J. Invest. Dermatol.* 2009;129(1):248–50
- Becker JC, Lorenz E, Ugurel S, Eigentler TK, Kiecker F, Pföhler C, et al. Evaluation of real-world treatment outcomes in patients with distant metastatic Merkel cell carcinoma following second-line chemotherapy in Europe. *Oncotarget.* 2017;8(45):79731–41
- Becker JC, Zur Hausen A. Cells of origin in skin cancer. *J. Invest. Dermatol.* 2014;134(10):2491–3
- Beckervordersandforth J, Pujari S, Rennspiess D, Speel EJM, Winnepenninckx V, Diaz C, et al. Frequent detection of human polyomavirus 6 in keratoacanthomas. *Diagn. Pathol.* 2016;11(1):58
- Behr DS, Peitsch WK, Hametner C, Lasitschka F, Houben R, Schönhaar K, et al. Prognostic value of immune cell infiltration, tertiary lymphoid structures and PD-L1 expression in Merkel cell carcinomas. *Int. J. Clin. Exp. Pathol.* 2014;7(11):7610–21

Bellizzi AM. SATB2 in Neuroendocrine Neoplasms: Strong Expression is Restricted to Well-Differentiated Tumors of Lower Gastrointestinal Tract Origin and is More Frequent in Merkel Cell Carcinoma among Poorly Differentiated Carcinomas. *Histopathology*. 2019;

Bellott TR, Baez CF, Almeida SG, Venceslau MT, Zalis MG, Guimarães MA, et al. Molecular prevalence of Merkel cell polyomavirus in nonmelanoma skin cancer in a Brazilian population. *Clin. Exp. Dermatol.* 2017;42(4):390–4

Ben-nun-Shaul O, Bronfeld H, Reshef D, Schueler-Furman O, Oppenheim A. The SV40 capsid is stabilized by a conserved pentapeptide hinge of the major capsid protein VP1. *J. Mol. Biol.* 2009;386(5):1382–91

Berrios C, Padi M, Keibler MA, Park DE, Molla V, Cheng J, et al. Merkel Cell Polyomavirus Small T Antigen Promotes Pro-Glycolytic Metabolic Perturbations Required for Transformation. *PLoS Pathog.* 2016;12(11) Available from: <https://www.ncbi.nlm.nih.gov/pmc/articles/PMC5120958/>

de Biase D, Ragazzi M, Asioli S, Eusebi V. Extracutaneous Merkel cell carcinomas harbor polyomavirus DNA. *Hum. Pathol.* 2012;43(7):980–5

Bichakjian CK, Olencki T, Aasi SZ, Alam M, Andersen JS, Blitzblau R, et al. Merkel Cell Carcinoma, Version 1.2018, NCCN Clinical Practice Guidelines in Oncology. *J. Natl. Compr. Cancer Netw. JNCCN.* 2018;16(6):742–74

Borchert S, Czech-Sioli M, Neumann F, Schmidt C, Wimmer P, Dobner T, et al. High-affinity Rb binding, p53 inhibition, subcellular localization, and transformation by wild-type or tumor-derived shortened Merkel cell polyomavirus large T antigens. *J. Virol.* 2014;88(6):3144–60

Bossuyt W, Kazanjian A, De Geest N, Van Kelst S, De Hertogh G, Geboes K, et al. Atonal homolog 1 is a tumor suppressor gene. *PLoS Biol.* 2009;7(2):e39

Boulais N, Pereira U, Lebonvallet N, Gobin E, Dorange G, Rougier N, et al. Merkel cells as putative regulatory cells in skin disorders: an in vitro study. *PLoS One.* 2009;4(8):e6528

Boyd N, Dancey JE, Gilks CB, Huntsman DG. Rare cancers: a sea of opportunity. *Lancet Oncol.* 2016;17(2):e52–61

Brew BJ, Davies NWS, Cinque P, Clifford DB, Nath A. Progressive multifocal leukoencephalopathy and other forms of JC virus disease. *Nat. Rev. Neurol.* 2010;6(12):667–79

Brewer JD, Shanafelt TD, Otley CC, Roenigk RK, Cerhan JR, Kay NE, et al. Chronic lymphocytic leukemia is associated with decreased survival of patients with malignant melanoma and Merkel cell carcinoma in a SEER population-based study. *J. Clin. Oncol. Off. J. Am. Soc. Clin. Oncol.* 2012;30(8):843–9

Brownell, I. How the paranuclear cytokeratin dot may be blocking apoptosis in MCC. 2019.

Buck CB, Van Doorslaer K, Peretti A, Geoghegan EM, Tisza MJ, An P, et al. The Ancient Evolutionary History of Polyomaviruses. *PLoS Pathog.* 2016;12(4):e1005574

Busam KJ, Jungbluth AA, Rekhman N, Coit D, Pulitzer M, Bini J, et al. Merkel cell polyomavirus expression in merkel cell carcinomas and its absence in combined tumors and pulmonary neuroendocrine carcinomas. *Am. J. Surg. Pathol.* 2009;33(9):1378–85

Buscone S, Garavello W, Pagni F, Gaini RM, Cattoretti G. Nasopharyngeal tonsils (adenoids) contain extrathymic corticostimulatory cells. *PLoS One.* 2014;9(5):e98222

Calabrese LH, Molloy E, Berger J. Sorting out the risks in progressive multifocal leukoencephalopathy. *Nat. Rev. Rheumatol.* 2015;11(2):119–23

Calder KB, Coplowitz S, Schlauder S, Morgan MB. A case series and immunophenotypic analysis of CK20-/CK7+ primary neuroendocrine carcinoma of the skin. *J. Cutan. Pathol.* 2007;34(12):918–23

Carter JJ, Daugherty MD, Qi X, Bheda-Malge A, Wipf GC, Robinson K, et al. Identification of an overprinting gene in Merkel cell polyomavirus provides evolutionary insight into the birth of viral genes. *Proc. Natl. Acad. Sci. U. S. A.* 2013;110(31):12744–9

Carter MD, Gaston D, Huang W-Y, Greer WL, Pasternak S, Ly TY, et al. Genetic Profiles of Different Subsets of Merkel Cell Carcinoma Show Links between Combined and Pure MCPyV-negative Tumors. *Hum. Pathol.* 2017;

Cason C, Monasta L, Zanotta N, Campisciano G, Maestri I, Tommasino M, et al. Antibody response to polyomavirus primary infection: high seroprevalence of Merkel cell polyomavirus and lymphoid tissue involvement. *J. Neurovirol.* 2018;24(3):314–22

Caulin C, Ware CF, Magin TM, Oshima RG. Keratin-dependent, epithelial resistance to tumor necrosis factor-induced apoptosis. *J. Cell Biol.* 2000;149(1):17–22

Champaneria MC, Modlin IM, Kidd M, Eick GN. Friedrich Feyrter: a precise intellect in a diffuse system. *Neuroendocrinology.* 2006;83(5–6):394–404

Chan JK, Suster S, Wenig BM, Tsang WY, Chan JB, Lau AL. Cytokeratin 20 immunoreactivity distinguishes Merkel cell (primary cutaneous neuroendocrine) carcinomas and salivary gland small cell carcinomas from small cell carcinomas of various sites. *Am. J. Surg. Pathol.* 1997;21(2):226–34

Chang W, Kanda H, Ikeda R, Ling J, DeBerry JJ, Gu JG. Merkel disc is a serotonergic synapse in the epidermis for transmitting tactile signals in mammals. *Proc. Natl. Acad. Sci. U. S. A.* 2016;113(37):E5491-5500

Chen Z, Gu J. Immunoglobulin G expression in carcinomas and cancer cell lines. *FASEB J. Off. Publ. Fed. Am. Soc. Exp. Biol.* 2007;21(11):2931–8

Chen Z, Li J, Xiao Y, Zhang J, Zhao Y, Liu Y, et al. Immunoglobulin G locus events in soft tissue sarcoma cell lines. *PLoS One.* 2011;6(6):e21276

Chen H-Z, Tsai S-Y, Leone G. Emerging roles of E2Fs in cancer: an exit from cell cycle control. *Nat. Rev. Cancer.* 2009;9(11):785–97

Cheng Y-F. Atoh1 regulation in the cochlea: more than just transcription. *J. Zhejiang Univ. Sci. B.* 2019;20(2):146–55

Cheng J, Park DE, Berrios C, White EA, Arora R, Yoon R, et al. Merkel cell polyomavirus recruits MYCL to the EP400 complex to promote oncogenesis. *PLoS Pathog.* 2017;13(10):e1006668

Cheng J, Rozenblatt-Rosen O, Paulson KG, Nghiem P, DeCaprio JA. Merkel cell polyomavirus large T antigen has growth-promoting and inhibitory activities. *J. Virol.* 2013;87(11):6118–26

Cheng Y-F, Tong M, Edge ASB. Destabilization of Atoh1 by E3 Ubiquitin Ligase Huwe1 and Casein Kinase 1 Is Essential for Normal Sensory Hair Cell Development. *J. Biol. Chem.* 2016;291(40):21096–109

Cheuk W, Kwan MY, Suster S, Chan JK. Immunostaining for thyroid transcription factor 1 and cytokeratin 20 aids the distinction of small cell carcinoma from Merkel cell carcinoma, but not pulmonary from extrapulmonary small cell carcinomas. *Arch. Pathol. Lab. Med.* 2001;125(2):228–31

Chittick P, Williamson JC, Ohl CA. BK virus encephalitis: case report, review of the literature, and description of a novel treatment modality. *Ann. Pharmacother.* 2013;47(9):1229–33

Chou T-C, Tsai K-B, Wu C-Y, Hong C-H, Lee C-H. Presence of the Merkel cell polyomavirus in Merkel cell carcinoma combined with squamous cell carcinoma in a patient with chronic arsenism. *Clin. Exp. Dermatol.* 2016;41(8):902–5

Chteinberg E, Sauer CM, Rennspiess D, Beumers L, Schiffelers L, Eben J, et al. Neuroendocrine Key Regulator Gene Expression in Merkel Cell Carcinoma. *Neoplasia N. Y. N.* 2018;20(12):1227–35

Clark JJ, Bowen AR, Bowen GM, Hynstrom JR, Hadley ML, Duffy K, et al. Cutaneous carcinosarcoma: a series of six cases and a review of the literature. *J. Cutan. Pathol.* 2017;44(1):34–44

Coleman DV, Mackenzie EF, Gardner SD, Poulding JM, Amer B, Russell WJ. Human polyomavirus (BK) infection and ureteric stenosis in renal allograft recipients. *J. Clin. Pathol.* 1978;31(4):338–47

Coleman CB, Nealy MS, Tibbetts SA. Immature and transitional B cells are latency reservoirs for a gammaherpesvirus. *J. Virol.* 2010;84(24):13045–52

Collina G, Eusebi V, Capella C, Rosai J. Merkel cell differentiation in trichoblastoma. *Virchows Arch. Int. J. Pathol.* 1998;433(4):291–6

Cook M, Baker K, Redman M, Lachance K, Nguyen MH, Parvathaneni U, et al. Differential Outcomes Among Immunosuppressed Patients With Merkel Cell Carcinoma: Impact of Immunosuppression Type on Cancer-specific and Overall Survival. *Am. J. Clin. Oncol.* 2019;42(1):82–8

Czapiewski P, Majewska H, Kutzner H, Kazakov D, Renkielska A, Biernat W. TTF-1 and PAX5 Are Frequently Expressed in Combined Merkel Cell Carcinoma. *Am. J. Dermatopathol.* 2016;38(7):513–6

Dalle S, Parmentier L, Moscarella E, Phan A, Argenziano G, Thomas L. Dermoscopy of Merkel cell carcinoma. *Dermatol. Basel Switz.* 2012;224(2):140–4

D'Angelo SP, Russell J, Lebbé C, Chmielowski B, Gambichler T, Grob J-J, et al. Efficacy and Safety of First-line Avelumab Treatment in Patients With Stage IV Metastatic Merkel Cell Carcinoma: A Preplanned Interim Analysis of a Clinical Trial. *JAMA Oncol.* 2018;4(9):e180077

Dehority WN, Eickman MM, Schwalm KC, Gross SM, Schroth GP, Young SA, et al. Complete genome sequence of a KI polyomavirus isolated from an otherwise healthy child with severe lower respiratory tract infection. *J. Med. Virol.* 2017;89(5):926–30

Deichmann M, Kurzen H, Egner U, Altevogt P, Hartschuh W. Adhesion molecules CD171 (L1CAM) and CD24 are expressed by primary neuroendocrine carcinomas of the skin (Merkel cell carcinomas). *J. Cutan. Pathol.* 2003;30(6):363–8

Dela Cruz FN, Giannitti F, Li L, Woods LW, Del Valle L, Delwart E, et al. Novel polyomavirus associated with brain tumors in free-ranging raccoons, western United States. *Emerg. Infect. Dis.* 2013;19(1):77–84

Delbue S, Ferrante P, Provenzano M. Polyomavirus BK and prostate cancer: an unworthy scientific effort? *Oncoscience.* 2014;1(4):296–303

Diaz J, Wang X, Tsang SH, Jiao J, You J. Phosphorylation of large T antigen regulates merkel cell polyomavirus replication. *Cancers.* 2014;6(3):1464–86

Domínguez-Malagón HR, Michal M, Kazakov DV, Caro-Sánchez CH, Lino-Silva LS. Utility of CD99 Paranuclear Expression in the Differential Diagnosis of Merkel Cell Carcinoma. *Int. J. Surg. Pathol.* 2016;24(4):293–6

Dong HY, Liu W, Cohen P, Mahle CE, Zhang W. B-cell specific activation protein encoded by the PAX-5 gene is

commonly expressed in merkel cell carcinoma and small cell carcinomas. *Am. J. Surg. Pathol.* 2005;29(5):687–92

Doucet YS, Woo S-H, Ruiz ME, Owens DM. The Touch Dome Defines an Epidermal Niche Specialized for Mechanosensory Signaling. *Cell Rep.* 2013;3(6):1759–65

Duncavage EJ, Magrini V, Becker N, Armstrong JR, Demeter RT, Wylie T, et al. Hybrid capture and next-generation sequencing identify viral integration sites from formalin-fixed, paraffin-embedded tissue. *J. Mol. Diagn. JMD.* 2011;13(3):325–33

Dye KN, Welcker M, Clurman BE, Roman A, Galloway DA. Merkel cell polyomavirus Tumor antigens expressed in Merkel cell carcinoma function independently of the ubiquitin ligases Fbw7 and β -TrCP. *PLoS Pathog.* 2019;15(1):e1007543

Eid M, Nguyen J, Brownell I. Seeking Standards for the Detection of Merkel Cell Polyomavirus and its Clinical Significance. *J. Invest. Dermatol.* 2017;137(4):797–9

Eisemann N, Waldmann A, Geller AC, Weinstock MA, Volkmer B, Greinert R, et al. Non-melanoma skin cancer incidence and impact of skin cancer screening on incidence. *J. Invest. Dermatol.* 2014;134(1):43–50

Engels EA, Frisch M, Goedert JJ, Biggar RJ, Miller RW. Merkel cell carcinoma and HIV infection. *Lancet Lond. Engl.* 2002;359(9305):497–8

Erard V, Storer B, Corey L, Nollkamper J, Huang M-L, Limaye A, et al. BK virus infection in hematopoietic stem cell transplant recipients: frequency, risk factors, and association with postengraftment hemorrhagic cystitis. *Clin. Infect. Dis. Off. Publ. Infect. Dis. Soc. Am.* 2004;39(12):1861–5

Fahsbender E, Altan E, Estrada M, Seguin MA, Young P, Leutenegger CM, et al. Lyon-IARC Polyomavirus DNA in Feces of Diarrheic Cats. *Microbiol. Resour. Announc.* 2019;8(29)

Falto Aizpurua LA, Wang M, Ruiz HA, Sánchez JL, Chan MP, Andea AA, et al. A case of combined Merkel cell carcinoma and squamous cell carcinoma: Molecular insights and diagnostic pitfalls. *JAAD Case Rep.* 2018;4(10):996–9

Fan K, Gravemeyer J, Ritter C, Rasheed K, Gambichler T, Moens U, et al. MCPyV Large T antigen induced atonal homolog 1 (ATOH1) is a lineage-dependency oncogene in Merkel cell carcinoma. *J. Invest. Dermatol.* 2019;

Fanning E, Zhao K. SV40 DNA replication: from the A gene to a nanomachine. *Virology.* 2009;384(2):352–9

Feng H, Kwun HJ, Liu X, Gjoerup O, Stolz DB, Chang Y, et al. Cellular and viral factors regulating Merkel cell polyomavirus replication. *PLoS One.* 2011;6(7):e22468

Feng H, Shuda M, Chang Y, Moore PS. Clonal integration of a polyomavirus in human Merkel cell carcinoma. *Science.* 2008a;319(5866):1096–100

Feng H, Shuda M, Chang Y, Moore PS. Clonal integration of a polyomavirus in human Merkel cell carcinoma. *Science.* 2008b;319(5866):1096–100

Fernández-Figueras M-T, Puig L, Musulén E, Gilaberte M, Lerma E, Serrano S, et al. Expression profiles associated with aggressive behavior in Merkel cell carcinoma. *Mod. Pathol. Off. J. U. S. Can. Acad. Pathol. Inc.* 2007a;20(1):90–101

Feyrter F. Über diffuse endokrine epithelia- le Organe. Leipzig, Barth; 1938;

Fields RC, Busam KJ, Chou JF, Panageas KS, Pulitzer MP, Allen PJ, et al. Five hundred patients with Merkel cell carcinoma evaluated at a single institution. *Ann. Surg.* 2011;254(3):465–73; discussion 473–475

Fitzgerald TL, Dennis S, Kachare SD, Vohra NA, Wong JH, Zervos EE. Dramatic Increase in the Incidence and Mortality from Merkel Cell Carcinoma in the United States. *Am. Surg.* 2015;81(8):802–6

Fletcher CDM. The evolving classification of soft tissue tumours: an update based on the new WHO classification. *Histopathology.* 2006;48(1):3–12

Forget A, Bihannic L, Cigna SM, Lefevre C, Remke M, Barnat M, et al. Shh signaling protects Atoh1 from degradation mediated by the E3 ubiquitin ligase Huwe1 in neural precursors. *Dev. Cell.* 2014;29(6):649–61

Foschini MP, Eusebi V. Divergent differentiation in endocrine and nonendocrine tumors of the skin. *Semin. Diagn. Pathol.* 2000;17(2):162–8

Foulongne V, Kluger N, Dereure O, Mercier G, Molès JP, Guillot B, et al. Merkel cell polyomavirus in cutaneous swabs. *Emerg. Infect. Dis.* 2010;16(4):685–7

Fradette J, Godbout MJ, Michel M, Germain L. Localization of Merkel cells at hairless and hairy human skin sites using keratin 18. *Biochem. Cell Biol. Biochim. Biol. Cell.* 1995;73(9–10):635–9

Fukuhara M, Agnarsdóttir M, Edqvist P-H, Coter A, Ponten F. SATB2 is expressed in Merkel cell carcinoma. *Arch. Dermatol. Res.* 2016a;308(6):449–54

Fukuhara M, Agnarsdóttir M, Edqvist P-H, Coter A, Ponten F. SATB2 is expressed in Merkel cell carcinoma. *Arch. Dermatol. Res.* 2016b;308(6):449–54

Fusumae T, Tanese K, Takeuchi A, Takasugi A, Kawakita R, Shiraishi J, et al. High-grade trichoblastic carcinoma arising through malignant transformation of trichoblastoma: Immunohistochemical analysis and the expression

of p53 and phosphorylated AKT. *J. Dermatol.* 2019;46(1):57–60

Gambichler T, Mohtezabsade S, Wieland U, Silling S, Höh A-K, Dreißigacker M, et al. Prognostic relevance of high atonal homolog-1 expression in Merkel cell carcinoma. *J. Cancer Res. Clin. Oncol.* 2016;

García-Caballero T, Pintos E, Gallego R, Parrado C, Blanco M, Bjornhagen V, et al. MOC-31/Ep-CAM immunoreactivity in Merkel cells and Merkel cell carcinomas. *Histopathology.* 2003;43(5):480–4

García-Mesa Y, García-Piqueras J, García B, Feito J, Cabo R, Cobo J, et al. Merkel cells and Meissner's corpuscles in human digital skin display Piezo2 immunoreactivity. *J. Anat.* 2017;231(6):978–89

Gardair C, Samimi M, Touzé A, Coursaget P, Lorette G, Caille A, et al. Somatostatin Receptors 2A and 5 Are Expressed in Merkel Cell Carcinoma with No Association with Disease Severity. *Neuroendocrinology.* 2015;101(3):223–35

Gardner SD, Field AM, Coleman DV, Hulme B. New human papovavirus (B.K.) isolated from urine after renal transplantation. *Lancet Lond. Engl.* 1971;1(7712):1253–7

Gazdar AF, Bunn PA, Minna JD. Small-cell lung cancer: what we know, what we need to know and the path forward. *Nat. Rev. Cancer.* 2017;17(12):725–37

Gheit T, Dutta S, Oliver J, Robitaille A, Hampras S, Combes J-D, et al. Isolation and characterization of a novel putative human polyomavirus. *Virology.* 2017;506:45–54

Giacinti C, Giordano A. RB and cell cycle progression. *Oncogene.* 2006;25(38):5220–7

Gjoerup O, Chang Y. Update on human polyomaviruses and cancer. *Adv. Cancer Res.* 2010;106:1–51

Godlewski J, Kowalczyk A, Koziellec Z, Pidsudko Z, Kmieć A, Siedlecka-Kroplewska K. Plasticity of neuropeptidergic neoplasm cells in the primary and metastatic Merkel cell carcinoma. *Folia Histochem. Cytobiol.* 2013;51(2):168–73

Goh S, Lindau C, Tiveljung-Lindell A, Allander T. Merkel Cell Polyomavirus in Respiratory Tract Secretions. *Emerg. Infect. Dis.* 2009;15(3):489–91

Goh G, Walradt T, Markarov V, Blom A, Riaz N, Doumani R, et al. Mutational landscape of MCPyV-positive and MCPyV-negative Merkel cell carcinomas with implications for immunotherapy. *Oncotarget.* 2016a;7(3):3403–15

González-Vela MDC, Curiel-Olmo S, Derdak S, Beltran S, Santibañez M, Martínez N, et al. Shared Oncogenic Pathways Implicated in Both Virus-Positive and UV-Induced Merkel Cell Carcinomas. *J. Invest. Dermatol.* 2017;137(1):197–206

Goto K, Anan T, Nakatsuka T, Kaku Y, Sakurai T, Fukumoto T, et al. Low-Grade Neuroendocrine Carcinoma of the Skin (Primary Cutaneous Carcinoid Tumor) as a Distinctive Entity of Cutaneous Neuroendocrine Tumors: A Clinicopathologic Study of 3 Cases With Literature Review. *Am. J. Dermatopathol.* 2017;39(4):250–8

Goyal A, Solus JF, Chan MP, Doyle LA, Schaffer A, Thakuria M, et al. Cytokeratin 17 is highly sensitive in discriminating cutaneous lymphadenoma (a distinct trichoblastoma variant) from basal cell carcinoma. *J. Cutan. Pathol.* 2016;43(5):422–9

Grachtchouk M, Pero J, Yang SH, Ermilov AN, Michael LE, Wang A, et al. Basal cell carcinomas in mice arise from hair follicle stem cells and multiple epithelial progenitor populations. *J. Clin. Invest.* 2011;121(5):1768–81

Grausam KB, Dooyema SDR, Bihannic L, Premathilake H, Morrissy AS, Forget A, et al. ATOH1 Promotes Leptomeningeal Dissemination and Metastasis of Sonic Hedgehog Subgroup Medulloblastomas. *Cancer Res.* 2017;77(14):3766–77

Grichnik JM, Ali WN, Burch JA, Byers JD, Garcia CA, Clark RE, et al. KIT expression reveals a population of precursor melanocytes in human skin. *J. Invest. Dermatol.* 1996;106(5):967–71

Griffiths DA, Abdul-Sada H, Knight LM, Jackson BR, Richards K, Prescott EL, et al. Merkel cell polyomavirus small T antigen targets the NEMO adaptor protein to disrupt inflammatory signaling. *J. Virol.* 2013;87(24):13853–67

Grim M, Halata Z. Developmental origin of avian Merkel cells. *Anat. Embryol. (Berl.).* 2000;202(5):401–10

Gross L. A filterable agent, recovered from Ak leukemic extracts, causing salivary gland carcinomas in C3H mice. *Proc. Soc. Exp. Biol. Med. Soc. Exp. Biol. Med. N. Y. N.* 1953;83(2):414–21

Hafner C, Houben R, Baeurle A, Ritter C, Schrama D, Landthaler M, et al. Activation of the PI3K/AKT pathway in Merkel cell carcinoma. *PLoS One.* 2012;7(2):e31255

Haigis K, Sage J, Glickman J, Shafer S, Jacks T. The related retinoblastoma (pRb) and p130 proteins cooperate to regulate homeostasis in the intestinal epithelium. *J. Biol. Chem.* 2006;281(1):638–47

Halata Z, Grim M, Bauman KI. Friedrich Sigmund Merkel and his “Merkel cell”, morphology, development, and physiology: review and new results. *Anat. Rec. A. Discov. Mol. Cell. Evol. Biol.* 2003a;271(1):225–39

Halata Z, Grim M, Christ B. Origin of spinal cord meninges, sheaths of peripheral nerves, and cutaneous receptors including Merkel cells. An experimental and ultrastructural study with avian chimeras. *Anat. Embryol. (Berl.).* 1990;182(6):529–37

Harms PW, Collie AMB, Hovelson DH, Cani AK, Verhaegen ME, Patel RM, et al. Next generation sequencing of

Cytokeratin 20-negative Merkel cell carcinoma reveals ultraviolet-signature mutations and recurrent TP53 and RB1 inactivation. *Mod. Pathol. Off. J. U. S. Can. Acad. Pathol. Inc.* 2016a;29(3):240–8

Harms PW, Harms KL, Moore PS, DeCaprio JA, Nghiem P, Wong MKK, et al. The biology and treatment of Merkel cell carcinoma: current understanding and research priorities. *Nat. Rev. Clin. Oncol.* 2018a;15(12):763–76

Harms PW, Harms KL, Moore PS, DeCaprio JA, Nghiem P, Wong MKK, et al. The biology and treatment of Merkel cell carcinoma: current understanding and research priorities. *Nat. Rev. Clin. Oncol.* 2018b; Harms KL, Healy MA, Nghiem P, Sober AJ, Johnson TM, Bichakjian CK, et al. Analysis of Prognostic Factors from 9387 Merkel Cell Carcinoma Cases Forms the Basis for the New 8th Edition AJCC Staging System. *Ann. Surg. Oncol.* 2016b;23(11):3564–71

Harms PW, Patel RM, Verhaegen ME, Giordano TJ, Nash KT, Johnson CN, et al. Distinct gene expression profiles of viral- and nonviral-associated merkel cell carcinoma revealed by transcriptome analysis. *J. Invest. Dermatol.* 2013;133(4):936–45

Harms PW, Vats P, Verhaegen ME, Robinson DR, Wu Y-M, Dhanasekaran SM, et al. The Distinctive Mutational Spectra of Polyomavirus-Negative Merkel Cell Carcinoma. *Cancer Res.* 2015a;75(18):3720–7

Harms PW, Vats P, Verhaegen ME, Robinson DR, Wu Y-M, Dhanasekaran SM, et al. The Distinctive Mutational Spectra of Polyomavirus-Negative Merkel Cell Carcinoma. *Cancer Res.* 2015b;75(18):3720–7

Harold A, Amako Y, Hachisuka J, Bai Y, Li MY, Kubat L, et al. Conversion of Sox2-dependent Merkel cell carcinoma to a differentiated neuron-like phenotype by T antigen inhibition. *Proc. Natl. Acad. Sci. U. S. A.* 2019; Harrison CJ, Meinke G, Kwun HJ, Rogalin H, Phelan PJ, Bullock PA, et al. Asymmetric assembly of Merkel cell polyomavirus large T-antigen origin binding domains at the viral origin. *J. Mol. Biol.* 2011;409(4):529–42

Harting MS, Ludgate MW, Fullen DR, Johnson TM, Bichakjian CK. Dermatoscopic vascular patterns in cutaneous Merkel cell carcinoma. *J. Am. Acad. Dermatol.* 2012;66(6):923–7

Hartschuh W, Grube D. The Merkel cell—a member of the APUD cell system. Fluorescence and electron microscopic contribution to the neurotransmitter function of the Merkel cell granules. *Arch. Dermatol. Res.* 1979;265(2):115–22

Haugg AM, Rennspiess D, zur Hausen A, Speel E-JM, Cathomas G, Becker JC, et al. Fluorescence in situ hybridization and qPCR to detect Merkel cell polyomavirus physical status and load in Merkel cell carcinomas. *Int. J. Cancer.* 2014;135(12):2804–15

Haugg AM, Speel E-JM, Pantulu ND, Pallasch C, Kurz AK, Kvasnicka HM, et al. Fluorescence in situ hybridization confirms the presence of Merkel cell polyomavirus in chronic lymphocytic leukemia cells. *Blood.* 2011;117(21):5776–7

Haymerle G, Fochtmann A, Kunstfeld R, Pammer J, Erovcic BM. Management of Merkel cell carcinoma of unknown primary origin: the Vienna Medical School experience. *Eur. Arch. Oto-Rhino-Laryngol. Off. J. Eur. Fed. Oto-Rhino-Laryngol. Soc. EUFOS Affil. Ger. Soc. Oto-Rhino-Laryngol. - Head Neck Surg.* 2015;272(2):425–9

Heath M, Jaimes N, Lemos B, Mostaghimi A, Wang LC, Peñas PF, et al. Clinical characteristics of Merkel cell carcinoma at diagnosis in 195 patients: the AEIOU features. *J. Am. Acad. Dermatol.* 2008;58(3):375–81

Henseleit U, Zhang J, Wanner R, Haase I, Kolde G, Rosenbach T. Role of p53 in UVB-induced apoptosis in human HaCaT keratinocytes. *J. Invest. Dermatol.* 1997;109(6):722–7

Hesbacher S, Pfitzer L, Wiedorfer K, Angermeyer S, Borst A, Haferkamp S, et al. RB1 is the crucial target of the Merkel cell polyomavirus Large T antigen in Merkel cell carcinoma cells. *Oncotarget.* 2016;7(22):32956–68

Hillen LM, Rennspiess D, Speel E-J, Haugg AM, Winnepeninckx V, Zur Hausen A. Detection of Merkel Cell Polyomavirus in Seborrheic Keratosis. *Front. Microbiol.* 2017;8:2648

Hirsch HH. BK virus: opportunity makes a pathogen. *Clin. Infect. Dis. Off. Publ. Infect. Dis. Soc. Am.* 2005;41(3):354–60

Ho J, Jedrych JJ, Feng H, Natalie AA, Grandinetti L, Mirvish E, et al. Human polyomavirus 7-associated pruritic rash and viremia in transplant recipients. *J. Infect. Dis.* 2015;211(10):1560–5

Ho S-Y, Tsai Y-C, Lee M-C, Guo H-R. Merkel cell carcinoma in patients with long-term ingestion of arsenic. *J. Occup. Health.* 2005;47(2):188–92

Hoefler H, Kerl H, Rauch HJ, Denk H. New immunocytochemical observations with diagnostic significance in cutaneous neuroendocrine carcinoma. *Am. J. Dermatopathol.* 1984;6(6):525–30

Houben R, Adam C, Baeurle A, Hesbacher S, Grimm J, Angermeyer S, et al. An intact retinoblastoma protein-binding site in Merkel cell polyomavirus large T antigen is required for promoting growth of Merkel cell carcinoma cells. *Int. J. Cancer.* 2012a;130(4):847–56

Houben R, Angermeyer S, Haferkamp S, Aue A, Goebeler M, Schrama D, et al. Characterization of functional domains in the Merkel cell polyoma virus Large T antigen. *Int. J. Cancer.* 2015;136(5):E290-300

Houben R, Dreher C, Angermeyer S, Borst A, Utikal J, Haferkamp S, et al. Mechanisms of p53 restriction in

Merkel cell carcinoma cells are independent of the Merkel cell polyoma virus T antigens. *J. Invest. Dermatol.* 2013;133(10):2453–60

Houben R, Michel B, Vetter-Kauczok CS, Pföhler C, Laetsch B, Wolter MD, et al. Absence of classical MAP kinase pathway signalling in Merkel cell carcinoma. *J. Invest. Dermatol.* 2006;126(5):1135–42

Houben R, Ortmann S, Schrama D, Herold MJ, Berberich I, Reichardt HM, et al. Activation of the MAP kinase pathway induces apoptosis in the Merkel cell carcinoma cell line UIISO. *J. Invest. Dermatol.* 2007;127(9):2116–22

Houben R, Schrama D, Becker JC. Molecular pathogenesis of Merkel cell carcinoma. *Exp. Dermatol.* 2009;18(3):193–8

Houben R, Shuda M, Weinkam R, Schrama D, Feng H, Chang Y, et al. Merkel cell polyomavirus-infected Merkel cell carcinoma cells require expression of viral T antigens. *J. Virol.* 2010;84(14):7064–72

Houcine Y, Chelly I, Zehani A, Belhaj Kacem L, Azzouz H, Rekik W, et al. Neuroendocrine differentiation in basal cell carcinoma. *J. Immunoassay Immunochem.* 2017;38(5):487–93

Howard RA, Dores GM, Curtis RE, Anderson WF, Travis LB. Merkel cell carcinoma and multiple primary cancers. *Cancer Epidemiol. Biomark. Prev. Publ. Am. Assoc. Cancer Res. Cosponsored Am. Soc. Prev. Oncol.* 2006;15(8):1545–9

Hunter DV, Smaila BD, Lopes DM, Takatoh J, Denk F, Ramer MS. Advillin Is Expressed in All Adult Neural Crest-Derived Neurons. *eNeuro.* 2018;5(5)

Husein-ElAhmed H, Ramos-Pleguezuelos F, Ruiz-Molina I, Civico-Amat V, Solis-García E, Galán-Gutierrez M, et al. Histological Features, p53, c-Kit, and Poliovirus Status and Impact on Survival in Merkel Cell Carcinoma Patients. *Am. J. Dermatopathol.* 2016;38(8):571–9

Iaria M, Caccuri F, Apostoli P, Giagulli C, Pelucchi F, Padoan RF, et al. Detection of KI WU and Merkel cell polyomavirus in respiratory tract of cystic fibrosis patients. *Clin. Microbiol. Infect. Off. Publ. Eur. Soc. Clin. Microbiol. Infect. Dis.* 2015;21(6):603.e9-15

Ikeda R, Cha M, Ling J, Jia Z, Coyle D, Gu JG. Merkel cells transduce and encode tactile stimuli to drive A β -afferent impulses. *Cell.* 2014;157(3):664–75

Inman GJ, Wang J, Nagano A, Alexandrov LB, Purdie KJ, Taylor RG, et al. The genomic landscape of cutaneous SCC reveals drivers and a novel azathioprine associated mutational signature. *Nat. Commun.* 2018;9

Inoue T, Shimono M, Takano N, Saito C, Tanaka Y. Merkel cell carcinoma of palatal mucosa in a young adult: immunohistochemical and ultrastructural features. *Oral Oncol.* 1997;33(3):226–9

International Committee on Taxonomy of Viruses, Van Regenmortel MHV, International Union of Microbiological Societies, editors. *Virus taxonomy: classification and nomenclature of viruses: seventh report of the International Committee on Taxonomy of Viruses.* San Diego: Academic Press; 2000.

Ishibashi F, Shimizu H, Nakata T, Fujii S, Suzuki K, Kawamoto A, et al. Contribution of ATOH1+ Cells to the Homeostasis, Repair, and Tumorigenesis of the Colonic Epithelium. *Stem Cell Rep.* 2018;10(1):27–42

Islam MN, Chehal H, Smith MH, Islam S, Bhattacharyya I. Merkel Cell Carcinoma of the Buccal Mucosa and Lower Lip. *Head Neck Pathol.* 2018;12(2):279–85

Iwasaki T, Kodama H, Matsushita M, Kuroda N, Yamasaki Y, Murakami I, et al. Merkel cell polyomavirus infection in both components of a combined Merkel cell carcinoma and basal cell carcinoma with ductal differentiation; each component had a similar but different novel Merkel cell polyomavirus large T antigen truncating mutation. *Hum. Pathol.* 2013a;44(3):442–7

Iwasaki T, Matsushita M, Kuwamoto S, Kato M, Murakami I, Higaki-Mori H, et al. Usefulness of significant morphologic characteristics in distinguishing between Merkel cell polyomavirus-positive and Merkel cell polyomavirus-negative Merkel cell carcinomas. *Hum. Pathol.* 2013c;44(9):1912–7

Iyer JG, Parvathaneni K, Bhatia S, Tarabardkar ES, Blom A, Doumani R, et al. Paraneoplastic syndromes (PNS) associated with Merkel cell carcinoma (MCC): A case series of 8 patients highlighting different clinical manifestations. *J. Am. Acad. Dermatol.* 2016;75(3):541–7

Iyer J, Storer B, Paulson K, Lemos B, Phillips J, Bichakjian C, et al. Relationships between primary tumor size, number of involved nodes and survival among 8,044 cases of Merkel cell carcinoma. *J. Am. Acad. Dermatol.* 2014;70(4):637–43

Jalilian C, Chamberlain AJ, Haskett M, Rosendahl C, Goh M, Beck H, et al. Clinical and dermoscopic characteristics of Merkel cell carcinoma. *Br. J. Dermatol.* 2013;169(2):294–7

Jeffers L, Webster-Cyriaque JY. Viruses and salivary gland disease (SGD): lessons from HIV SGD. *Adv. Dent. Res.* 2011;23(1):79–83

Jia Y, Gu D, Wan J, Yu B, Zhang X, Chiorean EG, et al. The role of GLI-SOX2 signaling axis for gemcitabine resistance in pancreatic cancer. *Oncogene.* 2019;38(10):1764–77

Jirásek T, Matej R, Pock L, Knotková I, Mandys V. [Merkel cell carcinoma--immunohistochemical study in a

group of 11 patients]. *Cesk. Patol.* 2009;45(1):9–13

Johansson E, Andersson L, Örnros J, Carlsson T, Ingesson-Carlsson C, Liang S, et al. Revising the embryonic origin of thyroid C cells in mice and humans. *Dev. Camb. Engl.* 2015;142(20):3519–28

Johansson B, Sahi H, Koljonen V, Böhling T. The expression of terminal deoxynucleotidyl transferase and paired box gene 5 in Merkel cell carcinomas and its relation to the presence of Merkel cell polyomavirus DNA. *J. Cutan. Pathol.* 2018;

Johnson EM. Structural evaluation of new human polyomaviruses provides clues to pathobiology. *Trends Microbiol.* 2010;18(5):215–23

Jour G, Aung PP, Rozas-Muñoz E, Curry JL, Prieto V, Ivan D. Intraepidermal Merkel cell carcinoma: A case series of a rare entity with clinical follow up. *J. Cutan. Pathol.* 2017;44(8):684–91

Kanitakis J. [Merkel cell carcinoma: a human tumour induced by a new polyomavirus (MCV)]. *Med. Sci. MS.* 2008;24(6–7):570–1

Kanitakis J, Bouchany D, Faure M, Claudy A. Merkel cells in hyperplastic and neoplastic lesions of the skin. An immunohistochemical study using an antibody to keratin 20. *Dermatol. Basel Switz.* 1998;196(2):208–12

Kanitakis J, Joly MO, Chouvet B, Euvrard S, Claudy A. Merkel cell carcinoma in immunocompetent and organ-transplant recipients do not harbor HPV. *Eur. J. Dermatol. EJD.* 2006;16(4):445–6

Kantola K, Sadeghi M, Lahtinen A, Koskenvuo M, Aaltonen L-M, Möttönen M, et al. Merkel cell polyomavirus DNA in tumor-free tonsillar tissues and upper respiratory tract samples: implications for respiratory transmission and latency. *J. Clin. Virol. Off. Publ. Pan Am. Soc. Clin. Virol.* 2009;45(4):292–5

Kaplan DR, Whitman M, Schaffhausen B, Pallas DC, White M, Cantley L, et al. Common elements in growth factor stimulation and oncogenic transformation: 85 kd phosphoprotein and phosphatidylinositol kinase activity. *Cell.* 1987;50(7):1021–9

Kaplan-Lefko PJ, Chen T-M, Ittmann MM, Barrios RJ, Ayala GE, Huss WJ, et al. Pathobiology of autochthonous prostate cancer in a pre-clinical transgenic mouse model. *The Prostate.* 2003;55(3):219–37

Kardas P, Leboeuf C, Hirsch HH. Optimizing JC and BK polyomavirus IgG testing for seroepidemiology and patient counseling. *J. Clin. Virol. Off. Publ. Pan Am. Soc. Clin. Virol.* 2015;71:28–33

Kassem A, Pantulu D, Technau K, Kurz AK, Diaz C, Hörster S, et al. Merkel cell polyomavirus in naevoid basal cell carcinoma syndrome-associated basal cell carcinomas and sporadic trichoblastomas. *J. Dermatol. Sci.* 2010;59(2):140–2

Kaufman HL, Hunger M, Hennessy M, Schlichting M, Bharmal M. Nonprogression with avelumab treatment associated with gains in quality of life in metastatic Merkel cell carcinoma. *Future Oncol. Lond. Engl.* 2018a;14(3):255–66

Kaufman HL, Russell J, Hamid O, Bhatia S, Terheyden P, D'Angelo SP, et al. Avelumab in patients with chemotherapy-refractory metastatic Merkel cell carcinoma: a multicentre, single-group, open-label, phase 2 trial. *Lancet Oncol.* 2016;17(10):1374–85

Kaufman HL, Russell JS, Hamid O, Bhatia S, Terheyden P, D'Angelo SP, et al. Updated efficacy of avelumab in patients with previously treated metastatic Merkel cell carcinoma after ≥1 year of follow-up: JAVELIN Merkel 200, a phase 2 clinical trial. *J. Immunother. Cancer.* 2018b;6(1):7

Kazakov DV. Brooke-Spiegler Syndrome and Phenotypic Variants: An Update. *Head Neck Pathol.* 2016;10(2):125–30

Kelley WL, Georgopoulos C. The T/t common exon of simian virus 40, JC, and BK polyomavirus T antigens can functionally replace the J-domain of the Escherichia coli DnaJ molecular chaperone. *Proc. Natl. Acad. Sci. U. S. A.* 1997;94(8):3679–84

Kenan DJ, Mieczkowski PA, Latulippe E, Côté I, Singh HK, Nickeleit V. BK Polyomavirus Genomic Integration and Large T Antigen Expression: Evolving Paradigms in Human Oncogenesis. *Am. J. Transplant. Off. J. Am. Soc. Transplant. Am. Soc. Transpl. Surg.* 2017;17(6):1674–80

Kervarrec T, Gaboriaud P, Berthon P, Zaragoza J, Schrama D, Houben R, et al. Merkel cell carcinomas infiltrated with CD33+ myeloid cells and CD8+ T cells are associated with improved outcome. *J. Am. Acad. Dermatol.* 2018a;78(5):973-982.e8

Kervarrec T, Samimi M, Guyétant S, Sarma B, Chéret J, Blanchard E, et al. Histogenesis of Merkel cell carcinoma: a comprehensive review. *Front. Oncol. Accepted Manuscript.* 2019;

Kervarrec T, Tallet A, Miquelstorena-Standley E, Houben R, Schrama D, Gambichler T, et al. Diagnostic accuracy of a panel of immunohistochemical and molecular markers to distinguish Merkel cell carcinoma from other neuroendocrine carcinomas. *Mod. Pathol. Off. J. U. S. Can. Acad. Pathol. Inc.* 2018b;

Kervarrec T, Zaragoza J, Gaboriaud P, Le Gouge A, Beby-Defaux A, Le Corre Y, et al. Differentiating Merkel cell carcinoma of lymph nodes without a detectable primary skin tumor from other metastatic neuroendocrine carcinomas: The ELECTHIP criteria. *J. Am. Acad. Dermatol.* 2018c;78(5):964-972.e3

Kieny A, Cribier B, Meyer N, Velten M, Jégu J, Lipsker D. Epidemiology of Merkel cell carcinoma. A population-based study from 1985 to 2013, in northeastern of France. *Int. J. Cancer*. 2019;144(4):741–5

Kim HY, Ahn BY, Cho Y. Structural basis for the inactivation of retinoblastoma tumor suppressor by SV40 large T antigen. *EMBO J*. 2001;20(1–2):295–304

Klöppel G. Neuroendocrine Neoplasms: Dichotomy, Origin and Classifications. *Visc. Med*. 2017;33(5):324–30

Knapp AC, Franke WW. Spontaneous losses of control of cytokeratin gene expression in transformed, non-epithelial human cells occurring at different levels of regulation. *Cell*. 1989;59(1):67–79

Knight LM, Stakaityte G, Wood JJ, Abdul-Sada H, Griffiths DA, Howell GJ, et al. Merkel cell polyomavirus small T antigen mediates microtubule destabilization to promote cell motility and migration. *J. Virol*. 2015;89(1):35–47

Koba S, Nagase K, Ikeda S, Aoki S, Misago N, Narisawa Y. Merkel cell carcinoma with glandular differentiation admixed with sweat gland carcinoma and spindle cell carcinoma: histogenesis of merkel cell carcinoma from hair follicle stem cells. *Am. J. Dermatopathol*. 2015;37(3):e31–36

Köksal Y, Toy H, Talim B, Unal E, Akçören Z, Cengiz M. Merkel cell carcinoma in a child. *J. Pediatr. Hematol. Oncol*. 2009;31(5):359–61

Koljonen V, Haglund C, Tukiainen E, Böhling T. Neuroendocrine differentiation in primary Merkel cell carcinoma--possible prognostic significance. *Anticancer Res*. 2005a;25(2A):853–8 8

Koljonen V, Rantanen M, Sahi H, Mellekjær L, Hansen BT, Chen T, et al. Joint occurrence of Merkel cell carcinoma and non-Hodgkin lymphomas in four Nordic countries. *Leuk. Lymphoma*. 2015;56(12):3315–9

Kontochristopoulos GJ, Stavropoulos PG, Krasagakis K, Goerdts S, Zouboulis CC. Differentiation between merkel cell carcinoma and malignant melanoma: An immunohistochemical study. *Dermatol. Basel Switz*. 2000;201(2):123–6

Kotteas EA, Pavlidis N. Neuroendocrine Merkel cell nodal carcinoma of unknown primary site: management and outcomes of a rare entity. *Crit. Rev. Oncol. Hematol*. 2015;94(1):116–21

Krump NA, Liu W, You J. Mechanisms of persistence by small DNA tumor viruses. *Curr. Opin. Virol*. 2018;32:71–9

Kurzen H, Esposito L, Langbein L, Hartschuh W. Cytokeratins as markers of follicular differentiation: an immunohistochemical study of trichoblastoma and basal cell carcinoma. *Am. J. Dermatopathol*. 2001;23(6):501–9

Kuwamoto S, Higaki H, Kanai K, Iwasaki T, Sano H, Nagata K, et al. Association of Merkel cell polyomavirus infection with morphologic differences in Merkel cell carcinoma. *Hum. Pathol*. 2011a;42(5):632–40

Kwok CK-M, Tam PK-H, Ngan ES-W. Potential use of skin-derived precursors (SKPs) in establishing a cell-based treatment model for Hirschsprung's disease. *J. Pediatr. Surg*. 2013;48(3):619–28

Kwun HJ, Chang Y, Moore PS. Protein-mediated viral latency is a novel mechanism for Merkel cell polyomavirus persistence. *Proc. Natl. Acad. Sci. U. S. A*. 2017;114(20):E4040–7

Kwun HJ, Guastafierro A, Shuda M, Meinke G, Bohm A, Moore PS, et al. The minimum replication origin of merkel cell polyomavirus has a unique large T-antigen loading architecture and requires small T-antigen expression for optimal replication. *J. Virol*. 2009;83(23):12118–28

Kwun HJ, Shuda M, Camacho CJ, Gamper AM, Thant M, Chang Y, et al. Restricted protein phosphatase 2A targeting by Merkel cell polyomavirus small T antigen. *J. Virol*. 2015;89(8):4191–200

Kwun HJ, Shuda M, Feng H, Camacho CJ, Moore PS, Chang Y. Merkel cell polyomavirus small T antigen controls viral replication and oncoprotein expression by targeting the cellular ubiquitin ligase SCFFbw7. *Cell Host Microbe*. 2013;14(2):125–35

Lach B, Joshi SS, Murty N, Huq N. Transformation of Merkel cell carcinoma to ganglioneuroblastoma in intracranial metastasis. *Hum. Pathol*. 2014;45(9):1978–81

Laga AC, Lai C-Y, Zhan Q, Huang SJ, Velazquez EF, Yang Q, et al. Expression of the embryonic stem cell transcription factor SOX2 in human skin: relevance to melanocyte and merkel cell biology. *Am. J. Pathol*. 2010;176(2):903–13

Langan EA, Philpott MP, Kloepper JE, Paus R. Human hair follicle organ culture: theory, application and perspectives. *Exp. Dermatol*. 2015;24(12):903–11

Lasithiotaki I, Tsitoura E, Koutsopoulos A, Lagoudaki E, Koutoulaki C, Pitsidianakis G, et al. Aberrant expression of miR-21, miR-376c and miR-145 and their target host genes in Merkel cell polyomavirus-positive non-small cell lung cancer. *Oncotarget*. 2017;8(68):112371–83

Lau PP-L, Ting SH, Ip YT, Tsang WYW, Chan JKC. Merkel cell carcinosarcoma: Merkel cell carcinoma with embryonal rhabdomyosarcoma-like component. *Ann. Diagn. Pathol*. 2012;16(5):388–91

Laude HC, Jonchère B, Maubec E, Carlotti A, Marinho E, Couturaud B, et al. Distinct merkel cell polyomavirus molecular features in tumour and non tumour specimens from patients with merkel cell carcinoma. *PLoS Pathog*. 2010;6(8):e1001076

Leblebici C, Bambul Sıgırcı B, Kelten Talu C, Koca SB, Huq GE. CD10, TDAG51, CK20, AR, INSM1, and Nestin Expression in the Differential Diagnosis of Trichoblastoma and Basal Cell Carcinoma. *Int. J. Surg. Pathol.* 2019a;27(1):19–27

Leblebici C, Yeni B, Savli TC, Aydın Ö, Güneş P, Cinel L, et al. A new immunohistochemical marker, insulinoma-associated protein 1 (INSM1), for Merkel cell carcinoma: Evaluation of 24 cases. *Ann. Diagn. Pathol.* 2019b;40:53–8

Lesko MH, Driskell RR, Kretzschmar K, Goldie SJ, Watt FM. Sox2 modulates the function of two distinct cell lineages in mouse skin. *Dev. Biol.* 2013;382(1):15–26

Lewis JS, Duncavage E, Klonowski PW. Oral cavity neuroendocrine carcinoma: a comparison study with cutaneous Merkel cell carcinoma and other mucosal head and neck neuroendocrine carcinomas. *Oral Surg. Oral Med. Oral Pathol. Oral Radiol. Endod.* 2010;110(2):209–17

Li M, Feng D-Y, Ren W, Zheng L, Zheng H, Tang M, et al. Expression of immunoglobulin kappa light chain constant region in abnormal human cervical epithelial cells. *Int. J. Biochem. Cell Biol.* 2004;36(11):2250–7

Li J, Wang X, Diaz J, Tsang SH, Buck CB, You J. Merkel Cell Polyomavirus Large T Antigen Disrupts Host Genomic Integrity and Inhibits Cellular Proliferation. *J. Virol.* 2013;87(16):9173–88

Li Z, Yang J-J, Wu M. Collision tumor of primary merkel cell carcinoma and chronic lymphocytic leukemia/small lymphocytic lymphoma, diagnosed on ultrasound-guided fine-needle aspiration biopsy: a unique case report and review of literature. *Diagn. Cytopathol.* 2015;43(1):66–71

Lien HC, Tsai TF, Lee YY, Hsiao CH. Merkel cell carcinoma and chronic arsenicism. *J. Am. Acad. Dermatol.* 1999;41(4):641–3

Lill C, Schneider S, Item CB, Loewe R, Houben R, Halbauer D, et al. P53 mutation is a rare event in Merkel cell carcinoma of the head and neck. *Eur. Arch. Oto-Rhino-Laryngol. Off. J. Eur. Fed. Oto-Rhino-Laryngol. Soc. EUFOS Affil. Ger. Soc. Oto-Rhino-Laryngol. - Head Neck Surg.* 2011;268(11):1639–46

Lilo MT, Chen Y, LeBlanc RE. INSM1 Is More Sensitive and Interpretable than Conventional Immunohistochemical Stains Used to Diagnose Merkel Cell Carcinoma. *Am. J. Surg. Pathol.* 2018a;42(11):1541–8

Liu X, Hein J, Richardson SCW, Basse PH, Toptan T, Moore PS, et al. Merkel cell polyomavirus large T antigen disrupts lysosome clustering by translocating human Vam6p from the cytoplasm to the nucleus. *J. Biol. Chem.* 2011;286(19):17079–90

Liu W, Yang R, Payne AS, Schowalter RM, Spurgeon ME, Lambert PF, et al. Identifying the Target Cells and Mechanisms of Merkel Cell Polyomavirus Infection. *Cell Host Microbe.* 2016;19(6):775–87

Liu H, Zheng H, Li M, Hu D, Tang M, Cao Y. Upregulated expression of kappa light chain by Epstein-Barr virus encoded latent membrane protein 1 in nasopharyngeal carcinoma cells via NF-kappaB and AP-1 pathways. *Cell. Signal.* 2007;19(2):419–27

Logan GJ, Wright MC, Kubicki AC, Maricich SM. Notch pathway signaling in the skin antagonizes Merkel cell development. *Dev. Biol.* 2018;434(2):207–14

Lucarz A, Brand G. Current considerations about Merkel cells. *Eur. J. Cell Biol.* 2007;86(5):243–51

Mancuso G, Antona J, Sirini C, Salvo M, Giacometti L, Olivero C, et al. Frequent detection of Merkel cell polyomavirus DNA in tissues from 10 consecutive autopsies. *J. Gen. Virol.* 2017;98(6):1372–6

Mariño-Enríquez A, Bovée JVMG. Molecular Pathogenesis and Diagnostic, Prognostic and Predictive Molecular Markers in Sarcoma. *Surg. Pathol. Clin.* 2016;9(3):457–73

Martel-Jantin C, Filippone C, Tortevoeye P, Afonso PV, Betsem E, Descorps-Declere S, et al. Molecular epidemiology of merkel cell polyomavirus: evidence for geographically related variant genotypes. *J. Clin. Microbiol.* 2014;52(5):1687–90

Martel-Jantin C, Pedergrana V, Nicol JTJ, Leblond V, Trégouët D-A, Tortevoeye P, et al. Merkel cell polyomavirus infection occurs during early childhood and is transmitted between siblings. *J. Clin. Virol. Off. Publ. Pan Am. Soc. Clin. Virol.* 2013;58(1):288–91

Martin B, Poblet E, Rios JJ, Kazakov D, Kutzner H, Brenn T, et al. Merkel cell carcinoma with divergent differentiation: histopathological and immunohistochemical study of 15 cases with PCR analysis for Merkel cell polyomavirus. *Histopathology.* 2013a;62(5):711–22

Martincorena I, Roshan A, Gerstung M, Ellis P, Van Loo P, McLaren S, et al. Tumor evolution. High burden and pervasive positive selection of somatic mutations in normal human skin. *Science.* 2015;348(6237):880–6

McCluggage WG, Kennedy K, Busam KJ. An immunohistochemical study of cervical neuroendocrine carcinomas: Neoplasms that are commonly TTF1 positive and which may express CK20 and P63. *Am. J. Surg. Pathol.* 2010;34(4):525–32

McNiff JM, Eisen RN, Glusac EJ. Immunohistochemical comparison of cutaneous lymphadenoma, trichoblastoma, and basal cell carcinoma: support for classification of lymphadenoma as a variant of

trichoblastoma. *J. Cutan. Pathol.* 1999;26(3):119–24

Meder L, König K, Ozretić L, Schultheis AM, Ueckerth F, Ade CP, et al. NOTCH, ASCL1, p53 and RB alterations define an alternative pathway driving neuroendocrine and small cell lung carcinomas. *Int. J. Cancer.* 2016;138(4):927–38

van der Meijden E, Janssens RWA, Lauber C, Bouwes Bavinck JN, Gorbalenya AE, Feltkamp MCW. Discovery of a new human polyomavirus associated with trichodysplasia spinulosa in an immunocompromized patient. *PLoS Pathog.* 2010;6(7):e1001024

Mertz KD, Junt T, Schmid M, Pfaltz M, Kempf W. Inflammatory monocytes are a reservoir for Merkel cell polyomavirus. *J. Invest. Dermatol.* 2010;130(4):1146–51

Mertz KD, Paasinen A, Arnold A, Baumann M, Offner F, Willi N, et al. Merkel cell polyomavirus large T antigen is detected in rare cases of nonmelanoma skin cancer. *J. Cutan. Pathol.* 2013;40(6):543–9

Mhaweche-Fauceglia P, Saxena R, Zhang S, Terracciano L, Sauter G, Chadhuri A, et al. Pax-5 immunoeexpression in various types of benign and malignant tumours: a high-throughput tissue microarray analysis. *J. Clin. Pathol.* 2007;60(6):709–14

Mikami Y, Fujii S, Nagata K, Wada H, Hasegawa K, Abe M, et al. GLI-mediated Keratin 17 expression promotes tumor cell growth through the anti-apoptotic function in oral squamous cell carcinomas. *J. Cancer Res. Clin. Oncol.* 2017;143(8):1381–93

Miller RW, Rabkin CS. Merkel cell carcinoma and melanoma: etiological similarities and differences. *Cancer Epidemiol. Biomark. Prev. Publ. Am. Assoc. Cancer Res. Cosponsored Am. Soc. Prev. Oncol.* 1999;8(2):153–8

Miner AG, Patel RM, Wilson DA, Procop GW, Minca EC, Fullen DR, et al. Cytokeratin 20-negative Merkel cell carcinoma is infrequently associated with the Merkel cell polyomavirus. *Mod. Pathol. Off. J. U. S. Can. Acad. Pathol. Inc.* 2015;28(4):498–504

Mishra N, Pereira M, Rhodes RH, An P, Pipas JM, Jain K, et al. Identification of a Novel Polyomavirus in a Pancreatic Transplant Recipient With Retinal Blindness and Vasculitic Myopathy. *J. Infect. Dis.* 2014;210(10):1595–9

Mitteldorf C, Mertz KD, Fernández-Figueras MT, Schmid M, Tronnier M, Kempf W. Detection of Merkel cell polyomavirus and human papillomaviruses in Merkel cell carcinoma combined with squamous cell carcinoma in immunocompetent European patients. *Am. J. Dermatopathol.* 2012;34(5):506–10

Modlin IM, Champaneria MC, Bornschein J, Kidd M. Evolution of the diffuse neuroendocrine system--clear cells and cloudy origins. *Neuroendocrinology.* 2006;84(2):69–82

Moens U, Calvignac-Spencer S, Lauber C, Ramqvist T, Feltkamp MCW, Daugherty MD, et al. ICTV Virus Taxonomy Profile: Polyomaviridae. *J. Gen. Virol.* 2017a; Available from: <http://www.microbiologyresearch.org/content/journal/jgv/10.1099/jgv.0.000839.v1>

Moens U, Krumbholz A, Ehlers B, Zell R, Johne R, Calvignac-Spencer S, et al. Biology, evolution, and medical importance of polyomaviruses: An update. *Infect. Genet. Evol. J. Mol. Epidemiol. Evol. Genet. Infect. Dis.* 2017b;54:18–38

Mogha A, Fautrel A, Mouchet N, Guo N, Corre S, Adamski H, et al. Merkel cell polyomavirus small T antigen mRNA level is increased following in vivo UV-radiation. *PLoS One.* 2010;5(7):e11423

Moll I, Kuhn C, Moll R. Cytokeratin 20 is a general marker of cutaneous Merkel cells while certain neuronal proteins are absent. *J. Invest. Dermatol.* 1995;104(6):910–5

Moll I, Lane AT, Franke WW, Moll R. Intraepidermal formation of Merkel cells in xenografts of human fetal skin. *J. Invest. Dermatol.* 1990;94(3):359–64

Moll I, Roessler M, Brandner JM, Eispert A-C, Houdek P, Moll R. Human Merkel cells--aspects of cell biology, distribution and functions. *Eur. J. Cell Biol.* 2005;84(2–3):259–71

Moll I, Troyanovsky SM, Moll R. Special program of differentiation expressed in keratinocytes of human haarscheiben: an analysis of individual cytokeratin polypeptides. *J. Invest. Dermatol.* 1993;100(1):69–76

Morgan GJ. Ludwik Gross, Sarah Stewart, and the 1950s discoveries of Gross murine leukemia virus and polyoma virus. *Stud. Hist. Philos. Sci. Part C Stud. Hist. Philos. Biol. Biomed. Sci.* 2014;48:200–9

Morrison KM, Miesegaes GR, Lumpkin EA, Maricich SM. Mammalian Merkel cells are descended from the epidermal lineage. *Dev. Biol.* 2009;336(1):76–83

Moshiri AS, Doumani R, Yelistratova L, Blom A, Lachance K, Shinohara MM, et al. Polyomavirus-Negative Merkel Cell Carcinoma: A More Aggressive Subtype Based on Analysis of 282 Cases Using Multimodal Tumor Virus Detection. *J. Invest. Dermatol.* 2017;137(4):819–27

Mouchet N, Coquart N, Lebonvallet N, Le Gall-Ianotto C, Mogha A, Fautrel A, et al. Comparative transcriptional profiling of human Merkel cells and Merkel cell carcinoma. *Exp. Dermatol.* 2014;23(12):928–30

Müller DC, Rämö M, Naegele K, Ribi S, Wetterauer C, Perrina V, et al. Donor-derived, metastatic urothelial cancer after kidney transplantation associated with a potentially oncogenic BK polyomavirus. *J. Pathol.*

2018;244(3):265–70

Mulvaney J, Dabdoub A. Atoh1, an essential transcription factor in neurogenesis and intestinal and inner ear development: function, regulation, and context dependency. *J. Assoc. Res. Otolaryngol. JARO*. 2012;13(3):281–93

Murakami I, Takata K, Matsushita M, Nonaka D, Iwasaki T, Kuwamoto S, et al. Immunoglobulin expressions are only associated with MCPyV-positive Merkel cell carcinomas but not with MCPyV-negative ones: comparison of prognosis. *Am. J. Surg. Pathol.* 2014;38(12):1627–35

Nagase K, Kimura H, Yonekura N, Koba S, Inoue T, Narisawa Y. Large-cell neuroendocrine carcinoma of the skin: ultrastructural and immunohistochemical findings. *J. Cutan. Pathol.* 2016;43(11):1067–73

Nagase K, Kimura-Kaku H, Inoue T, Shinogi T, Narisawa Y. Usefulness of ulceration and hyperkeratosis as clinical predictors of Merkel cell polyomavirus-negative and combined Merkel cell carcinoma: A retrospective study. *J. Dermatol.* 2019;46(2):103–9

Nakamura T, Sato Y, Watanabe D, Ito H, Shimonohara N, Tsuji T, et al. Nuclear localization of Merkel cell polyomavirus large T antigen in Merkel cell carcinoma. *Virology*. 2010;398(2):273–9

Narisawa Y, Inoue T, Nagase K. Evidence of proliferative activity in human Merkel cells: implications in the histogenesis of Merkel cell carcinoma. *Arch. Dermatol. Res.* 2018;

Narisawa Y, Koba S, Inoue T, Nagase K. Histogenesis of pure and combined Merkel cell carcinomas: An immunohistochemical study of 14 cases. *J. Dermatol.* 2015;42(5):445–52

Naska S, Yuzwa SA, Johnston APW, Paul S, Smith KM, Paris M, et al. Identification of Drugs that Regulate Dermal Stem Cells and Enhance Skin Repair. *Stem Cell Rep.* 2016;6(1):74–84

Neu U, Hengel H, Blaum BS, Schowalter RM, Macejak D, Gilbert M, et al. Structures of Merkel cell polyomavirus VP1 complexes define a sialic acid binding site required for infection. *PLoS Pathog.* 2012;8(7):e1002738

Nghiem PT, Bhatia S, Lipson EJ, Kudchadkar RR, Miller NJ, Annamalai L, et al. PD-1 Blockade with Pembrolizumab in Advanced Merkel-Cell Carcinoma. *N. Engl. J. Med.* 2016;374(26):2542–52

Nghiem P, Bhatia S, Lipson EJ, Sharfman WH, Kudchadkar RR, Brohl AS, et al. Durable Tumor Regression and Overall Survival in Patients With Advanced Merkel Cell Carcinoma Receiving Pembrolizumab as First-Line Therapy. *J. Clin. Oncol. Off. J. Am. Soc. Clin. Oncol.* 2019;37(9):693–702

Nghiem P, Kaufman HL, Bharmal M, Mahnke L, Phatak H, Becker JC. Systematic literature review of efficacy, safety and tolerability outcomes of chemotherapy regimens in patients with metastatic Merkel cell carcinoma. *Future Oncol. Lond. Engl.* 2017;13(14):1263–79

Nguyen MB, Cohen I, Kumar V, Xu Z, Bar C, Dauber-Decker KL, et al. FGF signalling controls the specification of hair placode-derived SOX9 positive progenitors to Merkel cells. *Nat. Commun.* 2018;9(1):2333

Nguyen KD, Lee EE, Yue Y, Stork J, Pock L, North JP, et al. Human polyomavirus 6 and 7 are associated with pruritic and dyskeratotic dermatoses. *J. Am. Acad. Dermatol.* 2017;76(5):932–940.e3

Nguyen BD, McCullough AE. Imaging of Merkel cell carcinoma. *Radiogr. Rev. Publ. Radiol. Soc. N. Am. Inc.* 2002;22(2):367–76

Nguyen ND, Simmons DB, Bersabe AR, Duginski TM, Sladky JH, Walton D, et al. Lambert-Eaton myasthenic syndrome and merkel cell carcinoma. *Cutis.* 2019;103(5):E19–23

Nicol JTJ, Robinot R, Carpentier A, Carandina G, Mazzoni E, Tognon M, et al. Age-specific seroprevalences of merkel cell polyomavirus, human polyomaviruses 6, 7, and 9, and trichodysplasia spinulosa-associated polyomavirus. *Clin. Vaccine Immunol. CVI.* 2013;20(3):363–8

Niv Y, Goel A, Boland CR. JC virus and colorectal cancer: a possible trigger in the chromosomal instability pathways. *Curr. Opin. Gastroenterol.* 2005;21(1):85–9

Ollier J, Kervarrec T, Samimi M, Benlalam H, Aumont P, Vivien R, et al. Merkel cell carcinoma and cellular cytotoxicity: sensitivity to cellular lysis and screening for potential target antigens suitable for antibody-dependent cellular cytotoxicity. *Cancer Immunol. Immunother. CII.* 2018;67(8):1209–19

Oronsky B, Ma PC, Morgensztern D, Carter CA. Nothing But NET: A Review of Neuroendocrine Tumors and Carcinomas. *Neoplasia N. Y. N.* 2017;19(12):991–1002

Oser MG, Niederst MJ, Sequist LV, Engelman JA. Transformation from non-small-cell lung cancer to small-cell lung cancer: molecular drivers and cells of origin. *Lancet Oncol.* 2015;16(4):e165–172

Ostrowski SM, Wright MC, Bolock AM, Geng X, Maricich SM. Ectopic Atoh1 expression drives Merkel cell production in embryonic, postnatal and adult mouse epidermis. *Dev. Camb. Engl.* 2015;142(14):2533–44

Ota S, Ishikawa S, Takazawa Y, Goto A, Fujii T, Ohashi K, et al. Quantitative analysis of viral load per haploid genome revealed the different biological features of Merkel cell polyomavirus infection in skin tumor. *PLoS One.* 2012;7(6):e39954

Padgett BL, Walker DL, ZuRhein GM, Eckroade RJ, Dessel BH. Cultivation of papova-like virus from human brain with progressive multifocal leucoencephalopathy. *Lancet Lond. Engl.* 1971;1(7712):1257–60

Pan Z, Chen Y-Y, Wu X, Trisal V, Wilczynski SP, Weiss LM, et al. Merkel cell carcinoma of lymph node with unknown primary has a significantly lower association with Merkel cell polyomavirus than its cutaneous counterpart. *Mod. Pathol. Off. J. U. S. Can. Acad. Pathol. Inc.* 2014;27(9):1182–92

Pantulu ND, Pallasch CP, Kurz AK, Kassem A, Frenzel L, Sodenkamp S, et al. Detection of a novel truncating Merkel cell polyomavirus large T antigen deletion in chronic lymphocytic leukemia cells. *Blood.* 2010;116(24):5280–4

Papadimitriou JC, Randhawa P, Rinaldo CH, Drachenberg CB, Alexiev B, Hirsch HH. BK Polyomavirus Infection and Renourinary Tumorigenesis. *Am. J. Transplant. Off. J. Am. Soc. Transplant. Am. Soc. Transpl. Surg.* 2016;16(2):398–406

Park DE, Cheng J, Berrios C, Montero J, Cortés-Cros M, Ferretti S, et al. Dual inhibition of MDM2 and MDM4 in virus-positive Merkel cell carcinoma enhances the p53 response. *Proc. Natl. Acad. Sci. U. S. A.* 2019;116(3):1027–32

Park K-S, Liang M-C, Raiser DM, Zamponi R, Roach RR, Curtis SJ, et al. Characterization of the cell of origin for small cell lung cancer. *Cell Cycle Georget. Tex.* 2011;10(16):2806–15

Pasternak S, Carter MD, Ly TY, Doucette S, Walsh NM. Immunohistochemical profiles of different subsets of Merkel cell carcinoma. *Hum. Pathol.* 2018a;82:232–8

Pastrana DV, Tolstov YL, Becker JC, Moore PS, Chang Y, Buck CB. Quantitation of human seroresponsiveness to Merkel cell polyomavirus. *PLoS Pathog.* 2009;5(9):e1000578

Paulson KG, Carter JJ, Johnson LG, Cahill KW, Iyer JG, Schrama D, et al. Antibodies to merkel cell polyomavirus T antigen oncoproteins reflect tumor burden in merkel cell carcinoma patients. *Cancer Res.* 2010;70(21):8388–97

Paulson KG, Iyer JG, Blom A, Warton EM, Sokil M, Yelistratova L, et al. Systemic immune suppression predicts diminished Merkel cell carcinoma-specific survival independent of stage. *J. Invest. Dermatol.* 2013;133(3):642–6

Paulson KG, Park SY, Vandeven NA, Lachance K, Thomas H, Chapuis AG, et al. Merkel cell carcinoma: Current US incidence and projected increases based on changing demographics. *J. Am. Acad. Dermatol.* 2018;78(3):457-463.e2

Pearse AG. Common cytochemical and ultrastructural characteristics of cells producing polypeptide hormones (the APUD series) and their relevance to thyroid and ultimobranchial C cells and calcitonin. *Proc. R. Soc. Lond. B Biol. Sci.* 1968;170(1018):71–80

Pearse AG. The cytochemistry and ultrastructure of polypeptide hormone-producing cells of the APUD series and the embryologic, physiologic and pathologic implications of the concept. *J. Histochem. Cytochem. Off. J. Histochem. Soc.* 1969;17(5):303–13

Perdigoto CN, Bardot ES, Valdes VJ, Santoriello FJ, Ezhkova E. Embryonic maturation of epidermal Merkel cells is controlled by a redundant transcription factor network. *Dev. Camb. Engl.* 2014;141(24):4690–6

Perdigoto CN, Dauber KL, Bar C, Tsai P-C, Valdes VJ, Cohen I, et al. Polycomb-Mediated Repression and Sonic Hedgehog Signaling Interact to Regulate Merkel Cell Specification during Skin Development. *PLoS Genet.* 2016;12(7):e1006151

Peterson SC, Eberl M, Vagnozzi AN, Belkadi A, Veniaminova NA, Verhaegen ME, et al. Basal cell carcinoma preferentially arises from stem cells within hair follicle and mechanosensory niches. *Cell Stem Cell.* 2015;16(4):400–12

Pilotti S, Rilke F, Bartoli C, Grisotti A. Clinicopathologic correlations of cutaneous neuroendocrine Merkel cell carcinoma. *J. Clin. Oncol. Off. J. Am. Soc. Clin. Oncol.* 1988;6(12):1863–73

Pipas JM. Common and unique features of T antigens encoded by the polyomavirus group. *J. Virol.* 1992;66(7):3979–85

Pipas JM. SV40: Cell transformation and tumorigenesis. *Virology.* 2009;384(2):294–303

Poulin DL, DeCaprio JA. Is there a role for SV40 in human cancer? *J. Clin. Oncol. Off. J. Am. Soc. Clin. Oncol.* 2006;24(26):4356–65

Pulitzer MP, Brannon AR, Berger MF, Louis P, Scott SN, Jungbluth AA, et al. Cutaneous squamous and neuroendocrine carcinoma: genetically and immunohistochemically different from Merkel cell carcinoma. *Mod. Pathol. Off. J. U. S. Can. Acad. Pathol. Inc.* 2015a;28(8):1023–32

Rajagopalan A, Browning D, Salama S. CD99 expression in Merkel cell carcinoma: a case series with an unusual paranuclear dot-like staining pattern. *J. Cutan. Pathol.* 2013;40(1):19–24

Rascovan N, Monteil Bouchard S, Grob J-J, Collet-Villette A-M, Gaudy-Marqueste C, Penicaud M, et al. Human Polyomavirus-6 Infecting Lymph Nodes of a Patient With an Angiolymphoid Hyperplasia With Eosinophilia or Kimura Disease. *Clin. Infect. Dis. Off. Publ. Infect. Dis. Soc. Am.* 2016;62(11):1419–21

Reddi DM, Puri PK. Expression of focal TTF-1 expression in a case of CK7/CK20-positive Merkel cell carcinoma. *J. Cutan. Pathol.* 2013;40(4):431–3

Reichgelt BA, Visser O. Epidemiology and survival of Merkel cell carcinoma in the Netherlands. A population-based study of 808 cases in 1993-2007. *Eur. J. Cancer Oxf. Engl.* 1990. 2011;47(4):579–85

Rekhtman N, Pietanza MC, Hellmann MD, Naidoo J, Arora A, Won H, et al. Next-Generation Sequencing of Pulmonary Large Cell Neuroendocrine Carcinoma Reveals Small Cell Carcinoma-like and Non-Small Cell Carcinoma-like Subsets. *Clin. Cancer Res. Off. J. Am. Assoc. Cancer Res.* 2016;22(14):3618–29

Rennspiess D, Pujari S, Keijzers M, Abdul-Hamid MA, Hochstenbag M, Dingemans A-M, et al. Detection of human polyomavirus 7 in human thymic epithelial tumors. *J. Thorac. Oncol. Off. Publ. Int. Assoc. Study Lung Cancer.* 2015;10(2):360–6

Reploeg MD, Storch GA, Clifford DB. Bk virus: a clinical review. *Clin. Infect. Dis. Off. Publ. Infect. Dis. Soc. Am.* 2001;33(2):191–202

Requena L, Jaqueti G, Rütten A, Mentzel T, Kutzner H. Merkel cell carcinoma within follicular cysts: report of two cases. *J. Cutan. Pathol.* 2008;35(12):1127–33

Rodig SJ, Cheng J, Wardzala J, DoRosario A, Scanlon JJ, Laga AC, et al. Improved detection suggests all Merkel cell carcinomas harbor Merkel polyomavirus. *J. Clin. Invest.* 2012;122(12):4645–53

Rouanet J, Aubin F, Gaboriaud P, Berthon P, Feltkamp MC, Bessenay L, et al. Trichodysplasia spinulosa: a polyomavirus infection specifically targeting follicular keratinocytes in immunocompromised patients. *Br. J. Dermatol.* 2016;174(3):629–32

Royal I, Gourdeau H, Blouin R, Marceau N. Down-regulation of cytokeratin 14 mRNA in polyoma virus middle T-transformed rat liver epithelial cells. *Cell Growth Differ. Mol. Biol. J. Am. Assoc. Cancer Res.* 1992;3(9):589–96

Samimi M. Immune Checkpoint Inhibitors and Beyond: An Overview of Immune-Based Therapies in Merkel Cell Carcinoma. *Am. J. Clin. Dermatol.* 2019;

Samimi M, Molet L, Fleury M, Laude H, Carlotti A, Gardair C, et al. Prognostic value of antibodies to Merkel cell polyomavirus T antigens and VP1 protein in patients with Merkel cell carcinoma. *Br. J. Dermatol.* 2016;174(4):813–22

Samimi M, Touzé A, Laude H, Le Bidre E, Arnold F, Carpentier A, et al. Vitamin D deficiency is associated with greater tumor size and poorer outcome in Merkel cell carcinoma patients. *J. Eur. Acad. Dermatol. Venereol. JEADV.* 2014;28(3):298–308

Santini R, Pietrobono S, Pandolfi S, Montagnani V, D'Amico M, Penachioni JY, et al. SOX2 regulates self-renewal and tumorigenicity of human melanoma-initiating cells. *Oncogene.* 2014;33(38):4697–708

Saraggi D, Salmaso R, Valentini E, Munari G, Vindigni V, Rügge M, et al. Pigmented trichoblastoma developed in a sebaceous nevus: HRAS mutation as a common molecular driver. *Pathol. Res. Pract.* 2017;213(7):860–2

Sastre-Garau X, Peter M, Avril M-F, Laude H, Couturier J, Rozenberg F, et al. Merkel cell carcinoma of the skin: pathological and molecular evidence for a causative role of MCV in oncogenesis. *J. Pathol.* 2009;218(1):48–56

Sauer CM, Haugg AM, Chteinberg E, Rennspiess D, Winnepeninckx V, Speel E-J, et al. Reviewing the current evidence supporting early B-cells as the cellular origin of Merkel cell carcinoma. *Crit. Rev. Oncol. Hematol.* 2017;116:99–105

Scalettar BA, Jacobs C, Fulwiler A, Prah L, Simon A, Hilken L, et al. Hindered submicron mobility and long-term storage of presynaptic dense-core granules revealed by single-particle tracking. *Dev. Neurobiol.* 2012;72(9):1181–95

Schadendorf D, Lebbé C, Zur Hausen A, Avril M-F, Hariharan S, Bharmal M, et al. Merkel cell carcinoma: Epidemiology, prognosis, therapy and unmet medical needs. *Eur. J. Cancer Oxf. Engl.* 1990. 2017;71:53–69

Schmidt U, Müller U, Metz KA, Leder LD. Cytokeratin and neurofilament protein staining in Merkel cell carcinoma of the small cell type and small cell carcinoma of the lung. *Am. J. Dermatopathol.* 1998;20(4):346–51

Schowalter RM, Buck CB. The Merkel cell polyomavirus minor capsid protein. *PLoS Pathog.* 2013;9(8):e1003558

Schowalter RM, Pastrana DV, Buck CB. Glycosaminoglycans and sialylated glycans sequentially facilitate Merkel cell polyomavirus infectious entry. *PLoS Pathog.* 2011;7(7):e1002161

Schowalter RM, Pastrana DV, Pumphrey KA, Moyer AL, Buck CB. Merkel cell polyomavirus and two previously unknown polyomaviruses are chronically shed from human skin. *Cell Host Microbe.* 2010;7(6):509–15

Schowalter RM, Reinhold WC, Buck CB. Entry tropism of BK and Merkel cell polyomaviruses in cell culture. *PLoS One.* 2012;7(7):e42181

Schrama D, Groesser L, Ugurel S, Hafner C, Pastrana DV, Buck CB, et al. Presence of human polyomavirus 6 in mutation-specific BRAF inhibitor-induced epithelial proliferations. *JAMA Dermatol.* 2014;150(11):1180–6

Schrama D, Hesbacher S, Angermeyer S, Schlosser A, Haferkamp S, Aue A, et al. Serine 220 phosphorylation of the Merkel cell polyomavirus large T antigen crucially supports growth of Merkel cell carcinoma cells. *Int. J. Cancer.* 2016;138(5):1153–62

Schrama D, Peitsch WK, Zapatka M, Kneitz H, Houben R, Eib S, et al. Merkel cell polyomavirus status is not associated with clinical course of Merkel cell carcinoma. *J. Invest. Dermatol.* 2011;131(8):1631–8

Schrama D, Sarosi E-M, Adam C, Ritter C, Kaemmerer U, Klopocki E, et al. Characterization of six Merkel cell polyomavirus-positive Merkel cell carcinoma cell lines: Integration pattern suggest that large T antigen truncating events occur before or during integration. *Int. J. Cancer*. 2019;

Scola N, Wieland U, Silling S, Altmeyer P, Stücker M, Kreuter A. Prevalence of human polyomaviruses in common and rare types of non-Merkel cell carcinoma skin cancer. *Br. J. Dermatol.* 2012;167(6):1315–20

Sebastian A, Volk SW, Halai P, Colthurst J, Paus R, Bayat A. Enhanced Neurogenic Biomarker Expression and Reinnervation in Human Acute Skin Wounds Treated by Electrical Stimulation. *J. Invest. Dermatol.* 2017;137(3):737–47

Seo GJ, Chen CJ, Sullivan CS. Merkel cell polyomavirus encodes a microRNA with the ability to autoregulate viral gene expression. *Virology*. 2009;383(2):183–7

Shamir ER, Devine WP, Pekmezci M, Umetsu SE, Krings G, Federman S, et al. Identification of high-risk human papillomavirus and Rb/E2F pathway genomic alterations in mutually exclusive subsets of colorectal neuroendocrine carcinoma. *Mod. Pathol. Off. J. U. S. Can. Acad. Pathol. Inc.* 2018;

Shaw M, Warren S, Groben P, Gully ML. No evidence of Epstein-Barr virus association with Merkel cell carcinoma. *J. Cutan. Pathol.* 2006;33(9):624–8

Shen A-S, Peterhof E, Kind P, Rütten A, Zelger B, Landthaler M, et al. Activating mutations in the RAS/mitogen-activated protein kinase signaling pathway in sporadic trichoblastoma and syringocystadenoma papilliferum. *Hum. Pathol.* 2015;46(2):272–6

Sheu JC, Tran J, Rady PL, Dao H, Tying SK, Nguyen HP. Polyomaviruses of the skin: integrating molecular and clinical advances in an emerging class of viruses. *Br. J. Dermatol.* 2019;180(6):1302–11

Shi X, Zhang Z, Zhan X, Cao M, Satoh T, Akira S, et al. An epigenetic switch induced by Shh signalling regulates gene activation during development and medulloblastoma growth. *Nat. Commun.* 2014;5:5425

Shikova E, Emin D, Alexandrova D, Shindov M, Kumanova A, Lekov A, et al. Detection of Merkel Cell Polyomavirus in Respiratory Tract Specimens. *Intervirolgy*. 2017;60(1–2):28–32

Shuda M, Chang Y, Moore PS. Merkel cell polyomavirus-positive Merkel cell carcinoma requires viral small T-antigen for cell proliferation. *J. Invest. Dermatol.* 2014;134(5):1479–81

Shuda M, Feng H, Kwun HJ, Rosen ST, Gjoerup O, Moore PS, et al. T antigen mutations are a human tumor-specific signature for Merkel cell polyomavirus. *Proc. Natl. Acad. Sci. U. S. A.* 2008;105(42):16272–7

Shuda M, Guastafierro A, Geng X, Shuda Y, Ostrowski SM, Lukianov S, et al. Merkel Cell Polyomavirus Small T Antigen Induces Cancer and Embryonic Merkel Cell Proliferation in a Transgenic Mouse Model. *PLoS One*. 2015a;10(11):e0142329

Shuda M, Kwun HJ, Feng H, Chang Y, Moore PS. Human Merkel cell polyomavirus small T antigen is an oncoprotein targeting the 4E-BP1 translation regulator. *J. Clin. Invest.* 2011b;121(9):3623–34

Sieber-Blum M, Szeder V, Grim M. The role of NT-3 signaling in Merkel cell development. *Prog. Brain Res.* 2004;146:63–72

Sirohi D, Vaske C, Sanborn Z, Smith SC, Don MD, Lindsey KG, et al. Polyoma virus-associated carcinomas of the urologic tract: a clinicopathologic and molecular study. *Mod. Pathol. Off. J. U. S. Can. Acad. Pathol. Inc.* 2018;31(9):1429–41

Spurgeon ME, Cheng J, Bronson RT, Lambert PF, DeCaprio JA. Tumorigenic activity of merkel cell polyomavirus T antigens expressed in the stratified epithelium of mice. *Cancer Res.* 2015a;75(6):1068–79

Stanoszek LM, Chan MP, Palanisamy N, Carskadon S, Siddiqui J, Patel RM, et al. Neurofilament is superior to cytokeratin 20 in supporting cutaneous origin for neuroendocrine carcinoma. *Histopathology*. 2019;74(3):504–13

Stanoszek LM, Wang GY, Harms PW. Histologic Mimics of Basal Cell Carcinoma. *Arch. Pathol. Lab. Med.* 2017;141(11):1490–502

Starrett GJ, Marcelus C, Cantalupo PG, Katz JP, Cheng J, Akagi K, et al. Merkel Cell Polyomavirus Exhibits Dominant Control of the Tumor Genome and Transcriptome in Virus-Associated Merkel Cell Carcinoma. *mBio*. 2017;8(1)

Stewart SE, Eddy BE, Borgese N. Neoplasms in mice inoculated with a tumor agent carried in tissue culture. *J. Natl. Cancer Inst.* 1958;20(6):1223–43

Su LD, Fullen DR, Lowe L, Uherova P, Schnitzer B, Valdez R. CD117 (KIT receptor) expression in Merkel cell carcinoma. *Am. J. Dermatopathol.* 2002;24(4):289–93

Sunshine JC, Jahchan NS, Sage J, Choi J. Are there multiple cells of origin of Merkel cell carcinoma? *Oncogene*. 2018;37(11):1409–16

Sutherland KD, Proost N, Brouns I, Adriaensen D, Song J-Y, Berns A. Cell of origin of small cell lung cancer: inactivation of Trp53 and Rb1 in distinct cell types of adult mouse lung. *Cancer Cell*. 2011;19(6):754–64

Sweet BH, Hilleman MR. The vacuolating virus, S.V. 40. *Proc. Soc. Exp. Biol. Med. Soc. Exp. Biol. Med. N. Y. N.*

1960;105:420–7

Swick BL, Ravdel L, Fitzpatrick JE, Robinson WA. Platelet-derived growth factor receptor alpha mutational status and immunohistochemical expression in Merkel cell carcinoma: implications for treatment with imatinib mesylate. *J. Cutan. Pathol.* 2008;35(2):197–202

Swick BL, Srikantha R, Messingham KN. Specific analysis of KIT and PDGFR-alpha expression and mutational status in Merkel cell carcinoma. *J. Cutan. Pathol.* 2013;40(7):623–30

Syder AJ, Karam SM, Mills JC, Ippolito JE, Ansari HR, Farook V, et al. A transgenic mouse model of metastatic carcinoma involving transdifferentiation of a gastric epithelial lineage progenitor to a neuroendocrine phenotype. *Proc. Natl. Acad. Sci. U. S. A.* 2004;101(13):4471–6

Szedler V, Grim M, Halata Z, Sieber-Blum M. Neural crest origin of mammalian Merkel cells. *Dev. Biol.* 2003;253(2):258–63

Tadmor T, Aviv A, Polliack A. Merkel cell carcinoma, chronic lymphocytic leukemia and other lymphoproliferative disorders: an old bond with possible new viral ties. *Ann. Oncol. Off. J. Eur. Soc. Med. Oncol.* 2011;22(2):250–6

Takahashi K, Yamanaka S. Induction of pluripotent stem cells from mouse embryonic and adult fibroblast cultures by defined factors. *Cell.* 2006;126(4):663–76

Tan TH, Wallis J, Levine AJ. Identification of the p53 protein domain involved in formation of the simian virus 40 large T-antigen-p53 protein complex. *J. Virol.* 1986;59(3):574–83

Tang CK, Toker C. Trabecular carcinoma of the skin: an ultrastructural study. *Cancer.* 1978;42(5):2311–21

Tellechea O, Cardoso JC, Reis JP, Ramos L, Gameiro AR, Coutinho I, et al. Benign follicular tumors. *An. Bras. Dermatol.* 2015;90(6):780–96; quiz 797–8

Testa U, Castelli G, Pelosi E. Lung Cancers: Molecular Characterization, Clonal Heterogeneity and Evolution, and Cancer Stem Cells. *Cancers.* 2018;10(8)

Tilling T, Moll I. Which are the cells of origin in merkel cell carcinoma? *J. Skin Cancer.* 2012a;2012:680410

Tilling T, Wladykowski E, Failla AV, Houdek P, Brandner JM, Moll I. Immunohistochemical analyses point to epidermal origin of human Merkel cells. *Histochem. Cell Biol.* 2014;141(4):407–21

Tischler AS. Small cell carcinoma of the lung: cellular origin and relationship to other neoplasms. *Semin. Oncol.* 1978;5(3):244–52

Toker C. Trabecular carcinoma of the skin. *Arch. Dermatol.* 1972;105(1):107–10

Tolstov YL, Knauer A, Chen JG, Kensler TW, Kingsley LA, Moore PS, et al. Asymptomatic primary Merkel cell polyomavirus infection among adults. *Emerg. Infect. Dis.* 2011;17(8):1371–80

Tolstov YL, Pastrana DV, Feng H, Becker JC, Jenkins FJ, Moschos S, et al. Human Merkel cell polyomavirus infection II. MCV is a common human infection that can be detected by conformational capsid epitope immunoassays. *Int. J. Cancer.* 2009;125(6):1250–6

Toptan T, Yousem SA, Ho J, Matsushima Y, Stabile LP, Fernández-Figueras M-T, et al. Survey for human polyomaviruses in cancer. *JCI Insight.* 2016;1(2)

Touzé A, Gaitan J, Arnold F, Cazal R, Fleury MJ, Combelas N, et al. Generation of Merkel cell polyomavirus (MCV)-like particles and their application to detection of MCV antibodies. *J. Clin. Microbiol.* 2010;48(5):1767–70

Touzé A, Le Bidre E, Laude H, Fleury MJ, Cazal R, Arnold F, et al. High levels of antibodies against merkel cell polyomavirus identify a subset of patients with merkel cell carcinoma with better clinical outcome. *J. Clin. Oncol. Off. J. Am. Soc. Clin. Oncol.* 2011;29(12):1612–9

Tsang SH, Wang X, Li J, Buck CB, You J. Host DNA damage response factors localize to merkel cell polyomavirus DNA replication sites to support efficient viral DNA replication. *J. Virol.* 2014;88(6):3285–97

Tsang SH, Wang R, Nakamaru-Ogiso E, Knight SAB, Buck CB, You J. The Oncogenic Small Tumor Antigen of Merkel Cell Polyomavirus Is an Iron-Sulfur Cluster Protein That Enhances Viral DNA Replication. *J. Virol.* 2016;90(3):1544–56

Tseng YD, Apisarnthanarax S, Liao JJ, Bhatia S, Nghiem PT, Parvathaneni U. Factors influencing radiation treatment recommendations in early-stage Merkel cell carcinoma: a survey of US-based radiation oncologists. *Expert Rev. Anticancer Ther.* 2017;17(3):281–7

Van Gele M, Leonard JH, Van Roy N, Cook AL, De Paepe A, Speleman F. Frequent allelic loss at 10q23 but low incidence of PTEN mutations in Merkel cell carcinoma. *Int. J. Cancer.* 2001;92(3):409–13

Van Keymeulen A, Mascre G, Youseff KK, Harel I, Michaux C, De Geest N, et al. Epidermal progenitors give rise to Merkel cells during embryonic development and adult homeostasis. *J. Cell Biol.* 2009;187(1):91–100

Vela-Romera A, Carriel V, Martín-Piedra MA, Aneiros-Fernández J, Campos F, Chato-Astrain J, et al. Characterization of the human ridged and non-ridged skin: a comprehensive histological, histochemical and immunohistochemical analysis. *Histochem. Cell Biol.* 2018;

Verhaegen ME, Mangelberger D, Harms PW, Eberl M, Wilbert DM, Meireles J, et al. Merkel cell polyomavirus small T antigen initiates Merkel cell carcinoma-like tumor development in mice. *Cancer Res.* 2017a;77(12):3151–7

Verhaegen ME, Mangelberger D, Harms PW, Vozheiko TD, Weick JW, Wilbert DM, et al. Merkel cell polyomavirus small T antigen is oncogenic in transgenic mice. *J. Invest. Dermatol.* 2015;135(5):1415–24

Vidal VPI, Ortonne N, Schedl A. SOX9 expression is a general marker of basal cell carcinoma and adnexal-related neoplasms. *J. Cutan. Pathol.* 2008;35(4):373–9

Vinik A. Diffuse Hormonal Systems. In: Feingold KR, Anawalt B, Boyce A, Chrousos G, Dungan K, Grossman A, et al., editors. *Endotext*. South Dartmouth (MA): MDText.com, Inc.; 2000 [cited 2019 Aug 21]. Available from: <http://www.ncbi.nlm.nih.gov/books/NBK279025/>

Visvader JE. Cells of origin in cancer. *Nature.* 2011;469(7330):314–22

Vitalis T, Alvarez C, Chen K, Shih JC, Gaspar P, Cases O. Developmental expression pattern of monoamine oxidases in sensory organs and neural crest derivatives. *J. Comp. Neurol.* 2003;464(3):392–403

Walsh NM. Primary neuroendocrine (Merkel cell) carcinoma of the skin: morphologic diversity and implications thereof. *Hum. Pathol.* 2001;32(7):680–9

Wang X, Li J, Schowalter RM, Jiao J, Buck CB, You J. Bromodomain protein Brd4 plays a key role in Merkel cell polyomavirus DNA replication. *PLoS Pathog.* 2012;8(11):e1003021

Wendzicki JA, Moore PS, Chang Y. Large T and small T antigens of Merkel Cell Polyomavirus. *Curr. Opin. Virol.* 2015;11:38–43

WHO. WHO classification of skin tumours. 4th edition. Elder DE, Massi D, Scolyer RA, Willemze R, editors. Lyon: International Agency for Research on Cancer; 2018.

Wiedinger K, Bitsaktsis C, Chang S. Reactivation of human polyomaviruses in immunocompromised states. *J. Neurovirol.* 2014;20(1):1–8

Wieland U, Mauch C, Kreuter A, Krieg T, Pfister H. Merkel cell polyomavirus DNA in persons without merkel cell carcinoma. *Emerg. Infect. Dis.* 2009;15(9):1496–8

Willmes C, Adam C, Alb M, Völkert L, Houben R, Becker JC, et al. Type I and II IFNs inhibit Merkel cell carcinoma via modulation of the Merkel cell polyomavirus T antigens. *Cancer Res.* 2012;72(8):2120–8

Winkelman RK. The Merkel cell system and a comparison between it and the neurosecretory or APUD cell system. *J. Invest. Dermatol.* 1977b;69(1):41–6

Wong SQ, Waldeck K, Vergara IA, Schröder J, Madore J, Wilmott JS, et al. UV-Associated Mutations Underlie the Etiology of MCV-Negative Merkel Cell Carcinomas. *Cancer Res.* 2015;75(24):5228–34

Wright MC, Logan GJ, Bolock AM, Kubicki AC, Hemphill JA, Sanders TA, et al. Merkel cells are long-lived cells whose production is stimulated by skin injury. *Dev. Biol.* 2017;422(1):4–13

Xiao Y, Thoresen DT, Williams JS, Wang C, Perna J, Petrova R, et al. Neural Hedgehog signaling maintains stem cell renewal in the sensory touch dome epithelium. *Proc. Natl. Acad. Sci. U. S. A.* 2015a;112(23):7195–200

Xiao Y, Williams JS, Brownell I. Merkel cells and touch domes: more than mechanosensory functions? *Exp. Dermatol.* 2014;23(10):692–5

Yang S-B, Chen X, Wu B-Y, Wang M-W, Cai C-H, Cho D-B, et al. Immunoglobulin kappa and immunoglobulin lambda are required for expression of the anti-apoptotic molecule Bcl-xL in human colorectal cancer tissue. *Scand. J. Gastroenterol.* 2009;44(12):1443–51

Yarchoan M, Albacker LA, Hopkins AC, Montesion M, Murugesan K, Vithayathil TT, et al. PD-L1 expression and tumor mutational burden are independent biomarkers in most cancers. *JCI Insight.* 2019;4(6)

Yazawa T. Recent advances in histogenesis research of lung neuroendocrine cancers: Evidence obtained from functional analyses of primitive neural/neuroendocrine cell-specific transcription factors. *Pathol. Int.* 2015;65(6):277–85

Yesner R. Are small-cell carcinomas of the lung derived from neural crest? *N. Engl. J. Med.* 1980;303(1):51

Yoshimoto T, Motoi N, Yamamoto N, Nagano H, Ushijima M, Matsuura M, et al. Pulmonary Carcinoids and Low-Grade Gastrointestinal Neuroendocrine Tumors Show Common MicroRNA Expression Profiles, Different from Adenocarcinomas and Small Cell Carcinomas. *Neuroendocrinology.* 2018;106(1):47–57

Youlenden DR, Soyer HP, Youl PH, Fritschi L, Baade PD. Incidence and survival for Merkel cell carcinoma in Queensland, Australia, 1993-2010. *JAMA Dermatol.* 2014;150(8):864–72

Zaragoza J, Kervarrec T, Touzé A, Avenel-Audran M, Beneton N, Esteve E, et al. A high neutrophil-to-lymphocyte ratio as a potential marker of mortality in patients with Merkel cell carcinoma: A retrospective study. *J. Am. Acad. Dermatol.* 2016;75(4):712-721.e1

Zheng X, Liu D, Fallon JT, Zhong M. Distinct genetic alterations in small cell carcinoma from different anatomic sites. *Exp. Hematol. Oncol.* 2015;4:2

Zheng Y, Tian Q, Wang J, Dong X, Jing H, Wang X, et al. Differential diagnosis of eccrine spiradenoma: A case

report. *Exp. Ther. Med.* 2014;8(4):1097–101

Zur Hausen A, Rennspiess D, Winnepenninckx V, Speel E-J, Kurz AK. Early B-cell differentiation in Merkel cell carcinomas: clues to cellular ancestry. *Cancer Res.* 2013a;73(16):4982–7

WHO CLASSIFICATION OF SKIN TUMOURS. S.I.: WORLD HEALTH ORGANIZATION; 2018.

ABSTRACT

Merkel cell carcinoma (MCC) is a rare and aggressive skin cancer. In approximately 80% of cases, genomic integration of the Merkel cell polyomavirus (MCPyV) is observed and overexpression of the two MCPyV T antigens (TAg) is regarded as the main oncogenic determinant of MCPyV-positive MCC cases. However, the nature of the cells from which MCC arises is unknown. Therefore, the goal of the present work was to determine the cell of origin of MCC.

First, we characterized MCC patients' tumors and demonstrated a high similarity of MCPyV-negative MCC with extracutaneous neuroendocrine carcinoma while MCPyV-positive MCC differs from these two groups with respect to morphology, immunohistochemical profile, genetics, origin and behavior. Based on the analysis of a trichoblastoma/MCC combined tumor, we demonstrated that a MCPyV-positive MCC can arise following MCPyV integration in an epithelial cell. In addition, the high similarity between trichoblastoma cells and Merkel cell (MC) progenitors of the hair follicle suggests that these hair follicle cells may represent a general start point for the development of MCPyV-positive MCC. A contribution of the viral TAg to the development of the characteristic Merkel cell-like MCC phenotype is suggested by experiments demonstrating induction of Merkel cell markers upon TAg expression in human primary keratinocytes or hair follicle cells. As potential mechanisms mediating these phenotypic changes, we identified the capability of MCPyV LT to repress degradation of master regulator of MC development, i.e. the transcription factor ATOH1.

To conclude, our work suggests that MCPyV integration in epithelial cells of the hair follicle may represent an important path for MCC development.

ABSTRAKT

Das Merkelzellkarzinom (MCC) ist ein seltener und aggressiver Hautkrebs. In etwa 80% der Fälle wird die genomische Integration des Merkelzell-Polyomavirus (MCPyV) beobachtet und die Überexpression der beiden MCPyV-T-Antigene (TAGs) gilt als die wichtigste onkogene Determinante der MCPyV-positiven MCC-Fälle. Die Ursprungszelle des MCC ist jedoch bisher unbekannt. Daher war das Ziel der vorliegenden Arbeit, die Hinweise auf die Herkunftszelle zu generieren.

Zuerst charakterisierten wir deshalb Tumore von MCC-Patienten und konnten dabei eine hohe Ähnlichkeit von MCPyV-negativem MCC mit extrakutanem neuroendokrinem Karzinom zeigen, während sich MCPyV-positive MCC von diesen beiden Gruppen in Bezug auf Morphologie, immunhistochemisches Profil, Genetik, Herkunft und Verhalten unterscheidet. Basierend auf der Analyse eines kombinierten Trichoblastom/MCC-Tumors konnten wir nachweisen, dass nach der MCPyV-Integration in eine Epithelzelle ein MCPyV-positives MCC entstehen kann. Darüber hinaus deutet die hohe Ähnlichkeit zwischen Trichoblastomzellen und Merkelzellen (MC)-Vorläufern des Haarfollikels darauf hin, dass diese Haarfollikelzellen einen allgemeinen Ausgangspunkt für die Entwicklung von MCPyV-positivem MCC darstellen könnten. *In vitro* Experimente zeigten den Beitrag der viralen TAGs zur Entwicklung des charakteristischen Merkelzell-ähnlichen MCC-Phänotyps, denn durch TAG-Expression in menschlichen primären Keratinozyten oder Haarfollikelzellen kam es zur Induktion von Merkelzellmarkern. Als einen potenziellen Mechanismus, der diese phänotypischen Veränderungen vermittelt, identifizierten wir die Fähigkeit von MCPyV LT, die Degradation des Transkriptionsfaktors ATOH1, den Masterregulator der MC-Entwicklung, zu unterdrücken. Zusammenfassend lässt sich sagen, dass die MCPyV-Integration in Epithelzellen des Haarfollikels einen wichtigen Beitrag zur MCC-Entwicklung darstellen könnte.